TEXT FLY WITHIN
THE BOOK ONLY

AERODYNAMICS

By the Same Author

A Complete Course in Elementary Aerodynamics with Experiments and Examples

AERODYNAMICS

BY

N. A. V. PIERCY

D.Sc., M.Inst.C.E., M.I.Mech.E., F.R.Ae.S.

Reader in Aeronautics in the University of London
Head of the Department of Aeronautics, Queen Mary College
Member of the Association of Consulting Engineers

SECOND EDITION

THE ENGLISH UNIVERSITIES PRESS LTD
LONDON

First Printed 1937
Reprinted 1943
Second Edition, Revised and Enlarged 1947

Made and Printed in Great Britain by
Hazell, Watson & Viney Ltd., London and Aylesbury.

PREFACE TO SECOND EDITION

THE present edition is enlarged to provide, in the first place, an introduction to the mathematical and experimental study of compressible flow, subsonic and supersonic. This and other matters now becoming prominent are not collected in a supplementary section but incorporated in place as additional articles or short chapters. Following a well-established practice, the numbering of original articles, figures and chapters is left undisturbed as far as possible, interpolations being distinguished by letter-suffixes. It is hoped this procedure will ensure a minimum of inconvenience to readers familiar with the earlier edition. To some extent the unlettered articles indicate a first course of reading, though a modern view of Aerodynamics requires consideration of Mach numbers equally with Reynolds numbers almost from the outset.

Other matters now represented include various theories of thin aerofoils and the reduction of profile drag. The brief account of the laminar-flow wing is in general terms, but the author has drawn for illustrations on the conformal system, in the development of which he has shared more particularly.

The original text is revised to bring it up to date, and also in the following connection. Experience incidental to the use of the book at Cambridge and London Universities isolated certain parts where the treatment was insufficiently detailed for undergraduates ; these are now suitably expanded.

The aim of the book remains unchanged. It does not set out to collect and summarise the researches, test results and current practice of the subject, but rather to provide an adequate and educational introduction to a vast specialist literature in a form that will be serviceable for first and higher degrees, and like purposes, including those of the professional engineer.

N. A. V. PIERCY.

TEMPLE,
October, 1946.

PREFACE TO FIRST EDITION

FIRST steps towards formulating the science of Aerodynamics preceded by only a few years the epoch-making flight by the Wright brothers in 1903. Within a decade, many fundamentals had been established, notably by Lanchester, Prandtl, Joukowski, and Bryan. Yet some time elapsed before these essentially mathematical conceptions, apart from aircraft stability, were generally adopted. Meanwhile, development proceeded largely by model experiment. To-day, much resulting empiricism has been superseded and the subject is unique among those within the purview of Engineering in its constant appeal to such masters as Helmholtz and Kelvin, Reynolds and Rankine. A complete theory is still far out of reach ; experiment, if no longer paramount, remains as important as analysis ; and there is a continual swinging of the pendulum between these two, with progress in aviation marking time.

This book presents the modern science of Aerodynamics and its immediate application to aircraft. The arrangement is based on some eighteen years' organisation of teaching and research in the University of London. The first five chapters, and the simpler parts of Chapters VI–XII, constitute an undergraduate course ; more advanced matters are included to serve especially the Designer and Research Engineer. No attempt has been made to summarise reports from the various Aerodynamic Laboratories, which must be consulted for design data, but the treatment is intended to provide an adequate introduction to the extensive libraries of important original papers that now exist in this country and abroad.

To facilitate reference, symbols have been retained, for the most part, in familiar connections, though duplication results in several instances, as shown in the list of notations. Of the two current systems of force and moment coefficients, the American or Continental, associated with " C," will probably supersede the British, distinguished by " k." No great matter is involved, a C-coefficient being derived merely by doubling the corresponding k-coefficient. However, so many references will be made in this country to literature using the " k " notation that the latter has been given some preference.

My thanks are due to Professor W. G. Bickley for reading the proof sheets and making many suggestions ; also to The English Universities Press for unremitting care and consideration.

N. A. V. PIERCY.

TEMPLE.

CONTENTS

CHAPTER I

AIR AT REST, THE ATMOSPHERE AND STATIC LIFT

CHAPTER II

AIR FLOW AND AERODYNAMIC FORCE

CHAPTER III

WIND-TUNNEL EXPERIMENT

CHAPTER III A

EXPERIMENT AT HIGH SPEEDS

CHAPTER IV

AIRCRAFT IN STEADY FLIGHT

CHAPTER V

FUNDAMENTALS OF THE IRROTATIONAL FLOW

CHAPTER VI

TWO-DIMENSIONAL AEROFOILS

CHAPTER VI A

THIN AEROFOILS AT ORDINARY SPEEDS

CHAPTER VI B

COMPRESSIBLE INVISCID FLOW

CHAPTER VI C

THIN AEROFOILS AT HIGH SPEEDS

CHAPTER VII

VORTICES AND THEIR RELATION TO DRAG AND LIFT

CHAPTER VIII

WING THEORY

CHAPTER IX

VISCOUS FLOW AND SKIN DRAG

CHAPTER IX A

REDUCTION OF PROFILE DRAG

CHAPTER X

AIRSCREWS AND THE AUTOGYRO

CHAPTER XI

PERFORMANCE AND EFFICIENCY

CHAPTER XII

SAFETY IN FLIGHT

NOTATION

(Some of the symbols are also used occasionally in connections other than those stated below.)

A . . .	Aerodynamic force; aspect ratio; transverse moment of inertia.
A.R.C.R. & M.	Aeronautical Research Committee's Reports and Memoranda.
A.S.I. . .	Air speed indicator.
a . . .	Axial inflow factor of airscrews; leverage of Aerodynamic force about C.G. of craft; slope of lift curve of wings; velocity of sound in air.
a' . . .	Slope of lift curve of tail plane.
α . . .	Angle of incidence.
α_t . . .	Tail-setting angle.
B . . .	Gas constant; longitudinal moment of inertia; number of blades of an airscrew.
B_1, B_2 . .	Stability coefficients.
b . . .	Rotational interference factor of airscrews.
β . . .	Transverse dihedral; twice the mean camber of a wing.
C . . .	Directional moment of inertia; sectional area of tunnel.
C.A.T. . .	Compressed air tunnel.
C_1, C_2 . .	Stability coefficients.
C_L, C_D, etc. .	Non-dimensional coefficients of lift, drag, etc., on basis of stagnation pressure.
C.G. . .	Centre of gravity.
C.P. . .	Centre of pressure.
c . . .	Chord of wing or aerofoil; molecular velocity.
γ . . .	Ratio of specific heats; $\tan^{-1}$ (drag/lift).
D . . .	Diameter; drag.
D_1, D_2 . .	Stability coefficients.
Δ, δ . .	Thickness of boundary layer; displacement thickness.
E . . .	Elasticity; kinetic energy.
E_1, E_2 . .	Stability coefficients.

e . . . Base of the Napierian logarithms.
ε . . . Angle of downwash.
F . . . Skin friction (in Chapter II) ; Froude Number.
$\sim$ . . Frequency.
ζ . . . Vorticity.
g . . . Acceleration due to gravity.
H . . . Horse power ; the boundary layer ratio δ/θ.
h . . . Aerodynamic gap ; height or altitude.
η . . . A co-ordinate ; efficiency ; elevator angle.
θ . . . Airscrew blade angle ; angle of climb ; angular co-ordinate ; temperature on the Centigrade scale ; momentum thickness.
I . . . Impulse ; second moment of area.
i . . . $\sqrt{-1}$; as suffix to D: denoting induced drag ; incidence of autogyro disc.
J . . . The advance of an airscrew per revolution in terms of its diameter.
K . . . Circulation.
k . . . Radius of gyration ; roughness.
k_A, k_B, k_C . Inertia coefficients.
k_L, k_D, etc. . Non-dimensional coefficients of lift, drag, etc., on basis of twice the stagnation pressure.
k_x, k_z . . British drag and lift coefficients of autogyro rotor.
L . . . Lift ; rolling moment.
l . . . Length ; leverage of tail lift about C.G. of craft.
λ . . . Damping factor ; mean free path of molecule ; mean lift per unit span.
M . . Pitching moment ; Mach number.
m . . . Mass ; with suffix: non-dimensional moment derivative ; Mach angle.
μ . . . Coefficient of viscosity ; 'relative density of aeroplane' ; a co-ordinate.
N . . . Yawing moment.
N.A.C.A. . National Advisory Committee for Aeronautics, U.S.A.
N.P.L. . . National Physical Laboratory, Teddington.
n . . . Distance along a normal to a surface ; revolutions per sec.
ν . . . Kinematic coefficient of viscosity ; a co-ordinate.
ξ . . . A co-ordinate.
P . . . Pitch of an airscrew ; pressure gradient ; total pressure.

p . . . Angular velocity of roll ; pressure or stress.
ρ . . . Density of air in slugs per cu. ft.
Q . . . Torque.
q . . . Angular velocity of pitch ; resultant fluid velocity.
R . . . Radius ; Reynolds number.
R_1, R_2 . . Routh's discriminant.
R.A.E. . . Royal Aircraft Establishment, Farnborough.
r . . . Angular velocity of yaw ; lift/drag ratio ; radius.
r_a . . . Over-all lift/drag ratio.
S . . . Area, particularly of wings.
s . . . Distance along contour or streamline ; semi-span.
σ . . . Density of air relative to sea-level standard ; Prandtl's biplane factor ; sectional area of vortex ; solidity of an airscrew.
T . . . Thickness ; thrust.
t . . . Period of time in sec. ; the complex co-ordinate $\xi + i\eta$.
t_0 . . . Unit of time in non-dimensional stability equations.
τ . . . Absolute temperature ; skin friction in Chapter IX ; tail angle of aerofoil section ; tail volume ratio.
ϕ . . . Aerodynamic stagger ; angle of bank ; angle of helical path of airscrew element ; velocity
[illegible]tial.
[illegible]ion ; yaw.
[illegible]f undisturbed velocity in the direc-
[illegible], Oz.
[illegible]city of a body.
[illegible]
[illegible]ircraft.
[illegible] components in the directions Ox,
[illegible]).
[illegible]city ; mean loading of wing in
[illegible]: potential function $\phi + i\psi$.
[illegible]f force.
[illegible]f stability charts.
[illegible]dinates ; with suffixes : non-dimen-
derivatives.

z . . .	The complex co-ordinate $x + iy$.
Ω . . .	Angular velocity of an airscrew.
ω . . .	Angular velocity.
ϖ . . .	Impulsive pressure.
∇^2 . .	$\partial^2/\partial x^2 + \partial^2/\partial y^2$.
∇^4 . .	$(\partial^2/\partial x^2 + \partial^2/\partial y^2)(\partial^2/\partial x^2 + \partial^2/\partial y^2)$.

Chapter I

AIR AT REST, THE ATMOSPHERE AND STATIC LIFT

1. Air at sea-level consists by volume of 78 per cent. nitrogen, 21 per cent. oxygen, and nearly 1 per cent. argon, together with traces of neon, helium, possibly hydrogen, and other gases. Although the constituent gases are of different densities, the mixture is maintained practically constant up to altitudes of about 7 miles in temperate latitudes by circulation due to winds. This lower part of the atmosphere, varying in thickness from 4 miles at the poles to 9 miles at the equator, is known as the troposphere. Above it is the stratosphere, a layer where the heavier gases tend to be left at lower levels until, at great altitudes, such as 50 miles, little but helium or hydrogen remains. Atmospheric air contains water-vapour in varying proportion, sometimes exceeding 1 per cent. by weight.

From the point of view of kinetic theory, air at a temperature of 0° C. and at standard barometric pressure (760 mm. of mercury) may be regarded statistically as composed of discrete molecules, of mean diameter $1{\cdot}5 \times 10^{-5}$ mil (one-thousandth inch), to the number of $4{\cdot}4 \times 10^{11}$ per cu. mil. These molecules are moving rectilinearly in all directions with a mean velocity of 1470 ft. per sec., i.e. one-third faster than sound in air. They come continually into collision with one another, the length of the mean free path being 0·0023 mil.

2. Density

Air is thus not a continuum. If it were, the density at a point would be defined as follows: considering the mass M of a small volume V of air surrounding the point, the density would be the limiting ratio of M/V as V vanishes. But we must suppose that the volume V enclosing the point is contracted only until it is small compared with the scale of variation of density, while it still remains large compared with the mean distance separating the molecules. Clearly, however, V can become very small before the continuous passage of molecules in all directions across its bounding surface can make indefinite the number of molecules enclosed and M or M/V uncertain. Density is thus defined as the ratio of the

mass of this very small, though finite, volume of air—i.e. of the aggregate mass of the molecules enclosed—to the volume itself.

Density is denoted by ρ, and has the dimensions M/L^3. In Aerodynamics it is convenient to use the slug-ft.-sec. system of units.* At 15° C. and standard pressure 1 cu. ft. of dry air weighs 0·0765 lb. This gives $\rho = 0{\cdot}0765/g = 0{\cdot}00238$ slug per cu. ft.

It will be necessary to consider in many connections lengths, areas, and volumes that ultimately become very small. We shall tacitly assume a restriction to be imposed on such contraction as discussed above. To take a further example, when physical properties are attached to a ' point ' we shall have in mind a sphere of very small but sufficient radius centred at the geometrical point.

3. Pressure

Consider a small rigid surface suspended in a bulk of air at rest. The molecular motion causes molecules continually to strike, or tend to strike, the immersed surface, so that a rate of change of molecular momentum occurs there. This cannot have a component parallel to the surface, or the condition of rest would be disturbed. Thus, when the gas is apparently at rest, the aggregate rate of change of momentum is normal to the surface; it can be represented by a force which is everywhere directed at right angles towards the surface. The intensity of the force per unit area is the pressure p, sometimes called the hydrostatic or static pressure.

It is important to note that the lack of a tangential component to p depends upon the condition of stationary equilibrium. The converse statement, that fluids at rest cannot withstand a tangential or shearing force, however small, serves to distinguish liquids from solids. For gases we must add that a given quantity can expand to fill a volume, however great.

It will now be shown that the pressure at a point in a fluid at rest is uniform in all directions. Draw the small tetrahedron ABCO, of

* In this system, the units of length and time are the foot and the second, whilst forces are in pounds weight. It is usual in Engineering, however, to omit the word ' weight,' writing ' lb.' for ' lb.-wt.,' and this convention is followed. The appropriate unit of mass is the ' slug,' viz. the mass of a body weighing g lb. Velocities are consistently measured in ft. per sec., and so on. This system being understood, specification of units will often be omitted from calculations for brevity. For example, when a particular value of the kinematic viscosity is given as a number, sq. ft. per sec. will be implied. It will be desirable occasionally to introduce special units. Thus the size and speed of aircraft are more easily visualised when weights are expressed in tons and velocities in miles per hour. The special units will be duly indicated in such cases. Non-dimensional coefficients are employed wherever convenient.

which the faces OAB, OBC, OCA are mutually at right angles (Fig. 1). Denote by S the area of the face ABC. With the help of OD drawn perpendicular to this face, it is easily verified from the figure that the area OCA is $S \cdot \cos\alpha$. The pressure p_{ABC} on the S-face gives rise to a force $p_{ABC} \cdot S$ which acts parallel to DO. From the pressures on the other faces, forces similarly arise which are wholly perpendicular to the respective faces.

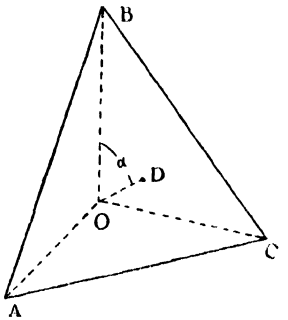

FIG. 1.

Resolving in the direction BO, for equilibrium

$$W + p_{ABC} \cdot S \cdot \cos\alpha - p_{OCA} \cdot S \cdot \cos\alpha = 0,$$

where W is a force component on the tetrahedron arising from some general field of force in which the bulk of air may be situated ; such might be, for example, the gravitational field, when W would be the weight of the tetrahedron if also OB were vertical. But W is proportional to the volume of the tetrahedron, i.e. to the third order of small quantities, and is negligible compared with the other terms of the equation, which are proportional to areas, i.e. to the second order of small quantities. Hence :

$$p_{ABC} = p_{OCA}.$$

Similarly :

$$p_{ABC} = p_{OAB} = p_{OBC}.$$

4. It will be of interest to have an expression for p in terms of molecular motions.

Considering a rigid plane surface suspended in air, draw Oy, Oz mutually at right angles in its plane and Ox perpendicular to it (Fig. 2). Erect on a unit area S of the plane, and to one side of it a right cylinder of unit length, so that it encloses unit volume of air. If m is the mass of each molecule, the total number N of molecules enclosed is ρ/m. They are moving in all directions with mean velocity c along straight paths of mean length λ.

At a chosen instant the velocities of all the molecules can be resolved parallel to Ox, Oy, Oz. But, since N is very large, it is equivalent to suppose that $N/3$ molecules move parallel to each of the co-ordinate axes with velocity c during the short time Δt required to describe the mean free path. Molecules moving parallel to Oy, Oz cannot impinge on S ; we need consider only molecules moving

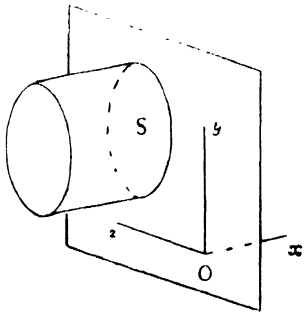

FIG. 2.

parallel to Ox, and of these only one-half must be taken as moving towards S, i.e. in the specific direction Ox (Fig. 2).

The interval of time corresponding to the free path is given by—

$$\Delta t = \lambda/c.$$

During this interval all those molecules moving in the direction Ox which are distant, at the beginning of Δt, no farther than λ from S, will strike S. Their number is evidently $\lambda N/6$. Each is assumed perfectly elastic, and so will have its velocity exactly reversed. Thus the aggregate change of momentum at S in time Δt is $2mc \,.\, \lambda N/6$. The pressure p, representing the rate of change of momentum, is thus given by :

$$\begin{aligned} p &= \frac{2mc\lambda N}{6\,.\,\Delta t} \\ &= \tfrac{1}{3}Nmc^2 \\ &= \tfrac{1}{3}\rho c^2. \quad . \quad . \quad . \quad . \quad . \quad (1) \end{aligned}$$

Thus the pressure amounts to two-thirds of the molecular kinetic energy per unit volume.

5. The Hydrostatic Equation

We now approach the problem of the equilibrium of a bulk of air at rest under the external force of gravity. g has the dimensions of an acceleration, L/T^2. Its value depends slightly on latitude and altitude, increasing by 0·5 per cent. from the equator to the poles and decreasing by 0·5 per cent. from sea-level to 10 miles altitude. At sea-level and 45° latitude its value is 32·173 in ft.-sec. units. The value 32·2 ft./sec.^{2} is sufficiently accurate for most purposes.

Since no horizontal component of external force acts anywhere on the bulk of air, the pressure in every horizontal plane is constant, as otherwise motion would ensue. Let h represent altitude, so that it increases upward. Consider an element-cylinder of the fluid with axis vertical, of length δh and cross-sectional area A (Fig. 3). The pressure on its curved surface clearly produces

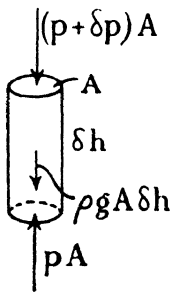

FIG. 3.

no resultant force or couple. If p is the pressure acting upward on the lower end of the cylinder, the pressure acting downward on its upper end will be $p + \frac{dp}{dh}\delta h$. These pressures give a resultant downward force: $A\frac{dp}{dh}\delta h$. The gravity force acting on the cylinder is $\rho g \,.\, A\delta h$. Therefore, for equilibrium—

$$A\frac{dp}{dh}\delta h + \rho g \,.\, A\delta h = 0,$$

or

$$\frac{dp}{dh} = -\rho g. \quad . \quad . \quad . \quad (2)$$

Thus the pressure decreases with increase of altitude at a rate equal to the local weight of the fluid per unit volume.

6. Incompressibility Assumption in a Static Bulk of Air

Full use of (2) requires a knowledge of the relationship existing between p and ρ, but the particular case where ρ is constant is important. We then have

$$\int dp = -\rho g \int dh + \text{const.}$$

or for the change between two levels distinguished by the suffixes 1 and 2:

$$p_1 - p_2 = \rho g(h_2 - h_1). \quad . \quad . \quad . \quad (3)$$

This equation is exact for liquids, and explains the specification of a pressure difference by the head of a liquid of known density which the pressure difference will support. In the mercury barometer, for example, if $h_2 > h_1$, $p_2 = 0$ and p_1 is the atmospheric pressure which supports the otherwise unbalanced column of mercury. At 0° C. the density of mercury relative to that of water is 13·596. When $h_2 - h_1 = 760$ mm., p_1 is found from (3) to be 2115·6 lb. per sq. ft. at this temperature.

7. Measurement of Small Pressure Differences

Accurate measurement of small differences of air pressure is often required in experimental aerodynamics. A convenient instrument is the Chattock gauge (Fig. 4). The rigid glasswork AB forms a U-tube, and up to the levels L contains water, which also fills the central tube T. But above L and the open mouth of T the closed vessel surrounding this tube is filled with castor oil. Excess of air pressure in A above that in B tends to transfer water from A to B

by bubbling through the castor oil. But this is prevented by tilting the heavy frame F, carrying the U-tube, about its pivots P by means of the micrometer screw S, the water-oil meniscus M being observed for accuracy through a microscope attached to F. Thus the excess air pressure in A is compensated by raising the water level in B above that in A, although no fluid passes. The wheel W fixed to S is graduated, and a pressure difference of 0·0005 in. of water is easily

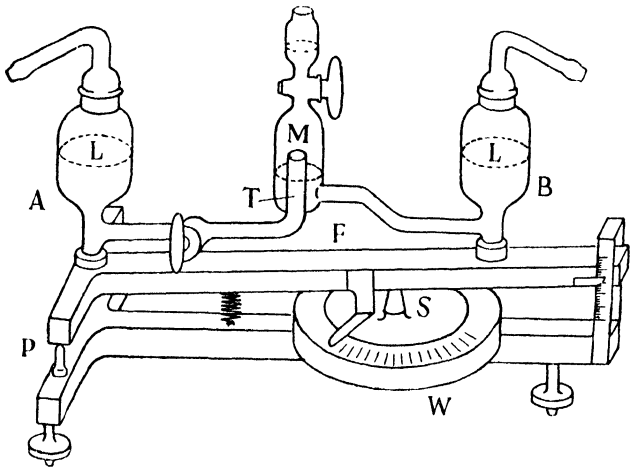

FIG. 4.—CHATTOCK GAUGE.

detected. By employing wide and accurately made bulbs set close together, constantly removing slight wear, protecting the liquids against appreciable temperature changes and plotting the zero against time to allow for those that remain, the sensitivity * may be increased five or ten times. These gauges are usually constructed for a maximum pressure head of about 1 in. of water. Longer forms extend this range, but other types are used for considerably greater heads.

At 15° C. 1 cu. ft. of water weighs 62·37 lb. Saturation with air decreases this weight by about 0·05 lb. The decrease of density from 10° to 20° C. is 0·15 per cent. A 6 or 7 per cent. saline solution is commonly used instead of pure water in Chattock gauges, however, since the meniscus then remains clean for a longer period.

8. Buoyancy of Gas-filled Envelope

The maximum change of height within a balloon or a gas-bag of an airship is usually sufficiently small for variation of density to be

* Cf. also Cope and Houghton, *Jour. Sci. Instr.*, xiii, p. 83, 1936.

neglected. Draw a vertical cylinder of small cross-sectional area A completely through the envelope E (Fig. 5), which is filled with a light gas of density ρ', and is at rest relative to the surrounding atmosphere of density ρ. Let the cylinder cut the envelope at a lower altitude-level h_1 and at an upper one h_2, the curves of inter-

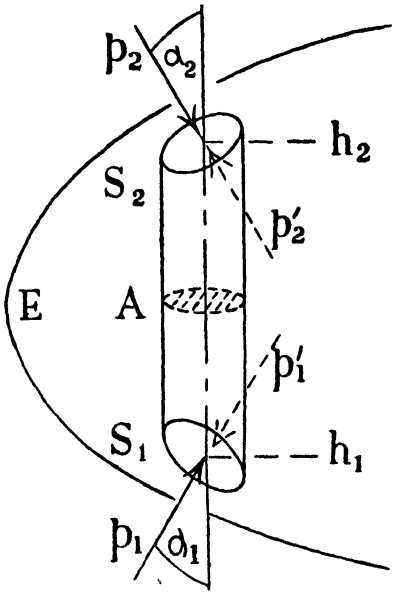

FIG. 5.

section enclosing small areas S_1, S_2, the normals to which (they are not necessarily in the same plane) make angles α_1, α_2 with the vertical. On these areas pressures p'_1, p'_2, act outwardly due to the gas, and p_1, p_2 act inwardly due to the atmosphere.

There arises at h_2 an upward force on the cylinder equal to

$$(p'_2 - p_2)S_2 \cos \alpha_2.$$

The similar force arising at h_1 may be upward or downward, depending on the position of S_1 and whether an airship or a balloon is considered, but in any case its upward value is—

$$(p_1 - p'_1)S_1 \cos \alpha_1.$$

Since $S_2 \cos \alpha_2 = A = S_1 \cos \alpha_1$, the resultant upward force on the cylinder due to the pressures is

$$[p_1 - p_2 - (p'_1 - p'_2)]A.$$

Substituting from (3), if ΔL denotes the element of lift—

$$\Delta L = (\rho - \rho')g(h_2 - h_1)A.$$

The whole volume of the envelope may be built up of a large number of such cylinders, and its total lift is :

$$L = (\rho - \rho')g\Sigma(h_2 - h_1)A$$
$$= (\rho - \rho')gV' \quad . \quad . \quad . \quad . \quad . \quad (4)$$

where V' is the volume of gas enclosed. For free equilibrium a weight of this amount, less the weight of the envelope, must be attached.

The above result expresses, of course, the Principle of Archimedes. It will be noted that the lift acts at the centre of gravity of the enclosed gas or of the air displaced, called the centre of buoyancy, so that a resultant couple arises only from a displacement of the centre of buoyancy from the vertical through the centre of gravity of the attached load plus gas. For stability the latter centre of gravity must be below the centre of buoyancy.

If W is the total load supported by the gas and σ' the density of the gas relative to that of the surrounding air, (4) gives

$$W = \rho g V'(1 - \sigma'). \quad . \quad . \quad . \quad . \quad (5)$$

For pure hydrogen, the lightest gas known, $\sigma' = 0{\cdot}0695$. But hydrogen is inflammable when mixed with air and is replaced where possible by helium, for which $\sigma' = 0{\cdot}138$ in the pure state.

9. Balloons and Airships

In balloons and airships the gas is contained within envelopes of cotton fabric lined with gold-beaters' skins or rubber impregnated. Diffusion occurs through these comparatively impervious materials, and, together with leakage, contaminates the enclosed gas, so that densities greater than those given in the preceding article must be assumed.

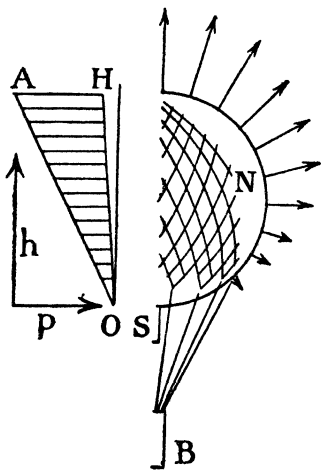

FIG. 6.

Practical values for lift per thousand cubic feet are 68 lb. for hydrogen and 62 lb. for helium, at low altitude. Thus the envelope of a balloon weighing 1 ton would, in the taut state at sea-level, have a diameter of 39·8 ft. for hydrogen and 41·1 ft. for helium ; actually it would be made larger, filling only at altitude and being limp at sea-level.

Referring to Fig. 6, OA represents

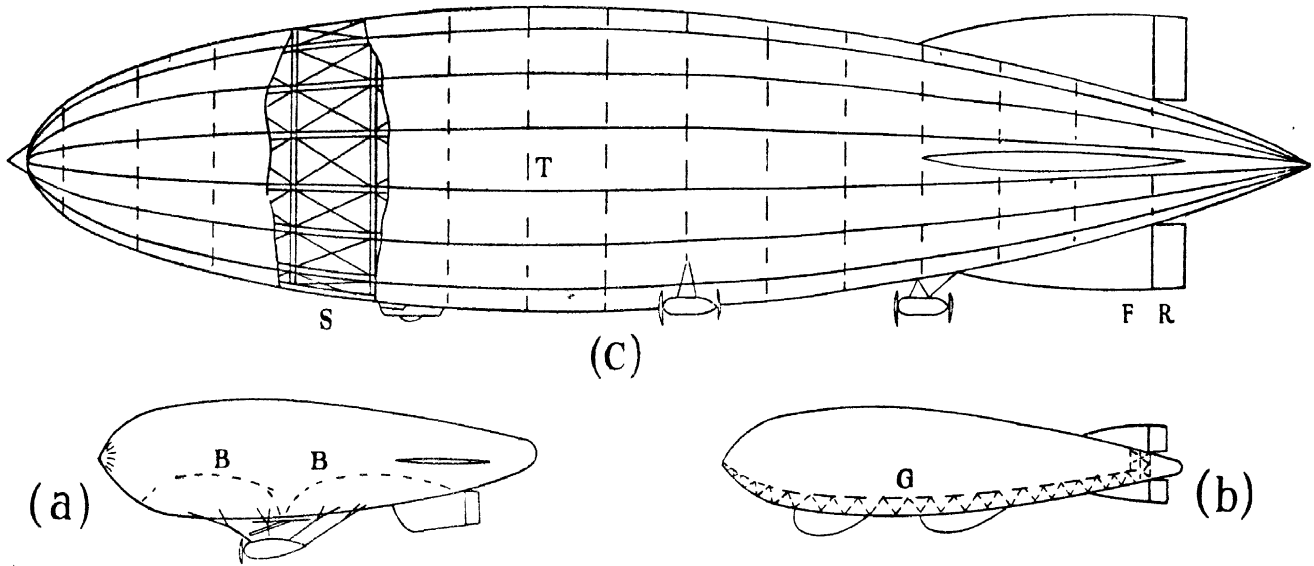

FIG. 7.—AIRSHIP TYPES.

(*a*) Non-rigid ; B, B, ballonets.
(*b*) Semi-rigid ; G, internal keel.
(*c*) Modern rigid airship ; T, transverse frames ; S, outline view of structure with outer covering removed ; F, fin ; R, rudder.

the variation of atmospheric pressure from the level of the top of the open filling sleeve S to that of the crest of the balloon, *OH* the corresponding variation of pressure through the bulk of helium filling the envelope. The difference between these external and internal pressures acts radially outward on the fabric as shown to the right. The upward resultant force and part of the force of expansion are supported by the net N, from which is suspended the basket or gondola B, carrying ballast and the useful load.

Balloons drift with the wind and cannot be steered horizontally. Airships, on the other hand, can maintain relative horizontal velocities by means of engines and airscrews, and are shaped to streamline form for economy of power. Three classes may be distinguished.

The small non-rigid airship, or dirigible balloon (Fig. 7(*a*)) has a faired envelope whose shape is conserved by excess gas pressure maintained by internal ballonets which can be inflated by an air scoop exposed behind the airscrew. Some stiffening is necessary, especially at the nose, which tends to blow in at speed. A gondola, carrying the power unit, fuel, and other loads, is suspended on cables from hand-shaped strengthening patches on the envelope. (Only a few of the wires are shown in the sketch.)

In the semi-rigid type (*b*) some form of keel is interposed between the envelope and gondola, or gondolas, enabling excess gas pressure to be minimised. Several internal staying systems spread the load carried by the girder over the envelope, the section of which is not as a rule circular.

The modern rigid airship (*c*) owes its external form entirely to a structural framework covered with fabric. Numerous transverse frames, binding together a skeleton of longitudinals or stringers, divide the great length of the hull into cells, each of which accommodates a gas-bag, which may be limp. Single gas-bags greatly exceed balloons in size, and are secured to the structure by nets. Some particulars of recent airships are given in Table I.

TABLE I

Airship	Zeppelins		R101	Akron (U.S.A.)
	Graf	Hindenburg		
Length (ft.)	776	800	777	785
Max. diam. (ft.)	100	135	132	133
Gas used	Hydrogen	Hydrogen	Hydrogen	Helium
Volume (cu. ft.)	$3{\cdot}7 \times 10^6$	$6{\cdot}7 \times 10^6$	$5{\cdot}5 \times 10^6$	$6{\cdot}5 \times 10^6$
Approximate gross lift (tons)	112	203	167	180

The largest single gas-bag in the above has a lift of 25 tons.

10. Centre of Pressure

The point on a surface exposed to pressure through which the resultant force acts is called the centre of pressure. The centres of pressure with which we are concerned relate to the pressure difference, often called the gas pressure, unevenly spread over part of an envelope separating gas from the atmosphere. Gas pressures are small at the bottom of an envelope and reach a maximum at the top, as illustrated in Fig. 6, and positions of the centres of pressure are usually high.

The high centres of the total gas pressures exerted on walls which restrain a gas-bag, as in the case of the wire bulkheads or transverse frames of a rigid airship, lead to moments internal to the structure.

BCDE (Fig. 8) is a (full) gas-bag of an airship which is pitched at angle α from a level keel. The longitudinal thrusts P, P' from the

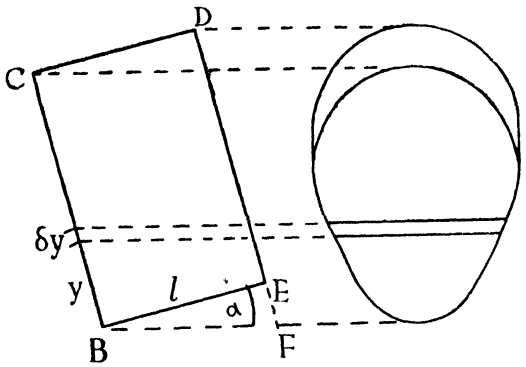

FIG. 8.

' gas pressure ' are supported by bulkheads BC and DE of areas A, A', assumed plane, B and E being lowest and C and D highest points. The gas is assumed to be at rest, so that pressure is constant over horizontal planes, and its pressure at B, the bottom of the bag, is taken as equal to that of the atmosphere. Let p be the excess pressure at height h above the level of B. Then from (3) $p = \rho_1 g h$, where ρ_1 is the difference in the densities of the gas and the surrounding air.

Lower Bulkhead BC.—Let δA be the area of a narrow horizontal strip of BC distant y from a horizontal axis in its plane through B. Then $h = y \cos \alpha$, and the total thrust on BC is given by :

$$P = \int_B^C p \, dA = \rho_1 g \cos \alpha \int_B^C y \, dA$$
$$= \rho_1 g \cos \alpha \, . \, A y_0 \quad . \quad . \quad \text{(i)}$$

where y_0 is the distance of the centroid of BC from the axis through B.

Let the centre of pressure of P be distant $y_0 + \Delta y$ from the B-axis, and take moments about this axis.

$$P(y_0 + \Delta y) = \int_B^C py\, dA = \rho_1 g \cos\alpha \int_B^C y^2\, dA$$
$$= \rho_1 g \cos\alpha \,.\, I_B \quad . \quad \text{(ii)}$$

where I_B is the second moment of the area about the B-axis. If I_0 is this moment about a parallel axis through the centroid, $I_B = I_0 + Ay_0^2$. Substituting in (ii):

$$\Delta y = \frac{\rho_1 g \cos\alpha\,(I_0 + Ay_0^2)}{P} - y_0.$$

Hence from (i):

$$\Delta y = \frac{I_0}{Ay_0} = \frac{k_0^2}{y_0} \quad . \quad . \quad . \quad . \quad . \quad (6),$$

where k_0 is the radius of gyration.

The result is independent of pitch. For a circular bulkhead of radius r, for example, $I_0 = \pi r^4/4$ and $\Delta y = r/4$. In practice, however, an excess pressure is often introduced, so that p_B is not zero, when a correction must be made, as will be clear from the following:

Upper Bulkhead DE.—Measuring now y in the plane of ED from a parallel horizontal axis through E, we have:

$$p = \rho_1 g(y \cos\alpha + l \sin\alpha),$$

where l is the distance apart of the bulkheads.

$$P' = \rho_1 g \int_E^D (y \cos\alpha + l \sin\alpha) dA$$
$$= \rho_1 g A'(y_0' \cos\alpha + l \sin\alpha).$$
$$P'(y_0' + \Delta y') = \rho_1 g \int_E^D (y^2 \cos\alpha + yl \sin\alpha) dA$$
$$= \rho_1 g[(I_0' + A'y_0'^2) \cos\alpha + A'y_0' l \sin\alpha].$$

This gives

$$\Delta y' = \frac{(k_0'^2 + y_0'^2) + y_0' l \tan\alpha}{y_0' + l \tan\alpha} - y_0'$$
$$= \frac{k_0'^2}{y_0' + l \tan\alpha} \quad . \quad . \quad . \quad . \quad . \quad (7)$$

The additional term in the denominator is EF. Hence (6) is generalised by (7), since it is always possible to draw a horizontal line BF at which any super pressure would vanish.

11. Relation between Pressure, Density, and Temperature of a Gas

By the experimental laws of Boyle and Charles, for constant temperature the pressure of a gas is proportional to its density; for constant volume the pressure of a gas is proportional to its absolute temperature. The absolute temperature is denoted by τ and, if θ is the temperature on the centigrade scale, is given by

$$\tau = \theta + 273.$$

Combining these laws, we have, for a given mass of a particular gas:

$$p V = B\tau, \quad . \quad . \quad . \quad . \quad (8)$$

where V is the volume, or, if V is the volume of 1 lb.,

$$p/\rho = gB\tau. \quad . \quad . \quad . \quad . \quad (9)$$

B is a constant which is made characteristic of a particular gas by treating 1 lb. of the gas; it is then evaluated from measurements of pressure and volume at a known temperature. It follows that B will vary from one gas to another in inverse proportion to the density under standard conditions of pressure and temperature.

If N is the number of molecules in V, N will, by Avogadro's law, be the same for all gases at constant p and τ. Hence, writing $pV/N = B'\tau$, B' is an absolute constant having the same value for all gases. Equation (9) is more convenient, however, and the variation of B is at once determined from a table of molecular weights. Some useful data are given in Table II. It will be noticed that, if p is kept constant, B measures the work done by the volume of gas in expanding in consequence of being heated through unit temperature change. The units of B are thus ft.-lb. per lb. per degree centigrade, or ft. per ° C.

TABLE II

Fluid	At 0° C. and 760 mm. mercury			B ft./°C.
	lb./cu. ft.	cu. ft./lb.	ρ slugs/cu. ft.	
Dry air . . .	0·0807	12·39	0·00251	96·0
Hydrogen . . .	0·00561	178·3	0·000174	1381
Helium . . .	0·01113	89·8	0·000346	696
Water-vapour . .	0·0501	19·95	0·00156	155

12. Isothermal Atmosphere

We now examine the static equilibrium of a bulk of gas under gravity, taking into account its compressibility. Equation (2)

applies, but specification is needed of the relationship between p and ρ. The simple assumption made in the present article is that appropriate to Boyle's law, viz. constant temperature τ_0, so that p/ρ remains constant. From (2):

$$\frac{dp}{\rho g} = -dh.$$

From (9):

$$\frac{1}{\rho g} = \frac{B\tau_0}{p}.$$

Hence:

$$B\tau_0 \frac{dp}{p} = -dh.$$

Integrating between levels h_1 and h_2, where $p = p_1$ and p_2 respectively,

$$B\tau_0 \log (p_1/p_2) = h_2 - h_1 \quad . \quad . \quad . \quad (10)$$

The logarithm in this expression is to base e. Throughout this book Napierian logarithms will be intended, unless it is stated otherwise. The result (10) states that the pressure and therefore the density of a bulk of gas which is everywhere at the same temperature vary exponentially with altitude.

The result, although accurately true only for a single gas, applies with negligible error to a mass of air under isothermal conditions, provided great altitude changes are excluded. The stratosphere is in conductive equilibrium, the uniform temperature being about — 55° C. The constitution of the air at its lowest levels is as given in Article 1. As altitude increases, the constitution is subject to Dalton's law: a mixture of gases in isothermal equilibrium may be regarded as the aggregate of a number of atmospheres, one for each constituent gas, the law of density variation in each atmosphere being the same as if it constituted the whole. Hence argon and other heavy gases and subsequently oxygen, nitrogen, and neon will become rarer at higher levels. The value of B for the atmosphere will consequently increase with altitude, although we have assumed it constant in order to obtain (10). The variation of B for several miles into the stratosphere will, however, be small. At greater altitudes still the temperature increases again.

13. The Troposphere

The atmosphere beneath the stratified region is perpetually in process of being mechanically mixed by wind and storm. When a bulk of air is displaced vertically, its temperature, unlike its pressure, has insufficient time for adjustment to the conditions obtaining at the

new level before it is moved away again. The properties of this part of the atmosphere, to which most regular flying so far has been restricted, are subject to considerable variations with time and place, excepting that B varies only slightly, depending upon the humidity. There exists a temperature gradient with respect to altitude, and on the average this is linear, until the merge into the stratosphere is approached. It will be found in consequence that the pressure and density at different levels obey the law—

$$p/\rho^n = k, \quad . \quad . \quad . \quad . \quad (11)$$

where k and n are constants. This relationship we begin by assuming.

Substituting for ρ from (11) in (2) leads to

$$k^{1/n}\int p^{-1/n}dp = -g\int dh\ ;$$

or

$$\frac{nk^{\frac{1}{n}}}{n-1}\cdot p^{\frac{n-1}{n}} = -gh + \text{const.}$$

Putting $p = p_0$ when $h = 0$ gives for the constant of integration—

$$\frac{nk^{\frac{1}{n}}}{n-1}\cdot p_0^{\frac{n-1}{n}}.$$

Therefore :

$$p^{\frac{n-1}{n}} = p_0^{\frac{n-1}{n}} - \frac{n-1}{nk^{1/n}}\cdot gh \quad . \quad . \quad . \quad (12)$$

To evaluate k let ρ_0, τ_0, be the density and absolute temperature at $h = 0$. By (11) :

$$p/\rho^n = p_0/\rho_0^n = k$$

while by (9) :

$$p_0/\rho_0 = gB\tau_0.$$

Hence :

$$\frac{1}{\rho_0^n} = \left(\frac{gB\tau_0}{p_0}\right)^n$$

and

$$k = (gB\tau_0)^n p_0^{1-n}$$

or

$$\frac{1}{k^{1/n}} = \frac{p_0^{\frac{n-1}{n}}}{gB\tau_0}$$

Substituting in (12)

$$\frac{p}{p_0} = \left(1 - \frac{n-1}{n}\cdot\frac{h}{B\tau_0}\right)^{\frac{n}{n-1}} \quad . \quad . \quad . \quad (13)$$

The temperature gradient is found as follows. From (9) and (11):

$$\frac{\tau}{\tau_0} = \frac{p}{\rho} \cdot \frac{\rho_0}{p_0} = \frac{p}{p_0}\left(\frac{p_0}{p}\right)^{\frac{1}{n}}$$

$$= \left(\frac{p}{p_0}\right)^{\frac{n-1}{n}} \quad . \quad . \quad . \quad . \quad . \quad . \quad (14)$$

Substituting in (13)

$$\frac{\tau}{\tau_0} = 1 - \frac{n-1}{n} \cdot \frac{h}{B\tau_0},$$

or

$$\tau - \tau_0 = \theta - \theta_0 = -\frac{n-1}{n} \cdot \frac{h}{B} \quad . \quad . \quad . \quad (15)$$

θ denoting temperature in °C. This shows that while n remains constant:

$$\frac{d\tau}{dh} = \frac{d\theta}{dh} = -\frac{n-1}{nB} \quad . \quad . \quad . \quad (16)$$

i.e. the temperature variation is linear.

As the stratosphere is approached, the law changes, the gradient becoming less and less steep.

14. The International Standard Atmosphere

It is necessary to correct observations of the performance of aircraft for casual atmospheric variation, and for this purpose the device of a standard atmosphere is introduced. A number of countries have agreed upon the adoption of an international standard, representing average conditions in Western Europe. This is defined by the temperature-altitude relationship:

$$\theta = 15 - 0{\cdot}00198_{115}h \quad . \quad . \quad . \quad (17)$$

h being in feet above sea-level (the number of significant figures given is due to h being expressed in the metric system in the original definition). The dry air value of B, viz. 96·0, is also assumed.

This definition leads to the following approximations:

From (16)	$n = 1{\cdot}235$	
From (13)	$p/p_0 = (1 - 0{\cdot}00000688h)^{5\cdot256}$	. . (18)
From (14)	$p/p_0 = (\tau/288)^{5\cdot256}$	
Similarly	$\rho/\rho_0 = (\tau/288)^{4\cdot255}$	

Some numerical results are given in Table III.

TABLE III

h (ft.)	θ (° C.)	p/p_0	$\sigma = \rho/\rho_0$
0	15·0	1·000	1·000
5,000	5·1	0·832	0·862
10,000	− 4·8	0·688	0·738
15,000	− 14·7	0·564	0·629
20,000	− 24·6	0·459	0·534
25,000	− 34·5	0·371	0·448
30,000	− 44·4	0·297	0·375
35,000	− 54·3	0·235	0·310
40,000	− 55	0·185	0·244
45,000	− 55	0·145	0·192
50,000	− 55	0·115	0·151

15. Application to Altimeters

A light adaptation of the aneroid barometer is used on aircraft, with the help of a thermometer, to gauge altitude. To graduate the instrument, increasing pressure differences are applied to it, and the dial is marked in intervals of h according either to the isothermal or to the standard atmosphere laws.

In the former case, the uniform temperature requiring to be assumed is usually taken as 10° C. From (10) and Table III the altitudes indicated are then excessive, on the basis of the standard atmosphere, by about 1·6, 5·7, and 10 per cent. at altitudes of 10,000, 20,000 and 30,000 ft. respectively. Correction for decrease of temperature with increase of altitude is made by assigning estimated mean temperatures to successive intervals of altitude. Thus, if τ_M applies to the true increase of altitude ΔH, corresponding to a decrease of p from p_1 to p_2, while Δh is indicated by the altimeter whose calibration temperature is τ_0, we have from (10)

$$\Delta H = \Delta h \,.\, \frac{\tau_M}{\tau_0} \quad . \quad . \quad . \quad . \quad (19)$$

Readings of altimeters with a standard atmosphere scale require correction for casual variation of temperature. Let H, τ_H, and p denote the true altitude, temperature, and pressure respectively, and h the altimeter reading corresponding to p and the graduation temperature τ. Use suffix 0 for sea-level and write s for the temperature lapse rate, so that $\tau - \tau_0 = -sh$. Then from (14), if s remains constant—

$$\frac{\tau}{\tau_0} = \frac{\tau_H}{\tau_{H0}} = \left(\frac{p}{p_0}\right)^{\frac{n-1}{n}} \quad . \quad . \quad (i)$$

Hence:

$$1 - \frac{sh}{\tau_0} = 1 - \frac{sH}{\tau_{H0}}$$

giving

$$H = h\frac{\tau_{H0}}{\tau_0} = h\frac{\tau_H}{\tau_0 - sh} \quad . \quad . \quad . \quad (20)$$

by (i).

16. Gas-bag Lift in General

The assumption of constant density made in Article 8 to obtain expression (4) for the lift L of a gas-filled envelope may now be examined. Although a balloon of twice the size has been constructed, 100 ft. may be taken as a usual height of large gas-envelopes. The maximum variation from the mean of the air density then follows from the formulæ (18). At sea-level, where it is greatest, it amounts to 0·15 per cent. approximately. Similarly, the maximum variation of the air pressure from the mean is found to be less than 0·2 per cent. Equation (3) shows that the corresponding variations in the gas will be smaller still.

Although the buoyancy depends on differences between atmospheric and gas pressures, these are negligible compared with variations caused in both by considerable changes in altitude. Gas-bags should be only partly filled at sea-level, so that the gas can, on ascent, expand to fill an increased volume without loss.

To study the condition of a constant weight W' of gas enclosed, (4) is conveniently written:

$$L = W'\left(\frac{1}{\sigma'} - 1\right) . \quad . \quad . \quad . \quad (21)$$

We also have from (9), always distinguishing the gas by accented symbols:

$$\frac{1}{\sigma'} = \frac{\rho}{\rho'} = \frac{B'\tau'}{B\tau}$$

at all pressures, and, therefore, altitudes. So (21) becomes

$$L = W'\left(\frac{B'\tau'}{B\tau} - 1\right) \quad . \quad . \quad . \quad (22)$$

and it is seen that since B, B' are constants, L remains constant in respect of change of altitude, provided that no gas is lost and that no temperature difference arises between the gas and the surrounding air. The last requirement involves very slow ascent or descent to

allow sufficient transference of heat through the envelope, or the envelope must be held at a new altitude—as is possible by aerodynamic means with airships—until such transference has taken place.

Gas-bags are too weak to support a considerable pressure, and safety valves operate when they become full, leading to a loss of gas. Thus the volume held in reserve at sea-level decides the maximum altitude permissible without loss of gas. This is called the static ceiling. A lighter-than-air craft can be forced to still greater altitudes by the following means : aerodynamic lift ; heating of the gas by the sun ; entering a cold atmospheric region ; or by discharging ballast. The condition then is that V' remains constant. Excluding the case of variation of weight, we find from (4) that the gas lift will remain constant only if $\rho - \rho'$ remain constant or, by (9) if $p\left(\frac{1}{B\tau} - \frac{1}{B'\tau'}\right)$, i.e. if $\rho\left(1 - \frac{B\tau}{B'\tau'}\right)$ remain constant. Hence, from (11) the condition is that $\left(1 - \frac{B\tau}{B'\tau'}\right)$ must vary inversely as $p^{\frac{1}{n}}$. In this way it is simple to calculate the excess gas temperature required for static equilibrium at a given altitude in excess of the static ceiling. Gas having been lost, when the temperature difference vanishes ballast must be released for static equilibrium to occur at any altitude.

17. Vertical Stability

The foregoing conditions depend upon the absence of a propulsive or dragging force ; the envelope must move with the wind, otherwise a variation of external pressure, different from that investigated, may contribute to lift. A difference between gas-lift and total weight, brought about by release of gas, for instance, or discharge of ballast, creates vertical acceleration which leads to vertical velocity relative to the surrounding air, equilibrium again being attained by the supervention of an aerodynamic force due to the relative motion. Variation of weight carried or of gas provides control of altitude, but even if, as in the case of airships, vertical control by aerodynamic means is also possible, the practical feasibility of lighter-than-air craft requires further investigation, since their level of riding is not obviously fixed, as is the case with ships only partly immersed in water. The first question is whether, in a stationary atmosphere, a balloon would hunt upwards and downwards, restricting time in the air through rate of loss of gas due to the need for con-

tinual control. A second question is whether the atmosphere is liable to continual up and down currents. These would have the same effect on the duration of flight of a balloon, but the second question has a wider significance, since such currents, if sufficiently violent, would make flight by heavier-than-air craft also impossible.

Consider the rapid ascent of an envelope without loss of gas from altitude h_1, where the atmospheric pressure $p = p_1$ and the absolute temperature $\tau = \tau_1$, to h_2, where $p = p_2$. When the atmosphere is in standard condition we have :

$$\frac{\tau_2}{\tau_1} = \left(\frac{p_2}{p_1}\right)^{\frac{n-1}{n}} = \left(\frac{p_2}{p_1}\right)^{0\cdot1903}.$$

For the gas within the envelope the thermal conductivity is so small that heat transference can be neglected. The gas then expands according to the adiabatic law :

$$\frac{p}{\rho^\gamma} = \text{const.}$$

Distinguishing properties by accented symbols, we have, since $\gamma = 1\cdot405$:

$$\frac{\tau_2'}{\tau_1'} = \left(\frac{p_2'}{p_1'}\right)^{0\cdot288}.$$

Now assume that initially $\tau_1' = \tau_1$. Very closely, $p_1 = p_1'$ and $p_2 = p_2'$. Since $p_2 < p_1$, we then have that $\tau_2' < \tau_2$. Hence, by Article 16 the gas-bag will sink, the load attached to it being constant. Conversely, a rapid descent of a gas-bag results in temporary excessive buoyancy.

Thus a lighter-than-air craft riding below its static ceiling tends to return to its original altitude if displaced, provided displacement is sufficiently rapid for passage of heat through the envelope to be small. It is said to be stable in respect of vertical disturbance. The state of the atmosphere is part and parcel of the question, for a necessary proviso is seen to be that $n < \gamma$.

If the craft is above its static ceiling, the stability in face of downward disturbance is the same, since no further gas is lost. But for upward displacement the stability is greater, since the weight of gas enclosed decreases.

18. Atmospheric Stability and Potential Temperature

The foregoing reasoning may be applied to the rapid vertical displacement of a bulk of the atmosphere, and we find that if, for the

atmosphere, n has a value less than 1·405, up and down currents are damped out. If $n = 1{\cdot}405$, the stability is neutral ; the atmosphere is then said to be in convective equilibrium. When $n > \gamma$, a condition that may arise from local or temporary causes, vertical winds occur and make aeronautics dangerous, if not impossible.

The condition for atmospheric stability is discussed alternatively in terms of ' potential temperature.' The potential temperature at a given altitude is defined as the temperature which a given bulk of air at that altitude would attain if displaced to a standard altitude, such as sea-level, the compression taking place without loss or gain of heat. We see that for $n = \gamma$ the potential temperature would be the same for all altitudes. For $n < \gamma$ the potential temperature increases upward. An atmosphere is stable when the potential temperature is greater the greater the altitude. It will be noticed that the stratosphere is more stable than the troposphere.

19. Bulk Elasticity

Fluids at rest possess elasticity in respect of change of volume. The modulus of elasticity E is defined as the ratio of the stress causing a volumetric strain to the strain produced. An increase of pressure from p to $p + \delta p$ will change a volume V to $V - \delta V$. The strain is $-\delta V/V$ and E is given by

$$E = dp \Big/ \left(-\frac{dV}{V}\right).$$

Since

$$-\frac{dV}{V} = \frac{d\rho}{\rho}$$

$$E = \rho \frac{dp}{d\rho}. \quad . \quad . \quad . \quad . \quad (23)$$

In the case of liquids the compressibility is very small, and (23) sufficiently defines E, but with gases we must specify the thermal conditions under which the compression is supposed to take place. The interest of E in Aerodynamics is chiefly in respect of changes of pressure, and therefore of density, occurring in air moving at approximately constant altitude. The changes are usually too rapid for appreciable heat to be lost or gained, having regard to the small thermal conductivity of air. In these typical circumstances the adiabatic law is again assumed, viz. $p = k\rho^{\gamma}$, so that from (23)

$$E = \gamma k \rho^{\gamma}$$
$$= \gamma p \, . \quad . \quad . \quad . \quad . \quad (24)$$

20. Velocity of Sound

The condition under which (24) has been derived is ideally realised in the longitudinal contractions and expansions produced in elements of the air by the passage of waves of sound. Newton demonstrated the following law for the velocity a of such waves in a homogeneous fluid :

$$a = \sqrt{(E/\rho)}.$$

Thus for gases, from (24)—

$$a = \sqrt{\gamma p/\rho} \quad . \quad . \quad . \quad . \quad (25)$$

or, substituting from (9),

$$a = \sqrt{\gamma g B \tau}. \quad . \quad . \quad . \quad . \quad (26)$$

The velocity of sound is seen to depend on the nature of the gas and its temperature only.

We shall always employ the symbol a for the velocity of sound in air. With $\gamma = 1{\cdot}405$, $g = 32{\cdot}173$ and $B = 96{\cdot}0$,

$$a = 65{\cdot}9\sqrt{\tau} \quad . \quad . \quad . \quad . \quad (27)$$

nearly. For 15° C., $\tau = 288$,

$$a = 1118 \text{ ft. per sec.} \quad . \quad . \quad . \quad (28)$$

A disturbing force or pressure suddenly applied to a part of a solid body is transmitted through it almost instantaneously. From the preceding article we infer that through air such a disturbance is propagated more slowly, but yet at a considerably greater rate than the velocities common in aeronautics. Disturbance of the stationary equilibrium of a bulk of air follows from swift but not instantaneous propagation through it of pressure changes. It may be noted, for example, that a moving airship disturbs the air far in front of it ; a fast bullet, on the other hand, overtakes its propagation of disturbance and fails to do so. This change assumes great significance in connection with stratospheric flying, for two reasons : a decreases to between 970 and 975 ft. per sec., the flight speeds of low altitude are at least doubled to compensate for the reduced density of the air.

Chapter II

AIR FLOW AND AERODYNAMIC FORCE

21. Streamlines and Types of Flow

It is familiar that motions of air vary considerably in character. Means of discriminating with effect between one kind of flow and another will appear as the subject develops, but some preliminary classification is desirable.

Streamlines.—Discussion is facilitated by the conception of the streamline. A streamline is a line drawn in the moving fluid such that the flow *across* it is everywhere zero at the instant considered.

Uniform Flow.—The simplest form of flow is uniform motion. By this we mean that the velocity of all elements is the same in magnitude and direction. It follows that the streamlines are all parallel straight lines, although this is not sufficient in itself to distinguish uniform motion.

Laminar Parallel Flow.—There are other motions whose streamlines are parallel straight lines, in which the velocity of the element, although uniform in direction, depends upon distance from some fixed parallel axis or plane. Such motions are properly called laminar, although the name laminar is nowadays frequently used in a wider sense, strictly laminar motions being characterised as 'parallel.'

Both uniform and laminar motions are steady, i.e. the velocity at any chosen *position* in the field of flow does not vary in magnitude or direction with time. They are more than this, however, for the velocity of any chosen *element of fluid* does not vary with time as it proceeds along its path. (It is specifically in this respect that wider use is commonly made of the name laminar.)

General Steady Flow.—We may have a steady motion which is neither uniform nor strictly laminar. The streamlines then form a picture of the flow which does not vary with time, but the velocity along a streamline varies from one position to another. Thus the elements of fluid have accelerations. The streamlines are not parallel and in general are not straight. It is this more general kind of flow that is usually intended by the term 'steady motion' used without qualification.

Unsteadiness and Path-lines.—Steady motions are often called 'streamline.' All steady motions have one feature in common: the streamlines coincide with the paths of elements, called path-lines.

Unsteady motions are common in Aerodynamics, and in these the path-lines and streamlines are not the same. The velocity varies with both space and time. At a chosen instant streamlines may be drawn, but each streamline changes in shape before an element has time to move more than a short distance along it. An unsteady motion may be such that an instantaneous picture of streamlines recurs at equal intervals of time; it is then said to be periodic or eddying, though use of the latter term is less restricted.

Turbulence.—When unsteadiness of any kind prevails, the motion is often called turbulent. In addition to periodic we may have irregular fluctuations. These may occur on such a scale that transient streamlines might conceivably be determined. But in other cases the fluctuations are much more finely grained, conveying the impression of a chaotic intermingling of very small masses of the fluid accompanied by modifications of momentum. This last type of unsteadiness is, unfortunately, at once the most difficult to understand and the most important in practical Aerodynamics. It has come to be the form usually intended by the name turbulence.

Stream-tube.—A conception of occasional use in discussing steady flow is the stream-tube. This may be defined as an imaginary tube drawn in the fluid, of small but not necessarily constant section, whose walls are formed of streamlines. Clearly, no fluid can enter or leave the tube through the walls except in respect of molecular agitation.

Two-dimensional Flow.—Another conception, of which we shall make very frequent use, is that of two-dimensional flow. Consider fixed co-ordinate axes Ox, Oy, Oz drawn mutually at right angles in the fluid. Let the velocity components of any element in the directions of these axes be u, v, and w, respectively. Two of the directions, say Ox and Oy, are open to selection, the third then following. If the motion is such that we can select Ox, Oy in such a way that $w = 0$ for all elements at all times, and also if neither u nor v then vanishes, the motion is of general two-dimensional form. The streamlines drawn in all planes parallel to a selected xy-plane will be the same. It is then sufficient to study the motion in the xy-plane, tacitly assuming that we are dealing with a slice of the fluid in motion of unit thickness perpendicular to this plane.

If besides $w = 0$ we have another velocity component, say v,

everywhere vanishing, the motion is strictly laminar, or parallel, and we may have u depending either upon distance from the plane xOz or upon distance from the axis Ox. In the former case, where u is a function of y only, the motion is two-dimensional ; in the latter, the flow is of the kind that occurs *in certain circumstances* along straight pipes of uniform section, when it is sufficient to consider unit length of the pipe because the distribution of flow will be the same through all cross-sections.

22. Absence of Slip at a Boundary

The theorem of Article 3 holds equally for a fluid in uniform motion if the rigid surface exposed in the fluid moves exactly with it. The pressure in uniform motion is thus constant and equal in all directions. Unless the whole motion is uniform, however, the theorem fails, and considerable investigation is necessary to establish precisely what we then mean by ' pressure.'

Imagine a small, rigid, and very thin material plate to be immersed and held stationary in the midst of a bulk of air in motion ; let its plane be parallel to the oncoming air, considered for simplicity to be in uniform motion. The disturbance caused by the plate might, on account of its extreme thinness, be expected to be negligible. This would, however, be completely at variance with experimental fact. Experiment clearly shows that the fluid coming into contact with the tangential surfaces of the plate is brought to rest, whilst fluid that passes close by has its velocity substantially reduced.

To explain this phenomenon in molecular terms we may suppose the plate to be initially chemically clean, each surface being a lattice-work of atoms of the substance of which the plate is made. As such it exposes a close distribution of centres of adhesive force. The force of adhesion is very intense at distances from the surface comparable with the size of a molecule, and a molecule of gas impinging on the surface is held there for a time. Considering the whole lattice-work, we may say that the air is condensed on it, since the molecules no longer possess a free path. But the layer of condensed gas receives energy, partly from the body of the plate and partly from bombardment by free gas molecules, and where the energy attains to the latent heat of evaporation the molecules free themselves and return to the bulk of the gas—thereby only giving place, however, to others. Thus the film of condensed gas molecules is in circulation with the external free gas.

Regarding the action of the plate on the stream of air, we must

suppose, therefore, two effects to result from molecular constitution : (*a*) impinging air molecules are brought to rest relative to the bulk or mass motion—just as they are, for a time, in regard to the molecular motion ; (*b*) air molecules released from the plate are deprived of mass motion, and, requiring to be accelerated by the other molecules, retard the general flow to an appreciable depth. Thus the rate of change of molecular momentum at the plate is no longer normal to its surface, but has a tangential component ; in other words, the ' pressure ' on the plate is oblique. Further, the retardation occurring at some distance into the fluid shows that the pressure in this affected region away from the plate cannot be equal in all directions. It will be noted that the mass flow is no longer uniform ; its initial uniformity has been destroyed by introducing the plate which has a relative velocity.

The phenomenon of absence of slip at the surface of separation of a material body from a surrounding fluid occurs quite generally and is of fundamental importance in Aerodynamics. It is known as the boundary condition for a real fluid. No matter how fast a fluid, gaseous or liquid, is forced to rush through a pipe, for example, the velocity at the wall is zero. The velocity of the air immediately adjacent to the skin of an aeroplane at any instant is equal to that of the aeroplane itself.

Thus a uniform fluid motion cannot persist in the presence of a material boundary which is not moving with the same velocity (although the motion may remain steady). The ' pressure ' at a point in the unevenly moving fluid will depend upon the direction considered. The matter is further investigated in the following articles.

VISCOSITY

23. Nature of Viscosity

If air is moving in other than uniform motion, a further physical property is brought into play in consequence of the molecular structure of the fluid. Its nature will be discussed with reference to laminar (or parallel) two-dimensional flow. Let this flow be in the direction Ox, and draw Oy so that u, the mass velocity, is a function of y only.

Consider an imaginary plane, say $y = y'$, perpendicular to Oy (Fig. 9). This plane is formed of streamlines, but owing to molecular motion, molecules are continually darting across it in all directions. Density remains uniformly distributed, and this condition entails that the same number of molecules crosses a chosen area of

the plane in unit time from either side. The molecules possess, in addition to their molecular velocity, a superposed mass velocity u, which by supposition is different on one side of the plane from on the other. Hence molecules crossing in one direction carry away, per unit area of the plane and in unit time, a different quantity of mass momentum from that which those crossing in the opposite direction bring with them. Hence momentum is being transported across the direction of flow. This phenomenon is called the viscous effect. Clearly, it exists only in the presence of a velocity gradient, which it tends to destroy in course of time.

Qualitative Theory of Viscosity

Consider an imaginary right cylinder (Fig. 9) of unit length and unit cross-section, whose ends are parallel to and, say, equidistant from the imaginary plane $y = y'$. Denote by S the unit area of the plane which the cylinder encloses. If ρ is the density of the air and m the mass of each molecule, the number of molecules within the cylindrical space is ρ/m and is constant. These molecules are moving in all directions with a mean molecular velocity c along straight paths of mean length λ. They have in addition a superposed mass velocity u whose magnitude depends upon their values of y at the instant considered, subject to the consideration that the u of any particular molecule cannot be modified while it is in process of describing a free path, for changes can come only from collisions.

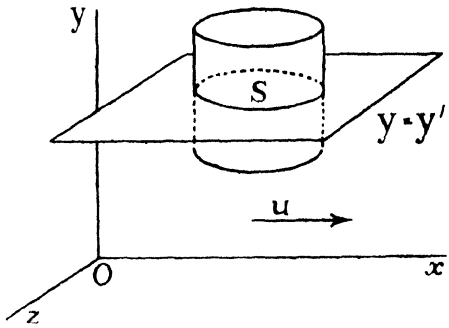

FIG. 9.

The molecular velocities of all the ρ/m molecules can be resolved at any instant parallel to Ox, Oy, Oz, but, as in Article 4, the number being very large, this procedure may be replaced statistically by imagining that $\rho/6m$ molecules move at a velocity c in each of the two directions which are parallel to each of the three co-ordinate axes. This equivalent motion must be supposed to extend through the interval of time Δt which is required for a displacement of the molecules through a distance λ. Thus $\Delta t = \lambda/c$. At the end of this interval collision occurs generally.

We are concerned only with molecules which cross S, and so ignore

all moving parallel to Ox, Oz. Of molecules moving parallel to Oy, only those within a distance λ of $y = y'$ can cross during Δt. Thus, S being unity and there being no displacement of mass, $\lambda\rho/6m$ molecules cross in each direction during this time. For clarity we shall speak of y increasing as 'upward' and assume u to increase upward. There is also no loss of generality in supposing that all molecules penetrating S from above or below y' start at distance λ from that plane, the velocity at $y = y'$ being u.

Consider a single exchange by the fluid above y'. It loses on account of the downward-moving molecule momentum $= m\left(u + \lambda\frac{du}{dy}\right)$, whilst it receives by the upward-moving molecule momentum $= mu$, a loss on this account of $m\lambda\frac{du}{dy}$. But in addition it must, by collision at the end of Δt, add momentum to the incoming molecule to the amount $m\lambda\frac{du}{dy}$. Thus the total change in the momentum of the fluid above y' in respect of a single molecule exchanged with one from below is a loss amounting to $2m\lambda\frac{du}{dy}$. Summing for all pairs, the aggregate loss is :

$$\frac{\lambda\rho}{6m} \cdot 2m\lambda\frac{du}{dy}.$$

The rate of this loss is :

$$\frac{1}{\Delta t} \cdot \frac{\rho\lambda^2}{3}\frac{du}{dy}$$

or, since $\Delta t = \lambda/c$, the rate is

$$\tfrac{1}{3}\rho\lambda c\frac{du}{dy}.$$

The rate of change of mass momentum being parallel to Ox, it may be represented by a force in the fluid at $y = y'$ acting tangentially on the fluid above. If the intensity of this traction is F, we have, since $S = 1$,

$$F = \tfrac{1}{3}\rho\lambda c\frac{du}{dy}. \quad . \quad . \quad . \quad . \quad (29)$$

The direction of F is such as to oppose the motion of the fluid above.

Similarly, we find that the fluid below y' gains momentum at the same rate. We note the passage downward of momentum and that the traction F acts at S in the opposite direction on the fluid below, urging it forward.

The coefficient by which du/dy is to be multiplied in order to determine F is called the *coefficient of viscosity*, and is denoted by μ. Its dimensions are $(M/L^3) \cdot (L/T) \cdot L = M/LT$.

24. Maxwell's Definition of Viscosity

The following example is instructive from several points of view. A number of layers of air, each of thickness h, are separated from one another by a series of infinite horizontal plates. Alternate plates are fixed, while the others are given a common velocity U in their own planes. The resulting conditions in all layers will be the same except for a question of sign, and we shall investigate one layer only.

Draw Ox (Fig. 10) in the fixed plate (taken to be the lower one)

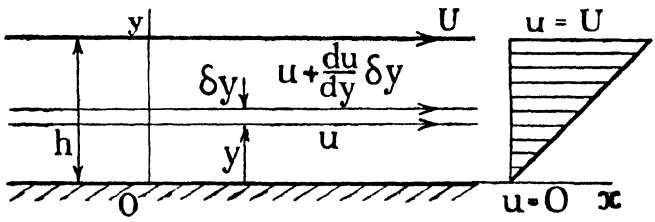

FIG. 10.

and in the direction of motion of the other, and Oy vertically upward. By Article 22 air touching the fixed plate has a velocity $u = 0$, while for air touching the moving plate $u = U$, and the fluid between is urged forward from above, but the ensuing motion is retarded from below.

Now it is assumed that, after sufficient time has elapsed, the motion in the layer becomes steady. In these circumstances consider a stratum of air of thickness δy between the plates and parallel to them. If the velocity at the lower face distant y from Ox is u, that on the upper face is $u + \frac{du}{dy}\delta y$. The intensity of traction F on the lower face is equal in magnitude to $\mu\frac{du}{dy}$, and retards the stratum; that on the upper face is $\mu\frac{d}{dy}\left(u + \frac{du}{dy}\delta y\right)$, and tends to accelerate the stratum. The resultant traction on the stratum in the direction Ox is $\mu\left\{\frac{d}{dy}\left(u + \frac{du}{dy}\delta y\right) - \frac{du}{dy}\right\} = \mu\frac{d^2u}{dy^2}\delta y$. But as the motion is steady,

there cannot be a resultant force on the stratum. Hence :

$$\frac{d^2u}{dy^2} = 0.$$

Integrating twice,

$$u = Ay + B$$

where A and B are constants of integration. Now insert in this equation for u the special values which are known, viz. $u = 0$ when $y = 0$, $u = U$ when $y = h$. Two equations result, viz. :

$$0 = 0 + B$$
$$U = Ah + B$$

which are sufficient to determine A and B. We find :

$$B = 0$$
$$A = U/h.$$

Inserting these values in the original equation for u,

$$u = \frac{U}{h}y. \quad . \quad . \quad . \quad . \quad (30)$$

Thus the fluid velocity between the plates is proportional to y. The distribution of velocity is plotted in the figure.

Let F be, as before, the intensity of traction, and reckon it positive in the direction Ox. The traction exerted on the fluid adjacent to the lower plate by the fluid above is given by

$$F = \mu\left(\frac{du}{dy}\right)_{y=0}.$$

This traction is transmitted to the lower plate and a force of equal intensity must be applied in the opposite direction to prevent it from being dragged in the Ox direction. Similarly, it is found that a force

$$F = \mu\left(\frac{du}{dy}\right)_{y=h}$$

must be applied to the upper plate to maintain the motion. But from (30)—

$$\left(\frac{du}{dy}\right)_{y=0} = \frac{U}{h} = \left(\frac{du}{dy}\right)_{y=h}.$$

Hence the forces on the plates are equal and opposite, as is otherwise obvious. F is, in fact, uniform throughout the fluid. Hence this case of motion is known as uniform rate of shearing.

If $U = 1 = h$, the intensity of either force is equal to μ. Hence, Maxwell's definition of the coefficient of viscosity as the tangential

force per unit area on either of two parallel plates at unit distance apart, the one being fixed while the other moves with unit velocity, the fluid filling the space between them being in steady motion.

In the general case the moving plate does work on the layer of fluid at the rate $\mu U^2/h$ per unit area of the plate. The result is a gradual rise in temperature of the fluid unless the heat generated is conducted away.

25. Laws of Viscosity

The traction on a bounding surface past which a fluid is flowing is called the *skin friction*. It differs in nature from the rubbing friction between two dry surfaces, but is essentially the same as the friction of a lubricated surface, such as that of a shaft in a bearing.

In certain cases of laminar flow, as will be seen in Chapter IX, the boundary value of the velocity gradient can be calculated in terms of a total rate of flow which can be measured experimentally, while the skin friction can also be measured. Hence the value of μ can be deduced without reference to the theory of Article 23. By varying the density, pressure, and temperature of the fluid in a series of experiments, empirical laws expressing the variation of μ can be built up.

The experimental value of μ for air at 0° C. is given by

$$\mu_0 = 3{\cdot}58 \times 10^{-7} \text{ slug/ft. sec.} \quad . \quad . \quad (31)$$

It is interesting to compare this with a numerical value obtainable from the qualitative theory. Equations (1) and (9) of Chapter I together give

$$c^2 = 3gB\tau \quad . \quad . \quad . \quad . \quad . \quad (32)$$

The value of c calculated from this expression for 0° C., viz. 1591 ft. per sec., is greater than the mean molecular velocity given in Article 1 for this temperature, because it is a root-mean-square value. Hence, according to (29)—

$$\mu = \rho\lambda\sqrt{\tfrac{1}{3}gB\tau}$$
$$= 32{\cdot}1\rho\lambda\sqrt{\tau} \quad . \quad . \quad . \quad (i)$$

giving, for 0° C., $\mu = 2{\cdot}58 \times 10^{-7}$. The error, amounting to 28 per cent., is removed by more elaborate analysis, which shows that the mean free path must effectively be increased in the viscosity formula. But this mathematical development is not required in Aerodynamics, since μ can be measured accurately.

The first law of viscosity is that the value of the coefficient is independent of density variation at constant temperature. This

surprising law is expressed in (i), because it is obvious that λ must be inversely proportional, approximately, to ρ. After predicting the law, Maxwell showed it experimentally to hold down to pressures of 0·02 atmosphere. It tends to fail at very high pressures.

According to (i) a second law would be $\mu \propto \sqrt{\tau}$, but experiment shows μ to vary more rapidly with the temperature. An empirical law for air is

$$\mu = \mu_0 \left(\frac{\tau}{273}\right)^{3/4} \quad . \quad . \quad . \quad . \quad (33)$$

(Rayleigh), where μ_0 is the value of the coefficient at 0° C.

PRESSURE IN AIR FLOW

26. Relation between Component Stresses

We now prove a relationship that exists between the stresses on an element (in the sense of Article 2) of a fluid in any form of two-dimensional motion. In the general case we have four component stresses to deal with, and a certain nomenclature is adopted, as follows. For a face drawn perpendicular to Ox, the normal pressure on it in the direction Ox is denoted by p_{xx} and the tangential component in the direction Oy by p_{xy}. The corresponding normal and tangential pressures on a face perpendicular to Oy are p_{yy} and p_{yx}.

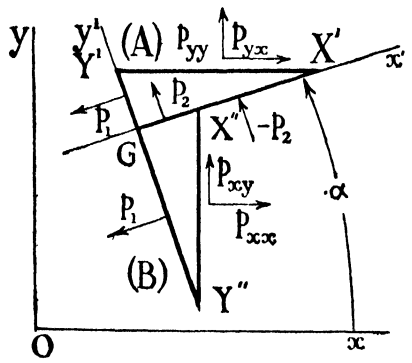

FIG. 11.

It will always be possible to find two axes at right angles to one another, moving with the element, such that, at the instant considered, the pressures in these directions tend to produce either simple compression or simple dilatation in the element. These axes are called principal axes and the pressures in their directions principal stresses.

Let G be the centre of the element which is moving in any manner in the plane xOy. Let Gx', Gy' be the principal axes at any instant, inclined at some angle α to the fixed axes of reference Ox, Oy. Denote by p_1 (Fig. 11) the principal pressure parallel to Gx' and by p_2 that parallel to Gy', and take a negative sign to indicate that the

pressure is tending to compress the element and a positive sign that it is tending to dilate it.

Adjacent to G draw $X'Y'$ perpendicular to Oy and $X''Y''$ of equal length perpendicular to Ox, forming with the principal axes the element-triangles $GY'X'$ and $GX''Y''$ (Fig. 11). These triangles are to be regarded as the cross-sections of prisms A and B, respectively, which have the same motion as that of G and whose faces are perpendicular to the xy-plane. Let $X'Y' = X''Y'' = \Delta$, then Δ is equal to the area of each of these two particular faces of the prisms per unit length perpendicular to the xy-plane. Similarly the area per unit length of the GX' face = that of the GY'' face = $\Delta \cos \alpha$, etc.

The prisms of fluid form part of the general motion and have accelerations. The forces arising from these are proportional, however, to mass, i.e. to Δ^2, and, as Δ is supposed very small, are negligible compared with forces arising from the stresses, which are proportional to Δ^2. Hence the stresses are related by the condition for static equilibrium.

For the equilibrium of prism A we have, first, resolving in the direction Ox—

$$p_{yx} \cdot \Delta - p_1 \cdot \Delta \sin \alpha \cdot \cos \alpha + p_2 \cdot \Delta \cos \alpha \cdot \sin \alpha = 0,$$

or

$$p_{yx} = (p_1 - p_2) \sin \alpha \cos \alpha.$$

Resolving in the direction Oy, we have, in regard to the equilibrium of B—

$$p_{xy} \cdot \Delta - p_1 \cdot \Delta \cos \alpha \cdot \sin \alpha + p_2 \cdot \Delta \sin \alpha \cdot \cos \alpha = 0,$$

or

$$p_{xy} = (p_1 - p_2) \sin \alpha \cos \alpha.$$

Hence :

$$p_{xy} = p_{yx} = \tfrac{1}{2}(p_1 - p_2) \sin 2\alpha. \quad . \quad . \quad (34)$$

The pressure p_{xy} is identical with the tractional stress F of equation (29) and involves an equal tractional stress at right angles. This conversely is the condition for principal axes to exist.

With regard again to the equilibrium of A, but resolving now in the direction Oy—

$$p_{yy} \cdot \Delta - p_1 \cdot \Delta \sin^2 \alpha - p_2 \cdot \Delta \cos^2 \alpha = 0,$$

while resolving parallel to Ox with regard to B—

$$p_{xx} \cdot \Delta - p_1 \cdot \Delta \cos^2 \alpha - p_2 \cdot \Delta \sin^2 \alpha = 0.$$

These two equations together give :

$$p_{xx} + p_{yy} = p_1 + p_2. \quad . \quad . \quad . \quad (35)$$

This equation is independent of α. Hence the arithmetic mean of the normal components of pressure on any pair of perpendicular faces through G is the same.

27. The Static Pressure in a Flow

Let us write:

$$-p = \tfrac{1}{2}(p_1 + p_2) = \tfrac{1}{2}(p_{xx} + p_{yy}) \quad . \quad . \quad (36)$$

where, it has been found possible to say, x and y are any directions at right angles to one another. Then p does not depend upon direction and is the compressive pressure we shall have in mind when referring to the 'static pressure,' or simply the pressure, at a point of a fluid in motion. (The system of signs adopted in the last article will be found convenient in a later chapter.) It will be noted that, if the fluid were devoid of viscosity, p would be the pressure acting equally in all directions at a chosen point, although not necessarily equally at all points.

The basis of the experimental measurement of p is as follows. The mouth of the short arm of an L-shaped tube is sealed, and a ring of small holes is drilled through the tube wall a certain distance from the closed mouth. The long arm is connected to a pressure gauge, so that the outer air communicates with the gauge through the ring of holes. The other side of the gauge is open to the atmosphere. The tube is then set in motion in the direction of its short arm through approximately stationary air. It is apparent, from Article 22, that the pressure acting through the ring of holes will not in general be the same as with the tube stationary. Nevertheless, a design for the short arm can be arrived at by experiment, such that the gauge shows no pressure difference when the tube is given any velocity, large or small. Adding to the whole system of tube and air a velocity equal and opposite to that of the tube converts the case of motion to that of a stationary tube immersed in an initially uniform air-stream. The pressure communicated is then the same when the tube is immersed in uniform flow or in stationary air. Thus the tube correctly transmits the static pressure of a uniform motion. To cope with motions in which the static pressure varies from point to point, the tube may be reduced to suitably small dimensions; even 0·5 mm. diameter is practicable, the ring of holes then degenerating to one or two small perforations.

28. Forces on an Element of Moving Fluid

The forces on the three-dimensional element $\delta x \delta y \delta z$ are conveniently grouped as due to (*a*) external causes, such as gravity,

(*b*) variation of the static pressure p through the field of flow, (*c*) tractions on the faces.

In regard to (*a*) it may be remarked generally that, although aircraft traverse large changes of altitude, the air motions to which they give rise are conveniently considered with the aircraft assumed at constant altitude and generalised subsequently. The air will be deflected upward or downward, but its changes of altitude are then sufficiently small for variations of density or pressure on this account to be neglected. An element of air may be regarded as in neutral equilibrium so far as concerns the gravitational field, its weight being supposed always exactly balanced by its buoyancy.

(*b*) We shall require very frequently to write down the force on an element due to space variation of p. Choose Ox in the direction in which p is varying and consider the forces due to p only on the faces of the element $\delta x\delta y\delta z$. The forces on all the $\delta x\delta y$ and $\delta x\delta z$ faces cancel, because p is varying only in the x-direction. On the $\delta y\delta z$ face that is nearer the origin, the force is $p\,.\,\delta y\delta z$, while on that farther from the origin the force is $\left(p + \frac{dp}{dx}\,\delta x\right)\,\delta y\delta z$.

The resultant force in the direction Ox is thus

$$p\,.\,\delta y\delta z - \left(p + \frac{dp}{dx}\,\delta x\right)\delta y\delta z$$

$$= -\frac{dp}{dx}\,.\,\delta x\delta y\delta z\ ,$$

$$= -\frac{dp}{dx} \times \text{the volume of the element}\ . \qquad (37)$$

This result should be remembered.

(*c*) The tractions have already been discussed to some extent. They are proportional to μ, which is small for air. Close to the surfaces of wings and other bodies studied in Aerodynamics, the velocity gradients are steep and the tractions large. Away from these boundaries, however, the velocity gradients are usually sufficiently small for the modification of the motion of the element due to the tractions to be neglected.

BERNOULLI'S EQUATION

29. Derivation of Bernoulli's Equation

The following five articles treat of flow away from the vicinity of material boundaries, and such that the tractions on the element can

be neglected, i.e. the pressure p is assumed to act equally in all directions at any point. It is also assumed that the flow is steady.

Consider steady flow of air at velocity q within a stream-tube (Article 21) of cross-sectional area A (Fig. 12). Denote by s distance measured along the curved axis of the tube in the direction of flow. The condition of steady motion means that ρ, q, p, A may vary with s, but not, at any chosen position, with time. Since fluid does not collect anywhere—

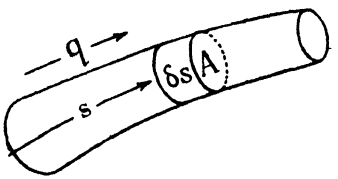

FIG. 12.

$$\rho q A = \text{constant} \quad . \quad . \quad . \quad . \quad (38)$$

The volume of a small element δs of the air filling the stream-tube is $A\delta s$, and the force on it in the direction of flow due to the pressure variation is $-\frac{dp}{ds} . A\delta s$, by (37). The mass of the element is $\rho A\delta s$, and its acceleration is dq/dt. By Newton's second law of motion—

$$-\frac{dp}{ds} . A\delta s = \rho A\delta s \cdot \frac{dq}{dt}.$$

But

$$\frac{dq}{dt} = \frac{dq}{ds} \cdot \frac{ds}{dt} = q\frac{dq}{ds}.$$

Hence :

$$\frac{1}{\rho}\frac{dp}{ds} + q\frac{dq}{ds} = 0. \quad . \quad . \quad . \quad . \quad (39)$$

Integrating along the stream-tube, which may now be regarded as a streamline—

$$\int \frac{dp}{\rho} + \tfrac{1}{2}q^2 = \text{constant}. \quad . \quad . \quad . \quad (40)$$

This is the important equation of Bernoulli. Evaluation of the remaining integral requires a knowledge of the relationship between p and ρ. The constant appertains, unless proved otherwise, only to the particular streamline chosen ; it must be regarded in general as varying from one streamline to another of the same flow. Another form is obtained by integrating (39) between any two values of s, where the conditions are denoted by 1 and 2 :

$$\int_1^2 \frac{dp}{\rho} + \frac{q_2^2 - q_1^2}{2} = 0. \quad . \quad . \quad . \quad . \quad (41)$$

30. Variation of Density and Temperature

1°.—Let us first assume the flow to be isothermal, so that p and ρ obey Boyle's law: $dp/d\rho = \text{constant}$. The integral remaining in (40) may then be written:

$$\int \frac{dp}{d\rho} \cdot \frac{d\rho}{\rho} = \frac{a^2}{\gamma} \int \frac{d\rho}{\rho}$$

from (25), a being the velocity of sound and γ the ratio of the specific heats = 1·405. This reduction is possible because (Article 20) a remains constant under the isothermal condition. Hence (41) becomes, on evaluating the integral—

$$\frac{a^2}{\gamma} \log \frac{\rho_2}{\rho_1} + \frac{q_2^2 - q_1^2}{2} = 0$$

or

$$\frac{\rho_2}{\rho_1} = e^{-\gamma \frac{q_2^2 - q_1^2}{2a^2}} \quad . \quad . \quad . \quad . \quad . \quad (42)$$

Expanding in an exponential series—

$$\frac{\rho_2}{\rho_1} = 1 - \gamma \frac{q_2^2 - q_1^2}{2a^2} + \frac{1}{\lfloor 2} \left(\gamma \frac{q_2^2 - q_1^2}{2a^2} \right)^2 - \ldots . \quad (43)$$

under isothermal conditions.

2°.—Density variations actually occur so rapidly in most aerodynamical motions that the isothermal assumption is inappropriate, and, in fact, the condition is closely approached that no heat is lost or gained. The adiabatic law then relates the pressure to the density, viz.:

$$p = k\rho^\gamma \quad . \quad . \quad . \quad . \quad (44)$$

The absolute temperature τ now varies from point to point according to

$$\frac{\tau_2}{\tau_1} = \left(\frac{p_2}{p_1} \right)^{\frac{\gamma - 1}{\gamma}} = \left(\frac{\rho_2}{\rho_1} \right)^{\gamma - 1} \quad . \quad . \quad . \quad . \quad (45)$$

From (44):

$$dp = \gamma k \rho^{\gamma - 1} d\rho.$$

Thus:

$$\int_1^2 \frac{dp}{\rho} = \gamma k \int_1^2 \rho^{\gamma - 2} d\rho$$

$$= \frac{\gamma k}{\gamma - 1} (\rho_2^{\gamma - 1} - \rho_1^{\gamma - 1})$$

or, eliminating k by (44),

$$\int_1^2 \frac{dp}{\rho} = \frac{\gamma}{\gamma - 1} \cdot \frac{p_1}{\rho_1} \left\{ \left(\frac{\rho_2}{\rho_1} \right)^{\gamma - 1} - 1 \right\}$$

$$= \frac{a_1^2}{\gamma - 1} \left\{ \left(\frac{\rho_2}{\rho_1} \right)^{\gamma - 1} - 1 \right\} \quad . \quad . \quad . \quad (46)$$

where, it will be noted, the velocity of sound introduced from (25) refers to the position s_1, where $\tau = \tau_1$.

Substitution in (41) leads to—

$$\frac{\rho_2}{\rho_1} = \left\{ 1 - (\gamma - 1) \frac{q_2^2 - q_1^2}{2a_1^2} \right\}^{\frac{1}{\gamma - 1}} \quad . \quad . \quad (47)$$

Finally, expanding by the Binomial Theorem—

$$\frac{\rho_2}{\rho_1} = 1 - \frac{q_2^2 - q_1^2}{2a_1^2} + \frac{2 - \gamma}{\lfloor 2} \left(\frac{q_2^2 - q_1^2}{2a_1^2} \right)^2 - \ldots . \quad (48)$$

Comparison with (42) and (43) shows density variation now to be less, also that the convenient expression—

$$\frac{\rho_2}{\rho_1} = e^{-\frac{q_2^2 - q_1^2}{2a_1^2}} \quad . \quad . \quad . \quad . \quad (49)$$

applies closely to adiabatic flow, provided the velocity change is not great. If $q_2^2 - q_1^2$ amounts to $\frac{1}{2}a_1^2$ the error in (49) is only 1·3 per cent.; this would occur, for example, if $q_2 = 2q_1 = 912$ ft. per sec., or if $q_2 = 3q_1 = 838$ ft. per sec.

There is an important limit to the application of (47); q_2 cannot exceed a_2, because a_2 gives the limiting velocity with which pressure waves can be propagated. It will be noted that, since the temperature is reduced on expansion, $a_2 < a_1$. When $q_2 = a_2$ and $q_1 = 0$, we find the minimum value of the density ratio:

$$\frac{\rho_2}{\rho_1} = \left[1 - (\gamma - 1) \tfrac{1}{2} \left(\frac{a_2}{a_1} \right)^2 \right]^{\frac{1}{\gamma - 1}}.$$

But

$$\left(\frac{a_2}{a_1} \right)^2 = \frac{\tau_2}{\tau_1} = \left(\frac{\rho_2}{\rho_1} \right)^{\gamma - 1}.$$

Hence:

$$\text{Minimum } \frac{\rho_2}{\rho_1} = \left(\frac{2}{1 + \gamma} \right)^{\frac{1}{\gamma - 1}} \quad . \quad . \quad . \quad (50)$$

If $\tau_1 = 288$, i.e. $\theta_1 = 15°$ C., this gives 0·634 and q_2 max. $= a_2 =$

1019 ft. per sec. The final temperature is — 33·7° C., a drop of 48·7° C.

The examples worked out in Table IV further illustrate adiabatic flow. Two cases of common occurrence are studied: (*a*) a stream brought to rest ($q_2 = 0$), (*b*) the velocity doubled ($q_2 = 2q_1$). In all cases the initial conditions assumed are: $p_1 = 760$ mm. mercury, $\theta_1 = 15°$ C. The values of A_2/A_1 are obtained from (38), by which, since $q_2 = 2q_1$, $A_2/A_1 = \frac{1}{2}(\rho_1/\rho_2)$.

TABLE IV

EXAMPLES OF ADIABATIC FLOW

q_2	q_1 (ft. per sec.) .	100	200	300	400	521
0	$\frac{\rho_2 - \rho_1}{\rho_1}$ (per cent.) .	0·4	1·6	3·6	6·5	11·1
0	θ_2 (° C.) . . .	15·4	16·8	19·2	22·5	27·7
$2q_1$	$\frac{\rho_1 - \rho_2}{\rho_1}$ (per cent.) .	— 1·2	— 4·7	— 10·5	— 18·2	— 30
$2q_1$	θ_2 (° C.) . . .	13·6	9·4	2·4	— 7·4	— 23·1
$2q_1$	A_2/A_1 . . .	0·506	0·525	0·56	0·61	0·71

The variation of temperature affects such questions as the troublesome formation of ice on wings and the location of convective radiators. Otherwise it is ignored.

31. Variation of Pressure—Comparison with Incompressible Flow

Equations for pressures corresponding to those of the preceding article for densities are obtained in a similar way. They follow immediately, however, by use of the relations: $p_1/p_2 = \rho_1/\rho_2$ for isothermal and $p_1/p_2 = (\rho_1/\rho_2)^\gamma$ for adiabatic flow. Thus Bernoulli's equation for adiabatic flow, which alone will now be considered, is found, with the help of (46), to be—

$$\frac{a_1^2}{\gamma - 1}\left\{\left(\frac{p_2}{p_1}\right)^{\frac{\gamma-1}{\gamma}} - 1\right\} + \frac{q_2^2 - q_1^2}{2} = 0. \quad . \quad . \quad (51)$$

This gives, corresponding to (47)—

$$\frac{p_2}{p_1} = \left\{1 - (\gamma - 1)\frac{q_2^2 - q_1^2}{2a_1^2}\right\}^{\frac{\gamma}{\gamma-1}} . \quad . \quad . \quad (52)$$

Now an outstanding result of the investigation of density variation is that it is small provided velocities do not approach that of sound.

The condition ρ = constant is then a first approximation. Making this assumption gives at once, from (40)—

$$p + \tfrac{1}{2}\rho q^2 = \text{constant} \quad . \quad . \quad . \quad (53)$$

for incompressible flow along a particular streamline, provided always that tractions can be neglected. (41) becomes—

$$p_2 - p_1 = \tfrac{1}{2}\rho(q_1^2 - q_2^2), \quad . \quad . \quad . \quad (54)$$

of which convenient non-dimensional forms are

$$\frac{p_2 - p_1}{\rho q_1^2} = \tfrac{1}{2}\left\{1 - \left(\frac{q_2}{q_1}\right)^2\right\} \quad . \quad . \quad . \quad (55)$$

or

$$\frac{p_2 - p_1}{\rho q_2^2} = \tfrac{1}{2}\left\{\left(\frac{q_1}{q_2}\right)^2 - 1\right\} \quad . \quad . \quad . \quad (56)$$

These alternative expressions of Bernoulli's theorem for an incompressible fluid are of great importance.

We now determine the error involved in applying (53) to a gas which is flowing adiabatically. Expanding (52) by the binomial theorem—

$$\frac{p_2}{p_1} = 1 - \frac{\gamma}{2}\frac{q_2^2 - q_1^2}{a_1^2} + \frac{\gamma}{8}\left(\frac{q_2^2 - q_1^2}{a_1^2}\right)^2 - \ldots\ldots$$

or

$$p_2 - p_1 = p_1\left(\frac{p_2}{p_1} - 1\right)$$
$$= \frac{\gamma p_1}{2a_1^2}(q_1^2 - q_2^2)\left\{1 + \frac{1}{4a_1^2}(q_1^2 - q_2^2) + \ldots\ldots\right\}.$$

Since $\gamma p_1/a_1^2 = \rho_1$ by (25), this reduces, with r written for q_2/q_1, to

$$\frac{p_2 - p_1}{\rho q_1^2} = \tfrac{1}{2}(1 - r^2)\left\{1 + \tfrac{1}{4}\left(\frac{q_1}{a_1}\right)^2(1 - r^2) + \ldots\ldots\right\}. \quad (57)$$

A similar expression is readily obtained to compare with (56).

The above series is rapidly convergent, and the equation indicates that the error involved in applying (55) to a gas in adiabatic flow is small, provided that q_1^2 is small compared with a_1^2. Since a_1 is only approached by q_1 in particular cases, as for example at the tips of airscrews, it follows that air in motion may usually be treated as an incompressible fluid, such as water.

As an example, consider the case $q_2 = 2q_1$. The error involved in employing (55) instead of (57) is as follows :

q_1 (ft. per sec.) :	100	200	300	400
q_2 (ft. per sec.) :	200	400	600	800
error (per cent.) :	0·6	2·4	5·5	10

32. The Pitot Tube and the Stagnation Point

Consider an L-shaped tube immersed and held stationary in a stream, one arm being parallel to it with open mouth directly facing the oncoming air ; suppose the other end to be connected to a pressure gauge so that no air can flow through. There must exist an axial streamline about which fluid approaching the mouth divides in order to flow past. Air following that streamline will arrive at some point within the mouth of the tube, where the time-average of the velocity is zero ; we refrain from saying that the velocity will be zero, because some unsteadiness may possibly exist in the mouth of the tube ; but we can assert that the time-average of the square of the velocity will be negligible in ordinary circumstances, compared with the square of the velocity of the oncoming stream. Denote by p, q, ρ, a the pressure, velocity, density, and the velocity of sound at a point of the streamline far upstream, and use suffix 0 for the mouth of the tube. Ignoring the small unsteadiness that may arise, and also, for the moment, variation of density, the pressure p_0 in the mouth of the tube is given from Article 31 by :

$$p_0 = p + \tfrac{1}{2}\rho q^2 \quad . \quad . \quad . \quad . \quad (58)$$

Such a tube is called a pitot tube (after its eighteenth-century inventor), and p_0 the pitot head, or total head, for air flow whose changes of pressure due to variation of altitude can be neglected. Comparing with (53), we note that the constant of that equation is measured by a pitot tube. Variation of p_0 from one streamline to another is readily determined by a pitot tube in experiment, its diameter being made very small where the space-variation of total head is rapid. For accurate work the tube must be oriented to lie parallel to the local streamlines of the flow.

Variations of p_0 are small compared with p, and it is convenient to deal with the quantity $p_0 - p$, sometimes called the dynamic head. For incompressible flow, to which Bernoulli's equation applies, we have $p_0 - p = \frac{1}{2}\rho q^2$. For the corresponding flow of a gas we find, in the same way as for (57) :

$$p_0 - p = \tfrac{1}{2}\rho q^2 \left\{ 1 + \tfrac{1}{4}\left(\frac{q}{a}\right)^2 + \ldots . \right\} . \quad . \quad . \quad (59)$$

Putting $a = 1118$ ft. per sec., the value appropriate to 15° C., gives, for example :

q (ft. per sec.) :	100	200	400
$(p_0 - p)/\frac{1}{2}\rho q^2$:	1·002	1·008	1·032

Thus the correction on (58) due to compressibility remains small for moderately large velocities.

In the above case of motion the dividing streamline is obviously straight, and collinear with the axis of the tube. Imagine a solid of revolution, of the shape of an airship envelope, for instance, having this same axis and situated with its nose at the mouth of the tube. The pressure in the tube remains unchanged, and indicates a pressure increase of $\frac{1}{2}\rho q^2$ occurring at the nose of the body. An airship nose requires special strengthening to withstand this pressure (cf. Fig. 7). If the body and tube are tilted with respect to the oncoming stream, i.e. are given an 'angle of incidence,' the pressure in the tube decreases. But it must then be possible to find a new position for the tube, in the neighbourhood of the nose of the body, such that the pressure difference in the tube is again $\frac{1}{2}\rho q^2$, for there must still exist a dividing streamline, although now it may be curved (Fig. 13). Experiment confirms this conclusion.

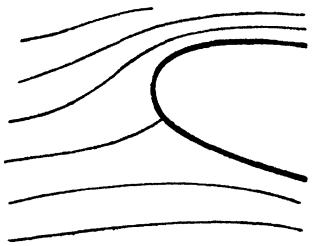

FIG. 13.—FRONT STAGNATION POINT.

The point at which the dividing streamline meets the nose of an immersed body is called the front stagnation point. The increase of pressure there is known as the stagnation pressure. The fact that a stagnation point must exist is of considerable help in constructing curves of pressure variation round the contour of a body from meagre experimental data.

33. Basis of Velocity Measurement

The undisturbed static pressure of a stream is measured as described in Article 27. A combination of a pitot tube and a static pressure tube, called a pitot-static tube, enables local velocity to be measured if ρ is known. For from (58)

$$q = \sqrt{\frac{2}{\rho}(p_0 - p)}. \quad . \quad . \quad . \quad (60)$$

The velocity thus obtained may be corrected, if need be, for compressibility by (59). A concentric form of pitot-static tube is shown in Fig. 14; other designs exist.

Other methods of measuring velocity are readily devised, although none is so convenient. The present method has a theoretical advantage in determining directly not q but ρq^2. It is usually the latter

quantity that is required to be known with accuracy in Aerodynamics ; often a comparatively rough knowledge of q itself is sufficient.

Various problems in connection with the use of pitot-static tubes are described later ; but a certain limitation may be referred to here.

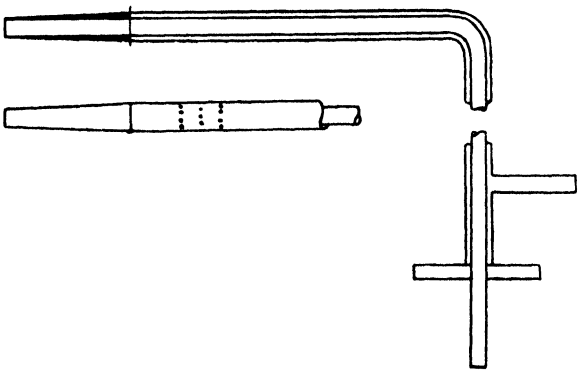

FIG. 14.—N.P.L. PITOT-STATIC PRESSURE TUBE.

Putting $q = 10$ ft. per sec. gives for standard conditions at sea-level $p_0 - p = 0{\cdot}119$ lb. per sq. ft. This pressure difference balances a head of water $= 0{\cdot}023$ in. only. Gauges (compare, for instance, Article 7) can be devised to measure such a pressure with high accuracy, but the required sensitivity makes simple forms unsuited to rapid laboratory use, owing to various small disturbing factors, which are usually negligible, beginning to become important. Variation of temperature, vibration, and slight wear are instances. 1 or 2 per cent. of the above head is a convenient limit to sensitivity. It follows that the pitot-static tube becomes unsuitable for smaller velocities, and other means of measurement are then substituted. Of these, the change in electrical resistance of a fine heated wire due to forced convection in a stream has proved most convenient.

A pitot-static tube, usually of divided type, is employed on aircraft to indicate speed. Wherever located within practical limitations, it is subject to disturbance from near parts of the craft to an extent depending on speed. Especially if fitted to an aeroplane, the tube can only be tangential to the local stream at one speed. Errors due to an inclination of 10° amount to 2–3 per cent., depending upon the type of tube. A mean alignment is adopted, but for the several reasons stated calibration in place is necessary for accurate readings.

The tube is connected with a pressure gauge of aneroid barometer type, deflection of a diaphragm of thin corrugated metal moving a

needle over a scale calibrated in miles per hour. The reading is termed indicated air speed (A.S.I.), and gives the true speed of the craft relative to the air at low altitude only. If true speed is required at considerable altitudes, readings must be increased in the ratio $\sqrt{1/\sigma}$, where σ is the relative air density.

Special forms of pressure tube also exist for aircraft, designed to permit use of a more robust gauge. Since increase of pressure cannot exceed $\frac{1}{2}\rho q^2$, except on account of compressibility, the static tube is replaced by a device giving less than static pressure. This sometimes consists of a single or double venturi tube. Particulars of venturis for this and other purposes are given in the paper cited * (as exposed on aircraft they are not constrained to 'run full'). A formula for the pitot pressure at speeds exceeding the velocity of sound is given later.

SUBDIVISION OF FLOW PAST BODIES

34. Taking advantage of the outstanding result of Article 30, it will now be assumed, except where stated otherwise, that the fluid is sensibly homogeneous and flows incompressibly. From Article 31, maximum velocities must not approach that of sound in air. A very useful expression of the assumption is obtained as follows.

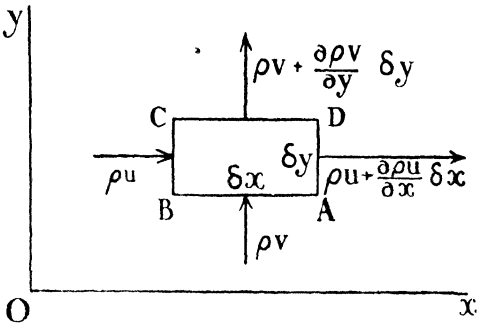

FIG. 15.

Consider part of the field of a two-dimensional flow enclosed within any small rectangle ABCD (Fig. 15), of sides δx, δy, u, v being the components parallel to Ox, Oy of the resultant velocity. The rate at which fluid mass tends to be exhausted from the rectangle owing to difference in velocities and densities at BC and DA is $\left(\rho u + \frac{\partial \rho u}{\partial x}\,\delta x\right)\delta y - \rho u \delta y = \frac{\partial \rho u}{\partial x}\,\delta x \delta y$. Comparing similarly the mass-flow across the sides AB and CD, the rate at which matter is exhausted from the rectangle on this account is $\frac{\partial \rho v}{\partial y}\,\delta x \delta y$. Now density

* Piercy and Mines, A.R.C.R. & M. 664, 1919.

is assumed to remain constant. Hence :

$$\frac{\partial u}{\partial x} + \frac{\partial v}{\partial y} = 0. \quad . \quad . \quad . \quad . \quad (61)$$

This expression is known as the *equation of continuity* for an incompressible fluid.

35. When a wind divides to flow past an obstacle, such as an airship, held stationary within it, the inertia of the air tends to localise to the vicinity of the body the large deflections that must occur in the stream, so that laterally distant parts are little affected. Imagine a hoop of diameter several times as great as the maximum transverse dimension of the body to be held across the stream, enclosing the body. The volume of air flowing through the hoop per sec. is little diminished by the presence of the body, the air flowing faster to make up for the obstructed area. As the diameter of the hoop is decreased, this statement becomes less true, but at first only slowly. In other words, the increase of speed increases as the body is approached. If there were no friction at the surface of the body, the speed would reach a maximum there. But (Article 22) the air is stationary on the surface, and is retarded for some distance into the fluid. We are concerned with the manner in which such retardation consorts with the more distant, though still close, increases of speed, which are often large.

36. Experimental Streamlines

It is always possible to plot the streamlines for a steady motion from experimental knowledge of the velocity distribution. Fig. 16 has been prepared from actual measurements of the approximately two-dimensional motion in the median plane of a scale model of an aeroplane wing of the section shown. The model wing, or aerofoil, was immersed in a stream whose velocity U and pressure p_0 were initially uniform. Explorations of the magnitude and direction of the disturbed velocity q were made along several normals to the wing surface ; values of $q \sin \alpha/U$ are plotted for the two shown, viz. S_1N_1 and S_2N_2, distance from the surface along either normal being denoted by n and the angle between q and the normal by α.

The flow across any part of a normal is given by the value of the integral

$$\int q \sin \alpha \, dn$$

over that part. Choose a point A_1 on S_1N_1 through which it is desired that a streamline shall pass. Evaluate graphically

$$\int_{S_1}^{A_1} q_1 \sin\alpha \, dn = k, \text{ say.}$$

For n small, $\sin\alpha = 1{\cdot}0$. Now find a point A_2 on S_2N_2 such that

$$\int_{S_2}^{A_2} q_2 \sin\alpha \, dn = k,$$

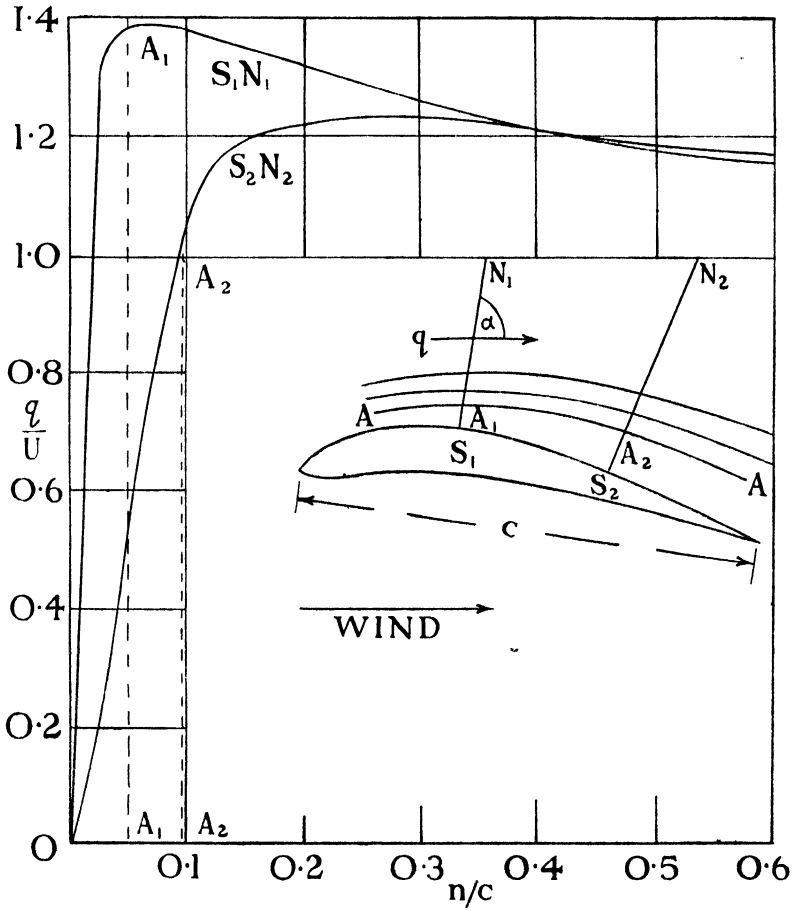

FIG. 16.

i.e. find the line $n = A_2$ (Fig. 16), such that the area OA_2A_2 equals the area OA_1A_1. Similarly, determine points A, A . . . along other normals. Now there is no flow across the aerofoil contour. Therefore there is no flow across the curve AA_1A_2A . . . Hence this curve is a streamline.

Successive streamlines follow by changing k to k', k'' . . . It is

convenient to make $k = k' - k = k'' - k' = \ldots$, for then, if the intervals are sufficiently small, the velocity is inversely proportional to the distance apart of successive streamlines. A second streamline is, of course, most conveniently constructed from the first, a third from the second, and so on.

37. The Stream Function

It would be possible to fit to an experimental streamline a formula $f(x, y) = \text{constant}$. The fit would not be so close, however, nor the original measurements so accurate as to ensure obtaining another streamline by equating the same function of x and y to another constant. In a motion that is known analytically, on the other hand, these difficulties disappear. We then have a function of x and y, $\psi(x, y)$, which, on equating to any constant, gives corresponding values of x and y for points lying on one of the streamlines of the motion. ψ is called the stream function of the motion.

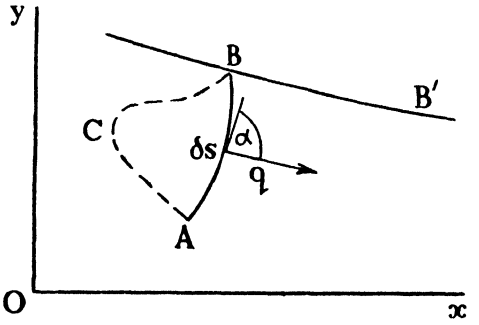

FIG. 17.

Consider a steady two-dimensional motion in the xy-plane. Let A and B be two points, not on the same streamline; join them by any curve (Fig. 17), and let q make an angle α with an element δs of the curve. Define the flow across this curve by $\psi_B - \psi_A$, i.e.

$$\psi_B - \psi_A = \int_A^B q \sin \alpha \, ds.$$

This value is unique, for the flow across AB is independent of the shape of the curve, being the same as that across any other curve, such as ACB, joining the points, since otherwise fluid would be compressed within, or exhausted from, the area ACBA.

With A fixed let B move in such a manner that the above flow remains constant. Then B traces out a streamline, because there is no flow across its path. If the value of $\psi(x, y)$ at $A = k$, for all points on the streamline BB′,

$$\psi = k + \psi_B - \psi_A.$$

It follows that the equation to all streamlines is

$$\psi = \text{constant} \quad . \quad . \quad . \quad . \quad (62)$$

the constant changing from one to another. A definite value is assigned to the constant of a particular streamline by agreeing to denote some chosen streamline by $\psi(x, y) = 0$. A question of sign is involved; the increment of ψ is taken as positive if the flow is in a clockwise direction about the origin, but sign is determined generally by (63) below.

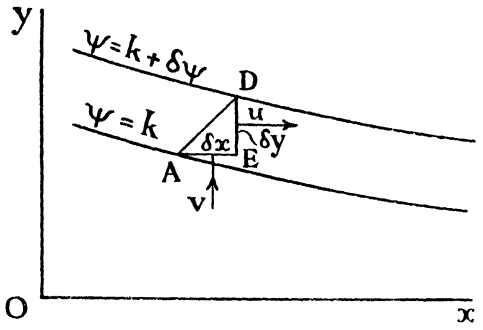

FIG. 18.

38. Let A and D be adjacent points on two streamlines: $\psi = k$ and $\psi = k + \delta\psi$. The co-ordinates of A are x and y, those of D $x + \delta x$, $y + \delta y$. From Fig. 18, the flow across AD = that across ED less that across AE. Hence if u, v are the components parallel to Ox, Oy, respectively, of the velocity q,

$$\delta\psi = u\delta y - v\delta x.$$

Now $\delta\psi$ is the total variation of a function of the two independent variables x and y. It is assumed that the partial derivatives $\partial\psi/\partial x$ and $\partial\psi/\partial y$ are also continuous functions of x and y. It is shown in text-books on Calculus that then

$$\delta\psi = \frac{\partial\psi}{\partial x}\delta x + \frac{\partial\psi}{\partial y}\delta y.$$

Hence:

$$u = \frac{\partial\psi}{\partial y}$$
$$v = -\frac{\partial\psi}{\partial x}. \qquad \ldots\ldots \quad (63)$$

As an example, suppose $\psi = Uy$, where U is a constant. From (63) $u = U$, $v = 0$, and the flow evidently consists of uniform motion at constant velocity U in the direction Ox. Putting $\psi/U = 0, 1, 2 \ldots$ gives a series of streamlines all parallel to Ox and spaced equally apart. Again, consider the flow $\psi = Cy^2$, where C is a constant. Putting $\psi/C = 0, 1, 2 \ldots$ again gives streamlines parallel to Ox, but at a decreasing distance apart (Fig. 19). From (63) $u = 2Cy$, $v = 0$, and we recognise the flow as including that of

Article 24, where $2C = U/h$, and there are certain restrictions on the area occupied by the flow.

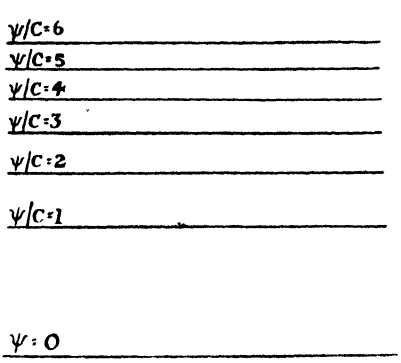

FIG. 19.—STREAMLINES FOR UNIFORM SHEARING.

39. Circulation and Vorticity

So far we have dealt with the line integral of the normal velocity component across a curve drawn in the field of flow. The line integral of the tangential velocity component once round any *closed* curve is called the circulation round that circuit and is denoted by K. If δs is an element of length of the closed curve of the circuit, q the velocity, and α the angle which q makes with δs,

$$K = \int_C q \cos\alpha \, ds \quad . \quad . \quad . \quad . \quad (64)$$

There is again a question of sign, and this is taken as positive if K has a counter-clockwise sense.

Let us calculate the circulation δK round the small rectangle ABCD (Fig. 20), of sides δx, δy. The sides AD and CB together contribute to counter-clockwise circulation an amount $u\delta x - \left(u + \frac{\partial u}{\partial y}\delta y\right)\delta x = -\frac{\partial u}{\partial y}\delta x\delta y$. Similarly DC and BA together contribute $\frac{\partial v}{\partial x}\delta x\,\delta y$. Hence:

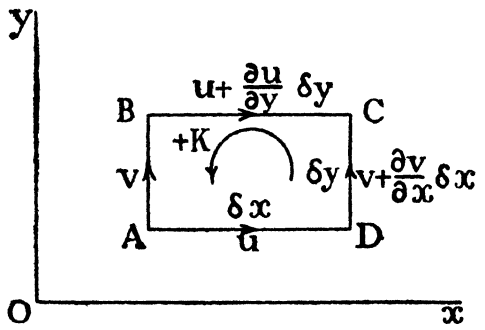

FIG. 20.

$$\frac{\delta K}{\delta x \delta y} = \frac{\partial v}{\partial x} - \frac{\partial u}{\partial y}.$$

The finite limit to which the left-hand side tends as the area decreases is called the vorticity at the point and has the symbol ζ. Thus:

$$\zeta = \frac{\partial v}{\partial x} - \frac{\partial u}{\partial y}. \quad . \quad (65)$$

In words, the vorticity of an element is the ratio to its area of the

circulation round its contour. Choose the element as circular, of radius r, and so small that its angular velocity ω can be considered constant. Then K is due to ω alone. Writing S for area,

$$\delta K = 2\pi r \,.\, \omega r \,;\; dK/dS = 2\omega$$

or

$$\zeta = 2\omega.$$

Thus the vorticity of an element is twice its angular velocity.

In the first example of Article 38, where $u = U$, a constant, and $v = 0$, we now have from (65) $\zeta = 0$ everywhere ; the elements of fluid are devoid of spin. For the second example, $u = 2Cy$, $v = 0$ and (65) gives $\zeta = -2C$, a constant, or there is a uniform distribution of vorticity. Applying the latter result to the motion of Article 24, $\zeta = -U/h$. Imagine the moving plate in Article 24 to be started from rest. Initially $u = v = 0$ and the fluid is devoid of vorticity, but after a sufficient time a uniform distribution of vorticity is generated, arising from the boundary condition of zero slip and the action of viscosity. We are thus able to trace the generation of the vorticity to viscosity. If the pressure had acted equally in all directions, it would have exerted no couple on any element of fluid which, being originally devoid of vorticity, would have remained so.

40. Extension of Bernoulli's Equation

We are now in a position to prove a theorem of practical importance in connection with flow that is sufficiently distant from bodies and other boundaries. A distribution of vorticity is assumed to exist, but tangential components of stress are neglected.

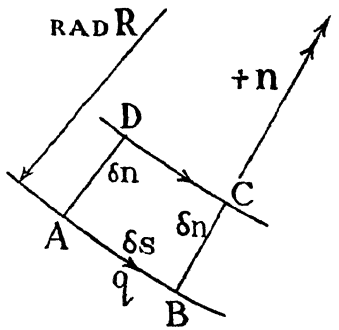

FIG. 21.

Consider the fluid element ABCD (Fig. 21), bounded by two adjacent streamlines and the normals thereto. Let the radius of curvature, assumed large, of the streamline AB be R. Let s denote length measured along AB, DC, and n denote length measured along either of the normals towards the centre of curvature. Let q be the velocity along AB. Tangential components being neglected, the pressures act normally to the faces of the element.

The element exerts a centrifugal force $\rho\delta s\delta n q^2/R$ which, the flow

being steady, is balanced by a force due to the difference of the pressures on the faces AB, CD, i.e. by the force $-\delta s\delta n(\partial p/\partial n)$ (Article 28). Hence :

$$-\frac{\partial p}{\partial n} = \rho\frac{q^2}{R}. \quad . \quad . \quad . \quad . \quad (66)$$

Now calculate the circulation δK round the element. There is no flow along the normals ; hence :

$$\delta K = q \,.\, AB - \left(q + \frac{\partial q}{\partial n}\delta n\right) CD \quad . \quad . \quad (i)$$

From the figure—

$$\frac{CD}{AB} = \frac{CD}{\delta s} = 1 - \frac{\delta n}{R}.$$

Substituting in (i)

$$\delta K = \left\{q - \left(q + \frac{\partial q}{\partial n}\delta n\right)\left(1 - \frac{\delta n}{R}\right)\right\}\delta s$$

$$= \left\{-\frac{\partial q}{\partial n} + \frac{q}{R} + \frac{\partial q}{\partial n}\cdot\frac{\delta n}{R}\right\}\delta s\delta n.$$

The last term is evidently negligible compared with the others. Hence, finally :

$$\zeta = \frac{q}{R} - \frac{\partial q}{\partial n}. \quad . \quad . \quad . \quad . \quad (67)$$

Multiply both sides of (67) by $-\rho q$ and substitute from (66) for $1/R$. (67) becomes

$$-\rho q\zeta = \frac{\partial p}{\partial n} + \rho q\frac{\partial q}{\partial n}$$

$$= \frac{\partial}{\partial n}(p + \tfrac{1}{2}\rho q^2). \quad . \quad . \quad . \quad (68)$$

Now $p + \frac{1}{2}\rho q^2$ is the pitot head (Article 32). Thus, across the streamlines the pitot head has a gradient proportional to the product of the velocity and the vorticity, provided tractions can be neglected. If, on traversing a pitot tube across a field of flow, the pitot head remains constant, then the flow is devoid of vorticity so far as it is explored.

41. Irrotational Flow

An irrotational motion is one in which it is everywhere true that $\zeta = 0$. Where velocity gradients exist, this condition usually

appears as an ideal which is not exactly attained by a real fluid, but many motions of great Aerodynamic interest approximate closely to the irrotational state. These are discussed theoretically in later chapters. Meanwhile, we note that the theorem of the preceding article leads, as described, to a convenient method of investigating experimentally whether a given flow, or what part of it, is approximately irrotational.

42. Subdivision of Flow Past Bodies

It will now be shown, on experimental grounds, as will be proved theoretically in a later chapter, that Aerodynamic types of flow can

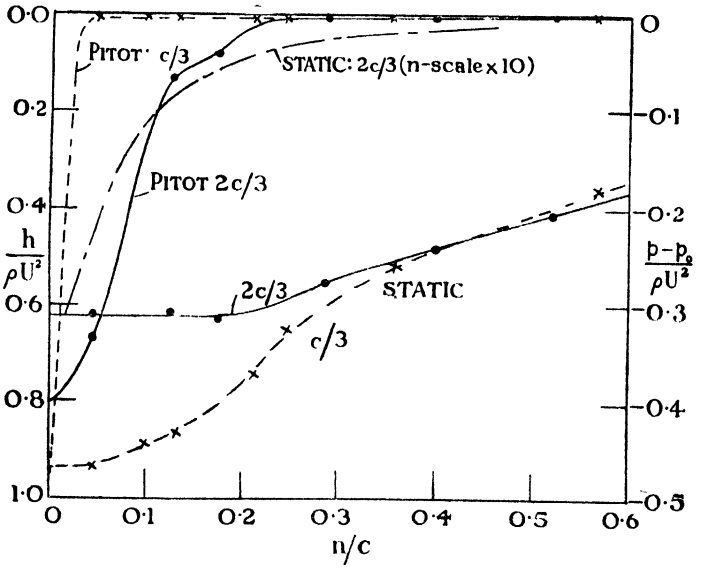

FIG. 22.

be separated into two parts: an outer irrotational motion and an inner flow characterised by the presence of vorticity. For this purpose a particular, but typical, case will be described in some detail. The flow selected is that above the aerofoil of Article 36. This aerofoil was small, having a chord c (length of section) of $1\frac{1}{2}$ in. It was set at an incidence (angle made with the oncoming stream by the common tangent to its lower surface) of 9·5° in an initially uniform air-stream of velocity $U = 41$ ft. per sec. and pressure p_0. The undisturbed stream was verified to be sensibly irrotational by tracking across it a pitot tube, the pitot head being found to be constant.

The same two normals, S_1N_1 and S_2N_2, distant $c/3$ and $2c/3$, respectively, from the leading edge, were selected for study as those for which the variation of velocity (q) has been given in Article 36. What will now be described is the variation that was found along them of pitot head and static pressure (p). In Fig. 22 the first of these is given in the form :

$$\frac{h}{\rho U^2} = \frac{p_0 + \frac{1}{2}\rho U^2 - (p + \frac{1}{2}\rho q^2)}{\rho U^2},$$

h, then, being the loss of pitot head caused by the model ; the second is conveniently expressed as $(p - p_0)/\rho U^2$, both quantities being non-dimensional.

It is seen from the figure that the aerofoil causes negligible change of pitot head beyond $n = 0{\cdot}04c$ for the upstream and $n = 0{\cdot}2c$ for the downstream normal. Beyond these limits the stream is concluded to be irrotational, approximately ; just within them the velocity gradients are not large and the tractions may be expected to be small, so that, from (68), we infer vorticity to be present. By traversing a fine pitot tube along a number of other normals, or lines across the stream, a number of similarly critical points for pitot head can be found. A line drawn through all such points forms a loop which wraps itself very closely round the nose of the model (where a special form of pitot tube is necessary for detection), widens as the trailing edge is approached, and finally marks out a wake behind the aerofoil. Fig. 23 shows the wake located in this way behind another aerofoil set at smaller incidence. The complete loop may be called, for short, the pitot boundary * and is one way of marking out an internal limitation to irrotational flow.

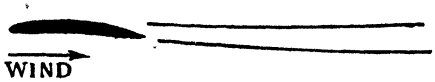

FIG 23.—PITOT BOUNDARY MARKING WAKE OF AEROFOIL.

The pressure decrease $p_0 - p$ builds up along the normals as the aerofoil is approached to maxima at the pitot boundary. Actually there was no reason to measure the pressure and velocity separately in the outer irrotational region except as a check, for here the one can be calculated from the other by Bernoulli's theorem. The maximum pressure changes generated at the pitot boundary are transmitted without further variation along normals to the aerofoil surface. This important point is clearly seen from the pressure

* For further illustrations see Piercy, *Jour. Roy. Aero. Soc.*, October 1923.

curve for the more downstream normal, the three readings nearest the surface being

$$\begin{array}{lccc} n/c = & 0{\cdot}047 & 0{\cdot}127 & 0{\cdot}173 \\ \dfrac{p_0 - p}{\rho U^2} = & 0{\cdot}310 & 0{\cdot}308 & 0{\cdot}312 \end{array}$$

A pressure change of $0{\cdot}47\ \rho U^2$ is transmitted to the surface along the more upstream normal. Within the pitot boundary adjacent to the aerofoil the velocity (Fig. 16) and the pitot head (Fig. 22) fall away rapidly. The first, as already seen, vanishes on the surface ; the second decreases from $p_0 + \frac{1}{2}\rho U^2$ to p', the value of the static pressure on the pitot boundary opposite the position round the contour of the aerofoil considered.

The chain-line curve (Fig. 22) gives a wider view of the manner in which the static pressure drop is built up.

An aeroplane was fitted with wings of the shape of the aerofoil, and some measurements were made in flight. These showed the velocities and pressures, non-dimensionally expressed, to be different from those observed with the model but not greatly so. The pitot boundary was found to be much closer to the full-scale wing surface than it was to the model surface when expressed as a fraction of the chord.

43. The Boundary Layer

From the many experiments which have been made on lines similar to the foregoing, we draw the following preliminary conclusions regarding motions of Aerodynamic interest past bodies :

1. There exists an outer irrotational flow.

2. This is separated from the body by a sheath of fluid infected with vorticity arising from the boundary condition of no slip and the action of viscosity. This sheath or film of fluid increases in thickness from the nose to the tail of the body, but is nowhere thick and is called the Boundary Layer. It merges into the wake.

3. Changes in static pressure are built up in the outer flow, related to the velocity changes there by Bernoulli's equation, and are transmitted to the surface of the body through the boundary layer.

AERODYNAMIC FORCE AND SCALE

44. The Aerodynamic force on a body is that resultant force on it which is due solely to motion relative to the fluid in which it is

immersed. Thus forces acting on the body due to gravity, buoyancy, etc., are excluded. Aerodynamic force arises on the body in two ways: (*a*) from the static pressures over the surface, sometimes called the normal pressures; (*b*) from a distribution of skin friction over the surface.

Consider, for example, an aeroplane wing of uniform section. Let δs denote the area, per unit of span, of an element of the contour of

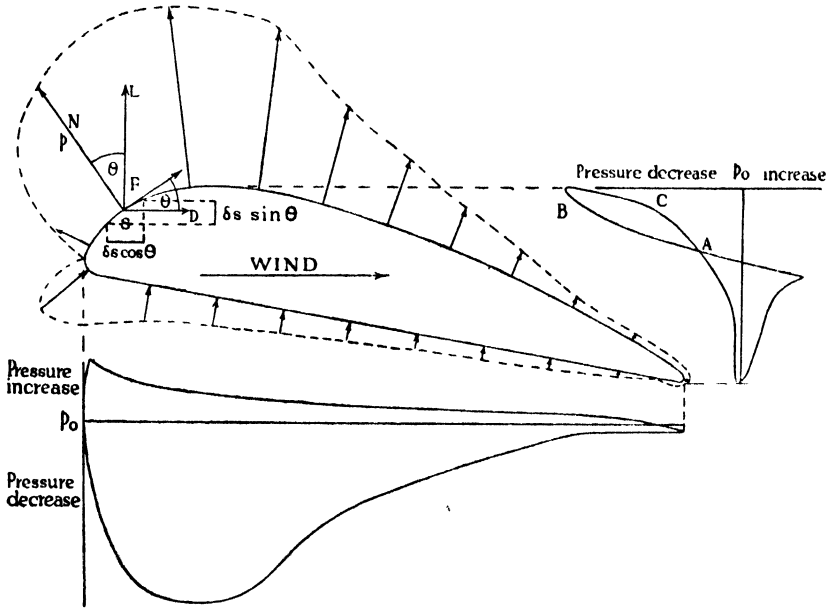

FIG. 24.—EXPERIMENTAL PRESSURE DISTRIBUTION ROUND SECTION OF AEROFOIL, SHOWING INTEGRATION OF PRESSURE DRAG AND LIFT.

the section at S (Fig. 24), and θ the angle which the normal SN at δs makes with SL, the perpendicular to the direction of the relative undisturbed wind. For convenience, subtract from the pressure acting on the surface the static pressure of the oncoming stream, and let p be the normal component of the remainder and F the tangential component. The variation of p is shown by the dotted line in the figure. The force on the element is compounded of $p.\delta s$, outwardly directed along SN and $F.\delta s$, perpendicular thereto. For simplicity we shall assume the flow to be two-dimensional, so that F has no component parallel to the span. p and F vary from point to point over the wing, leading to a variation of force from one element to another in both magnitude and direction. To obtain the resultant force we require to effect a summation of the forces on all elements.

Evaluation is usefully simplified in the following way: components of the resultant force are determined parallel to SL drawn perpendicular to the relative wind and to the aerofoil span, and SD in the direction of the relative wind. The first component is the *lift*, the second the *drag*. It will especially be noted that the Aerodynamic lift of a wing, unlike the static lift of a gas-bag, is not constrained to be vertical, nor even does its direction necessarily lie in a vertical plane; it is perpendicular to the span of the wing and also to the relative wind, and is taken as positive if it is directed upward when the wing is the right way up.

Denoting lift by L and drag by D, we have for δs

$$\delta L = (p \cos \theta + F \sin \theta)\, \delta s$$
$$\delta D = (-p \sin \theta + F \cos \theta)\, \delta s$$

Now $\delta s \sin \theta$ and $\delta s \cos \theta$ are the projections of δs perpendicular and parallel to SL. Hence, if the aerofoil section is drawn accurately to scale and all points on the contour at which p is known are projected upon a line perpendicular to SL (i.e. upon a line parallel to the undisturbed relative wind) and p is set up normally to this line, the area enclosed by the curve obtained by joining the points, completed so as to represent the whole contour, is proportional to that part of the lift which is due to p. If similar projections are made along a line parallel to SL, and p is set up normally to this line and a closed curve is obtained by joining all points and completing so as to include all positions round the contour, the net area enclosed by the curve is proportional to the contribution to drag by p. As regards drag, the simplest curve found for an aerofoil is of figure-of-eight form, one loop of which is positive and the other negative; the net area is conveniently obtained by tracing the point of a planimeter round the diagram in a direction corresponding to one complete circuit of the aerofoil contour. The contributions of skin friction to lift and drag are similarly determined, but the directions of projection are interchanged. The sense of F depends upon that of the velocity gradient with which it is associated. However, the correct sense is easily decided by inspection.

45. An example of the variation of p round the median section of an aerofoil at a certain angle of incidence, experimentally determined at a certain speed, is given in Fig. 24. Curves are also shown obtained by projection perpendicular to and in the direction of the oncoming stream, the areas under which are proportional to the lift and drag per foot run of the span at the median section, the area ABC giving negative contributions to drag. Apart from scientific

interest, investigations of distribution of force are of technical importance, especially in the case of aerofoils, providing data essential to the design of sufficiently strong structural members of minimum weight for the corresponding aeroplane wing. Such analysis is usually required at several angles of incidence. Since the pressure will most conveniently be found at the same points round the contour for all incidences, labour is saved by projecting along and normal to the chord of the wing, resolving subsequently in the wind direction and perpendicular thereto. Graphical processes of integration convenient for bodies other than wings will be left for the reader to devise.

46. Some limiting cases may be mentioned. When a fluid flows through a straight pipe or past a thin flat plate at zero incidence—i.e. parallel to the oncoming stream—the drag must be wholly frictional. Such drag is small with air as fluid. At the other extreme, the drag of a thin flat plate set normal to the undisturbed stream must arise wholly from unequal distribution of pressure. This drag is comparatively large, but is less than that of a cup-shaped body with the concavity facing the direction of flow, as instanced by a parachute. Referring to aerofoils, the contribution of skin friction to lift is negligible. The area enclosed by the negative drag loop of the projected pressure curve (e.g. ABC of Fig. 24) may approach that of the positive loop, when the contribution of the pressures to drag will be small. For this condition to be realised, the flow must envelop the back of the body closely, i.e. without ' breaking away ' from the profile. Negative drag loops are absent from the normal plate and very small for the circular cylinder.

A quantity of significance descriptive of an aerofoil is the ratio of the lift L to the drag D, i.e. L/D. Since $D = L \div L/D$, for a given lift the drag is smaller the greater L/D. Considering a flat plate at any incidence α and neglecting skin friction, and writing P for the total force due to variations of pressure over the two surfaces, we have $L = P \cos \alpha$, $D = P \sin \alpha$. However P varies with α, $L/D = \cot \alpha$. Values given by this formula must always be excessive, greatly so at small incidences when the neglected skin friction becomes relatively important. Nevertheless, at flying incidences the L/D of a wing, skin friction included, greatly exceeds cot α. A wing having also essentially more lifting power than a flat plate, this comparison is often given as illustrating the superiority of the aerofoil over the flat plate for aeroplane wings. The advantage is seen to arise from the pressure distribution round the forward part of the upper surface of the aerofoil, providing positive lift and negative drag.

As a matter of experiment it is found that the pressure drag of a carefully shaped airship envelope almost vanishes, although the pressure varies considerably from nose to tail, and the drag is almost wholly frictional ; it may amount to less than 2 per cent. of the drag of a normal disc of diameter equal to the maximum diameter of the envelope. The example illustrates the great economy in drag which can be achieved by careful shaping, a process known as fairing or streamlining. So exacting is this process that it pays to shape the contour of a wing, strut section, engine egg, or other exposed part of an aircraft by some suitable formula, instead of using french curves, so as to avoid sharp changes of curvature which, although scarcely apparent to the eye, may increase drag considerably.

47. Rayleigh's Formula

Further investigation of how Aerodynamic force depends upon shape is left to subsequent chapters. The knowledge required for practical use will result partly from theory and partly from experiment. For both lines of enquiry we need to establish a proper scale in terms of which Aerodynamic force may be measured. For this purpose we keep the geometrical shape of the body and its attitude to the wind constant, but allow its size to vary ; in other words, we consider a series of bodies of different sizes made from a single drawing, immersed, one after another, at the same incidence in a uniform stream of air. Geometrical similarity must include roughness of surface, unless effects of variation are known in a given case to be negligible ; a caution is also necessary against tolerating any lack of uniformity in the oncoming stream. But the velocity of the stream may vary and also the physical condition of the air ; in fact, the bodies may be supposed immersed in uniform streams of different fluids, liquid or gaseous. But it is assumed for simplicity, and as representing a common condition in Aerodynamics, that maximum velocities attained are small compared with the velocity of sound in the fluid concerned, so that compressibility may be neglected.

Preceding articles have shown that the Aerodynamic force A arises from pressure variation and skin friction. The pressure will depend upon the density ρ and the undisturbed velocity U. The skin friction has been seen to depend upon U and the viscosity μ. Comparing different fluids, or air in different states, the general effect of viscosity depends on the ratio of the internal tractions to the inertia, which is proportional to ρ. Hence it is convenient to substitute for μ the quantity

$$\nu = \mu/\rho \quad . \quad . \quad . \quad . \quad (69)$$

called the *kinematic coefficient of viscosity*, whose dimensions are (cf. Article 23) $M/LT \div M/L^3 = L^2/T$. The Aerodynamic force, since it results from the surface integration of pressure and skin friction, will also depend upon the size of the body, which is specified by any agreed representative length l, because the geometrical shape is constant.

It is concluded, then, that :

$$A \text{ depends upon } \rho, U, l, \nu \quad . \quad . \quad . \quad (70)$$

and on nothing else. This conclusion, which is essential to the investigation, can be arrived at in other ways ; e.g. by appeal to simple experiments. Thus, if a bluff shape, such as a normal plate, is moved by hand through air, drag can be felt to depend upon size and velocity. If it is then moved through water, a great increase occurs mainly as a result of increased density. Moving the plate finally through thick oil instead of water shows that drag also depends upon viscosity, for density need scarcely have changed. The importance of the more careful consideration that we have given to the question lies in the assurance that no important factor has been omitted.

It is desired to obtain a general formula for A, connecting it with ρ, U, l, ν. This may contain a number of terms, any one of which can be written in the form :

$$\rho^p U^q l^r \nu^s. \quad . \quad . \quad . \quad . \quad . \quad (71)$$

Now A, being a force, has the dimensions of mass $\times$ acceleration, i.e. ML/T^2. The principle of homogeneity of dimensions asserts that all terms in the formula for A must have the same dimensions. Writing (71) in dimensional form :

$$\frac{ML}{T^2} = \left(\frac{M}{L^3}\right)^p \left(\frac{L}{T}\right)^q L^r \left(\frac{L^2}{T}\right)^s.$$

For the dimensions of the term to be ML/T^2, it is required that

on account of the M's, $p = 1$,
on account of the L's, $-3p + q + r + 2s = 1$,
on account of the T's, $-q - s = -2$,

giving

$$p = 1$$
$$q = r = 2 - s.$$

Hence the formula for A is :

$$A = \Sigma\rho\, U^{2-s} l^{2-s} \nu^s$$
$$= \Sigma\rho\, U^2 l^2 \left(\frac{Ul}{\nu}\right)^{-s}$$

or
$$A = \rho U^2 l^2 . f\left(\frac{Ul}{\nu}\right), \quad . \quad . \quad . \quad (72)$$

where $f(Ul/\nu)$ means some particular function of the one variable Ul/ν.

This important relationship is the simplest case of Rayleigh's formula. The investigation equally leads to

$$A = \Sigma \rho \nu^2 \left(\frac{Ul}{\nu}\right)^{2-s}$$
$$= \rho \nu^2 . f_1\left(\frac{Ul}{\nu}\right) . \quad . \quad . \quad . \quad (72a)$$

an alternative form of particular use where change of fluid is involved. It will be noted that Aerodynamic force cannot vary with the area of the body or the square of the velocity exactly unless it is independent of viscosity, which is absurd.

48. Reynolds Number—Simple Similar Motions

The quantity Ul/ν is called the *Reynolds number* after Osborne Reynolds, who first discovered its significance, and is written R. Writing (72) as

$$\frac{A}{\rho U^2 l^2} = f(R) \quad . \quad . \quad . \quad . \quad (73)$$

we have, on the left-hand side, a coefficient of Aerodynamic force whose value for any shape of body and value of R can be found if required by actual measurement.

Still keeping shape constant, let us investigate what similarity exists in the flow of different fluids at different velocities past bodies of different sizes, subject to the restriction that R remains constant.

Considering any particular position in the field of flow past the particular shape, the method of Article 47 readily gives for any velocity component there, for instance u,

$$u = U . f_2(R).$$

Hence, from consideration of velocity components at right angles at geometrically similarly situated points, called corresponding points, one in each of a series of fields of flow past bodies of the same shape (and attitude) at the same Reynolds number, the resultant velocity there is the same in direction. Since this is true of all sets of corresponding points, the streamlines present the same picture, though to different geometric scales. The magnitude of the velocity at corres-

ponding points $\propto U$; and the pressure $\propto \rho U^2$, as may be shown directly.

It follows that at corresponding points on the contours of the bodies the pressure $\propto \rho U^2$ and the skin friction $\propto \mu U/l \propto \rho\nu U/l$, and that part of A resulting from pressure variation $\propto \rho U^2 l^2$, while that part due to skin friction $\propto \rho\nu Ul \propto \rho U^2 l^2$, since $\nu \propto Ul$, because R is constant. Hence $A \propto \rho U^2 l^2$, or the left-hand side of (73) is constant.

Example: if also the fluid is constant, show that A is constant.

The foregoing assumes the motions to be steady. Now let them have frequencies $\sim$ (dimensions: $1/T$). With frequency assumed to depend only on ρ, U, l, ν, the method of Article 47 gives:

$$\sim = \frac{U}{l} f_3(R).$$

While R remains constant, $\sim \propto U/l$ in periodic motions. If also the fluid be given so that ν, and therefore Ul, remain constant, $\sim \propto U^2 \propto 1/l^2$. The streamlines pass through the same sequence of transient configurations but at different rates; if cinema films were taken of the motions, any picture in one film would be found in the others, but it would recur at a different, though related, frequency. Similarity of streamlines, etc., as described above, then occurs at the same phase. The result: $A \propto \rho U^2 l^2$ is now true of the Aerodynamic force at any phase and also of the mean value, with which we are usually concerned.

The motions considered in this article provide an example of what are termed *dynamically similar* motions. Constancy of the left-hand side of (73) is also found by experiment for R constant when the bodies produce flow that varies rapidly in an irregular manner.

49. Aerodynamic Scale

When the Reynolds number changes, there is no reason to expect the coefficient of Aerodynamic force to remain constant, and it is found to vary, sometimes very little through a limited range of R, sometimes sharply, depending upon the shape of the body (or its attitude) and the mean value of R. Now, if by a series of experiments or calculations we obtain a number of values of A for a given shape, work out the coefficients and plot these against R, it is clear from Article 48 that all coefficients will lie on a single curve. This curve is the graphical representation of $f(R)$ through the range explored.

Fig. 25 gives as an example the variation of (drag $\div \rho U^2 l^2$) with R for long circular cylinders set across the stream. In order to fix

the numerical scales, it has been chosen quite arbitrarily to use the diameter of the cylinder in specifying R and the square of the diameter for l^2, but the drag then relates to a length of the cylinder equal to its diameter. The full line results from a great number of observations. These are not shown, but they fit the curve closely, though a cluster of points round a particular Reynolds number may include great

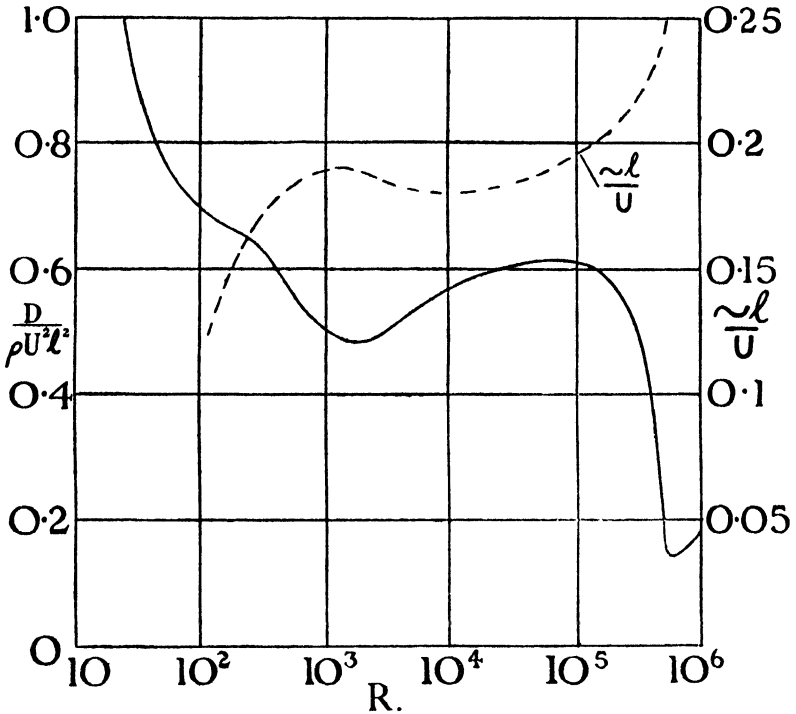

FIG. 25.—DRAG OF LONG CIRCULAR CYLINDERS SET ACROSS STREAM AND FREQUENCY OF FLOW IN WAKE (l = DIAMETER).

variation in, for instance, diameter. The rapid rise of drag at $R = 10^6$ flattens again at $1{\cdot}3 \times 10^6$ with a value of about 0·3 for the coefficient. The broken line gives the variation of frequency, the flow eddying for $R > 100$.

Similar success has been obtained experimentally in many other cases, and we conclude that the theory of Article 47 can be accepted with confidence. When observations at constant Reynolds number disagree with one another, the cause is to be sought in the particular circumstances of the experiments ; if geometrical similarity is truly realised and velocities are demonstrably too small for appreciable

compressions and expansions, the cause may be traced to considerable variation of unsteadiness in the oncoming streams.

Finally, it becomes evident that, with moderate velocities, the Reynolds number provides a proper scale for Aerodynamic motions. Circumstances in which this scale is not suitable are described in the following articles.

The principle of dimensional homogeneity is often employed to express in a rational formula the results of a series of experiments on a given shape. The process usually depends upon discovery of a constant index for one of the variables, although this restriction is not necessary. It should carefully be noted that such formulæ apply only through the range for which they have been shown to hold; large errors often result from extrapolation. Thus, such formulæ amount to no more than a convenient mental note of the results from which they are derived; they constitute merely an approximation to part of the $f(R)$ curve for the shape concerned.

The outstanding practical significance of general formulæ such as (72) is to establish the basis on which single experiments on scale models of aircraft or their component parts should, if possible, be carried out. Provided the model is tested at the same Aerodynamic scale, experimental measurements are accurately related to corresponding quantities at the full scale; otherwise corrections are necessary. The proviso can by no means always be satisfied even when the gauge of Aerodynamic scale is simply the Reynolds number. The more complicated formulæ completing this chapter will show that the Reynolds number alone is often insufficient; the position then becomes more difficult and experiment requires planning with judicious care.

49A. Rayleigh's Formula—High Speeds

If the compressibility of the air cannot be neglected, its modulus of bulk elasticity E must be admitted and the typical term in the new formula for Aerodynamic force becomes

$$\rho^p U^q l^r \nu^s E^t \qquad . \quad . \quad . \qquad \text{(i)}$$

The dimensions of E are M/LT^2, and the method of Article 47 gives

$$\begin{aligned} (M) \quad 1 &= p + t \\ (L) \quad 1 &= -3p + q + r + 2s - t \\ (T) \quad -2 &= -q - s - 2t, \end{aligned}$$

i.e.,

$$\begin{aligned} p &= 1 - t \\ q &= 2 - s - 2t \\ r &= 2 - s, \end{aligned}$$

giving the result—

$$\rho^{1-t}U^{2-s-2t}l^{2-s}\nu^{s}E^{t} = \rho U^{2}l^{2}\left(\frac{Ul}{\nu}\right)^{-s}\left(\frac{\rho U^{2}}{E}\right)^{-t}.$$

By Article 20, $E = \rho a^2$, where a is the velocity of sound, i.e. $\rho U^2/E = (U/a)^2$. The ratio U/a is called the *Mach number* and denoted by M, and the formula becomes finally

$$A = \rho U^{2}l^{2}.f(R, M). \quad . \quad . \quad . \quad . \quad . \quad (73A)$$

There being five unknowns and only three dimensional equations to relate them, the new function has two arguments; A depends upon both and, theoretically, this dependence cannot be separated. From calculation of the stagnation pressure, an inference has been made in a preliminary way that compressibility can be ignored for speeds little greater than 250 m.p.h. at low altitude, i.e. for values of M less than $\frac{1}{3}$, and considerably greater values produce in some cases only negligible effects on A. Formerly, the airscrew provided almost the only occasion calling for a formula of the type (73A), speeds towards the tips of their blades being so high as to make M approach unity. In modern Aeronautics, however, the importance of the formula is much wider. Considering, for example, a stratospheric aeroplane flying at the moderate indicated air speed of 200 m.p.h. at an altitude of 40,000 ft., where the relative density of the air is $\frac{1}{4}$, $U = (22/15) \cdot (200/\sqrt{\frac{1}{4}}) = 587$ ft. per sec., whilst a is reduced by the low temperature to the value 975 ft. per sec., giving $M > 0{\cdot}6$ for every part of the aeroplane. Now in full-scale flight at little more than this Mach number the effect of varying M may be much more important than that of varying R. Thus, while (72) can still be relied upon in a great variety of practical circumstances, the occasions on which it is superseded by (73A) are multiplying.

For two motions 1 and 2 to be dynamically similar, both R and M must be the same, leading to

$$\frac{l_1}{\nu_1} = \frac{l_2}{\nu_2} \cdot \frac{a_2}{a_1}.$$

For a dynamically similar experiment on a model of an aircraft it will be plain from the next chapter that the power required to produce the artificial wind is economised chiefly by reducing the speed. But this would involve employing very cold air. In

these circumstances and in view of the labour involved, the task of constructing a data sheet such as Fig. 25, which would now embrace a series of curves for a body of given shape, is abandoned, and experiments on the effect of high Mach numbers are usually carried out with no more than the precaution of avoiding very small Reynolds numbers.

49B. Some Other Conditions for Similitude occurring in Aerodynamics

(1) When a seaplane float or flying-boat hull moves partly immersed in water, waves formed cause variation of pressure over horizontal planes due to the weight of the heaped liquid. Thus gravity comes into the problem of similarity. Approximate treatment ignores air drag of parts projecting above the surface and also surface tension. Then ρ, U, l, ν refer to the water only and, with g added, we write any term in the formula for drag as

$$\rho^p\, U^q\, l^r\, \nu^s\, g^t.$$

Dimensional theory at once gives:

$$\begin{aligned} (M) \quad & 1 = p \\ (L) \quad & 1 = -3p + q + r + 2s + t \\ (T) \quad & -2 = -q - s - 2t \end{aligned}$$

whence

$$\begin{aligned} p &= 1 \\ q &= 2 - s - 2t \\ r &= 2 - s + t \end{aligned}$$

and the term becomes

$$\rho U^2 l^2 \left(\frac{Ul}{\nu}\right)^{-s} \left(\frac{U^2}{gl}\right)^{-t}$$

leading to the following formula for drag:

$$D = \rho U^2 l^2 . f\left(R, \frac{U^2}{gl}\right). \qquad . \qquad . \qquad . \quad (73B)$$

The drag is made up of two parts: (*a*) a part akin to Aerodynamic force but modified by (*b*) wave-making resistance, which again is modified by (*a*). U^2/gl is called the Froude number, F.

For dynamical similarity both arguments of the function must be kept constant. For change of size the second argument gives $U \propto \sqrt{l}$ since g is practically constant, and then by the first $\nu \propto \sqrt{l^3}$, i.e. the fluid must be changed when $D \propto \rho\nu^2 \propto \rho l^2$. A change from water is not

convenient, however, and it has been found sufficient, as originally suggested by Froude, to assume the two kinds of resistance to be independent of one another, i.e. to write (73B) as

$$D = \rho U^2 l^2 \left[f_1(R) + f_2\left(\frac{U^2}{gl}\right)\right]. \quad . \quad . \quad (73C)$$

This is convenient in regard to the wave-making resistance, because a model of scale e can be towed in a ship tank at the low corresponding speed: $U\sqrt{e}$, where U is the full-scale speed.

One 'ship' tank (U.S.A.) is 1980 ft. long, 24 ft. wide, and 12 ft. deep, with a maximum towing speed of 60 m.p.h. Another tank (R.A.E.) has rather more than one-third these dimensions, with a maximum speed of 27 m.p.h. In the latter a $\frac{1}{9}$th scale model of a large hull is feasible, when its maximum model speed would correspond to 81 m.p.h. full scale.

The wave-making resistance is assessed by subtracting from the total drag measured an estimated Reynolds resistance. The wave-making resistance is simply related to that under full-scale conditions, to which the Reynolds resistance is added after correction for change of scale.

(2) Froude's law of corresponding speeds reappears, unconnected with wave-making, in wind-tunnel tests on unsteady motions of aircraft. The subject is discussed under Stability and Control, but a simple example will shortly be provided by the 'spinning tunnel.'

49C. The airscrew is a twisted aerofoil, each section of the blades moving along a helical path defined by the radius, the revolutions per second n, and the forward speed U. To secure geometrical similarity in experiments on airscrews of different sizes, each made from the same drawing, it is therefore necessary that U/nl be constant. Thus a third argument must be added to (73A). The diameter D is chosen for convenience to specify l, and the non-dimensional parameter U/nD is given the symbol J. It is also convenient to replace U as far as possible by n. Now n^2D^4 has the same dimensions as U^2l^2, and the formula becomes—

$$A = \rho n^2 D^4 . f(R, M, J). \quad . \quad . \quad (73D)$$

Derivation from first principles on the assumption that A depends on ρ, U, l, ν, E and n presents no difficulty. But it will now have become apparent that formulæ even more complicated than (73D) can be constructed from dimensional considerations almost by inspection.

The following extension of Table III relates to the standard atmosphere and gives approximate values of various quantities which are constantly required in calculations of Aerodynamic scale.

TABLE III A

Altitude (ft.) ÷ 1000	$\sqrt{\sigma}$	$\frac{1}{\sqrt{\sigma}}$	$\frac{\nu}{\nu_0}$	$1/\nu$ (ft.²/sec.)$^{-1}$ ÷ 1000	$1/a$ (ft./sec.)$^{-1}$ × 1000
0	1·00	1·00	1·00	6·4	0·89
10	0·86	1·16	1·29	5·0	0·93
20	0·73	1·37	1·68	3·8	0·96
30	0·61	1·63	2·24	2·9	1·00
40	0·495	2·02	3·33	2·0	1·03
50	0·39	2·57	5·37	1·2	1·03

Chapter III

WIND-TUNNEL EXPERIMENT

50. Nature of Wind-tunnel Work

The calculation of Aerodynamic force presents difficulties even in simple cases. Great progress has been made with this problem, as will be described in subsequent chapters, and designers of aircraft now rely on direct calculation in several connections. Theoretical formulæ are improved, however, by experimentally determined corrections that take neglected factors into account, while other formulæ are based as much on experiment as on theory. Yet many effects of change of shape or Reynolds number are of so complicated a nature as entirely to elude theoretical treatment and to require direct measurement. Measurements can be made during full-scale flight by weighing, pressure plotting, comparison of performance, etc. This method is employed occasionally, but is economically reserved where possible to the final stages of investigations carried out primarily on models made strictly to scale. Thus model experiment, which formerly provided the whole basis of Aerodynamics, apart from the theoretical work of Lanchester in England and Prandtl in Germany, still occupies an important place.

In early days of the science, models were sometimes studied out-of-doors when flying freely (cf. Lanchester's experiments), suspended from a balance in a natural wind (Lilienthal), during fall from a considerable height (Eiffel), or towed. Calm days are few, however, and unsteadiness of winds was soon found to cause large errors, so that experiments came to be carried out in laboratories. In the Whirling Arm method (Langley and others), models attached to a balance were swung uniformly round a great horizontal circle ; a disadvantage, additional to mechanical difficulties arising from centrifugal force, lay in the swirl imparted to the air by the revolving apparatus and the flight of models in their own wakes after the first revolution. Experiments are now nearly always made in an artificial wind generated by or within a wind tunnel. This method was introduced during the second half of the nineteenth century and wind tunnels were built in various countries during the first decade

of the present century. A matter of great historic interest is that the Wright Brothers carried out numerous experiments in a diminutive wind tunnel, less than 2 square feet in sectional area, in preparation for their brilliant success in the first mechanically propelled aeroplane, which flew in 1903. The tunnel method of experiment has since been developed to a magnificent degree.

The artificial wind should be steady and uniform, for otherwise superposing a velocity cannot change the circumstances of experiment exactly to those of flight through still air. Tunnels can be designed to achieve a fair approximation to this requirement. Through the part of the stream actually used for experiment, the maximum variation of time-average velocity need not exceed $\pm$ 1 per cent. and the variation of instantaneous velocity at any one point, though more difficult to suppress, can be reduced to $\pm$ 2 per cent. This standard of steadiness may be relaxed for experiments in which it is not of prime importance. The wide range of modern experiment has led on economic grounds to the evolution of several specialised forms for the wind tunnel, as will be described, although in a small Aeronautical laboratory a single tunnel must serve a variety of widely different uses.

In elementary Aerodynamics it is advisable to carry out many experiments* which mathematical treatment renders unnecessary in a more advanced course, but there still remains unlimited scope for wind-tunnel work on scientific matters in which analysis is of little avail or particularly complicated. Questions of this nature will appear as the subject proceeds, and it will only be remarked here that their investigation invites originality of method and ingenuity in the design of special apparatus.

Another and equally important domain of model experiment lies in direct application to specific designs of aircraft. The Aerodynamic balances and other measuring apparatus surrounding the working section of a tunnel have usually been installed with this purpose primarily in view.

A more or less complete model of an aircraft can be suspended in a wind-tunnel stream of known speed and its reaction measured. It can be pitched, yawed, rolled about its longitudinal axis, or oscillated in imitation of a variety of circumstances arising in free flight, and its response accurately determined. A special technique described in a later chapter enables due allowance to be made for the limited lateral extent of the stream. Yet with every precaution

* A programme of experimental studies requiring only simple apparatus is given in a companion volume to this book.

the interpretation of the observations in terms of full-scale flight is attended with uncertainty. Two outstanding reasons are as follows. Experiments on complete models, even in national tunnels, can only cross the threshold of large full-scale Reynolds numbers, and fall far short in more modest tunnels. Secondly, the initial turbulence remaining in an artificial wind is sufficient to produce a marked difference in some connections from flight at the same Reynolds number.

The first difficulty can be circumvented in the case of small component parts of an aircraft by employing enlarged models ; for test in an artificial wind of normal density they would be larger than full-scale. The drag of the complete aircraft is then built up from piecemeal tests on its parts. A new problem introduced is to determine how each part will affect a neighbouring part or one to which it is joined. Such mutual effect is called *interference* and becomes familiar in wind-tunnel work, for in principle it enters into all experiments in which a model is supported in the stream by exposed attachments. The same device may be applied to wings and tail-planes by testing short spanwise-lengths of large chord under two-dimensional conditions. The consequent problem in this case is the change from two- to three-dimensional conditions and is left to calculation. For reliable data on wings at greater incidences or on long bodies, there is no alternative to large or costly wind tunnels except flying tests.

The above expedients leave the second main difficulty still to be faced, viz. the effect of initial turbulence. This question is many-sided and its consideration must be deferred, but there is evidently need to ascertain by suitable tests the degree of turbulence characterising the particular tunnel employed.

Finally, fast aircraft are considerably affected, especially at high altitudes, by the compressibility of the air. It was found in the preceding chapter that for dynamical similarity under these conditions both the Reynolds and Mach numbers require to be maintained. Tunnels capable of realising even moderate Reynolds numbers at high speeds are particularly expensive to construct and operate, and experiments are usually carried out in small streams, Reynolds numbers being ignored, and the effects of compressibility determined as corrections of a general nature.

It will be seen that, whilst the principles and phenomena of Aerodynamics can be illustrated qualitatively with ease in a modest wind tunnel, the constant need for quantitative information makes more serious demands and creates a study within itself.

51. Atmospheric Wind Tunnels—Open-Return Type

The cross-section of the experimental part of a wind-tunnel stream may be square, round, elliptic, oval, octagonal, or of other shape. The size of a tunnel is specified by the dimensions of this cross-section. Apart from small high-speed tunnels actuated by a pressure reservoir, the flow past the model is induced by a tractor airscrew located downstream. The airscrew is made as large as possible, if only to minimise noise, and its shaft is coupled direct to the driving motor, the speed of which is controlled preferably by the Ward-Leonard, Kramer, or similar electrical system. If C is the cross-sectional area and V the velocity of the experimental part of the stream, the ' power factor ' P is usually defined as

$$P = \frac{550 \times \text{input b.h.p.}}{\frac{1}{2}\rho V^3 C}.$$

But in some publications the reciprocal of this ratio is intended.

The term *atmospheric* applied to a wind tunnel means that the density of its air stream is approximately the same as that of the surrounding atmosphere. Some tunnels employ compressed or rarified air, but they are few, and so the term is commonly omitted in referring to the atmospheric class.

For some years many of the wind tunnels built were of the type shown in Fig. 26, described as ' straight-through ' or ' open-return.'

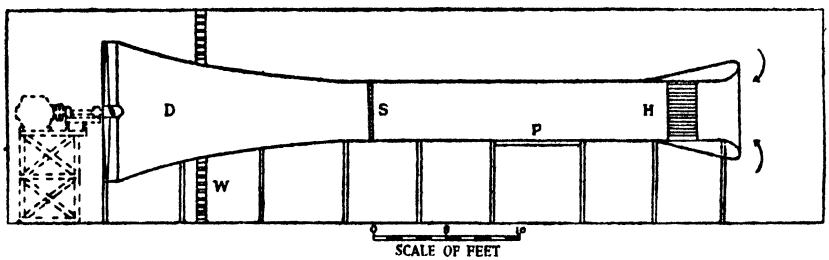

FIG. 26.—4-FT. OPEN-RETURN WIND TUNNEL.
H, inlet honeycomb ; P, plane table ; S, guard grid ; D, regenerative cone ; W, honeycomb wall.

Though the design has been superseded, numerous examples are still in use. Air is drawn from the laboratory into a short straight tunnel through a faired intake and wide honeycomb, the location of the latter being adjusted to spread the flow evenly over the working section. Subsequently the stream has most of its kinetic energy reconverted into pressure energy in a divergent duct D, from

which the airscrew exhausts the air into a 'distributor,' a large chamber enclosed by perforated walls W. The distributor returns the air, with disturbances due to the airscrew much reduced, over a wide area to the laboratory, which conveys it evenly and slowly back to the intake and thus forms an integral part of the circuit. A consequent disadvantage is that the laboratory requires to be reasonably clear of obstructions, symmetrically laid out, and also large; approximate dimensions for a tunnel of size x are: over-all length, including diffuser, $14x$; height and width, $4\frac{1}{2}x$. A second disadvantage is lack of economy in running, the power factor P having the high-value unity. In small sizes, however, the type is simple to construct and convenient in use.

A boundary layer of sluggish air lines the tunnel walls, but away from this Bernoulli's equation holds closely, showing a wide central stream almost devoid of vorticity. This stream slightly narrows along the tunnel owing to increasing thickness of the boundary layer. Thus the streamlines are slightly convergent; velocity increases and pressure decreases along the parallel length. To compensate for this characteristic variation, tunnels are sometimes made slightly divergent.

The static pressure is obviously less within the tunnel than outside. At first sight it may appear feasible to calculate the velocity at the working section from a measurement of the difference in static pressure between there and some sheltered corner of the laboratory. But losses in total energy occurring at the intake, principally through the honeycomb, prevent this. The pressure in a pitot tube within the working stream is less than the static pressure in the room. A small hole is drilled through the side of the tunnel several feet upstream from the working section, and the pressure drop in a pipe connected with it is calibrated against the appropriate mean reading of a pitot-static tube traversed across the working section (excluding, of course, the boundary layer). By this means velocities can afterwards be gauged without the obstruction of a pitot-static tube in the stream.

52. Closed-Return Tunnels

In the more modern tunnels of Fig. 27, the return flow is conveyed within divergent diffuser ducts to the mouth of a convergent nozzle, which accelerates the air rapidly into the working section. A ring of radial straighteners is fitted behind the airscrew to remove spin and the circulating stream is guided round corners by cascades

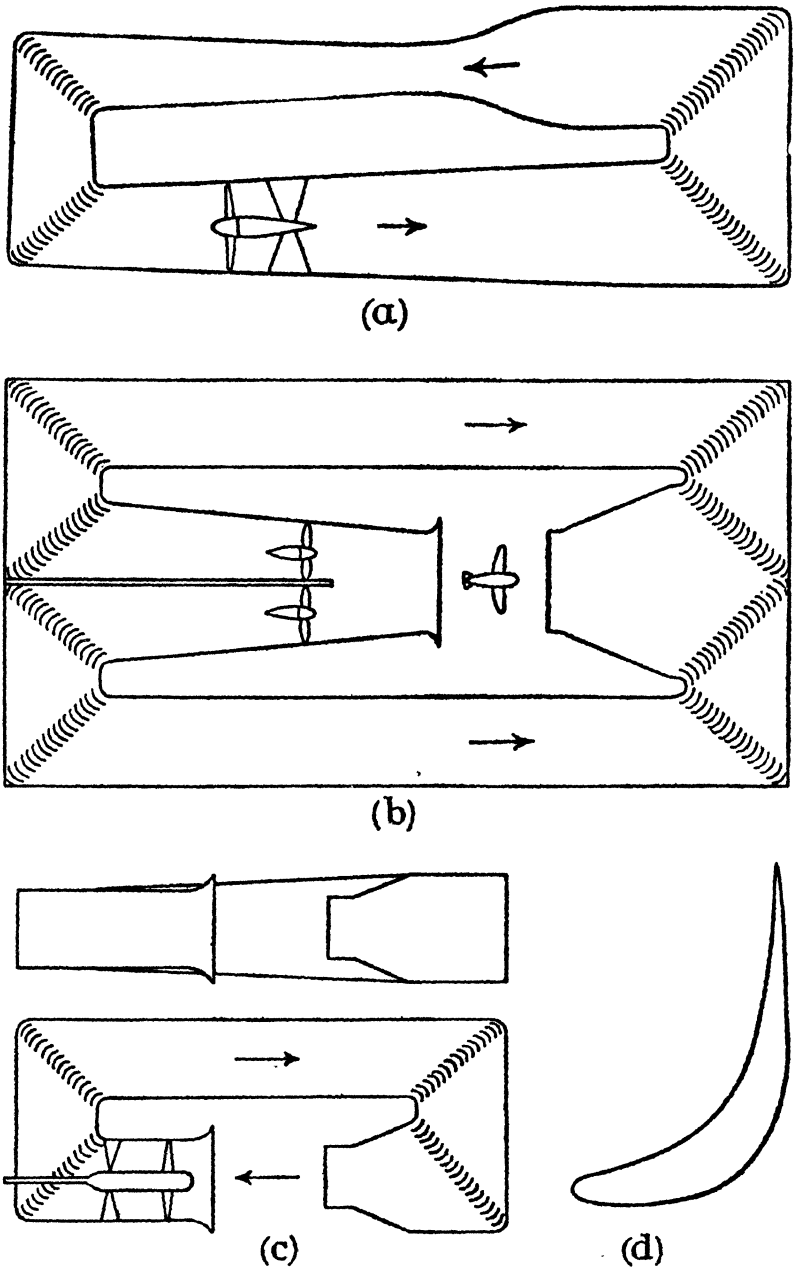

FIG. 27.—RETURN-CIRCUIT WIND TUNNELS.
(a), enclosed section; (b), full-scale open jet; (c), compact open jet; (d), corner vane.

of aerofoils or guide-vanes (see (*d*) in the figure for a suitable section), which maintain a fairly even distribution of velocity over the gradually expanding cross-section. The experimental part of the stream is preferably enclosed, as at (*a*), but sometimes takes the form of an open jet, as at (*b*) and (*c*). An open jet is distorted by a model and is resorted to only when accessibility is at a premium.

These tunnels are often known as of 'closed-return' or 'race-course' type. They effect a great economy in laboratory space, only a small room being required round the working section, and also in running costs, P having approximately the value $\frac{1}{3}$. Wood is not a suitable material for construction, though often used, because during a long run the air warms and produces cracks which are destructive to efficient working since the ducts support a small pressure.

A characteristic of prime importance is the *contraction ratio* of the tunnel, defined as the ratio of the maximum cross-sectional area attained by the stream to the cross-sectional area of the experimental part. A large contraction ratio effectively reduces turbulence but increases the over-all length of a tunnel of given size, since divergent ducts must expand slowly to prevent the return flow separating from the walls. A rather long tunnel has the advantage of preventing disturbances from a high-drag model being propagated completely round the circuit. Modern designs usually specify a contraction ratio greater than 5; values for the tunnels (*a*), (*b*), (*c*) in the figure are $6\frac{1}{2}$, 5, and $3\frac{1}{2}$, respectively. (*a*) may be regarded as suitable for general purposes. (*b*) illustrates the full-scale tunnel at Langley Field, U.S.A., which has an oval jet 60 ft. by 30 ft. in section, an over-all length of some 430 ft., and a speed of 175 ft. per sec. with a power input of 8,000 h.p. (*c*) indicates the maximum possible compactness for this type of tunnel; developed at the R.A.E., it has been used for sizes up to 24-ft. diameter.

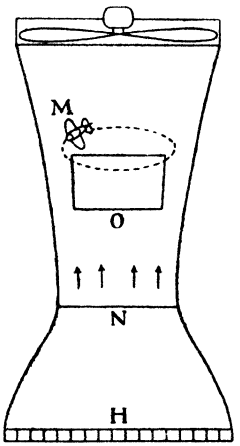

FIG. 28.—SPINNING TUNNEL.

M, flying model; O, observation window; N, net for catching model; H, honeycomb.

53. Spinning Tunnel

A few vertical tunnels have been built, as shown schematically in Fig. 28, for spinning tests. An aeroplane may fly in a vertical spiral with a velocity of descent V_F, say. A

question arising is whether operation of the aerodynamic control surfaces will steer the craft into a normal flight path. To investigate this, a light model of balsa wood, similar in disposition of mass as well as in form, is set into corresponding spiral flight, a camera mechanism operating the controls after a delay. Ignoring the effects of viscosity, the Froude number V^2/lg must be the same for craft and model. If the latter is made to $\frac{1}{16}$th scale, its velocity of descent $= \frac{1}{4}V_F$. This is a small speed, and it is feasible to employ a wide vertical tunnel with an upwardly directed stream, so that the model does not lose height and the action can be observed conveniently. The difficulty with these tunnels is to prevent the model from (*a*) flying into the wall, (*b*) spinning upwards or downwards. According to tests carried out on model tunnels, (*a*) can be overcome by a suitable distribution of velocity along the radius, and (*b*) by making the tunnel slightly divergent, which gives stability in respect of vertical displacement, since the rising model then loses flying speed, and vice versa.

54. Coefficients of Lift, Drag, and Moment *

In the general case of a body suspended in a wind tunnel Aerodynamic force is not a pure drag, but is inclined, often steeply, to the direction of flow. This inclination is not constant for a given shape and attitude of the body, but is a function of the Reynolds number.

When the flow has a single plane of symmetry for all angles of incidence of the body, the Aerodynamic force can be resolved into two components in that plane, parallel and perpendicular to the relative wind—the drag and lift, respectively. By Article 47 we find for any particular shape and incidence a lift coefficient:

$$\tfrac{1}{2}C_L = k_L \equiv \frac{\text{Lift } (L)}{\rho V^2 l^2} = f_1(R) \quad . \quad . \quad . \quad (74)$$

and a drag coefficient:

$$\tfrac{1}{2}C_D = k_D \equiv \frac{\text{Drag } (D)}{\rho V^2 l^2} = f_2(R). \quad . \quad . \quad (75)$$

* There are two systems of coefficients in Aerodynamics. In the now prevailing system, associated with the symbol C, forces and moments are divided by the product of the stagnation pressure for incompressible flow, viz. $\frac{1}{2}\rho V^2$ (cf. Art. 32), and l^2 or l^3; in an earlier system, distinguished by the symbol k, the quantity ρV^2 takes the place of the stagnation pressure. Thus a k-coefficient $= \frac{1}{4} \times$ the corresponding C-coefficient, as indicated in (74), (75), and (77). Neither system has an advantage over the other, but to secure a universal notation C-coefficients have superseded k-coefficients in this country since 1937. They are generally adopted in this book, but some matters are still expressed in the older system.

Most bodies tested are parts of aircraft, and L is then positive if it supports weight when the aircraft is right way up. For any chosen Reynolds number, we have

$$\text{Aerodynamic force } (A) = \tfrac{1}{2}\rho V^2 l^2 \sqrt{C_L^2 + C_D^2}$$

and, if its inclination to the direction of lift is γ (Fig. 29),

$$\tan\gamma = C_D/C_L \quad . \quad . \quad (76)$$

$k_L/k_D = C_L/C_D$ is called the lift-drag ratio and $= L/D$.

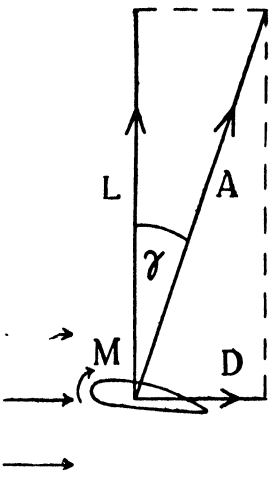

FIG. 29.

Without a plane of symmetry as above, A will have a third component, called the crosswind force.

Again assuming this plane of symmetry, the line of action of A can be found from its magnitude and direction and the moment about some axis in the body perpendicular to the plane, usually through the quarter-chord point. This moment is called the pitching moment M. The method of Article 47 gives for any particular shape and attitude a coefficient:

$$\tfrac{1}{2}C_M = k_M \equiv \frac{M}{\rho V^2 l^3} = f_3(R). \quad . \quad . \quad . \quad (77)$$

M is positive when it tends to increase angle of incidence, i.e. to turn the body clockwise in the figure.

Other moment coefficients will be introduced later when the motion of aircraft is considered in greater detail. It should carefully be noted that C_L, C_D, C_M are different functions of R; we shall often omit a distinguishing suffix to f without implying equality.

It has been stated that any agreed length may be adopted for l to specify the size of a body of given shape and attitude. More generally, any agreed area may be used for l^2, or volume for l^3. Practice varies in the choice made. C_L, C_D are always calculated for single wings on the area S projected on a plane containing the span and central chord (line drawn from nose to tail of median section). The length of the chord c is introduced as the additional length required for C_M (although not for other moment coefficients, when the semi-span is used). Thus for wings:

$$C_L = L/\tfrac{1}{2}\rho V^2 S,\ C_D = D/\tfrac{1}{2}\rho V^2 S,\ C_M = M/\tfrac{1}{2}\rho V^2 Sc.$$

The parasitic, or 'extra-to-aerofoil,' drag of a complete aeroplane, i.e. the drag of all parts other than the wings, may sometimes for convenience be referred to S. But usually for fuselages (aeroplane bodies), struts, and the like, and sometimes for airship envelopes, l^2 is specified by the maximum sectional area across the stream. Another area frequently used for airship envelopes is $(\text{volume})^{2/3}$, enabling the drags of different shapes to be compared on the basis of equal static lift. It is seldom suitable to employ the same l to specify both R and the coefficients; for R, the length from nose to tail is usually chosen.

55. Suspension of Models

It is evident that the foregoing and other coefficients can be determined through a range of R by direct measurement, given suitable balances. These are grouped round the working section of the tunnel, and the model is suspended from them. Their design and arrangement are partly determined by the following consideration.

Suppose the true drag D of a model in a tunnel is required. Let the suspension attachments (called, for short, the holder) have a drag d when tested alone. Let the drag of holder and model be D'. Except under special conditions we cannot write: $D = D' - d$; the combination represents a new shape not simply related to either part. The mutual effect of d on D, or vice versa, is termed the mutual interference. An example is as follows. If a 6-in. diameter model of an airship envelope be suspended by fine wires, and a spindle, the size of a pencil, made to approach its side end-on, the drag of the airship may increase as much as 20 per cent. before contact occurs.

The approximation used in general depends upon the interference being local. A second holder is attached to a different part of the model and a test made with both holders in place. Removing the original holder and testing again with only the second holder fitted gives a difference which is applied as holder correction to a third test in which the original holder alone is present. The approximation gives good results, provided neither holder creates much disturbance, to ensure which fine wires or thin streamline struts are used.

Fig. 30 shows as a simple illustration an arrangement suitable for a heavy long body having small drag. Near the nose the body is suspended by a wire from the tunnel roof, while a 'sting' screwed into the tail is pivoted in the end of a streamline balance arm, for the most part protected from the wind by a guard tube. If the guard

tube is of sufficient size to deflect the stream appreciably, a dummy is fixed above in an inverted position. Sensitivity, in spite of the heavy weight of the body, is achieved by calculating the fore-and-aft location of the wire to make, following small horizontal displacement, the horizontal component of its tension only just overcome that of the compression in the balance arm. To find the effective

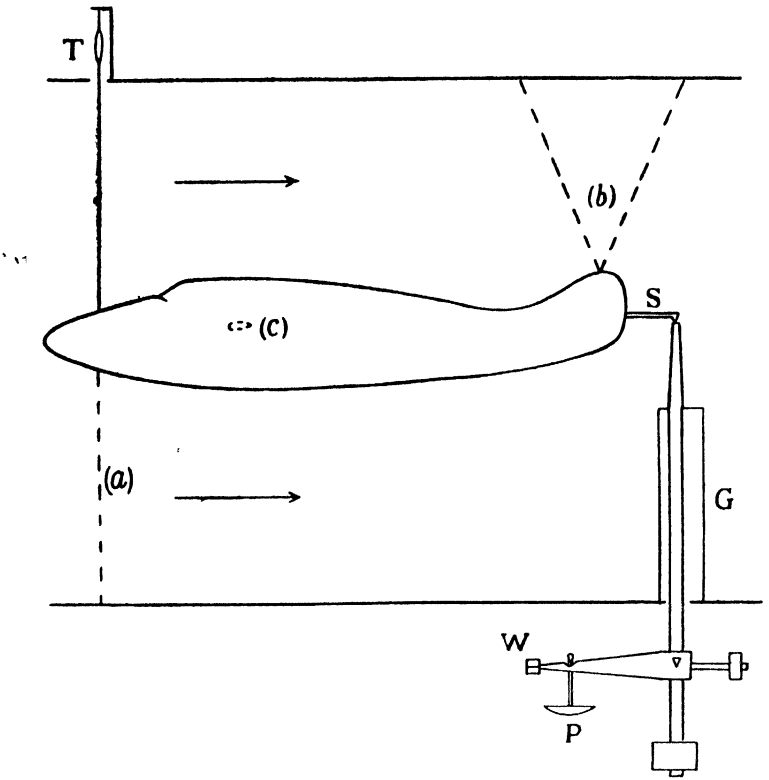

FIG. 30.—TESTING A HEAVY MODEL OF LOW DRAG.
G, guard tube ; P, scale pan ; S, sting ; T, turnbuckle ; W, cross-hair.

drag of the wire, another test is made with a second wire hung from the nose as shown at (*a*) and attached to the floor of the tunnel. Next, the sting is separated slightly from the balance arm, support being by the wires (*b*) from the roof, and the effective drag of the balance arm measured with the body almost in place. Finally, the model can be suspended altogether differently, from a lift-drag balance as at (*c*), the wires and original balance arm being removed, and the small effective drag of the sting estimated by testing with it

in place and away. At the same time special experiments can be made to investigate the interference, neglected above, between the sting and the original balance arm. It will be appreciated that the reason why the arrangement (*c*) is avoided except for corrections is that the spindle, although of streamline section, would split the delicate flow near the body, and artificially increase its drag. The model fuselage shown may have a small lift. To prevent consequent error in drag measurement, the wire and balance arm must be accurately vertical for a horizontal wind. This is verified by hanging a weight on the body without the wind, when no drag should be registered.

56. The Lift-drag Balance

When several force and couple components act on a model it is desirable for accuracy to measure as many as possible without disturbing the setting of the model. Omnibus balances designed for this purpose tend to be complicated, and reference must be made to original descriptions. An indispensable part of the equipment of a tunnel, however, is an Aerodynamic balance that will measure lift and drag simultaneously and preferably at least one moment at the same time.

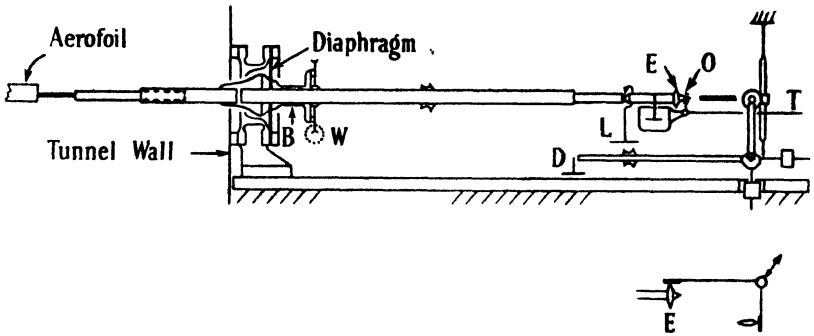

FIG. 31.—SIMPLE LIFT-DRAG BALANCE.

A simple form of lift-drag balance is illustrated in Fig. 31. The main beam passes through a bearing B centrally fixed to a hard copper diaphragm, 5 in. diameter and 0·003 in. thick, clamped to a flange of a casting which abuts on a side wall of the tunnel through soft packing to absorb vibration. The diaphragm gives elastically, permitting the beam to deflect in any direction almost freely between the fine limits imposed by the annular stop O which is opened by the

lever T while observations are being taken. The diaphragm suspension prevents leak into the enclosed-type tunnel assumed ; it may be replaced, if desired, by a gymbals with an open-jet tunnel, but sensitivity is then more difficult to maintain with large forces. The sensitivity of the balance described is 0·0003 lb. The bearing permits of turning the beam about its axis quickly and accurately by means of the worm gear W, an angular adjustment that is often useful, e.g. when testing an aerofoil of the form which can be suspended by screwing a spindle into a wing-tip as shown in the figure. Lift is measured by adjusting a lift rider on the main beam and by weights on the scale pan L. The free end of the main beam carries a knife-wheel E, engaging a hardened and ground plate at one end of a horizontal bell-crank lever, of sufficient leverage to ensure that the small end movement of the main beam is negligible. This lever is mounted on vertical knife edges, and transmits drag to a subsidiary balance, with a drag rider and scale pan D.

Horizontal lift-drag balances are simple to construct and also particularly convenient for testing square-ended aerofoils, negligible interference occurring between the aerofoil and a spindle screwed into its tip. They are inconvenient for aerofoils having thin tips and are not readily adaptable to measure pitching moments. Their usefulness is enlarged in combination with a simple steelyard mounted on the roof of the tunnel, as described in the next article. But experience with this double-balance method of testing suggested the more adaptable modern types of balance described in principle later.

57. Double Balance Method of Testing an Aerofoil

The distinguishing feature of a good aerofoil, or model wing, at fairly large Reynolds numbers is that its Aerodynamic force A is, at small angles of incidence, nearly perpendicular to the stream ; L/D may then be 25 and γ of (76) 2·3°. The point P (Fig. 32), at which A intersects the chord, of length c, is called the centre of pressure and NP/c the centre of pressure coefficient k_{CP}. The method described enables L, D and P and consequently M to be determined with only a simple roof balance and a lift-drag balance. The aerofoil is suspended from the former by wires attached to sunk eye-screws at W and from the latter through a sting pivoted at E. A drum carried by the roof balance enables the length of the wires to be adjusted and hence the incidence α. The model is suspended upside down to avoid the use of a heavy counterpoise, although a small one is desirable with a

light model for safety, to keep the wires taut, and to permit measurement of small upward forces—negative lifts.

Part L' of the lift L is taken at W, the remainder L'' at E. The wires are set truly vertical at some small incidence α, when they will be also vertical at a small negative α, but at no other incidence. Let

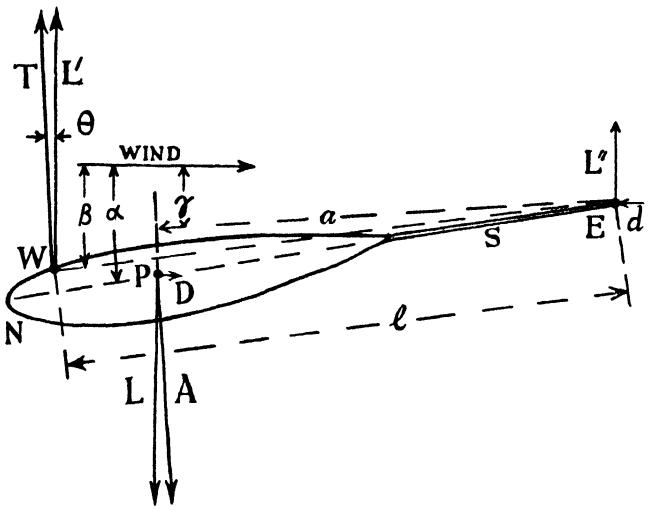

FIG. 32.

θ be their small inclination to the vertical, the stream being assumed truly horizontal, and T that part of their tension due to A. They support a part T sin θ of the drag D, only the remaining part d being supported at E. The lift-drag balance connected to E provides the only means of measuring D. Thus θ must be corrected for accurately and the method adopted is as follows. At any setting of the aerofoil the zeros of the lift-drag balance are observed, before starting the wind, with and without a known weight hooked on the model. An apparent drag is thus found for a known value of T at the particular value of θ corresponding to α, but which need not be known. A proportionate correction appropriate to the value of T measured when the wind is on can then be applied to drag observed at E. This correction requires to be determined for all values of α.

Measurements of drag must further be corrected for (*a*) part of the drag of the wires, for which purpose the measurements may be repeated with additional wires attached in a similar manner, or a calculation may be made based on Fig. 25, the geometry of the rig and the thickness of the tunnel boundary layer; (*b*) the effective

drag of the lift-drag balance arm, determined as in Article 55, α being varied through the complete range studied; (*c*) the effective drag of the sting, obtained by measuring drag with and without the sting in place at all incidences with the model suspended in some other manner, e.g. by a spindle fastened to a wing-tip.

Referring to Fig. 32, $L = L' + L''$, and taking moments about E we have

$$L' \,.\, l \cos \beta = A \,.\, a = Tl \cos (\beta - \theta)$$

giving

$$L' = T(1 + \theta \tan \beta)$$

since θ is small. Also $D = T\theta + d$

$$a = \frac{Tl}{A}(\cos \beta + \theta \sin \beta)$$

where $A = \sqrt{(L^2 + D^2)}$

and $\gamma = \tan^{-1}(D/L)$.

Finally $NP = c - \{a \sec (\alpha - \gamma) - s\}$.

58. Aerodynamic Balances

The foregoing method is simplified by fixing W and adjusting α by displacing E; the front wires may then form two longitudinal vees, and a vertical sting wire at E replace the lift-drag balance arm. The whole of the drag, as well as the major part of the lift, is taken by the vee-wires, and the sting wire supports only the remainder of the lift.

This in brief is the principle of the Farren balance, shown schematically at (*a*) in Fig. 32A. Part of the lift and the entire drag are communicated by two parallel pairs of vee-wires, intersecting at W, to the frame F located above the tunnel and pivoted vertically above W. The drag is transmitted by an increase of tension in the front wires of the vees and a decrease of tension in the back wires, and thus a counterpoise must be suspended from a light model of high drag in order to keep the back wires taut. Such a counterpoise is advisable in any case as a safeguard, and then care need not be taken to locate W well in front of the centre-of-pressure. The frame is weighed in the balances L and D for the lift and drag communicated to it. The sting wire, shown fastened at E to the fuselage of a complete model in the figure, remains truly vertical with change of incidence by virtue of being raised or lowered by a stirrup R which is parallel to EW and pivoted vertically above W. The familiar problem is to measure the remaining part

of the lift supported by the sting wire without interfering with the drag balance. This is achieved by pivoting the bell-crank lever, which supports the stirrup, level with the pivot of the frame F. Thus these two pivot lines are coincident, although in the figure they are shown slightly displaced from one another for clearness. If the pivot of the bell-crank lever is carried on the lift beam, the whole of the lift is transmitted to that beam, and the balance marked M is used only to determine the pitching moment of the Aerodynamic force about W.

The balance shown at (*b*) in the figure makes use of a different system, enabling all pivots to be located outside the tunnel. The model is suspended from the platform F by any convenient means and, provided the two lift beams shown are of equal length, the true lift and drag are measured whatever the position of the model relative to F. However, the pitching moment is determined about the line joining the intersections of the

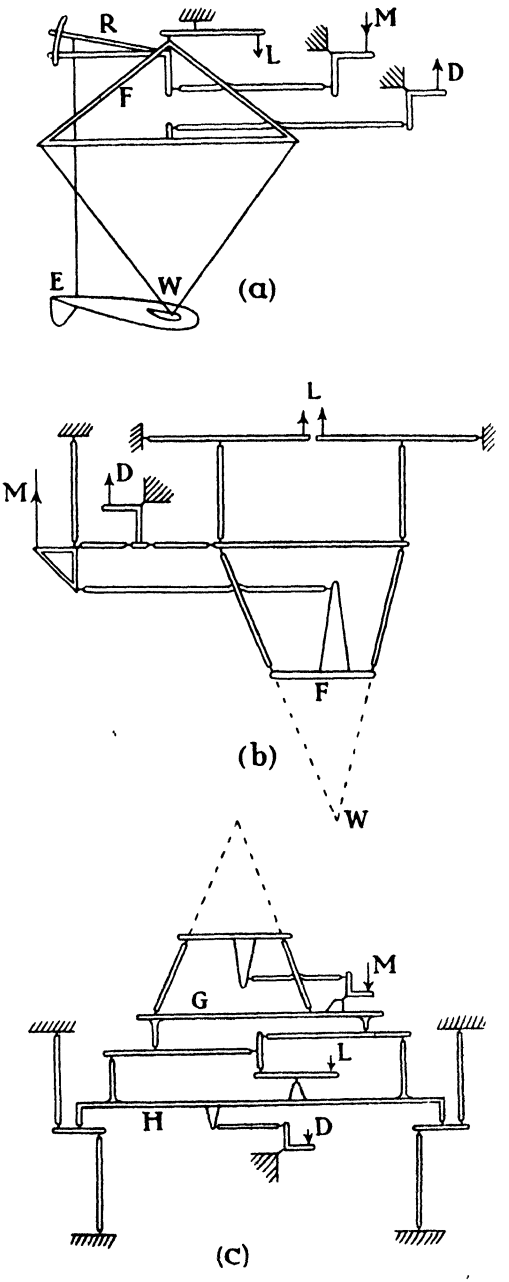

FIG.—32A. AERODYNAMIC BALANCES

centre-lines produced of the two inclined pairs of sloping struts which support F, i.e. about W in the figure. This is readily verified by considering the effect of a load acting in any direction through W; it would evidently cause tensions and compressions in the sloping struts but no force in the moment linkage. Hence the suspension from the platform will in practice usually be so arranged that the pitching moment is measured about a significant point in the model. The linkage connecting the drag and moment balances should ensure that these give the drag and moment separately, i.e. without interfering with one another.

The third balance (*c*) is an inverted form of (*b*) with other modifications. The moment balance is mounted on the lift platform G instead of being attached to a fixed point, a step which eliminates the necessity for a linkage to prevent interference between the moment and drag measurements. All weights used on the moment balance are stored on the lift platform so that their adjustment will not affect the lift reading. The drag frame H is supported in a parallel linkage so that fore and aft movements can occur without vertical displacement, and in consequence excessive static stability is avoided without the use of counterpoises.

The foregoing illustrates only a few of the many devices put to use in the design of a modern Aerodynamic balance. For clearness, the three balances have been described in 3-component form, but all are readily adaptable to cope with additional components. The following constructional features may also be noted. Elastic pivots are preferred to knife-edges or conical points and commonly take the form of two crossed strips of clock-spring. The amount of damping required is extremely variable, and therefore the electromagnetic method is preferred to a plunger working in oil. When a balance is inaccessible or there is need to save time in operation, weighing and recording can be carried out mechanically.

59. Given tunnel determinations of lift, drag, etc., freed from parasitic effects, various corrections are necessary before they can be applied to free air conditions at the same Reynolds number. These are in respect of: (1) choking of the stream by a body of relatively considerable dimensions, (2) deviation of the undisturbed stream from the perpendicular to the direction in which lift is measured, (3) variation of static pressure in the undisturbed stream, (4) effects of the limited lateral extent of the stream, applying principally to wings, and developed in Chapter VIII. A further cause of difference is introduced in Article 65.

(1) It is possible to express the argument of Article 35 in approxi-

mate numerical form for a given shape, when it is seen to follow that the choke correction is small. For a body whose diameter is $\frac{1}{4}$ that of the tunnel the correction is usually < 1 per cent.

(2) Let the stream be inclined downward from the horizontal at a small angle β, and, taking the familiar case of an aerofoil upside down, let its aerodynamic force be A and its true lift and drag L and D, respectively. The apparent lift and drag measured, however, are L_a and D_a (Fig. 33). We have, assuming β small—

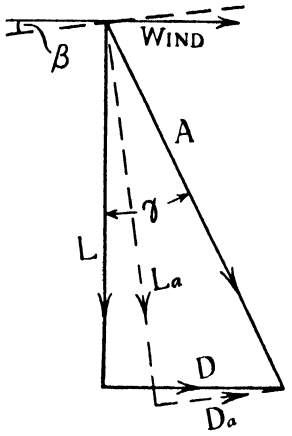

FIG. 33.

$$L = A\cos\gamma \qquad D = A\sin\gamma$$
$$L_a = A\cos(\gamma - \beta)$$
$$D_a = A\sin(\gamma - \beta)$$
$$= A(\sin\gamma - \beta\cos\gamma)$$
$$= D - \beta L.$$

Thus the error in L_a is negligible, but this may be far from true of D_a, for we have

$$\frac{D - D_a}{D} = \beta\frac{L}{D} \qquad . \qquad . \qquad (78)$$

Upward inclination of the stream leads to an error in drag of the same magnitude but opposite in sign.

Example: If $\beta = \frac{1}{2}°$, and $L/D = 20$, the error in D is $\pm 17\frac{1}{2}$ per cent.

This error can be removed by testing the model right way up and upside down, and taking the mean. The process is laborious, however, and a correction factor for general use is worked out by an initial test of this kind. Where their design permits, balances are carefully set on installation so as to eliminate the error as far as possible.

(3) Convergence or divergence of the stream leads to an error due to the pressure gradient that exists in the direction of flow prior to introducing the model. In the former, the more usual case, pressure decreases downstream (x increasing). Owing to the short length of the model dp/dx may be assumed constant, and to this approximation is easily determined experimentally. The maximum convergence in a parallel-walled tunnel is only about $\frac{1}{4}°$.

Complete analysis of the problem presents difficulty, but an inferior limit to the correction is readily calculated by a method that will now be familiar. Considering an element cylinder of the body, of cross-section ΔS and length l, parallel to the direction of flow and

coming to ends on the surface of the body, the downstream force on it, if we apply a method analogous to that of Article 8, is readily found to be $-(dp/dx)\ (\Delta S\ .\ l)$. The whole volume V can be made up of such cylinders, giving for the downstream force on the model $-(dp/dx)V$, which is essentially positive for convergence. This force has nothing to do with drag, vanishing when the stream is parallel or the model moves through free air, and measurements must be decreased on its account. The correction is important for low resistance shapes such as airship envelopes and good aeroplane bodies and wings at high-speed attitudes.

Further analysis shows that the volume should be greater than that of the body, an increase of 5–10 per cent. being required for long bodies of revolution, 10–15 per cent. for wings, and 30 per cent. for compact strut shapes, approximately. The correction does not vanish in the case of bluff shapes of small volume, but it is then numerically unimportant. (See also Article 230B.)

59A. Pitot Traverse Method

The drag of a two-dimensional aerofoil can be estimated from an exploration of the loss of pitot head through a transverse section of its wake. This loss will be denoted by a non-dimensional coefficient h, as follows. Let U, p_0 be the undisturbed velocity and pressure, respectively, and q, p the corresponding quantities at any point in the wake. Then the loss of pitot head at the point is

$$p_0 + \tfrac{1}{2}\rho U^2 - (p + \tfrac{1}{2}\rho q^2) = h\ .\ \tfrac{1}{2}\rho U^2.$$

It is much more marked close behind the aerofoil than farther downstream, where the wake has diffused outward.

Consider first a section of the wake sufficiently far behind the aerofoil for the pressure to be equal to p_0 and the velocity to have become parallel again to the relative motion, a state distinguished by writing $q = u$. Through an element δy of this section, of unit length parallel to the span of the aerofoil, the mass passing in unit time is $\rho u \delta y$, and the rate of loss of momentum parallel to the relative motion is $\rho u \delta y\ .\ (U - u)$. Hence the drag D_0 of unit length of the aerofoil is given by

$$D_0 = \rho \int u(U - u)dy$$

or

$$\frac{D_0}{\rho U^2} = \int \frac{u}{U}\left(1 - \frac{u}{U}\right) dy \quad . \quad . \qquad \text{(i)}$$

But $u/U = (1 - h)^{\frac{1}{2}}$. Hence

$$\frac{D_0}{\rho U^2} = \int \left\{ h - \left[1 - (1 - h)^{\frac{1}{2}} \right] \right\} dy.$$

Far behind the aerofoil h will be small and the term in the square brackets can be expanded as follows—

$$1 - (1 - \tfrac{1}{2}h - \tfrac{1}{8}h^2 + \ldots) = \tfrac{1}{2}h,$$

approximately, so that in this case

$$\frac{D_0}{\rho U^2} = \tfrac{1}{2}\int h dy. \quad . \quad . \quad . \quad \text{(ii)}$$

Defining a drag coefficient C_{DO} as equal to $D_0/\frac{1}{2}\rho U^2 c$, where c is the aerofoil chord, the result can be written

$$C_{DO} = \frac{1}{c}\int h dy \quad . \quad . \quad . \quad \text{(iii)}$$

This coefficient is known as the *profile drag coefficient* of the aerofoil. It includes the entire drag under two-dimensional conditions but only part of the drag under three-dimensional conditions, except at the incidence for zero lift ; at other incidences a wing has in addition an *induced drag coefficient*, arising from the continuous generation of lift Aerodynamically and appearing as a modification of the

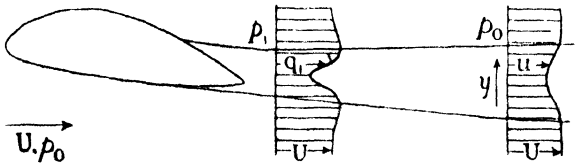

FIG. 33A.

pressure distribution for two-dimensional flow. The pitot traverse method finds uses in the wind tunnel, where two-dimensional flow can be simulated, but its chief application is to flight experiments. Exploration on the above lines of the wake of a wing can give only its profile drag, but its induced drag can be estimated separately by calculation, as will be found in Chapter VIII. A difficulty arising in flight is that the pitot traverse must be made close behind the wing, so that the pressure differs from p_0 and a correction to (iii) becomes necessary. The experimental section near the wing will be distinguished by suffix 1, see Fig. 33A.

This correction is rather uncertain. Jones* has suggested ignoring the turbulence in the wake and relating the pressure and velocity

* Jones (Sir Melvill), A.R.C.R. & M. No. 1688, 1936.

at section 1 to those at the distant section, where $p = p_0$, by Bernoulli's equation, applied along a suppositious mean stream-tube. Then:

$$p_1 + \tfrac{1}{2}\rho q_1^2 = p_0 + \tfrac{1}{2}\rho u^2.$$

Writing

$$k_1 = \frac{p_1 - p_0}{\tfrac{1}{2}\rho U^2},$$

this gives

$$\frac{u}{U} = \left\{k_1 + \left(\frac{q_1}{U}\right)^2\right\}^{\frac{1}{2}} \quad . \quad . \quad . \quad \text{(iv)}$$

Again,

$$h_1 = \{p_0 + \tfrac{1}{2}\rho U^2 - (p_1 + \tfrac{1}{2}\rho q_1^2)\}/\tfrac{1}{2}\rho U^2$$
$$= 1 - k_1 - \left(\frac{q_1}{U}\right)^2,$$

so that

$$\frac{q_1}{U} = (1 - h_1 - k_1)^{\frac{1}{2}} \quad . \quad . \quad . \quad \text{(v)}$$

Let n denote distance perpendicular to the direction of mean motion at section 1. Then for incompressible flow $q_1 \delta n = u \delta y$ and (i) becomes

$$\frac{D_0}{\rho U^2} = \int \frac{q_1}{U}\left(1 - \frac{u}{U}\right) dn.$$

Substituting from (iv) and (v) and again introducing the drag coefficient,

$$C_{D0} = \frac{2}{c}\int (1 - h_1 - k_1)^{\frac{1}{2}}\left[1 - (1 - h_1)^{\frac{1}{2}}\right] dn \quad . \quad (79)$$

This result is known as Jones' formula. Tested in a full-scale wind tunnel, it was found* to be accurate within experimental errors along the middle three-quarters of the span of a rectangular wing. Nearer the wing-tips the induced flow associated with the production of lift under three-dimensional conditions makes the method inapplicable. Restrictions of another kind have been discussed by Taylor.†

A different treatment of the problem has been given by Betz.‡ His formula includes provision for dealing with the induced flow caused by three-dimensional production of lift.

* Goett, N.A.C.A. Report No. 660, 1939.
† Taylor (Sir Geoffrey), A.R.C.R. & M. No. 1808, 1937.
‡ Betz, Z.F.M., vol. 16, 1925; *see* Arts. 79–81 by Prandtl in Tietjens, 'Applied Hydro- and Aero-Mechanics.'

The pitot traverse method of drag measurement offers such manifold advantages that the subject is an old one and has received attention on many occasions. The exact theory is complicated, however, and formulæ obtained by simple means require to be established by experiment. The method can be relied upon to give a close estimate of drag under fairly favourable conditions ; viz. briefly when the pressure in the wake differs little from p_0 and the velocity trough is rather shallow. These conditions imply, especially if C_{DO} has a considerable value, that the traverse should be made well downstream, but this is obviously inconvenient in flight, whilst in tunnel experiment it may sometimes vitiate the two-dimensional assumption. Again, the section behind which a traverse is made may not be truly representative of the average section of a wing or aerofoil. Such difficulties partly explain discrepancies that are found to exist.

The exploring pitot tube should be fine in order to avoid a systematic experimental error. The effect of compressibility on the method has also been examined.* The estimates are not affected by any pressure gradient that may exist in the empty tunnel.

60. An example of wing characteristics obtainable by the method of Article 57 at small scale, e.g. in a 6-ft. open-jet tunnel at 100 ft. per sec., is given in Fig. 34, corrections noted in Article 59 having been made so that the results apply to free air conditions at a small Reynolds number. The aerofoil is of the section shown, known as Clark YH, with a ratio of span to chord, called aspect ratio, of 6.

Features fairly typical of aerofoils in general may be noted.

Zero lift occurs at a negative incidence, usually small. The value $-3°$ shown in the present case is arbitrary, in the sense that it depends upon how α is measured. The present aerofoil has a partly flat lower surface, which is used to define inclination to the wind. Another aerofoil might have a slight concavity in the lower surface, when the common tangent would be employed. Most aerofoils are bi-convex, however, when the line joining the centres of curvature of the extreme nose and tail defines α.

Lift attains a maximum at a moderate angle, 15° in the present instance, after which it falls. This incidence is known as the critical or stalling angle and, combined with the maximum value attained by C_L, is of importance in connection with slow flying. The open-jet tunnel determines this feature more reliably † than the enclosed-

* Young, A.R.C.R. & M. No. 1881, 1938.
† Bradfield, Clark, and Fairthorne, A.R.C.R. & M., 1363, 1930.

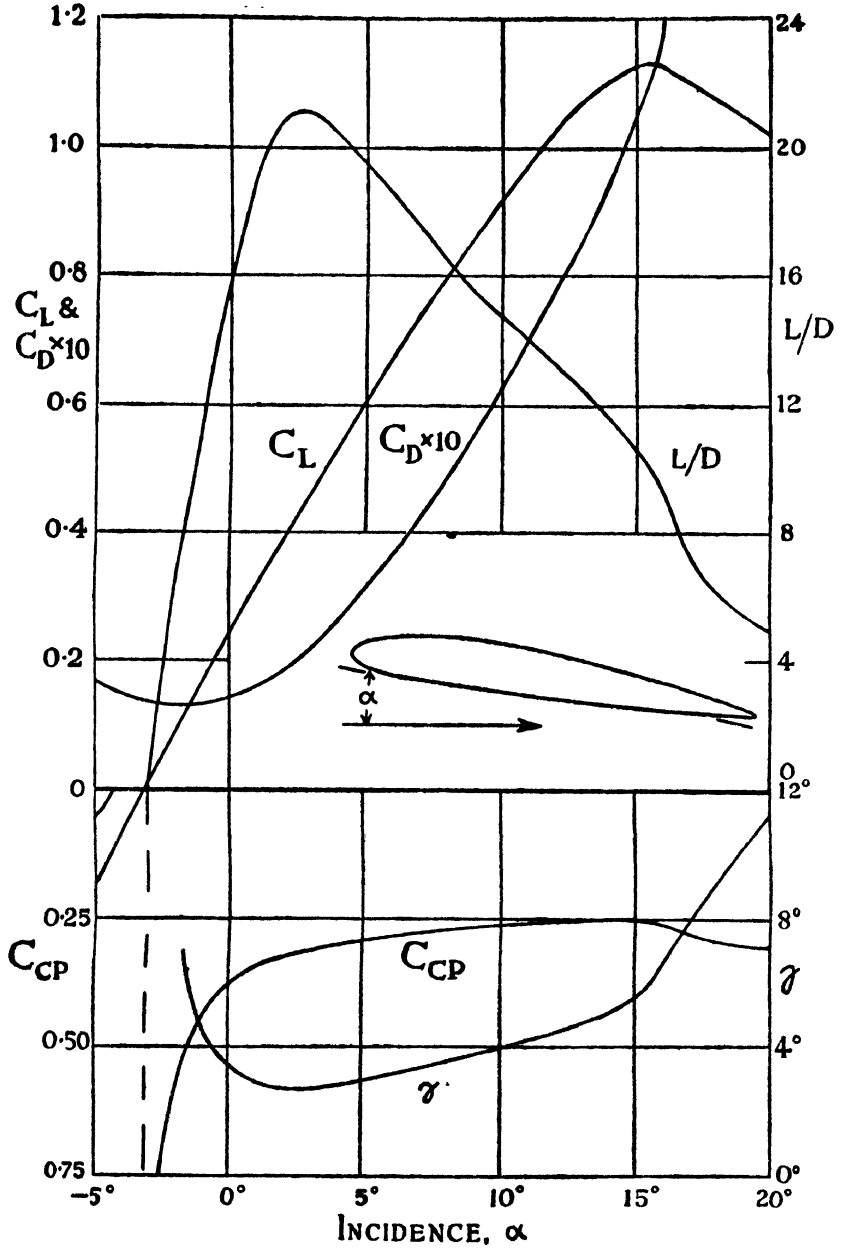

FIG. 34.—CHARACTERISTICS OF CLARK YH WING (ASPECT RATIO 6) AT SMALL SCALE (6-FT. OPEN-JET TUNNEL AT 100 FT. PER SEC.).

section tunnel, which tends to flatter compared with free air. The flow is often delicate in this region, some lift curves branching, and different coefficients being obtained according as to whether α is increasing or decreasing.

Minimum drag occurs when the lift is small but maximum L/D at a considerably larger incidence. Drag and the angle γ begin to increase rapidly at the critical angle.

At $-1{\cdot}3°$ the centre of pressure is midway along the chord. It moves forward as incidence is increased up to the critical angle, and then back. This travel results from striking changes which occur in the shape of the pressure diagram, illustrated for a rather similar aerofoil in Fig. 35. Between $-2{\cdot}7°$ and $-4{\cdot}5°$, approximately,

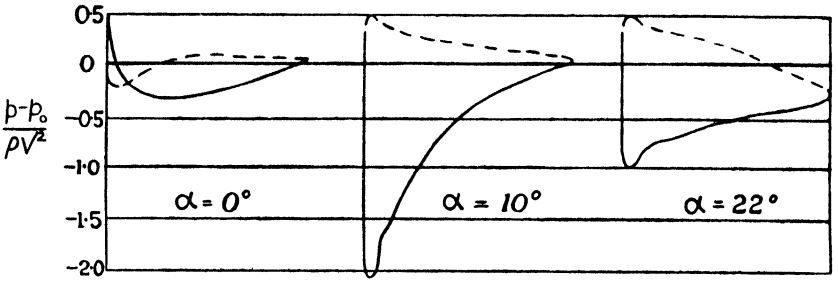

FIG. 35.—LIFT PRESSURE DIAGRAMS FOR THE MEDIAN SECTION OF AN AEROFOIL (BROKEN LINE APPLIES TO LOWER SURFACE).

the C.P. is off the aerofoil. $C_{CP} = \pm\infty$ at $\alpha = -3°$, meaning that when the resultant force is a pure drag, lift being zero, there is a couple on the aerofoil; the two loops seen in the pressure diagram for $0°$ become so modified at $-3°$ as to enclose equal areas. Thus the C.P. curve has two branches asymptotic to the broken line in Fig. 34; part of the negative lift branch is shown near the left-hand zero of the scales.

The travel of the C.P. for $\alpha < 15°$ indicates a form of instability. To see this, imagine the aerofoil to be pivoted in the tunnel about a line parallel to the span and distant 0·3 chord from the leading edge, and to be so weighted that it is in neutral equilibrium for all angles without the wind (an experiment on these lines is easy to arrange). If now the model be held lightly at $\alpha = 5°$, the incidence at which the C.P. is cut by the pivot line, and the wind started, a couple tending to increase or decrease α will instantly be felt, small disturbance of α displacing the C.P. in such a direction as to increase the disturbance. The aerofoil will ride in stable equilibrium, however, at $\alpha = 20°$. It would also be stable

if pivoted in front of 0·25 chord, but this case is only of interest in connection with the auxiliary control surfaces of aircraft. The C.P. curve is physically indefinite, in so far as it would have a different shape if we defined the C.P. as the intersection by A of some line parallel to the chord but displaced from it. Thus in the above experiment different results would be obtained if the pivot line were displaced from the chord plane.

Fig. 36 contains the essential information of Fig. 34 plotted in more compact and practical form, C_L being more generally useful than α as the independent variable. The moment coefficient given defines the pitching moment about a line one-quarter chord behind the leading edge of the aerofoil, often preferred for greater precision to that of Article 54. Its middle point is called the Aerodynamic centre.

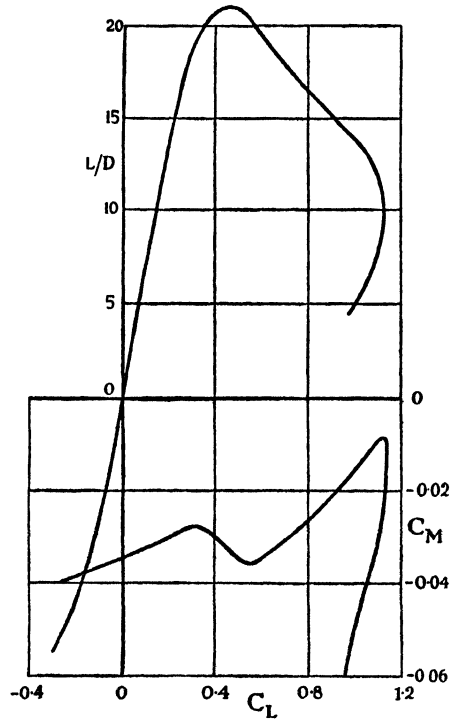

FIG. 36.—CHARACTERISTICS OF CLARK YH WING (ASPECT RATIO 6) AT THE SMALL SCALE OF FIG. 34.

C_M = pitching moment coefficient about a line $\frac{1}{4}$ chord behind the leading edge.

61. Application of Complete Model Data

Where $f(R)$ has been found in the tunnel through a sufficient range, calculations may be made for the shape of body concerned in a variety of practical circumstances, as illustrated in the two examples following.

(*a*) A temporary wire, $\frac{1}{8}$ in. diameter and 2 ft. long, is fixed parallel to the span of a wing just outside its boundary layer, above a position where the pressure drop amounts to 15·36 lb. per sq. ft. when the aeroplane is flying at 100 m.p.h. at low altitude. Find the drag of the wire under these conditions.

First determine the relative velocity of the wire. Writing p, V for the local pressure and velocity (ft. per second) where it is ex-

posed, and distinguishing normal values by suffix 0, by Bernoulli's theorem

$$\tfrac{1}{2}\rho(V^2 - V_0^2) = p_0 - p = 15{\cdot}36 \text{ lb./sq. ft.},$$

giving $V = 185{\cdot}5$ ft. per sec.

Now l = diameter of wire $= \frac{1}{96}$ ft., $\nu = 1{\cdot}56 \times 10^{-4}$ sq. ft. per sec. Hence :

$$R = \frac{185{\cdot}5 \times 10^4}{1{\cdot}56 \times 96} = 1{\cdot}23 \times 10^4,$$

giving, from Fig. 25, $C_D = 1{\cdot}16$

$$\text{Drag} = \frac{0{\cdot}58 \times 0{\cdot}00238(185{\cdot}5)^2 \times 2}{96} = 0{\cdot}99 \text{ lb.}$$

(*b*) The lift coefficient of a wing of the section shown (known as R.A.F. 48) and span/chord ratio (aspect ratio) = 6, set at 15° incidence, is found in the wind tunnel to vary as in Fig. 37, through

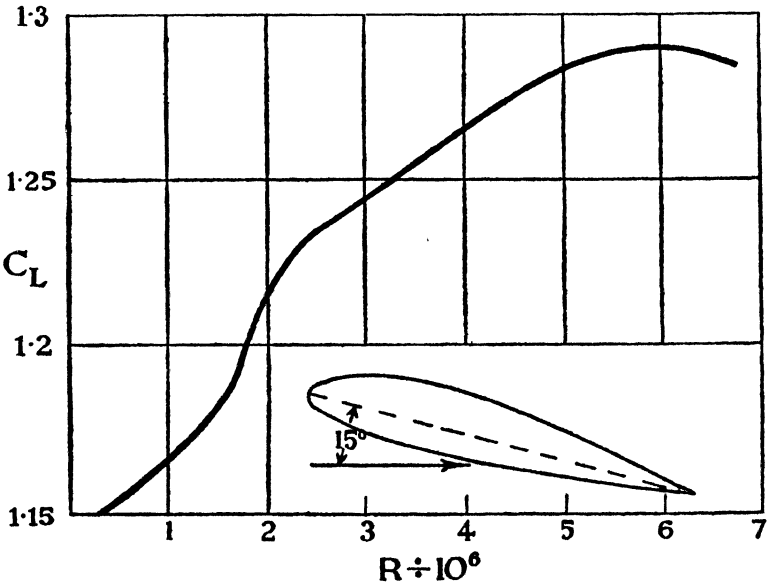

FIG. 37.—APPROXIMATE SCALE EFFECT ON LIFT COEFFICIENT OF R.A.F. 48 WING AT 15° INCIDENCE.

the range of R given. A parasol monoplane fitted with a wing of this shape, chord = 6 ft., is required to approach a landing field situated at 5000 ft. altitude at the same incidence and 60 m.p.h. A.S.I. (indicated air speed). What lift will the wing exert when standard atmospheric conditions prevail ?

From Table III, Article 14, temperature is 5·1° C. and relative density 0·862.

$$\nu = \frac{\mu}{\rho} = 3{\cdot}58 \times 10^{-7}\left(\frac{278{\cdot}1}{273}\right)^{3/4}\frac{1}{0{\cdot}00238 \times 0{\cdot}862}$$
$$= 1{\cdot}77 \times 10^{-4} \text{ sq. ft. per sec.}$$

(cf. Article 25). 60 m.p.h. = 88 ft. per sec. and the true velocity

$$V = \frac{88}{\sqrt{0{\cdot}862}} = 94{\cdot}8 \text{ ft. per sec.}$$

$$R = \frac{94{\cdot}8 \times 6 \times 10^4}{1{\cdot}77} = 3{\cdot}21 \times 10^6.$$

Hence, from the figure $C_L = 1{\cdot}248$, and, since wing area = $(6 \times 6)6 = 216$ sq. ft.,

$$L = 0{\cdot}624 \times 0{\cdot}00238(88)^2 \times 216 = 2484 \text{ lb.}$$

or 11·5 lb. per sq. ft.

The following may also be verified. A scale model of 1 ft. chord would have, at 60 m.p.h. at sea-level, a Reynolds number = $0{\cdot}55 \times 10^6$. Its C_L would be 1·154, and it would lift 10·63 lb. per sq. ft. or a total of 63·8 lb. The same fairly low Reynolds number would apply to the full-scale wing held in a natural wind of 10 m.p.h., when the total lift would be the same and its mean intensity 0·295 lb. per sq. ft.

62. Arrangement of Single Drag Experiment

Such complete data as in the last article are rare. Frequently the drag of some aircraft part is desired accurately only under particular conditions, e.g. at top speed at a certain altitude. From these specifications and the size of the part the full-scale Reynolds number can be calculated, and sometimes a single decisive test arranged in the wind tunnel under dynamically similar conditions.

Examples: the drags are required of the following aircraft parts exposed at A.S.I. = 150 m.p.h. at 10,000 ft. altitude: (*a*) a streamline static balance weight of 2 in. diameter, (*b*) a long strut whose streamline section is 6 in. in length. Arrange suitable experiments in a 4-ft. wind tunnel at sea-level working at 50 ft. per sec.

The true relative velocity of the craft is, from Article 33,

$$\frac{150}{\sqrt{0{\cdot}738}} \times \frac{88}{60} = 256 \text{ ft. per sec.}$$

Assuming standard atmospheric conditions, the temperature = − 4·8° C. and, as in Article 61 (*b*), ν is found to be $2{\cdot}01 \times 10^{-4}$. For the tunnel 15° C. may be assumed, so that $\nu = 1{\cdot}56 \times 10^{-4}$.

Models geometrically similar to the parts will be tested in the tunnel. Distinguishing experiment by suffix T and full scale by suffix F, for dynamical similarity we have $R_T = R_F$.

(*a*) Let d be the diameter of the model of the balance weight. Then

$$\frac{d \times 50}{1{\cdot}56} = \frac{(1/6) \times 256}{2{\cdot}01}$$

or

$$d = 0{\cdot}662 \text{ ft.} = 8 \text{ in.}$$

The drag coefficient measured on a model 4 times as large as the actual weight will apply exactly to full scale under the prescribed conditions. From (72a) the forces on the model and the weight will be in the ratio

$$\frac{1}{0{\cdot}738}\left(\frac{1{\cdot}56}{2{\cdot}01}\right)^2 = 0{\cdot}816.$$

(*b*) Similarly the tunnel model of the strut should be larger than full scale in the ratio 4. Applying the factor to the strut section gives a model section of length $4 \times 6 = 24$ in. Since only a short axial length can be accommodated in the tunnel, the test is arranged under two-dimensional conditions, i.e. experiment is limited to finding the drag per ft. run of the strut well away from its ends. Fig. 38 shows the rig. A model of axial length 2 ft. 6 in., say, swings with small clearance between shoulders of the same section fixed to the tunnel walls. These dummy ends separate the model from the walls, eliminating error due to the tunnel boundary layer. Suspension may be by wires and sting, or by a spindle passing through one of the shoulders, which will then act as a guard tube.

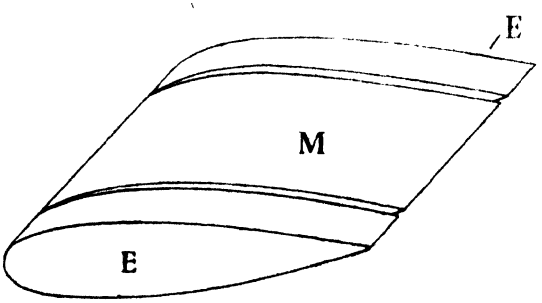

FIG. 38.—ARRANGEMENT FOR TESTING UNDER APPROXIMATELY TWO-DIMENSIONAL CONDITIONS.
M, model; E, E, shoulders or dummy ends fixed to wind-tunnel walls.

The drag coefficient determined will apply exactly to the full-scale strut at the speed and altitude given, except near its sockets. The force measured will be simply related to that on a length 2 ft. 6 in. $\div$ 4 = 0·625 ft. run of the actual strut.

63. Compressed-air Tunnel

The foregoing examples illustrate that, to secure dynamical similarity, models will not as a rule be smaller than full-scale parts. The restriction is unimportant in the case of small components, but destructive for large parts, such as wings. An element of the span of the full-scale wing of a small aeroplane can be tested under two-dimensional conditions in a 4–5-ft. tunnel as described above for a strut model, provided incidence is closely that for zero lift. It will be found later on that Aerofoil Theory and Skin Friction Analysis can then be used to deduce the drag of the wing in free flight through a useful range of incidence. But certain important phenomena occurring at considerable incidences must be measured directly on models of complete wings. Not more than 8-in. chord could then be used in a 5-ft. tunnel. Thus a model wing is seldom larger than $\frac{1}{8}$th and may be smaller than $\frac{1}{20}$th scale. To realise full-scale Reynolds numbers by testing at speeds six to twenty times as great as those of flight is impracticable both on economic grounds and as vitiating the incompressible flow assumption.

In some national tunnels, however, the air circulates in a compressed state, pressures of 25 atmospheres being reached. By Maxwell's Law (Article 25) μ is independent of density at constant temperature, when $\nu \propto 1/\rho$ and $R \propto \rho$. Hence for R constant

$$\frac{V_T}{V_F} = \frac{l_F}{l_T} \cdot \frac{\nu_T}{\nu_F} = \frac{l_F}{l_T} \cdot \frac{\rho_F}{\rho_T},$$

where suffix T refers to the model and F to full scale. If, for example, the last factor is $\frac{1}{25}$ and $l_T/l_F = \frac{1}{10}$, $V_T/V_F = \frac{2}{5}$.

Fig. 39 illustrates the compressed air tunnel at the N.P.L. It is of annular return flow type, the working jet being 6 ft. diameter and the enclosing steel shell 18 ft. diameter and $2\frac{1}{2}$ in. thick in its cylindrical part. A 450-h.p. motor gives a wind velocity of 90 ft. per sec. through the working section. After rigging a model, the tunnel is sealed and pumped up by a large compressor plant in an adjoining room. Forces and moments are measured by special balances located within the shell and controlled electrically.* The exhaust from the tunnel, after the test, is utilised to drive small high-speed tunnels.

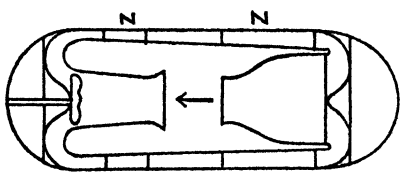

FIG. 39.—COMPRESSED-AIR TUNNEL.

N, N, radial vanes to prevent swinging of flow.

* Relf, *Jour. Roy. Aero. Soc.*, Jan. 1935.

If b is the compression ratio required in the C.A.T. to secure a full-scale low-altitude value of R, so that Vl for the model is $1/b$ times that for full scale, then by (72) the ratio of any component force on the model to the corresponding full-scale component is also $1/b$. For example, with $b = 25$ the aerofoil lift (L_T) for a wing of 5 tons lift (L_F) would be 448 lb. If the geometrical scale of the model were $\frac{1}{16}$th we should have for the ratio of the mean intensities of lift

$$\frac{L_T/l_T^2}{L_F/l_F^2} = \frac{16^2}{25}$$

or the loading on the model would be 10 times that on the full-scale wing, and might reach 4 cwt. per sq. ft. Such intense forces readily distort C.A.T. models, which are therefore often shaped from metal castings.

64. Practical Aspect of Aerodynamic Scale

Table V relates to aeroplane wings and complete models of wings, and indicates the maximum Reynolds numbers obtained in various types of wind tunnel and the range of Reynolds numbers characterising various aircraft categories. R is specified on the mean chord. Maximum sizes are assumed for the models and involve important corrections for the limited width of the tunnel stream (Chapter VIII).

TABLE V

REYNOLDS NUMBERS OF WINGS

	Speed (ft. per sec.)	$R \div 10^6$
Tunnel Experiment:		
12–36 h.p. 4 ft. enclosed-section (A)	100	$\frac{1}{4}$
600 h.p. 5–6 ft. open-jet (A)	300	$1\frac{1}{4}$
12,000 h.p. 60 × 30 ft. open-jet (A)	200	$9\frac{1}{2}$
600 h.p. 6 ft. jet (25 atmospheres)	100	$10\frac{1}{2}$
9,000 h.p. 13 × 9 ft. enclosed-section (4 atmospheres)	300	$11\frac{1}{2}$
Full Scale Flight:		
Small and light aeroplanes	80–250	$2\frac{1}{2}$–7
Small fast aeroplanes	100–600	4–25
Medium-size aeroplanes	110–450	9–35
Medium-size (stratospheric)	700	16
Specially large aeroplanes	130–400	15–45

(A) denotes atmospheric pressure.

In compiling this list, which is by no means exhaustive, some known extreme cases have been omitted in order to preserve a

generally representative view of the position. The tunnels are not confined to existing plant ; that last mentioned is designed primarily for high Mach numbers (as will be described later) but can be used as a compressed-air tunnel, as shown. The comparatively small Reynolds number typical of stratospheric flight is due to the large value of ν at 40,000 ft. altitude ; in regard to flight at this altitude, an atmospheric tunnel has a compression ratio of 4. All the other aircraft data relate to comparatively low altitudes.

It will be seen that a small tunnel using highly compressed air is much the most economical for a straightforward test on an aerofoil when the Mach number can be ignored. The 6-ft. size with pressures up to 25 atmospheres covers the entire range of Reynolds number for small aeroplanes of low power, and the landing conditions and stratospheric Reynolds numbers of all but the largest aeroplanes, for experimental Reynolds numbers can be increased to about 25 million for small incidences by testing under two-dimensional conditions and applying a theoretical correction for the change to three dimensions, checked experimentally in the same tunnel at a smaller scale. A very large tunnel is desirable in other connections, e.g. when access is required to the stream during a test, or details are concerned which cannot be reproduced in small models ; instances of such details are engine cowlings and Aerodynamic controls ; but it is often claimed that these purposes can be served without going to the extreme of a full-scale tunnel. The relative advantages of the two methods have, indeed, long been contended. For very high compressions, models are expensive to construct and the exceedingly heavy air creates experimental difficulties, in connection with deflections, that are sometimes serious ; there is a case for restricting the compression to less than 8 atmospheres, and increasing the size, though the advantage in respect of power is then greatly reduced. On the other hand, an aeroplane cannot in general be tested in a full-scale tunnel, under conditions quite different from those of flight, without special strengthening, a process which is not simple to carry out. Further reference to the matter will be made in the chapter on testing at high speeds. Meanwhile the conclusion will be drawn that wind tunnels, of whatever kind, capable of realising full-scale Reynolds numbers are costly, and that experiments will usually be made, therefore, at much smaller Reynolds numbers.

65. Scale Effects (*a*)

Since tunnel measurements are made in general at too low a Reynolds number, important differences are to be expected on the

craft. These are termed scale effects. By 'scale' is meant, of course, Aerodynamic scale. But the practical term has two meanings, of which we now consider the first, i.e. the total change in $f(R)$ through the interval of R between experiment and flight.

Rapid changes often occur in a 5-ft. atmospheric tunnel of moderate speed, e.g. the dip in the C_M curve of Fig. 36 quickly disappears on increasing scale. Thus it is advisable to test at as large a scale as possible, however far this may be from that of flight. Certain

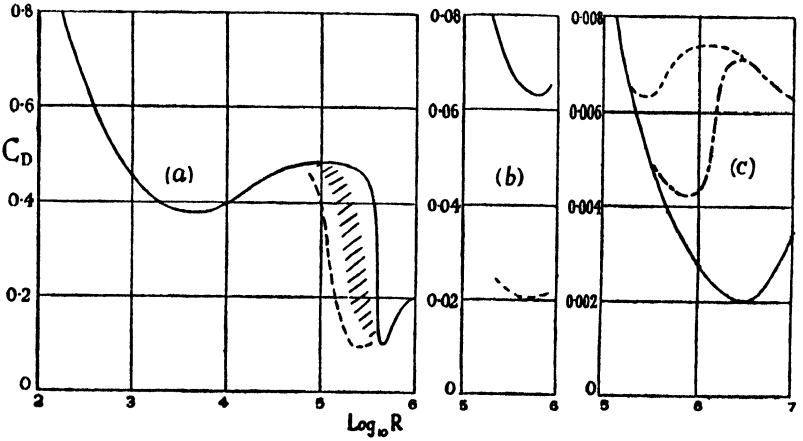

FIG. 40.—EXAMPLES OF SCALE EFFECT.

(*a*) Spheres. Full line: smooth flow; dotted line: turbulent wind tunnel; hatched area: steadier tunnels.

(*b*) Streamline strut of fineness ratio 3. Full line: C_D reckoned on maximum sectional area across the stream; dotted line: C_D reckoned on maximum sectional area parallel to the stream.

(*c*) Smooth tangential boards or plates. Full line: smooth flow; dotted line: turbulent tunnel; chain line: some experiments under fairly steady conditions.

subsequent changes can be estimated from theory, as we shall find later on, but others, of which Fig. 37 is an example, rest entirely on experiment or engineering experience.

Fig. 40 gives further examples of $f(R)$. C_D is reckoned for (*a*) and the upper full-line curve of (*b*) on maximum sectional area across the stream; for (*c*) on maximum area projected perpendicular to the stream. To facilitate comparison a lower broken line curve has been added for (*b*) calculated on the second basis (for (*a*) there would be no difference).

Two important considerations, to some extent interconnected, may be introduced here. The curves given relate, where possible, to bodies of studiedly smooth surface in streams comparatively free from turbulence. By turbulence is deliberately meant, as before, an

unsteadiness that is finely grained in comparison with the size of the body, and not comparatively large-scale fluctuations of velocity such as eddying might produce. We could make a smooth and steady tunnel stream turbulent by interposing upstream of the body a mesh screen of cords. Alternatively we could give it large and fairly rapid fluctuations of velocity by operating quickly an electrical resistance in series with the armature or field of the driving motor. But the second form of unsteadiness is not turbulence. Again, the natural wind is subject to considerable variation in magnitude and direction of velocity, but except very close to the ground it is free of turbulence in comparison with all ordinary tunnel streams.

Now the initial turbulence in a stream approaching a body is found to affect drag (or lift, etc.), particularly at scales where $f(R)$ changes sharply. The sphere at *circa* 3×10^5 affords a good example; change is here so sharp that drag actually decreases with increase of speed, as occurs also with the circular cylinder at much the same Reynolds number. In Fig. 40(*a*) the full-line curve shows the variation in $C_D (= D/\frac{\pi}{4}\frac{1}{2}\rho V^2 d^2$, for diameter d) against $R (= Vd/\nu)$ for smooth flow, as obtained by towing a sphere freely through the atmosphere. A notably turbulent tunnel would give, on the other hand, the left-hand dotted curve; the shaded area indicates common variation in different tunnels. Similar remarks could be made in connection with the example (*c*). We note immediately that at critical scales (1) tunnels of different turbulence will disagree with one another, (2) free air values of $f(R)$ may differ from those determined in any tunnel. Furthermore, if in a given tunnel size be greatly varied, the relative scale of the turbulence will change and the tunnel will disagree with itself, though R remain constant. Thus in general a $f(R)$ curve in a given tunnel is a narrow band of readings; the same curve for many tunnels would be a wider band.

Effects on drag are expected to be produced chiefly by the turbulence in parts of the stream that pass the body closely. To make an initially smooth stream effectively turbulent, our mesh screen might be reduced to diminutive proportions if suitably located. In the limit it might be replaced by a thin wire bound round the forepart of the body. We infer (and may check by direct experiment) that roughness of surface modifies $f(R)$. This is to be expected, since geometrical shape is changed, but it may be noted that very slight roughness may increase drag remarkably—e.g. with wings at

$R > 10^6$. Thus aerofoils are often polished or plated if they are to be tested at large Reynolds numbers.

While postponing further investigation of the foregoing, we may note that from the engineering point of view knowledge of $f(R)$ in a given case may not be necessary. The engineer is commonly faced with inadequate data which he must extrapolate, whatever the risk, to a flight scale. A controlled turbulence in the tunnel may ease in some cases this difficult process, though introducing artificiality at model scale. By convention the degree of turbulence in a particular tunnel is gauged by the Reynolds number at which C_D for spheres is 0·3 (= 385,000 in the atmosphere). Spheres are supported from the back to obviate effects of attached wires; the drag can be inferred from the pressure at the back.

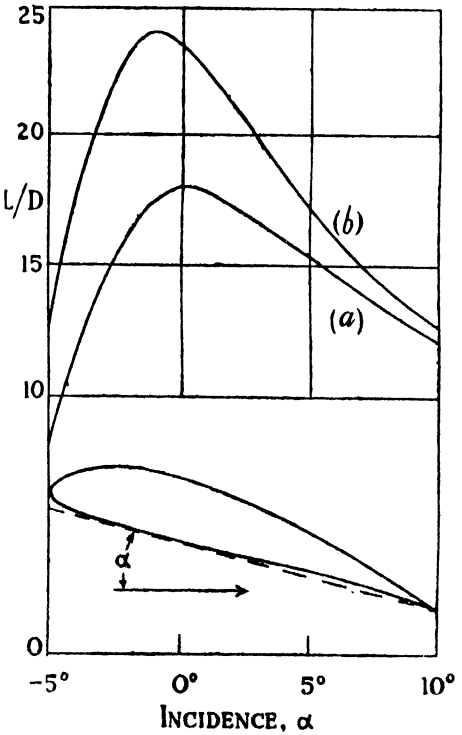

FIG. 41.—SCALE EFFECT ON L/D FOR GÖTTINGEN 387 WING.
(*a*) 5-ft. low-speed wind tunnel corrected to free air.
(*b*) Small full scale.

Scale Effects (*b*)

The second meaning of 'scale effect' is of a more applied nature and reserved chiefly to wings and the like. The aeroplane wing sometimes preserves a single shape, but always assumes various attitudes in course of flight. Accordingly, a wide view must be taken of its performance before choice can be made for a particular craft. Features of engineering interest include maximum lift coefficient, maximum lift-drag ratio, the drag coefficient at certain small lift coefficients, etc., and at what incidences these occur is often immaterial. Rayleigh's formula can only, of course, be applied to a given wing shape at constant incidence, so that in practice we have to deal with a series of $f(R)$ curves for a single wing. Now it always happens that scale effect is more advantageous at some

incidences than at others, so that max. L/D, for example, occurs at one incidence in the tunnel and at a different incidence in flight (see Fig. 41, for example). The change from model to full scale of max. L/D, max. C_L, or other characteristic, is then called scale effect irrespective of modification of incidence.

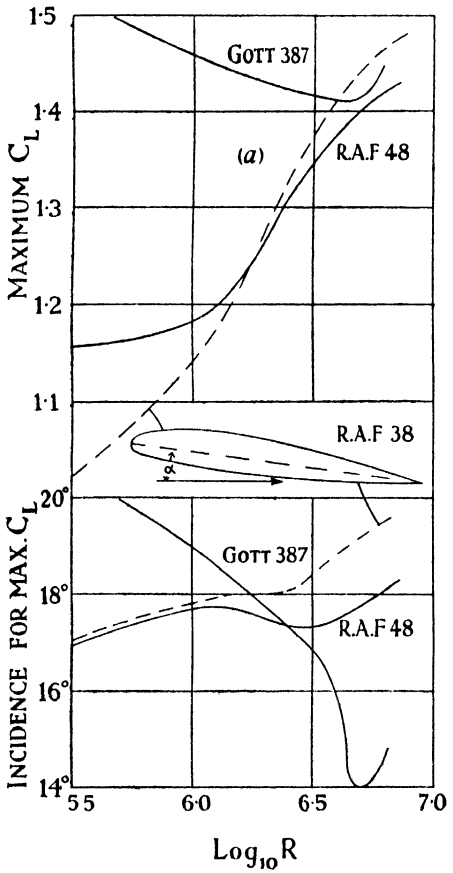

FIG. 42.—APPROXIMATE SCALE EFFECTS ON MAXIMUM C_L FOR THREE AEROFOILS (ASPECT RATIO 6).

Further examples * of scale effect with this wider meaning are given in Fig. 42. The results shown at (*a*) illustrate a difficulty that will be now thoroughly appreciated in interpreting ordinary wind-tunnel results in terms of full scale. Assuming choice to be required between the wings R.A.F. 38 and R.A.F. 48, and max. lift to be the overruling consideration, experiments at $R < 2 \times 10^6$ would give preference to the second, while actually it should be given to the first.

Again, from the same point of view, tests would be required at $R > 3\frac{1}{2} \times 10^6$ to decide definitely between R.A.F. 38 and the wing Göttingen 387. Nevertheless, tests through a range of much smaller Reynolds numbers, within the compass of a high-speed 5-ft. open-jet tunnel, would show max. C_L decreasing with increase of R for Göttingen 387. suggesting that it *might* not maintain its great advantage at the small scale over R.A.F. 38, whose max. C_L would be shown increasing sharply. Such evidence, though inconclusive, provides a better guide than comparison at a single small scale.

* These and other examples given are based on Relf, Jones, and Bell, A.R.C.R. & M., 1627.

Chapter III A

EXPERIMENT AT HIGH SPEEDS

66. Variable-density Tunnel

High-speed phenomena in Aerodynamics are usually studied in two parts : appreciably below the velocity of sound, or well above it. Comparatively few quantitative measurements have been made for Mach numbers within the range 0·9 to 1·3 owing to lack of sufficient stability of flow. High-speed tunnels are consequently divided into two distinct groups : the subsonic and the supersonic. Of these the former is the more important, as exploring the compressible flow that immediately precedes critical Mach numbers at which is experienced *shock*, a phenomenon that is accompanied by great increase of drag and decrease of lift.

One method of obtaining subsonic speeds for experiment is to employ a tunnel of the ' race-course ' design partially evacuated. Adaptation to withstand a crushing pressure of some 12 lb. per sq. in. permits alternative use under a bursting pressure of a few atmospheres. The term *variable density* is often applied to tunnels arranged only for compressed air, and justifiably so since their pressure is varied, but it is gradually becoming reserved for those in which the density can also be reduced.

In examining tunnels of this type we have to take into account that at high speeds the density ρ, the absolute temperature τ, and the velocity of sound a in the experimental part of the stream are much less than in the return flow just before contraction. The latter state will be distinguished by suffix 1.

The power required to maintain a stream of section C and velocity V, the power factor being defined as in Article 51, is

$$\text{b.h.p.} = \frac{PC}{1100}\,\rho V^3.$$

If M denotes the Mach number V/a, the formula may be rearranged as

$$\begin{aligned}\text{b.h.p.} &= \frac{PC\rho_1}{1100}\,M^3 . \frac{\rho}{\rho_1}\,a^3 \\ &= \frac{PC\rho_1 a_1^3}{1100}\,M^3 . \left(\frac{\rho}{\rho_1}\right)^{3\gamma/2 - 1/2} \qquad \text{(i)}\end{aligned}$$

by Article 30. Assuming a substantial contraction ratio, as is specially desirable with this kind of tunnel, V_1^2 can be neglected in comparison with V^2 and, introducing also the approximation $\gamma = 1{\cdot}4$, (47) of Article 30 then gives

$$\frac{\rho}{\rho_1} = \left\{1 - \frac{1}{5}M^2\left(\frac{a}{a_1}\right)^2\right\}^{5/2}$$

i.e.,

$$\left(\frac{\rho}{\rho_1}\right)^{2/5} = \frac{1}{1 + M^2/5} \quad . \quad . \quad . \quad . \quad \text{(ii)}$$

Substituting in (i),

$$\text{b.h.p.} = \frac{PC\rho_1 a_1^3}{1100} \cdot \frac{M^3}{(1 + M^2/5)^4} \quad . \quad . \quad \text{(iii)}$$

If we further assume $P = \frac{1}{3}$, $\tau_1 = 288°$, and write σ for the ratio of ρ_1 to the standard air density at sea-level, (iii) yields the approximate formula

$$\text{b.h.p.} = 1000\sigma C \frac{M^3}{(1 + M^2/5)^4} \quad . \quad . \quad \text{(iv)}$$

Calculations by means of these formulæ speedily show that a large power is required to maintain a high Mach number in a stream of moderate size in spite of considerable rarefaction. Thus for $M = 0{\cdot}8$, $C = 100$ sq. ft., and $\sigma = \frac{1}{4}$, the h.p. required is nearly 8000 for the empty tunnel and would need further increase to cope with the high drag of models under test. The large power, and the consequently elaborate measures necessary to cool the relatively small circulating mass of air, comprise the principal disadvantages of this type of tunnel. On the other hand, the type possesses the advantage of combining, in a single installation, provisions for high Mach numbers at a reasonable experimental Reynolds number with a complete model, and also for high experimental Reynolds numbers when low Mach numbers can be accepted.

This can be verified as follows. Using (ii), the Reynolds number R is given by

$$R = \frac{\rho l M a}{\mu} = \frac{\rho_1 a_1 l}{\mu} \cdot \frac{M}{(1 + M^2/5)^3} \quad . \quad . \quad \text{(v)}$$

Now μ is the coefficient of viscosity for air in the state prevailing at the working section ; i.e. from (31) and (33)—

$$\mu = 3{\cdot}72 \times 10^{-7}(\tau/288)^{3/4}$$

where

$$\tau = \tau_1(\rho/\rho_1)^{2/5} = \tau_1/(1 + M^2/5).$$

Hence, introducing σ as before and assuming $\tau_1 = 288^0$,

$$R = 7{\cdot}17 \times 10^6 \sigma l \frac{M}{(1+M^2/5)^{9/4}} \cdot \quad . \quad . \quad . \quad \text{(vi)}$$

Referring to the numerical example above, $R > 1\frac{1}{2}$ million could be expected with a complete model at $M = 0{\cdot}8$. Again, putting $\sigma = 4$ instead of $\frac{1}{4}$ in (iv) leads for the same case to $M = 0{\cdot}28$, and the expectation of a Reynolds number of 11 or 12 million with a complete model. The Mach number is then so low as to have no significance, and the same Reynolds number could be realised with 25 atmospheres pressure in a tunnel of approximately half the size and one-third the speed, entailing an expenditure of only some 450 h.p. But turning this small compressed-air tunnel into a variable-density tunnel would enable only a small Reynolds number to be reached with a complete model at a Mach number of 0·8, and the h.p. would be increased to upwards of 2000.

It can now be seen that adjusting the density of the air used for experiment presents opportunities for economy in two directions, viz. by employing light air for high Mach numbers and heavy air for high Reynolds numbers. Excessive use of either expedient is to be avoided, however. A very low density leads to unacceptably small Reynolds numbers at high Mach numbers, and a small mass of attenuated air in which mechanical energy is being converted into heat at a great rate is difficult to cool. Difficulties arising at the other extreme have already been mentioned. Thus a compromise is sought between apparent economy, on the one hand, and the advantages of moderate compressions and rarefactions on the other. It is unfortunate, in view of the evident utility of the variable-density tunnel, that these considerations point to a power equipment of some 10,000 h.p. The number of such tunnels is likely, therefore, always to be limited.

66A. Induced-flow Subsonic Tunnel

The imposing installations necessary to maintain experimental streams of ordinary size at high speeds have led to the development of small induction tunnels in which subsonic winds are produced for short periods at a time by the exhaustion of reservoirs of compressed air. Such tunnels are small, often about 1 sq. ft. in cross-sectional area, and the limited supply of compressed air is expended economically by use of the injector principle, a sheath of high-velocity air from a pressure chamber entraining the flow of a much greater volume from rest in the atmosphere. Reservoirs

should be large and pumping plants powerful in order to provide runs of sufficient duration at reasonable intervals, but only a moderate pressure is called for.

These tunnels may have round, square, or other sections. A vertical rectangular form has been developed at the National Physical Laboratory for experiments on aerofoils under two-dimensional conditions. Being of outstanding interest and suitable for wide reproduction, it will be described * in some detail.

Fig. 42A indicates the main points of the apparatus. The section is 17½ in. by 8 in., and the plane of the figure is parallel to the wide sides. The downstream end of the tunnel is surrounded by a distributing box or pressure chamber C, which receives compressed air from a large reservoir and exhausts it through injector slots J, about 4·2 millimetres wide, into a long divergent diffuser D. The injector stream induces the flow of atmospheric air into the flared intake A through a box baffle B of fine gauze screens which raise the turbulence Reynolds number to the satisfactory value of 290,000 (cf. Article 65). The aerofoil stretches from one wide wall to the other, and these walls are flat and parallel. The narrow walls, opposite the upper and lower surfaces of the aerofoil, are made from metal strip and can be adjusted separately to streamline forms, as indicated by dotted lines in the figure, by means of closely spaced micrometer screws. If they are shaped to lie along streamlines appropriate to the aerofoil in the absence of walls, the condition of free flight will be simulated, the permissible chord of the aerofoil increased, and best use made of the restricted cross-sectional area of the tunnel. Towards the outlet, the adjustable walls may converge to a throat, where the stream attains to the velocity of sound and creates a shock wave which has a beneficial effect in steadying the flow upstream.

Mach numbers exceeding 0·9 can be produced by an injector pressure of 80–90 lb. per sq. in., which appears to be the optimum pressure for this tunnel with the model in ; the blowing pressure for the empty tunnel is 30–40 lb. per sq. in. For measurements of lift, drag, and pitching moment at the small incidences of interest in connection with high Mach numbers, the permissible aerofoil chord is 5 in. By (vi) of the preceding article with $\sigma = 1$, this gives a Reynolds number of 1·8 million at a Mach number of 0·8. An

* A preliminary description of this tunnel is included by kind permission of the Aeronautical Research Council. The author's acknowledgments are also due to the following, whose papers have been read:—Bailey and Wood, A.R.C.R. & M., Nos. 1791 and 1853 ; Beavan and Hyde, A.R.C. Rept. No. 5622, 1942 ; and Lock and Beavan, A.R.C. Rept. No. Ae. 2640, 1944.

aerofoil of more than twice the above chord can be tested at zero incidence with only manageable difficulties, increasing the Reynolds number at need to 4 million.

Adjustment of Walls.—For various reasons these tunnels are usually vertical, but for brevity and clarity the side opposite the upper surface of the aerofoil will be referred to as the roof and that opposite its lower surface as the floor. The roof and floor alone are adjustable in shape, the wider sides remaining flat. The approximately free-air shape for a non-lifting aerofoil is determined in steps, as follows.

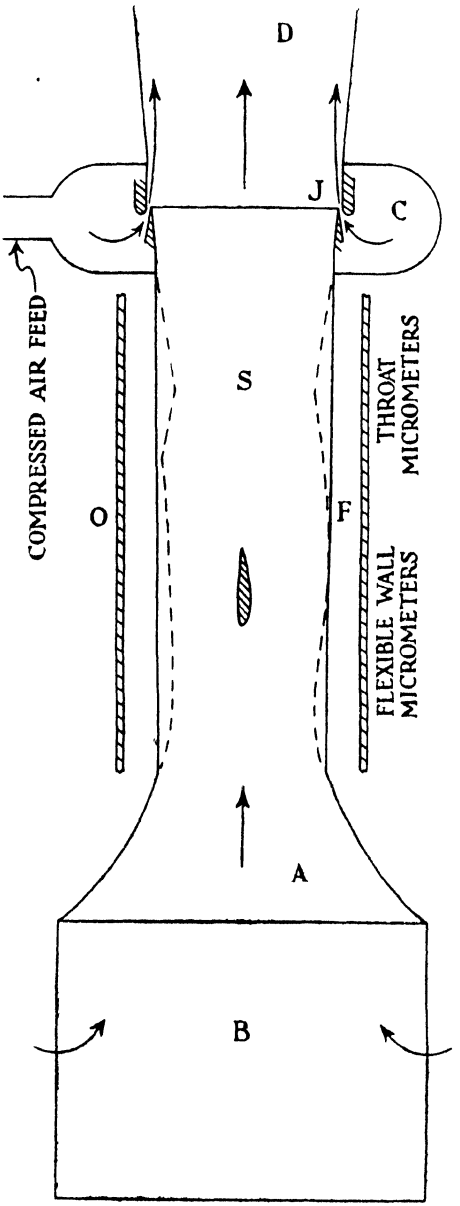

FIG 42A.—N.P.L. SUBSONIC TUNNEL.
A, intake; B, fine gauze screens; C, pressure chamber; J, jets; D, divergent diffuser; F, flexible walls; O, outer walls fitted with micrometer screws; S, sonic throat.

The roof and floor are first adjusted to give constant pressure (zero longitudinal pressure gradient) with the tunnel empty. Owing to thickening boundary layers along all four sides and the compressible nature of the flow, the required shape is neither simple nor predictable, but it is easily arrived at by experiment.

Inserting the aerofoil varies the pressures along roof and floor

from the constant values found for the empty tunnel, as illustrated by curve (*a*) of Fig. 42B. The increment of speed at the edge of the boundary layers of the roof and floor is much greater than would exist at the same distance from the aerofoil in free flight and indicates the difficulty experienced by the air in flowing past the aerofoil in the presence of the tunnel. This is termed *blockage*; the peak effect opposite the aerofoil is called solid blockage, and the maintained effect behind, the wake blockage. Clearly, the back part of the tunnel requires widening in the presence of the aerofoil. As a second step, the roof and floor are again adjusted in shape to give constancy of pressure along them, the amount of readjustment necessary being accurately noted from the graduated heads of the micrometer screws used for the purpose. Finally, the roof and floor are set to shapes approximately midway between those for constant pressure with the tunnel empty and with it containing the aerofoil, respectively (the factor 0·5 is for greater accuracy replaced by 0·6).

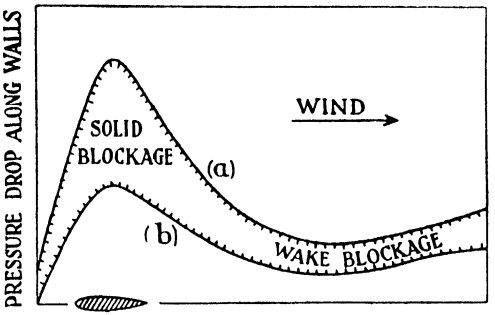

FIG. 42B.—BLOCKAGE IN SUBSONIC TUNNEL.
(a) Pressure along 'flat' wall; (b) pressure along streamline wall.

The last step gives effect to a theoretical calculation by Taylor and Goldstein concerning compressible flow between two parallel walls, one flat and the other corrugated. This showed that, under certain conditions, one-half of the pressure distribution along the flat wall is caused by the corrugation of the other wall and one-half by the constraint which the flat wall itself exerts on the flow. Hence, a wall shaped to lie along free streamlines should exhibit, under these conditions, one-half the pressure changes caused along a flat wall by a disturbance. The roof and floor of the tunnel adjusted to constant pressure with the tunnel empty are regarded as flat in this sense, and linear variation of pressure change with shape is assumed.

Blockage is then eliminated, the pressure distributions on roof and floor being reduced to curve (*b*) of Fig. 42B, which accords approximately with absence of constraint. A greater speed becomes possible in the tunnel. But the essential point is that the flow past

the aerofoil should now be characteristic of free flight, a large exaggeration due to tunnel interference having been removed. A test of the sufficiency of the measures adopted is described in Article 66C. Different settings of the roof and floor are required for different aerofoils, or incidences, as well as for considerably different Mach numbers with the same aerofoil.

The shape of the roof is the same as that of the floor for an aerofoil of symmetrical section at zero incidence, to which the above description applies, but is different if a lift exists. Free streamline shapes for a lifting aerofoil involve bending the axis of the tunnel, which is inconvenient, and an approximate process is adopted. The principle of this further step will appear in later chapters, and reference may be made to the papers cited for the best method of application.

Methods of Measurement.—An Aerodynamic balance could be used to weigh the force components on the aerofoil as with an ordinary wind tunnel, except that it would require to be enclosed or specially designed to take account of the large drop of pressure in the tunnel. Forces are actually measured by wake exploration for drag and by pressure plotting the aerofoil for lift and moment. The lift of the aerofoil per unit length midway between the side walls can also be determined by connecting a multiple-tube manometer to a line of holes in the roof and in the floor and subtracting the integrals of the pressure changes so recorded; this known method is illustrated quantitatively in Chapter VII, but obviously the aerofoil lift must be supported on a long floor and roof by pressure changes, and the only question arising is whether an allowance must be made for restricted length.

66B. The Supersonic Tunnel

Raising the injector pressure of a subsonic tunnel of the type just described fails to increase its speed appreciably. Tunnels that provide wind speeds in excess of the velocity of sound are actuated by connecting them directly to large reservoirs of compressed air, or to receivers evacuated by pumps. Making extravagant use of high-pressure storage space, they are kept very small, only a few inches in width.

In Fig. 42c the reservoir or region of higher pressure is at O, and a convergent nozzle N leads through a throat T to a long divergent duct D, which is open to the atmosphere or region of lower pressure at R. The location of quantities is distinguished below by use of these letters as suffixes. Suffix O refers to air sufficiently removed

from the vicinity of the intake for its velocity V_0 to be negligibly small. When a supersonic tunnel is working satisfactorily the entire flow, apart from a thin boundary layer, is irrotational; the pressure is related to the velocity by Bernoulli's equation and to the density by the adiabatic law. The boundary layer will be ignored and the tunnel assumed to run full with constant velocity over each cross-section.

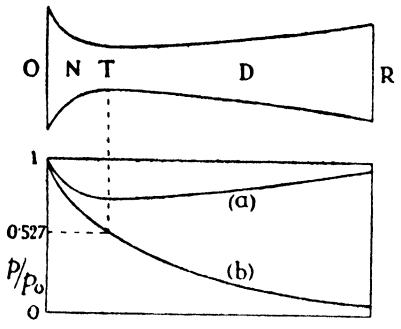

FIG. 42c.—SUPERSONIC WIND TUNNEL.

For p_0 little greater than p_R the apparatus works as a subsonic tunnel or venturi tube, a large pressure drop at the throat where the speed is a maximum being mostly recovered in the divergent duct, along which the kinetic energy is gradually reduced. This state is indicated schematically by curve (*a*) in the figure. Increasing p_0/p_R at first merely increases the pressure drop at the throat and the speed. But a limiting condition is reached when $V_T = a_T$, the velocity of sound in air of the low temperature then attained at the throat. The corresponding minimum value of p_T/p_0 follows immediately from (50) of Article 30 as—

$$\min.\frac{p_T}{p_0} = \min.\left(\frac{\rho_T}{\rho_0}\right)^{\gamma} = \left(\frac{2}{1+\gamma}\right)^{\frac{\gamma}{\gamma-1}} = 0{\cdot}527. \quad . \quad \text{(i)}$$

Any further increase of p_0/p_R fails to produce a larger pressure drop at the throat or to make V_T exceed a_T. But if $p_0 - p_R$ be made substantially greater than $0{\cdot}473p_0$, further expansion of the air occurs along a suitable divergent duct in place of the former compression, as indicated schematically by curve (*b*) in the figure. Supersonic speeds result from the air expanding more rapidly than the cross-sectional area of the duct. The expansion further reduces the temperature of the air, and therefore the local velocity of sound, by (27). Hence the significant ratio V_D/a_D is increased on two counts. This ratio will be denoted by M.

Wide scope exists provided p_0/p_R can be made large. For $V_0 = 0$, (51) of Article 31 gives

$$\left(\frac{V_D}{a_0}\right)^2 = \frac{2}{\gamma-1}\left\{1 - \left(\frac{p_D}{p_0}\right)^{\frac{\gamma-1}{\gamma}}\right\},$$

and, remembering that the second term in the curly brackets is equal to $(a_D/a_O)^2$, the expression can be changed to

$$M^2 = \frac{2}{\gamma - 1}\left\{\left(\frac{p_O}{p_D}\right)^{\frac{\gamma-1}{\gamma}} - 1\right\} \quad . \quad . \quad \text{(ii)}$$

with the understanding that M applies to the position along the duct at which the pressure is p_D. Putting $p_O/p_D = 10$ and 20, for example, yields $M = 2{\cdot}15$ and $2{\cdot}60$, respectively. Greater values, between 3 and 4, have been obtained in practice. At the other extreme, $M = \sqrt{2}$ appears as a matter of recent experience to be approximately the lowest Mach number at which the flow through a supersonic tunnel is sufficiently stable for accurate experiments to be made, and it gives $p_O/p_D = \gamma^{\frac{\gamma}{\gamma-1}} = 3\frac{1}{4}$.

Let S_T be the cross-sectional area of the throat. For any value of p_O/p_R greater than that required to secure $V_T = a_T$, the mass flow per second through the tunnel remains constant. It will be denoted by C, and from (i)

$$C = S_T\rho_T a_T = S_T\rho_O a_O\left(\frac{2}{\gamma+1}\right)^{\frac{\gamma+1}{2(\gamma-1)}} \quad . \quad \text{(iii)}$$

Now the mass flow through every cross-section must be the same. Hence, neglecting the boundary layer,

$$C = S_D\rho_D V_D = S_D\cdot\rho_O\left(\frac{p_D}{p_O}\right)^{\frac{1}{\gamma}} \cdot a_O\left(\frac{2}{\gamma-1}\right)^{\frac{1}{2}}\left[1 - \left(\frac{p_D}{p_O}\right)^{\frac{\gamma-1}{\gamma}}\right]^{\frac{1}{2}}.$$

Substituting for C from (iii),

$$\left(\frac{S_T}{S_D}\right)^2 = \frac{2}{\gamma-1}\left(\frac{\gamma+1}{2}\right)^{\frac{\gamma+1}{\gamma-1}}\left(\frac{p_D}{p_O}\right)^{\frac{2}{\gamma}}\left[1 - \left(\frac{p_D}{p_O}\right)^{\frac{\gamma-1}{\gamma}}\right] \quad \text{(iv)}$$

This result applies to all subsonic tunnels of the type considered and is plotted in Fig. 42D. An approximate value for the constant coefficient is 14·7. To find the expansion of the tunnel area required for a given value of M, p_D/p_O is first found from (ii) and then S_D/S_T from(iv). The particular manner in which it is chosen to expand the tunnel beyond the throat will

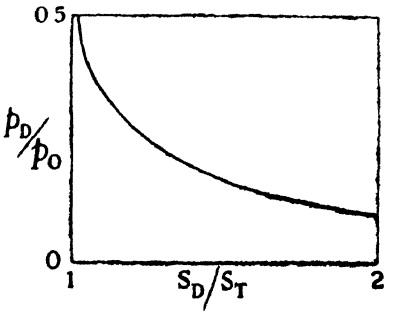

FIG. 42D.—PRESSURE ALONG SUPERSONIC TUNNEL.

then fix the position of the experimental station along the divergent duct. Correction is required on account of the boundary layer.

Downstream of the experimental station the duct expands further in some continuous manner to a maximum cross-sectional area S' before discharging into the atmosphere or low-pressure receiver. The flow can remain irrotational throughout the length only if the pressure p' at S' also satisfies (iv). A shock wave is likely to occur somewhere within D if $p_R > p'$, and travel upstream towards the throat if p_R is increased further. In Fig. 42E, (*a*) is the continuous pressure curve along a tunnel in which p_R is not greater than p'; (*b*) is the discontinuous pressure curve appropriate to a shock wave forming at B; (*c*) shows an earlier failure due to a still greater value of p_R. Irrotational flow is possible only as far as the wave front. If $p_R < p'$, M will not be increased, but a shock wave can be expected in the issuing jet.

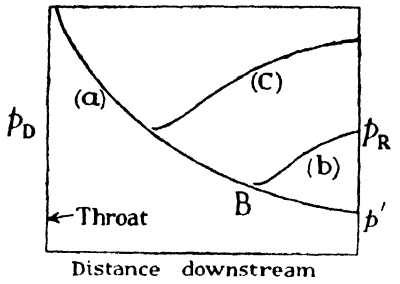

FIG. 42E.—SHOCK WAVE IN SUPERSONIC TUNNEL.

It will be seen that only one value of M is possible at a fixed experimental station along a given tunnel. Displacing the station along the divergent duct is usually inconvenient. But the small size of the tunnel enables large variations of M to be obtained readily by employing alternative divergent ducts, provided p_0/p_R is sufficiently large. From this point of view, and also to lengthen the necessarily brief time of a run even at a comparatively small Mach number, the reservoirs (in the common case of tunnels exhausting into the atmosphere) should be capable of withstanding air pressures of many atmospheres and possess a large capacity, suggesting a battery of long boiler shells of moderate diameter together with pumps of substantial power. But for visual purposes in a small laboratory a modest equipment will provide a very small supersonic stream for, say, a minute at a time. For quantitative two-dimensional work with larger apparatus, the section will be put to best use if made deeply rectangular in shape, or fitted with adjustable sides as described for the N.P.L. subsonic tunnel.

66C. Illustrative Results

Published experiments of aeronautical interest at high Mach numbers are sparse and largely confined to two-dimensional tests.

The illustrations now given are no more than typical in a qualitative way.

As a first example, the left-hand side of Fig. 42F gives the drag curves for certain symmetrical aerofoils of three different thickness ratios (maximum thickness of section expressed in terms of the chord) tested at zero incidence through a range of high subsonic speeds. C_D remains almost constant until, at some critical Mach number depending on the section, there occurs what is known as the *compressibility* or *shock stall*. Thereafter C_D increases very rapidly; some tests suggest to five or more times its value for incompressible flow. Supersonic tests are difficult to carry out for $M < 1{\cdot}4$, as already mentioned, but it is clear that after a peak value C_D decreases as indicated qualitatively on the right-hand side of the figure, though not to its small initial value.

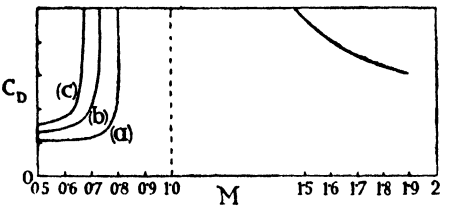

FIG. 42F.—CRITICAL MACH NUMBERS.
The curves (a), (b), (c), are for symmetrical aerofoils in ascending order of thickness.

The determination of the critical Mach number is evidently a matter of first importance and likely to be affected by the presence of tunnel walls. Fig. 42G reproduces some of the results of an investigation * of the reliability in this connection of the small N.P.L. tunnel described in Article 66A. Curve (*a*) was obtained with an aerofoil chord of 12 in. and curve (*c*) with one of 5 in., both with streamlined walls. Curve (*b*) applies to 12-in. chord with the walls shaped to give constant pressure in the absence of the aerofoil. Comparison shows the magnitude of the correction achieved in a rather extreme case (the depth of the tunnel being only 17½ in.) by streamlining the walls, and the fair agreement reached as to the critical Mach number for the given aerofoil section with a test employing a much-reduced chord, for which the corresponding correction is relatively small. Thus the test on the

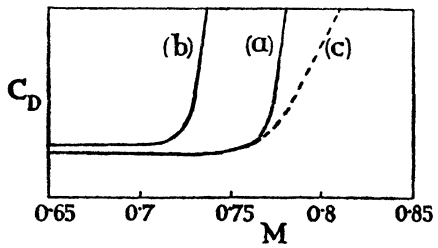

FIG. 42G.—CHECK ON STREAMLINING WALLS.

* Lock and Beavan, *loc. cit.*, p. 106.

smaller aerofoil can be regarded with some confidence as approximating to free-air conditions. Apart from its immediate interest, the investigation illustrates the care that should be taken to establish the validity of wind-tunnel experiments in general.

Fig. 42H illustrates the nature of the lift curve obtained for a fairly thin cambered aerofoil at a small angle of incidence. C_L increases strongly at first, but the shock stall causes a rapid loss of lift. The initial increase is of special importance in the design of airscrews. Beyond the velocity of sound, recovery of lift is poor, drag remains high, and the maximum lift-drag ratio obtainable with any aerofoil has a much-reduced value.

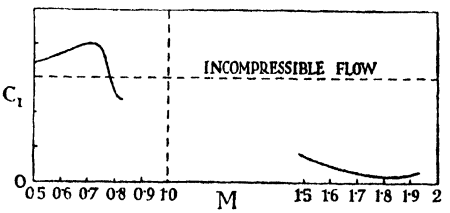

FIG. 42H.—SHOCK STALL.

It is possible to gain a preliminary idea of the nature of the shock stall by visually inspecting the flow under suitable illumination; for this reason high-speed tunnels may be fitted with glass sides opposite the aerofoil. The critical Mach number is associated with the generation of a shock wave, which extends from the aerofoil for some distance into the stream and casts a shadow.* The wave changes the Bernoulli constant for flow passing through it, creating the compressibility wake already noted. With further increase of Mach number the wave penetrates more deeply into the stream and becomes rapidly displaced backward. In a tunnel, a stage is soon reached when it extends right across to the roof, and experiment becomes more difficult. The stall is easily caused to occur early by employing a bluff section; e.g. a circular cylinder gives a shock wave at *circa* $M = 0{\cdot}45$. It can also be delayed to some extent by reducing thickness ratio, as illustrated in Fig. 42F, and by shaping the profile to minimise the maximum velocity attained by the wind in flowing past. At supersonic speeds a shock wave is formed in front of the body. These considerations apply not only to models but equally to any exposed attachment used to support them in the stream or to explore the flow in their vicinity.

66D. The Pitot Tube at Supersonic Speeds

The speed of supersonic tunnels is inferred from the static pressure drop at the experimental station as obtained from a hole in the wall.

* See frontispiece.

However, a pitot tube may be used in experiment, and then a special formula is required to deduce the speed from its pressure P, the shock wave formed in front causing P to differ considerably from the pitot pressure for irrotational compressible flow. If p denotes the static pressure of the oncoming wind upstream of the wave, the formula is, in approximate terms,

$$\left(\frac{P}{p}\right)^{2/7} = 0{\cdot}617\left(7M^2 - 1\right)^{2/7}\left(1 + \frac{1}{7M^2 - 1}\right) \quad . \quad (81)$$

To much the same approximation, (52) of Article 31 gives for irrotational flow

$$\left(\frac{P}{p}\right)^{2/7} = 1 + \frac{1}{5}M^2$$

and the loss of pitot head implied in (81) becomes large at Mach numbers considerably greater than unity. The formula may also be used to estimate the speed of an aircraft diving at a supersonic speed, and the pressure at a front stagnation point.

The theory is due to Rankine and Rayleigh and is summarised below, partly in view of the importance of the case and partly as illustrating, with a minimum of analytical complication, the nature of the phenomena occurring at very high speeds. Simplification arises from the legitimate assumption that though the wave is in fact flatly conical, only the bluntly rounded apex of the cone, immediately in front of the mouth of the tube, is likely to be effective, and that this may be treated as plane and normal to the direction of motion.

Rankine's Relationship.—Fig. 421 shows, in front of the pitot tube, part of an infinite plane shock wave which is stationary and normal to the wind. Through the very small thickness the velocity of the air is diminished from V to V_1, and its pressure and density increased from p, ρ to p_1, ρ_1. Up to the wave and beyond it the pressure and density are related by the adiabatic law, i.e. the flow is isentropic, but the air increases in entropy on penetrating the wave.

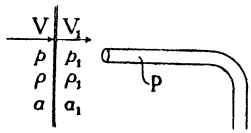

FIG. 421.

Consider unit area of the wave, and let m be the mass of air crossing this area per second. In doing work against the increase of pressure at the rate

$$pV - p_1V_1,$$

kinetic energy is lost at the rate

$$\tfrac{1}{2}m\left(V^2 - V_1^2\right)$$

and the air also loses internal energy at the rate

$$\frac{m}{\gamma - 1}\left(\frac{p}{\rho} - \frac{p_1}{\rho_1}\right),$$

by Article 30. The principle of the conservation of energy demands, therefore, that

$$pV - p_1V_1 + \tfrac{1}{2}m(V^2 - V_1^2) + \frac{m}{\gamma - 1}\left(\frac{p}{\rho} - \frac{p_1}{\rho_1}\right) = 0 \quad \text{(i)}$$

Now the increase of pressure is equal to the rate of loss of momentum per unit area, i.e.

$$p_1 - p = m(V - V_1), \quad . \quad . \quad \text{(ii)}$$

so that the loss of kinetic energy can be expressed as

$$\tfrac{1}{2}(p_1 - p)(V + V_1) = -(pV - p_1V_1) + \tfrac{1}{2}(p + p_1)(V - V_1),$$

and since

$$m = \rho V = \rho_1 V_1, \quad . \quad . \quad . \quad \text{(iii)}$$

$$V - V_1 = m\left(\frac{1}{\rho} - \frac{1}{\rho_1}\right).$$

Hence (i) reduces to

$$\tfrac{1}{2}(p + p_1)\left(\frac{1}{\rho} - \frac{1}{\rho_1}\right) + \frac{1}{\gamma - 1}\left(\frac{p}{\rho} - \frac{p_1}{\rho_1}\right) = 0 . \quad \text{(iv)}$$

This is the Rankine,* or Rankine-Hugoniot, relationship between the pressures and densities on the two sides of the wave. It readily gives

$$\frac{\rho_1}{\rho} = \frac{(\gamma - 1)p + (\gamma + 1)p_1}{(\gamma + 1)p + (\gamma - 1)p_1}, \quad \text{(v)}$$

or approximately—

$$\frac{\rho_1}{\rho} = \frac{6(p_1/p) + 1}{(p_1/p) + 6}, \qquad \frac{p_1}{p} = -\frac{6(\rho_1/\rho) - 1}{(\rho_1/\rho) - 6}.$$

The Pitot Pressure.—From (ii) and (iii),

$$p_1 - p = \rho V^2\left(1 - \frac{V_1}{V}\right) = \rho V^2\left(1 - \frac{\rho}{\rho_1}\right)$$

whence

$$M^2 \equiv \frac{V^2}{a^2} = \frac{\rho V^2}{\gamma p}$$

$$= \frac{1}{\gamma p} \cdot \frac{p_1 - p}{1 - \rho/\rho_1}.$$

* Phil. Trans. Roy. Soc., vol. 160, 1870.

On substituting for ρ/ρ_1 from (v), this gives

$$M^2 = \frac{1}{2\gamma}\left[(\gamma+1)\frac{p_1}{p} + \gamma - 1\right]. \quad . \quad \text{(vi)}$$

In like manner

$$M_1^2 \equiv \frac{V_1^2}{a_1^2} = \frac{\rho_1 V_1^2}{\gamma p_1}$$

$$= \frac{1}{2\gamma}\left[(\gamma+1)\frac{p}{p_1} + \gamma - 1\right]. \quad . \quad \text{(vii)}$$

Now, the pitot pressure P can be obtained by Articles 30 and 31 in terms of quantities on the far side of the wave as

$$M_1^2 = \frac{2}{\gamma - 1}\left\{\left(\frac{P}{p_1}\right)^{\frac{\gamma-1}{\gamma}} - 1\right\} \quad . \quad \text{(viii)}$$

since the flow between the wave and the pitot tube is isentropic. Equating (vii) and (viii),

$$\left(\frac{P}{p_1}\right)^{\frac{\gamma-1}{\gamma}} = \frac{\gamma+1}{4\gamma}\left[(\gamma-1)\frac{p}{p_1} + \gamma + 1\right]$$

and, multiplying through by $\left(\frac{p_1}{p}\right)^{\frac{\gamma-1}{\gamma}}$, we have finally *

$$\left(\frac{P}{p}\right)^{\frac{\gamma-1}{\gamma}} = \frac{(\gamma+1)^2}{4\gamma}\left(\frac{p_1}{p}\right)^{\frac{\gamma-1}{\gamma}}\left[\frac{\gamma-1}{\gamma+1}\cdot\frac{p}{p_1} + 1\right]. \quad \text{(ix)}$$

M is obtained from p_1/p by (vi). With the approximation 1·4 for γ,

$$\frac{p_1}{p} = \frac{7M^2 - 1}{6}$$

and (ix) reduces to (81), closely.

* Rayleigh, Proc. Roy. Soc., A, vol. 84, 1910.

Chapter IV

AIRCRAFT IN STEADY FLIGHT

67. Aircraft

Examples of airships have been given in Fig. 7. Heavier-than-air craft are illustrated in Fig. 43. These depend for lift entirely upon motion through the atmosphere either as a whole, as with aeroplanes, seaplanes, and flying boats, or in respect of their lifting surfaces which then have a relative motion, as with autogyros and helicopters. Description of the latter type must refer to Airscrew Theory, and so is deferred. Investigations of the present chapter are for the most part expressed in terms of the aeroplane, but apply equally to the seaplane and flying boat with modifications in detail only. Many of the principles established also apply in a general way to autogyros and helicopters.

All heavier-than-air flying depends first and foremost on the lift of wings of bird-like section, which has already received preliminary discussion (cf. Article 46) and the theory of which, the subject of later chapters, mathematically resembles that of the electric motor. The utility of wings of this kind was first realised by Horatio Phillips and their principle by Lanchester. Most aircraft avoid flapping as a matter of structural and mechanical expediency. Aircraft wings are much more heavily loaded than those of birds to improve performance and minimise structural weight. Useful flying depends acutely upon extremely light power plant. Specialised development of reliable engines has been remarkable, and large units, complete with metal airscrews of variable pitch, now weigh less than $1\frac{1}{2}$ lb. per brake h.p. It may be said that, following the work of the pioneers, high-performance flying first waited upon engine design, then upon Aerodynamics,* whilst now further improvement is equally concerned with Aerodynamics and new methods of propulsion.

No attempt is made in this book to describe the work of the pioneers of aviation; even a cursory record of their gallant and brilliant achievements would occupy much space. But in no department

* Cf. Relf, Institution of Civil Engineers, James Forrest Lecture, 1936.

were their experiences more valuable than in relation to means of control, and here especially, perhaps, may tribute be paid to the Wright Brothers. Safety in the air is a first consideration and depends notably on an inherent stability of the craft, tending to conserve any of the various forms of flight to which it may be set, and also on the provision of adequate means of control.

There has long existed a successful Theory of Stability due to Bryan and Bairstow. The layouts of the craft illustrated, in regard to the proportions and positions of the stabilising surfaces considered in conjunction with the location of the centre of gravity and the moments of inertia about the three principal axes, express a convenient and usual (though not the only) manner in which the principles established are given effect.

Control surfaces, adjustable from the pilot's cockpit, are indicated and named in Fig. 43. The *rudder*, attached to a fixed fin, gives directional control in a familiar way. Orientation of the craft in plan to the flight path is known as yaw, and angular velocity, producing a change of yaw, as yawing. Horizontal rudders, called *elevators*, are hinged to a fixed or only slowly adjustable tail plane, and control attitude or incidence to the flight path in side elevation. This is termed pitch, and angular motion that varies pitch is called pitching. The *ailerons* move differentially, rolling the craft about its longitudinal axis. A fourth control is provided by the engine throttle.

68. An aircraft cannot maintain exactly a steady state of motion. Disturbances arise from many causes and a continuous adjustment takes place through either its inherent stability or judicious use of controls by the pilot. Flight consequently proceeds in a series of oscillations or wide corrected curves. Nevertheless, whether by stability or control, uniform flight is closely approximated to for short periods under favourable atmospheric conditions. It is assumed to persist in the present chapter.

Study of an aircraft in these circumstances has for immediate objects the determination of equilibrium and control and the estimation of performance. These enquiries can quickly assume a rather complicated character, and only first principles will occupy us for the present. Early study of the elements of flight is desirable, however, to obtain a general view which will be a guide to the practical aims of the theories that follow in subsequent chapters.

Various assumptions are introduced in order to avoid detail. It is assumed, for instance, that the aircraft in straight flight has a plane of symmetry, a characteristic that can hold exactly only in the

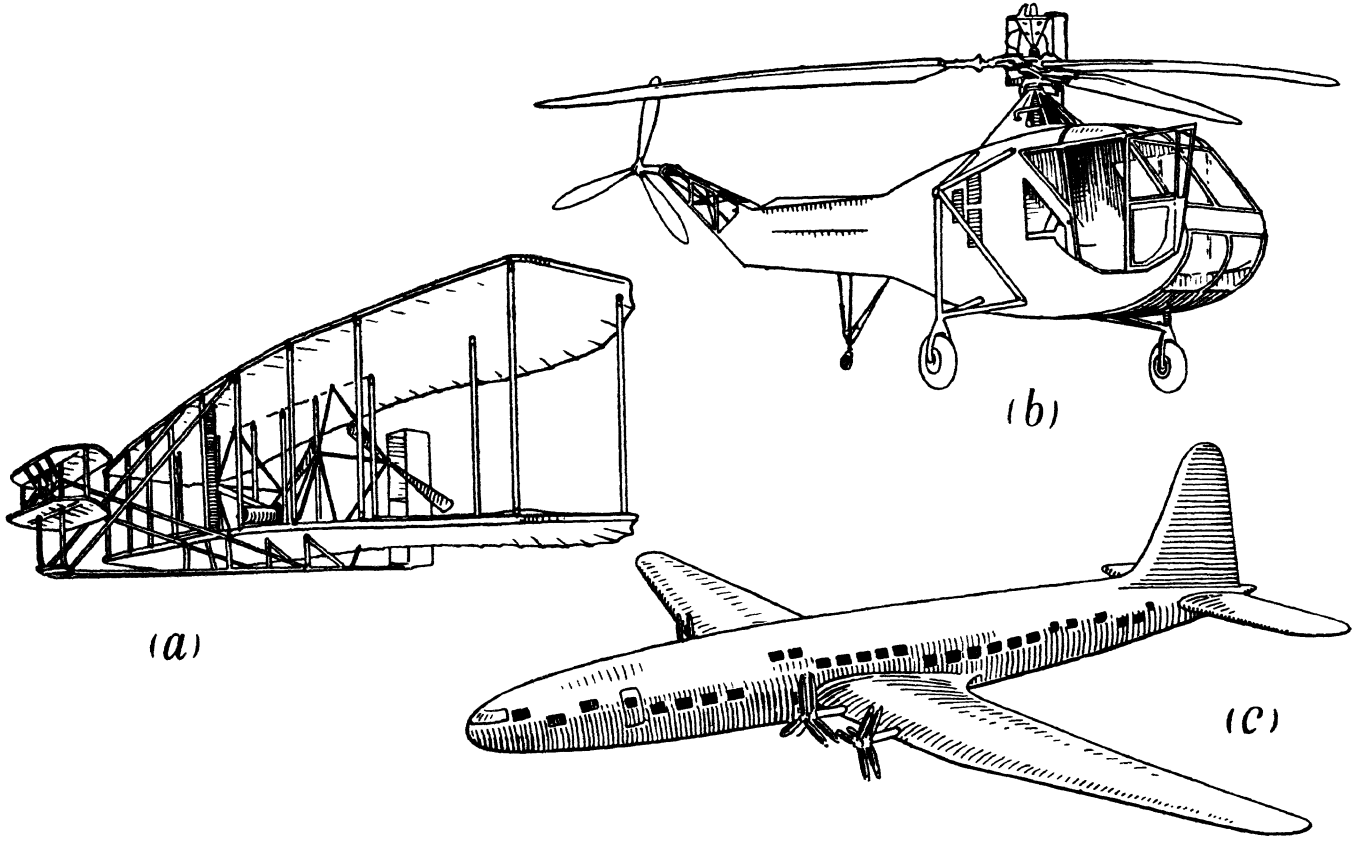
(a)
(b)
(c)

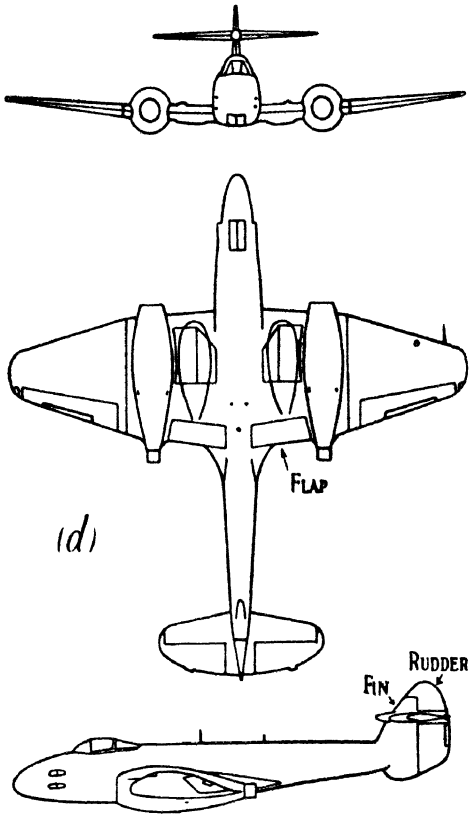

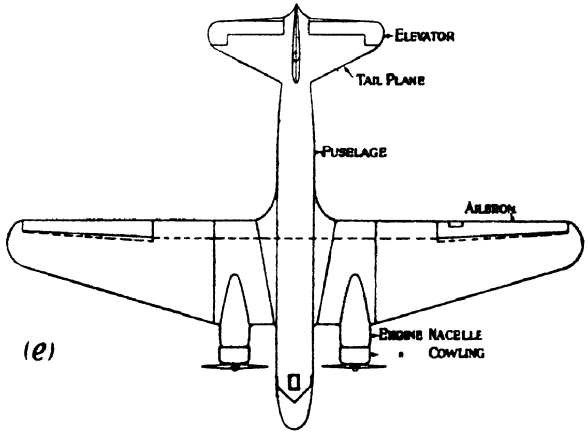

FIG. 43.—EXAMPLES OF AIRCRAFT.

(*a*) Wright Biplane. (*b*) Voight Helicopter. (*c*) One model of the Brabazon Air-liner. (*d*) Meteor jet-propelled fighter (the central view is from beneath showing flaps, undercarriage doors, etc.). (*e*) Early form of Douglas.

absence of airscrew torque. Flight in this plane is known as symmetric flight; roll, yaw, rolling, yawing, and crosswind force must all be absent. Asymmetric flight, which includes such common motions as turning and side slipping, can also be uniform.

Some simple unsteady motions are referred to briefly, but adequate study of manœuvring, and the transient air loads to which it gives rise, is postponed.

69. Except for temporary purposes, Aerodynamic lift is unnecessary for airships, and the investigation of their equilibrium and performance is consequently straightforward. The continuous generation of Aerodynamic lift by aeroplanes and flying-boats, on the other hand, results in peculiarities which have no counterpart in other forms of transport. These characteristics are implied in the standard coefficients determined from experiments on models in wind tunnels, which readily suffice to reveal the main features of aeroplane flight, and are used both in the present chapter and in technical performance calculations. But a preliminary discussion in more general terms introduces an alternative method, which, though of less technical accuracy, has the advantage of explaining the reason for the above distinguishing features.

The duty of an aircraft is to carry a large useful or disposable load from one place to another quickly and at low cost in fuel. The tare weight W_t and the drag D should clearly be minimised in comparison with the lift L, provided the true air speed V is not unduly decreased. High speed is especially necessary for aircraft, since the velocity of every head wind must be subtracted in full; and it is also their prerogative, being most economically and safely attained in their case.

Consider two series of geometrically similar aircraft, a sequence of airships and another of aeroplanes, in straight and level flight, so that in every case $L = W$, the total weight. Denote size by l, and let this be sufficiently large for the materials of construction to be used economically. Then approximately, $W_t \propto l^3$, though in practice this relationship is considerably affected by variations in requisite structural strength and by 'fixed' weights, i.e. those of components or equipment which depend little on aircraft size.

For the airships, assuming the same gas and a constant ceiling, $L \propto l^3$, whence W_t/L is approximately constant.

The lift of the aeroplanes depends on speed as well as size, but is equal to Sw, where S is the wing area and w the *wing-loading* $W/S = L/S$, in straight, level flight. Since $L/w \propto l^2$, W_t/L will be constant in their case only if $w \propto L^{1/3}$. This slow increase of wing-

loading with lift entails faster landing speeds for big aircraft, as will be investigated later, but is evidently not an unreasonable requirement within limits. It may be mentioned at once that in 1903 the loading per square foot of wing area was 2 lb. (the Wright biplane), by 1933–4 (the end of the biplane period) it had reached 15 lb., and a year or two later $\frac{1}{4}$ cwt., whilst now wing-loadings of about $\frac{1}{2}$ cwt. are in use and $\frac{3}{4}$ cwt. per square foot are contemplated. As a matter of experience, aeroplanes or flying-boats exceeding 50 tons in weight can realise as small values of W_t/L as can airships of 2–3 times the weight. Aeroplanes cannot indefinitely increase in size as, theoretically, can airships, but the disparity in gross weight between practicable airships and the largest aeroplanes capable of realising acceptable values of W_t/L is decreasing. Thus it is reasonable to compare the two types on the basis of lift.

Neglecting Aerodynamical scale effects, the drag of the airships is given by—

$$D = C\rho V^2 l^2, \quad . \quad . \quad . \quad \text{(i)}$$

where C is a non-dimensional coefficient and constant for the shape concerned. $D/L \propto \rho V^2/l$. But $\rho V^2 \propto \rho_0 V_i^2$, ρ_0 being the standard density of the air at sea-level and V_i the indicated air speed. Thus alternatively $D/L \propto V_i^2/l$. The evident advantage of increasing size arises geometrically from the linear reduction of the ratio of surface area to volume. The fact that small indicated air speeds give very small values of D/L is without interest because of head winds. The question of interest is: At what speed (if any) does D/L become prohibitively large?

Turning to aeroplanes for an answer, we have first to note that only part of their drag, called the *total parasitic drag* D_P, can be expressed in the form (i). This form is also restricted, as will be illustrated in due course, to the upper two-thirds of their speed range owing to increased form drag at the large incidences necessary for lower speeds. The remaining part of the drag, viz. the *induced drag* D_i (Article 59A), arises in a complicated manner and takes an entirely different form. Adequate investigation must be postponed, but the principle underlying its peculiar nature may readily be seen by reference to an artificial system in which the action of the wings in generating lift is represented as imparting a uniform downward velocity v to all elements of a mass m of air per second, so that $L = mv$. In the actual system, lift is derived by the same principle, but the air flown through is affected unequally.

This action communicates kinetic energy to the atmosphere at

the rate $\frac{1}{2}mv^2$, which must be equal to the rate of doing work against D_i, i.e. to D_iV, whence—

$$D_i = \tfrac{1}{2}\frac{m}{V}v^2. \quad . \quad . \quad . \quad \text{(ii)}$$

Ignoring the effects of viscosity, the velocity v is essentially residual and cannot come into being suddenly at the wings; we must assume that a pressure field, travelling with the wings, starts the mass into motion some distance in front and leaves it with the velocity v only at some distance behind. Let v' be the uniform downward velocity of the mass m in the vicinity of the wings, and assume v'/V to be small. Then another expression for the induced drag can be constructed from the reflection that it must be equal to the resolved part of the Aerodynamic force on the wings, which is sensibly equal to the lift. The alternative expression is—

$$D_i = \frac{v'}{V}L = \frac{v'}{V}mv.$$

Comparison with (ii) gives $v' = \frac{1}{2}v$, and the second expression becomes—

$$D_i = \tfrac{1}{2}\frac{v}{V}L. \quad . \quad . \quad . \quad \text{(iii)}$$

Considering change of size and speed with constant shape, the volume of air affected each second, viz. m/ρ, $\propto Vl^2$, whence (ii) can be written $D_i = \frac{1}{2}k\rho v^2l^2$, and combining with (iii) gives—

$$v = \frac{L}{k\rho Vl^2}.$$

Substituting in (iii) and writing A for $1/2k$,

$$D_i = \frac{A}{\rho V^2}\left(\frac{L}{l}\right)^2. \quad . \quad . \quad \text{(iv)}$$

When it becomes possible to take the unequal motion of the air into account, (iv) will be verified to have the correct form. Thus the formula for the total drag of each of these similar aeroplanes may be taken as—

$$D = D_i + D_P = \frac{A}{\rho V^2}\left(\frac{L}{l}\right)^2 + B\rho V^2l^2, \quad . \quad . \quad \text{(v)}$$

where A and B are constant coefficients in so far as Aerodynamical scale effects and incidence effects on form drag can be neglected.

For any aeroplane of the series, l and L are constant in straight,

level flight, and differentiation with respect to ρV^2 gives the drag to be a minimum for that aeroplane when—

$$\rho V^2 = \frac{L}{l^2}\left(\frac{A}{B}\right)^{1/2}. \quad . \quad . \quad . \quad . \quad \text{(vi)}$$

and— minimum $D = 2L\sqrt{AB}$, . . . (vii)

so that— minimum $D/L = 2\sqrt{AB}$. . . . . (viii)

It is useful to notice that, since $\rho V^2 = \rho_0 V_i^2(22/15)^2$, (vi) gives very closely—

$$V_i = 14\left(\frac{A}{B}\right)^{1/4}\left(\frac{L}{l^2}\right)^{1/2}\text{(m.p.h.)}. \quad . \quad . \quad \text{(ix)}$$

This indicated air speed for minimum drag will be denoted by V_{i0}.

Thus the essential peculiarity of an aeroplane or flying-boat as a means of transport is that minimum drag occurs at a certain intermediate speed; in other words, that D actually decreases when V increases, so long as $V_i < V_{i0}$. For a given shape of aeroplane, l^2 is proportional to the wing area, and (ix) can be written in the form—

$$V_{i0} = hw^{1/2}. \quad . \quad . \quad . \quad \text{(x)}$$

Thus we have that the minimum value of D/L is a constant for that shape, and the speed at which it is realised can be adjusted in so far as w can be varied. Subsequent calculations will show that limitations imposed on the increase of w keep V_{i0} too small for low-altitude flying, judged by modern standards of aircraft speed, though it is much larger than the speed of a 200-ton airship (about 100 m.p.h.), for which the value of D/L would be the same. Aeroplanes fly faster than V_{i0}, incurring considerably more than the minimum drag, but putting to use the whole, or part, of a large margin of engine power which must in any case be carried in order to provide for doing work against gravity at a sufficient rate to gain altitude quickly when required.

When V_i is much greater than V_{i0}, the first term on the right of (v) becomes small in comparison with the second, and the drag of aeroplanes tends to become more nearly expressible in the form (i). Assuming clean cantilever wings and rigid airship hulls, no great difference exists between the coefficients B and C specified on the surface area, but the aeroplanes have less values of D/L than would airships at such speeds because their surface area for a given lift is much smaller. A further advantage to be derived from increasing wing-loading is thus perceived.

The first term on the right of (v) predominates, on the other hand, when V_i is much less than V_{i0}; if aeroplanes could be designed to fly really slowly, their drag would become prohibitively large. Aeroplanes become inferior to airships on the present basis at speeds less than 100 m.p.h. (or 75 m.p.h., if small airships are admitted for comparison). The reason is partly that already stated and partly due to B becoming greater than C when, in order to economise in the weight of large lightly loaded wings, the clean cantilever design suitable for substantial wing-loadings gives place first to external bracing and finally to biplane design.

70. Airship in Straight Horizontal Flight on Even Keel

A rigid airship can be trimmed by movement of ballast or fuel, a dirigible balloon by transference of air between forward and aft ballonets. On an even keel there is least resistance to motion. Let this drag at velocity V relative to the wind be D, W the total weight, L' the gas lift, T the resultant thrust of the airscrews. For steady rectilinear horizontal flight—

$$W = L', T = D$$

and T satisfies—

$$\frac{TV}{550} = H$$

where H is the thrust h.p., i.e. the total b.h.p. of the engines $\times$ the efficiency of the airscrews. It is also required that no resultant couple act. The centre of buoyancy B, (Fig. 44), is above the centre

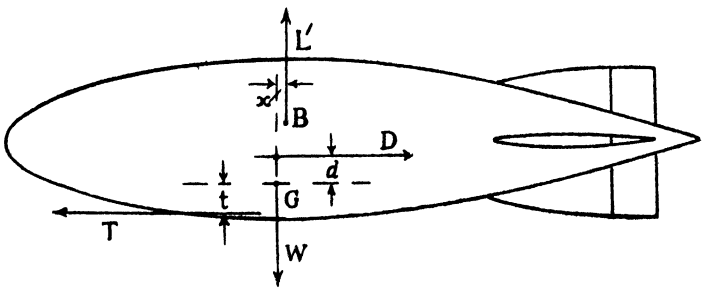

FIG. 44.

of volume of the envelope; the C.G. (G) is low, but possibly above the line of action of T; D is the sum of the drags of envelope, tail unit, gondolas, and airscrew struts, and its line of action is appreciably below the centre of volume, because the envelope and fin drag,

acting axially, constitutes only 80 per cent. of the whole. Taking moments about G and using the notation of the figure—

$$Tt + Dd - L'x = 0$$

or

$$D(t + d) = Wx.$$

If there is no tail lift, G is forward of B, but only slightly in a practical case. For example, W might be 150 tons, $t + d$ 40 ft., $T = D =$ 15,000 lb.; when $x = 1{\cdot}79$ ft., or 0·25 per cent., perhaps, of the total length.

The drag coefficient varies in a complicated manner through the very wide range of Reynolds number (R) occurring in practice (from 0 at zero speed to 6×10^8, if length of hull be used in specifying R). Direct model experiment can give only a rough estimate of full-scale drag ; this is matter for semi-empirical theory and full-scale experiment. From 15 to 25 b.h.p. per ton are usually supplied.

71. Airship Pitched

Now consider steady straight horizontal flight, but with the airship pitched nose up. Fig. 45 gives the normal pressure difference

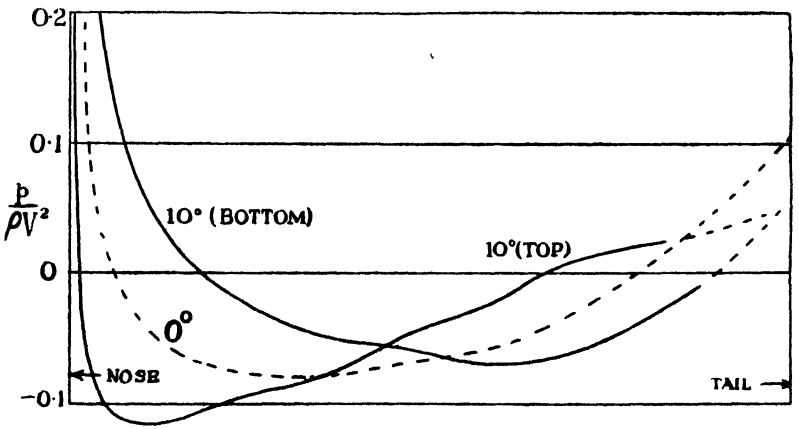

FIG. 45.—PRESSURE DISTRIBUTION ALONG AIRSHIP.

along the top and bottom of the hull of Fig. 7 (c), when level and when pitched at $\alpha = 10°$, showing Aerodynamic lift (L) in the latter case. Associated with this is an Aerodynamic pitching moment M. Referring to Fig. 46, x has increased owing to the pitch. An Aero-

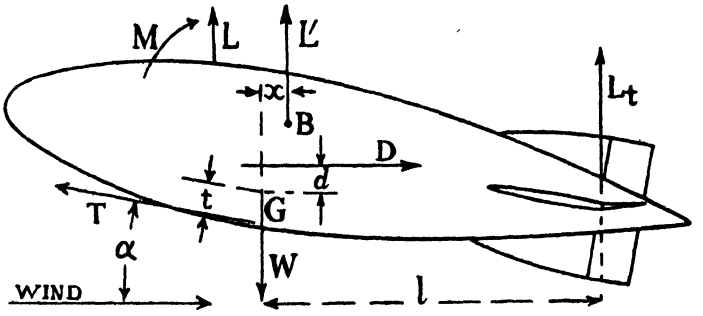

FIG. 46.

dynamic force L_t, exerted by the horizontal fins and elevators, acts at a distance l behind G, maintaining the pitch. From Fig. 46:

$$W = L' + L + L_t + T \sin \alpha$$
$$T \cos \alpha = D$$
$$Tt + Dd + M - L'x - L_t l = 0.$$

The lengths, etc., denoted by these symbols are not the same, of course, as in the preceding article, but T must satisfy the same h.p. equation as before.

With increase of α, D tends to increase, so that V must diminish. Thus L increases on account of α, but decreases on account of V, and a maximum value will evidently occur at some particular α and corresponding V, assuming the elevators to be sufficiently large to permit the last equation to be satisfied.

The airship illustrated in Fig. 7 (*c*) had $L' = 157$ tons and maximum b.h.p. = 4200; the curve of *possible* Aerodynamic lift against speed has been estimated as in Fig. 47. It appears that L may here exceed 12 per cent. of L', but the large decrease in speed will be noted. With less engine power available this maximum percentage would be less.

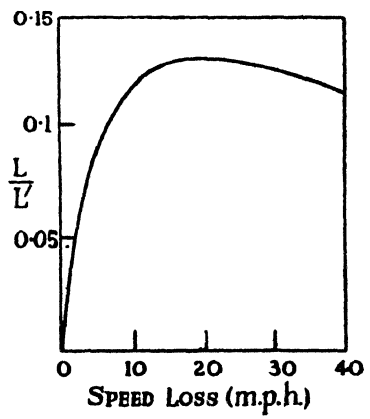

FIG. 47.

Little speed is lost, on the other hand, at a small angle of pitch, giving, for example, one-third of the maximum Aerodynamic lift. Airships fly *cabré* (tail down) commonly for three reasons: (1) decreased gas lift, resulting from either general loss of gas or consider-

able and sharp change of temperature, (2) transient overload at the beginning of a long flight due to fuel, (3) failure of a gas-bag. In the last case the shift of the centre of buoyancy may be sufficient, depending upon the fore and aft position of the fault, to prevent the elevators from holding the craft to the required pitch for equilibrium.

72. Aerodynamic Climb of an Airship

While the gas-bags remain only partly full, an airship can be steered to higher altitudes. If ballast is discharged during flight at zero pitch, the craft rises until the gas-bags fill, and an equal mass of gas is valved. Temperature lag in the gas, described in Article 17, results in slow attainment of ultimate altitude. Thus, rapid climb to a given altitude by discharge of ballast entails subsequent slow ascent, with a loss of gas that may be needless. Such waste is minimised by Aerodynamic climb, when positive pitch to the upwardly inclined flight path provides Aerodynamic lift, supporting excess ballast until the gas has time to complete expansion appropriate to the new pressure and temperature.

The conditions for steady climb at any instant are simply stated. Resolving along and perpendicular to the path, inclined at θ to the horizon—

$$L' \cos \theta + L = W \cos \theta$$
$$L' \sin \theta + T = W \sin \theta + D,$$

since L is perpendicular to the direction of motion. During such a climb L must gradually be increased, however, to compensate for decreasing gas lift. The engines now do work against gravity in respect of the excess ballast.

73. Aeroplane in Straight Level Flight

The vertical position of the C.G. of a heavier-than-air craft varies considerably with type, but longitudinal position is restricted by

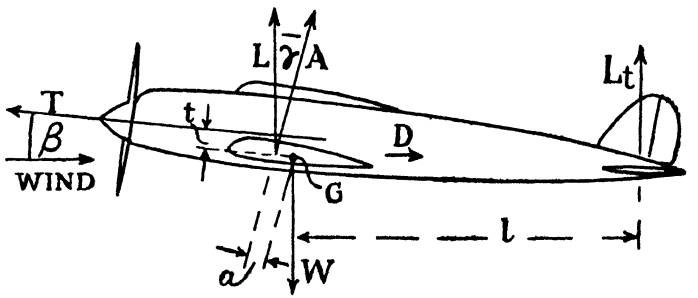

FIG. 48.

Aerodynamic conditions. In the normal case, travel of the centre of pressure, already described, leads to unstable moments about the C.G., which require to be counteracted by the tail plane.

Fig. 48 refers to a low-wing monoplane of weight W acting at G. A is the resultant Aerodynamic force on the whole craft, excluding the airscrew thrust T and the tail lift L_t. Thus, with these exclusions, L is the lift and $D = L \tan \gamma$ is the drag of the whole craft. It is assumed that crosswind force and couples about vertical and longitudinal axes vanish. Then for steady horizontal rectilinear flight at velocity V, with leverages as indicated in the figure—

$$W = L + L_t + T \sin \beta \quad . \quad . \quad . \quad (82)$$

$$T \cos \beta = D \quad . \quad . \quad . \quad . \quad . \quad (83)$$

$$Aa = L_t l + Tt \quad . \quad . \quad . \quad . \quad (84)$$

with $$T = 550\ H/V \quad . \quad . \quad . \quad . \quad (85)$$

where H is the total thrust h.p. as before.

First Approximation.—The above equations present no difficulties given adequate data, but they are complicated by technical detail. A first approximation follows the assumptions: (1) that a is small compared with l and that L_t can be neglected in comparison with L, (2) that the sum total of the lifts of all components of the craft other than the wings and tail plane can be neglected in comparison with the lift L_w of the wings, (3) that β and t may be ignored. Then the equations become:

$$W = L_w = C_L \cdot \tfrac{1}{2}\rho V^2 S \quad . \quad . \quad . \quad . \quad (86)$$

$$T = D = 550\ H/V \quad . \quad . \quad . \quad . \quad (87)$$

$$Aa = L_t l \quad . \quad . \quad . \quad . \quad . \quad . \quad (88)$$

where S is the area of the wings and C_L their lift coefficient.

In order to describe the primary characteristics of aeroplane flight, we adopt these simplified expressions together with the further approximations:

$$W = \text{const.} \quad . \quad . \quad . \quad . \quad . \quad . \quad (89)$$

$$D = D_w + D_B = \frac{L_w}{r} + D'_B \sigma \left(\frac{V}{V'}\right)^2 \quad . \quad . \quad (90)$$

where D_w is the drag of the wings according to data appropriate to a single Aerodynamic scale within the speed range of the craft, r is the lift-drag ratio of the wings only, D_B is the 'extra-to-wing' drag, i.e. the drag apart from the wings, and D'_B its value at standard density and a particular speed V', preferably within the range. It will be observed that we neglect scale effects through the flying range of scale. This applies also to the lift curve of the wings, but the

scale chosen in their case is at least that for the minimum flying speed. In (89) we ignore loss of weight through consumption of fuel. In (90) we also omit to take into account variation in airscrew slipstream effects ; these will be allowed for in estimating H.

If at constant altitude V changes from V_1 to V_2, the corresponding lift coefficients are related by :

$$\frac{C_{L2}}{C_{L1}} = \left(\frac{V_1}{V_2}\right)^2 \quad . \quad . \quad . \quad . \quad (91)$$

provided S remains constant, which with present aircraft is implied conventionally in C_L. D_{B2} follows from D_{B1} by the relation

$$\frac{D_{B2}}{D_{B1}} = \left(\frac{V_2}{V_1}\right)^2 = \frac{C_{L1}}{C_{L2}} \quad . \quad . \quad . \quad . \quad (92)$$

These expressions are independent of the shape of the wings or constancy of that shape. But resulting values of wing drag and incidence depend upon shape. If this is constant, r is conveniently read from an $r - C_L$ curve ; if it is continuously variable for changing flight, r may be read from the evolute of a family of such curves, one for each shape, but the result will express an ideal that the pilot may not quite realise in practice. Incidence is similarly determined.

Before the performance of any given aeroplane is examined, it is necessary to know S. Considerations affecting choice of area are discussed in the following three articles.

74. Minimum Flying Speed and Size of Wings of Fixed Shape

While, as is either true or implied in C_L, S remains constant, from (86) V is a minimum for a particular craft in steady level flight when $C_L\rho$ is a maximum, i.e. at low altitude when C_L is a maximum. The speed at which C_L reaches its maximum value is called the stalling speed ; further loss of speed leads to $L_w < W$ and descent occurs.

Typical examples are given in Fig. 42 of full-scale maximum values of C_L for wings of fixed shape, according to the compressed-air tunnel. Without special devices the value 1·5 for C_L is not easily exceeded, even in the case of large monoplanes for which $R = 10^7$ at minimum speed. In terms of $w = W/S$, the wing-loading already introduced, (86) becomes

$$w = C_L \cdot \tfrac{1}{2}\rho V^2 \quad . \quad . \quad . \quad . \quad (93)$$

The following table gives, for various speeds chosen as minima, approximate corresponding values of w, S, and span (on the basis of an aspect ratio of 7), for $W = 10$ tons, assuming maximum $C_L = 1{\cdot}50$.

V (ft. per sec.)	w (lb. per sq. ft.)	S (sq. ft.)	Span (ft.)
106	20·0	1120	89
80	11·4	1960	117
60	6·4	3485	156

The smallest span given may be regarded as roughly the greatest for which a reasonably light wing structure of sufficient strength could be expected without external bracing. To economise on wing weight and for other reasons it is advisable, indeed, to have $w > 20$, and often w exceeds 40 lb. per sq. ft. On the other hand, high minimum speeds lead to danger in forced landings on unprepared ground. Such comparisons lead to two general conclusions : Really low stalling speeds cannot be designed for economically in aeroplanes, seaplanes, and flying-boats. Special devices to reduce such speeds by adapting wing shape are important.

75. Landing Conditions

Reference to Fig. 42 shows that maximum C_L may require the incidence α of the wing to exceed 18°. Now $\alpha = 0$, approximately, for high speeds, when the fuselage or body should be horizontal in level flight, for low drag. The C.P. of the tail plane is usually distant 0·4 to 0·5 of the span behind the C.G. of the craft. Further, unless a nose-wheel exists undercarriage wheels must be located considerably in front of the C.G. to prevent overturning on the ground, due to running the engines at full power with wheels chocked, or applying brakes. Thus, to land at 18° would mean a high and heavy undercarriage : 13° is often the economic limit.

Fig. 49 gives $C_L - \alpha$ curves for the wing Clark YH illustrated in Fig. 34 (aspect ratio 6) for a small aeroplane (5-ft. chord) with low stalling speed (48 m.p.h.)—lower curve ; and for a larger craft of higher stalling speed—upper curve. At the greater Aerodynamic scale, C_L drops from 1·48 at 18·3° to $< 1·20$ at 13°. The lift coefficient available for landing is apparently, therefore, considerably less than the maximum.

This disadvantage may be offset by an increase that occurs in maximum C_L when a wing is in motion only a few feet above the ground. (It will be recalled that an aerofoil usually gives an appreciably greater maximum lift coefficient between the walls of an enclosed-section wind tunnel than in an open jet.) The tail plane may also contribute to lift.

A further correction exists in the hands of experienced pilots who

land aeroplanes with great skill in an unsteady motion, realising landing speeds which are often lower than designers have reason to expect and which scarcely exceed the stalling speeds.

One other point must be mentioned. At stalling speed the various Aerodynamic controls of a craft tend to become inefficient. A pilot therefore 'brings an aeroplane in,' i.e. descends preparatory to landing, considerably faster; 20 per cent. excess over stalling speed is not uncommon, when by (91) C_L would have 0·7 of its maximum value, corresponding to less than 11° incidence with the Clark YH wing, or 2° less, perhaps, than the standing angle. Speed is still high after flattening out the flight path to within a few feet above the ground. Moreover, so far removed from the stall, the lift-drag ratio is high. Little drag exists and the aeroplane tends to 'float,' i.e. to proceed a considerable distance before actually landing. Yet it is essential with high landing speeds to make contact with the ground quickly after flattening out, so that the brakes can bring the craft to a standstill within the distance prescribed by the aerodrome. It is desirable to have large drag on landing, and this, together with reduction in speed of approach and a further advantage to be described later, is conveniently effected by use of flaps.*

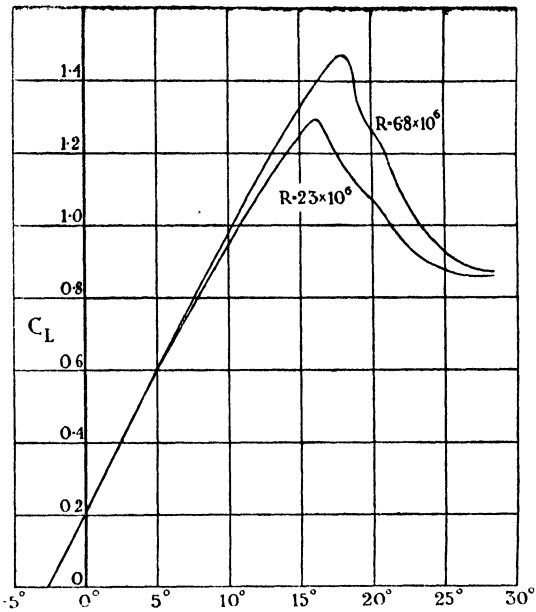

FIG. 49.—LIFT CURVES AT TWO SCALES FOR CLARK YH AEROFOIL (ASPECT RATIO 6).

76. Flaps

Wing flaps exist in many different forms. They commonly extend along the inner two-thirds or so of the span and are retracted

* The variable-pitch airscrew also provides, as one of its applications, additional and powerful means for restricting landing runs.

into the wing section except when required for landing, slow flying, or take-off. Size is specified by width expressed in terms of the wing chord, and angle by the downward rotation from the withdrawn position. Flaps should be located well aft. Several forms move aft on opening, increasing the wing area; in such cases coefficients are reckoned on the original wing area.

In an early scheme for modifying wing sections during flight, the

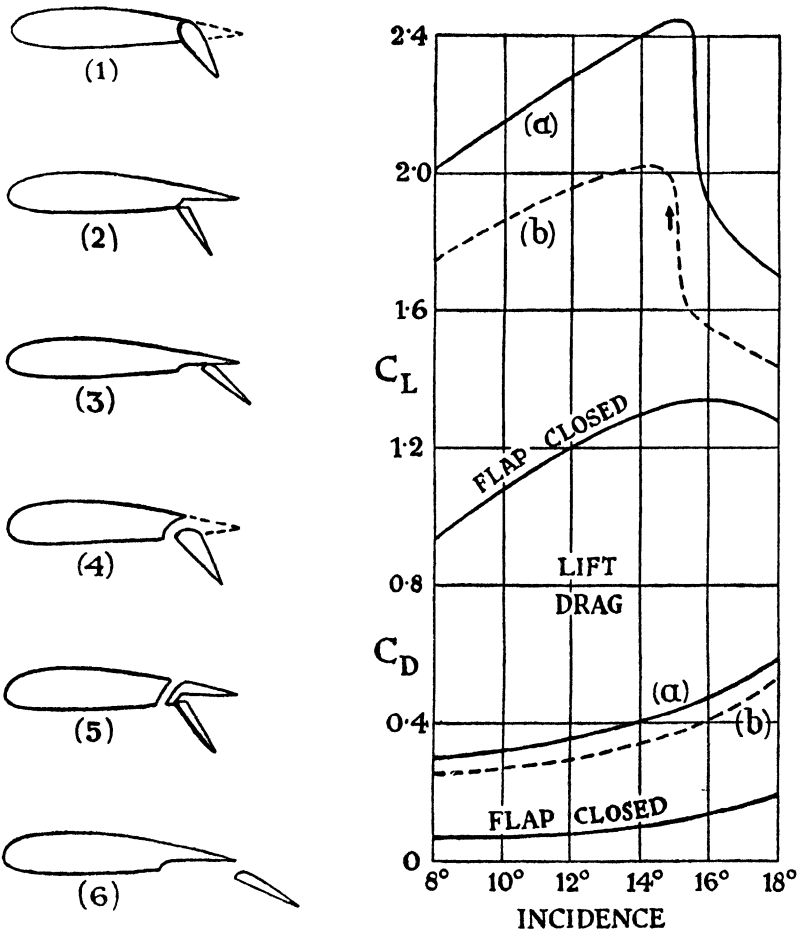

FIG. 50.—WING FLAPS OF VARIOUS TYPES.

(1) Original form; (2) Split flap;
(3) Split flap with displacement;
(4) Original form slotted;
(5) Split type slotted;
(6) Split with displacement and trailing edge slot.

C_L and C_D at $R = 1{\cdot}7 \times 10^6$:

(*a*) 20 per cent. flap type (6) at 30°.
(*b*) 20 per cent. flap type (2) at 45°. (Partial span.)

ailerons were rotated together to give maximum lift-drag ratio at each speed before differential use for control, and depressed together to assist landing. But the need to retain lateral control kept angles far too small for the attainment of large lift and drag coefficients.

This original type, (1) of Fig. 50, could be employed at large angles between the ailerons but is less effective than the 'split' flap (2) of the same figure, which was invented (Dayton Wright) in 1921 and, like most ensuing types, leaves the upper surface of the wing undisturbed. The split flap was adopted generally in 1934 and enabled much larger wing-loadings to be employed without increase of landing speeds. With its aid, the two wings of a monoplane give as much maximum lift as the four wings of an unflapped biplane, leading to greater maximum speeds by reducing skin friction and the parasitic drag of external bracing (cf. Article 69). Thus landing flaps have so far been applied to improve high-speed performance, and development tends to continue on these lines, but their reverse use is always available to produce aeroplanes that will land especially slowly.

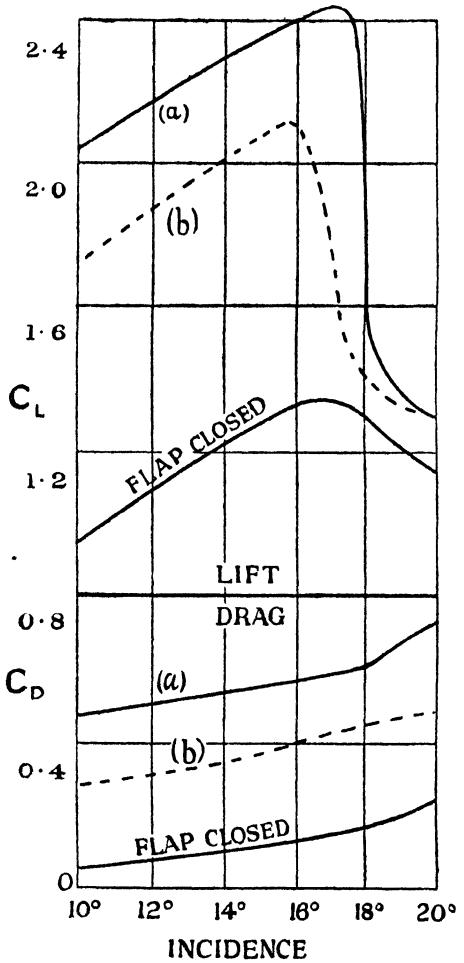

FIG. 51.—FULL-SPAN FLAPS ON CLARK YH AEROFOIL AT $R = 3{\cdot}9 \times 10^6$.
(*a*) 40 per cent. flap type (3) at 45°.
(*b*) 10 per cent. flap type (2) at 90°.

The dotted curves (*b*) of Figs. 50 and 51 relate to split flaps and show (1) a large and approximately constant increase of C_L at all flying incidences, enabling high lift to be realised without a high and heavy undercarriage, (2) little effect on stalling angle, (3) little increase of C_L beyond the stall, and (4) a great increase of drag at large flap

angles. The severe drop of lift beyond the stall can be mitigated by a so-called 'cut' slot through the wing immediately in front of the flap. Little is to be gained in lift as a rule by increasing flap angles beyond 60°–70°, but larger angles may be used to augment drag. Again, increase of width much beyond 20 per cent. of the wing chord is seldom justifiable in view of extra weight and operational difficulties.

With improved aerodromes, limitation of landing speeds is chiefly important in connection with forced landings from low altitudes, especially soon after take-off; in normal circumstances weight is much reduced by consumption of fuel before landing at the end of a journey. Hence the very high wing-loadings frequently employed for first-line aircraft present a more pressing problem in connection with take-off than with landing. For this reason flaps are commonly adjustable to give high lift and high drag for landing, with alternatively fairly high lift without undue drag for take-off. At (4) in Fig. 50 is shown a type that is more useful for take-off than for landing, a cut slot being fitted to the original form (1) and the hinge being displaced backward and downward so that the slot remains closed when the flap is not in use. At (6) is shown another form capable of adjustment for the two purposes; lift coefficients exceeding 3 have been obtained with large flaps of this type extending over the full span.

Comparison with Air Brakes.—Before flaps came into general use, air brakes of various forms were employed in addition to the mechanical brakes fitted to undercarriage wheels. The extra drag is readily seen to be small, unless the high-resistance area exposed is large. Choose an aeroplane of 5000 lb. weight with a flap as given by Fig. 51 (*b*), but extending over the inner half of the span and assumed to have one-half the effect. At 13° incidence the basic wing shape gives $r = 14$, approximately, or, while the craft is still air-borne just prior to landing, $D_w = 5000/14 = 357$ lb. With the flap, $r = 7{\cdot}8$ and $D_w = 641$ lb., an increase of 284 lb. This is independent of the speed, which depends upon the wing area S. Fix this at 75 m.p.h. with flap. Since $C_L = 1{\cdot}56$, $S = 5000/(1{\cdot}56.\frac{1}{2}\rho V^2)$ $= 222$ sq. ft. $= 7c^2$ for chord c and aspect ratio 7, so that $c = 5{\cdot}63$ ft. and the span $= 39{\cdot}4$ ft. The area of the flap $= 0{\cdot}1 \times 5{\cdot}63 \times \frac{1}{2} \times 39{\cdot}4 = 11{\cdot}1$ sq. ft., a large area for so small a craft unless continuously supported, as is possible with a flap. It is easily verified that this area would not be reduced appreciably if the flap were separated from the wing in the form of a simple air brake. For a long normal plate, free along both edges, $C_D = 1{\cdot}9$, so that for the above area

$D = 0{\cdot}95\rho V^2 \times 11{\cdot}1 = 304$ lb. at 75 m.p.h., little greater than the effective drag of 284 lb. in position.

Spoilers.—These consist of long narrow strips, projected from the forward part of the upper surface of the wings when the craft is close to the ground and ready to land. Though themselves of small area, they split the flow over the wing, causing the critical angle to occur early, partly destroying lift and greatly increasing drag. Thus the craft is let down to the ground quickly, giving wheel brakes opportunity to shorten landing run. But they do not permit the craft to be brought in slowly.

Tabs.—Tabs may be regarded as very narrow flaps which are fitted close to the trailing edges of control surfaces. Operated from the cock-pit, servo tabs enable large control surfaces to be rotated (in the opposite sense) with little effort, and trimming tabs alter the zero positions of controls. Balance tabs are linked to control surfaces to reduce operational effort in another way.

77. Power Curves

From preceding articles it appears that a maximum C_L of 2·0 is readily feasible with a large monoplane using a small flap. This will be assumed. It also appears that minimum flying speed forms a better gauge for wing area than landing speed.

Practical questions regarding aeroplane performance often lead through equations (86)–(90) to cubic equations. Graphical presentation avoids these. The process will be illustrated in the case of an aeroplane weighing 10 tons, with reciprocating engines totalling 2000 b.h.p., and having a minimum flying speed of 60 m.p.h. Extra-to-wing drag is assumed to be assessed at some high speed and to decrease, in accordance with (90), to 110 lb. at minimum speed.

TABLE VI

α (deg.)	C_L	$L/D = r$	D_w (lb.)	D_B (lb.)	D_T (lb.)	$\left(\frac{V}{V_{min.}}\right)^2$	V (m.p.h.)	Thrust h.p. required
− 1·0	0·14	13·0	1723	1571	3294	14·29	227	1990
− 0·7	0·16	15·1	1483	1375	2858	12·50	212	1620
− 0·2	0·20	18·4	1217	1100	2317	10·00	190	1170
+ 1·1	0·30	22·2	1009	733	1742	6·67	155	720
2·8	0·44	23·2	966	500	1466	4·55	128	500
7·7	0·80	18·1	1238	275	1513	2·50	95	383
10·4	1·00	15·0	1493	220	1713	2·00	85	388
13·3	1·20	12·6	1778	183	1961	1·67	77·5	405
16·7	1·40	10·8	2074	157	2231	1·43	72	426
18·3	1·48	10·0	2240	149	2389	1·35	69·5	444
19·2	1·30	6·5	3446	169	3615	1·54	74·5	717

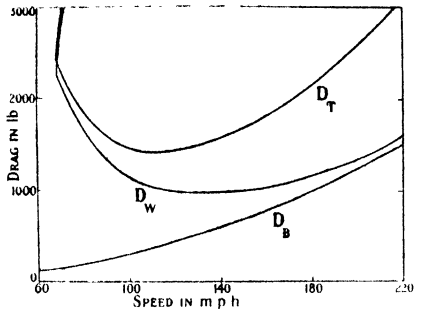

FIG. 52.

Given the first three columns of Table VI, defining the characteristics of the wings, subsequent columns are compiled from equations (89) to (92). All quantities relate to low altitude. Columns 4–6 may be evaluated before the speed, as tabulated, or afterwards. The first column is of no interest, except in locating the wings on the body and in assessing the C_L available for landing. 19·2° is beyond the critical angle.

Drag of wings (flaps closed), of body, and total drag are plotted against speed in Fig. 52. The variation of D_B is parabolic within the approximation contained in (90). D_w decreases by more than 50 per cent. while speed increases from 70 to 128 m.p.h.; subsequently it increases, at first slowly, but at high speeds quickly. At 70 m.p.h. the body contributes < 7 per cent. to the total drag, but at 220 m.p.h. it contributes 48 per cent. These results, though special to the present example, are fairly typical of modern craft of medium speed and fine lines; with low-speed craft body drag often appears in considerably greater proportion, mounting to high values at a comparatively early stage. An effect of adding D_B to D_w is to decrease the speed for minimum drag—from 128 m.p.h. to 112 m.p.h. in the present example; greater parasitic resistance would produce a greater change.

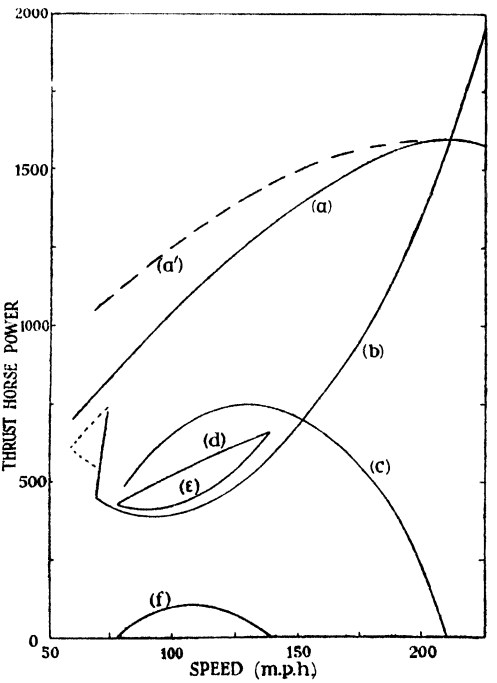

FIG. 53.

The thrust h.p. required for horizontal flight is plotted as curve (*b*) in Fig. 53. Curve (*a*) gives the thrust h.p. available from fixed-pitch airscrews, less losses through extra drag of aircraft parts within their slipstreams. The curve (*a'*) relates to constant-speed airscrews and assumes a continuously variable pitch. It will be seen that the power available at intermediate speeds is greatly reduced by a fixed pitch.

The dotted elbow in the h.p. required curve between 70 and 60 m.p.h. applies to flaps in use. There is only 100 h.p. to spare at 60 m.p.h. with a fixed pitch. It is by no means impossible for an aeroplane to have wings equal to a lower horizontal speed than the power units can manage (see p. 126).

78. Top Speed

The h.p.'s available and required are equal at 211 m.p.h., the maximum speed that can be reached under standard conditions in straight horizontal flight; if it is exceeded the craft must descend. It occurs at a small negative incidence of the wings, viz. $-0{\cdot}7°$. The lift-drag ratio of the wings is then 15—far less than the maximum; in craft of larger speed range the difference is greater.

Had only top speed been required, the first four rows of the Table would have been sufficient. Complete curves have been obtained for future reference. But to answer isolated questions it is economical to anticipate the result from inspection of the character of the craft, and then to solve graphically through a short range of speed, or, which comes to the same thing, of lift coefficient. This remark also applies, of course, to the further analysis below.

79. Rate of Climb

It has been assumed, in preparing Fig. 53, that (88) or, more generally, (84) can be satisfied at all flight speeds. Means for ensuring this will be described later. Now assume flight to be taking place at top speed and tail lift to be changed so as to satisfy (84) only at some lower speed. If steady conditions are to result, speed must decrease to an appropriate extent. If the engines are left at full throttle, they will exert more power than is required for horizontal flight and the craft will climb.

Alternatively, let the craft be flying at some speed lower than its maximum with engines throttled, full power not being required. Now let the engines be opened fully out without modifying tail lift. Speed will remain practically unchanged from the value appropriate to the tail lift, and consequently the work done per second in over-

coming drag will hardly change. Hence the additional power must produce climb.

A close approximation to the rate of climb is often obtained from the assumption that speed is the same for given incidence, whether climbing or flying horizontally. Then if H_r is the excess thrust h.p. available at a given speed over and above that required for horizontal flight at that speed, and v is the rate of climb in ft. per sec. :

$$v = 550\ H_r/W. \quad . \quad . \quad . \quad . \quad (94)$$

The reserve power is zero at maximum, and may be small at minimum speed, but it attains a large maximum at some intermediate speed with a craft of large speed range. The rate of climb is then a maximum. In Fig. 53, curve (*c*) gives the reserve power for fixed-pitch airscrews, attaining a maximum of 750 thrust h.p. at 128 m.p.h. when $v = 550 \times 750/22400 = 18{\cdot}4$ ft. per sec. Rate of climb is expressed in ft. per min. and the maximum rate of climb of the craft is 1104 ft. per min. The angle of climb is $\sin^{-1}(18{\cdot}4/187) = 5{\cdot}6°$, but this is not the maximum angle.

80. Climbing, Correction for Speed

With the simplifications already discussed, Fig. 54 shows the forces acting on an aeroplane whose flight path is inclined upwards

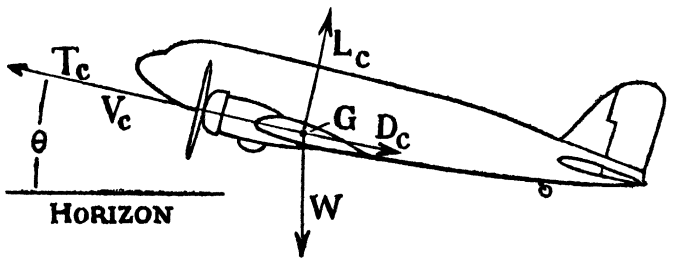

FIG. 54.

at angle θ to the horizon. Comparison will be made with horizontal flight at the same angle of incidence of the wings. Climbing conditions are distinguished by suffix *c*, and it is only assumed that weight, together with the coefficients appropriate to the constant incidence, remain unchanged. For steady climbing—

$$L_c = C_L\, \tfrac{1}{2}\rho V_c^2 S = W \cos\theta \quad . \quad . \quad . \quad . \quad (95)$$

$$T_c = 550\ H_c/V_c = D_c + W \sin\theta \quad . \quad . \quad . \quad (96)$$

It is seen that lift requires to be less than for horizontal flight at the same incidence. This means a lower speed, the relation being—

$$V_c = V\sqrt{\cos\theta} \quad . \quad . \quad . \quad . \quad . \quad (97)$$

and we have—

$$L_c/L = D_c/D = \cos\theta,$$

so that in climbing flight the thrust can be expressed as—

$$T_c = D_c\left(1 + \frac{W}{D_c}\sin\theta\right) = D\cos\theta(1 + r_a\tan\theta)$$

whence it immediately follows that—

$$\frac{H_c}{H} = (1 + r_a\tan\theta)\sqrt{\cos^3\theta} \quad . \quad . \quad . \quad (98)$$

r_a being the lift-drag ratio of the complete aeroplane at the incidence considered.

The approximate estimate of the preceding article can be written in the form—

$$H_c = H + Wv/550$$

or—

$$\frac{H_c}{H} = 1 + \frac{W}{T}\cdot\frac{v}{V} = 1 + r_a\sin\theta.$$

Hence it is a conservative estimate. The errors in H_c/H for 5°, 10°, and 15° climbing angles are 0·4, 1·2, and 3·4 per cent., respectively, for $r_a = 15$.

A difficulty is sometimes felt with the implications of (98), in that for a range of values of H_c/H there are two values of θ, while for others there is no solution. Thus, writing $H_c/H = 2$ and $r_a = 15$, we find $\theta = 4°$ or 89°, approximately. The small angle refers to flight of the kind under discussion. At the large angle the craft would be almost hovering, and would be of different form, of the type known as a helicopter, and then practical difficulties in design would prevent its taking up the corresponding horizontal flight. Thus, certain second angles given by the equation lack practical interest.

Fig. 55 gives the form of (98) for various values of r_a. Differentiating—

$$\frac{d(H_c/H)}{d\theta} = \frac{1}{\sqrt{\cos\theta}}\left[-\tfrac{3}{2}\sin\theta(\cos\theta + r_a\sin\theta) + r_a\right].$$

This is a maximum when—

$$\sin\theta(\cos\theta + r_a\sin\theta) = \tfrac{2}{3}r_a$$

or— $$\tfrac{1}{3}r_a\tan^2\theta + \tan\theta - \tfrac{2}{3}r_a = 0\ ;$$

i.e. when— $$\tan\theta = \frac{-1 + \sqrt{1 + \frac{8}{9}r_a^2}}{\frac{2}{3}r_a}.$$

It will be seen, from the figure or otherwise, that for all practical aeroplanes θ for maximum H_c/H lies between 50° and 53°, and that

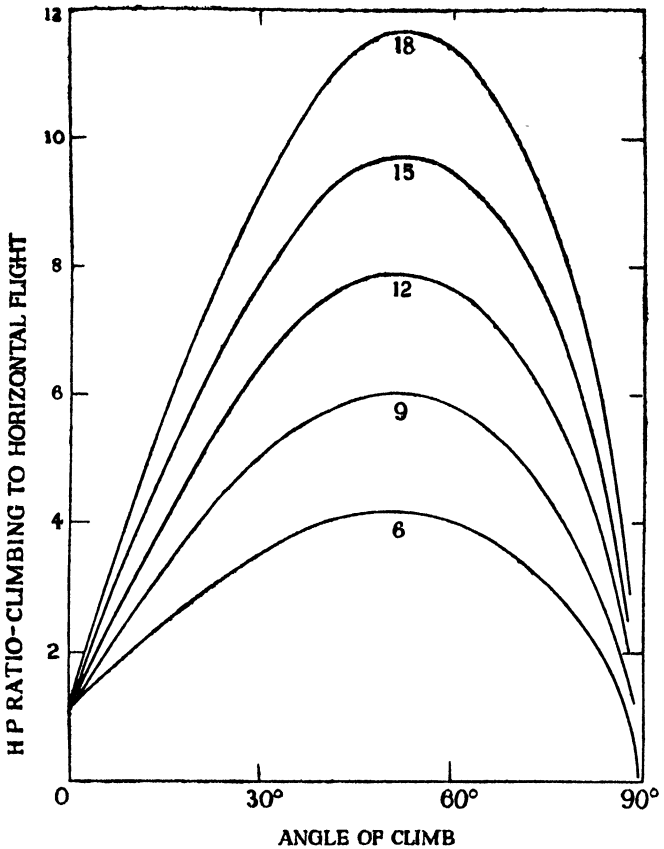

FIG. 55.—NUMBERS ATTACHED TO CURVES GIVE OVERALL LIFT-DRAG RATIOS.

maximum $H_c/H = 0{\cdot}618r_a + 0{\cdot}5$, approximately. It would be feasible to construct a craft with sufficient power to exceed this ratio. Incidence could not then be maintained and rectilinear climb result; if it were not decreased, the craft would begin a loop. With reciprocating engines, the useful load of such a craft would be very small, and one-half of the supposed power equipment considerably exceeds the economic limit with present-day aeroplanes intended for high-speed transport. On the other hand, the restriction does not apply to military aeroplanes fitted with jet or rocket propulsion. Gas turbines and jets, in course of development, will enable large angles of climb to be attained by civil aircraft.

Referring to the example of Fig. 53, and taking Fig. 52 into account, there are two speeds at which $r_a = 15$, viz. 97 and 132 m.p.h., the h.p. ratios being 2·65 and 2·35, and the climbing angles

6·3° and 5·1°, respectively. In a favourable case, variable-pitch airscrews might be arranged to give 1300 effective thrust h.p., on the present basis at the lower speed, when the h.p. ratio would be 3·4 and the angle of climb 8·9°. The direct importance of angle of climb to civil aviation is largely in connection with take-off. Reciprocating engines are sometimes boosted for short periods to provide additional power for this purpose.

81. Effects of Altitude

So far, low altitude has been assumed. If altitude be increased, air density diminishes (Article 14). Equation (86) then shows that horizontal flight at a given C_L, i.e. at a given α, can only continue on increasing V, so that ρV^2 remains constant. With this proviso, L_w, D_w and D_B are independent of altitude, ignoring modifications in coefficients due to increased Aerodynamic scale. H, however, increases as V, i.e. as $\sqrt{1/\sigma}$, where σ is the density relative to that at ground level.

Every point on a h.p. required curve (see Fig. 53) corresponds to a particular incidence. Considering the effect of increased altitude on any one such point, its ordinate and abscissa are both increased in the ratio $\sqrt{1/\sigma}$.

Had $H\sqrt{\sigma}$ been plotted against $V\sqrt{\sigma}$ in Fig. 53, one h.p. required curve would have sufficed for all altitudes. But on the basis of that figure new curves for increasing altitudes can rapidly be derived. Minimum h.p. will always occur at the same C_L, and can be plotted

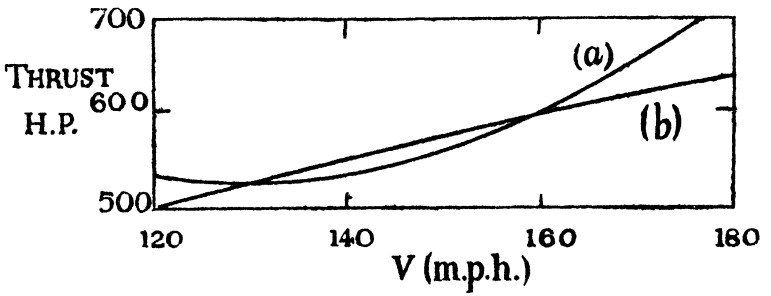

FIG. 56.

separately against altitude if desired. Part of the curve of Fig. 53 is replotted for 20,000 ft. altitude in Fig. 56, curve (*a*).

Variation of performance with altitude depends more acutely, however, on the power units. H.p. available decreases for altitudes higher than that for which the engines are supercharged more rapidly than the atmospheric pressure. Examination for a given

engine and airscrew, or for a given type, involves technical questions which will not be discussed at the present stage. But the rough formula—thrust h.p. available $\propto \sigma^{1\cdot6}$—is sufficiently representative, for present purposes, of normally aspirated engines developing full power at low altitude. The h.p. available curve of Fig. 53 has been replotted on this assumption for 20,000 ft. altitude in Fig. 56, curve (*b*).

It will be seen that, at the chosen high altitude, minimum flying speed is increased to 129 m.p.h., top speed decreased to 159 m.p.h., and rate of climb decreased to 23 ft. per min. At approximately 20,500 ft. the curves have a common tangent at 145 m.p.h.; the craft will just fly horizontally at full power at this speed; at any other it must descend. The altitude at which the rate of climb is zero is known as the absolute ceiling of the craft.

The reserve h.p. can be worked out by the above method for various altitudes less than the absolute ceiling, and a curve giving rate of climb against altitude follows. Fig. 57 gives this variation without supercharging. Since a craft approaches its absolute ceiling asymptotically, a 'service' ceiling is introduced, defined by the altitude at which the rate of climb falls to 100 ft. per min. This is 18,300 ft. in the example.

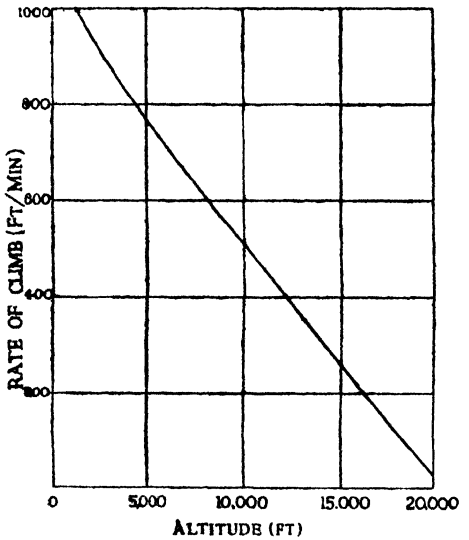

FIG. 57.

Time of Climb.—The time required by an aeroplane to climb through a given change of altitude is clearly given by—

$$\int \frac{1}{v}\, dh$$

where h denotes altitude, and limits are inserted as given. The time may be determined by plotting the reciprocal of v against h and measuring the area under the curve between the limits prescribed.

For a normally aspirated engine, however, there is substantially a linear variation of v with h, as illustrated in Fig. 57, so that—

$$\frac{dh}{dt} = v = v_0\left(1 - \frac{h}{h_1}\right),$$

h_1 denoting the absolute ceiling and v_0 the rate of climb at ground level. If t is the time from ground level to altitude h', by integration—

$$t = \frac{h_1}{v_0}\int_0^{h'} \frac{1}{h_1 - h}\,dh = \frac{h_1}{v_0}\log\frac{1}{1 - h'/h_1} \quad . \quad . \quad (99)$$

82. Variation of Load

When the disposable load carried by an aeroplane is increased, the abscissæ and ordinates of points on the h.p. required curve at any altitude both increase, the first because of the greater speed necessary at any incidence, the second partly for the same reason and also because D_w increases. Keeping incidence constant, we have $D \propto L \propto V^2$ and $H \propto V^3 \propto \sqrt{L^3}$. Consequently—

$$\frac{W}{W_1} = \left(\frac{H}{H_1}\right)^{2/3} \quad . \quad . \quad . \quad . \quad (100)$$

enabling a h.p. required curve to be derived rapidly for any new total weight. In the limit this curve will have a common tangent with the h.p. available curve, when the absolute ceiling of the craft will be at ground level. A near approach to this condition would be dangerous, since the rate of climb would be very small.

The practical case arising is concerned with the maximum permissible total weight for a minimum value of the maximum rate of climb, prescribed by local conditions or official regulations. The method of solution will be obvious. A maximum weight is first assumed from experience and parts of the h.p. required and available curves are plotted, whence an estimate follows of the probable h.p. available and incidence required in the limiting condition. An equation can then be framed in W, having one term dependent on the h.p. required for horizontal flight at the assumed incidence and a second on the prescribed rate of climb. The solution can afterwards be improved if need be.

83. Partial Engine Failure

Multi-engined aeroplanes must be designed to maintain altitude in the event of one engine failing. The worst case is that of the twin-engined craft with fixed-pitch airscrews. The h.p. available is then cut by 50 per cent., whilst also the total drag is appreciably increased by the head resistance of the useless airscrew. The drag coefficient C_D reckoned on projected blade area may be as great as 0·75, but is usually somewhat less.

Twin-engined layout has been assumed for the example of Fig. 53. For moderate airscrew drag the h.p. required with one engine out of action is represented by curve (*e*). Curve (*d*) gives that available with only one engine, and (*f*) the reserve h.p. with a fixed pitch. The maximum reserve at low altitude is 107 h.p., indicating an absolute ceiling of 5000 ft. An estimate on these lines of performance with outboard engine failure must usually, however, be reduced owing to the following consideration.

Airscrew thrust that is asymmetrical in plan leads to a yawing moment on the craft, which is balanced by an equal moment arising chiefly from a crosswind force on the rudder and fin. The resultant of the two forces is inclined across the craft in plan, so that the craft flies crabwise at a small angle of yaw. Total drag may be appreciably greater in the yawed attitude.

It is often deduced from the above that three engines provide an especially good layout. But it may be stated here that practical conditions often dictate that there shall be an even number.

84. Straight Descent at Moderate Angles

If the flight path be inclined downward at θ to the horizon, the equations of Article 80 become (suffix e denoting descent) :—

$$L_e = C_L \tfrac{1}{2}\rho V_e^2 S = W \cos\theta$$
$$T_e = 550 H_e/V_e = D_e - W \sin\theta.$$

A descent with engines on is known as a power dive. Particular solutions follow readily from power-curve analysis, but reciprocating engines must be taken into account. Maximum permissible engine revolutions are attained at a small angle of dive, and throttle must be used for steeper angles until eventually the airscrews work as powerful windmills, finally contributing a considerable fraction of the whole drag. In very steep dives the above equations are insufficient ; this case is considered in a later article.

There is a particular interest when $T = 0$, i.e. when the engines are turning just sufficiently fast to prevent the airscrews from contributing either thrust or drag, and when the angle of descent is small. The case of engines off may be included, body drag being increased on account of the airscrew blades. This form of flight is known as gliding, and the equations give

$$r_a = \cot\theta. \quad . \quad . \quad . \quad . \quad (101)$$

θ is a minimum when r_a is a maximum, corresponding to a certain incidence for a particular craft, whence the speed of this flattest glide follows. Thus, in the example of Fig. 52, airscrew thrust being

supposed zero, minimum $\theta = \tan^{-1}(1420/22400) = 3{\cdot}65°$, $C_L = 0{\cdot}50$ approximately, and V_s is only $\frac{1}{4}$ per cent. less than the speed of 112 m.p.h. indicated in the figure for minimum drag in horizontal flight. Two aspects of minimum gliding angle may be noticed. Theoretically, it can be used to determine by observation in full-scale experiment the maximum lift-drag ratio of a complete aeroplane. But difficulties appear in practice. It is not easy to ensure that $T = 0$, while also, as we shall find later, small upward trend of the wind introduces large error. In case of complete engine failure at a given altitude, minimum gliding angle determines the maximum area from which the pilot can select suitable ground for a forced landing.

Steeper descent is, of course, feasible, and there are then two incidences from which to choose, corresponding to alternative speeds for a given θ. It is desirable to be able to approach a confined landing-ground at a steep angle and a low speed while avoiding very large incidence in consideration of the comfort of passengers. For this purpose r_a must be low and C_L large at a moderate incidence, conditions which are excellently realised by using flaps.

84A. Induced-drag Method

The example of Article 77 may also be used to illustrate the utility of the formula (v) of Article 69. Remembering that minimum drag occurs when the induced drag D_i is equal to the total parasitic drag D_P, and using the data deduced in the preceding article from Table VI, each part of the total drag is equal to 710 lb. at 112 m.p.h. But for a given aeroplane in straight and level flight $D_i \propto 1/V^2$ and $D_P \propto V^2$ to the present approximation, and hence at any speed V m.p.h.—

$$D_T = D_i + D_P = 710\left[\left(\frac{112}{V}\right)^2 + \left(\frac{V}{112}\right)^2\right].$$

This formula reproduces with the following errors various values of D_T listed in Table VI :—

V (m.p.h.) :	85	95	128	155	190	212
Error (%) :	$-4\frac{1}{3}$	-1	$+\frac{1}{3}$	$-\frac{2}{3}$	-1	-4

Discrepancies are seen to be small through the major part of the speed range. An isolated investigation of the present kind by no means establishes the method, but similar examples combine to

verify that it can often be employed with fair accuracy except at large or negative incidences.

Applications of the complete formula (v) of Article 69 to matters such as those considered by other means in above articles will be evident. For example, if the total weight of an aeroplane is increased from W_1 to W_2, then the additional horse-power required for the same speed is—

$$\frac{V}{550} D_{i1} \left[\left(\frac{W_2}{W_1} \right)^2 - 1 \right],$$

D_P remaining constant provided no great increase of incidence is involved. The value of D_i at V with the weight equal to W_1 may be found as indicated above (methods of direct calculation are given in a later chapter).

85. Effects of Wind

Aircraft speeds are always to be reckoned, of course, relative to the wind. Ground speeds are obtained by adding vectorially the wind velocity, provided that it has no vertical component. The proviso is of great importance and seldom holds in practice. The presence of an upward wind inclines the lift in horizontal flight forward of the vertical, the aeroplane descending through the atmosphere, and increased speed results for the same engine power towards whatever point of the compass the aeroplane flies. One method of calculating the effect follows from Article 59. Another is as follows:

If v denote the upward component of the wind velocity, (101) shows that an aeroplane will fly horizontally with zero thrust at an incidence such that $r_a = V/v$, approximately. The magnitude of v required for sustentation can be deduced from the engine power calculated as necessary at that incidence and speed for level flight without upward wind, and any less upwind may be regarded as leaving a corresponding proportion of the power available for increase of speed. A greater upwind means that the aeroplane would climb without airscrew thrust.

Powerless Gliders.—The foregoing principle is put to use in the motorless glider. Gliders have essentially the same form as aeroplanes. But they are very lightly constructed, carry a minimum of load, and have comparatively large wings, so that wing loading is small and speed low. It is possible to realise high lift-drag ratios in their case, especially in view of the absence of engine nacelles.

Consequently, a small value of v suffices for level, or even climbing, flight. The latter is called soaring in the present case. Again, a comparatively small head-wind enables them to hover. Rising currents sufficient for soaring are found to the windward side of rising ground, and in many other circumstances, but they are especially strong and extensive through cumulus cloud, and before the cold air fronts of line-squalls; with their aid great altitudes may be gained, permitting cross-country glides exceeding 100 miles. Gliding, by which intrepid pioneers explored the possibilities of flying before the introduction of the light petrol engine, has now become a recognised sport.

It will be appreciated that observations of top speed of engined aircraft require correction for upwind if representative performance figures are required. Another assumption in foregoing articles, peculiarly affecting rate of climb, is that the horizontal wind remains constant in respect of altitude. Suppose an aeroplane climbing against a head-wind which increases (as is usual) with altitude. With constant air speed, horizontal speed relative to the ground becomes less with increasing altitude. The craft loses kinetic energy, while its potential energy is increased by the wind at a like rate. Thus the observed rate of climb is fictitiously great. Correction at altitude is easily made in this case, however, by repeating a climb downwind and taking a mean of the observed rates. The effect is of importance in the study* of the take-off of aeroplanes, and may greatly increase rate of climb near the ground.

86. Downwash

We proceed to study longitudinal balance, which has so far been assumed. Although tail-less aircraft exist, longitudinal balance is commonly secured by a tail plane fitted with elevators. These are essentially affected by downwash from the wings, however, which calls for prior consideration. Downwash is usually defined by the angular deflection of the air in a downward direction from its undisturbed direction of flow, the craft being regarded as stationary, and is denoted by ε.

It is evident that wings lift by virtue of downward momentum given at an appropriate rate to the air through which they fly. The form this superposed air flow takes is complicated and its study is deferred, but the downwash is, to a first approximation, constant

* Rolinson, A.R.C.R. & M., 1406, 1931.

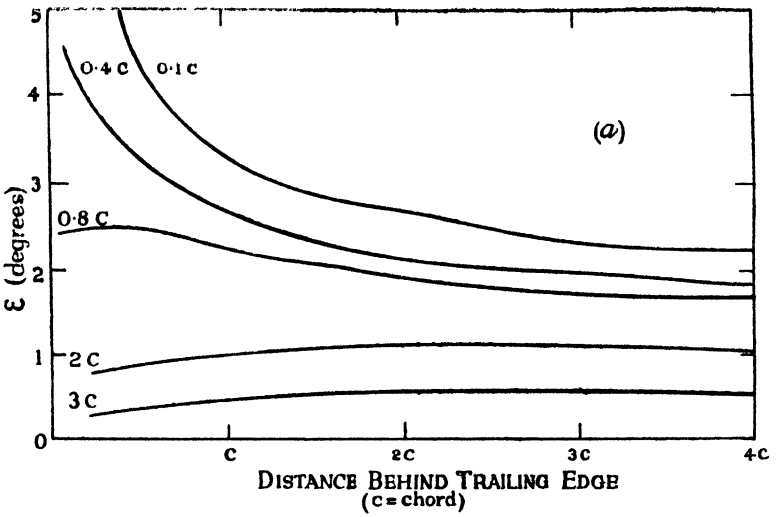

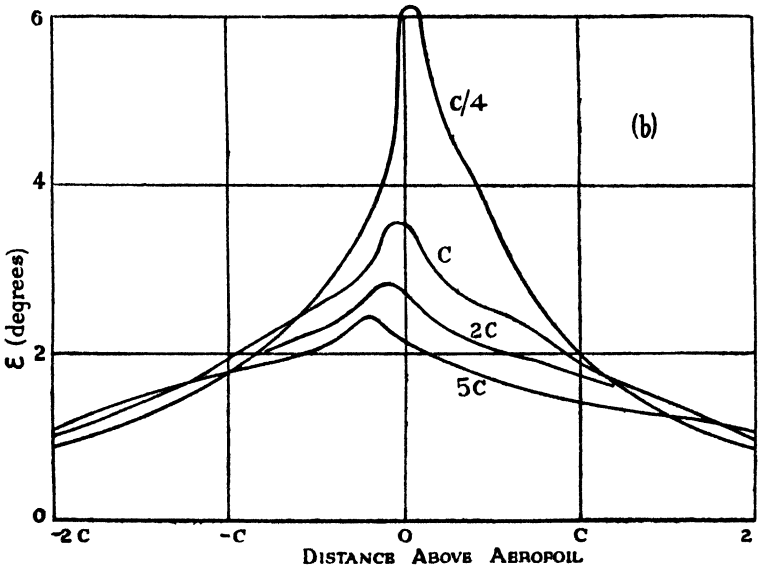

Fig. 58.—Downwash behind an Aerofoil in a Wind Tunnel, $C_L = 0{\cdot}50$.

(*a*) Numbers attached to curves give levels above trailing edge.
(*b*) Numbers attached to curves give distances behind aerofoil.

through the region occupied by a particular tail plane, if of small span, and equal to that at its centre.

Fig. 58* gives the downwash as measured in a 4-ft. enclosed-section wind tunnel in the median plane behind a thin aerofoil of 18-in. span set at 3° incidence ($C_L = 0{\cdot}50$), showing variation

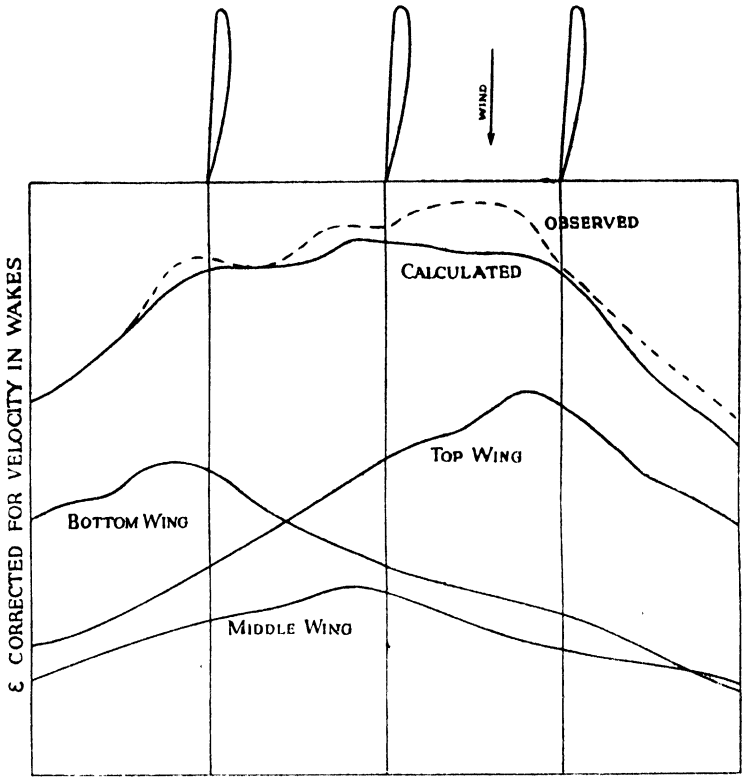

FIG. 59.—DOWNWASH 5 CHORDS BEHIND TRIPLANE IN WIND TUNNEL.

The curve marked 'top wing' applies to a monoplane aerofoil of different section (lift coefficient = C_{L_1}) occupying the position of the top wing of the triplane. The other two of the three lower curves are derived by reducing the top wing curve in proportion to the known distribution of lift between the planes of the triplane and displacing them to the levels of the appropriate planes. The curve marked 'calculated' is obtained by adding the ordinates of the three lower curves and reducing the sum by the factor: $C_{L_2}/C_{L_1} = 0{\cdot}76$, C_{L_2} being the mean lift coefficient of the triplane.

(*a*) with distance downstream at various levels above the aerofoil, (*b*) perpendicular to the span at various distances behind.

Well downstream, the distribution of ϵ is little affected by minor

* The reader already acquainted with Aerodynamics or Hydrodynamics will at once observe evidence in favour of the circulation theory of wing lift originally advanced by Lanchester, developed by Prandtl and his colleagues, and now in universal use. The observations recorded formed, indeed, some of the earliest experimental corroborations advanced in support of the theory in this country. (Piercy, *Adv. Com. for Aeronautics*, R. & M., 578, 1918.)

changes in aerofoil section, provided incidence is adjusted for constant C_L. As incidence (or, within limits, the section) changes, aspect ratio remaining constant, the downwash at any fixed point varies closely as C_L through normal flying angles. Deviation from this law occurs near the critical angle, and may also do so to a less extent close to the incidence for no lift. Given the downwash distribution for a monoplane at a known C_L, that for a biplane or multiplane wing system may be obtained by superposition, provided that the C_L of each member is known. Fig. 59* gives the results of superposition by the proportionality law, together with direct measurements made as a check.

Increase of ε occurs locally in reduced velocity wakes. The wake of a monoplane can sometimes be avoided by assigning a favourable position to the tail plane, also desirable for other reasons. But it will be seen that no reasonable position can be found that is removed from the effects of downwash.

If at some wing incidence α_0, when the downwash at the tail plane is ε_0, no lift is required from a tail plane of symmetrical section, it must be set at the angle ε_0 to the undisturbed flow, i.e. at $\alpha_0 - \varepsilon_0$ to the wing. It is not as a rule fixed to the body of an aircraft at the same incidence as the wings, and the difference is termed the tail setting angle and denoted by α_t. If wing incidence change, ε will change in the same direction, though at a less rate. Thus the effective change of incidence of a tail plane is less than the geometrical change, and area has to be increased on this account.

87. Elevator Angle

To secure longitudinal equilibrium at wing incidence α_0 at a particular angle θ of the flight path to the horizon, the tail plane and elevators provide a particular moment about the C.G. of the craft, balancing a contrary moment M_0 that arises from other parts, particularly the wings. The tail plane is at incidence $\alpha' = \alpha_0 + \alpha_t - \varepsilon_0$ to the local wind. If α_0 is inadvertently changed to α, α' becomes $\alpha + \alpha_t - \varepsilon$ and M_0 changes to M, but the tail plane has at least sufficient area to provide a force at its new incidence sufficient (taking account of leverage about the C.G.) to overcome $M - M_0$ and to right the craft to α_0. In symbols, $dM/d\alpha < -dM_t/d\alpha$, the minus being introduced because the moments are of opposite sign. Stability in regard to flight at α_0 does not necessarily follow, but the above is an important condition to that end.

If it is *desired* to change from α_0 to α, the righting moment towards

* Piercy, *Adv. Com. for Aer.*, R. & M., 634, 1919.

α_0 must be offset. This is achieved by adjusting the elevator angle (measured between the centre-lines of the fixed part of the tail plane and of the elevators) from η_0, say, to η. By this means the tail lift, positive or negative, is reduced to precisely the amount required for the new compensating moment. If now α change without change of η, the complete tail plane will right the aeroplane back to α. It will be seen that the rôle of the elevators is to work against the fixed part of the tail plane when required.

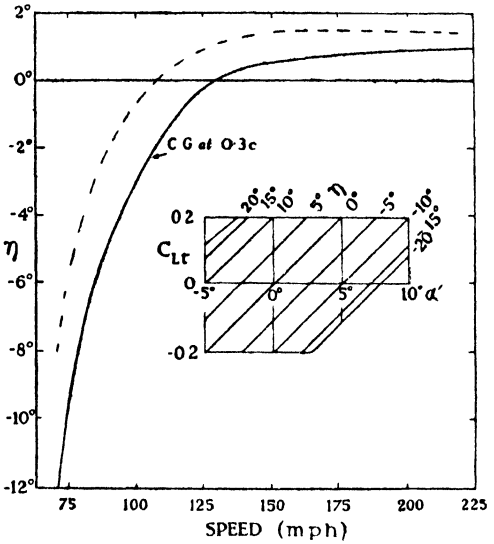

FIG. 60.—ELEVATOR CURVE.

Now α_0, α correspond to particular speeds of flight at particular values of θ. Thus the foregoing argument may equally well be expressed in terms of speed if θ remain constant.

For small values of θ we may ignore the difference between $\cos\theta$ and unity. In these circumstances we deduce that for a given craft η determines the speed of flight, while it is the airscrews and vertical wind which determine whether the craft shall fly level, or climb or descend, at this speed.

Of course, with an unstable aeroplane, both α and θ would be indeterminate, and the maintenance of any average form of flight would depend upon the skill of the pilot.

88. Example

Fig. 60 gives (inset) the lift coefficient C_{Lt} of a tail plane of aspect ratio 3, free of downwash effects, through a restricted range of incidence α' and elevator angle η. The curves would be more openly spaced with larger elevators. Increase of either α' or η results in closer spacing, until eventually the tail plane stalls.

The 10-ton aeroplane of Article 73 in horizontal flight with flaps closed is chosen to illustrate a usual method of investigating elevator angle. Lengths are referred to a plane parallel to the wing chord and passing through the C.G. of the craft. The C.P. travel in this

plane for the complete craft less tail-plane is given in the third column of Table VII, the first two columns of which are copied from Table VI. The C.G. is located at $0{\cdot}3c$ behind the leading edge of the wings of chord c, whence column 4 of the Table, x denoting the distance of the C.P. measured in the plane in the upstream direction from the C.G. No righting moment is required at 128 m.p.h., and it is chosen to have the elevators neutral at this speed.

TABLE VII

α (deg.)	V (m.p.h.)	$k_{C.P.}$	$\frac{x}{c}$	α' (deg.)	C_{Lt}	η (deg.)
− 1·0	227	0·48	− 0·18	− 2·5	− 0·078	1·1
− 0·7	212	0·45	− 0·15	− 2·3	− 0·074	0·9
− 0·2	190	0·40	− 0·10	− 2·0	− 0·062	0·7
+ 1·1	155	0·335	− 0·035	− 1·1	− 0·032	0·6
2·8	128	0·300	0	0	0	0
7·7	95	0·277	+ 0·023	+ 3·2	+ 0·056	− 3·6
10·4	85	0·272	0·028	4·9	0·086	− 5·5
13·3	77·5	0·269	0·031	6·8	0·114	− 7·9
18·3	69·5	0·266	0·034	10·0	0·154	− 12·2

The value 0·35, a theoretical result for a monoplane of aspect ratio 6, is assumed for $d\varepsilon/d\alpha$, α being the wing incidence, whence follows the column of values of α' relative to the local stream. To realise these, the tail setting angle α_t must be $-0{\cdot}8°$; for zero lift occurs with the wings at $\alpha = -3°$, so that 128 m.p.h. applies to $5{\cdot}8°$ increase of incidence, when $\varepsilon = 0{\cdot}35 \times 5{\cdot}8° = 2° =$ the incidence of the tail plane to the direction of motion, whence $\alpha_t = \alpha' - \alpha_0 + \varepsilon = -2{\cdot}8° + 2° = -0{\cdot}8°$.

S_t, the tail plane area including elevators, is taken as 13 per cent. of that of the wings. Its C.P. is assumed to be fixed and distant $l = 2\frac{1}{2}c$ behind the C.G. of the craft measured in the plane. The product of this length and S_t is called the tail volume. Further assumptions made in order to avoid unnecessary detail are that the tail plane avoids the wake of the wings; that L_t, the tail lift, may be neglected in comparison with L_w, the wing lift, so that $L_w = W$; and that moments of drags and of the airscrew thrust about the C.G. may be ignored.

We then have, taking moments about the C.G.—

$$L_w \,.\, x \cos\alpha = L_t \,.\, l \cos\alpha;$$

or—

$$\frac{W}{\rho V^2} \cdot \frac{x}{c} = \frac{L_t}{\rho V^2} \cdot \frac{l}{c};$$

or—

$$C_{Lt} \equiv \frac{2L_t}{\rho V^2 S_t} = \frac{2W}{\rho V^2} \cdot \frac{x}{c} \cdot \frac{c}{lS_t} = \frac{2Wx}{\rho V^2 m} = \frac{C_L S x}{m} \quad . \quad (102)$$

if m is the tail volume. Values of $W/\rho V^2$ are calculated immediately from Table VI, and column 6 of Table VII follows, or C_{L_t} may be calculated directly by the relation: $C_{L_t} = 3{\cdot}08 C_L \cdot x/c$.

Finally, corresponding elevator angles are found from Fig. 60 by interpolation, α' and C_{L_t} being now known. The same figure shows η plotted against speed (full-line curve). The curve is of typical shape. The tail plane gives a righting moment against disturbance at all speeds investigated, but the craft is very sensitive to longitudinal control at speeds > 150 m.p.h., when $\frac{1}{2}°$ movement of the elevators suffices to add 60 m.p.h., although 5° movement is necessary to decrease speed by the same amount. Control is still satisfactory at 70 m.p.h., but is tending to become sluggish.

89. The student is recommended to work out further examples, and should verify particularly that, although insufficient tail volume must be avoided, another very important variable is the fore and aft position of the C.G. This is nominally at the choice of the designer, but a desired position cannot always be maintained under varying conditions of loading; for instance, 2 tons of fuel might be consumed by the above craft during a non-stop flight of 1000 miles, whilst structural difficulties might prevent balancing this bulk precisely about a set C.G. Tail lift may be adjusted by trimming tabs from the cockpit to compensate for shift of the C.G. during flight or on changing disposable load. But this affects only in a secondary way the problem before the designer, which is to determine what displacement of the C.G. from its chosen position can be tolerated for a given weight, having regard to the safety of the craft—here represented by righting moment—comfort, and ease of control. The broken line in Fig. 60 gives the result of moving the C.G. farther back by 2 per cent. of the chord. Stability becomes neutral for $V >$ 150 m.p.h.

90. Nose Dive

The circumstances of an aeroplane in a very steep dive are exceptional. An interesting case is that in which the craft descends steadily at fastest speed, engines off, a condition known as the terminal nose dive. The flight path is then usually within 5° of the vertical, so that the total drag is nearly equal to the weight. The wings are nearly at the incidence for no lift, whence a first approximation to the high speed attained readily follows. But it is easily seen that L_w, the wing lift, will not exactly vanish. For if it did so there would remain a pitching moment due to the wings, which, together

with the moment of the body drag, now no longer negligible, must be balanced by a tail moment. L_w is consequently required in general to secure zero component force across the flight path.

The centre of pressure coefficient for the wings may be expressed in the form $A + B/C_L$, where A often lies between 0·22 and 0·25 and B between 0·02 and 0·10. For the very small lift coefficients concerned, the C.P. of the wings may be near or even behind the tail plane. Tail lift, L_t, may reach considerable values, and a practical interest concerned with the strength of the structure centres in determining its maximum value.

Let l be the leverage of L_t, D_T the total drag, including the windmill resistance of the airscrews, M_T the total pitching moment, excluding that of L_t. Neglecting body lift, we have—

$$W = \sqrt{D_T^2 + (L_w + L_t)^2}$$
$$M_T = L_t l \quad . \quad . \quad . \quad . \quad . \quad \text{(i)}$$

whence—

$$L_t = \frac{M_T}{l} \cdot \frac{W}{\sqrt{\{D_T^2 + (L_w + L_t)^2\}}}$$

or, dividing numerator and denominator by $\frac{1}{2}\rho V^2 S$—

$$L_t = \frac{C_{MT}}{l/c} \frac{W}{\sqrt{\left\{C_{DT}^2 + \left(C_L + \frac{C_{MT}}{l/c}\right)^2\right\}}} \quad . \quad (103)$$

c being the wing chord, by (i). Calculations to determine the maximum value proceed by assuming small increasing values for C_L. All the coefficients are expressed in terms of wing area and chord, but it must be remembered that they are composite, and include the drag and moment of drag of the body.

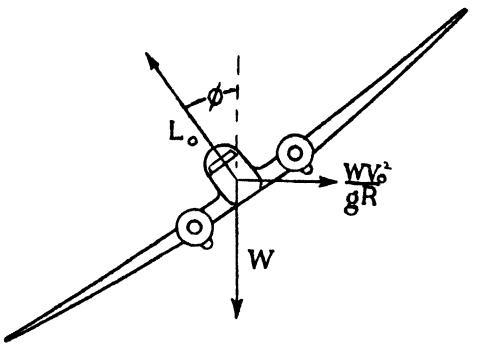

FIG. 61.

91. Circling Flight

For an aeroplane of weight W to fly uniformly at speed V_0 in a horizontal circle of radius R, lift and airscrew thrust must balance, in addition to W and the total drag D_0, a centrifugal force WV_0^2/gR. With R large, crosswind force due to flat yaw can be utilised for this purpose, the craft sideslipping, but

the normal course, necessary for smaller radii, is to bank the craft at an angle ϕ (Fig. 61), such that no sideslipping occurs. Then, if L_0 is the lift—

$$L_0 \cos \phi = W \quad . \quad . \quad . \quad \text{(i)}$$

$$L_0 \sin \phi = WV_0^2/gR \quad . \quad . \quad \text{(ii)}$$

so that— $$\tan \phi = V_0^2/gR. \quad . \quad . \quad . \quad (104)$$

But the equation— $$D_0V_0 = 550H \quad . \quad . \quad . \quad \text{(iii)}$$

must also be satisfied. For the moment we assume the further conditions regarding couples to be satisfied.

Comparing with straight horizontal flight at the same incidence and altitude, since—

$$\frac{L_0}{L} = \frac{D_0}{D} = \sec \phi = \sqrt{1 + \left(\frac{V_0^2}{gR}\right)^2},$$

$$V_0 = V\sqrt{\sec \phi}$$

and— $$\frac{H_0}{H} = \frac{D_0V_0}{DV} = \sqrt{\sec^3 \phi} \quad . \quad . \quad . \quad . \quad (105)$$

The abscissæ of points on a h.p. required curve for a particular craft in straight level flight are to be increased in the ratio $1/\sqrt{\cos \phi}$ and the ordinates in the cube of this ratio. New h.p. required curves are thus immediately constructed for increasing values of ϕ, corresponding to decreasing values of R at constant speeds.

Although h.p. required increases on turning into circling flight at the same incidence, this is due, as the equations show, to the necessary increase of speed. Comparing at constant speed, on the other hand, gives—

$$\frac{L_0}{L} = \frac{C_{L0}}{C_L} = \sqrt{1 + \left(\frac{V^2}{gR}\right)^2} \quad . \quad . \quad . \quad (106)$$

Incidence must be increased for $C_{L0} > C_L$.

The increase of power required on changing from straight and level to level circling flight at constant speed V is most readily found from (v) of Article 69. Assuming that the increase of incidence is not large, D_P remains constant while D_i increases in the ratio $(L_0/W)^2 = 1/\cos^2 \phi$. Hence the additional power is—

$$\frac{V}{550} D_i \left(\frac{1}{\cos^2 \phi} - 1\right) = \frac{VD_i}{550} \tan^2 \phi$$

$$= \frac{V^5 D_i}{550g^2R^2}.$$

D_i is the induced drag in straight and level flight at the speed concerned and may be found as already indicated.

Rewriting (i) and substituting from (104) gives—

$$C_{L_0}\tfrac{1}{2}\rho(gR\tan\phi)S = W/\cos\phi\,;$$

or—

$$R\sin\phi = k/C_{L_0},$$

k being a constant depending on wing loading and altitude. For a given craft at constant altitude the equation may appear to suggest $R\sin\phi$ to be a minimum when incidence increases on circling to the stalling angle, and then R a minimum when $\phi = 90°$. But increase of speed and drag prevent (iii) from being satisfied at a much smaller angle of bank. Thus power-curve analysis decides minimum radius of uniform turning subject to limitation of L_0/W.

Of course, the direction of motion of an aeroplane can be reversed, for instance, very quickly by using vertical bank and large incidence, but the motion is unsteady, loss of altitude and speed taking place.

During circling, one wing tip is moving faster than the other and a yawing moment arises, requiring to be balanced by the rudder. Again, the tendency to greater lift of the faster wing must be compensated by adjustment of the ailerons. Since also incidence is increased, we see that all the controls are put into use.

92. Helical Descent

Direct descent preparatory to landing is conveniently effected by flying down in a more or less vertical helix. Resolving along and perpendicular to the helical flight path, angles of bank and descent being ϕ and θ, respectively—

$$L\cos\phi = W\cos\theta$$
$$L\sin\phi = WV^2/gR$$
$$T = D - W\sin\theta,$$

where R, the radius of curvature of the path, exceeds the radius of the helix in the ratio $1/\cos^2\theta$. Compared with level circling, $\tan\phi$ is increased by the factor $\sec\theta$.

Notable effects occur when the wing incidence exceeds the critical angle. Following a slight initial disturbance, the wings may then produce a stable rolling motion about a longitudinal axis, known as autorotation, and θ and ϕ may approach 70° or 80°, the radius of the helix decreasing to a fraction of the span of the craft. This form of flight is known as the spin, and in certain circumstances may involuntarily result from stalling the wings at altitude. The matter is investigated further in the following article.

93. Rolling and Autorotation

Let a monoplane of constant chord c, flying at speed V, receive an angular velocity p about its longitudinal axis, so that the wing on

one side, beating downward, experiences a graded increase of incidence, while on the other side incidence is decreased. Consider a pair of wing-elements (Fig. 62), distant y on opposite sides of the axis. The change of incidence $\Delta\alpha$ at these positions amounts to $\pm yp/V$. For a span of $2s$ the maximum values of this quantity are $\pm sp/V$ and occur at the wing tips. Provided the new incidence at

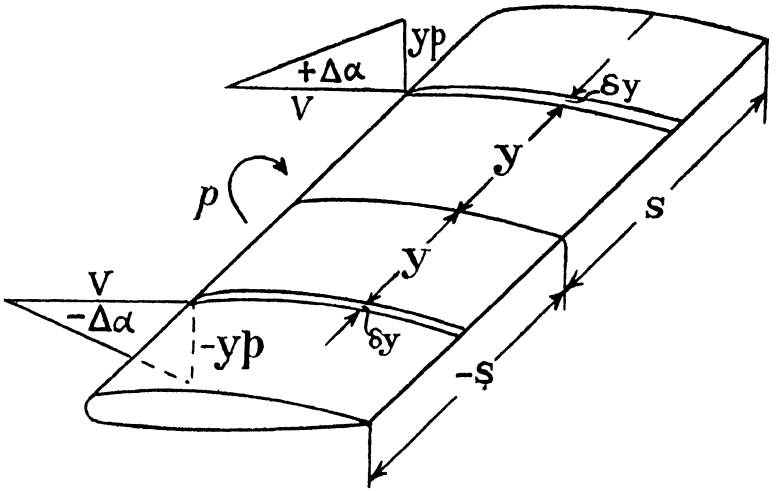

FIG. 62.

the downward-moving tip is considerably less than the critical angle, we can regard $dC_L/d\alpha$ as constant along the span to a first approximation. Then the lift coefficients of the elements at $\pm y$, originally the same, are changed by the amount $\pm (dC_L/d\alpha)(yp/V)$, giving rise to a couple :

$$\rho V^2 . c\, \delta y . \frac{dC_L}{d\alpha} . \frac{yp}{V} . y.$$

(α must be expressed in radians in this and similar expressions.) Hence, neglecting the body, we have for the whole span the couple—

$$\rho Vpc \frac{dC_L}{d\alpha} \int_0^s y^2\, dy = \tfrac{1}{3}\rho Vpc \frac{dC_L}{d\alpha} s^3. \quad . \quad . \quad (107)$$

This is seen to be of large magnitude on inserting some practical numbers, and evidently tends to damp out the rolling motion very quickly.

If, however, the monoplane is flying, prior to receiving the rolling disturbance, at a low speed and a large incidence α_0, a small value of sp suffices to invalidate the above method of calculation, and we obtain a quite different result. Let us suppose the monoplane first to be accidentally stalled, the constant incidence increasing to α_0'.

and then to receive a small p. For a lift curve of the type shown in Figs. 49 or 63, downward-moving elements will now suffer decrease of lift, while along the upward-moving wing some elements will increase their lift. Considering again two elements distant $\pm y$ from the axis, their changes of lift will now be different. Let ΔC_L be the whole difference of lift coefficient between them. The expression for the rolling moment becomes—

$$\tfrac{1}{2}\rho V^2 c \int_0^s \Delta C_L \cdot y dy,$$

which may be rewritten as :

$$\tfrac{1}{2}\frac{\rho V^4 c}{p^2}\int_0^{\frac{sp}{V}} \Delta C_L \cdot \frac{yp}{V}\, d\left(\frac{yp}{V}\right), \quad . \quad . \quad . \quad (108)$$

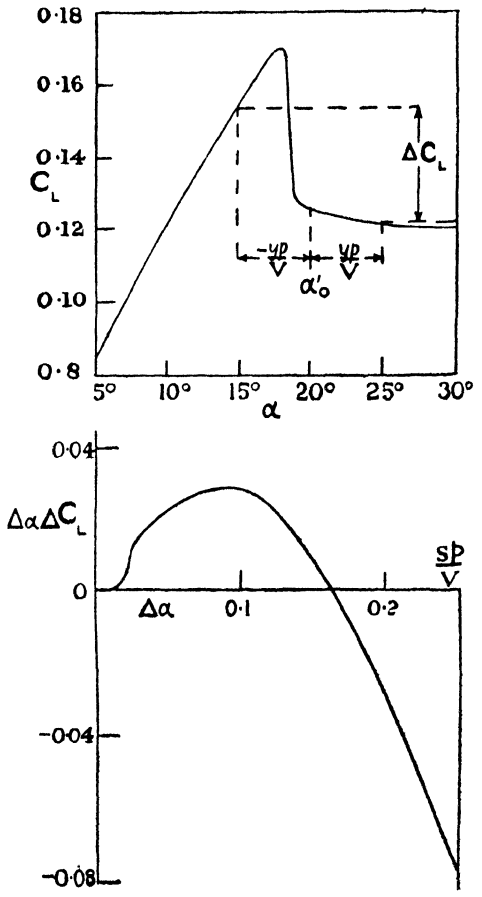

FIG. 63.

a form suitable for graphical integration. Plotting $\Delta C_L \cdot yp/V$ against yp/V, the area under the curve (Fig. 63) as far as sp/V is proportional to the rolling moment at constant p and V. As p increases for a given craft at a given speed, the couple tends still further to increase p at first, but a limit is reached when the couple is zero, the integral vanishing as is shown in the figure. This corresponds to a particular angular velocity, and the motion is evidently stable, for any further increase of p would produce a damping couple.

This striking result is readily demonstrated in a wind tunnel. An aerofoil, or model of an aeroplane, is mounted at a suitably large incidence in such a way as to be free

to rotate about an axis parallel to the wind. Slight disturbance results in the model gathering angular velocity until a certain p is reached, which it will maintain indefinitely. Timing this and comparing with the value estimated as above usually shows good agreement.

94. The Handley Page Slot

Recovery from a spin can usually be effected by decreasing incidence, and nose diving to recover speed, but at low altitudes there is no space for this manœuvre. Thus it is important to retain lateral control in case of inadvertent stalling near the ground. This insurance is admirably effected by the Handley Page slot, a false nose to the wing in front of the ailerons, which, on opening, considerably delays the stall. We are not here concerned with the theory of the working of the device, but Fig. 64 shows the effect in a particular case, the slot extending the whole length of the aerofoil. Associated with an increase of lift on opening the slot of a stalled wing there occurs also a decrease of drag. This we shall find also to be a feature of efficient lateral control, the wing that is made to rise pushing forward relative to the other, so that the craft turns in a direction natural to the bank; the yawing moment might easily have been in the opposite direction, necessitating compensation by use of the rudder.

As a result of this brief investigation, we note that delay of stall is important, though not of use in landing. The ordinary flap is liable to stall and induce autorotation. To remove this disadvantage, while retaining high drag when required, is the next step in its development

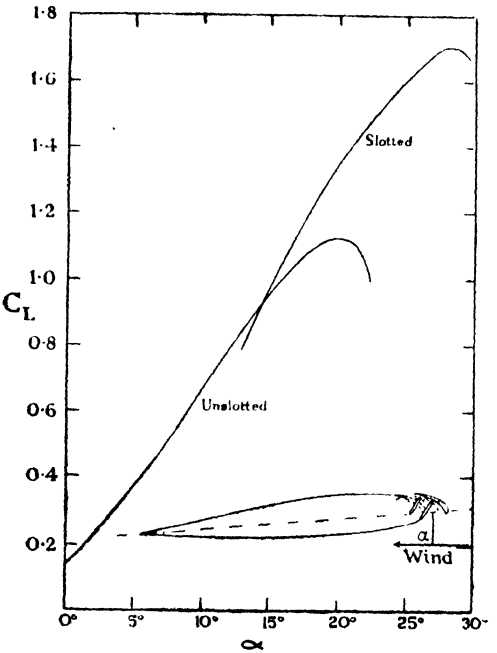

FIG. 64.—EFFECT OF HANDLEY PAGE SLOT ON LIFT CURVE.

and may be achieved by a slot system.* One form of slotted flap has already been illustrated.

95. The Dihedral Angle

A damped roll by an aeroplane at normal incidence leaves the wings banked, and, lift being inclined away from the vertical, sideslip occurs, the lower wing tip leading. Let the velocity of sideslip be v. The wings may be regarded in the result as yawed at an angle $\sin^{-1}(v/V)$, the lower wing leading, and air passes the trailing edge of the lower wing nearer to the body than it passes the leading edge. If, when span is horizontal, each wing is inclined upward towards the tip by a small angle β to the horizon, in the yaw equivalent to the sideslip the incidence of the leading wing is increased approximately by the amount $\beta(v/V)$. The incidence of the trailing wing is similarly decreased.

Considering a pair of elements of span δy distant $\pm y$ from the longitudinal axis, they give rise to a couple—

$$\rho V^2 . c\delta y . \frac{dC_L}{d\alpha} \Delta\alpha . y,$$

assuming incidence to be sufficiently small for the slope of the lift curve to be constant. Hence the total rolling couple is—

$$\tfrac{1}{2}\rho V c \frac{dC_L}{d\alpha} \beta v s^2. \quad . \quad . \quad . \quad . \quad (109)$$

The sense of this couple is clearly to right the aeroplane and stop the sideslipping. Inserting practical numbers into the expression shows the righting rolling moment to be powerful with the small values of β used (cf. Fig. 61). The above estimate tends to be excessive, in some cases by 30 per cent., owing to various neglected factors, but a slight increase of β readily makes up for any such deficiency.

The angle 2β is called the dihedral angle of the wings. As will be anticipated, it becomes of great importance in the study of stability. We shall note further here only that its magnitude requires adjusting with some care ; too large a dihedral angle results in an unstable motion of the craft.

* Cf. Nazir, *Flight*, Dec. 31st, 1936.

Chapter V

FUNDAMENTALS OF THE IRROTATIONAL FLOW

96. In Chapter II we found from experiment that the flow past bodies shaped for low resistance comprises two dissimilar parts: (*a*) a thin boundary layer, dominated by viscosity and merging into the wake; (*b*) an external motion, in which viscous effects are scarcely measurable. In (*b*) occur the important pressure changes which, transmitted through (*a*), account for part of the Aerodynamic force on the body. Investigation will now be directed towards this external flow. The fluid is assumed to be devoid of viscosity, so that at any point the pressure acts equally in all directions. It will later be proved that if an undisturbed stream of this inviscid fluid is irrotational, it will remain irrotational in flowing past an immersed body, since no tractions come into play which could generate vorticity. Thus the total pressure head given by Bernoulli's equation remains constant throughout the flow. To take account of the shape of immersed bodies, we must suppose that their surfaces are closely approached, but not so closely as to enter the boundary layer. This is tantamount to assuming that the boundary layer is everywhere very thin and that no wake exists. In the limit the fluid may be regarded as slipping with perfect ease over the surfaces of immersed bodies. The boundary condition for the idealised fluid is, then, simply that the velocity component normal to the surface vanishes. Attention is confined to two-dimensional conditions, and compressibility of the fluid is neglected.

97. The Velocity-potential

A and B, Fig. 65 (*a*), are two points in a field of two-dimensional irrotational flow parallel to the xy-plane. For the present the region is assumed to be occupied wholly by fluid. Join the points by any curve, and let the velocity q make an angle α with the element δs of this curve. Write:

$$\phi_B - \phi_A = \int_A^B q \cos \alpha \, ds \quad . \quad . \quad . \quad (110)$$

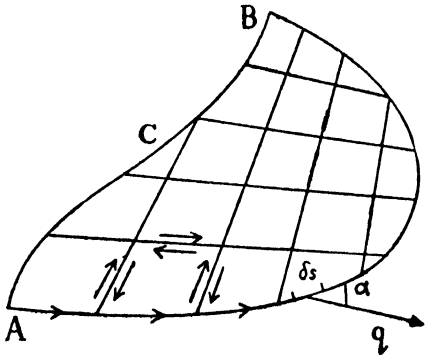

(a)

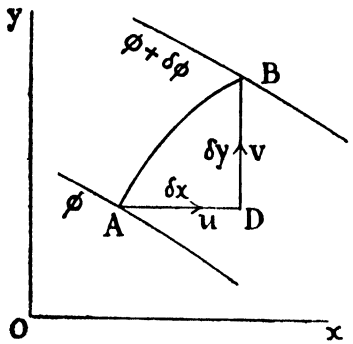

(b)

FIG. 65.

This quantity will be shown to have a unique value, independent of the curve drawn, as a consequence of the flow being irrotational.

Let ACB be another curve joining the points, and consider the line integral of the tangential velocity component once round the complete circuit ABCA. The area enclosed may, since it does not include the section of a body, be divided into a large number of small fluid parts by a fine network of lines. The circulatory velocities round the elements of area so formed will cancel at all common edges. Therefore, the circulation round the circuit equals, in the end, the sum of the circulations round all the elements enclosed. Now it is assumed that $\zeta = 0$ everywhere, so that the element-circulations all vanish separately; therefore, the circulation round ABCA is zero. Hence $\phi_B - \phi_A$ is the same whether evaluated along AB or ACB, or along any curve joining the points. Its value is therefore definite, and is called the change of velocity-potential.

If A be fixed and B moved in such a manner that $\phi_B - \phi_A$ remains constant, B will trace out a line of constant ϕ, and conversely. Thus the region of flow can be mapped out with contours of ϕ, which are known as lines of equi-velocity-potential, or, shortly, equipotentials. If zero value of ϕ be assigned to one of these lines, a numerical value follows for the velocity-potential along any other line.

Now let A and B be adjacent points not on the same ϕ-contour.

If $\delta\phi$ be the change of velocity-potential from A to B, we may calculate it along AD, DB, Fig. 65 (*b*), finding—

$$\delta\phi = u\delta x + v\delta y.$$

But—

$$\delta\phi = \frac{\partial\phi}{\partial x}\delta x + \frac{\partial\phi}{\partial y}\delta y.$$

Hence—

$$u = \frac{\partial\phi}{\partial x},\ v = \frac{\partial\phi}{\partial y} \quad . \quad . \quad . \quad . \quad (111)$$

98. Physical Meaning of ϕ

Any incompressible flow having a definite velocity-potential could be generated instantaneously from rest by a suitable system of impulsive pressures. These might be applied from the surface of a rigid body which is suddenly set in motion. At the point (x, y) in the fluid let ϖ be the impulsive pressure and u, v the velocity components immediately after the impulse. An impulse is measured by the change of momentum produced. Considering the element $\delta x\delta y$, the change of momentum parallel to x is $\rho u\delta x\delta y$, while that parallel to y is $\rho v\delta x\delta y$. The impulsive forces in these directions are, by Article 28, $-\frac{\partial\varpi}{\partial x}\delta x\delta y$ and $-\frac{\partial\varpi}{\partial y}\delta x\delta y$, respectively. Hence—

$$\rho u\delta x\delta y = -\frac{\partial\varpi}{\partial x}\delta x\delta y$$

with a similar expression for v, or—

$$u = -\frac{1}{\rho}\frac{\partial\varpi}{\partial x}$$

$$v = -\frac{1}{\rho}\frac{\partial\varpi}{\partial y}.$$

Now comparing these equations with (111), we immediately find—

$$\varpi = -\rho\phi + \text{const.} \quad . \quad . \quad . \quad (112)$$

The arbitrary constant refers to the general hydrostatic pressure, and, if ρ is given its proper value, may be neglected while the assumption of incompressible flow holds good.

This interpretation of ϕ will be of particular interest later on, but the following may be noted: (1) The equations for u and v above neglect all forces which are small compared with the very large force acting for a short time which constitutes an impulse. Viscous

stresses would be in this category. Thus the equations certainly apply *momentarily* to air. (2) Rotational motion has no velocity-potential, and could neither be generated nor brought to rest by impulsive pressures alone.

Irrotational flow is often called *potential flow.*

99. Since there is no flow along any part of a line of constant velocity-potential, streamlines cross that line everywhere at right angles. If the equi-velocity-potentials are closely mapped over a field of irrotational flow, the system of curves that cut orthogonally at all points of intersection will represent the streamlines. In Article 38 the velocity components were related to the stream function ψ by the following:

$$u = \frac{\partial \psi}{\partial y}, \quad v = -\frac{\partial \psi}{\partial x}. \qquad . \quad . \quad . \quad (113)$$

Hence—

$$\frac{\partial \phi}{\partial x}\frac{\partial \psi}{\partial x} + \frac{\partial \phi}{\partial y}\frac{\partial \psi}{\partial y} = -uv + vu = 0,$$

which expresses the above result.

If the spacing of the curves accords with equal intervals of ϕ and ψ, the resultant velocity q at any point, seen in Article 36 to be inversely proportional to the distance apart of neighbouring streamlines, will also be inversely proportional to the distance apart of neighbouring equipotentials. Mathematically, if δs, δn are elements of length of adjacent streamlines and equi-velocity-potentials, respectively,

$$q = \frac{\partial \psi}{\partial n} = \frac{\partial \phi}{\partial s} \qquad . \quad . \quad . \quad . \quad (114)$$

100. Substituting from (111) in (61) gives for the equation of continuity for incompressible flow which is also irrotational—

$$\frac{\partial^2 \phi}{\partial x^2} + \frac{\partial^2 \phi}{\partial y^2} = 0.$$

This important equation, which occurs frequently in physics and engineering, is known after Laplace. It is written for short—

$$\nabla^2 \phi = 0 \qquad . \quad . \quad . \quad . \quad (115)$$

the symbol ∇^2 standing for $\partial^2/\partial x^2 + \partial^2/\partial y^2$.

For irrotational incompressible flow Laplace's equation must also be satisfied by the stream function. For substituting from (113) in (65) gives—

$$\nabla^2 \psi = 0 \qquad . \quad . \quad . \quad . \quad (116)$$

It follows that either the ϕ-lines or the ψ-lines may be chosen as streamlines, so that if the solution of one problem of irrotational flow is known, the solution of a complementary problem also exists.

Every solution of Laplace's equation may be taken as representing an irrotational motion. But to be of practical interest the solution is additionally required to satisfy certain boundary conditions. The straightforward calculation of ϕ and ψ in a complicated case where the boundary conditions are prescribed is beyond the scope of this book. But the solutions of several simple problems are easily found. These are additive, because the equations involved are linear, and hence more complicated motions can be built up. The final result cannot as a rule be arranged exactly to comply with prescribed conditions, but for many purposes it will give a sufficiently close approximation.

101. Source

A source has no physical significance, but may be regarded as a small circular area from which fluid flows out equally in all directions in the xy-plane. Its strength is defined by the volume m of fluid, per unit length perpendicular to the xy-plane, sent out per second. The streamlines are obviously straight lines radiating from the centre of the source, and at radius r the velocity $q = m/2\pi r$ and is wholly radial. Suppose the source to be situated at the origin and choose Ox for the streamline $\psi = 0$. The flux across any curve drawn from Ox will equal that across the arc of a circle of any radius subtending the same angle θ at the centre O; this follows from there being no flow across a radial line (Fig. 66). Therefore—

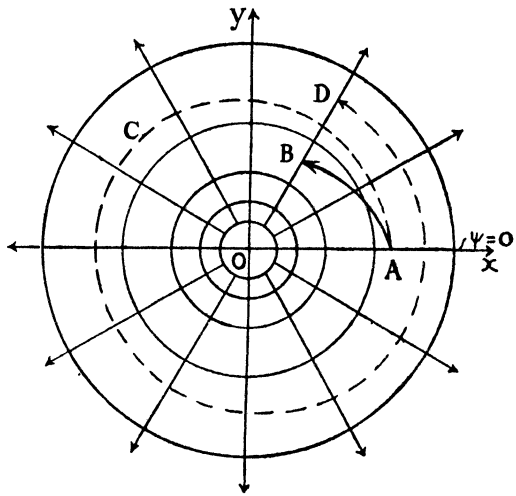

FIG. 66.

$$\psi = m\frac{\theta}{2\pi} \quad . \quad . \quad . \quad . \quad (117)$$

Evaluating (110) along any radial streamline gives—

$$\phi_B - \phi_A = \frac{m}{2\pi}\int_A^B \frac{dr}{r} = \frac{m}{2\pi}[\log r]_A^B$$

so that the equipotentials are concentric circles, as is otherwise obvious. Choosing for $\phi = 0$ the circle of radius unity—

$$\phi = \frac{m}{2\pi}\log r \quad . \quad . \quad . \quad . \quad (118)$$

For equal intervals of ψ the streamlines are inclined to one another at equal angles, and for equal intervals of ϕ the logs (to base e) of the radii will increase by a constant.

If the value of ψ (Fig. 66) is evaluated from the flux across AB, it will differ by m from the value obtained from the curve ACD. Evidently the value of ψ for any streamline may be increased or decreased by any multiple of m. The uncertainty is removed by agreeing that θ shall lie between 0 and 2π and ψ, consequently between 0 and m. Other cases will occur where, as here, the value of ψ or of ϕ is unique, except for the addition of a 'cyclic' constant.

102. Sink

Changing the sign of m in Article 101 makes the source into a sink, a point or small circular area towards which fluid is flowing equally in all radial directions in the xy-plane and at which it is supposed to be disappearing.

A three-dimensional sink is a point or small sphere, the centre of a symmetrical radial flow from all directions. The flow across all surfaces completely surrounding the point will be the same. If this is denoted by m, m is the strength of the sink, and the velocity at radius r is $m/4\pi r^2$.

Away from the immediate vicinity of the source or sink, where the large velocities attained would make untenable the assumption of incompressible flow, Bernoulli's equation applies in the simple form $p + \frac{1}{2}\rho q^2 = \text{const.}$ It is easily found that the pressure drop varies as $1/r^2$ for a two-dimensional, and as $1/r^4$ for a three-dimensional source or sink.

Application to Experiment.—Measurements of drag are often made in a stream of air which is slightly convergent in three dimensions. A close approximation to the conditions is obtained by assuming the body to be situated at a large distance r_0 from a sink. If s denotes distance downstream measured from the position of the body towards the sink—

$$q \propto 1/(r_0 - s)^2.$$

Therefore—

$$\frac{d}{ds}(r_0 - s)^2 q = -2(r_0 - s)q + \frac{dq}{ds}(r_0 - s)^2 = 0$$

or—

$$\frac{dq}{ds} = \frac{2q}{r_0 - s}.$$

But since $p + \frac{1}{2}\rho q^2 = \text{const.}$, differentiating—

$$\frac{dq}{ds} = -\frac{1}{\rho q} \cdot \frac{dp}{ds}.$$

Hence—

$$\frac{dp}{ds} = -\frac{2\rho q^2}{r_0 - s} = -\frac{2\rho q^2}{r_0} \quad . \quad . \quad . \quad (119)$$

approximately. Experiments with tunnels of parallel-walled type show $dp/ds \propto q^2$, giving r_0 constant for a given tunnel. With tunnels of the type illustrated in Fig. 26, r_0 commonly amounts to 110 × width of section.

An apparent drag arises on a body in a convergent stream. Since this drag is inwardly directed, whether the flow is assumed to be towards a sink or from a source, it can have nothing to do with Aerodynamic force; it vanishes when $r_0 = \infty$, i.e. when the stream is parallel. Article 59 (3) shows how measurements of Aerodynamic force in a convergent or divergent stream require correction for pressure gradient.

103. Irrotational Circulation round a Circular Cylinder

Interchanging the meanings of ϕ and ψ in Article 101, so that the equi-velocity-potentials become the streamlines, we have the case of fluid circulating irrotationally about a centre, and—

$$\psi = \frac{m}{2\pi} \log r, \qquad \phi = \frac{m}{2\pi}\theta,$$

where m is now a constant whose meaning it is required to investigate. The velocity q is perpendicular to r. Taken as positive in the counter-clockwise sense, it is given by—

$$q = -\frac{\partial \psi}{\partial r} = -\frac{m}{2\pi r}$$

and is constant if r is constant. Thus the circulation K round any concentric circle is

$$K = 2\pi r \,.\, q = -m, \text{ a const.}$$

The circulation round all concentric circles being the same, it follows that the circulation is the same round all circuits, of whatever shape,

which may be drawn enclosing the centre, for any such circuit is equivalent to one made up of arcs of concentric circles and of radial elements, and along the latter there is no flow. To the value of ϕ for any radial line may be added a cyclic constant as for ψ in Article 101, but the convention there mentioned is again adopted.

On approaching the centre about which the fluid is circulating, the velocity, which $\propto 1/r$, and the pressure drop, by Bernoulli's equation, both become great. Apart from other considerations we should expect to find eventually a hole in the fluid, because the general hydrostatic pressure would be insufficient to support the loss associated with the high velocity, a phenomenon known as cavitation. The condition for the centre to be formed of fluid will be discussed later under vortices. For the present we assume the centre to be isolated by a concentric circle, the trace of a circular cylinder, of sufficient radius to prevent the velocity exceeding that which is consistent with the assumption of incompressible flow when the fluid is air. If the radius of the circle is a and this circle is chosen for $\psi = 0$, then for a greater radius r—

$$\psi = -\frac{K}{2\pi}\log\frac{r}{a}. \quad . \quad . \quad . \quad (120)$$

If $a = 1$, $\psi = -(K/2\pi)\log r$.

A difficulty is sometimes experienced on a first reading in seeing the necessity for irrotational circulation to have the above form. An element of fluid circulating round the circular cylinder is in equilibrium under its centrifugal force and the radial pressure gradient. Thus, if V is its volume and r the radius of its path—

$$\rho V.\frac{q^2}{r} - V\frac{dp}{dr} = 0.$$

From (120) $q = -d\psi/dr = K/2\pi r$. Substitution leads to—

$$dp = \frac{\rho K^2}{4\pi^2 r^3}\,dr\,;$$

and on integrating—

$$p = -\frac{\rho K^2}{8\pi^2 r^2} + \text{const.}$$

Let $p = P$ when $r = \infty$. Then the const. $= P$ and—

$$P - p = \frac{\rho K^2}{8\pi^2 r^2}. \quad . \quad . \quad . \quad (121)$$

Now, because the flow is irrotational, this result must satisfy Bernoulli's equation. When $r = \infty$, $q = 0$, and we must have—

$$P + 0 = p + \tfrac{1}{2}\rho q^2.$$

On substitution this is seen to agree with the above result, explaining the form determined for the circulation.

The motion investigated is an example of what is often called cyclic flow, the cyclicity occurring in the value of ϕ. Conversely, a flow that is devoid of circulation is termed acyclic.

104. Combination of Source and Sink

The foregoing motions are supposed to be isolated. A source A together with a sink B of equal strength provide an important combined motion. Let A and B be situated on the x-axis at equal distances from the origin (Fig. 67). With A, B as centres, draw arcs

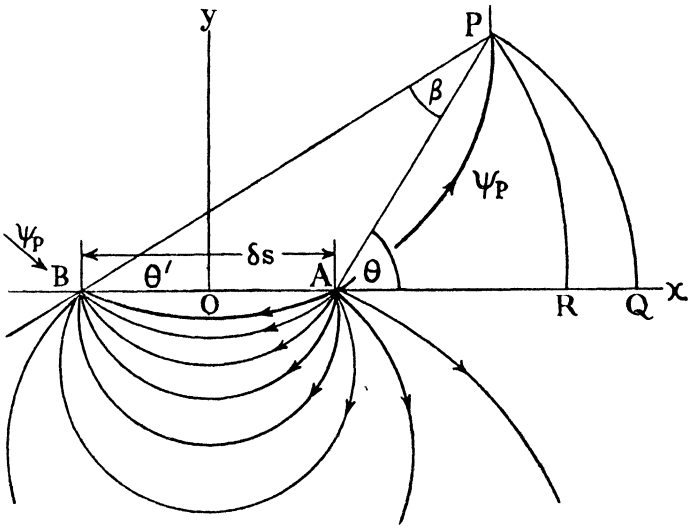

FIG. 67.

PQ, PR from any point P (x, y) to Ox, and let Ax, which is evidently a streamline, be $\psi = 0$. The flux across any line drawn from P to Ax will equal the outward flow across PQ due to A, less the inward flow across PR due to B, or—

$$\psi = \frac{m}{2\pi}(\theta - \theta') = \frac{m}{2\pi}\beta. \quad . \quad . \quad . \quad (122)$$

The streamline through P is $\beta = \text{const.}$, i.e. the circular arc joining A to B through P. Streamlines for half the field of flow are shown in the figure. The equi-velocity-potentials are the orthogonal systems of co-axial circles with A and B as limiting points. It will be noted that (122) could have been obtained by simply adding together the functions for a separate source and sink.

105. Doublet

Let A and B of the preceding article approach one another indefinitely, so that the streamlines become the family of circles touching the x-axis at the origin, as included in Fig. 71. Let m increase as AB, which we will now write δs, diminishes, so that in the limit, when δs becomes infinitely small and m infinitely great, the product $m\delta s$ remains finite and $= \mu$, say. When β is small—

$$\theta - \theta' = \tan(\theta - \theta') = \frac{y \,.\, \delta s}{x^2 + y^2 - (\frac{1}{2}\delta s)^2}$$

and as δs vanishes—

$$\psi = \frac{\mu}{2\pi \,.\, \delta s}(\theta - \theta') = \frac{\mu}{2\pi r}\sin\theta. \quad . \quad . \quad (123)$$

A source and sink combined in this way is known as a doublet of strength μ.

106. The foregoing simple motions will now be combined with a uniform stream of velocity U in the direction $-Ox$, i.e. $-U$, whose stream function is $-Uy$. The stream function of a resultant flow is immediately obtained, as explained in Article 100, by adding together the stream functions of its component parts, Laplace's equation being linear. Details of the motion may be investigated either analytically or mostly by graphical means, and the examples given will illustrate both methods.

Flow over Symmetrically Faired Nose of Long Board or Plate.—Consider a simple source at the origin added to the stream. The stream function is—

$$\psi = -Uy + \frac{m}{2\pi}\theta. \quad . \quad . \quad . \quad (124)$$

Consider the streamline $\psi = 0$. Either $y = 0$ or $\theta = 2\pi Uy/m$. Thus this streamline consists of the x-axis, together with the curve—

$$\frac{\theta}{\pi} = \frac{2U}{m}y = \frac{2U}{m}r\sin\theta. \quad . \quad . \quad (i)$$

The curve is drawn in Fig. 68. It attains maximum values of $y = \pm m/2U$, when $\theta = \pm\pi$ and $r = \infty$, i.e. at a large distance downstream. Where the curve crosses the x-axis, a stagnation point occurs, for here the velocity due to the source cancels that due to the oncoming stream, i.e.—

$$-U + \frac{m}{2\pi x_0} = 0$$

giving—

$$x_0 = \frac{m}{2\pi U}.$$

Other streamlines are shown in the figure. The method of obtaining these graphically is described in Article 107. Any of them may be replaced wholly or in part by a rigid boundary without modifying the others, because the fluid is assumed to slip without friction along a material surface. Let us choose a boundary in the position of the curved part of $\psi = 0$, and assume it to represent the shaped contour of a solid board or plate which extends infinitely in the direction $-Ox$ and also perpendicularly to the xy-plane. The streamlines internal to the curve, of which four are shown dotted, then cease to exist, and the source becomes an artifice used to calculate the external streamlines, which give the inviscid flow towards and over the nose of the board. The maximum thickness of the board is seen to be 2π times the distance of the stagnation point from the imaginary source.

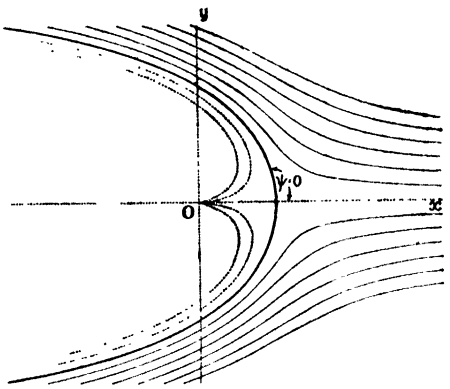

FIG. 68.

Differentiating (124):

$$u = \frac{\partial\psi}{\partial y} = -U + \frac{m}{2\pi}\frac{\partial\theta}{\partial y} = -U + \frac{m}{2\pi}\cdot\frac{\cos\theta}{r}$$

$$v = -\frac{\partial\psi}{\partial x} = -\frac{m}{2\pi}\frac{\partial\theta}{\partial x} = \frac{m}{2\pi}\frac{\sin\theta}{r}.$$

Hence, for the resultant velocity q at any point r, θ—

$$q^2 = u^2 + v^2 = U^2 + \frac{m^2}{4\pi^2 r^2} - \frac{mU}{\pi}\frac{\cos\theta}{r} \quad . \qquad \text{(ii)}$$

Substitute in Bernoulli's equation:

$$p + \tfrac{1}{2}\rho q^2 = P + \tfrac{1}{2}\rho U^2,$$

where P is the undisturbed pressure, and obtain—

$$\frac{p - P}{\rho U^2} = \tfrac{1}{2}\cdot\frac{m}{2\pi r U}\left(2\cos\theta - \frac{m}{2\pi r U}\right) \quad . \qquad \text{(iii)}$$

enabling the pressure to be found at any point. But on the boundary, i.e. over the surface of the board, $m/2\pi rU = \sin\theta/\theta$ by (i) and—

$$\frac{p - P}{\rho U^2} = \left(\frac{\sin\theta}{\theta}\right)^2 (\theta \cot\theta - \tfrac{1}{2}). \qquad \text{(iv)}$$

The pressure on the board equals P when $\theta \cot\theta = \frac{1}{2}$, i.e. when $\pm\theta = 1{\cdot}166$ radians $= 66{\cdot}8°$. From these points it increases towards the extreme nose by $\frac{1}{2}\rho U^2$, while downstream it decreases at first, but finally again approaches P.

We shall now investigate the drag D of the board. This will equal, since skin friction is excluded, the total pressure exerted by the shaped nose on the remainder. By Article 44 :

$$D = \int (p - P)\, dy.$$

The pressure difference given by (iv) is plotted against y in Fig. 69, and the area enclosed is seen to vanish. Thus the drag is zero.

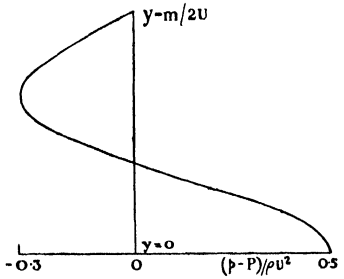

FIG. 69.

The result of zero drag is a direct consequence of Bernoulli's equation applying exactly throughout the fluid, so that the fluid loses no mechanical energy. But the pressure-drag of the nose of a board shaped in this way would be expected to be small with air as fluid and with the real boundary condition of absence of slip ; a drag would exist, but this would approximate to the skin friction. In the present example the pressures given by (iv) would, at least as far along the board as the points of minimum pressure, differ little from those which would be transmitted through the boundary layer in experiment. For a board of finite length, if the section were sufficiently long, the presence of a tail would not greatly modify the pressures near the nose. Thus the distribution found approximates to that existing over the fore-part of a symmetrical tail plane.

The x-axis beyond the stagnation point, together with the part of the curve of $\psi = 0$ to one side of the axis, might be chosen alternatively as boundary. Half the field of flow would then approximate to the flow of a uniform wind from a plain or sea over a cliff of the section bounded by the curve. The application of this interesting interpretation to motorless gliding is developed in the late Mr. Glauert's *Aerofoil and Airscrew Theory*. Again, if the external streamlines be ignored, we have the case of flow from a source

within a barrier, circumscribing the whole flow from the source. Since the expanse of fluid is infinite in the complete problem, the flow far downstream must be uniform and of velocity U. Hence, the maximum width of the barrier is m/U as before.

107. Oval Cylinder

Assume a source and sink situated on the x-axis, the source at $x = +s$, the sink at $x = -s$. Combining with uniform flow in the direction Ox, we have—

$$\psi = -Uy + \frac{m}{2\pi}\beta. \quad . \quad . \quad . \quad (125)$$

This problem will be developed by the graphical method.

The streamlines of the combined source and sink and of the uniform flow are known. Superpose these as shown in the lower half of Fig. 70, attaching to each streamline its value of ψ. The

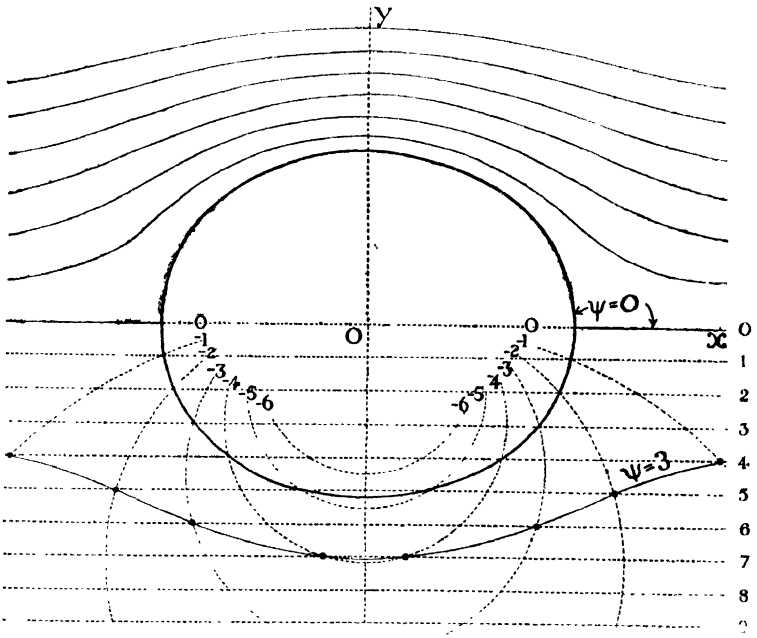

FIG. 70.—ABOVE: STREAMLINES FOR POTENTIAL FLOW PAST OVAL CYLINDER. BELOW: GRAPHICAL CONSTRUCTION.

closeness of packing of either set for equal intervals of ψ is open to choice, but, together with the distance $2s$, controls the final form of the streamlines. At any point of intersection the value of ψ equals

the sum of the two values of ψ of the streamlines crossing at that point. Draw a smooth curve through all points of intersection that give in this way a constant resultant value of ψ, and repeat the process for different constant values. Then the curves obtained are the resultant streamlines, shown in the upper half of the figure.

The streamline $\psi = 0$ consists of the x-axis, excluding the length $2s$, together with the oval curve shown. A set of streamlines internal to this oval are ignored. Substituting a rigid boundary for the oval, it becomes the contour of the section of a cylinder. The condition determining the position of the front stagnation point occurring on the axis Ox is that the sum of the velocities due to the stream, source, and sink vanishes, i.e. if it is distant x_0 from the origin—

$$-U + \frac{m}{2\pi}\left(\frac{1}{x_0 - s} - \frac{1}{x_0 + s}\right) = 0$$

or—

$$x_0 = \pm s\sqrt{1 + \frac{m}{\pi U s}}.$$

The condition fixes also a back stagnation point situated at an equal distance on the other side of the origin.

The ratio of the length of the section to its maximum width across the stream is known as the fineness ratio. The flow past cylinders of different fineness ratios is obtained by varying the quantity m/Us. Cylinders of elliptic section are treated in Articles 117 and 125. The case of a cylinder of oval section moving broadside-on appears in Article 149.

108. Circular Cylinder

A doublet of strength μ fixed at the origin with its axis (the line joining the source to the sink) in the direction $-Ox$, together with uniform streaming of velocity $-U$, gives for the combined motion—

$$\psi = -Uy + \frac{\mu}{2\pi}\frac{\sin\theta}{r} = -Uy\left(1 - \frac{\mu}{2\pi r^2 U}\right). \quad . \quad (126)$$

Putting $\psi = 0$, we have for that streamline either $y = 0$ or $r = \sqrt{\left(\frac{\mu}{2\pi U}\right)}$, a const. $= a$, say. Thus a circle of radius a with centre at the origin is a streamline. Let this be a boundary and ignore the internal motion. Then the streamlines obtained from (126), or by the graphical method of the preceding article, give the

flow past a long circular cylinder (Fig. 71), where are also shown the streamlines for the doublet alone. (126) becomes—

$$\psi = -U\left(r - \frac{a^2}{r}\right)\sin\theta \quad . \quad . \quad . \quad (127)$$

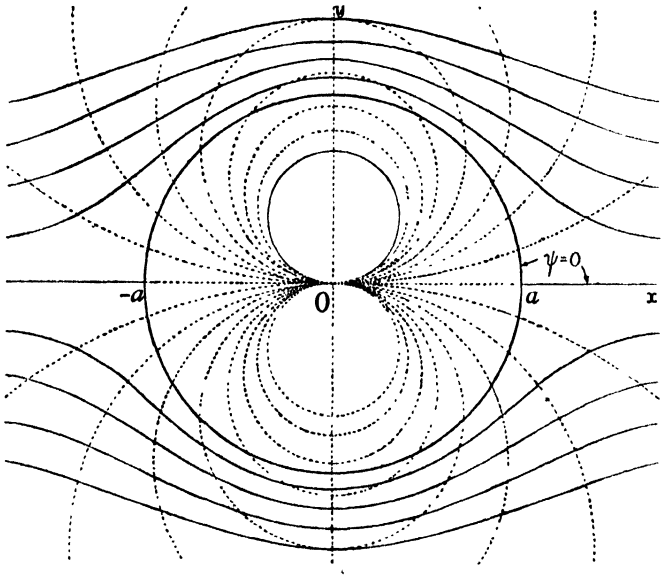

FIG. 71.—POTENTIAL FLOW PAST CIRCULAR CYLINDER.
Dotted : streamlines for doublet.

To obtain the velocity q_a round the periphery, we have—

$$q_a = \left[-\frac{\partial\psi}{\partial r}\right]_{r=a} = \left[U\left(1 + \frac{a^2}{r^2}\right)\sin\theta\right]_{r=a}$$
$$= 2U\sin\theta \quad . \quad . \quad . \quad . \quad (128)$$

giving stagnation points when $\theta = 0$ and π, i.e. where the circle cuts the x-axis. From Bernoulli's equation the difference between the pressure at any point on the surface of the cylinder and P, the undisturbed pressure, is—

$$\frac{p - P}{\rho U^2} = \tfrac{1}{2}\left(1 - q_a^2/U^2\right) = \tfrac{1}{2}\left(1 - 4\sin^2\theta\right). \quad . \quad (129)$$

The variation round the cylinder is plotted in Fig. 72, together with some experimental measurements. There is fair agreement over

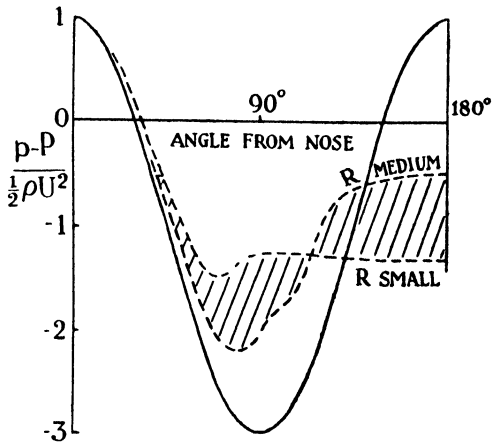

FIG. 72.—NORMAL PRESSURE ROUND CIRCULAR CYLINDER.

Hatched area includes experiments with R ranging from 2×10^4 to 2×10^5. Original papers should be consulted for variation in experimental data.

the front part of the cylinder which may be extended at greater Reynolds numbers, but a real fluid breaks away. From considerations of symmetry it is apparent at once that the drag for irrotational flow is zero. Thus the present theory gives no help in calculating the drag of a cylinder. Nevertheless, we shall find important uses for the above results.

109. Circular Cylinder with Circulation

On adding a counter-clockwise circulation K round the cylinder of the preceding article we obtain from (120)—

$$\psi = -U\left(r - \frac{a^2}{r}\right)\sin\theta - \frac{K}{2\pi}\log\frac{r}{a} \quad . \quad . \quad (130)$$

The tangential velocity at $r = a$ now comes to :

$$q_a = \left[U\left(1 + \frac{a^2}{r^2}\right)\sin\theta + \frac{K}{2\pi r}\right]_{r=a} = 2U\sin\theta + \frac{K}{2\pi a} \quad . \quad (131)$$

and for the pressure on the surface—

$$\frac{p - P}{\rho U^2} = \tfrac{1}{2}\left(1 - 4\sin^2\theta - \frac{2K\sin\theta}{\pi a U} - \frac{K^2}{4\pi^2 a^2 U^2}\right) \quad . \quad (132)$$

The stagnation points no longer lie on a diameter, but approach one another, being situated (if they remain on the surface of the cylinder) at points given by $q_a = 0$ or

$$\sin\theta = -\frac{K}{4\pi a U} \quad . \quad . \quad . \quad (133)$$

an important result. When $K = 4\pi aU$, $\sin\theta = -1$ and they coincide on the bottom of the cylinder. If K/U be further increased, (133) does not apply; they still coincide on the axis of y, but occur in the fluid. The streamlines in the latter case are shown in Fig. 73, S being the stagnation point. The fluid between the cylinder and the loop encircling it from S circulates continuously round the cylinder, failing to pass downstream. The streamlines for a much smaller value of K/U are given in Fig. 74.

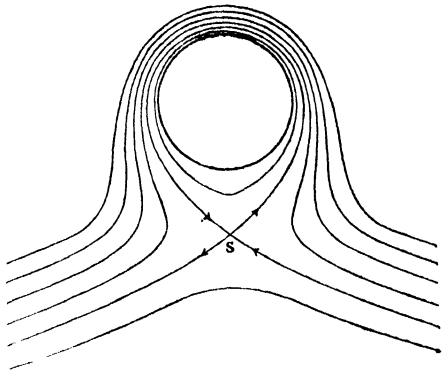

FIG. 73.—POTENTIAL FLOW PAST CIRCULAR CYLINDER WITH STRONG CIRCULATION.

It is again obvious from symmetry that the drag is zero. But the pressure is less on the upper half of the section than it is on the lower half. It is immediately found from (132), for example, that if p_1 be pressure at the top of the cylinder and p_2 that at the bottom:

$$\frac{p_2 - p_1}{\rho U^2} = \frac{2K}{\pi aU} = \frac{4q'}{U}$$

denoting by q' the velocity at $r = a$ of the circulation alone. Consequently, a lift L arises. To find this we note that the lift δL of an element δs ($= a \,.\, \delta\theta$, Fig. 75) of the contour is $-(p - P)\, a\delta\theta \sin\theta$, so that on substituting for $p - P$ from (132) and integrating with regard to θ between the limits 0 and 2π, all integrals except that derived from the third term of the R.H.S. of the equation vanish, since they contain $\sin\theta$ to an odd power. Hence:

$$L = \frac{\rho UK}{\pi}\int_0^{2\pi} \sin^2\theta\, d\theta = \rho UK. \quad . \quad (134)$$

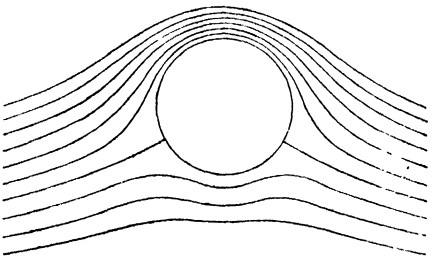

FIG. 74.—POTENTIAL FLOW PAST CIRCULAR CYLINDER WITH WEAK CIRCULATION

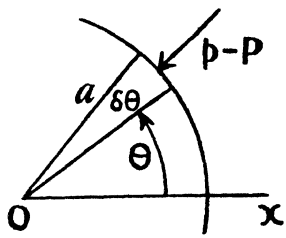

FIG. 75.

This gives a lift coefficient :

$$C_L \equiv \frac{L}{\frac{1}{2}\rho U^2 . 2a} = \frac{K}{aU} . \quad . \quad . \quad (135)$$

The above result is of great importance. The lift is independent of the size of the cylinder. A circulation can be generated by rotating a real circular cylinder in air, when, if it also moves as a whole, a lift of this kind appears, although the flow is not wholly irrotational. The principle finds practical expression in Flettner's sailless ship and in many ball games. We shall find that a cylinder of wing-shaped section moving through a viscous fluid has the property of generating a circulation by other means, and, with the help of an analytical process to be explained later, we shall be able to calculate the lift of wings with good accuracy from the basis provided by the foregoing results.

110. The Potential Function

The complex function $\phi + i\psi$, where i denotes $\sqrt{(-1)}$, is called the potential function of the irrotational flow. Let us equate it to any analytical function of the complex variable $x + iy$, say $f(x + iy)$, so that—

$$\phi + i\psi = f(x + iy). \quad . \quad . \quad (i)$$

Then we have—

$$\frac{\partial \phi}{\partial x} + i\frac{\partial \psi}{\partial x} = f'(x + iy)$$

and—

$$\frac{\partial \phi}{\partial y} + i\frac{\partial \psi}{\partial y} = if'(x + iy) = i\frac{\partial \phi}{\partial x} - \frac{\partial \psi}{\partial x}$$

Hence, equating real and imaginary parts—

$$\frac{\partial \psi}{\partial y} = \frac{\partial \phi}{\partial x}, \quad -\frac{\partial \psi}{\partial x} = \frac{\partial \phi}{\partial y}$$

which, Article 100, are the relations requiring to be satisfied for irrotational flow. Therefore, any assumption made in accordance with (i) leads to an irrotational motion. For shortness it is usual to write :

$$z = x + iy,$$
$$w = \phi + i\psi.$$

The function of z, $f(z)$, can always be separated into real and imaginary parts. Then from (i) we immediately obtain ϕ and ψ, which are real functions of x and y. It will be noticed, however, that the method can be applied only to two-dimensional problems.

It is shown in the theory of functions that if $w = f(z)$—

$$\frac{dw}{dz} \equiv \frac{d(\phi + i\psi)}{d(x + iy)} = \frac{\partial \phi}{\partial x} + i\frac{\partial \psi}{\partial x} = \frac{\partial \phi}{\partial x} - i\frac{\partial \phi}{\partial y}.$$

Thus, from (111) :

$$\frac{dw}{dz} = u - iv \quad . \quad . \quad . \quad . \quad (136)$$

111. As a first example it will be shown that—

$$w = f(z) = (A + iB)z \quad . \quad . \quad . \quad (137)$$

where A and B are real constants, covers all cases of uniform motion. We have—

$$\begin{aligned} \phi + i\psi &= A(x + iy) + iB(x + iy) \\ &= Ax - By + i(Bx + Ay). \end{aligned}$$

Equating real and imaginary parts—

$$\begin{aligned} \phi &= Ax - By \\ \psi &= Bx + Ay \end{aligned}$$

and—

$$u = \frac{\partial \phi}{\partial x} = A$$

$$v = \frac{\partial \phi}{\partial y} = -B.$$

Both velocity components are constant for chosen values of A and B and the flow is therefore uniform. If $B = 0$ the constant of (137) is wholly real and the flow is in the direction Ox with velocity $U = A$. If $A = 0$, the flow is parallel to Oy and of velocity $V = -B$. Generally, the flow is inclined to the x-axis by the angle $\tan^{-1}(-B/A)$, the velocity being equal to $\sqrt{(A^2 + B^2)}$.

112. It is often convenient to express the complex variable z in the polar form :

$$z = x + iy = r(\cos\theta + i\sin\theta).$$

Remembering that—

$$\cos\theta = \frac{e^{i\theta} + e^{-i\theta}}{2}$$

and—

$$\sin\theta = \frac{e^{i\theta} - e^{-i\theta}}{2i}$$

we note that—

$$\begin{aligned} \cos\theta + i\sin\theta &= e^{i\theta} \\ \cos\theta - i\sin\theta &= e^{-i\theta}. \end{aligned}$$

If we have z in the form $x + iy$, it can always be obtained in the form—

$$z = re^{i\theta}.$$

For, writing out both sides and equating real and imaginary parts, we find $x = r\cos\theta, y = r\sin\theta$, so that $r = \sqrt{(x^2 + y^2)}$, of which the positive root is taken, and these equations give a unique value of θ between 0 and 2π. r is called the modulus of z and is written mod z or $|z|$; θ is called the argument of z.

The complex co-ordinate z can be represented geometrically. For the operator -1 applied to Ox changes it to $-Ox$, i.e. turns it through the angle π. Since $-1 = i \times i$, the operator i turns a length through a right angle. Hence, to plot the point $x + iy$, x is measured along Ox and the increment y is measured at right angles thereto (Fig. 76). If P is the point represented by z, it will be seen that $OP = r$ and $\tan^{-1}(y/x) = \theta$. Thus z represents the vector OP, its length being $|z|$ and the angle it makes with Ox being θ.

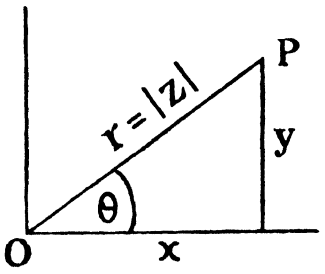

FIG. 76.

113. With this brief note on the complex variable, we proceed to consider the function—

$$w = f(z) = Az + A/z. \quad . \quad . \quad . \quad (138)$$

By Article 111 the first term on the R.H.S. represents steady streaming at velocity $U = A$, and to this is added a second motion. The combination may be written in the polar form :

$$w = A(re^{i\theta} + \frac{1}{r}e^{-i\theta})$$

and we have—

$$\phi + i\psi = Ar(\cos\theta + i\sin\theta) + \frac{A}{r}(\cos\theta - i\sin\theta).$$

Equating real and imaginary parts—

$$\phi = A(r + 1/r)\cos\theta$$
$$\psi = A(r - 1/r)\sin\theta.$$

Comparing with (127) or by considering the form of the streamline $\psi = 0$, we find that (138) gives the flow at velocity A past a circular cylinder of unit radius. It may be noted also that $w = A/z$ represents a doublet at the origin, as may be verified independently.

113A. Formulæ for Velocity

The velocity q at the general point in a two-dimensional irrotational flow can be expressed in various ways, of which the most useful are the following:

(*a*) Directly from (111), since $q^2 = u^2 + v^2$,

$$q = \left\{ \left(\frac{\partial \phi}{\partial x}\right)^2 + \left(\frac{\partial \phi}{\partial y}\right)^2 \right\}^{1/2} \quad . \quad . \quad \text{(i)}$$

(*b*) Denoting the components of q along and perpendicular to the radius r from the origin by u' and v', respectively,

$$u' = \frac{1}{r}\frac{\partial \psi}{\partial \theta} \text{ and } v' = -\frac{\partial \psi}{\partial r},$$

whence— $$q = (u'^2 + v'^2)^{1/2} = \left\{ \frac{1}{r^2}\left(\frac{\partial \psi}{\partial \theta}\right)^2 + \left(\frac{\partial \psi}{\partial r}\right)^2 \right\}^{1/2}. \quad \text{(ii)}$$

(*c*) By (136), $|dw/dz| = (u^2 + v^2)^{1/2}$. Hence— $q = \left|\frac{dw}{dz}\right|$ (iii)

For the potential function of the preceding article, for instance, (iii) gives, since—

$$\frac{dw}{dz} = A\left(1 - \frac{1}{z^2}\right) = A\left\{1 - \frac{1}{r^2}(\cos 2\theta - i \sin 2\theta)\right\},$$

$$q = A\left\{ \left(1 - \frac{1}{r^2}\cos 2\theta\right)^2 + \left(\frac{1}{r^2}\sin 2\theta\right)^2 \right\}^{1/2}$$

$$= A\left\{ \left(1 - \frac{1}{r^2}\right)^2 + \frac{4}{r^2}\sin^2\theta \right\}^{1/2} \quad . \quad . \quad . \quad \text{(iv)}$$

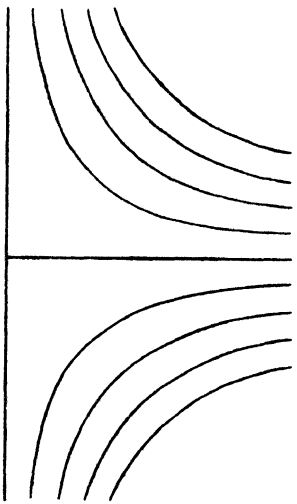

FIG. 76A.

As another example consider the function—

$$w = \frac{C}{n} z^n,$$

which yields a variety of irrotational motions on ascribing different values to n, choosing straight streamlines through the origin as boundaries, and interchanging if need be the meanings of ϕ and ψ; e.g. a doublet with $n = -1$, the streamlines (consisting of rectangular hyperbolas) in the vicinity of a stagnation point with $n = 2$, Fig. 76A, etc. For all these,

$$q = |dw/dz| = |Cz^{n-1}| = Cr^{n-1},$$

i.e. the velocity is constant at a given radius from the origin.

114. It will be convenient to have the potential function for a cylinder of unit radius with circulation K in a stream of velocity $-U$.

Let—

$$w = -i\frac{K}{2\pi}\log z. \quad . \quad . \quad . \quad (139)$$

Now the Napierian logarithm of $x+iy\,(=re^{i\theta})$ is $\log r+i\theta$. Hence—

$$\phi + i\psi = -i\frac{K}{2\pi}\log r + \frac{K}{2\pi}\theta$$

and—

$$\phi = \frac{K}{2\pi}\theta, \qquad \psi = -\frac{K}{2\pi}\log r$$

so that (139) gives circulation with strength K round the origin, and the expression for ψ is unchanged if the circulation is round a circle of unit radius.

Hence, for this circulation combined with translation we have, from Article 113—

$$w = -U\left(z + \frac{1}{z}\right) - i\frac{K}{2\pi}\log z. \quad . \quad . \quad (140)$$

115. Instead of w being expressed as a function of z, we may have z as a function of w.

Consider :

$$z = c\cosh w \quad . \quad . \quad . \quad . \quad (141)$$

Writing out—

$$\begin{aligned} x + iy &= c\cosh(\phi + i\psi) \\ &= c(\cosh\phi\cosh i\psi + \sinh\phi\sinh i\psi) \\ &= c[\cosh\phi\cos\psi + \sinh\phi\,(i\sin\psi)]. \end{aligned}$$

Equating real and imaginary parts—

$$\begin{aligned} x &= c\cosh\phi\cos\psi \\ y &= c\sinh\phi\sin\psi \quad . \quad . \quad . \end{aligned} \qquad (i)$$

Square and add to eliminate ψ, obtaining—

$$\frac{x^2}{c^2\cosh^2\phi} + \frac{y^2}{c^2\sinh^2\phi} = \cos^2\psi + \sin^2\psi = 1 \qquad (ii)$$

or square and subtract to eliminate ϕ, finding alternatively—

$$\frac{x^2}{c^2\cos^2\psi} - \frac{y^2}{c^2\sin^2\psi} = \cosh^2\phi - \sinh^2\phi = 1. \quad (iii)$$

Putting ϕ = a series of constants in (ii) gives a family of confocal ellipses (Fig. 77), the foci being at $x = \pm c$, $y = 0$. Choosing ϕ as the stream function, any one of these ellipses may be taken as

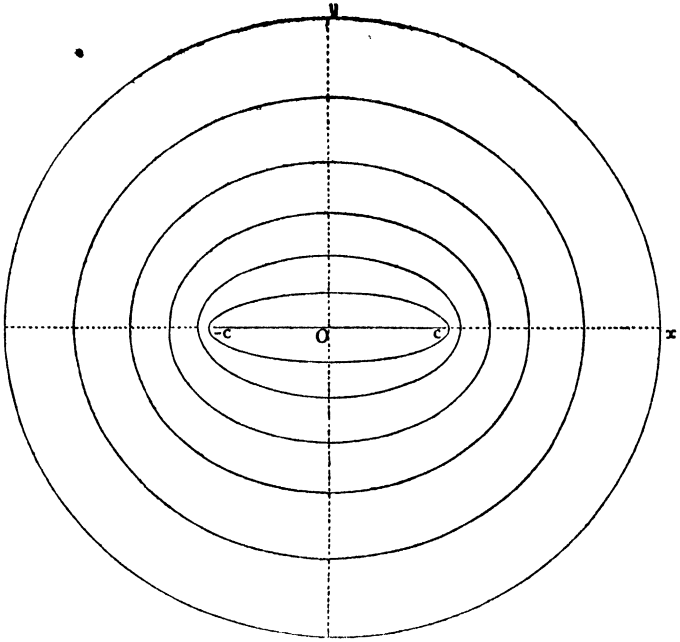

FIG. 77.—IRROTATIONAL CIRCULATION ROUND PLATE.

boundary, and we then have the streamlines for irrotational circulation round a cylinder of elliptic section. The line joining the foci may be taken as boundary, when the ellipses become the streamlines for circulation round a flat plate. It is readily seen by plotting or calculation that the velocity and the pressure reduction both become very large as the edges of the plate are closely approached, and we shall frequently have to remark on artificiality on this score. It will be noted that, at a large distance from the plate or elliptic cylinder, the streamlines become the same as for circulation round a circular cylinder.

Putting $\psi = \text{const.}$ in (iii) gives a family of hyperbolas having the same foci. These are everywhere orthogonal to the ellipses, and constitute the equipotentials of the circulation. If, however, they be interpreted as the streamlines, so that the ellipses become the equipotentials, we shall have the case of fluid flowing through the whole or part of the x-axis between $\pm c$. Choosing two hyperbolas equidistant from the y-axis as boundaries, we at once have the streamlines for flow through a long two-dimensional nozzle (Fig. 78). According to potential flow theory the nozzle may be made as sharp as we please, but a real flow breaks away from the divergent

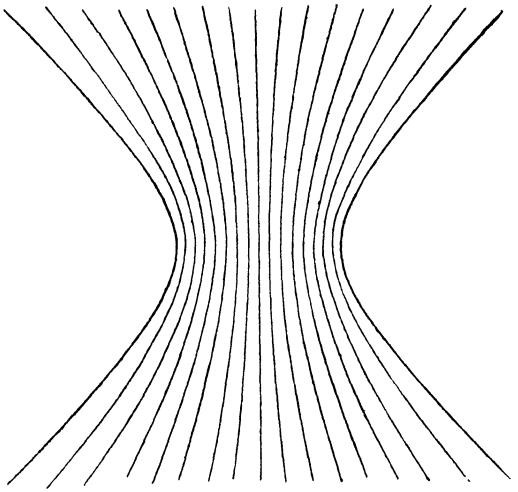

FIG. 78.—POTENTIAL FLOW THROUGH HYPERBOLIC CHANNEL.

walls, the flow ceasing to fill the channel, if the divergence is other than small. With this restriction, the three-dimensional analogue is applied in the design of high-speed wind tunnels. Recovery of pressure energy at the outlet from the kinetic energy generated at the throat leads to higher efficiency (Article 51), resulting in greater speed at the throat for a given expenditure of power, than if the tunnel were parallel-walled. The idea is of ancient origin. A cylindrical tunnel is often fitted with a divergent outlet only. Where smooth flow and high efficiency are urgent, it is advisable to shape, if possible, the divergent wall with some care. The inlet part is of less importance, and is often made of quite different form for other reasons.

The complete nozzle is known as a venturi or venturi-tube, and, in its three-dimensional form, has many practical applications. A pressure reduction obviously occurs at the throat, and, if it is known in a given instance to what extent the space between the walls is filled with continuous flow, this reduction follows at once from Bernoulli's equation. When the venturi forms part of a pipe-line conveying liquid, the convergent inlet is forced to run full. But if the venturi is short and is exposed in a stream, free to flow round it, little fluid may pass through, so that it by no means runs full.* Nevertheless, a pressure reduction still exists which can be used (after calibration) to measure velocity (Article 33), or again to supply power. Application to aircraft in the latter connection is associated with poor efficiency.

116. Motion of a Cylinder through Fluid

So far the immersed body has been assumed to be held in a stream. Sometimes it is desirable to consider the body as moving, the fluid

* Piercy and Mines, *loc. cit.*, p. 44.

being stationary at large distances away. If the solution be known in the former case, that in the latter may readily be deduced by the superposition of an additional stream function as already explained. But the direct solution may be simpler and a method for this will now be described.

The boundary condition can now be stated as follows: the resolved parts of the velocities of an element of the contour of the body and of the adjacent fluid, along a normal drawn from the element, must be the same.

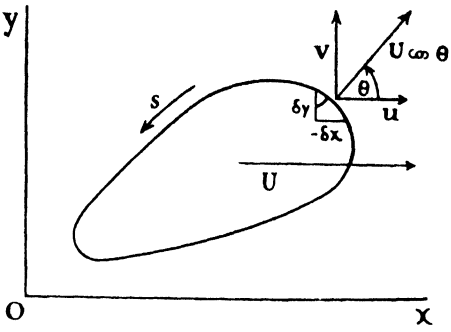

FIG. 79.

The contour shown in Fig. 79 is that of the cross-section of any cylinder supposed to move at uniform velocity U in the direction Ox. Distance measured round the curve in the direction of θ, increasing as shown, is denoted by s. Considering a small element δs, the velocity component of the cylinder along the normal from it is $U.\cos\theta$, while the velocity component of the fluid there in the same direction is $v\,.\sin\theta + u\,.\cos\theta$. Therefore—

$$v \sin\theta + u \cos\theta = U \cos\theta.$$

Substituting for u and v, and from the figure—

$$-\frac{\partial\psi}{\partial x}\left(-\frac{dx}{ds}\right) + \frac{\partial\psi}{\partial y}\cdot\frac{dy}{ds} = U\frac{dy}{ds},$$

noticing that x is decreasing at the element in the figure as s is increasing. Hence:

$$\frac{\partial\psi}{\partial x}dx + \frac{\partial\psi}{\partial y}dy = d\psi = U dy.$$

Finally, integrating round the boundary—

$$\psi = Uy + \text{const.} \quad . \quad . \quad . \quad . \quad (142)$$

Any form of ψ satisfying Laplace's equation (Article 100) gives from this expression a family of curves any one of which may become a boundary and, moved in the direction Ox, will give the path-lines $\psi =$ constant. A similar expression is obtained for motion parallel to the y-axis. Superposition of motions parallel to x and y enables path-lines to be obtained when the cylinder moves with its section

inclined. The streamlines for the body at rest are immediately found by the addition of an appropriate stream function affecting the fluid as a whole.

The method was employed by Rankine * to find mathematical shapes for ship lines. It is tentative or inverse in the sense that the form selected for ψ (and there is an infinite number) may well lead to a possible variety of shapes for the boundary, none of which has any bearing on Aerodynamics. The following classical example has a particular interest, and should be studied carefully, as we shall use it later on as a key to a difficult problem of the greatest practical importance in our subject.

117. Elliptic Cylinder and Plate in Motion

Assume for the potential function the form—

$$w = -Ae^{-(\xi + i\eta)} \quad . \quad . \quad . \quad \text{(i)}$$

where A is a real constant. We have—

$$\phi + i\psi = -Ae^{-\xi}(\cos\eta - i\sin\eta)$$

and on separation of real and imaginary parts—

$$\psi = Ae^{-\xi}\sin\eta \quad . \quad . \quad . \quad \text{(ii)}$$

The co-ordinates ξ, η, called elliptic co-ordinates, are related to x, y in the same way as ϕ, ψ were in Article 115, i.e.—

$$z = c\cosh(\xi + i\eta);$$

so that—

$$x = c\cosh\xi\cos\eta,$$
$$y = c\sinh\xi\sin\eta. \quad . \quad . \quad \text{(iii)}$$

As in that article, we find that $\xi = \text{const.} = \xi_0$, say, is the ellipse :

$$\frac{x^2}{c^2\cosh^2\xi_0} + \frac{y^2}{c^2\sinh^2\xi_0} = 1$$

which we shall write for short—

$$\frac{x^2}{a^2} + \frac{y^2}{b^2} = 1$$

so that—

$$a = c\cosh\xi_0,\ b = c\sinh\xi_0 \quad . \quad . \quad \text{(iv)}$$

are its semi-axes.

Now putting (ii), with $\xi = \xi_0$ so as to represent the boundary, in (142) gives, making use of the second formula of (iii)—

$$Ae^{-\xi_0}\sin\eta = Uc\sinh\xi_0\sin\eta + \text{const.};$$

* *Phil. Trans. Roy. Soc.*, 1864.

and since this must be satisfied for all values of η, we have—

$$\text{the const.} = 0,$$
$$A = Uce^{\xi_0} \sinh \xi_0.$$

Hence, in order that (i) should represent the case of the ellipse $\xi = \xi_0$—

$$\psi = Uce^{\xi_0 - \xi} \sinh \xi_0 \sin \eta \quad . \quad . \quad (v)$$

This result can be simplified, because, using (iv)—

$$ce^{\xi_0} \sinh \xi_0 = be^{\xi_0} = b(\cosh \xi_0 + \sinh \xi_0) = \frac{b}{c}(a + b);$$

and—

$$c^2 = a^2 - b^2.$$

Thus, finally—

$$\psi = Ub\sqrt{\frac{a+b}{a-b}} \cdot e^{-\xi} \sin \eta \quad . \quad . \quad (143)$$

and—

$$\phi = -Ub\sqrt{\frac{a+b}{a-b}} \cdot e^{-\xi} \cos \eta.$$

These expressions are for motion parallel to the major axis. Corresponding results are similarly obtained for motion in the direction of the minor axis. They come to—

$$\psi = -Va\sqrt{\frac{a+b}{a-b}} \cdot e^{-\xi} \cos \eta, \quad . \quad . \quad (144)$$
$$\phi = -Va\sqrt{\frac{a+b}{a-b}} \cdot e^{-\xi} \sin \eta.$$

The solution applies to all confocal ellipses, and so includes the case of a plate of chord $2c$ (cf. Article 115) moving broadside on. In this important case $b = 0$ and $a = c$, and the last formulæ become—

$$\psi = -Vc\, e^{-\xi} \cos \eta$$
$$\phi = -Vc\, e^{-\xi} \sin \eta. \quad . \quad . \quad . \quad (145)$$

The path-lines are shown in Fig. 80 for downward motion of the plate.

If the cylinder or plate has components of velocity U and V, i.e. if the line joining the foci, or the plane of the plate, be inclined to the direction of motion, the new stream function is written down immediately by superposition. But the stream-

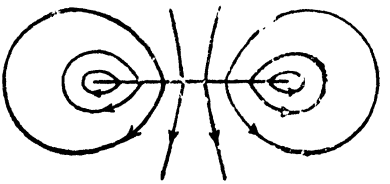

FIG. 80.—PATH-LINES FOR PLATE IN BROADSIDE-ON MOTION.

lines are more illustrative than the path-lines, and for these the additional stream function $Vx - Uy$, where x and y are given by (iii), must be superposed. In this way the streamlines for any angle of incidence α can be plotted; they are shown for a flat plate at $\alpha = 45°$ in Fig. 81, the oncoming stream being supposed horizontal. Another treatment is given in Article 124, where further details are obtained.

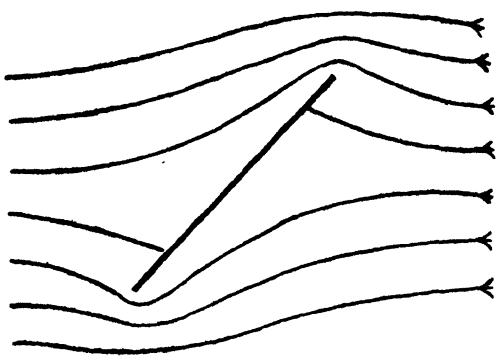

FIG. 81.

From symmetry, there is no component of force in any direction on the plate or cylinder, whatever its incidence, although, if it be inclined, a couple exists tending to produce broadside-on motion. This further instance of absence of force in steady motion is reviewed in the next article. A circulation might be added from Article 115, and a lift or transverse force would result; this will appear as a special case of a more general investigation in the next chapter.

118. It has been remarked several times that the only Aerodynamic force arising on a body in steady potential flow is that due to the superposition of circulation and translation, and is a transverse force. Absence of drag is especially striking, perhaps, in the example just considered of a flat plate moving at right angles to its plane, when the drag coefficient C_D has, in experimental fact, a value equal to 2, representing a particularly large force. It may be remarked in this case that high velocities are built up towards the edges which would invalidate the assumption of incompressible flow with air as fluid, and even with a liquid such pressure reductions would occur before the edges were reached as could not be supported by the general hydrostatic pressure. To avoid these objections, which would clearly prevent the flow from running smoothly to the back of the plate, we might round the edges, as, for instance, by substituting an elliptic cylinder. But the flow would still break away, as was seen to occur even with the circular cylinder. The subject of drag is complicated, and is postponed until later chapters. But it should not be inferred that failure to indicate drag prevents the foregoing theory from being of practical use. The methods discussed will

often suffice to calculate approximately the streamlines and velocity and pressure distribution over the fore-parts of bodies. They could readily be developed to a more effective stage. But this will be left to a reading of original papers, for, from the foregoing theory, we can proceed directly to a very powerful process of solution that readily gives essentially practical forms of potential flow. This is treated in the next chapter.

119. Acceleration from Rest

There is one circumstance, however, in which potential flow yields a drag, viz. during the time of its generation.

Consider a body at rest in an infinite bulk of stationary fluid. Its weight will be assumed to be balanced by its buoyancy or by mechanical means. Let it be given an impulse in any direction, i.e. let an indefinitely large force act upon it for an indefinitely short time τ, being withdrawn at the end of τ. The impulse is measured by the momentum produced. *In vacuo*, the impulse would be given by the momentum acquired by the body. But part of the impulse is absorbed in generating momentum in the fluid. This increment alone concerns us, and we shall denote it by I.

Now, regarding the flow generated in the fluid by the motion of the body under I, it can be proved that if the acyclic potential flow is known for that body, then the flow actually set up will be of that known form. We need not follow out the theoretical argument, because, as will be described in more detail later on, the result can be verified by experiment with a real fluid, whose viscosity requires appreciable time to take effect and so modify the flow. Thus, the present investigation relates to the initial motion of air, provided generation from rest is almost instantaneous.

Assuming that the body is of such a shape that the solution for irrotational flow exists, we know from Article 98 the distribution over its surface of the impulsive pressure which generates the flow. The pressure acts normally to the surface of the body at all points, and, on integration over the body (cf. Article 44), will give a resultant force which must exactly balance that part X of the external force applied which is not absorbed in producing momentum in the body, and we have—

$$X = \frac{dI}{dt}. \quad . \quad . \quad . \quad . \quad (146)$$

At the end of the short interval of time τ, when the impulsive force is removed, the motion of the body and the fluid becomes steady, if

the latter is inviscid, and the pressures round the body indicate zero resistance, as we have seen. With air, viscosity produces friction and soon modifies the flow, leading to pressure drag, as well as skin friction, as also we have noted. But the important result now obtained is that during instantaneous generation of flow from rest, whether the fluid possess viscosity or be conceived to be destitute of this property, a force must be applied whose magnitude, direction, and point of application can be calculated in suitable circumstances. It is clear that a linear impulse would be insufficient to generate some motions, and that an impulsive 'wrench' would sometimes be required. But the moment of the impulse may be found similarly.

Now during τ the impulse I does work on the fluid, evidenced by the appearance within the fluid of kinetic energy. Denote the kinetic energy at the end of τ by E. It is given by—

$$E = \tfrac{1}{2}\rho \iint q^2 \, dxdy \quad . \quad . \quad . \quad (147)$$

in the two-dimensional case, if E be reckoned for unit depth perpendicular to the xy-plane, q denote the velocity at any point, and the integration extend over the whole of the xy-plane that is not occupied by the section of the body.

The above integration is, in general, difficult to carry out. But E must equal the work done by the impulse during τ. Now a familiar theorem of Dynamics proves that the work done by a system of impulses operating from rest is equal to the sum of the products of each impulse and half the final velocity of its point of application. This theorem may be applied to the finite continuous distribution of impulse which we have to consider. If δn be an element of the normal drawn into the fluid from an element δs of the contour of the body, the final velocity at δs is $\partial\phi/\partial n$, while the 'impulse pressure' at δs is, by Article 98, $-\rho\phi$. Hence—

$$E = -\tfrac{1}{2}\rho \int \phi \frac{\partial \phi}{\partial n} ds \quad . \quad . \quad . \quad (148)$$

where the integration is to extend round the contour of the body. Thus the kinetic energy at the end of τ is at once calculated if ϕ be known.

With an inviscid fluid, E remains constant after τ. The flow might, however, provided it is irrotational, be brought instantaneously to rest by the application of a reverse impulsive wrench, which would do work in destroying the kinetic energy of the fluid. Thus the work done by an impulse is equal to the (positive or negative) increment of the kinetic energy.

A property shown by Kelvin to be characteristic of all Dynamical

systems started instantaneously from rest is that the kinetic energy generated is a minimum. The motions calculated in the present chapter have the least kinetic energy that could arise from the displacement of the body through the fluid.

120. Impulse and Kinetic Energy of the Flow Generated by a Normal Plate

The case of a plate set instantaneously from rest into motion at right angles to its plane provides an important example of the foregoing. Assume two-dimensional conditions; take the origin midway between the edges of the plate, draw Ox in its plane, and let $2c$ be its width and V its final velocity.

For the impulse I per unit length perpendicular to the xy-plane—

$$I = -\rho \int \phi \, ds \quad . \quad . \quad . \quad \text{(i)}$$

where the integration extends round the whole contour; i.e. from one edge along one face round the other edge and back again along the other face. From Article 117, on the plate, where $\xi = 0$—

$$\phi = -Vc \sin \eta \quad . \quad . \quad . \quad \text{(ii)}$$

and η ranges from 0 to 2π in the integration. Also from that article, $dx = -c \sin \eta \, d\eta$. Hence (i) gives—

$$I = \rho V c^2 \int_0^{2\pi} \sin^2 \eta \, d\eta$$

$$= \pi \rho V c^2 \quad . \quad . \quad . \quad . \quad . \quad (149)$$

Writing from (ii) $\sin \eta = -\phi/Vc$ and from Article 117 $x = c \cos \eta$ on the plate, where $\cosh \xi = 1$, we have—

$$\frac{\phi^2}{V^2 c^2} + \frac{x^2}{c^2} = \sin^2 \eta + \cos^2 \eta = 1$$

showing that the distribution across the plate of ϕ and, therefore, of the impulse is elliptic.

Half the final velocity of the impulse is constant across the plate and is equal to $\frac{1}{2}V$. Hence, from (149)—

$$E = \tfrac{1}{2} \pi \rho V^2 c^2 \quad . \quad . \quad . \quad . \quad (150)$$

Chapter VI

TWO-DIMENSIONAL AEROFOILS

121. The present chapter obtains the streamlines and other details of irrotational incompressible flow past streamline and aerofoil sections of practical forms. The process employed is an application of the methods of conformal transformation, the aim of which is to enable the flow in analytically complicated circumstances to be inferred from that in some simple case whose solution either is known or can readily be obtained. The method is applicable to two-dimensional conditions only, so that the shapes derived must be regarded as the sections of long cylinders whose generating lines are perpendicular to the xy-plane.

A simple type of conformal transformation will first be described as an introduction.

Every point in a field of two-dimensional irrotational flow has attached to it a particular value of $z = x + iy$ and of $w = \phi + i\psi$. The relationship between these is known at every point, if by the methods of the preceding chapter we can construct the equation—

$$w = f(z) \quad . \quad . \quad . \quad \text{(i)}$$

for the flow in question ; ϕ and ψ are separately obtainable as the real and imaginary parts, respectively, of the function of z.

We have seen how a particular point z' can immediately be plotted in the xy-plane, which will now be called the z-plane. In like manner w' may be regarded as the complex co-ordinate of the corresponding point in another plane, called the w-plane, whose rectangular co-ordinates, instead of being x and y, are ϕ and ψ. If a region of the flow in the z-plane be mapped with a network of equipotentials and streamlines, the whole network can accordingly be replotted in the w-plane.

Such an operation is called a transformation. It can only be carried out by means of a formula connecting the co-ordinates in the two planes, which is called the transformation formula. The process is, of course, reversible ; (i) equally enables a network to be transferred from the w- to the z-plane.

Now, in the simple transformation under discussion the network

in the w-plane can have only one form : it must consist of one group of straight lines parallel to the ϕ-axis and another group parallel to the ψ-axis. For equal intervals of ϕ and ψ the mesh will be square, whether it be fine or coarse. But this is not true of the corresponding network obtained by transformation to the z-plane.

Suppose, for instance, that it is desired to transform the square mesh net in the w-plane to the equipotentials and streamlines of the flow at unit velocity without circulation past a circular cylinder of radius a in the z-plane. We happen to know from Article 113 the form of (i), which will achieve the result ; it is :

$$w = z + a^2/z \quad . \quad . \quad . \quad \text{(ii)}$$

which can be written—

$$w = re^{i\theta} + a^2e^{-i\theta}/r. \quad . \quad . \quad \text{(iii)}$$

Fig. 82 shows the results of the transformation of part of the w-plane above the axis of ϕ. A very small square element of the w-plane will evidently transform to a small square element of the z-plane, although its size, orientation, and disposition geometrically relative to the axes are changed. On the other hand, a larger square element of the w-plane transforms to a distorted figure in the z-plane. This illustrates a characteristic of conformal transformation : corresponding elements are geometrically similar if infinitely small, but not so if finite.

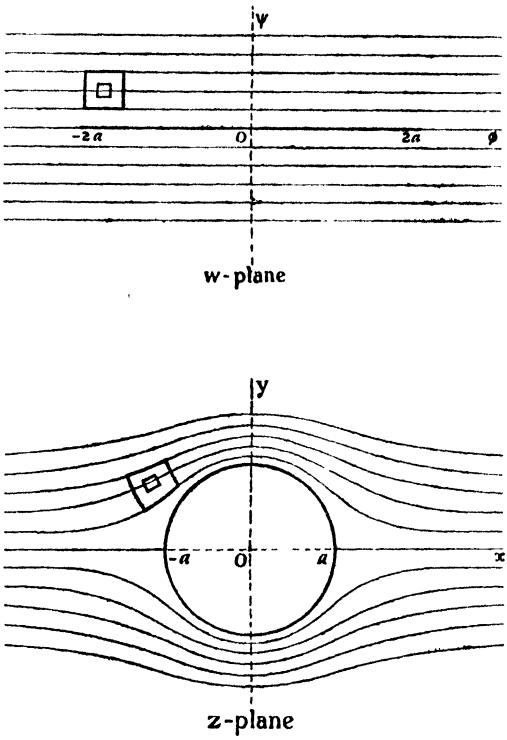

FIG. 82.

Another point in the present example is as follows : from (iii) we easily obtain, as in Article 113—

$$\phi = (r + a^2/r) \cos \theta$$
$$\psi = (r - a^2/r) \sin \theta$$

and on the circle, where $\psi = 0$ and $r = a$,

$$\phi = 2a \cos \theta \quad . \quad . \quad . \quad . \quad (151)$$

Since θ varies from 0 to 2π, the maximum and minimum values of ϕ on the circle are $\pm 2a$. Thus the circle itself corresponds to both sides of a line of length $4a$ lying on the ϕ-axis and bisected by the ψ-axis. Moreover, the formula (151) relates each point on this line to a corresponding point on the circle.

Now, the plot in the w-plane can be regarded as representing uniform flow parallel to $O\phi$ past a tangential plate of length $4a$. The formula (ii) then relates at every point this simple flow to the flow past a circular cylinder of radius a.

Similar results are obtained in dealing with a cylinder of any other shape if circulation is excluded. But as a rule the form of (1) is not known. If, however, we can find a means of opening out, as it were, a part of the ϕ-axis into some section that interests us, then a proper generalisation of the process gives the flow past the section. The example given is fully known in analytical terms. But in other cases of practical interest analytical treatment might be complicated, while a solution might more readily be obtainable by graphical means. An intermediate step is then required, however, as will be described in the following article.

It may here be remarked, however, that the transformation (i) becomes of direct use when the real flow in the z-plane is known, but is too complicated for the study of some added problem; the simplified flow obtained by transformation to the w-plane may permit of a solution there which can be transformed back. The transformation was so employed by the French engineer Boussinesq in his pioneering work on heat transfer, and is often known after him.

122. Conformal Transformation

Consider the transformation of part of the z-plane, where the co-ordinate of a point is $z = x + iy$, to the corresponding part of a t-plane, where the complex co-ordinate of a point is $t = \xi + i\eta$, so that the co-ordinates in the t-plane are ξ and η. Let—

$$t = f(z) \quad . \quad . \quad . \quad (i)$$

and assume that throughout the regions considered (i) leads to a unique relationship between z and t and that dt/dz has a definite value. Thus for the present we exclude transformation formulæ

such as $t = z^2$, while also we assume that in the parts of the planes considered dt/dz has neither zero nor infinite values.

As in Article 112 δt, δz may be interpreted as very small vectors. Applying the operator dt/dz to an element-vector in the one plane converts it to an element-vector in the other, and this transformation is independent of direction. Elementary lengths in the z-plane are increased on transformation in the ratio $\left|\frac{dt}{dz}\right| : 1$. Further, element-lines are rotated through an angle equal to the argument of dt/dz.

It follows at once that angles between adjacent short lines are unchanged by the transformation, so that infinitesimal corresponding areas are similar. Further, it follows that the magnitudes of very small corresponding areas are in the ratio $\left|\frac{dt}{dz}\right|^2 : 1$.

Such a transformation is said to be conformal.

Let ϕ and ψ, defined by—

$$w = F(t),$$

be the velocity potential and stream function of a motion in the t-plane and let the boundary there be $F_1(\xi, \eta) = \text{constant}$. From (i) we can substitute for t in terms of z and obtain—

$$w = f(z).$$

In the same way we can find a new boundary $f_1(x, y) = \text{constant}$ in the z-plane corresponding to that in the t-plane. The same functions ϕ and ψ then hold for the motion in the z-plane.

Considering a small area mapped with streamlines and equipotentials transformed by (i) from the z- to the t-plane, the distances separating streamlines or equipotentials diminish in the ratio $\left|\frac{dz}{dt}\right| : 1$. Therefore, velocities at corresponding points are increased in that ratio, i.e. at corresponding points—

$$q_t = q_z \left|\frac{dz}{dt}\right| \quad . \quad . \quad . \quad . \quad (152)$$

To make such increases in local velocity representative of the change in the boundary shape, we must arrange that the same velocity exists at infinity in the two planes. If when z is large $dt/dz = 1$, the transformation is sometimes known as one-to-one, but this term often signifies absence of double points.

The distribution of velocity in the z-plane, say, will be known, and that in the t-plane will immediately follow from (152). Application

of Bernoulli's equation then gives the distribution of pressure in the t-plane.

123. Singular Points

Reconsidering now the special assumptions made in the last article, we note first that the transformation formula may be of such a form that a point in the t-plane, as in the example mentioned, corresponds to two points in the z-plane, one-half of the one plane transforming to the whole of the other. The remaining half of the first plane may then be mapped, if it is required, on a second sheet of the other. A further example occurs in Article 117, if interpreted in this way, where the whole of the z-plane maps into a strip of the t-plane of width 2π.

Turning to the second assumption, we shall always find on extending the region transformed to cover the whole of one of the planes that certain points occur where dt/dz becomes zero or infinite. Such points are known as singular points, and the transformation ceases to be conformal there ; they must either receive special investigation or be specifically excluded.

An example occurs in Article 121. For clearness rewrite (ii) of that article as—

$$t = z + a^2/z \quad . \quad . \quad . \quad \text{(i)}$$

so that the w-plane of Fig. 82 becomes the t-plane. Differentiating—

$$dt/dz = 1 - a^2/z^2$$

and there are two singular points where $dt/dz = 0$, viz. $z = \pm a$; i.e. $x + iy = \pm a$ or $y = 0$, $x = \pm a$. In words, the circle of radius a cuts the x-axis in two singular points. It is seen at once that the transformation ceases to be conformal at these points ; for the angle between adjacent elements of the circle is everywhere π, while, although this also holds for the line as a whole, at its ends the angle becomes 2π. A singular point is seen to produce a discontinuity in the transformed contour.

124. Transformation of Circular Cylinder into Normal Plate

An alternative solution of the case of motion investigated in Article 117 will now be described briefly. The opportunity will be taken to effect certain calculations required later on, which were left over in anticipation. The article is of further interest in that in principle it forms a starting-point for more difficult work than is attempted in a first reading of the subject.

Flow past a circle of radius a at unit velocity parallel to Oy is

obtained from that parallel to Ox by multiplying the co-ordinate by i, giving—

$$w = iz + \frac{a^2}{iz} = i\left(z - \frac{a^2}{z}\right). \quad . \quad . \quad (i)$$

The circle itself is transformed into a line of length $4a$ on the ξ-axis of the t-plane by the formula—

$$t = z + a^2/z \quad . \quad . \quad . \quad (ii)$$

as we have seen, and transformation of the flow (i) by this formula will give in the t-plane the flow past a normal plate. To obtain the potential function of the flow in the t-plane, we require to eliminate z. Squaring both equations and adding—

$$w^2 + t^2 = 4a^2$$

or—

$$w = i\sqrt{t^2 - 4a^2} \quad . \quad . \quad . \quad (iii)$$

If u', v' are the ξ- and η-components of velocity in the t-plane from (136)—

$$\frac{dw}{dt} = u' - iv'.$$

Hence (iii) gives—

$$u' - iv' = \frac{it}{\sqrt{(t^2 - 4a^2)}}$$

$$= \frac{i(\xi + i\eta)}{\sqrt{\{(\xi + i\eta)^2 - 4a^2\}}}. \quad . \quad (iv)$$

In the plane of the plate $\eta = 0$ and we have—

$$u' - iv' = \frac{i\xi}{\sqrt{(\xi^2 - 4a^2)}} \text{ for } \xi > 2a$$

$$= \frac{\xi}{\sqrt{(4a^2 - \xi^2)}} \text{ for } \xi < 2a.$$

Hence beyond the edges of the plate, in its plane—

$$u' = 0,\ v' = -\xi/\sqrt{\xi^2 - 4a^2},$$

while over the surface of the plate—

$$v' = 0,\ u' = \xi/\sqrt{4a^2 - \xi^2} \quad . \quad . \quad . \quad (153)$$

The sign of u' depends upon which side and which face of the plate is considered, but is obvious on inspection. The expressions for u'

and v' have been obtained for unit velocity parallel to the y-axis; for any velocity V the right-hand sides are to be multiplied by V. If P is the undisturbed pressure of the stream of velocity V, Bernoulli's equation gives for the pressure p over the plate—

$$\frac{p - P}{\rho V^2} = \tfrac{1}{2}\left[1 - \frac{(\xi/2a)^2}{1 - (\xi/2a)^2}\right].$$

The further details calculated above for the normal plate will elucidate remarks made in Articles 117 to 119. For instance, (153) indicates clearly that the velocity tends to infinity at the edges. The calculated pressure is as shown in Fig. 83 and, being the same over both faces, gives zero drag. In experiment, when a permanent régime has become established, and the flow has broken away from the edges, the whole of the upstream face has an increased and the downstream face a decreased pressure, leading to the large drag measured.

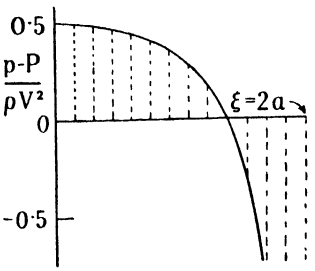

FIG. 83.—PRESSURE DISTRIBUTION OVER A NORMAL PLATE IN IRROTATIONAL FLOW.

The result (iii) is not in convenient form for plotting, elliptic co-ordinates being suitable for this as in Article 117. Instead of deriving these, an approximate graphical method of general utility will be described.

Fig. 84 shows in the z-plane the streamlines of (i) and, superposed, the ϕ- and ψ-lines of $w = z + a^2/z$. In the t-plane is shown as a background the entirely square network obtained by transforming the latter potential function by the formula (ii). Now follow any streamline of the flow (i). The plotting being close, the streamline nearly crosses at several points the intersection of a ϕ- and a ψ-line of the x-flow. Read off the pairs of values of ϕ and ψ where this occurs, and by their use plot points on the square network of the t-plane. One of the points so transferred is shown encircled. The points will be approximately on one of the streamlines of (iii) and a smooth curve may be drawn through them. The proof is left to the reader. The graphical method can be used to find the streamlines of flow without circulation past an inclined flat plate (cf. Article 117). For this purpose the direction of the flow in the z-plane to be transformed, instead of being rotated from the x-axis through 90° as in (i), is set at the appropriate angle.

An alternative graphical method is based on the fact that circles

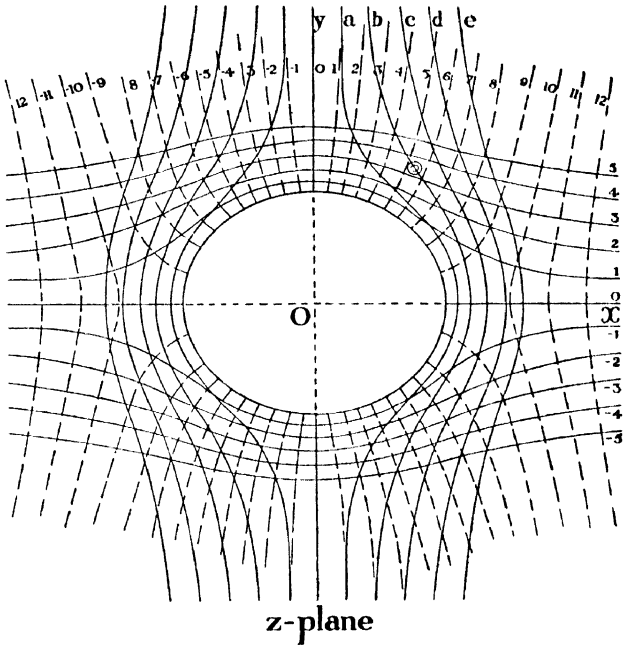

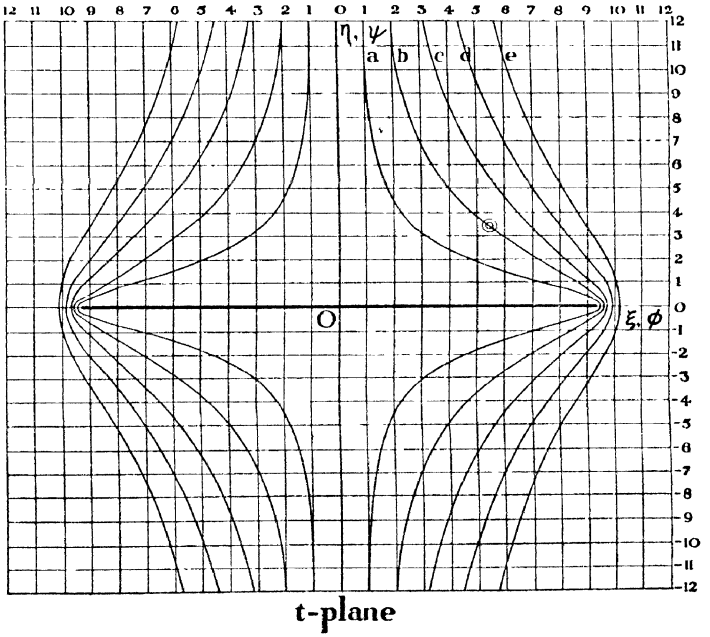

FIG. 84.—GRAPHICAL METHOD FOR OBTAINING THE STREAMLINES PAST A NORMAL PLATE.

with centres at the origin in the z-plane and the orthogonal system of radial lines become ellipses and hyperbolas, respectively, when transformed to the t-plane by formula (ii). For substituting $z = ae^{m+in}$, which represents circles of radii ae^m together with radial lines making angles n with the x-axis, the formula gives—

$$t = ae^{m+in} + ae^{-(m+in)} = 2a \cosh (m + in).$$

In the t-plane, therefore, m and n are the elliptic co-ordinates already employed in Article 117. Thus mapping the z-plane with a network of such circles and radial lines and the t-plane with the corresponding confocal ellipses and hyperbolas provides corresponding systems of co-ordinates which enable any curve drawn in the one plane to be transformed at once to the other plane.

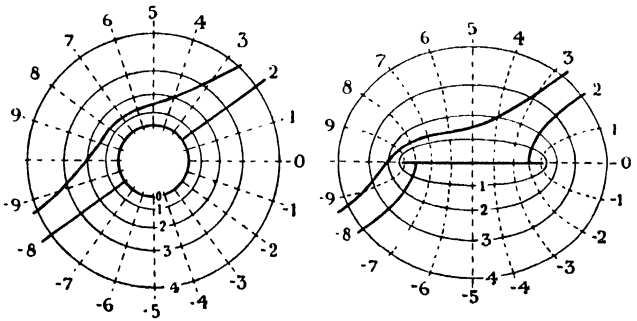

FIG. 84A.—ALTERNATIVE GRAPHICAL METHOD.

Fig. 84A illustrates the method in application to the problem of finding the streamlines of irrotational flow past a plate inclined at an angle θ. The t-plane is mapped for equal intervals of m and n, represented by the proportional numbers 1, 2, 3, . . . , and the plate is the straight line of length $4a$ joining the foci. The same values of m and n yield the network shown in the z-plane, where both sides of the straight line map into the circle of radius a. The transformation (ii) is such that the undisturbed streams are inclined at the same angle θ to the real axes in both planes. Hence any streamline may be drawn in the z-plane by Article 108 or otherwise. Values of m and n for points on this streamline are read off in the z-plane and replotted in the t-plane, yielding the corresponding streamline past the inclined plate. The streamlines leading to the stagnation points are radial for the circle and hyperbolic for the plate.

SYMMETRICAL STREAMLINE SECTIONS

125. Joukowski Sections

The transformation formula—

$$t = z + a^2/z \quad . \quad . \quad . \quad . \quad (154)$$

involves, as has been noted, singular points at $x = \pm a$, marked R and Q in Fig. 85. To avoid discontinuities in the t-plane contour, these points must be excluded from the area transformed. This is achieved by applying the formula to a circle of radius $> a$ enclosing Q and R. Describing such a circle with O as centre results in an ellipse, but displacing its centre a little upstream leads to a section of the streamline form found in experiment to give small drag. The flow to be transformed will now be that past this greater circle, of centre B and radius b, which will be called the b-circle to distinguish it from the a-circle that yields Q and R.

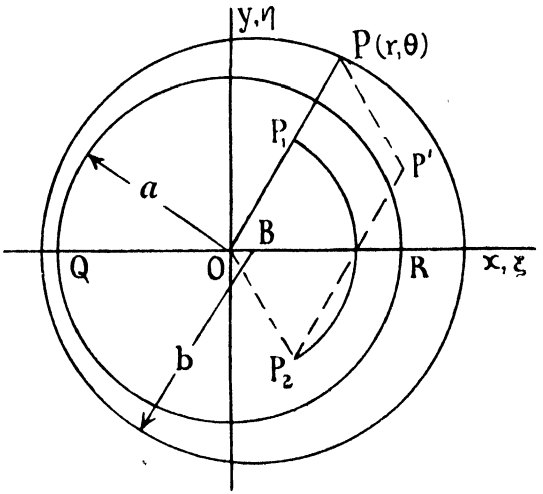

FIG. 85.

The form of (154) permits the contour in the t-plane to be found by a simple construction. Let P, Fig. 85, any point on the b-circle, become P' in the t-plane. We have for the co-ordinate of P—

$$z = re^{i\theta}$$

and for that of P'—

$$t = re^{i\theta} + \frac{a^2}{r} e^{-i\theta}.$$

Thus the co-ordinate of P' is the sum of two vectors, the first of which is identical with the vector OP. Dealing with the second component vector, the modulus a^2/r means * that P is to be reflected in the a-circle, giving P_1, while the argument $-\theta$ means that OP_1

* The relation $OP \cdot OP_1 = a^2$ is clearly necessary. Cf. also Art. 152.

so obtained is to be reflected in the x-axis, giving OP_2. The vector OP' is found by completing the parallelogram POP_2P'.

This graphical method can be applied, of course, to points outside the b-circle, so that any point on any streamline past the circle can immediately be transformed to the t-plane in the same way, its radius r' being written for r.

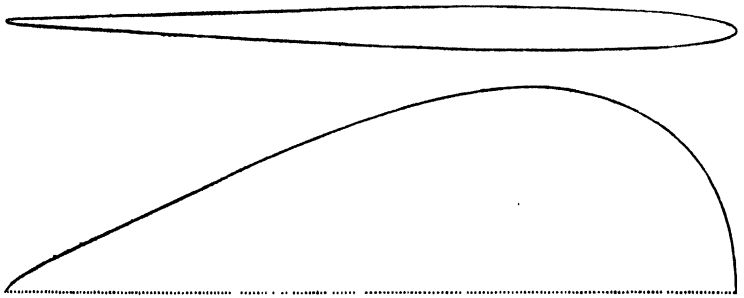

FIG. 86.—THIN JOUKOWSKI SECTION, BOTH POLES EXCLUDED.
One-half of the section is magnified transversely in the lower diagram to show details.

In Fig. 86 $b/a = 1{\cdot}05$, $OB/a = 0{\cdot}035$. The transformed section is of thin symmetrical streamline form, such as might be adopted for an aeroplane fin or tail-plane. Half the contour is also plotted with its thickness magnified ten times to show the slight rounding achieved at the trailing edge which is necessary for practical construction. Another point of practical interest is that an appreciable length of the rear part of the contour is very nearly straight.

Fig. 87 shows the streamlines round a thick section suitable for a strut, drawn by the same method. Here $b/a = 1{\cdot}24$, $OB/a = 0{\cdot}185$.

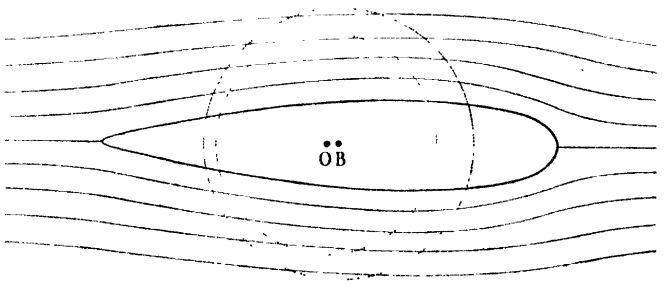

FIG. 87.—STREAMLINES PAST A JOUKOWSKI STRUT.

If the b-circle be so drawn as to enclose R only, passing through Q, a sharp trailing edge is obtained, as illustrated in Fig. 88. The

trailing edge is infinitely thin, both surfaces having a common tangent there, while the rear parts of the contour are concave outwards, making an unpractical shape. On the other hand, the section is analytically simple, and in some calculations may be substituted for a more complicated shape without serious error. A theoretical interest will also appear later in the sharp trailing edge. Unless otherwise stated, it is this particular type of section which will be referred to as a Joukowski symmetrical aerofoil.

FIG. 88.—STANDARD JOUKOWSKI SYMMETRICAL SECTION, ONE POLE ONLY EXCLUDED.

126. Approximate Dimensions

In many Aerodynamic applications of the foregoing the lines of sections are ' fine ' (cf. Article 107) and the reciprocal of the fineness ratio, called the thickness ratio, is then introduced. Thickness ratio is accordingly defined as the ratio of the maximum thickness of the section to the chord. For small thickness ratios b is little greater than a, and certain dimensions may be evaluated for the Joukowski symmetrical aerofoil.

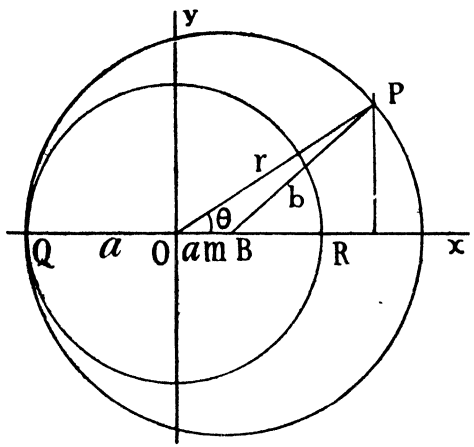

FIG. 89.

Let—

$$b = a(1 + m) \quad . \quad \text{(i)}$$

where m is small compared with a. Considering the point P (r, θ), Fig. 89—

$$(r \sin \theta)^2 + (r \cos \theta - am)^2 = b^2 = a^2 (1 + m)^2.$$

Neglecting the terms $(am)^2$ because m is small, this gives—

$$r^2 - 2ram \cos \theta = a^2 (1 + 2m) ;$$

or—

$$\frac{r^2}{a^2} - 2m \cos \theta \cdot \frac{r}{a} - (1 + 2m) = 0 \quad . \quad \text{(ii)}$$

Now r/a is positive. Again neglecting terms of order m^2—

$$\frac{r}{a} = m\cos\theta + \sqrt{(1+2m)}$$
$$= 1 + m(1+\cos\theta)$$

and—

$$\frac{a}{r} = 1 - m(1+\cos\theta) \quad . \quad . \quad \text{(iii)}$$

approximately.

Hence, in the t-plane we have for P', the point corresponding to P, remembering (154)—

$$\left.\begin{aligned} \xi &= a\cos\theta\left(\frac{r}{a}+\frac{a}{r}\right) = 2a\cos\theta \\ \eta &= a\sin\theta\left(\frac{r}{a}-\frac{a}{r}\right) = 2am\sin\theta(1+\cos\theta) \end{aligned}\right\} \quad \text{(iv)}$$

The first of these formulæ states that when m is small compared with a, the chord of the section is $4a$ to the first order. Again, the thickness ratio is the maximum value of $2\eta/4a$, and differentiating the right-hand side of the second formula with respect to θ and equating to zero gives $\cos\theta = \frac{1}{2}$, so that $\sin\theta = \frac{1}{2}\sqrt{3}$. Hence :

$$\text{Thickness ratio} = m \cdot \frac{\sqrt{3}}{2}(1+\tfrac{1}{2})$$
$$= \frac{3\sqrt{3}}{4}m = 1{\cdot}3\ m, \text{ approximately.} \quad (155)$$

The maximum thickness, occurring when $\cos\theta = \frac{1}{2}$, i.e. when $\xi = a$, is situated at one-quarter of the chord from the leading edge.

Eliminating θ leads to a simple formula by which narrow aerofoils of the cusped form shown in Fig. 88 can be plotted directly.

Let X be the distance from the trailing edge of a point on the chord-line, expressed non-dimensionally in terms of the chord. Then the first of (iv) gives—

$$X = \frac{2a+\xi}{4a} = \tfrac{1}{2}(1+\cos\theta).$$

Hence if Y denotes the ordinate at X, similarly expressed, the second of (iv) gives—

$$Y = \frac{\eta}{4a} = mX\sin\theta$$
$$= 2mX^{3/2}(1-X)^{1/2} \quad . \quad . \quad . \quad (156)$$

Rounded-tail Aerofoils.—Narrow sections derived by the Joukowski transformation from an eccentric circle enclosing both singular points, as in Fig. 85, can be treated similarly.

Let $b = a(1 + m)$ as before, and let $OB = al$, where $l < m$. The following expressions result in place of (iii)—

$$\frac{r}{a} = 1 + m + l\cos\theta$$

$$\frac{a}{r} = 1 - m - l\cos\theta.$$

Thus the first of (iv) remains unchanged, but the second becomes—

$$\eta = 2a\sin\theta(m + l\cos\theta). \quad . \quad . \quad \text{(v)}$$

Introducing X and Y as defined above and substituting,

$$Y = \tfrac{1}{2}\{1 - (2X - 1)^2\}^{1/2}\{m + l(2X - 1)\}$$
$$= (2lX + m - l)\,X^{1/2}\,(1 - X)^{1/2} \quad . \quad \text{(vi)}$$

The last expression can be rearranged as—

$$Y = 2lX^{3/2}\,(1 - X)^{1/2} + (m - l)X^{1/2}(1 - X)^{1/2}. \quad (157)$$

The first term on the right has the same form as in (156) and thus represents a thinner-cusped aerofoil. The second term is an ellipse. Hence the rounded-tail Joukowski symmetrical section can be described as a cusped aerofoil of reduced thickness enveloping, or built round, a core consisting of an ellipse of the same chord. The position of maximum thickness no longer occurs at one-quarter of the chord from the nose but farther back, depending upon the ratio m/l. Let X' denote the value of X for maximum thickness. Then by differentiating (157) and equating to zero,

$$\frac{1 - 8X'(1 - X')}{1 - 2X'} = \frac{m}{l}. \quad . \quad . \quad \text{(vii)}$$

For $m/l = 1$, $X' = \frac{3}{4}$, as already found. Reducing X' from this value soon causes m/l to increase rapidly, leading to predominance of the elliptic term in (157) and consequently to a notably blunt tail. The curve (a) of Fig. 90 is the half-profile of a symmetrical Joukowski

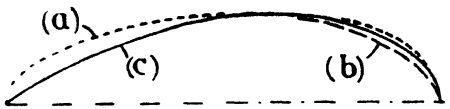

FIG. 90.—THICKNESS DISTRIBUTION OF SYMMETRICAL AEROFOILS WITH MAXIMUM THICKNESS AT 0·4 CHORD FROM NOSE.
(a) Joukowski, (b) Kármán-Trefftz, (c) Piercy.

aerofoil having a thickness ratio of 0·15 and the position of maximum thickness located at 0·4 of the chord from the nose ($X' = 0{\cdot}6$); in this case $m/l = 4{\cdot}6$. The curves (b) and (c) will be described later.

It will, of course, be noted that m is no longer connected with the thickness ratio by (155).

126A. Velocity and Pressure

The velocity q_t at any point in the flow past a symmetrical Joukowski section at zero incidence is calculated as follows:

The first step is to determine the point P (r, θ) in the z-plane of the circle corresponding to the given point ξ, η in the t-plane of the aerofoil. The transformation formula—

$$t = \xi + i\eta = z + a^2/z \quad . \quad . \quad \text{(i)}$$

gives on separation of real and imaginary parts—

$$\xi = (r + a^2/r)\cos\theta, \qquad \eta = (r - a^2/r)\sin\theta \quad . \quad \text{(ii)}$$

and combining these leads to—

$$\frac{\xi^2}{\cos^2\theta} - \frac{\eta^2}{\sin^2\theta} = 4a^2$$
$$\frac{\xi}{\cos\theta} + \frac{\eta}{\sin\theta} = 2r. \quad . \quad . \quad \text{(iii)}$$

θ is found from the first of (iii) and then r from the second.

The undisturbed velocity in the z-plane is taken as $-U$ and the circle as of radius b. The potential function of the flow past the circle is then—

$$w = \phi + i\psi = -U(z_1 + b^2/z_1), \quad . \quad \text{(iv)}$$

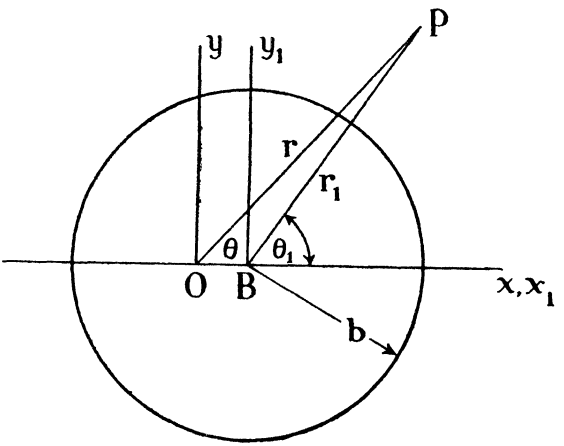

FIG. 90A.

in which $z_1 = x_1 + iy_1 = r_1 e^{i\theta_1}$ is the complex co-ordinate of a point referred to axes with B as origin parallel to Ox, Oy, B being the

centre of the circle, Fig. 90A. Considering the projections of OP, BP in the figure,

$$r\cos\theta = r_1\cos\theta_1 + OB$$
$$r\sin\theta = r_1\sin\theta_1,$$

so that—

$$\tan\theta_1 = \frac{r\sin\theta}{r\cos\theta - OB}, \qquad r_1 = \frac{r\sin\theta}{\sin\theta_1} \quad . \quad \text{(v)}$$

These together with (ii) enable the co-ordinate z_1 corresponding to the point given in the aerofoil-plane to be found.

The velocity q_z at P can now be obtained from (iv) by (iii) of Article 113A—

$$\left|\frac{dw}{dz_1}\right| = \left| - U(1 - b^2/z_1^2)\right|$$
$$= U\sqrt{\left\{\left(1 - \frac{b^2}{r_1^2}\right)^2 + 4\frac{b^2}{r_1^2}\sin^2\theta_1\right\}}. \quad . \quad . \quad \text{(vi)}$$

The transformation gives—

$$dt/dz = 1 - a^2/z^2 = 1 \text{ when } z \text{ is large.} \quad . \quad \text{(vii)}$$

Hence the undisturbed velocity is $-U$ in the t-plane as well as in the z-plane, and the velocity at the general point is given by (152) of Article 122, i.e.—

$$q_t = q_z \Big/ \left|\frac{dt}{dz}\right|.$$

In the same manner as for (vi) it is found that—

$$\left|\frac{dt}{dz}\right| = \sqrt{\left\{\left(1 - \frac{a^2}{r^2}\right)^2 + 4\frac{a^2}{r^2}\sin^2\theta\right\}}, \quad . \quad \text{(viii)}$$

the similarity to (vi), a feature of the Joukowski transformation, being due to the similarity between (i) and (iv).

These formulæ are general. But an important special case arises when the given point is on the profile of an aerofoil of normal thickness with a cusped tail and the corresponding point on the circular boundary. Then (vi) reduces to $q_z = 2U\sin\theta_1$, and $1 - 2m(1 + \cos\theta)$ can be substituted for a^2/r^2.

Finally, if P is the undisturbed pressure and p_t the pressure at the given point, Bernoulli's equation gives—

$$\frac{p_t - P}{\frac{1}{2}\rho U^2} = 1 - \left(\frac{q_t}{U}\right)^2. \quad . \quad . \quad \text{(ix)}$$

127. Kármán-Trefftz Symmetrical Sections

It has been seen that Joukowski sections suffer from practical limitations, briefly as follows. If the tail is sharp it is also cusped, and the shape of the profile is controlled by only one parameter, viz. m, which varies the thickness ratio; the position along the chord at which the maximum thickness of the section occurs is invariable and too far forward. Admitting a rounded tail is ineffectual because the tail becomes blunt, causing much form drag, when the position of maximum thickness is moved back appreciably. To overcome these and other drawbacks calls for more elaborate transformations.

An early improvement provided profiles which are known as extended or generalised Joukowski aerofoils, or after Kármán and Trefftz. The formula (154) is identical with—

$$\frac{t+2a}{t-2a} = \left(\frac{z+a}{z-a}\right)^2 \quad . \quad . \quad \text{(i)}$$

which is a special case of the transformation—

$$\frac{t+na}{t-na} = \left(\frac{z+a}{z-a}\right)^n \quad . \quad . \quad . \quad (158)$$

whose singular points are at $z = \pm a$ as before. Using (158) to transform a b-circle drawn through one of the singular points and enclosing the other, as shown in Fig. 89, enables the aerofoil to be given a 'tail angle' τ, defined as the angle at which the two sides of the section meet at the tail. The angle is secured by choosing for n a value less than 2 according to the relation—

$$n = 2 - \tau/\pi. \quad . \quad . \quad . \quad \text{(ii)}$$

Again, the position of maximum thickness can be adjusted while

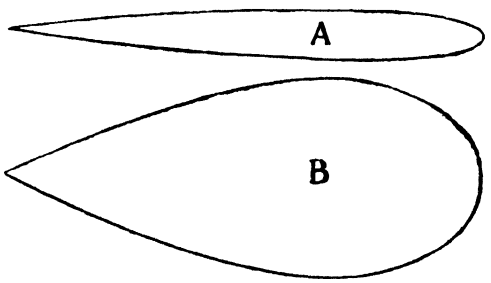

FIG. 91.—KÁRMÁN-TREFFTZ SECTIONS.

retaining a tail angle by suitably relating b/a to n; for example, $2n = 5 - b/a$ locates this position at one-third of the chord from

the nose. Two sections shown in Fig. 91 have the following characteristics:

Section	n	b/a	Thickness
A . . .	1·967	1·067	10 per cent.
B . . .	1·833	1·333	40 per cent.

The first might be suitable for a tail-plane; the second, better described as having a fineness ratio of 2·5, is rather thicker than would be used for a strut. But modern conditions usually require the maximum thickness to be located still farther back. The transformation (158) is insufficiently elastic from this point of view, as will be illustrated. Moreover, the simplicity distinguishing the Joukowski transformation is lost; (158) is best dealt with, indeed, as a special case of a more general transformation whose discussion is beyond the scope of this book. In these circumstances, the detailed treatment of these sections is left to further reading.*

It can be shown, however, that narrow Kármán-Trefftz sections accord closely with the formula—

$$Y = cX^{3/2}(1 - X)^{1/2} + sX(1 - X), \quad . \qquad (159)$$

where X and Y have the meanings defined in Article 126 and c and s are two parameters. The first term on the right is seen to have the same form as in (156), and the second term is a circular arc. Thus the section can be described as a cusped Joukowski aerofoil built round a core of the same chord formed by two segments of a circle. The non-dimensional distance X' of the position of maximum thickness from the tail is given by—

$$\frac{2(2X' - 1)\,(1 - X')^{1/2}}{(3 - 4X')X'^{\frac{1}{2}}} = \frac{c}{s}. \quad . \quad . \quad \text{(iii)}$$

As the position of maximum thickness is moved backward, c/s decreases, showing, in conjunction with (159), that the circular arc then tends to control the shape except close to the nose. The result is a flattening of the front part of the profile as illustrated by the half-profile (b) of Fig. 90, for which the maximum thickness is located at 0·4 of the chord from the nose ($c/s = 0·544$).

* Glauert, A.R.C.R. & M., No. 911; Fage, Falkner and Walker, A.R.C.R. & M., No. 1241.

128. Aerofoils inverted from Hyperbolas

A more amenable family * of aerofoils avoiding the defects of the Joukowski system is obtained by inverting one branch of an hyperbola. The shape is controlled by two independent parameters which may be arranged to secure a prescribed tail angle and position of maximum thickness of the section. The latter can usefully be varied between 0·3 and 0·45 of the chord from the nose (for farther back positions the nose sharpens rapidly). A description of the symmetrical form of this family is given in the following articles and provides an introduction to methods used in more advanced work, where the number of parameters is further increased.

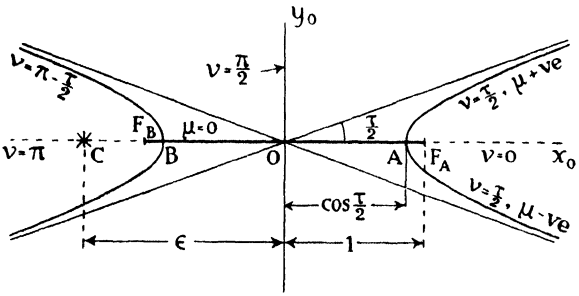

FIG. 92.—THE Z_0-PLANE.

Fig. 92 shows the two branches of an hyperbola whose centre is at the origin of a z_0-plane and whose 'transverse axis' AB lies on the x_0-axis. The foci are F_A, F_B and the angle between the asymptotes is τ. It is one of the family represented by the equation $x_0^2/\cos^2\frac{1}{2}\tau - y_0^2/\sin^2\frac{1}{2}\tau = 1$; $OF_A = 1$ and therefore $OA = \cos\tau/2$. The right-hand branch will be transformed into an aerofoil, for which purpose the complex co-ordinate $z_0 = x_0 + iy_0$ is suitable, but it will also be transformed into a circle and for this operation the complex co-ordinate is changed to $\zeta = \mu + i\nu$ by the formula $z_0 = \cosh\zeta$. Relations are readily found as in Articles 115 and 117 between x_0, y_0 and μ, ν, but the new co-ordinates differ from those of Article 117 in that μ may assume any real value, positive or negative, whilst ν is restricted to lie within the range O to π. It follows that ν = constant gives one of a system of confocal hyperbolas, the constant being equal to one-half the angle between the asymptotes, and that μ = constant gives the upper or lower half of one of a system of

* Piercy, Piper and Preston, *Phil. Mag.*, Ser. 7, vol. xxiv, p. 425 (1937). Piercy, Piper and Whitehead, *Aircraft Engineering*, November, 1938; Piper, *Phil. Mag.*, Ser. 7, vol. xxiv, p. 1114 (1937). For further generalisation and applications see later publications by Piercy and Whitehead (when released).

confocal ellipses, according to whether the latter constant is positive or negative, respectively.

Some other values of the co-ordinates are indicated in the figure. Along the x_0-axis : $\nu = 0$ and the sign of μ is indeterminate from F_A to infinity, ν increases from 0 to π and $\mu = 0$ from F_A to F_B, $\nu = \pi$ and the sign of μ is indeterminate from F_B to $-\infty$. Along Oy_0, $\nu = \pi/2$ and μ increases from 0 to ∞ ; along $-Oy_0$, $\nu = \pi/2$ and μ decreases from 0 to $-\infty$.

The hyperbola $\nu = \tau/2$ will be inverted with respect to a centre of inversion C located on the x_0-axis at a suitable distance ε from O, reckoned positive if C is to the left of the origin in the figure. Co-ordinates of C are distinguished by suffix c. If $\varepsilon < 1$, ζ_c lies between $i\tau/2$ and $i\pi$ since $\mu_c = 0$. If $\varepsilon > 1$, $\zeta_c = \mu_c + i\pi$, giving $z_{0c} = -\cosh \mu_c$, and this quantity is determinate although μ itself is rendered uncertain by the change of sign on crossing the x_0-axis beyond the focus.

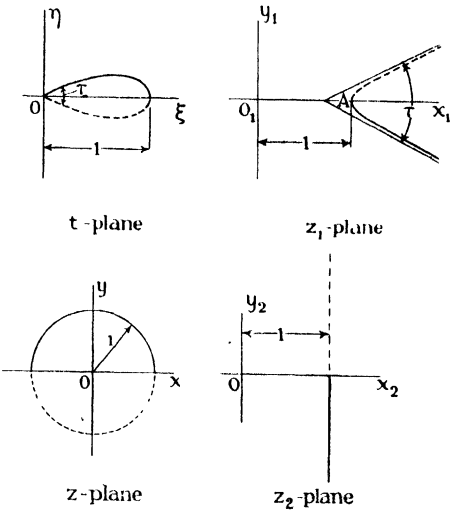

FIG. 92A.—THE AEROFOIL TO CIRCLE PLANES.

The right-hand branch of the hyperbola is replotted in the z_1-plane of Fig. 92A, where the origin O_1 is coincident with the centre of inversion C. Thus with $OF_A = 1$, the complex co-ordinate in this plane would be $z_1 = x_1 + iy_1 = \varepsilon + \cosh \zeta$, but a change of scale is made below to $O_1A = 1$, as marked in the figure.

In the t-plane of Fig. 92A is shown a symmetrical aerofoil obtained from the hyperbola by the formula—

$$tz_1 = 1. \quad . \quad . \quad . \quad (160)$$

Substituting $t = r_t e^{i\theta_t}$, $z_1 = r_1 e^{i\theta_1}$ leads at once to—

$$r_t = 1/r_1, \qquad \theta_t = -\theta_1. \quad . \quad . \quad . \quad (i)$$

Thus points remote from the origin in the z_1-plane are close to the origin in the t-plane, and vice versa ; remote parts of the hyperbola yield the back part of the aerofoil, and the part of the hyperbola in the neighbourhood of its vertex provides the rounded nose of the

aerofoil. The inversion is accompanied by reflection in the real axis, so that the upper side of the aerofoil corresponds to the lower side of the hyperbola, and vice versa. Thus μ is negative on the upper side of the aerofoil profile.

The chord c of the aerofoil is equal to the inverse of the x_1-axis beyond A, i.e. $1/O_1A$, and this is made equal to unity by multiplying lengths in the z_1-plane by $1/(\varepsilon + \cos \tau/2)$. Then the distance of C to the left of the centre of the hyperbola becomes $\varepsilon/(\varepsilon + \cos \tau/2)$, and the complex co-ordinate of the general point in the z_1-plane becomes—

$$z_1 = \frac{\varepsilon + \cosh \zeta}{\varepsilon + \cos \tau/2} \quad . \quad . \quad . \quad . \quad (161)$$

It will be seen that the tail angle τ of the aerofoil is equal to the angle τ between the asymptotes of the hyperbola. τ and ε comprise the two independent parameters of the family.

Plotting the Aerofoil Profile.—Any point on the hyperbolic boundary will be denoted by X_1, Y_1 and any point on the aerofoil profile by X, Y ; the co-ordinates are non-dimensionally expressed in terms of the chord, and X, Y have the same meanings as in Articles 126 and 127. With this notation, (160) gives—

$$X + iY = 1/(X_1 + iY_1) \quad . \quad . \quad \text{(ii)}$$

i.e., on rationalising the denominator on the right by multiplying by $X_1 - iY_1$ and separating real and imaginary parts,

$$X = X_1/R_1^2 \quad \text{and} \quad Y = -Y_1/R_1^2 \quad . \quad \text{(iii)}$$

where $R_1^2 = X_1^2 + Y_1^2$, and to map the aerofoil we have only to determine X_1 and Y_1. (161) gives, on separating real and imaginary parts,

$$X_1 = \frac{\varepsilon + \cosh \mu \cos \tau/2}{\varepsilon + \cos \tau/2} \text{ and } Y_1 = \frac{\sinh \mu \sin \tau/2}{\varepsilon + \cos \tau/2} \quad \text{(iv)}$$

for a chosen position of the centre of inversion and tail angle τ of the aerofoil. Eliminating μ yields the following relations between X_1 and Y_1 :

$$Y_1^2 = \varkappa^2(X_1 - 1)(X_1 + b) \quad . \quad . \quad . \quad \text{(v)}$$

where,

$$\varkappa = \tan \tau/2 \quad \text{and} \quad b = -\frac{\varepsilon - \cos \tau/2}{\varepsilon + \cos \tau/2}. \quad \text{(vi)}$$

The above method is exact, but an approximate formula which is more direct can usually be employed instead.

Noting that if $R^2 = X^2 + Y^2$ (ii) equally gives $X_1 = X/R^2$, etc., and substituting,

$$\frac{Y^2}{R^4} = \kappa^2\left(\frac{X}{R^2} - 1\right)\left(\frac{X}{R^2} + b\right). \quad . \quad \text{(vii)}$$

This expression also is exact. But it contains terms in Y^4 which may usually be neglected, leading to the approximate formula—

$$Y^2 = \frac{\kappa^2 X^2(1 - X)\,(1 + bX)}{1 - \kappa^2 X\{b(1 - X) - (1 + bX)\}}. \quad . \quad \text{(162)}$$

Further approximation is permissible in the case of very thin aerofoils, for which the denominator will differ little from unity, so that—

$$Y = \pm \kappa X(1 - X)^{1/2}(1 + bX)^{1/2}. \quad . \quad \text{(viii)}$$

But (162) should be employed for aerofoils having thickness ratios within the range 0·12 to 0·20 common in practice.

Parameters and Shape.—It is usually required to determine the parameters κ and b, whence τ and ε follow, for an aerofoil of chosen thickness ratio and position of maximum thickness. The condition for a maximum ordinate, i.e. $dY/dX = 0$, may be expressed as—

$$\frac{1}{Y_1} \cdot \frac{dY_1}{dX_1} = \frac{2X_1}{X_1^2 - Y_1^2}.$$

A second expression is obtained from (v), for differentiating both sides of that equation with respect to X_1 and dividing by $2Y_1^2$ gives—

$$\frac{1}{Y_1} \cdot \frac{dY_1}{dX_1} = \tfrac{1}{2}\,\frac{2X_1 + b - 1}{(X_1 - 1)(X_1 + b)}.$$

Equating the two expressions leads to—

$$b = \frac{Y_1^2(2X_1 - 1) + X_1^2(2X_1 - 3)}{X_1(4 - 3X_1) - Y_1^2} \quad \text{(ix)}$$

where the point X_1, Y_1 corresponds to the chosen co-ordinates X', Y' of the aerofoil profile at its position of maximum thickness. For an aerofoil so thin that Y_1^2 may be neglected, giving $X = 1/X_1$ approximately, (ix) reduces further to—

$$b = \frac{2 - 3X'}{X'(4X' - 3)}. \quad . \quad . \quad . \quad \text{(x)}$$

The curve (*c*) of Fig. 90 is the half-profile of an aerofoil of the present family with the position of maximum thickness located at 0·4 of the chord from the nose, and may be compared with the corresponding profiles (*a*) and (*b*) for the Joukowski and Kármán-Trefftz families, respectively, which have already been described.

129. Completion of the Transformation

The aerofoil cannot be transformed into a circle directly but only through the hyperbola, which is changed first into an infinite straight line in a z_2-plane, and then into the circle in a z-plane, Fig. 92A.

The first step is accomplished by the formula—

$$z_2 = \frac{1}{\varepsilon''}\left[\varepsilon'' + i \sinh \frac{\zeta - i\tau/2}{2 - \tau/\pi}\right], \quad . \quad . \quad (163)$$

where ζ has already been defined, being the complex $\mu + i\nu$ in which ν is restricted to lie between O and π. ε'' is a constant such as to ensure that the origins in the z_1- and z_2-planes shall be corresponding points. Hence, putting $z_1 = 0$ when $z_2 = 0$,

$$\varepsilon'' = - i \sinh \frac{\zeta_c - i\tau/2}{2 - \tau/\pi}. \quad . \quad . \quad (i)$$

This transformation may be regarded as changing the given hyperbola into the hyperbola which coincides with the y_0-axis in the z_0-plane, Fig. 92. However, in the z_2-plane it is defined by $\nu = \tau/2$, and the formula (163) arranges that the origin in this plane is at unit distance to the left of the straight line, as marked in Fig. 92A.

A circle inverts into a straight line if the centre of inversion lies upon the circle, and the formula—

$$z_2(z + 1) = 2 \quad . \quad . \quad . \quad (164)$$

inverts a circle of unit radius with centre at the origin in the z-plane into the straight line of the z_2-plane, and then the centre of inversion is at the point on the circle which corresponds to the origin in the t-plane.

This completes the transformation of the aerofoil of unit chord into the circle of unit radius. In the reverse order, (164) opens out the circle into an infinite straight line, (163) and (161) turn the straight line into one branch of an hyperbola, and (160) inverts the hyperbola into the aerofoil.

To enable the flow past the aerofoil to be inferred from the simple flow past the circle, the above process must conformally transform the region exterior to the circle into the region exterior to the aerofoil; all singularities must be excluded from these two regions except only the singularity yielding the sharp tail of the aerofoil. (164) transforms the region exterior to the circle into the region to the left of the infinite straight line in the z_2-plane, giving a singularity at the origin in the z_2-plane. (163) and (161)

transform this region into the entire region to the left of (or outside) the right-hand branch of the hyperbola, introducing no further singularity in the region considered not on the boundary. The singularity at the origin in the z_1- and z_2-planes occurs at corresponding points in those two planes and at infinity in the z- and t-planes, while the singularity on the circle and aerofoil boundaries occurs at corresponding points in the z- and t-planes and at infinity in the others.

The foregoing may be illustrated by considering the nature of the flow in each plane. The uniform flow at a large distance from the boundary in the z-plane becomes on inversion a doublet at the origin in the z_2-plane. The transformation from the z_2-plane to the z_1-plane carries over this doublet to the origin in the z_1-plane, only its strength being changed. The final inversion into the aerofoil plane reconverts the doublet into a uniform flow at infinity in that plane, though not of the same velocity as the uniform flow in the z-plane. The change of velocity between the circle and aerofoil planes must be allowed for but is easily determined, as in the next article.

129A. Velocity on the Aerofoil Boundary

Calculation of the velocity in the t-plane from that in the z-plane requires in the first place a relationship between the positions of corresponding points. For any point on the aerofoil boundary, μ can be found from (iii) and (iv) of Article 128, and this boundary value of μ is related as follows to the corresponding angle θ in the circle plane. Substituting $z = e^{i\theta}$ (since $r = 1$ on the circle) in (164) and, in the same equation, expressing z_2 in terms of $\zeta = \mu + i\tau/2$ from (163),

$$\tan\frac{\theta}{2} = -\frac{1}{\epsilon''}\sinh\frac{\mu}{2-\tau/\pi}. \quad . \quad . \quad \text{(i)}$$

The next step is to evaluate mod. dz/dt from—

$$\left|\frac{dz}{dt}\right| = \left|\frac{dz}{dz_2}\right| \cdot \left|\frac{dz_2}{d\zeta}\right| \cdot \left|\frac{d\zeta}{dz_1}\right| \cdot \left|\frac{dz_1}{dt}\right|. \quad . \quad . \quad \text{(ii)}$$

The transformation formulæ give—

$$\frac{dz}{dz_2} = -\tfrac{1}{2}(z+1)^2$$

$$\frac{dz_2}{d\zeta} = i\,\frac{1}{\epsilon''(2-\tau/\pi)}\cosh\frac{\zeta - i\tau/2}{2-\tau/\pi}$$

$$\frac{d\zeta}{dz_1} = \frac{\varepsilon + \cos \tau/2}{\sinh \zeta}$$

$$\frac{dz_1}{dt} = -\frac{1}{t^2}$$

whence (ii) yields after reduction—

$$\left|\frac{dz}{dt}\right| = A \cos^2 \frac{\theta}{2} \cosh \frac{\mu}{2 - \tau/\pi} \cdot \frac{R_1^2}{\sqrt{(\sinh^2 \mu + \sin^2 \tau/2)}}, \quad \text{(iii)}$$

where the constant coefficient has the value—

$$A = \frac{2(\varepsilon + \cos \tau/2)}{\varepsilon''(2 - \tau/\pi)}. \quad \text{(iv)}$$

The velocity $-U$ at infinity in the aerofoil plane is derived from the velocity $-U'$ at infinity in the circle plane by—

$$-U = -U' \left|\frac{dz}{dt}\right|_\infty. \quad \text{(v)}$$

For z and t large, z_1 and z_2 are the co-ordinates of the centre of inversion, and (ii) gives—

$$\left|\frac{dz}{dt}\right|_\infty = \frac{A}{4} \left|\left(\frac{z+1}{t}\right)^2\right|_\infty \cdot \frac{\left|\cosh \dfrac{\zeta_c - i\tau/2}{2 - \tau/\pi}\right|}{|\sinh \zeta_c|}. \quad \text{(vi)}$$

But from (v) we can write, owing to the large values of t and z,

$$\left[\frac{dt}{dz}\right]_\infty = \frac{t}{z} = \frac{t}{z+1}$$

and substituting in (vi) gives—

$$\left|\frac{dz}{dt}\right|_\infty = \frac{4}{A} \frac{|\sinh \zeta_c|}{\left|\cosh \dfrac{\zeta_c - i\tau/2}{2 - \tau/\pi}\right|},$$

which reduces to—

$$\left|\frac{dz}{dt}\right|_\infty = \frac{4}{A} \left(\frac{\varepsilon^2 - 1}{\varepsilon''^2 - 1}\right)^{1/2}. \quad \text{(vii)}$$

Thus the proportionate increase of velocity from the undisturbed speed U in the aerofoil plane, at the point t corresponding to the point z in the circle-plane where the ratio q_z/U' is known, is given by—

$$\frac{q_t}{U} = \frac{q_z}{U'} \cdot \left|\frac{dz}{dt}\right| \div \left|\frac{dz}{dt}\right|_\infty$$

$$= \frac{q_z}{U'} \cdot \left|\frac{dz}{dt}\right| \cdot \left(\frac{\varepsilon''^2 - 1}{\varepsilon^2 - 1}\right)^{1/2} \cdot \frac{A}{4}, \quad (165)$$

where the modulus on the right is given by (iii) and A by (iv).

129B. Comparison with Experiment and Example

Question arises as to how far calculations of velocity based upon the assumption of wholly irrotational flow agree with experiment in the case of streamline sections. A comparison between theory and experiment has been made* at the National Physical Laboratory in the case of the very thick Kármán-Trefftz aerofoil *B* of Fig. 91. The theoretical pressure distribution, ignoring the boundary layer and wake, is shown as the full-line in Fig. 92B. Experimental observations for this section obtained at a Reynolds number of 6×10^5 gave the broken line. Agreement is seen to be close over 80 per cent. of the contour. With a small thickness ratio experiment still diverges from the present theory as the tailing edge is approached, but to a much less extent than in the extreme case illustrated. Equally successful comparisons have also been made with symmetrical sections of the simple Joukowski type.

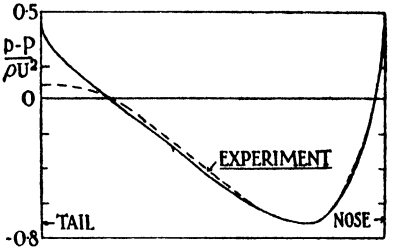

FIG. 92B.—PRESSURE DISTRIBUTIONS OF THEORY AND EXPERIMENT COMPARED FOR THE SECTION B OF FIG. 91.

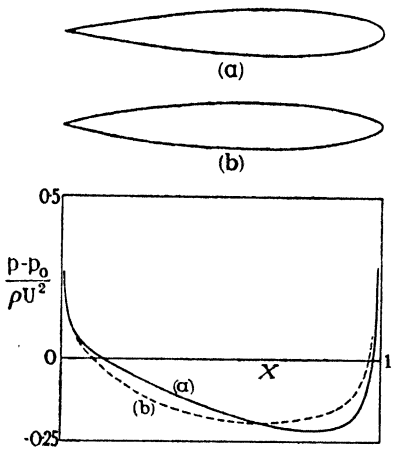

FIG. 92C.—PRESSURE DISTRIBUTIONS FOR MAXIMUM THICKNESS LOCATED AT (*a*) 0·35 CHORD AND (*b*) 0·425 CHORD FROM NOSE.

The important conclusion is that for the Reynolds numbers of Aeronautics the present methods enable reliable calculations to be made, except near the trailing edge, of the pressure round derived shapes of streamline form, and of the velocity field outside their boundary layers.†

In these circumstances the theory finds many Aerody-

* *Loc. cit.*, page 211.

† According to Piercy, Preston and Whitehead, *Phil. Mag.*, Ser. 7, vol. xxvi, p. 802 (1938), approximate allowance can be made for the wake of a bluff section by determining the potential function as for an imaginary elongated boundary, in which the back of the section is replaced by a narrow extension to infinity, representing the wake.

namical applications, one of which is indicated in Fig. 92c. In the figure there have been drawn two examples of the family of aerofoils inverted from hyperbolas. Both have a thickness ratio of 0·15, but for (*a*) the position of maximum thickness is at 0·35 chord from the nose, while for (*b*) it is at 0·425 chord from the nose. The distribution of the theoretical pressure distribution round the two boundaries is also shown and can be relied upon to agree fairly with experiment except in the region of the tail. The difference illustrates a decrease in the *maximum velocity ratio* achieved by displacing the position of maximum thickness backward. This decrease and the backward displacement of the position round the profile at which the maximum velocity occurs are of importance in designing sections for low drag and high speeds.

DERIVED WING SECTIONS

130. Circular Arc Skeletons—Joukowski Transformations

The straight lines to which the circle of radius a transforms by formulæ (154) or (158) are known as the skeletons of the symmetrical sections given by these formulæ when applied to a circle of greater radius b with centre on the x-axis. Skeletons of arched form are obtained by locating the centre B of the b-circle on the y-axis and drawing the b-circle through both the singular points Q and R, $x = \pm a$.

Dealing first with formula (154), and applying it to any point P (r, θ) on the b-circle so drawn (Fig. 93), we have as before for the co-

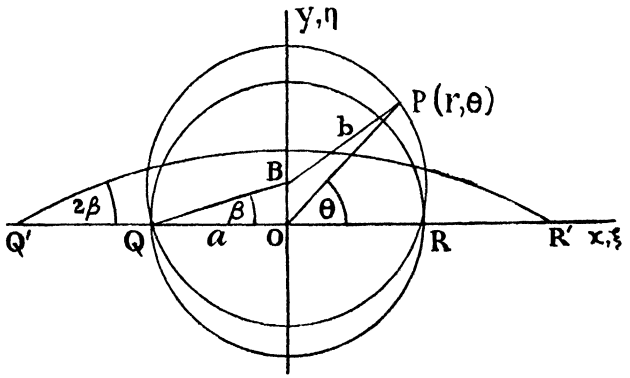

FIG. 93.

ordinates of the corresponding point P' in the t-plane—

$$\xi = (r + a^2/r) \cos \theta \quad . \quad . \quad \text{(i)}$$

$$\eta = (r - a^2/r) \sin \theta. \quad . \quad . \quad \text{(ii)}$$

From the triangles OQB, OBP with β as shown—

$$b^2 = a^2 \sec^2 \beta = r^2 + a^2 \tan^2 \beta - 2ra \tan \beta \sin \theta$$

or—

$$r - a^2/r = 2a \tan \beta \sin \theta$$

Hence from (ii):

$$\eta = 2a \tan \beta \sin^2 \theta \quad . \quad . \quad \text{(iii)}$$

showing that two points on the b-circle at $\pm \theta$ transform to a single point in the t-plane, and that the maximum ordinate of the transformed curve is situated on the η-axis ($\theta = \pi/2$) and equals $2 \, . \, OB$. Q and R transform to Q' and R' (Fig. 93), giving $Q'R' = 4a$, as seen from (i) and (ii). The ratio of the maximum ordinate of the arch to its chord is called the camber and from (iii) equals $\frac{1}{2} \tan \beta$.

Squaring (i) and (ii) and by subtraction we find—

$$\frac{\xi^2}{\cos^2 \theta} - \frac{\eta^2}{\sin^2 \theta} = 4a^2,$$

and eliminating θ by (iii) gives for the equation of the arch—

$$\xi^2 + (\eta + 2a \cot 2\beta)^2 = (2a \operatorname{cosec} 2\beta)^2 \, . \quad \text{(iv)}$$

a circle whose centre is on the η-axis at $\eta = -2a \cot 2\beta$. The tangent at Q' is inclined at the angle 2β to the ξ-axis.

Whilst the formula (154) thus transforms the b-circle passing through Q and R to both sides of a circular arc, formula (158) transforms it into two circular arcs (Fig. 94), which intersect at Q', R'

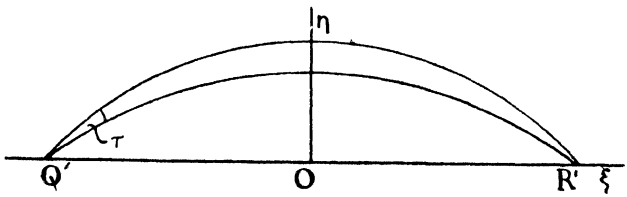

FIG. 94.

at the tail angle $\tau = \pi(2 - n)$. The figure is readily obtained by the methods of Article 127.*

These and other arched skeletons may be used to bend symmetrical aerofoil sections into cambered wing shapes. The modulus is not then known, however.

131. Joukowski Wing Sections

We now consider in some detail wing sections of a certain type introduced by Joukowski in 1910, which are susceptible to simple analysis.

To obtain these the formula (154) is applied to a b-circle passing

* The transformation is known after Kutta. Detailed investigation of this and other shapes is given in a paper by Mrs. Glauert, *Jour. R.Ae.S.*, July 1923, which should be read.

through one of the singular points, Q say, and enclosing the other, with centre B slightly displaced from both axes. For a section of normal proportions to result, the angle β which QB makes with Ox requires to be small and EB (Fig. 95) a small fraction of a.

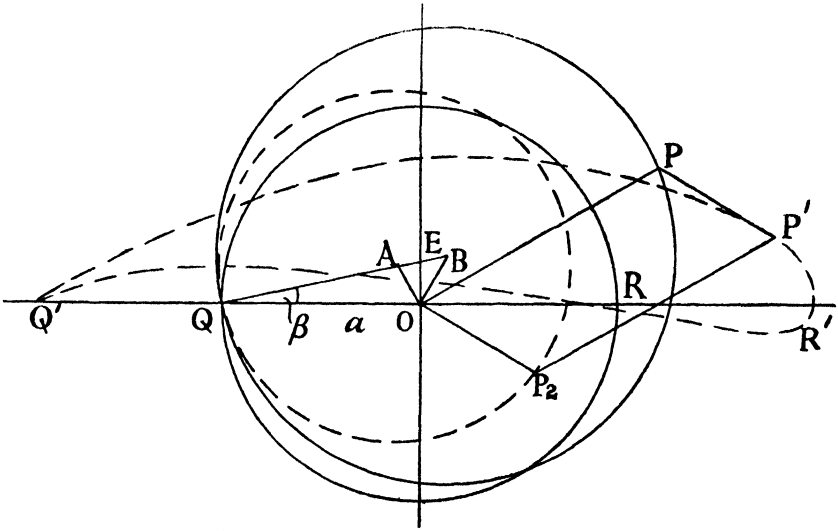

FIG. 95.—CONSTRUCTION FOR JOUKOWSKI CAMBERED WING.

A transformed profile of this class is shown in the figure. A point P' on it is found from the corresponding point P (r, θ) on the b-circle in the z-plane exactly as described in Article 125. It may be noted that the locus of P_1, the reflexion of P in the a-circle as it moves round the b-circle, is another circle of radius $< a$ whose centre lies on BO produced. The image in the x-axis of the centre of this latter circle, the point A on QB, is the centre of the equal circular locus of P_2, the reflexion of P_1 in the x-axis. The circle with centre A is called the auxiliary circle, and has a common tangent with the b-circle at Q. It is easily found that OA, OB make equal angles with Oy. With the help of the auxiliary circle, the locus of P', i.e. the aerofoil contour in the t-plane, is plotted rapidly.

Joukowski wing sections are infinitely thin at the trailing edge, like the corresponding symmetrical sections, as is evident from the preceding article.

132. Approximate formulæ for the co-ordinates ξ, η of any point P' on the wing are found as follows:

Let m be the small fraction that EB is of a, so that, since β is small we have approximately—

$$b = a(1 + m). \quad . \quad . \quad . \quad \text{(i)}$$

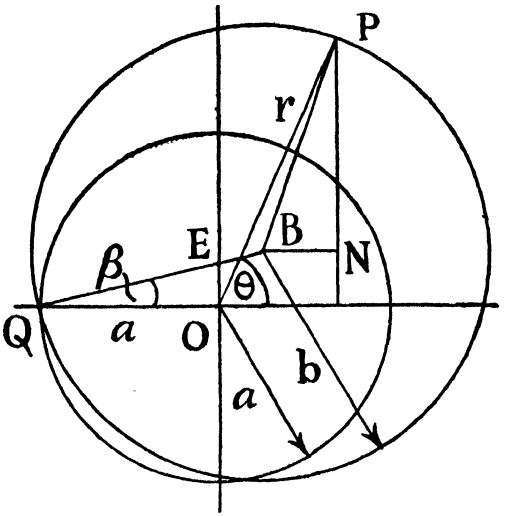

FIG. 96.

From Fig. 96 and (i)—

$$(PN)^2 = (r\sin\theta - ma\sin\beta - a\tan\beta)^2 = r^2\sin^2\theta - 2ra\beta\sin\theta$$
$$(BN)^2 = (r\cos\theta - ma\cos\beta)^2 = r^2\cos^2\theta - 2ram\cos\theta$$
$$(BP)^2 = b^2 = (QB)^2 = (a\sec\beta + ma)^2 = a^2 + 2ma^2.$$

The right-hand members are obtained by taking account of m and β being small and neglecting terms of smaller order.

Hence, since $(PN)^2 + (BN)^2 = (BP)^2$,

$$r^2 - 2ra(\beta\sin\theta + m\cos\theta) = a^2(1 + 2m)$$

or—

$$\left(\frac{r}{a}\right)^2 - 2\frac{r}{a}(\beta\sin\theta + m\cos\theta) - 1 - 2m = 0.$$

This gives:

$$\frac{r}{a} = 1 + \beta\sin\theta + m(1 + \cos\theta)$$
$$\frac{a}{r} = 1 - \beta\sin\theta - m(1 + \cos\theta)$$

to the first order.

Finally—

$$\xi = a\left(\frac{r}{a} + \frac{a}{r}\right)\cos\theta = 2a\cos\theta \quad . \quad \text{(ii)}$$
$$\eta = a\left(\frac{r}{a} - \frac{a}{r}\right)\sin\theta$$
$$= 2a\sin\theta\{m(1 + \cos\theta) + \beta\sin\theta\}. \quad . \quad \textbf{(166)}$$

These formulæ may be compared with those of Article 126 for a symmetrical Joukowski section. The first shows that the ξ-ordinate is the same to the approximation considered and the chord equal to $4a$ as before. The η-ordinate is increased by the term $2a\beta \sin^2 \theta$.

133. Shape of Joukowski Wings

The shape depends upon the particular values assumed for m and β. Provided always that these are small, certain characteristics may be conveniently expressed.

It is first seen that the thickness ratio is still given by (155). For, if η, η' are the ordinates of points on the upper and lower surfaces at any distance along the chord specified by ξ, the thickness T at that position is given by—

$$T = \eta - \eta'$$

and if η is transformed from a point on the b-circle whose radius makes an angle θ with Ox, the corresponding angle leading to η' will be $-\theta$. Hence from (166) of the preceding article :

$$T = 4am \sin \theta (1 + \cos \theta)$$

and, on comparison with Article 126 (iv), the result follows. The maximum thickness again occurs at one-quarter of the chord from the leading edge.

The mean camber is defined by the maximum value of $\frac{1}{2}(\eta + \eta')$ divided by the chord, or $(\eta + \eta')/8a$ for m, β small, and from the preceding article :

$$\eta + \eta' = 4a\beta \sin^2 \theta.$$

The maximum value of this, occurring when $\theta = \frac{1}{2}\pi$, is $4a\beta$. Hence :

$$\text{Mean camber} = \tfrac{1}{2}\beta \quad . \quad . \quad . \quad (167)$$

as is seen alternatively from Article 130.

Kármán-Trefftz Aerofoils

Wing sections of the generalised Joukowski type with finite tail angle result from transforming a b-circle whose centre is offset from both axes in the z-plane by the formula (158). The process is facilitated by the formulæ developed in the papers to which reference has already been made. Kármán-Trefftz cambered aerofoils have recently been developed further by introducing an additional parameter.*

* Betz and Keune, *Jahrbuch d. LFF.*, 1937.

133A. Cambered Aerofoils Inverted from Hyperbolas

Cambered aerofoils closely resembling the sections of modern wings result from inverting hyperbolas with respect to a centre of inversion which is displaced from the axis of symmetry. The transformation into a circle requires only slight modification of the formulæ given in Articles 128–9 for symmetrical aerofoils of the family.

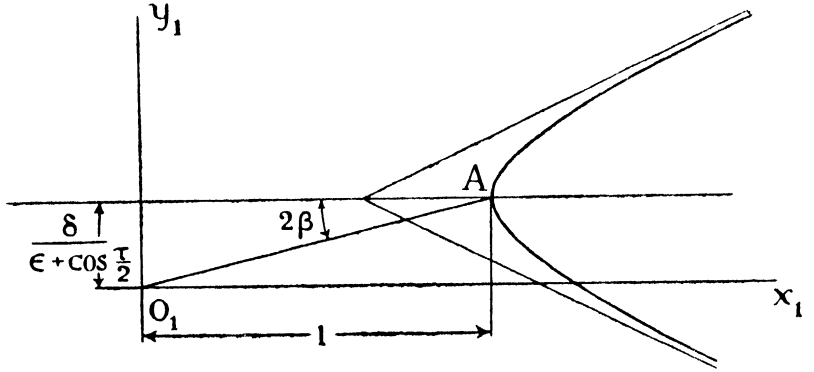

FIG. 96A.

Referring to the z_1-plane of Fig. 92A, let the axis of symmetry of the right-hand branch of the chosen hyperbola be displaced parallel to itself through a distance $\Delta y_1 = \delta$ such that the origin in this plane may still coincide with the centre of inversion. Fig. 96A illustrates the modification. The complex z_1 is then related to ζ by—

$$z_1 = \frac{\epsilon + i\delta + \cosh\zeta}{\epsilon + \cos\tau/2} \quad . \quad . \quad (161A)$$

in place of (161).

An aerofoil of zero thickness is obtained in the t-plane when the hyperbola degenerates into both sides of the part of the axis of symmetry beyond the focus, i.e. the line $\nu = 0$ (cf. Article 128). This straight line inverts into a circular arc in the t-plane.

A cambered aerofoil of small thickness results from $\nu = \tau/2$ where τ is small, and the above circular arc approximates closely to the median line of its section and is therefore called its camber-line. The camber-line may be slightly extended to intersect the aerofoil profile at the nose, the extension representing the inversion of the short length $F_A A$ of the x_1-axis, and then the co-ordinate of the front end of the camber-line, called the nose of the aerofoil, is $\zeta = i\tau/2$. The part of the line $O_1 A$ beyond the vertex A of the

hyperbola inverts into the chord-line of the cambered aerofoil, and the angle 2β between this line and $F_A A$ remains unchanged by the transformation close to the nose of the aerofoil. Hence, at the nose the camber-line makes with the chord-line the angle 2β defined by (see Fig. 96A)—

$$\tan 2\beta = \frac{\delta}{\epsilon + \cos \tau/2}$$

and it follows that the amount of camber, or the mean camber, is $\frac{1}{2}\beta$ as in (167).

For constant values of the parameters ϵ and τ, the maximum thickness and its position along the chord of an aerofoil are only slightly affected by camber. Thus appropriate values for the parameters may be determined by means of the formulæ already given for symmetrical sections of the family, whence δ follows on choosing the camber. If a bi-convex section is desired, the camber must be so restricted that the centre of inversion lies between the asymptotes produced of the hyperbola, i.e. δ must be less than $\epsilon \tan \tau/2$.

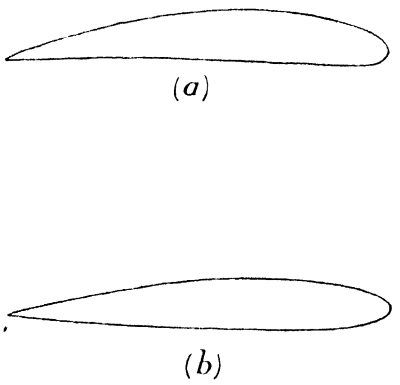

FIG. 96B.—EXAMPLES OF CAMBERED SECTIONS.
The value of δ is greater for (*a*) than for (*b*).

Retaining the same change of scale between the z_0- and z_1-planes, as adopted for the symmetrical sections, results in the distance between the centre of inversion and the vertex of the hyperbola being no longer equal to unity. The inversion formula (160) is accordingly modified for cambered aerofoils to—

$$tz_1 = 1 + i \tan 2\beta \quad . \quad . \quad . \quad (160A)$$

in order that they shall have unit chord. The change also rotates the aerofoil through the angle 2β so that the real axis of the t-plane contains its chord-line, which would otherwise be inclined thereto.

With this change the formulæ (ii) and (iii) of Article 128 become for points on the boundaries of cambered aerofoils—

$$X + iY = (1 + i \tan 2\beta)/(X_1 + iY_1) \quad . \quad (iiA)$$

and—

$$X = (X_1 + Y_1 \tan 2\beta)/R_1^2$$
$$Y = -(Y_1 - X_1 \tan 2\beta)/R_1^2, \quad \text{(iiiA)}$$

whilst to relate X_1, Y_1 to μ for points on the hyperbolic boundary we now have in place of (iv) of Article 128—

$$X_1 = \frac{\varepsilon + \cosh \mu \cos \tau/2}{\varepsilon + \cos \tau/2},$$
$$Y_1 = \tan 2\beta + \frac{\sinh \mu \sin \tau/2}{\varepsilon + \cos \tau/2}, \quad \text{(ivA)}$$

Thus the only modification of the values of X_1, Y_1 for points on the hyperbolic boundary is the inclusion of $\tan 2\beta$ in the expression for Y_1. It follows that the relation (v) of Article 128 between X_1 and Y_1 will be applicable to cambered aerofoils of the family if Y_1 is replaced by $Y_1 - \tan 2\beta$.

Fig. 96B shows two cambered aerofoils of this family.

LIFT OF WINGS OF INFINITE SPAN

134. Joukowski's Hypothesis

Suitable values being chosen for parameters and a definite aerofoil shape obtained in the t-plane, the same transformation process converts the streamlines past the circle to the corresponding streamlines past the aerofoil. Now when this process is applied to flow without circulation in the z-plane, results follow of which Fig. 97

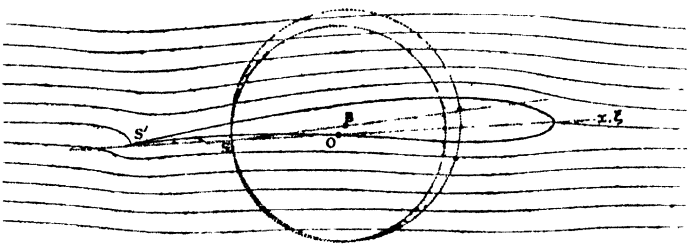

FIG. 97.—STREAMLINES PAST JOUKOWSKI AEROFOIL WITHOUT CIRCULATION.

is typical; the back stagnation point, S, on the circle transforms to the back stagnation point S' lying on the upper surface of the aerofoil some distance in front of its trailing edge. As with the thin plate, normal or inclined to a stream, fluid is asked to whip round a sharp edge, attaining an infinite velocity in the process.

It is easily proved, as follows, that for all conformal transformations the circulation round the aerofoil is the same as the circulation round the circle. Construct any two corresponding circuits enclosing the circle and aerofoil respectively. Then, since ϕ is the same at corresponding points (Article 122), the interval of ϕ round each circuit will be the same. But the circulation is the interval of ϕ round a complete circuit. It is important to note that this result is independent of the relationship between the undisturbed velocities in the two planes.

In Fig. 97, therefore, there is no circulation round the aerofoil, and it will shortly be proved generally that no force arises on the aerofoil in these circumstances. Now, the criticism that fluid cannot turn round the sharp trailing edge might be met by rounding that edge, which could be achieved by enclosing all singular points within the aerofoil, as we have seen. But the result of zero lift, incompatible with experiment, would still suggest the streamlines to be discordant with fact.

Modifying the streamlines past the circle by adding a small circulation K displaces the point S' backward, and a particular relationship between K and the undisturbed velocity makes S' coincide with the sharp trailing edge, so that the velocity there becomes finite.

Joukowski's hypothesis is that K is correctly and uniquely determined by the above consideration. Briefly, let Q be the point on the circle which transforms to Q' the trailing edge of the aerofoil. Since $dt/dz = 0$ at Q and

$$q_t = q_z \left| \frac{dz}{dt} \right|,$$

clearly only one condition permits of a finite velocity at Q', viz. when $q = 0$ at Q, i.e. the value of K to be added to the flow past the circle must be such as to make S coincide with Q. It is applicable only to wings with a sharp trailing edge, although a tail angle may exist. But it may be supposed that if we determine K for such a wing, and then slightly round the trailing edge for ease of construction, the effect of the modification will be small.

135. Calculation of K

Denote the undisturbed velocity by q_0, and let it be inclined at an angle α to the x-axis. With $K = 0$, the stagnation points on the circle are S_1, S (Fig. 98). These approach one another in that half

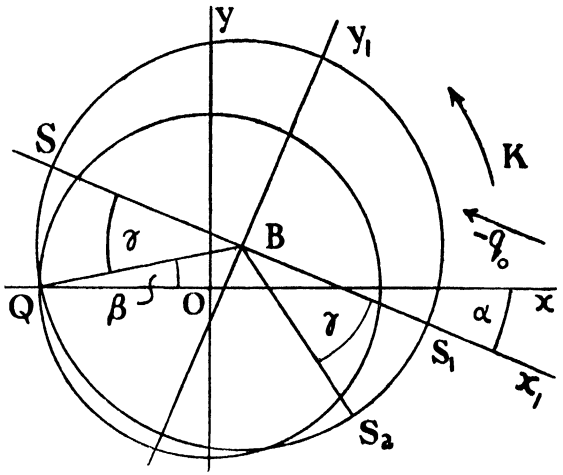

FIG. 98.

of the circle which transforms to the lower surface of the aerofoil when K is added in the direction shown.

Referred to axes Bx_1, By_1 through B as origin parallel and perpendicular to q_0, the flow past the circle is given by—

$$w = -q_0\left(z_1 + \frac{b^2}{z_1}\right) - i\frac{K}{2\pi}\log z_1 \quad . \quad \text{(i)}$$

whence—

$$\psi = -q_0\left(r - \frac{b^2}{r}\right)\sin\theta - \frac{K}{2\pi}\log r. \quad . \quad . \quad (168)$$

If q_b denote the peripheral velocity round the circle—

$$q_b = -\left[\frac{\partial\psi}{\partial r}\right]_{r=b} = 2q_0\sin\theta + \frac{K}{2\pi b},$$

giving—

$$q_b = 0 \text{ when } K = -4\pi b q_0 \sin\theta$$

(Cf. Article 109).

Hence, for the stagnation points to recede to Q, S_2—

$$\begin{aligned} K &= 4\pi b q_0 \sin\gamma \\ &= 4\pi b q_0 \sin(\alpha + \beta) \quad . \quad . \quad . \quad (169) \end{aligned}$$

from the figure, determining K in the z-plane.

The figure refers particularly to the Joukowski transformation, but the theorem is general. When less simple transformations are employed, however, care must be taken to note that the velocity

and angles of (169) refer to the circle-plane and may be changed in passing to the aerofoil-plane.

136. The Streamlines

Plotting (168) with the prescribed value of K/q_0 gives the streamlines appropriate to a chosen value of α in the z-plane (cf. Article 109). Transforming these gives the flow past the aerofoil. An example is shown in Fig. 99. The value of K/q_0 and, therefore, the

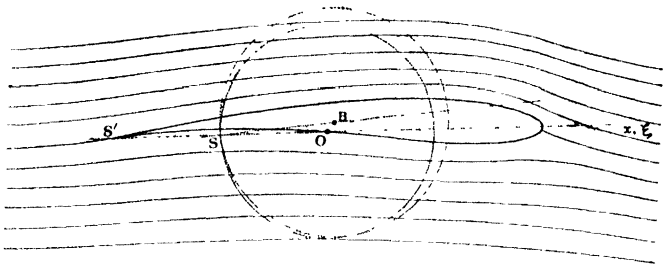

FIG. 99.—STREAMLINES PAST THE AEROFOIL OF FIG. 97 WITH CIRCULATION ACCORDING TO JOUKOWSKI'S HYPOTHESIS.

streamlines past the aerofoil, will change if α be varied. Thus the method is generalised as regards angle of incidence of the aerofoil.

In the z-plane there is a lift L per unit length of the circular cylinder given by—

$$L = \rho K q_0. \quad . \quad . \quad . \quad . \quad (170)$$

This force is perpendicular to the direction of q_0.

The velocity round the profile of the aerofoil may be obtained by the methods already described, and hence, from Bernoulli's equation, the variation of pressure. Finally, the lift may be evaluated by a graphical integration (cf. Article 44), and will be found to be the same as L for the same undisturbed velocity.

Analytical investigation is given in the following articles.

137. The Lift

In the t-plane draw a circle of large radius R enclosing the aerofoil at its centre (Fig. 100), and take axes $O\xi'$, $O\eta'$ parallel and perpendicular to q_0. Since R is great, the circulation velocity component at the circle is unaffected by the shape of the aerofoil (cf. Article 115). It equals $K/2\pi R$, and is perpendicular to R. At any point P (R, θ) it has components $\cos\theta \,.\, K/2\pi R$ perpendicular to q_0

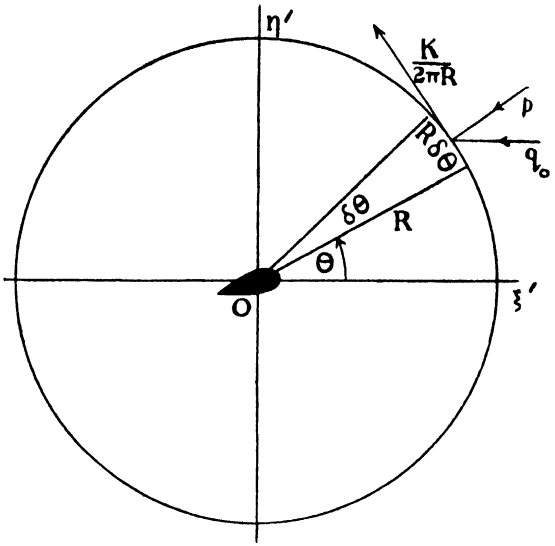

FIG. 100.

and sin θ . $K/2\pi R$ parallel to q_0. Thus the resultant velocity q at P is given by—

$$q^2 = \left(\frac{K}{2\pi R}\cos\theta\right)^2 + \left(\frac{K}{2\pi R}\sin\theta + q_0\right)^2. \quad . \quad \text{(i)}$$

Consider an element of the circle $R.\delta\theta$ at P, and let m be the fluid mass crossing it per second. We have—

$$m = \rho q_0 \,.\, R\delta\theta \,.\, \cos\theta. \quad . \quad . \quad \text{(ii)}$$

When P is on the upstream side of the aerofoil, the streamlines having an upward trend, passage across the element communicates upward momentum at the rate $m\cos\theta.K/2\pi R$ to the fluid within the circle. This calculation is correct wherever the element is situated. Hence the fluid within the circle will, on account of the flux of fluid across its whole contour, have its momentum in the direction $O\eta'$ increased at the rate—

$$\frac{\rho K q_0}{2\pi}\int_0^{2\pi}\cos^2\theta d\theta$$

$$= \tfrac{1}{2}\rho K q_0. \quad . \quad . \quad . \quad \text{(iii)}$$

We have omitted to attach a sign to q_0, and it is evident that this should be negative, since the velocity is in the direction $-O\xi'$. Hence the last member of (iii) when essentially positive gives the rate at which the fluid within the circle is receiving momentum from the aerofoil in a downward direction, i.e. in the direction $-O\eta'$. This

is checked by the fact that the aerofoil bends the streamlines downward.

The fluid outside the circle exerts, we shall also find, an upward force on the fluid within by virtue of the pressure p acting radially inward. This must also be taken into account.

Considering again the contour-element $R\delta\theta$, the upward force on it is $-p \sin\theta \,.\, R\delta\theta$. Integrating round the circle we find the whole force to amount to—

$$-R\int_0^{2\pi} p \sin\theta d\theta \quad . \quad . \quad . \quad \text{(iv)}$$

Now p is related to q by Bernoulli's equation. If p_0 is the undisturbed pressure of the stream, using (i)—

$$p + \tfrac{1}{2}\rho\left(\frac{K^2}{4\pi^2R^2} + \frac{K}{\pi R}q_0 \sin\theta + q_0^2\right) = p_0 + \tfrac{1}{2}\rho q_0^2$$

and since R is large, the velocity term in $1/R^2$ is negligible compared with that in $1/R$, so that—

$$p = p_0 - \rho\frac{K}{2\pi R}q_0 \sin\theta.$$

Substituting in (iv) we find for the upward force on the fluid within the circle—

$$\rho\frac{K}{2\pi}q_0\int_0^{2\pi}\sin^2\theta\, d\theta = \tfrac{1}{2}\rho K q_0. \quad . \quad . \quad \text{(v)}$$

Summing up, we find that the fluid within the circle receives downward momentum at the rate $\frac{1}{2}\rho K q_0$, while also it presses downwardly on the surrounding fluid with a force of the same magnitude. Hence the upward reaction L on the aerofoil in the t-plane is given by (170). It is important to remember that by 'upward' is meant the direction $O\eta'$ which is perpendicular to that of q_0.

The equality of the momentum and pressure integrals in the foregoing has no physical significance, following only from choosing a circle for ease of integration. Variations are dealt with in Tietjen's *Applied Hydro- and Aeromechanics*. A wing flying through the atmosphere must derive its lift eventually from a pressure integral over the ground or sea. This must amount to the same as the lift calculated above.

138. The important result of the preceding article does not depend upon the precise shape of the aerofoil. For aerofoils of the simple Joukowski type we may substitute from (169) in (170), obtaining—

$$L = 4\rho q_0^2 \,.\, \pi b \sin(\alpha + \beta) \quad . \quad . \quad . \quad \text{(171)}$$

Introducing the lift coefficient C_L, and remembering that $b/a = 1 + m$,

$$C_L \equiv \frac{L}{\frac{1}{2}\rho q_0^2 . 4a} = 2(1 + m)\pi \sin(\alpha + \beta)$$
$$= 2\pi(\alpha + \beta) \quad . \quad . \quad . \quad . \quad (172)$$

approximately, when α, β, and m are small. In these circumstances

$$\frac{dC_L}{d\alpha} = 2\pi, \quad . \quad . \quad . \quad . \quad (173)$$

i.e. if the angle of incidence of a Joukowski aerofoil of infinite span increase, the lift coefficient C_L increases at the rate 2π per radian, or 0·11 per degree.

139. Pitching Moment

The most general transformation formula by which the flow past aerofoil shapes may be derived from that past the circle is of the type—

$$t = z + \frac{C'}{z} + \frac{C''}{z^2} + \ldots . \quad . \quad . \quad (174)$$

where the coefficients are complex numbers. This gives

$$\frac{dt}{dz} = 1 - \frac{C'}{z^2} - \frac{2C''}{z^3} - \ldots . \quad . \quad (i)$$

and all the zeros, except that yielding the sharp trailing edge of the aerofoil, must be enclosed within the circle. The origin O is situated at the centroid of the zeros. Different sets of poles and circles may be chosen to give an infinite variety of aerofoil shapes. Further development of this wider view of a subject of considerable practical importance is left to subsequent reading and research.

The pitching moment about any point exerted by the pressures on a given aerofoil can be determined as an application of the process described in Article 136. General analytical investigation may proceed as follows:

Consider a great circle of radius R with centre at O. The pressures round it are everywhere radially directed and exert no moment on the fluid within. The pitching moment M_0 about O can be calculated from the rate of change of the moment of momentum of the fluid passing through. If the resultant velocity q at the point R, θ is inclined at ε to $O\xi$, the mass of fluid crossing the element $R\delta\theta$ per second is $\rho q . \cos(\varepsilon - \theta)R\delta\theta$, while its velocity perpendicular to R is $q . \sin(\varepsilon - \theta)$, and the moment of its momentum is accordingly $\frac{1}{2}\rho q^2 \sin 2(\varepsilon - \theta)R^2\delta\theta$. Integrating round the circle—

$$M_0 + \tfrac{1}{2}\rho R^2 \int_0^{2\pi} q^2 \sin 2(\varepsilon - \theta)d\theta = 0.$$

Now from (136), Article 110, if u and v are the velocity components in the t-plane of the aerofoil—

$$\frac{dw}{dt} = u - iv = q(\cos\varepsilon - i\sin\varepsilon) = qe^{-i\varepsilon}$$

whence—

$$-M_0 = \tfrac{1}{2}\rho R^2 \int_0^{2\pi} \left(\frac{dw}{dt}\right)^2 e^{2i\varepsilon} \sin 2(\varepsilon - \theta)d\theta \quad . \qquad \text{(ii)}$$

and the problem is resolved into finding a tractable expression for q with reference to the axes $O\xi$, $O\eta$ of the great circle.

The flow round the b-circle is given in Article 135 (i), referred to a z_1-plane, whose origin is at B, and whose axes are at the inclination α. This is transferred to axes through O parallel to $O\xi$, $O\eta$ by the substitution—

$$z_1 = (z - z_0)\, e^{i\alpha} \quad . \quad . \quad . \qquad \text{(iii)}$$

where z_0 is the co-ordinate of B, and becomes—

$$w = -q_0\left\{(z - z_0)\, e^{i\alpha} + \frac{b^2}{z - z_0}\, e^{-i\alpha}\right\} - \frac{iK}{2\pi}\left\{\log(z - z_0) + i\alpha\right\},$$

whence—

$$\frac{dw}{dz} = -q_0\left\{e^{i\alpha} - \frac{b^2}{(z - z_0)^2}\, e^{-i\alpha}\right\} - \frac{iK}{2\pi(z - z_0)} \quad . \qquad \text{(iv)}$$

Now—

$$\frac{dw}{dt} = \frac{dw}{dz} \cdot \frac{dz}{dt}$$

and on expanding (iv) in descending powers of z and making use of (i) we find—

$$\frac{dw}{dt} = -q_0 e^{i\alpha} - \frac{iK}{2\pi} \cdot \frac{1}{z} + \left(q_0 b^2 e^{-i\alpha} - q_0 C' e^{i\alpha} - \frac{iK}{2\pi} z_0\right)\frac{1}{z^2} + \ldots \text{(v)}$$

The integral in (ii) can be solved * after substitution from (v), with the result that M_0 comes to the imaginary part of the expression—

$$2\pi\rho q_0^2\, C' e^{2i\alpha} + iLz_0 e^{i\alpha}$$

where L is the lift. The second term represents the moment of the lift acting at B about the origin O. Omitting this, and writing $h^2 e^{2i\gamma}$ for C', we obtain for the moment M_B about B—

$$M_B = 2\pi\rho q_0^2 h^2 \sin 2(\alpha + \gamma) \quad . \quad . \quad . \qquad (175)$$

This result is quite general. As an example, it may be shown that for zero travel of the centre of pressure, a problem of practical importance, particularly in connection with the structural design of

* Mrs. Glauert, *loc. cit.*, p. 184. This proof is due to v. Mises. A different treatment is given by H. Glauert, *The Elements of Aerofoil and Airscrew Theory*, Chap. VII.

wings, we must have $\gamma = \beta$, which circumscribes the form of C' in (174). To see this, we note that for a fixed C.P. when drag is nil, the moment must vanish when the lift vanishes, and that the latter occurs at the incidence $-\beta$.

If we now restrict the result to the simple Joukowski transformation formula, so that $C' = a^2$, γ vanishes and—

$$M_B = 2\pi\rho q_0^2 a^2 \sin 2\alpha. \quad . \quad . \quad . \quad (176)$$

The moment coefficient C_m is sometimes defined from the moment M about the leading edge of the aerofoil. Since the leading edge is distant $2a$ from B, it is then given closely by—

$$\begin{aligned} M &= M_B - 2aL \\ &= M_B - 2a\pi(\alpha + \beta)\rho q_0^2 c \end{aligned}$$

from (172), where c is the chord $= 4a$. Hence, S being the area, $= c$ per unit of span—

$$C_m \equiv \frac{M}{\frac{1}{2}\rho q_0^2 Sc} = \frac{M}{\frac{1}{2}\rho q_0^2 (4a)^2} = 2\pi\left(\frac{\sin 2\alpha}{8} - \frac{\alpha + \beta}{2}\right)$$

$$= -\frac{\pi}{2}\beta - \frac{1}{4}C_L \quad . \quad . \quad (177)$$

approximately.

140. Comparison with Experiment

Comparisons with experiment of practical engineering interest will occur in Chapter VIII, after extension of the theory to three-dimensional aeroplane wings. Numerous successful checks on the theory at the present stage have been devised, however, by experiments arranged to imitate two-dimensional conditions of flow. Such investigations are easily carried out and form interesting laboratory work. A long aerofoil is made to a Joukowski section which has been worked out in detail on the drawing board, and is mounted to stretch between the walls of an enclosed-type tunnel or right through an open jet. Preferably it is carried on traversing gear, so that the velocity at a single point in the stream can be measured in direction and magnitude with the aerofoil in various relative positions. It is also fitted for measurements of normal pressure round its median section, or sections close thereto.

The fundamental conception that lift, per unit of span, $= \rho K \times$ velocity, is closely realised on assessing K by graphical determination from measurements of the line integral of the tangential velocity round any wide circuit enclosing the aerofoil and cutting the wake roughly at right angles. For circuits that approach the aerofoil

closely (without, of course, cutting the boundary layer) K may decrease by some 10 per cent. The lift is determined for purposes of comparison from the experimental pressure diagram, as already described.

On examination, the pressure diagram will be found to conform reasonably closely with that determined theoretically for the section and incidence. Observations tend, however, to lie within the calculated diagram, differences occurring chiefly near the crest and tail of the upper surface of the section. Thus the experimental lift is less than the theoretical, although it is in agreement with the observed circulation; the theory over-estimates what a given shape can do, owing to neglect of frictional effects. If the pressures be observed at various small incidences and suitably integrated, it will be found that the slope of the lift coefficient curve is less than 2π. The value 6 is often used instead, although even this value is too generous and $5\frac{1}{2}$ is much closer to fact. For incidences approaching the critical angle the theory completely breaks down.

Typical pressure diagrams are not illustrated, since they resemble those already given for the median sections of aerofoils of considerable aspect ratio. The essential difference is that, in the case of two-dimensional aerofoils whose camber and thickness ratio are small, the pressure drag becomes small at moderately high Reynolds numbers, whilst in the case of the median or other planes of a three-dimensional aerofoil it does not do so, though the section be the same, unless the incidence is such that the lift is also small.

Chapter VI A

THIN AEROFOILS AT ORDINARY SPEEDS

140A. The preceding chapter gives an introductory account of a method by which the potential flow of an incompressible fluid past aerofoil sections resembling those of aeroplane wings can be obtained accurately and without difficulty. The fully developed theory provides for some 9 parameters controlling the shape of the profile, so that given wing sections can if desired be fitted closely. Arbitrary shapes can also be dealt with by an approximate method due to Theodorsen, further developed by Goldstein. Again, the potential flow problem could be solved otherwise by determining an appropriate distribution of vorticity round the given boundary. For it can be proved * that every continuous irrotational motion of an incompressible fluid that extends to infinity and is at rest there may be regarded as due to a certain distribution of vorticity round the surface of the body producing the motion. The determination of the said distribution in a given case involves in general, however, an integral equation whose solution is laborious without special calculating machines, and therefore this line of approach is followed in this book only in the present chapter.

Consideration of cambered aerofoils has so far been limited to those whose camber-line is a circular arc, a shape that is unfavourable for practical use since it entails a large moment coefficient, cf. (177). There is no analytical need for this restriction, and development of the system of conformal transformation described in Articles 128–129A and 133A enables the camber-line to be varied in shape as desired without loss of ultimate accuracy. Such variation has several applications and particularly to the reduction of the pitching moment coefficient. When, for example, the crest of an unreflexed camber-line is advanced from the mid-chord point characterising the circular arc to a position one-sixth of the chord behind the nose, the moment at zero lift almost vanishes and the centre of pressure remains almost stationary at the quarter-chord point. So far forward a position for the crest of the camber-line is

* Lamb, *Hydrodynamics*, 6th Ed., p. 214.

often unacceptable for other reasons, but evidently some advance from the mid-chord point is important. Similarly, Piper * has extended the simple profiles of Article 133A so that a stationary centre of pressure is secured by reflexing the camber-line towards the tail and displacing its crest upstream. These and similar precise calculations accord with experimental results known for some time previously. But they also show † that for small cambers and thickness ratios the effect of the distribution of thickness of the section on the pitching moment is small compared with that of the shape of the camber-line. Hence a serviceable approximation to the moment should be obtainable in such cases by neglecting thickness altogether and regarding the aerofoil simply as a bent line, the median line of its upper and lower surfaces. Such a 'skeleton' is intended (in the present connection only) by the term 'thin aerofoil.' Thus the circular arc of Fig. 93, if restricted to a small camber, constitutes the thin aerofoil (in the present connection) for all the transformations considered in detail in Chapter VI. This may be thickened into a Joukowski section or into one whose profile is inverted from an hyperbola, and the moment at zero lift will be different in the two cases but negligibly so, compared with the difference that would result from changing the camber-line if both thickness and camber are small.

The bent line to which the aerofoil section is reduced may be regarded as the trace of a *surface of discontinuity* in the sense that the velocity of the fluid, though tangential to it at all points, differs in magnitude at adjacent points on the two sides of the line. This difference is determined by a distribution along the line of '$\log r$ sources,' or 'point vortices,' i.e. the simple element-motion described in Article 103 without restriction as to the minimum value of r except as stated in Article 39. The total circulation K round a circuit enclosing the line is equal to the sum of the circulations of all these elements (Article 97). Determining this by Joukowski's Hypothesis secures a finite velocity at the trailing edge but, since the front stagnation point is under the sharp nose, the velocity is infinite at the leading edge. A further approximation, as follows, is also introduced at the outset. Investigation being limited to small cambers, i.e. to small deviations of the camber-line from the chord-line of the section, it is assumed that the vorticity may, for purposes of calculation, be regarded as distributed along the chord.

* *Loc. cit.*, p. 212.
† Garrard, Ph.D. thesis, London, 1942.

140B. The Equations

Choose the origin midway along the chord ; draw Ox along the chord-line in the upstream direction ; and let the undisturbed velocity V make an angle α with Ox. Denote the chord by c, and let it be understood that the following integrations with respect to x are to extend from $x = -\frac{1}{2}c$ to $x = +\frac{1}{2}c$.

Let k be the local intensity of the circulatory function forming the surface of discontinuity, so that—

$$K = \int k dx. \quad . \quad . \quad . \quad \text{(i)}$$

The lift L per unit of span is—

$$L = \rho V \int k dx \quad . \quad . \quad . \quad \text{(ii)}$$

and, the local contribution to lift being proportional to k, the moment M about the mid-chord point is given by—

$$M = \rho V \int kx dx. \quad . \quad . \quad \text{(iii)}$$

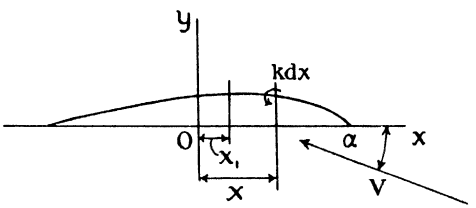

FIG. 100A.

The contribution, δv_1, of the element kdx to the normal velocity component v_1 at x_1 (see Fig. 100A) $= -kdx/2\pi(x - x_1)$, whence—

$$-v_1 = \frac{1}{2\pi} \int \frac{kdx}{x - x_1}. \quad . \quad . \quad \text{(iv)}$$

This velocity, though determined for the point x_1 on the chord, will be approximately the same at the corresponding point P on the thin aerofoil. But the resultant of v_1 and V must be parallel to the tangent at P. Now this tangent is inclined to V at the angle $\alpha + dy/dx$, so that the normal component of V at P is $V(\alpha + dy/dx)$. Thus the boundary condition requires—

$$V(\alpha + dy/dx) + v = 0,$$

or by (iv)—

$$\frac{1}{2\pi V}\int \frac{k\,dx}{x - x_1} = \alpha + \frac{dy}{dx_1} \quad . \quad . \quad \text{(v)}$$

and this equation is to be satisfied for all points on the thin aerofoil. Thus the complete solution of the problem follows the determination of the distribution of k along the chord which will satisfy (v) in respect of a specified thin aerofoil defined, in the present connection, by the variation of the slope dy/dx of the camber-line along the chord.

140C. Application to Circular Arc

Before attacking directly the problem presented by (v) of the preceding article, it is useful to investigate a case for which the solution is already known, viz. the circular-arc thin aerofoil of Article 130.

Generally, the assumption of small camber implies that the difference in the tangential velocities at the upper and lower surfaces of the thin aerofoil at a given point can arise only from the vorticity at that point, since other elements produce only normal velocities there. Hence k is proportional to this velocity difference, which is readily evaluated, as follows, for the case chosen.

Referring to Fig. 93 the circle with centre at B and passing through the two singular points Q and R is transformed by Joukowski's formula into the two sides of a circular arc of camber $\frac{1}{2}\beta$. In the nomenclature of the figure, let the chord $Q'R'$ be at a positive incidence α to a stream of velocity V coming from the right. With a circulation appropriate to Joukowski's Hypothesis, the velocity at any point P on the circular boundary is obtained from Article 135 as—

$$q_s = 2V[\sin(\theta_1 + \alpha) + \sin(\alpha + \beta)],$$

where θ_1 is the angle that BP makes with the x-axis. Or approximately, for α and β small,

$$q_s = 2V[\sin\theta_1 + \alpha(\cos\theta_1 + 1) + \beta]. \quad . \quad \text{(i)}$$

Now by Articles 132–3, to the first order, for a Joukowski aerofoil of vanishing thickness $r/b = r/a = 1 + \beta\sin\theta$ and $x/c = \frac{1}{2}\cos\theta$. Hence, and from the figure,

$$\sin\theta_1 = (r\sin\theta - a\beta)/b = \sin\theta - \beta\cos^2\theta,$$
$$\cos\theta_1 = (r\cos\theta)/b = \cos\theta + \beta\sin\theta\cos\theta.$$

Substituting in (i) gives—

$$q_s = 2V[\sin\theta(1 + \beta\sin\theta) + \alpha(1 + \cos\theta)], \quad . \quad \text{(ii)}$$

squares and products of the small quantities α and β being neglected.

To the same order the modulus of the transformation simplifies to—

$$\left|\frac{dt}{dz}\right| = 2 \sin \theta(1 - \beta \sin \theta),$$

so that the velocity on the boundary in the aerofoil plane is given by—

$$q_t = \frac{q_z}{|\, dt/dz \,|} = V\left[\frac{1 + \beta \sin \theta}{1 - \beta \sin \theta} + \alpha \frac{1 + \cos \theta}{\sin \theta(1 - \beta \sin \theta)}\right]$$

$$= V\left[1 + 2\beta \sin \theta + \alpha \frac{1 + \cos \theta}{\sin \theta}\right] \quad . \quad . \quad . \quad \text{(iii)}$$

for α and β small, and the last term can be reduced.

Now if for any point on the upper surface of the circular-arc aerofoil the corresponding point in the circle plane subtends the angle θ, the adjacent point on the lower surface has a corresponding point subtending the angle $-\theta$. Hence the difference between the increased velocity at the first point on the aerofoil and the reduced velocity at the second point is equal to—

$$2V[2\beta \sin \theta + \alpha \cot (\theta/2)], \quad . \quad . \quad \text{(iv)}$$

to which k is proportional. The first term arises from the camber and the second from the incidence. Only the second would be present in the case of an inclined flat plate.

It will be noticed that at the trailing edge, defined by $\theta = \pi$, the value of k is zero. This result is quite general, arising from the application of Joukowski's Hypothesis, for the velocity could not otherwise remain finite at the trailing edge.

140D. The General Case

The above result suggests that for more complicated thin aerofoils than the circular arc a suitable assumption regarding the variation of k along the chord is—

$$k = 2\pi V\left[A_0 \cot \frac{\theta}{2} + \Sigma A_n \sin n\theta\right],$$

where θ is now a variable related to the distance x measured along the chord from its mid-point by—

$$x = \tfrac{1}{2}c \cos \theta,$$

and only integral values of n are considered in the summation, so that the condition $k = 0$ at the trailing edge remains satisfied however many terms are included.

Substituting this assumed form for k in equation (v) of Article 140B gives the following expression for the slope dy/dx of the thin aerofoil, or camber-line—

$$\frac{dy}{dx} + \alpha = \int_0 \frac{A_0 \cot \frac{\theta}{2} + \Sigma A_n \sin n\theta}{\cos \theta - \cos \theta_1} \sin \theta d\theta. \qquad \text{(i)}$$

The evaluation of the integral gives rise to some difficulty owing to the singularity at $\theta = \theta_1$, where the denominator vanishes. We have to obtain the so-called principal value by evaluating the integral in two parts, between the limits 0 to $\theta_1 - \varepsilon$ and $\theta_1 + \varepsilon$ to π, and then evaluating the limit as ε becomes vanishingly small.

The principal values of the integral—

$$I_n = \int_0^\pi \frac{\cos n\theta}{\cos \theta - \cos \theta_1} \, d\theta$$

are*—

n	I_n
0	0
1	π
> 1	$\pi \dfrac{\sin n\theta_1}{\sin \theta_1}$

With the help of these, (i) can be re-expressed and reduced as follows :—

$$\frac{dy}{dx} + \alpha = \int_0^\pi \frac{A_0(1 + \cos \theta) + \frac{1}{2}\Sigma A_n[\cos (n-1)\theta - \cos (n+1)\theta]}{\cos \theta - \cos \theta_1} d\theta$$

$$= \pi \left\{ A_0 - \tfrac{1}{2}\Sigma A_n \frac{\sin (n+1)\theta_1 - \sin (n-1)\theta_1}{\sin \theta_1} \right\}$$

$$= \pi \{A_0 - \Sigma A_n \cos n\theta_1\}. \qquad \text{(ii)}$$

The values of the coefficients may be evaluated directly if the slope of the thin aerofoil can be expressed as a sum of cosines in this form. Alternatively, they may be found by the usual pro-

* Cf., for instance, Glauert, *Aerofoil and Airscrew Theory*.

cedure employed in the calculation of the coefficients of a Fourier series. Dropping suffix 1 as no longer necessary and integrating—

$$A_0 - \alpha = \frac{1}{\pi}\int_0^\pi \frac{dy}{dx}\, d\theta,$$

$$A_n = -\frac{2}{\pi}\int_0^\pi \cos n\theta \,.\, \frac{dy}{dx}\, d\theta.$$

140E. The Aerodynamical Coefficients and Centre

Equations (ii) and (iii) of Article 140B are now solved. Expressed in terms of coefficients, they give the following—

$$C_L = \frac{2K}{Vc} = 2\pi\int_0^\pi [A_0(1 + \cos\theta) + \Sigma A_n \sin n\theta \sin\theta]d\theta$$

$$= 2\pi^2(A_0 + \tfrac{1}{2}A_1). \quad . \quad . \quad . \quad . \quad . \quad . \quad \text{(i)}$$

Denoting by C_M' the moment coefficient about the mid-chord point,

$$C_M' = \pi\int_0^\pi [A_0(1 + \cos\theta) + \Sigma A_n \sin n\theta \sin\theta] \cos\theta\, d\theta$$

$$= \pi^2(\tfrac{1}{2}A_0 + \tfrac{1}{4}A_2). \quad . \quad . \quad . \quad . \quad . \quad \text{(ii)}$$

If C_M without an accent denotes the moment coefficient about a point one-quarter of the chord from the leading edge,

$$C_M = C_M' - \tfrac{1}{4}C_L$$

$$= \tfrac{1}{4}\pi^2 (A_2 - A_1). \quad . \quad . \quad . \quad . \quad . \quad \text{(iii)}$$

The last result is independent of incidence since only A_0 involves α. The quarter-chord point is therefore called the *Aerodynamic centre*. The value of C_M is a measure of the centre of pressure travel since the distance of the centre of pressure from the quarter-chord point is C_M/C_L. It will also be noticed from (iii) that a fixed centre of pressure requires that $A_2 = A_1$.

140F. Example

Let us assume for the camber-line a cubic curve of the form—

$$y/c = (\tfrac{1}{4} - x^2/c^2)\,(A + Bx/c),$$

so that—

$$\frac{dy}{dx} = -2(x/c)(A + Bx/c) + B(\tfrac{1}{4} - x^2/c^2)$$

$$= \tfrac{1}{4}B - 2Ax/c - 3Bx^2/c^2,$$

or, in terms of $\cos\theta$,

$$\frac{dy}{dx} = -\frac{1}{8}B - A\cos\theta - \frac{3}{8}B\cos 2\theta.$$

This gives—

$$A_1 = \frac{A}{\pi}, \; A_2 = \frac{3B}{8\pi}.$$

The condition for a fixed centre of pressure is thus $B = 8A/3$. We conclude that a camber-line of the type concerned will secure zero travel of the centre of pressure for a thin aerofoil provided its equation is—

$$y = C\left(\tfrac{1}{4} - \frac{x^2}{c^2}\right)\left(1 + \frac{8x}{3c}\right),$$

where C is a small coefficient. This shape of camber-line is illustrated in Fig. 100B, showing the magnitude of the reflexure towards the tail.

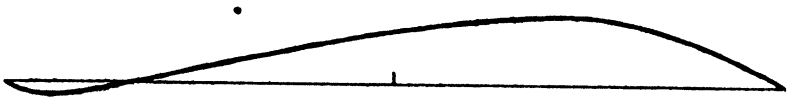

FIG. 100B.

Chapter VI B

COMPRESSIBLE INVISCID FLOW

140G. In Chapters V, VI, and VI A, the motion of the inviscid fluid considered was assumed to be irrotational and incompressible, steady and two-dimensional. The velocity potential that exists under these conditions satisfies Laplace's equation, making rapid progress possible, and the assumptions will often be reintroduced to obtain approximate solutions to practical problems. But in some circumstances they are inadmissible ; examples occur when high speeds cause appreciable variations of density, or when three-dimensional concentrations of vorticity exist in otherwise irrotational flow ; in the latter case there is no ' stationary ' streamline state, and we have to face unsteady as well as three-dimensional conditions.

The present chapter is concerned in the first place, therefore, with establishing a broader basis of fundamentals for guidance in later investigations. The fluid is still regarded as inviscid, so that the pressure acts equally in all directions at any point and there is no diffusion of any vorticity present. It is also assumed that the flow proceeds isentropically without shock (Chapter III), by which is meant generally a sudden large increase of density and decrease of velocity associated with a production of vorticity and other phenomena. In the succeeding chapter the general theory will be applied to two-dimensional aerofoils at high speeds.

140H. Generalised Equation of Continuity

Three-dimensional motions will be referred to fixed co-ordinate axes Ox, Oy, Oz, in the direction of which the velocity components at any instant are u, v, w. The equation of continuity for unsteady compressible flow depends on little more than the conservation of matter ; no special form is obtained for an inviscid fluid. Fixing attention on a box-like element of space, of sides δx, δy, δz, the mass enclosed at any instant is $\rho \,.\, \delta x \delta y \delta z$, and at the end of a brief interval of time δt this mass is increased by—

$$\frac{\partial \rho}{\partial t} \delta x \delta y \delta z \delta t. \quad . \quad . \quad . \quad . \quad \text{(i)}$$

Let the centre of the box be at the point (x, y, z) where, at any instant, the velocity components are u, v, w and the density is ρ. The mass entering the box during the time δt through the yz-face nearer to the origin is—

$$\left(\rho u - \tfrac{1}{2}\frac{\partial \rho u}{\partial x}\delta x\right)\delta y \delta z \delta t,$$

while the mass leaving the box through the opposite face is—

$$\left(\rho u + \tfrac{1}{2}\frac{\partial \rho u}{\partial x}\delta x\right)\delta y \delta z \delta t.$$

In respect of flow through this pair of faces, therefore, the mass of fluid within the box increases during δt by the amount—

$$-\frac{\partial \rho u}{\partial x}\delta x \delta y \delta z \delta t.$$

Extending the calculation to include also the other two pairs of faces, the total increase of mass during the time is—

$$-\left(\frac{\partial \rho u}{\partial x} + \frac{\partial \rho v}{\partial y} + \frac{\partial \rho w}{\partial z}\right)\delta x \delta y \delta z \delta t.$$

But this must be equal to (i). Hence—

$$\frac{\partial \rho}{\partial t} + \frac{\partial \rho u}{\partial x} + \frac{\partial \rho v}{\partial y} + \frac{\partial \rho w}{\partial z} = 0. \quad . \quad . \quad \text{(ii)}$$

This general equation of continuity for compressible flow can take various equivalent forms. Simplified for steady two-dimensional flow to compare with (61), it gives—

$$\frac{\partial u}{\partial x} + \frac{\partial v}{\partial y} = -\frac{1}{\rho}\left(u\frac{\partial \rho}{\partial x} + v\frac{\partial \rho}{\partial y}\right), \quad . \quad \text{(iii)}$$

showing a great change from the equation for incompressible flow.

1401. It is frequently required to know the component accelerations of a fluid element, and brief consideration shows that formulæ for this purpose can be constructed only by following the element for an instant along its path ; a simple example has already arisen in Article 29. The same position arises if it is desired to calculate the rate at which some property of the element other than its velocity is varying. We therefore examine the rate at which any function of position and time, $f(x, y, z, t)$, varies for a moving element.

If at time t a particle occupies the position (x, y, z), at time

$t + \delta t$ it will have moved to the position $(x + \delta x, y + \delta y, z + \delta z)$ and the function will have increased to—

$$f + \frac{\partial f}{\partial x}\delta x + \frac{\partial f}{\partial y}\delta y + \frac{\partial f}{\partial z}\delta z + \frac{\partial f}{\partial t}\delta t$$
$$= f + \frac{\partial f}{\partial x}u\delta t + \frac{\partial f}{\partial y}v\delta t + \frac{\partial f}{\partial z}w\delta t + \frac{\partial f}{\partial t}\delta t.$$

Writing the new value of the function in the form—

$$f + \frac{Df}{Dt}\delta t,$$

$$\frac{Df}{Dt} = \frac{\partial f}{\partial t} + u\frac{\partial f}{\partial x} + v\frac{\partial f}{\partial y} + w\frac{\partial f}{\partial z}.$$

The operator D/Dt, defined by—

$$\frac{D}{Dt} \equiv \frac{\partial}{\partial t} + u\frac{\partial}{\partial x} + v\frac{\partial}{\partial y} + w\frac{\partial}{\partial z}, \quad . \quad \text{(i)}$$

is sometimes known after Stokes, and its use is called a differentiation following the motion of the fluid. It is worth remembering.

For example, the rate at which the density of a moving element is increasing is—

$$\frac{D\rho}{Dt} = \frac{\partial \rho}{\partial t} + u\frac{\partial \rho}{\partial x} + v\frac{\partial \rho}{\partial y} + w\frac{\partial \rho}{\partial z}.$$

Substituting in (ii) of the preceding article gives—

$$\frac{D\rho}{Dt} = -\rho\left(\frac{\partial u}{\partial x} + \frac{\partial v}{\partial y} + \frac{\partial w}{\partial z}\right), \quad . \quad . \quad \text{(ii)}$$

providing an alternative, and often more convenient, form of the general equation of continuity.

140J. Euler's Dynamical Equations

From the preceding article, the component accelerations of an element are—

$$\begin{aligned}
\frac{Du}{Dt} &= \frac{\partial u}{\partial t} + u\frac{\partial u}{\partial x} + v\frac{\partial u}{\partial y} + w\frac{\partial u}{\partial z} \\
\frac{Dv}{Dt} &= \frac{\partial v}{\partial t} + u\frac{\partial v}{\partial x} + v\frac{\partial v}{\partial y} + w\frac{\partial v}{\partial z} \quad . \quad \text{(i)} \\
\frac{Dw}{Dt} &= \frac{\partial w}{\partial t} + u\frac{\partial w}{\partial x} + v\frac{\partial w}{\partial y} + w\frac{\partial w}{\partial z}
\end{aligned}$$

The force components producing these accelerations are, in the absence of viscosity, only of two kinds. The first arise from the pressure gradients, as described for one-dimensional motion in

Article 28, and are proportional to the volume of the element. The second are due to extraneous causes, such as gravity.

At any instant let p be the pressure, ρ the density, and X, Y, Z the components of extraneous force per unit mass at the point (x, y, z), and consider an element of volume V with its centre at this point. Resolving in the x-direction, $\rho V \,.\, Du/Dt = \rho V \,.\, X - V \,.\, \partial p/\partial x$ and similar expressions result from resolving in the y- and z-directions. Hence finally,

$$\left.\begin{aligned} \frac{Du}{Dt} &= X - \frac{1}{\rho}\frac{\partial p}{\partial x} \\ \frac{Dv}{Dt} &= Y - \frac{1}{\rho}\frac{\partial p}{\partial y} \\ \frac{Dw}{Dt} &= Z - \frac{1}{\rho}\frac{\partial p}{\partial z}. \end{aligned}\right\} \quad . \quad . \quad . \quad \text{(ii)}$$

These equations of motion are general, the only restriction being to an inviscid fluid. Substitutions for the left-hand sides will be made from (i) in accordance with given conditions; e.g. the terms in $\partial/\partial t$ will be omitted if the flow is steady, and those involving w if it is two-dimensional.

140K. Kelvin's (or Thomson's) Theorem

It will now be shown that under certain conditions the circulation round any circuit moving at every point with the fluid does not vary with time. This theorem was enunciated by Lord Kelvin when Sir William Thomson and is known under both names. It is of outstanding importance in Aerodynamics, exercising a directive influence on the theory and design of wings, airscrews, wind tunnels, etc. The above conditions are as follows: (*a*) The fluid is inviscid, though it may have any distribution of vorticity and is not constrained to be in steady motion; (*b*) There exists an integrable functional relation between the

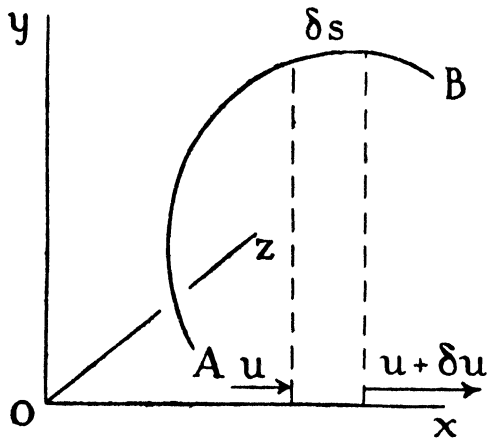

FIG. 100c.

pressure and density; (*c*) The extraneous forces are conservative.

Consider first any two separated points, A and B, Fig. 100c, themselves moving with the fluid and connected by any 'fluid line,' i.e. a line of which every point is moving with the fluid; thus the line selected will always consist of the same fluid particles, however its shape may vary with time.

The rate at which the flow along the fluid line from A to B increases is given by—

$$\frac{D}{Dt}\int_A^B (u\,dx + v\,dy + w\,dz). \quad . \quad . \quad \text{(i)}$$

Considering the first term of this expression,

$$\frac{D}{Dt}(u\delta x) = \frac{Du}{Dt}\delta x + u\frac{D\delta x}{Dt}.$$

But $(D/Dt)(\delta x)$ is the rate at which the projection of an element δs of the line on the x-axis is elongating, i.e. it is equal to δu. Hence—

$$\frac{D}{Dt}(u\delta x) = \frac{Du}{Dt}\delta x + u\delta u = \frac{Du}{Dt}\delta x + \tfrac{1}{2}\delta(u^2),$$

or, substituting from the equations of motion,

$$\frac{D}{Dt}(u\delta x) = \left(X - \frac{1}{\rho}\frac{\partial p}{\partial x}\right)\delta x + \tfrac{1}{2}\delta u^2$$

Differentiations following the motion of $v\delta y$ and $w\delta z$ are similarly expressed, yielding three such equations. It is assumed that the components of extraneous force per unit mass are derivable from a single-valued potential function Ω, so that $X = \partial\Omega/\partial x$, etc. Hence, adding the three equations together,

$$\begin{aligned}\frac{D}{Dt}(u\delta x + v\delta y + w\delta z) &= \frac{\partial\Omega}{\partial x}\delta x + \frac{\partial\Omega}{\partial y}\delta y + \frac{\partial\Omega}{\partial z}\delta z \\ &\quad - \frac{1}{\rho}\left(\frac{\partial p}{\partial x}\delta x + \frac{\partial p}{\partial y}\delta y + \frac{\partial p}{\partial z}\delta z\right) \\ &\quad + \tfrac{1}{2}\delta(u^2 + v^2 + w^2) \\ &= \delta\Omega - \frac{\delta p}{\rho} + \tfrac{1}{2}\delta q^2.\end{aligned}$$

Integrating along the entire fluid line gives finally—

$$\frac{D}{Dt}\int_A^B (u\,dx + v\,dy + w\,dz) = \left[\Omega - \int\frac{dp}{\rho} + \tfrac{1}{2}q^2\right]_A^B. \quad \text{(ii)}$$

Now let the fluid line be elongated to form a closed circuit, A and B becoming adjacent points. The left-hand side of (ii) then gives the rate at which the circulation K round this circuit varies with time. But the value of the right-hand side must be zero when B coincides with A, provided p is an integrable function of ρ, as assumed. Hence—

$$\frac{DK}{Dt} = 0, \qquad . \quad . \quad . \qquad \text{(iii)}$$

i.e. the circulation round a loop of fluid particles remains constant provided it does not enter a rotational field of extraneous force and the chain remains unbroken.

Applications of this result will be discussed in place, but the following may be noted at once. If the motion of a bulk of inviscid fluid is at any instant irrotational, then the circulations round all fluid loops that can be drawn within the bulk vanish for the reason discussed in Article 97. The theorem then asserts that these circulations remain zero under the conditions assumed, i.e. that the state of irrotational motion is maintained in that bulk of fluid.

IRROTATIONAL COMPRESSIBLE FLOW

140L. If at any instant all elements of the fluid (or of a given part of a fluid in motion, steady or not) are devoid of vorticity, it can be shown as before that a velocity potential then exists, since every closed circuit that can be drawn in the region occupied has zero circulation. But the argument can be shortened to the following.

If at any instant $udx + vdy + wdz$ is an exact differential $d\phi$, then $u = \partial\phi/\partial x$, $v = \partial\phi/\partial y$, $w = \partial\phi/\partial z$, and it follows immediately that—

$$\frac{\partial w}{\partial y} - \frac{\partial v}{\partial z} = 0, \qquad \frac{\partial u}{\partial z} - \frac{\partial w}{\partial x} = 0, \qquad \frac{\partial v}{\partial x} - \frac{\partial u}{\partial y} = 0. \quad \text{(i)}$$

The left-hand sides of these expressions are the components of vorticity of an element situated at (x, y, z). Assuming (i) in the first instance establishes the existence of a velocity potential at the given instant, irrespective of compressibility. The theorem of the preceding article then enables us to say that the bulk of fluid considered will continue to possess a velocity potential.

140M. Integration of the Equations of Motion

Euler's dynamical equations can be integrated through any part of a fluid in which a velocity potential exists. The need for this

step is not always apparent on a first reading of the subject in view of Articles 29 and 40. But it will be reflected that Bernoulli's equation was derived by integrating along a streamline, whilst in potential motions surrounding concentrations of vorticity, for example, streamlines in the sense implied do not in general exist, but only path-lines.

By virtue of (i) of the preceding article, the first of the equations of motion, viz.—

$$\frac{\partial u}{\partial t} + u\frac{\partial u}{\partial x} + v\frac{\partial u}{\partial y} + w\frac{\partial u}{\partial z} - X + \frac{1}{\rho}\frac{\partial p}{\partial x} = 0$$

can be changed to—

$$\frac{\partial^2 \phi}{\partial x \partial t} + u\frac{\partial u}{\partial x} + v\frac{\partial v}{\partial x} + w\frac{\partial w}{\partial x} - X + \frac{1}{\rho}\frac{\partial p}{\partial x} = 0.$$

Similarly, the second and third of the equations of motion can be rearranged to involve partial differentiations with regard to only y and z, respectively. Multiplying the first of these rearranged expressions by δx, the second by δy, the third by δz, and adding gives—

$$\delta\left(\frac{\partial \phi}{\partial t}\right) + u\delta u + v\delta v + w\delta w - (X\delta x + Y\delta y + Z\delta z) + \frac{\delta p}{\rho} = 0.$$

But $u\delta u = \frac{1}{2}\delta(u^2)$, etc., and $u^2 + v^2 + w^2 = q^2$. Hence, assuming that X, Y, Z have a potential Ω, say, so that $X = \partial\Omega/dx$, etc., the last equation becomes—

$$\delta\left(\frac{\partial \phi}{\partial t}\right) + \tfrac{1}{2}\delta(q^2) - \delta\Omega + \frac{\delta p}{\rho} = 0.$$

Integrating,

$$\frac{\partial \phi}{\partial t} + \tfrac{1}{2}q^2 - \Omega + \int \frac{dp}{\rho} = C. \quad . \quad . \quad \text{(i)}$$

In general C is an arbitrary function of time, and is therefore more accurately written as $F(t)$, or absorbed into $\partial\phi/\partial t$ with this understanding and the left-hand side of the expression then equated to zero. In this strict sense the left-hand side of (i) is constant for all particles only at any instant ; its value can be altered by, for example, changing the pressure throughout the bulk of fluid by extraneous means, such as a pump. But Aerodynamical calculations usually suppose an unrestricted expanse of fluid and exclude such external actions, when C becomes a constant.

For steady flow in the absence of extraneous forces the equation (i), obtained by integrating Euler's equations of motion, reduces to—

$$\int \frac{dp}{\rho} + \tfrac{1}{2}q^2 = \text{constant}, \quad . \quad . \quad \text{(ii)}$$

i.e. to the same form as Bernoulli's equation, found by integrating along a streamline, Article 29. The new result is less general in that it is restricted to potential flow, but it is more general in showing that with that type of compressible steady motion Bernoulli's constant has a single value for all particles.

As before, the pressure is assumed to be related to the density by the adiabatic law $p = k\rho^\gamma$, and expressions obtained in Articles 31 and 32 are applicable under steady conditions.

140N. Steady Irrotational Flow in Two Dimensions

The equation of continuity for steady compressible flow in two dimensions is, from Article 140H,

$$\frac{\partial u}{\partial x} + \frac{\partial v}{\partial y} = -\frac{1}{\rho}\left(u\frac{\partial \rho}{\partial x} + v\frac{\partial \rho}{\partial y}\right). \quad . \quad \text{(i)}$$

If the flow is irrotational, this becomes on substituting for u and v in terms of ϕ—

$$\nabla^2\phi = -\frac{1}{\rho}\left(\frac{\partial \phi}{\partial x}\frac{\partial \rho}{\partial x} + \frac{\partial \phi}{\partial y}\frac{\partial \rho}{\partial y}\right) \quad . \quad \text{(ii)}$$

where $\nabla^2 \equiv \partial^2/\partial x^2 + \partial^2/\partial y^2$.

Differentiating (ii) of the preceding article and remembering that $dp/d\rho = \gamma p/\rho = a^2$,

$$\frac{\partial q^2}{\partial x} = -\frac{2}{\rho}\frac{dp}{d\rho}\frac{\partial \rho}{\partial x} = -\frac{2a^2}{\rho}\cdot\frac{\partial \rho}{\partial x},$$

$$\frac{\partial q^2}{\partial y} = -\frac{2a^2}{\rho}\cdot\frac{\partial \rho}{\partial y},$$

where a is the local velocity of sound ; i.e. that for the air in the region where the velocity is q. Substituting in (ii),

$$\nabla^2\phi = \frac{1}{2a^2}\left(\frac{\partial \phi}{\partial x}\frac{\partial q^2}{\partial x} + \frac{\partial \phi}{\partial y}\frac{\partial q^2}{\partial y}\right). \quad . \quad \text{(iii)}$$

If the disturbed motion arises from a uniform stream of velocity U and in which the pressure is p_0, the density ρ_0 and the speed of sound a_0, then by Article 31—

$$\tfrac{1}{2}(q^2 - U^2) = \frac{\gamma}{\gamma - 1}\frac{p_0}{\rho_0}\left[1 - \left(\frac{p}{p_0}\right)^{\frac{\gamma-1}{\gamma}}\right]$$

$$= \frac{1}{\gamma - 1}(a_0^2 - a^2).$$

This expression enables substitution to be made in (iii) for the variable local speed of sound, giving—

$$[2 - (\gamma - 1)(q_a^2 - M^2)]\nabla^2\phi = \frac{\partial\phi}{\partial x}\frac{\partial}{\partial x}(q_a^2) + \frac{\partial\phi}{\partial y}\frac{\partial}{\partial y}(q_a^2), \quad \text{(iv)}$$

where q_a is written for the velocity ratio q/a_0 and M for the Mach number U/a_0.

This differential equation for ϕ, the counterpart, for compressible flow, of (115), has no general solution and is laborious to handle. ϕ is usually expanded in a series of terms of even powers of M, but convergence becomes slow as q approaches a; solutions * have been published only for the circular and elliptic cylinders, a Joukowski aerofoil and the sphere. A hodograph method, introduced by Tchapliguine in Russia (1904) has recently been developed † in the hope of enabling higher local speeds to be dealt with.

Whilst the exact calculation of compressible flow in two dimensions for given boundary conditions is intricate even under favourable conditions, there is no difficulty in appreciating qualitatively the effect of compressibility on the streamlines. As may be verified directly or inferred from the preliminary discussion of a general nature given in Chapter II, (iv) approximates closely to (115) for moderately small values of the Mach number $M = U/a_0$. The range depends upon the section of the body since the criterion is associated with the maximum value of q/a attained by the fluid in flowing past it; thus it may be more than twice as great for a wing section as it is for a circular cylinder. As M is increased, a stage is reached, early or late, when the variation of density is no longer negligible. The streamlines for incompressible flow are by then appreciably distorted. Let δs, δn be elements of length of adjacent streamlines and equipotentials, respectively. For incompressible flow, $q = d\phi/ds = d\psi/dn$. The first of these still holds for compressible flow, but variation of ρ must now be taken into account by defining $\delta\psi = \sigma q \,.\, \delta n$, where σ denotes the density relative to that of the undisturbed stream. Hence while formerly, with the density constant, ϕ and ψ varied equally through any small region, their variations are now inversely proportional to σ. Near the stagnation point, where the density increases, the streamlines close in, whilst near the shoulder of the body-section they separate

* Rayleigh (Lord), *Phil. Mag.*, vol. 32, 1916. Hooker, A.R.C.R. & M., No. 1684, 1936. Imai and Aihara, *Tokyo Univ. Rept.*, No. 199, 1940. Kaplan, N.A.C.A.T.N., No. 762, 1940. And others.

† Kármán and Tsien, see the former, *Jour. Aero. Sci.*, vol. 8, 1941, where further references are also given. The value of γ is changed by this method.

farther from each other in order to accommodate between them the same mass flow with a reduced density. The latter change is usually the more important in Aerodynamical applications, and so the main effect of compressibility is sometimes said to be an expansion of scale across the stream, but this statement is incomplete. Associated with the distortion of the streamlines, the pressure changes round the profile of the body are augmented so long as the flow remains irrotational.

1400. Analogies

These and similar considerations have led to the suggestion of certain analogies with a view to inferring from convenient experiments the effects of compressibility on irrotational flow. In an electrical analogy, an alternating current is passed through a layer of electrolytically conducting liquid contained in a bath having an insulating bottom, which can be shaped to represent the boundary condition in the flow case.* A trial exploration of the distribution of electrical potential (which is proportional to ϕ) enables the distribution of σ in the compressible flow to be assessed, and the bottom of the bath is then re-shaped to make the thickness of the electrolyte proportional to σ and the experiment repeated. There has also been suggested an incomplete analogy with the flow of water through an open channel,† as follows :

Hydraulic Analogy.—In comparing the two-dimensional flow of a gas and the flow of an incompressible fluid, say water, with a free surface along an open channel having vertical sides, an analogy will be found to exist between the variation of the density ρ within the compressible flow and the variation of the height h of the liquid surface above the floor of the channel, which is assumed to be flat and horizontal. The water is assumed to flow irrotationally and its velocity to be constant at all points along any one vertical line. Thus, if w is the component of the (horizontal) velocity in any direction across a vertical line whose total height above the channel floor is h', then the flux across a vertical strip of width b perpendicular to the direction of w is $w.h'\,b$.

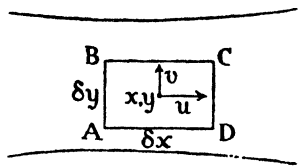

FIG. 100D.

Let x be measured in the direction of mean flow in the channel and y perpendicular thereto and horizontally, and consider a rect-

* Taylor (Sir Geoffrey) and Sharman, *Proc. Roy. Soc.*, A, vol. 121, 1928.

† Jouguet, *Jour. des. Math.*, 1920; see also Riaboushinsky, *Pub. Sci. et Tech.*, Ministre de l'air, No. 108, 1937.

angular space-element $ABCD$, Fig. 100D, whose centre is at x, y. If the height of the layer of water is h at x, y, its heights at the middle points of AB, CD, are $h \mp \frac{1}{2}\frac{\partial h}{\partial x}\delta x$, respectively, whilst the velocity components perpendicular to these faces at their middle points are $u \mp \frac{1}{2}\frac{\partial u}{\partial x}\delta x$, respectively. Hence the rate at which fluid is leaving the space-element in respect of flow across the faces AB and CD is, by the foregoing,

$$-\left(u - \tfrac{1}{2}\frac{\partial u}{\partial x}\delta x\right)\left(h - \tfrac{1}{2}\frac{\partial h}{\partial x}\delta x\right)\delta y + \left(u + \tfrac{1}{2}\frac{\partial u}{\partial x}\delta x\right)\left(h + \tfrac{1}{2}\frac{\partial h}{\partial x}\delta x\right)\delta y$$

$$= u\frac{\partial h}{\partial x}\delta x\delta y + h\frac{\partial u}{\partial x}\delta x\delta y,$$

to the first order. Adding the rate of outward flow, similarly calculated, across the pair of faces BC and DA, and expressing the fact that the volume of the incompressible liquid within the space-element cannot vary, we have finally—

$$u\frac{\partial h}{\partial x} + h\frac{\partial u}{\partial x} + v\frac{\partial h}{\partial y} + h\frac{\partial v}{\partial y} = 0$$

i.e.,

$$\frac{\partial}{\partial x}(hu) + \frac{\partial}{\partial y}(hv) = 0. \qquad . \qquad \text{(i)}$$

This result is identical with the equation of continuity for two-dimensional compressible flow if ρ replaces h.

Relations derived by virtue of the absence of vorticity are identical for the two cases of motion and, to establish the analogy, it remains only to compare the relation of h to the resultant velocity q in the channel, on the one hand, with the relation of the density ρ to the resultant velocity in the corresponding compressible flow, on the other hand. Suffix 0 will denote undisturbed conditions.

For the channel, Bernoulli's equation gives in the usual form employed in hydraulics and which is easily deduced from Article 140M :

$$\frac{p}{\rho_w} + \tfrac{1}{2}q^2 + gh = \frac{p_0}{\rho_w} + \tfrac{1}{2}q_0^2 + gh_0,$$

where ρ_w is the density of the water. Applying this equation to the free surface, where the pressures p and p_0 are identical, yields—

$$\frac{h}{h_0} = 1 - \frac{q^2 - q_0^2}{2gh_0}.$$

But gh_0 is equal to the square of the velocity of long waves of small amplitude in a channel, so that putting $gh_0 = c^2$—

$$\frac{h}{h_0} = 1 - \frac{q^2 - q_0^2}{2c^2}. \quad . \quad . \quad . \quad \text{(ii)}$$

The corresponding result for compressible flow has already been expressed in (47) as—

$$\frac{\rho}{\rho_0} = \left[1 - (\gamma - 1)\frac{q^2 - q_0^2}{2a_0^2}\right]^{\frac{1}{\gamma - 1}}, \quad . \quad \text{(iii)}$$

where a_0 is the velocity of sound in the gas where the temperature corresponds to ρ_0.

Thus (ii) is identical to (iii) if h is substituted for ρ, c for a_0 and if $\gamma = 2$. The value required for γ is substantially different from 1·405, and the analogy is therefore incomplete in this connection. This does not invalidate, however, its qualitative use. Moreover, we observe that the incompleteness is negligible if $q^2 - q_0^2$ is small compared with $2a_0^2$, for then (iii) can be expanded as—

$$\frac{\rho}{\rho_0} = 1 - \frac{q^2 - q_0^2}{2a_0^2} + \frac{2 - \gamma}{\underline{2}}\left(\frac{q^2 - q_0^2}{2a_0^2}\right)^2 + \ldots$$

If the density ratio is $\frac{3}{4}$, the term omitted in the analogy amounts in this case only to about 2 per cent. for air. Thus the analogy is close in the case of thin aerofoils and other slender bodies.

The formula quoted above for the velocity c of propagation of long shallow gravity-waves is easily derived as follows.

Imagine such a wave travelling upstream and adjust the speed of flow through the channel to c, so that the wave becomes stationary and the entire motion steady. The flux per unit width of the channel is then ch_0.

Let h denote the height of any point P on the surface of the wave above the bottom of the channel and q the fluid velocity at P. Under the conditions postulated, the horizontal component of velocity u is sensibly the same at all points of the vertical line drawn from P into the fluid and equal to q. Thus the flux across the transverse plane through P is qh per unit width, and $qh = ch_0$.

Bernoulli's equation gives for any streamline on the surface, the pressure being constant,

$$\tfrac{1}{2}c^2 + gh_0 = \tfrac{1}{2}q^2 + gh.$$

Substituting for q,

$$c^2 = \frac{2gh^2}{h + h_0}$$

This reduces approximately to the result stated, viz. $c^2 = gh_0$, on restricting the height h' of the crest of the wave so that $h'/h_0 - 1$ is small.

The velocity a of pressure-waves in the atmosphere cannot be calculated in this way without large error owing to the variation of temperature consequent upon adiabatic expansions and compressions. This matter has already been discussed and a reliable formula given. The correspondence between the gravity-waves in a channel and pressure- or sound-waves in air can be seen as follows.

Considering first a gravity-wave in slightly more detail, write $h_0 + z_1$ for h and let z denote height above the channel floor. Taking x in the direction of motion and assuming the disturbance to be small, the pressure increase at the level z is approximately equal to $g\rho_w\,(h_0 + z_1 - z)$, the static value, whence $\partial p/\partial x = g\rho_w.\partial z_1/\partial x$. This is independent of z, so that every particle in a vertical line is displaced equally.

Referring to the equations of motion given in Article 140J, all other terms can be neglected in comparison with $\partial u/\partial t$ and $\partial p/\partial x$; consequently—

$$\frac{\partial u}{\partial t} = -\frac{1}{\rho_w}\frac{\partial p}{\partial x} = -g\frac{\partial z_1}{\partial x} \quad . \quad . \quad \text{(iv)}$$

The upward velocity at P, viz. $\partial z_1/\partial t$, follows at once from the equation of continuity for incompressible flow and the result that $\partial u/\partial x$ is the same for all values of z since every particle on a vertical line moves equally. We have—

$$\frac{\partial z_1}{\partial t} = -\int_0^h \frac{\partial u}{\partial x}dz = -h\frac{\partial u}{\partial x} \quad . \quad . \quad \text{(v)}$$

Turning now to a plane wave of pressure disturbance moving normal to itself in the x-direction through the atmosphere, we restrict investigation to the case of a small disturbance so that $\rho/\rho_0 - 1$ is small; this quantity is known as the *condensation* and denoted by s.

With E written for the bulk elasticity $\rho dp/d\rho$ and with $u\partial u/\partial x$ neglected in comparison with $\partial u/\partial t$ as before, the equation of motion is

$$\frac{\partial u}{\partial t} = -\frac{1}{\rho}\frac{\partial p}{\partial x} = -\frac{E}{\rho^2}\frac{\partial \rho}{\partial x} \quad . \quad . \quad \text{(vi)}$$

The equation of continuity for compressible flow must be employed but, since the total variation in ρ is small (for which reason also a suffix to distinguish undisturbed conditions is unnecessary), this gives approximately—

$$\frac{1}{\rho}\frac{\partial \rho}{\partial t} = -\frac{\partial u}{\partial x} \quad . \quad . \quad . \quad \text{(vii)}$$

Now equations (vi) and (vii) can be reproduced from (iv) and (v) by substituting E/ρ for gh and s for z_1/h, establishing the analogy. If the disturbance in pressure is other than small, we have to return to the more complicated considerations set out for a plane shock wave in Article 66D. The present simplification will be found to possess, however, a surprising degree of utility.

In application to experiment, the floor of the channel will, of course, slope slightly downward to counteract approximately the effect of friction. The method has been widely employed, photographs being taken of flow patterns, especially of surface waves above the critical speed c, forces on models being measured, and surface configurations being used to estimate density ratios in the corresponding compressible flows. Apart from these important quantitative applications, the method is convenient to demonstrate changes in flow which occur as the velocity is increased from well below that of propagation of small waves in the medium to well above this speed, corresponding to change from subsonic to supersonic flow. For example, the flow in a convergent-divergent channel can be examined in this way and some aspects of the supersonic tunnel revealed.

Chapter VI C

THIN AEROFOILS AT HIGH SPEEDS

140P. Subsonic Speeds—Glauert's Theory

One application of conformal methods is found in the design of sections for wings and airscrew blades intended for such high speeds that account must be taken of the compressibility of the air. The primary aim is to avoid the formation of shock waves by restricting the maximum velocity ratio (cf. Article 129B) for a given lift coefficient. The flow outside the boundary layer then remains irrotational, as is assumed in the present Article. The difficulty in the way of obtaining even an approximate solution of the exact equation for ϕ is avoided by deriving in the first instance an approximate form of that equation suitable for thin aerofoils. Owing to the augmentation of pressure changes, modifications are required to formulæ (169)–(173) of Articles 135–138, and Glauert's Theory* is directed towards establishing the basis for these. The theorem proved in Article 137 for incompressible flow, and now written for convenience as $L = \rho_0 KU$, still holds when the undisturbed velocity U of the air stream is sufficiently high as to involve appreciable variation of ρ in the neighbourhood of the aerofoil from its initial value ρ_0. This generalisation is assumed below.†

Investigation is restricted to thin aerofoils at small incidences and having profiles that are everywhere inclined at only small angles to the x-direction of motion, so that the x-component u of the disturbed velocity is little greater than U and the y-component v is of the same order as $u - U$. The equation of continuity—

$$\frac{\partial}{\partial x}(\rho u) + \frac{\partial}{\partial y}(\rho v) = 0, \qquad . \quad . \qquad \text{(i)}$$

i.e.,
$$\frac{\partial u}{\partial x} + \frac{\partial v}{\partial y} + \frac{1}{\rho}\left(u\frac{\partial \rho}{\partial x} + v\frac{\partial \rho}{\partial y}\right) = 0,$$

may then be written approximately—

$$\frac{\partial u}{\partial x} + \frac{\partial v}{\partial y} + \frac{U}{\rho}\frac{\partial \rho}{\partial x} = 0. \qquad . \quad . \qquad \text{(ii)}$$

* *Proc. Roy. Soc.*, A, vol. 118, 1928.

† Proof is indicated by Taylor and Maccoll, *Aerodynamic Theory*, vol. III, Div. H.

Pressure and density variations are appropriately assumed to be governed by the adiabatic law and, if a_0 is the velocity of sound in the undisturbed stream, (47) of Article 30 gives with the present notation—

$$\left(\frac{\rho}{\rho_0}\right)^{\gamma-1} = 1 - \frac{\gamma-1}{2a_0^2}(u^2 - U^2).$$

Differentiating with respect to x,

$$\frac{1}{\rho}\frac{\partial \rho}{\partial x} = -\frac{\dfrac{u}{a_0^2}\dfrac{\partial u}{\partial x}}{1 - \dfrac{\gamma-1}{2a_0^2}(u^2 - U^2)}.$$

Now $(\gamma - 1)/2 = 1/5$ and $(u^2 - U^2)/a_0^2$ is always small. Therefore—

$$\frac{1}{\rho}\frac{\partial \rho}{\partial x} = -\frac{u}{a_0^2}\frac{\partial u}{\partial x} = -\frac{U}{a_0^2}\frac{\partial u}{\partial x}$$

closely. Writing M for the Mach number U/a_0 and substituting in (ii) gives approximately for the equation of continuity—

$$(1 - M^2)\frac{\partial u}{\partial x} + \frac{\partial v}{\partial y} = 0. \quad . \quad . \quad \text{(iii)}$$

Substitution in (iii) of—

$$v' = v/(1 - M^2)^{1/2} \quad \text{and} \quad y' = y(1 - M^2)^{1/2}$$

reduces that expression to—

$$\frac{\partial u}{\partial x} + \frac{\partial v'}{\partial y'} = 0$$

which has identically the same form as the equation of continuity for incompressible flow. The same substitution in the equation expressing the condition for irrotational flow, whether compressible or incompressible, viz.—

$$\text{vorticity} = \frac{\partial v}{\partial x} - \frac{\partial u}{\partial y} = 0,$$

gives—

$$\frac{\partial v'}{\partial x} - \frac{\partial u}{\partial y'} = 0,$$

and the form remains identically the same.

The circulation round the aerofoil—

$$K = \int_C (u\,dx + v\,dy)$$

remains unaltered by the substitution since v and y are changed in reciprocal ratios whilst u and x remain unchanged. Hence the lift of the aerofoil per unit of its length, being equal to $\rho_0 UK$, remains unaltered.

This mathematical analogy between compressible and incompressible flow at the same undisturbed speed past a thin aerofoil having the same circulation implies an important difference in order that the boundary condition may be satisfied in both cases. Since v/u in the compressible flow is everywhere less than v'/u, and the flow adjacent to the aerofoil profile must be tangential thereto, the incidence of the aerofoil section must be reduced in the same ratio, viz. $(1 - M^2)^{1/2} : 1$. Whilst this requirement can evidently be satisfied with vanishing camber and thickness, appreciable camber and thickness would usually involve as a secondary effect a change in the shape of the profile in the neighbourhood of the nose; but the analogy breaks down for another reason near the nose, viz. that neither v nor $u - U$ can be regarded as small in this region. The analogy also requires an expansion in the y-direction of the linear scale appropriate to the incompressible flow, and this is compatible with the reduction of incidence of the aerofoil because points on the profile, or on any other streamline, in the incompressible flow case do not correspond to points on a streamline in the compressible flow case.

Thus the effect of compressibility, consistently with the present approximation, is to enable a thin aerofoil to generate a given lift at an incidence reduced in the ratio $(1 - M^2)^{1/2} : 1$ compared with the incidence required with incompressible flow of the same speed. It follows that the lift-curve slope, $dC_L/d\alpha$, is increased by compressibility in the ratio $1 : (1 - M^2)^{1/2}$. This result is usually stated as an increase in the same ratio of the lift coefficient for a given incidence.

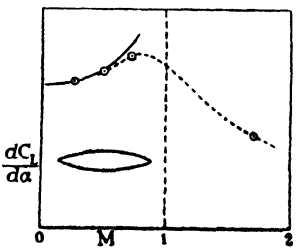

FIG. 100E.

140Q. *Comparison with experiment.*— Fig. 100E relates to some well-known experiments * at high speeds carried out at the National Physical Laboratory on an aerofoil having the section inset. The observations are shown as encircled points, while the increase of $dC_L/d\alpha$ according to the above theory is indicated by the full-line. Close agreement is seen between $M = 0{\cdot}25$ and $0{\cdot}5$. Between $0{\cdot}5$ and $0{\cdot}7$ the slope of the experimental lift-curve still increased

* Stanton, A.R.C.R. & M., No. 1130, 1928.

notably, but at less than the predicted rate. At some undetermined value of M in the neighbourhood of 0·7 the lift-curve slope began to decrease, as indicated schematically by the dotted extension to the experimental curve, to a much reduced value at $M = 1{\cdot}7$.

The section of the above aerofoil may be regarded as favourable to the conditions postulated in the theory except that the thickness ratio was necessarily too large (0·1). Another aerofoil, of more normal section, showed a less increase of $dC_L/d\alpha$ and an earlier maximum ; others have shown in more recent tests * a substantially greater rate of increase of lift-curve slope than the theory predicts. Thus experiments so far published suggest that the theory provides a fair indication, but no more, of the effects of compressibility on the lift of aerofoils up to moderate Mach numbers.

The value of M at which $dC_L/d\alpha$ changes sign is called the critical Mach number for the aerofoil and the phenomenon is known as the *shock stall* (Article 66C). It marks the formation of a shock wave, attached to the aerofoil at or near the position of maximum velocity round the profile. The critical Mach number is sometimes described as that at which this maximum velocity attains to the local velocity of sound. However, it has recently been questioned † whether a shock wave necessarily forms at this stage. In any case there appears no reason for supposing that the shock stall must occur at $M = 0{\cdot}6$–$0{\cdot}7$, as so often observed, but rather that aerofoil sections can be designed to delay this stall appreciably.

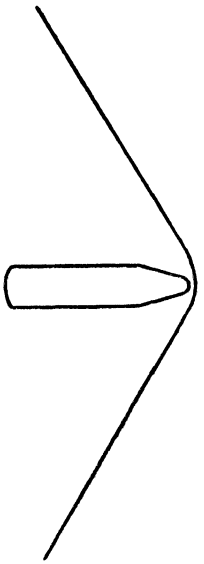

FIG. 100F. — SHOCK WAVE FORMED BY BULLET.

140R. Supersonic Speeds—The Mach Angle

When a body moves through air at a velocity greater than that of sound a shock wave precedes it in the form of a bow wave, in order to divide the air and deflect it round the nose. Such bow waves are familiar in photographs of fast-moving bullets, which show that the disturbance is confined to a thin sheet, Fig. 100F (cf. also Article 66C). Within the sheet, pressure, density, and velocity change with very great rapidity. Imagining the air to flow through a stationary shock wave, its velocity is suddenly decreased and its density

* E.g. Stack, Lindsey and Littell, N.A.C.A.T.R., No. 640, 1938.
† Kármán, *loc. cit.*, p. 253.

increased, part of its mechanical energy is converted into heat and it acquires vorticity. Bernoulli's equation can only be employed in these circumstances by introducing suitable changes in the constant, as illustrated in the case of the pitot tube, Article 66D. At some distance from the body, however, the disturbance becomes small and is propagated at the velocity of sound, whilst air passing through can satisfy Bernoulli's equation. But there is no preparatory formation of streamlines ahead such as characterises subsonic flow, for the body continually overtakes the wave it generates except for a central region of percussion. Behind the central region an additional wake is formed, and the streamlines are parallel to the surface.

Investigation of the complete problem is somewhat complicated, but progress can readily be made in the case of a thin aerofoil at small incidence by assuming that the disturbance consists only of a pressure wave, propagating at the speed of sound, and effecting only small changes.

It is then easily seen that the waves are inclined to the flight path at a definite angle. Let P, Fig. 100G, be any point on a body

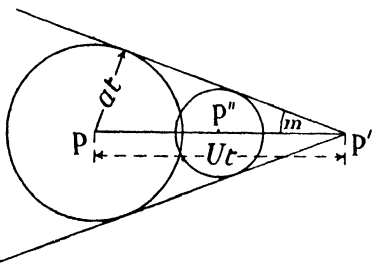

FIG. 100G.—THE MACH ANGLE.

moving steadily in the direction PP' at a supersonic speed U, and let it reach the position P' at the end of an interval of time t, so that $PP' = Ut$. A small disturbance of pressure starting from P will in the same interval of time travel a distance at, a being the velocity of sound, so that in the two-dimensional case the wave front will lie on a circular cylinder of radius at whose axis passes through P. Similarly, half-way through the interval of time when P has reached a point P'' such that $PP'' = \frac{1}{2}Ut$, the wave front will lie on a circular cylinder of radius $\frac{1}{2}at$ and axis at P'', and so on. Thus no disturbance can have been propagated during the time t beyond the pair of planes through P' tangential to all such circular cylinders. Each of these planes is inclined to the flight path at the angle $\sin^{-1}(a/U)$, which is known as the *Mach angle* and denoted

by m. The above argument is readily modified to apply to three dimensions, the wave front then becoming a cone of angle $2m$ at the vertex. The wave fronts are propagated normally to themselves, i.e. obliquely through the oncoming stream.

It must be observed that the foregoing result depends upon the loss of velocity normal to the wave suffered by the oncoming stream being small. In the case of a large disturbance the velocity of propagation may greatly exceed that of sound, so that the wave front is much more steeply inclined. The latter condition may be expected in the immediate vicinity of a fast-moving body, but since a large disturbance tends to die away as the wave proceeds, the Mach angle will still characterise the outer parts of the wave.

140S. Ackeret's Theory

The simplifying assumption above mentioned, viz. that for thin aerofoils such as those examined in Article 140P the disturbance may be regarded as everywhere small and the aerofoil flow as nearly uniform, was introduced by Ackeret * in advancing the following approximate method of calculating the lift, drag, and pitching moment at supersonic speeds.

Let the relative velocity U now exceed the velocity of sound a_0 in the undisturbed fluid, so that $M > 1$. The velocity potential is related in the same way to the relative motion as for incompressible flow, and substitution in (iii) of Article 140P gives, on writing n^2 for $M^2 - 1$,

$$\frac{\partial^2\phi}{\partial y^2} - n^2\frac{\partial^2\phi}{\partial x^2} = 0.$$

This equation has the general solution—

$$\phi = f_1(x - ny) + f_2(x + ny).$$

The solution over the upper surface of the aerofoil may be regarded as that for a uniform flow plus a function of the type f_1, whence it is seen that the increment of ϕ to be added to that for the uniform flow is constant along the straight lines $y = x/n +$ constant. These lines are inclined to the direction of motion of the aerofoil at the angle—

$$\tan^{-1}\frac{1}{n} = \sin^{-1}\frac{1}{\sqrt{(n^2+1)}} = \sin^{-1}\frac{a_0}{U} \quad . \qquad \text{(i)}$$

i.e. at the Mach angle m.

The wave under the aerofoil is similarly treated, leading to Fig. 100H, where lines have been drawn at the Mach angle from the nose and tail of the aerofoil. Each pair of lines contains between

* *Z.F.M.*, vol. 16, 1925.

them a sound-wave propagating obliquely upward from the upper surface and downward from the lower surface.

The increment of ϕ additional to that for a superposed uniform flow is constant along the wave front and along any line parallel thereto within the wave. Hence the additional velocity u is constant along, and directed normally to, all such lines. The magnitude of u appropriate to any such line is determined by the boundary condition and so depends upon the shape of the aerofoil profile. Considering an element of the profile inclined, as in the figure, at a small angle ε to the relative motion, the component of fluid velocity along the normal to the element is $u \cos (m - \varepsilon)$ and the component of the velocity of the element itself in the same direction is $U\varepsilon$. These must be equal, whence—

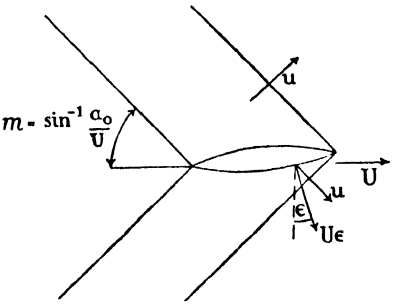

FIG. 100H.

$$u = U\varepsilon \sec m, \quad . \quad . \quad . \quad \text{(ii)}$$

provided ε is small.

Assuming now the air to be flowing past the stationary aerofoil, the pressure p within the standing sound-wave is related to the undisturbed pressure p_0 by (52) of Article 31, since increase of ρ is small; and $p - p_0$ may be expanded as described in that article since the resultant fluid velocity q within the wave differs little from U, giving approximately—

$$p - p_0 = \frac{\gamma p_0}{2a_0^2}(U^2 - q^2) = \tfrac{1}{2}\rho_0(U^2 - q^2).$$

Now q has the components $U - u \sin m$ and $u \cos m$, and substituting,

$$p - p_0 = \tfrac{1}{2}\rho_0\{U^2 - [(U - u \sin m)^2 + (u \cos m)^2]\}.$$

Since u is small, terms involving its square may be neglected, giving—

$$p - p_0 = \rho_0 U u \sin m.$$

Substituting for u in this equation from (ii),

$$p - p_0 = \rho_0 U^2 \varepsilon \tan m.$$

But by (i) $\tan m = a_0/(U^2 - a_0^2)^{1/2}$. Hence finally—

$$\frac{p - p_0}{\tfrac{1}{2}\rho_0 U^2} = \frac{2\varepsilon}{(M^2 - 1)^{1/2}}, \quad . \quad . \quad . \quad \text{(iii)}$$

where M, the Mach number, $= U/a_0$, as before.

The pressure coefficient, given by (iii), may be integrated round the profile of a given aerofoil section, in the manner described in Article 44, to yield estimations of the lift, drag, and pitching-moment coefficients, ignoring skin friction. For $M = 1{\cdot}7$, Taylor * examined from this point of view the biconvex circular-arc aerofoil of Fig. 100E, and obtained good agreement with Stanton's experiments. Approximately, the calculated value of $dC_L/d\alpha$ is 2·85 and the observed value 3. Comparison with the experimental value of 4·85 for $M = 0{\cdot}5$ illustrates the loss caused by the compressibility stall. At an incidence of $7\frac{1}{2}°$ the drag coefficeint (C_D) was observed to be nearly 0·1 and the calculated value, neglecting skin friction, is about 7 per cent. less. Few data have yet been published regarding tests on aerofoils of other sections at supersonic speeds.

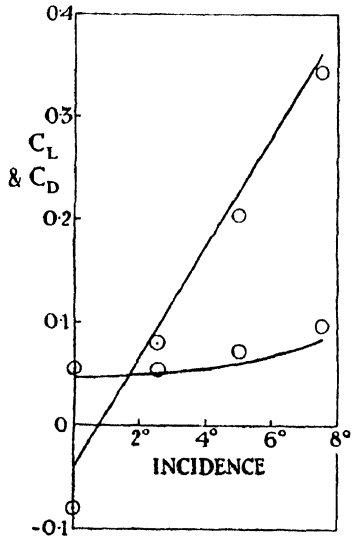

FIG. 100I.—BICONVEX AEROFOIL AT M = 1·7.

140T. Like Glauert's theory for thin aerofoils at subsonic speeds, Ackeret's theory for the higher range is regarded as an interesting and simple approach to a difficult matter, achieving success in favourable circumstances, and likely to be improved or adapted as more experience is gained in this comparatively new but important branch of our subject.

It is clear that the assumption of sound-waves cannot be justified in the region of the nose of the aerofoil at a very high speed, and that the shock wave there formed will involve considerations of the kind investigated for the pitot tube, Article 66D. More accurate methods due to Prandtl and Busemann are also available for determining the flow over the profile. The matter is developed further in a paper by Hooker,† from which Fig. 100I has been prepared with reference to the above biconvex aerofoil and Mach number. Considering that skin friction is neglected, the agreement between prediction and experiment is seen to be good. The maximum experimental L/D is only $3\frac{1}{2}$, but would be greater for a thinner section.

* A.R.C.R. & M. No. 1467, 1932. † A.R.C.R & M. No. 1721, 1936.

Chapter VII

VORTICES AND THEIR RELATION TO DRAG AND LIFT

GENERAL THEOREMS AND FORMULÆ

141. In Chapters V and VI the motion of the fluid was assumed to be wholly irrotational, but experiment shows motions of practical interest to comprise rotational and irrotational parts (Chapters II and VI B). While again assuming inviscid incompressible flow, we now extend its nature to this composite structure. In general the fluid motions will be unsteady but Bernoulli's equation will apply to irrotational regions, though not where vorticity exists ; through the latter there will be a variation of pitot head.

It will be proved that elements of fluid possessing vorticity are axially continuous with elements similarly characterised ; vorticity at a point in a cross-section of a bulk of fluid implies the existence of a string of rotating elements, cutting the section at the point. Such a string cannot terminate in the fluid, we shall find, but must either be re-entrant, forming a ring or loop, or else abut on a boundary. The line (in general curved) to which the axis of rotation of every element of the string is tangential is called a *vortex line.* If vortex lines be drawn through every point of the periphery of a very small area, they form a *vortex tube,* and the fluid, of which the small area is a cross-section, is called a *vortex filament,* or simply a *vortex.*

A difficulty is sometimes experienced at the outset with the foregoing definitions, because the tangible evidence of a real vortex in a wind is usually a widespread swirl of air. But in theory, as in fact, every vortex has inseparably associated with it an external motion ; for an inviscid fluid this is an irrotational circulation, a condition to which air flow approximates under aeronautical conditions.

We begin by considering in detail a simple type of theoretical vortex which long, straight parts of practical vortex loops resemble, known as Rankine's vortex.

142. Isolated Rectilinear Vortex of Circular Section and Uniform Vorticity

The vortex is assumed to be straight and infinitely long. If a is its radius and ζ its uniform vorticity, we have from Article 39 that ω, its

angular velocity, $= \frac{1}{2}\zeta$. The circulation K round its periphery is $2\pi a \,.\, \omega a$. Hence:

$$K = 2\omega \,.\, \pi a^2 = \zeta\sigma \quad . \quad . \quad . \quad (178)$$

writing σ for the area of cross-section. Any of these quantities defines the strength of the vortex, and this definition is carried over to vortices of cross-sectional area σ which are not straight.

Outside the vortex the flow is irrotational, and the velocity is assumed to be continuous at $r = a$. Therefore, an irrotational circulation of strength K must surround the vortex. If q is the velocity at any radius r, we have—

$$\text{for } r < a,\ q = \omega r = \frac{K}{2\pi a^2} r\,;$$

$$\text{for } r > a,\ q = \frac{K}{2\pi r}. \quad . \quad . \quad . \quad . \quad (179)$$

Let P be the pressure at $r = \infty$ when $q = 0$. Applying Bernoulli's equation through the outer flow gives for $r > a$—

$$P - p = \frac{\rho K^2}{8\pi^2 r^2} \,. \quad . \quad . \quad . \quad \text{(i)}$$

as was shown in Article 103 to be consistent with the element being in equilibrium under the pressure gradient and the centrifugal force. Within the vortex there is, of course, the same condition for equilibrium, but Bernoulli's equation does not apply. Since we have assumed constant angular velocity, however, for $r < a$—

$$\frac{dp}{dr} = \rho\omega^2 r.$$

Integrating and substituting for ω from (178)—

$$p = \frac{\rho K^2}{8\pi^2 a^4} r^2 + \text{const.}$$

Now this must give the same pressure as (i) when $r = a$. Therefore the constant $= P - \rho K^2/4\pi^2 a^2$. Hence, within the vortex—

$$P - p = \frac{\rho K^2}{4\pi^2 a^2}\left(1 - \frac{r^2}{2a^2}\right) \,. \quad . \quad . \quad . \quad (180)$$

Fig. 101 shows the variation of velocity and pressure through the vortex of the diameter shown. A practical vortex of sufficient size to investigate experimentally differs in that its spin is not constant and its periphery is less sharply defined.

The foregoing supplements Article 103, showing the simplest condition under which irrotational circulation can occur round a

fluid core. To prevent cavitation, P must exceed the pressure drop at the centre, which amounts to $\rho K^2/4\pi^2a^2$.

For the outer flow we have, from Article 103—

$$\psi = -\frac{K}{2\pi}\log\frac{r}{a} \quad . \quad . \quad \text{(ii)}$$

The stream function for the inner flow is obtained at once as—

$$\psi = -\int \omega r dr$$

$$= -\frac{K}{4\pi a^2}r^2 + \text{const.}, \quad \text{(iii)}$$

the negative sign following from choice of counter-clockwise sense for K positive. For (iii) to agree with (ii) when $r = a$, the constant $= K/4\pi$ and (iii) becomes—

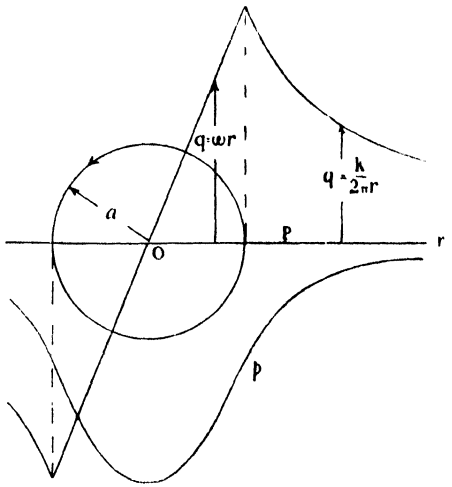

FIG. 101.—DISTRIBUTION OF VELOCITY AND PRESSURE THROUGH A RANKINE VORTEX.

$$\psi = \frac{K}{4\pi}\left(1 - \frac{r^2}{a^2}\right). \quad . \quad . \quad \text{(iv)}$$

143. A slight generalisation of the above has an experimental interest. In this the vortex is assumed to be vertical, and in a bulk of liquid on whose free surface it terminates.

To take account of the weight of the liquid, of density ρ_1, equations (i) and (180) of the preceding article become (cf. Article 6)—

$$\frac{P - p}{\rho_1} = \frac{K^2}{8\pi^2r^2} - gz, \qquad \text{for } r > a,$$

$$\frac{P - p}{\rho_1} = \frac{K^2}{4\pi^2a^2}\left(1 - \frac{r^2}{2a^2}\right) - gz, \quad \text{for } r < a,$$

where z is the depth below the general level of the surface.

Now, over the free liquid surface the pressure must be constant, and hence a dimple is formed. If z' denotes the depression of the surface through the dimple—

$$z' = \frac{K^2}{8g\pi^2r^2}, \qquad \text{for } r > a,$$

$$z' = \frac{K^2}{4g\pi^2a^2}\left(1 - \frac{r^2}{2a^2}\right), \text{ for } r < a.$$

The maximum depth of the dimple is $K^2/4g\pi^2a^2$

By observing dimples on the surface of water contained in a tank, the positions of the ends of vortices within the tank terminating on the surface can be found with some accuracy, although it is usually more convenient to sprinkle aluminium dust on the surface, which reveals the streamlines and facilitates photographs. If the vortices are in the atmosphere above the tank and terminate on the water surface, liquid is pressed a short distance up into their cores. When they form loops within an air stream, one way of making them visible is by introducing water-vapour, which tends to condense in the interior of the filaments.

144. An essential difference between a complete vortex and circulation around a solid core is that the latter may be fixed or constrained to a certain path, whilst the vortex is free to move. The outer irrotational flow associated with a vortex is called its *velocity field*, and the velocity at any point the *induced velocity*. The velocity at the centre of an isolated rectilinear vortex in an infinite expanse of fluid, which is stationary at a large distance from the vortex, or within a concentric cylindrical boundary, to take another example, is zero, and the vortex remains stationary. But this is not the case with a vortex ring or loop, or when one rectilinear vortex is near another or approaches a boundary.

Although requiring a knowledge of the strengths and instantaneous disposition of the vortices, Aerodynamical calculations are chiefly concerned with the velocity field, and it is nearly always permissible to neglect the effects of a vortex diameter and of the particular distribution of vorticity within a given vortex. In the following articles the vortex filaments are assumed to be thin and of uniform vorticity throughout any cross-section.

We proceed to prove a number of theorems. These are rigidly true only for the inviscid fluid assumed, but their direct application to air flow is remarkably fruitful in practical results. The theory of inviscid vortices was, in the first place, due to Helmholtz, although further developed by Kelvin.

145. The Strength of a Vortex is Constant throughout its Length

Fig. 102 shows part of a vortex filament, the circuit ABCDD'C' B'A'A being drawn on its surface. The lines AA', DD' are adjacent, so that ABCD and A'B'C'D' enclose two sections of the vortex. Let the circulation round the first section be K and that round the second K'.

It is clear that K, K' are the same as if evaluated round normal

cross-sections in the positions A, A′ along the vortex, because, if σ denote the normal cross-sectional area and ζ the vorticity at A, $K = \zeta\sigma$, by (178), which applies to a curved as well as to a straight vortex, and if the actual section be inclined at a small angle to the normal, the component of spin will be reduced below ζ by the same factor as that by which the area will be increased above σ, so that the product $\zeta\sigma$ remains independent of the angle. Hence K, K' give the strengths of the vortex at A, A′.

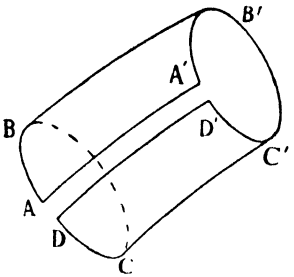

FIG. 102.

Now, the cylindrical surface having ABCDD′C′B′A′A as boundary may be split up into a large number of elements of area by a fine network of lines drawn in the surface, as was done in Article 97, and as in that article the circulation round the boundary will equal the sum of the circulations round the elements enclosed. But the surface does not penetrate into the vortex, and consequently the circulations round its elements are all separately zero. Hence the circulation round the boundary is zero. Also, the flow along AA′ cancels the flow along D′D. Therefore, the circulation round ABCD equals that round A′B′C′D′, i.e.—

$$K = K' \text{ or } \zeta\sigma = \zeta'\sigma'.$$

If the angular velocity within a vortex filament varies along its length, the cross-section also varies, or vice versa, in such a way that the product of the angular velocity and the cross-section remains constant.

146. Other Vortex Laws

A theorem given in Article 97 can now be re-stated as follows: The circulation round any circuit is equal to the sum of the strengths of the vortices it encloses. It should also be noted that this theorem is not restricted to two dimensions.

Let a wide circuit move at every point with the fluid and enclose a single isolated vortex section. Then by the above and Kelvin's Theorem (Article 140K) the strength of the vortex is *constant with respect to time*. Since also the strength of a vortex is constant along its length, a vortex cannot come to an end in a perfect fluid, but must either be re-entrant (like a smoke-ring) or abut on a boundary (as described, for instance, in Article 143).

Now reduce the circuit to a loop which at some instant encircles the isolated vortex section closely, and let the loop subsequently move with the fluid so that the circulation round it remains constant. But this circulation is equal to the strength of the vortex originally enclosed, itself constant. Hence the vortex remains enclosed ; i.e. a vortex *moves with the fluid.*

The above laws are of such outstanding importance in Aerodynamics that brief comment on their modification for a viscous fluid such as air may be interpolated here. In ordinary circumstances deviation from Kelvin's Theorem is negligible. On the other hand, concentrations of vorticity diffuse outward, like heat. Thus a real vortex tends to remain of constant strength but to increase in diameter. The laws for a perfect fluid are effectual in air away from boundaries, including that a vortex cannot originate or terminate within the fluid. Vortices may be built up slowly but originate from the surfaces of moving bodies by the action of viscosity in the presence of intense velocity gradients.

147. It is seen that the motion of a vortex arises, not from itself, but from the general field of flow, which may be due to a number of causes, such as sources, sinks, and other vortices. A vortex line very close to the surface of a body in motion through air actually also moves with the fluid, because of the real boundary condition of absence of slip and the action of viscosity in making the velocity of the fluid adjacent to the vortex line almost equal to that of the body. It will occasionally be convenient to treat of a vortex line constrained to move with a body, while ignoring viscosity and the real boundary condition. The vortex line is then said to be *bound.*

148. Formulæ for Induced Velocity of Short Straight Vortices

The derivation of formulæ for the velocity components at a point due to one or more vortex loops is beyond the scope of this book. It is shown in *Hydrodynamics* that each element of fluid possessing vorticity implies an associated increment of velocity in every other element of the fluid mass. The direction of this velocity increment at any point is perpendicular to the plane which contains the point and the axis of rotation of the vortex element. If δq denote the increment at P due to a small length, δs of a curved vortex filament of strength K distant r from P, and θ the angle between r and δs, it is found that—

$$\delta q = \frac{K \sin \theta \,.\, \delta s}{4\pi \quad r^2} \quad . \quad . \quad . \quad (181)$$

The total velocity q at P due to the whole filament is obtained by integrating along the filament.

In the case of a straight finite length QR of a vortex, the velocity at a point P distant h from its axis (see Fig. 103) is perpendicular to

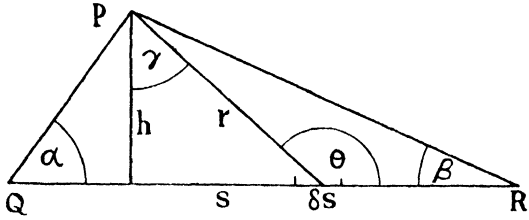

FIG. 103.

the plane PQR and from (181) amounts to :

$$q = \frac{K}{4\pi}\int_Q^R \frac{\sin\theta \,.\, ds}{r^2} = \frac{Kh}{4\pi}\int_Q^R \frac{ds}{r^3}.$$

Changing the variable from s to γ, since $ds/d\gamma = h\sec^2\gamma$—

$$q = \frac{Kh^2}{4\pi}\int \frac{\sec^2\gamma d\gamma}{r^3} = \frac{K}{4\pi}\int \frac{d\gamma}{r}$$

$$= \frac{K}{4\pi h}\int \cos\gamma d\gamma$$

where the limits are now from $-\left(\frac{\pi}{2} - \alpha\right)$ to $\frac{\pi}{2} - \beta$. Hence—

$$q = \frac{K}{4\pi h}(\cos\beta + \cos\alpha). \quad . \quad . \quad . \quad (182)$$

An application of this formula occurring frequently in aerofoil theory is when P is at a distance x, measured along the vortex, from one end of a straight vortex length, whose other end is a long distance away. We then have—

$$q = \frac{K}{4\pi h}\left\{1 + \frac{x}{\sqrt{(x^2 + h^2)}}\right\} . \quad . \quad . \quad (183)$$

If P is opposite the end of a semi-infinite straight length,

$$q = \frac{K}{4\pi h} \quad . \quad . \quad . \quad . \quad (184)$$

i.e. one-half the induced velocity for a rectilinear vortex.

149. We now consider some two-dimensional vortex fields and vortex motions of importance as leading to approximations to those

occurring in aerofoil theory. For ease of future reference, the vortex filaments are assumed to extend indefinitely in both directions parallel to the axis Ox. In the yz-plane perpendicular to them v is the velocity component in the direction Oy, w that in the direction Oz, and the third component $u = 0$.

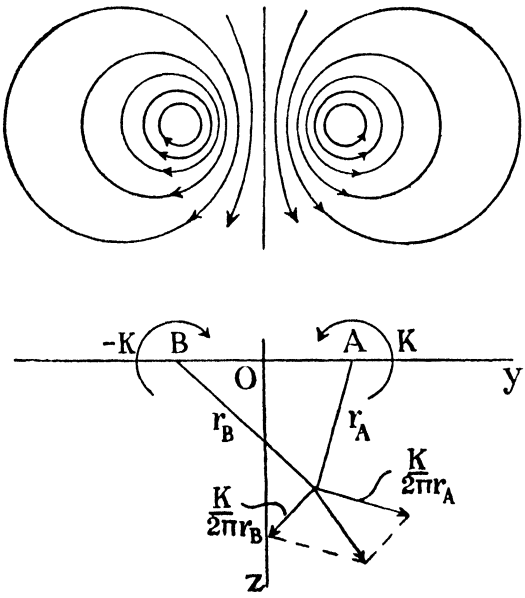

FIG. 104.—INSTANTANEOUS STREAMLINES OF A VORTEX PAIR.
Below: Construction for the resultant induced velocity.

Vortex Pair

The combination of two parallel rectilinear vortices of equal and opposite strengths is called a vortex pair. Let them be situated instantaneously on the y-axis at A and B (Fig. 104), equidistant from the origin and distant l apart, and let their strengths be $\pm K$ as shown. Neither has any motion due to itself, but each has a velocity induced by the other, given by—

$$w' = \frac{K}{2\pi l}, \qquad v = 0. \quad . \quad . \quad . \quad (185)$$

Thus the vortices move in the direction Oz, i.e. downward in the figure, at this constant velocity, remaining a constant distance apart.

Two sets of streamlines arise, viz. those relative to the fixed axes of reference and those relative to the vortices. The first are identical with the equipotentials of a source and sink occupying the positions of the vortices, and might be inferred from Article 104. But directly, since for A and B alone—

$$\psi = -\frac{K}{2\pi}\log r_A, \quad \psi = \frac{K}{2\pi}\log r_B,$$

respectively, we have for the combination—

$$\psi = -\frac{K}{2\pi}\log\frac{r_A}{r_B} \quad . \quad . \quad . \quad (186)$$

The streamlines are shown in Fig. 104, but represent only an instantaneous plotting, for A and B immediately move away from the y-axis. In accordance with Article 21 they are more appropriately called path-lines.

To obtain the steady streamlines relative to the vortex pair, we add to the field of flow a velocity $-w'$, or to ψ the increment $-w'y = -Ky/2\pi l$, obtaining—

$$\psi = -\frac{K}{2\pi}\left(\log\frac{r_A}{r_B} + \frac{y}{l}\right). \quad . \quad . \quad (187)$$

These streamlines are shown in Fig. 105. It will be noticed that fluid particles contained within a certain oval accompany the vortex pair in its career. The streamlines external to the oval represent the flow past a cylinder of this section broadside on to the stream. The dimensions of the oval are $1{\cdot}05l$ by $0{\cdot}87l$, approximately.

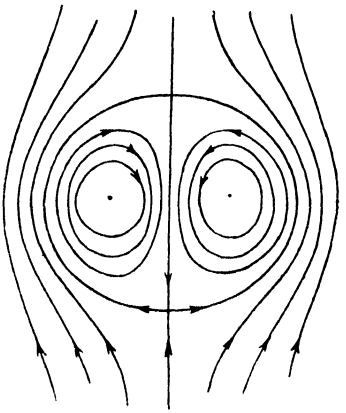

FIG 105.—STEADY STREAMLINES RELATIVE TO A VORTEX PAIR.

The instantaneous velocity relative to the fixed axes of reference at any point P (y, z) in the field is readily obtained by the construction shown in Fig. 104. Careful note should be made that the velocity of the vortices does not affect this velocity, just as the speed of a star makes no difference to the speed of the light it emits.

The velocity is equally simply found in analytical terms. For example, the component w at P is given by—

$$w = \frac{K}{2\pi}\left\{\frac{\frac{1}{2}l + y}{(\frac{1}{2}l + y)^2 + z^2} + \frac{\frac{1}{2}l - y}{(\frac{1}{2}l - y)^2 + z^2}\right\}. \quad . \quad (188)$$

Along the y-axis w represents the true instantaneous velocity, and the formula for it is—

$$w = \frac{K}{2\pi}\left\{\frac{1}{\frac{1}{2}l + y} + \frac{1}{\frac{1}{2}l - y}\right\} = \frac{K}{2\pi}\left\{\frac{l}{(\frac{1}{2}l)^2 - y^2}\right\} \quad . \quad (189)$$

The distribution of w along Oy is shown in Fig. 106, where the vortices have been given an appreciable size, but subsidiary effects of this size have been neglected. When P lies between A and B, w is positive, i.e. downwardly directed in the figure ; midway between them the velocity is four times as great as the velocity of the vortices.

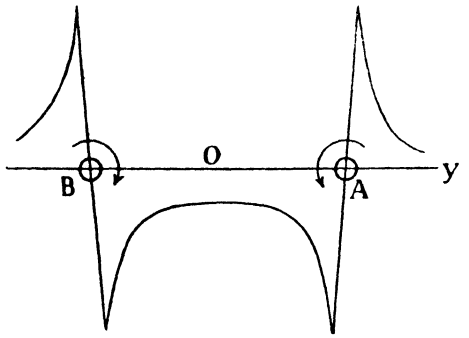

FIG. 106.—DISTRIBUTION OF VELOCITY THROUGH A VORTEX PAIR.

Beyond A or B, w is negative. The special interest of this example in connection with aeroplane wings will be described later.

150. If two vortices A, B distant l apart have strengths K_1, K_2, both of the same sign, the velocity of A will be $K_2/2\pi l$, while that of B will be $K_1/2\pi l$. Both velocities will be perpendicular to the line AB, but in opposite directions. Thus the line AB has a steady angular velocity and one point on it, which is easily found, remains fixed if a velocity is not induced there by other causes.

The instantaneous velocity at any point due to any number of parallel vortices may be found by the superposition of the velocities induced by the several filaments. The fixed point in the last example corresponds to the C.G. of the two vortices if each is imagined to be a gravitating line of mass equal to its strength. The analogy can be applied to more complicated dispositions of vortices, and so an axis, parallel to Ox, can be found for the system which remains fixed (in the absence of other disturbances) as the vortices move. But in the important case when the algebraic sum of the strengths vanishes, i.e. for a group of vortex pairs, the axis is at infinity.

There exists another analogy, of considerable experimental use, viz. that between a vortex filament and a wire conducting an electric current. The lines of magnetic force surrounding a current, or group of currents, which can readily be mapped out by experimental means, correspond exactly to the streamlines of the vortex case. The analogy finds practical expression in an apparatus called the 'electric tank.' *

EFFECT OF WALLS

151. Applications of the Method of Images

When a vortex approaches a parallel boundary which is not coaxial with it, the streamlines become distorted, and a motion is

* Relf, A.R.C.R. & M., 905, 1924.

induced in the vortex. These effects may sometimes be determined by the method of images. The question is one of outstanding interest, because Aerodynamical measurements of flow involving vortices are usually made in the presence of walls.

As a first example, let a single rectilinear vortex of strength K be distant $\frac{1}{2}l$ from a plane rigid wall parallel to its axis. The presence of a rigid boundary requires that at every point on it the normal component of velocity shall vanish. In the present case this is obviously satisfied by imagining a second vortex of strength $-K$ to be situated at a distance $\frac{1}{2}l$ beyond the boundary, opposite to the real vortex, i.e. by introducing the image of the vortex in the wall. The streamlines are determined by the two. The flow round, and the motion of, the real vortex will be exactly those that would obtain if it formed one member of a vortex pair. The solution is otherwise evident, for clearly the plane xOz in Article 149 might have been made rigid without effect.

152. Another example, which leads to an important case, is provided by a rectilinear vortex eccentrically situated within a long tunnel of circular section. The boundary takes the place of one of the co-axial circles of Fig. 104, which form the instantaneous streamlines of a vortex pair. The effects of the tunnel are reproduced by introducing the image of the vortex in the circular wall, an imaginary vortex of strength $-K$ situated at the inverse point.

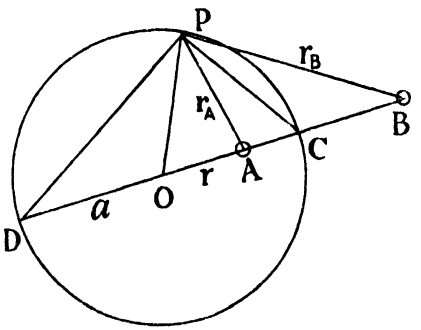

FIG. 107.

Let A, Fig. 107, be the real and B the imaginary vortex, and P any point on the boundary. The condition that the radial velocity component shall vanish at P whatever its position is that the locus of P be a streamline, and for this, $r_A/r_B = \text{const.}$

Bisect the $\angle BPA$ internally and externally by PC, PD; BA is then divided internally at C and externally at D, and—

$$\frac{BC}{CA} = \frac{BD}{DA} = \frac{r_B}{r_A} = \text{const.}$$

Thus C and D are fixed points and, since the $\angle CPD = \pi/2$, P traces a circle on CD as diameter. Let the radius of this circle

be a and its centre O. Then from the above equation and the figure—

$$OB = BD - a = \frac{DA \,.\, BC}{CA} - a$$
$$= \frac{(a + r)\,(OB - a)}{a - r} - a,$$

giving—

$$OB = \frac{a^2}{r} \quad . \quad . \quad . \quad . \quad . \quad (190)$$

Thus a vortex of strength K distant r from the centre of a tunnel of radius a moves in a concentric circular path with the constant velocity—

$$-\frac{K}{2\pi} \cdot \frac{1}{a^2/r - r} = -\frac{K}{2\pi} \cdot \frac{r}{a^2 - r^2}.$$

The instantaneous streamlines within the tunnel follow from Fig. 104.

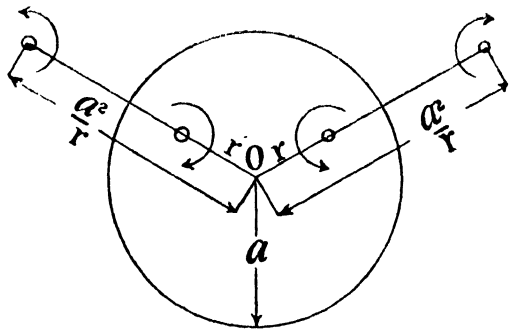

FIG. 108.—IMAGE SYSTEM FOR A VORTEX PAIR IN A CIRCULAR TUNNEL.

The image system for a vortex pair, each of whose members is distant r from the centre O of the tunnel is shown in Fig. 108, each of the two images being situated on the radial plane containing the corresponding real vortex and distant a^2/r from O. Each vortex describes in general a D-shaped path in its half of the tunnel section. But chief interest attaches to the effect of the tunnel on the velocity field. In, for example, the particular case where the vortices lie on a diameter, if their distance apart is then l, w at O is given by—

$$w = \frac{K}{2\pi}\left\{\frac{4}{l} - \frac{l}{a^2}\right\}. \quad . \quad . \quad . \quad (191)$$

Without a boundary we should have at O—

$$w = \frac{K}{2\pi}\left(\frac{4}{l}\right).$$

Thus the tunnel wall considerably reduces this velocity; when $l = a$, for example, the decrease amounts to one-quarter.

153. Some further examples of image systems will be referred to briefly.

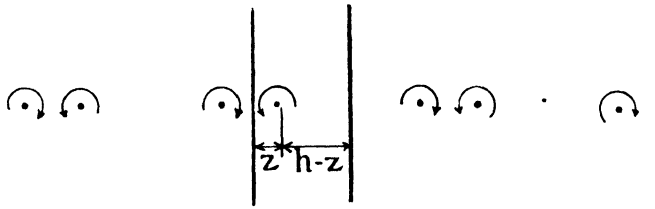

FIG. 109.—IMAGE SYSTEM FOR A RECTILINEAR VORTEX BETWEEN PARALLEL WALLS (THE ROW OF IMAGES EXTENDS TO INFINITY).

(1) A vortex parallel to two parallel plane walls gives rise to a doubly infinite row of images (Fig. 109). If h is the distance apart of the walls and z the distance of the vortex from one of them, the vortices are separated alternately by the distances $2z$ and $2(h - z)$.

(2) A vortex in the corner between two plane walls which meet at right angles calls for three images situated at the corners of a rectangle, as shown in Fig. 110.

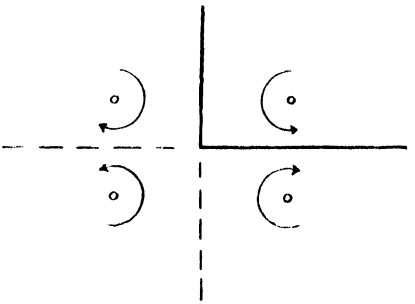

FIG. 110.—IMAGE SYSTEM FOR A RECTILINEAR VORTEX IN A RIGHT-ANGLED CORNER.

(3) The important case of a vortex pair contained within a rectangular tunnel leads to a complicated arrangement of images in doubly infinite columns and rows, as shown in Fig. 111. Reference will be made later to this case, when the subject will be systematised in connection with Wind-tunnel Interference. But when the sides of the rectangle are equal, or nearly so, it is often sufficient to substitute for the actual boundary an approximation consisting of a circle drawn fairly through the sides.

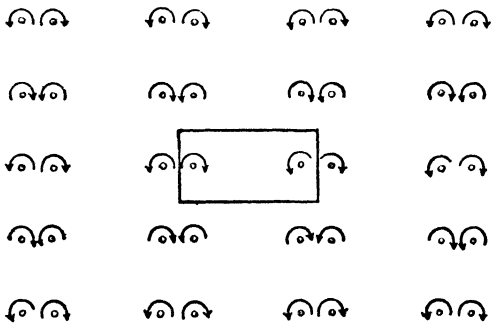

FIG. 111.—IMAGE SYSTEM FOR A VORTEX PAIR IN A RECTANGULAR WIND TUNNEL OF ENCLOSED TYPE (THE COLUMNS AND ROWS OF IMAGES EXTEND INFINITELY).

154. Application of Conformal Transformation

It will be apparent that the method of images is convenient in some cases of vortices near boundaries but cumbersome in others. The total effect of an infinite series of images may be difficult to sum while the step-by-step increments may converge so slowly as to make approximate calculation laborious. In some cases, again, an image system cannot be found. An alternative method of solution is provided by the use of conformal transformation which may be applied to parallel rectilinear vortices.

For ease of reference the vortices are now assumed to be perpendicular to the xy-plane, i.e. our real plane will be the z-plane of Article 122, where the co-ordinate of a point is $z = x + iy$, and transformation will be made to a t-plane where the co-ordinate is $t = \xi + i\eta$. If at any instant there is a vortex at the point z_1 in the real plane, at the same instant a vortex of equal strength will exist at the corresponding point t_1 in the transformed plane. There are several ways of proving this. The most direct is to note that outside the vortex a velocity potential ϕ exists; that the strength is equal to the interval in ϕ once round a circuit embracing the vortex; that ϕ has the same value at corresponding points in the two planes; and so, if the interval of ϕ be evaluated round corresponding circuits in the two planes, it will clearly come to the same thing. But it will be seen that, the transformation having changed the boundaries and the geometrical dispositions of other vortices that may be present, the vortex particularly considered will not move along a path in the t-plane which corresponds to its path in the z-plane. The two paths can be related, so that one can be drawn from the other, but, since in Aerodynamics we are chiefly concerned with instantaneous induced velocities, this development will be left to subsequent reading.*

The general aim in applying conformal transformation is to simplify the configuration of the real system, so that a convenient arrangement of images can be used; the difficulty, as in problems of potential flow, lies in finding the transformation formula. The simplest image system is that appropriate to a single vortex near a parallel plane wall. If in the z-plane the trace of the wall coincides with the x-axis and the real vortex of strength K is at the point x_1, y_1, the image of strength $-K$ will be at the point $x_1, -y_1$, and the stream function of the velocity field is obtained from (186) as—

$$\psi = -\frac{K}{2\pi} \log \frac{\sqrt{\{(x - x_1)^2 + (y - y_1)^2\}}}{\sqrt{\{(x - x_1)^2 + (y + y_1)^2\}}}$$

* Routh, *Proc. Lond. Math. Soc.*, t. XII, 1881.

$$= -\frac{K}{4\pi}\log\frac{(x-x_1)^2+(y-y_1)^2}{(x-x_1)^2+(y+y_1)^2}.$$

In the same way the identical system in the t-plane (*not* that obtained by transformation) gives—

$$\psi = -\frac{K}{4\pi}\log\frac{(\xi-\xi_1)^2+(\eta-\eta_1)^2}{(\xi-\xi_1)^2+(\eta+\eta_1)^2}, \quad . \quad . \quad (192)$$

the real vortex being situated at the point ξ_1, η_1, and the wall coinciding with the ξ-axis. If a transformation formula can be found to convert whatever configuration exists in the z-plane to this configuration, for instance, in the t-plane, the problem in the z-plane is at once solved.

155. Vortex Midway between Parallel Walls

The image system for this case follows from Article 153 (1), but we shall ignore this and solve the problem by the method of the preceding article. Assume that the distance apart of the walls is H. Choose Ox in the z-plane, so that $y = 0$, $y = H$ represent the walls and Oy passes through the vortex. Let $x' = x/H$, $y' = y/H$.

Consider the transformation formula—

$$\log t = \pi z/H \quad . \quad . \quad . \quad . \quad (193)$$

or—

$$\xi + i\eta = e^{\pi(x'+iy')} = e^{\pi x'} \cdot e^{i\pi y'}$$
$$= e^{\pi x'}(\cos \pi y' + i \sin \pi y').$$

Separating real and imaginary parts—

$$\xi = e^{\pi x'} \cos \pi y', \ \eta = e^{\pi x'} \sin \pi y'. \quad . \quad . \quad (i)$$

Corresponding to $y = 0$, we have $\xi = e^{\pi x'}$, $\eta = 0$, and corresponding to $y = H$ we have $\xi = -e^{\pi x'}$, $\eta = 0$. Thus both walls in the z-plane transform to the ξ-axis in the t-plane. The vortex of strength K at $x' = 0$, $y' = \frac{1}{2}$ in the z-plane transforms, using (i), to a vortex of strength K in the t-plane at the point $\xi = 0$, $\eta = 1$.

Thus, in the t-plane we have a vortex on the η-axis at unit distance from a single wall coinciding with the ξ-axis. Therefore, the stream function of the velocity field in this plane is given by (192), and comes to—

$$\psi = -\frac{K}{4\pi}\log\frac{\xi^2+(\eta-1)^2}{\xi^2+(\eta+1)^2}.$$

To find the stream function in the z-plane, substitute for ξ, η in terms of x', y' (cf. Article 122) from (i) obtaining—

$$\psi = -\frac{K}{4\pi}\log\frac{e^{2\pi x'}\cos^2\pi y' + (e^{\pi x'}\sin\pi y' - 1)^2}{e^{2\pi x'}\cos^2\pi y' + (e^{\pi x'}\sin\pi y' + 1)^2}$$
$$= -\frac{K}{4\pi}\log\frac{e^{2\pi x'} - 2e^{\pi x'}\sin\pi y' + 1}{e^{2\pi x'} + 2e^{\pi x'}\sin\pi y' + 1}.$$

This expression reduces on dividing the numerator and denominator of the logarithm by $2e^{\pi x'}$ to—

$$\psi = -\frac{K}{4\pi}\log\frac{\cosh\pi x/H - \sin\pi y/H}{\cosh\pi x/H + \sin\pi y/H}. \quad . \quad . \quad (194)$$

The path-lines are shown in Fig. 112.

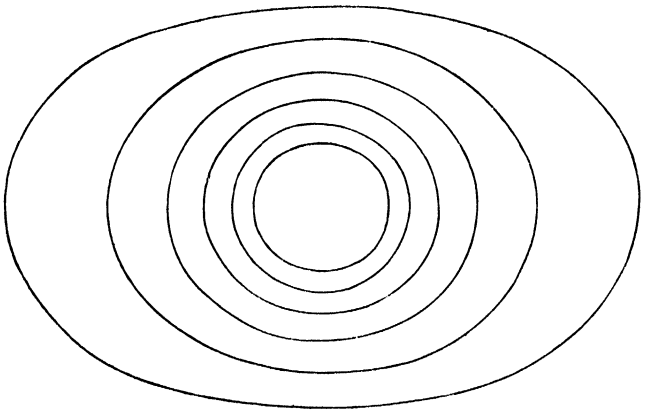

FIG. 112.—STREAMLINES FOR A RECTILINEAR VORTEX MIDWAY BETWEEN PARALLEL WALLS.

A particular interest centres in the effect of the walls on the velocity midway between them. This velocity is given by—

$$v' = -\frac{\partial\psi}{\partial x_{y=H/2}} = \frac{K}{2H}\left[\frac{\sinh\pi x/H\,.\,\sin\pi y/H}{\cosh^2\pi x/H - \sin^2\pi y/H}\right]_{y'=1/2}$$
$$= \frac{K}{2H}\cdot\frac{1}{\sinh\pi x/H} \quad . \quad . \quad . \quad . \quad . \quad . \quad (195)$$

In the absence of the walls, the velocity along this line would be equal to $K/2\pi x$. Hence the walls, if at distance H apart, reduce the velocity midway between them in the ratio—

$$\frac{\pi x/H}{\sinh\pi x/H}. \quad . \quad . \quad . \quad . \quad (196)$$

At a distance behind the vortex equal to its distance from either wall, for example, the reduction is over 30 per cent.

155A. Bound Vortex in Stream between Walls

The necessary modification of (194) to give the stream function for incompressible and irrotational flow past a bound vortex midway between parallel walls will be evident from the preceding article. Mention was made in Article 66A of a method of obtaining the lift of an aerofoil in a wind tunnel by integrating the changes of static pressure on the floor and roof of the tunnel. Further investigation in the present article will be directed more particularly to this question under the conditions stated and assuming the aerofoil to be small in chord, so that it may be replaced by a simple vortex.

The velocities along the floor and roof due to the vortex alone are, from (194),

$$u_{y'=0,\,1} = \left[\frac{\partial\psi}{\partial y}\right]_{y'=0,\,1} = \frac{K}{2H}\left[\frac{\cosh \pi x' \cos \pi y'}{\cosh^2 \pi x' - \sin \pi y'}\right]_{y'=0,\,1}$$

$$= \pm \frac{K}{2H \cosh \pi x'} \quad . \quad . \quad . \quad . \quad . \quad . \quad \text{(i)}$$

Adding a uniform stream of velocity $-U$ to produce an upward lift $L = \rho KU$ per unit length of the bound vortex gives for the resultant velocity along these walls—

$$q_0 = -U + u_0 \quad \text{and} \quad q_1 = -U + u_1, \quad . \quad \text{(ii)}$$

where the suffixes 0 and 1 distinguish the floor and roof, respectively.

Now, the flow being irrotational and incompressible, Bernoulli's equation gives—

$$\frac{p_0 - p_1}{\frac{1}{2}\rho U^2} = \left(\frac{q_1}{U}\right)^2 - \left(\frac{q_0}{U}\right)^2$$

$$= \left(\frac{K}{2UH \cosh \pi x'} + 1\right)^2 - \left(\frac{K}{2UH \cosh \pi x'} - 1\right)^2$$

by (i) and (ii), or—

$$p_0 - p_1 = \tfrac{1}{2}\rho U^2 \frac{2K}{UH \cosh \pi x'}$$

$$= \frac{L}{H \cosh \pi x'}. \quad . \quad . \quad . \quad . \quad . \quad \text{(iii)}$$

Thus if a gauge be connected between two static pressure holes at $x = 0$, one in the floor immediately below the lifting vortex and the other in the roof immediately above it, the lift per unit length will equal $H \times$ the pressure difference recorded. We also verify that—

$$L = \int_{-\infty}^{\infty} (p_0 - p_1)dx = \rho KU \int_{-\infty}^{\infty} \frac{dx'}{\cosh \pi x'}$$

$$= \rho KU.$$

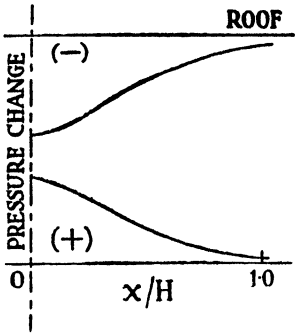

FIG. 112A.—LIFTING VORTEX BETWEEN PARALLEL WALLS.

A greater fraction of the lift will clearly be supported by the roof than by the floor, and the ratio of the two contributions to the total reaction is readily determined. The two pressure distributions are plotted in Fig. 112A. If the experimental exploration of $p_0 - p_1$ extends only to a distance X' on each side of the small aerofoil, the fraction of the lift obtained by integration will be—

$$\int_{-X'}^{X'} \frac{dx'}{\cosh \pi x'} = \frac{2}{\pi}\left[\tan^{-1} e^{\pi x'}\right]_{-X'}^{X'} \qquad \text{(iv)}$$

This result is plotted in Fig. 112B.

155B. Other Applications of the Transformation

In applying this method to other problems of flow between parallel walls it is sometimes advantageous to modify (193) to log $t = 2\pi z'$, which may be written, if r, θ are polar co-ordinates in the t-plane,

$$\log r + i\theta = 2(\pi x' + i\pi y'),$$

giving $\log r = 2\pi x'$, $\theta = 2\pi y'$. Thus $r = 1$ when $x = 0$, i.e. the y-axis of the z-plane corresponds to a circle of unit radius in the t-plane; also $\theta = 0$ when $y = 0$, and $\theta = \pm \pi$ when $y = \pm \frac{1}{2}H$. It follows that the *whole* of the t-plane yields in the z-plane an infinite strip of width H, as before, but with the x-axis midway between its edges (Fig. 112c). These edges are derived from the two sides of the negative half of the real axis in the t-plane. Hence the strip may be regarded as the section of a wind tunnel provided the corresponding flow in the t-plane makes the negative half of the real axis a streamline. A uniform flow between the parallel walls corresponds to a source at the origin in the t-plane since lines radiating at equal angle-increments from that origin transform

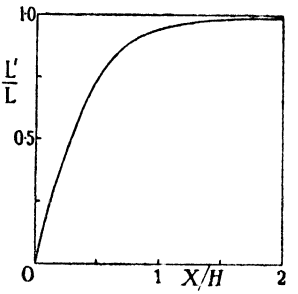

FIG. 112B.—INTEGRATED WALL PRESSURE.

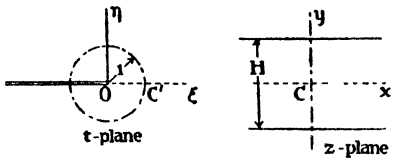

FIG. 112c.

to equally spaced lines parallel to the walls in the z-plane, and $r = 0$ corresponds to $x = -\infty$. If the uniform flow has a velocity U, the strength of the source is clearly UH.

(1) *Source in Uniform Stream.*—As a first example, let a source of strength m be located in the stream at the origin $z = 0$, which is not a singular point. The corresponding disturbance in the t-plane is an equal source at the point $t = 1$.

The potential function in the t-plane is—

$$w_t = \frac{UH}{2\pi} \log t + \frac{m}{2\pi} \log (t - 1).$$

Substituting gives for the z-plane—

$$w = Uz + \frac{m}{2\pi} \log (e^{2\pi z'} - 1)$$

so that the complex velocity $u - iv$ between the parallel walls is

$$\frac{dw}{dz} = U + \frac{m}{H} \frac{e^{2\pi z'}}{e^{2\pi z'} - 1}.$$

When z is large and negative, the velocity $= U$, as assumed, and when z is large and positive the velocity $= U + m/H$.

On the walls, $z = x \pm iH/2$, giving—

$$u = U + \frac{m}{H} \cdot \frac{e^{2\pi x'}}{e^{2\pi x'} + 1}$$

$$= U + \tfrac{1}{2}m(1 + \tanh \pi x')/H,$$

from which and Bernoulli's equation may be obtained the pressure distribution along the walls, illustrated in Fig. 112D. The streamline $\psi = 0$ will differ from that found in Article 106, becoming parallel more rapidly.

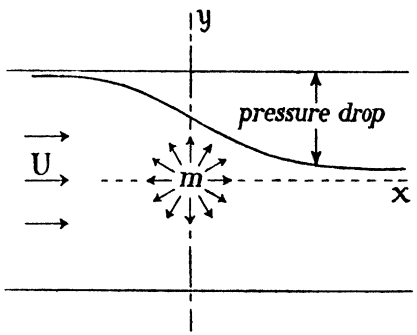

FIG. 112D.

(2) *Doublet in Uniform Stream.*—Let the source at $z = 0$ now be replaced by a doublet of strength $-\mu_s$. Then a doublet of strength μ_t appears at $t = 1$, and in that plane—

$$w_t = \frac{UH}{2\pi} \log t + \frac{\mu_t}{2\pi(t - 1)}$$

so that—

$$w = Uz + \frac{\mu_t}{2\pi} \cdot \frac{1}{e^{2\pi z'} - 1} \quad . \quad . \quad (i)$$

and—

$$u - iv = \frac{dw}{dz} = U - \frac{\mu_t}{H} \cdot \frac{e^{2\pi z'}}{(e^{2\pi z'} - 1)^2}.$$

On separating (i) into real and imaginary parts it is easily found that the streamline $\psi = 0$ is given by—

$$y = \frac{\mu_t}{4\pi U} \cdot \frac{\sin 2\pi y'}{\cosh 2\pi x' - \cos 2\pi y'}$$

This deformed circular boundary intersects the y-axis at points to be obtained from—

$$\frac{\pi y}{H} \tan \frac{\pi y}{H} = \frac{\mu_t}{4UH} \quad . \quad . \quad . \quad (ii)$$

and the x-axis at the points—

$$\sinh^2 \frac{\pi x}{H} = \frac{\mu_t}{4UH}. \quad . \quad . \quad . \quad (iii)$$

Substituting, for illustration, $y = \frac{1}{4}H$ in (ii) gives $\mu_t/U = \pi H$ and, by (iii), $x = 0{\cdot}254H$. Thus the deformation of a circle whose diameter is so great as one-half the height of the tunnel is small.*

It is assumed in the foregoing that the strength of a source, not situated at a singular point, remains unchanged on transformation. Proof follows immediately from that for a vortex (Article 154) on substituting ψ for ϕ. The same is not true, however, of a doublet since the strength of a doublet is proportional to the product of that of a source and an infinitesimal length. Thus whilst $q \propto 1/r$ for a source as for a vortex, $q \propto 1/r^2$ for a doublet. It follows that the strength μ_t in the t-plane is equal to $\mu|dt/dz|$, as may be proved in other ways. In the above example,

$$\frac{\mu_t}{\mu} = \left| \frac{dt}{dz} \right| = \frac{2\pi}{H}.$$

Investigations of the kind considered in this and the preceding article become of interest in the estimation of tunnel constraint on large two-dimensional models in comparatively small streams, and the use of adjustable walls to compensate (cf. Article 66A).

* Lamb, *Hydrodynamics*, 6th ed., p. 72, where the problem is solved by the method of images.

GENERATION OF VORTICES

156. As soon as an aeroplane, say, starting from rest, attains appreciable speed, the air flow induced past its various components becomes of the general nature described in Chapter II. But the wakes behind some of its parts—e.g. wings, wheel fairings, or thick exposed struts—are found to contain discrete vortices. The theory of the preceding articles then has a practical utility, which depends, however, upon a knowledge of the vortex distribution and strength. This information rests principally on observation, because it is difficult to calculate precisely how the vortices are formed, though it has been seen that they result from viscosity.

By starting a body of simple shape from rest in a tank of water, and sprinkling the water surface with aluminium dust, a cinema film can be taken of the accelerated motion. Under similar circumstances the same sequence of photographs will apply equally to air as fluid, but they are less easy to secure in air. Such films show vortices in various stages of growth, as will be described in the following articles.

It may be stated at once as a general result that photographs relating to a very early stage of motion accelerated from rest show path-lines which, even for bluff bodies, approximate closely to those of potential flow, as might have been anticipated on theoretical grounds (cf. Articles 98 and 119). The motions finally established may differ little or considerably from those of an inviscid fluid round the same shapes, but viscosity requires time in which to bring about the change.

157. Impulse

We shall have occasion to refer to the *impulse* of vortex loops. The external flow associated with an inviscid vortex loop is irrotational, and could be generated instantaneously from rest by an artificially arranged distribution of impulsive pressure, which can be calculated. The matter will be illustrated * with reference to the vortex pair.

Imagine a very long straight elastic membrane of width l immersed in stationary fluid. Let it be acted upon by a distribution of impulsive pressure, and let it bend transversely in the process in such a way that its final velocity at every point, attained at the end

* For rigorous mathematical investigation see Lamb's *Hydrodynamics*.

of the impulse, is exactly that appropriate to the fluid velocity field of a vortex pair situated along its edges. Finally, let the membrane vanish at the end of the impulse. The irrotational motion of a vortex pair results.

The impulsive pressure was identified in Article 98 with $-\rho\phi$. Considering any pair of adjacent points, A and B, on opposite faces of the membrane, the difference of impulsive pressure between them is $\rho(\phi_B - \phi_A)$, and this again is equal to ρK, if K be the magnitude of the eventual circulation round lines coincident with the long edges of the membrane. Now K is constant. Hence, per unit length—

$$\text{Impulse} = \rho K l \quad . \quad . \quad . \quad (197)$$

More generally it can be shown that the component in any direction of the impulse which would generate the velocity field of a vortex loop from rest is equal to—

$$\rho K S \quad . \quad . \quad . \quad . \quad . \quad (198)$$

where S is the projection in that direction of any area that is bounded by the vortex loop.

158. Vortex Sheets

A vortex sheet is a fluid layer, in general curved, containing a continuous, though not necessarily uniform, distribution of vorticity. Its two surfaces, a small but variable distance δn, say, apart, are formed of vortex lines. Consider a small length δs of the sheet perpendicular to the vortex lines. The circulation δK round the element $\delta n \delta s = (q - q')\,\delta s$, if q, q' denote the local velocities on the two surfaces of the sheet, for there is no flow along either of the δn-sides. Hence, writing 2ω for the vorticity—

$$2\omega \,.\, \delta n = q - q'. \quad . \quad . \quad . \quad (199)$$

Since the vortex lines move with the fluid, the sheet will not be stationary, but will locally have the velocity $\frac{1}{2}(q + q')$.

We have seen (Chapter II) an example of vortex sheet structure in the boundary layer. The term is more particularly reserved, however, for a sheet of vorticity out in the fluid, separating two regions of irrotational flow which have different adjacent velocities. The thickness δn may be considered to become indefinitely small while the product $2\omega \,.\, \delta n$ remains finite, when the sheet is formed simply of a single layer of vortex lines. It is then sometimes called a *surface of discontinuity*. In Chapter V the surfaces of bodies immersed in the stream were surfaces of discontinuity, but in Chapter II we saw that a boundary layer of small but measurable thickness represents

experimental conditions. A surface of discontinuity out in the fluid may be regarded as the ideally simplified, and a vortex sheet of finite thickness as the practical accompaniment of a sharp lateral change in velocity. The jump in velocity may be in respect of magnitude or direction.

159. Production and Disintegration of Vortex Sheets

Three ways may be distinguished in which vortex sheets are commonly produced.

(1) Considering, for example, a flat plate started from rest into broadside-on motion, the path-lines at an initial stage closely accord with those of potential flow (Fig. 80). But their persistence at the back of the plate calls for very high velocities near the edges, such as would lead to cavitation there. Thus the flow must break away, giving rise to surfaces of discontinuity which spring from the edges and separate flow from the front of the plate from fluid in the wake. This conception led Helmholtz and Kirchhoff to a theory of drag in inviscid flow, which, however, we shall not attempt to follow. We note that vortex sheets must be expected to replace the surfaces of discontinuity as viscosity makes its presence felt.

The phenomenon is not, of course, confined to the normal plate, but occurs whenever flow is asked to turn round a sharp edge. For this reason alone the streamlines of Figs. 81 and 97 could not persist.

(2) In potential flow completely surrounding a body, an element of fluid passing close to the front stagnation point arrives near to the back stagnation point with unimpaired energy. If the contour of the body is convex to the fluid, the element is accelerated during the first part of its transit by decreasing pressure, and gathers additional kinetic energy, which is converted without loss into pressure energy again during the second part of its transit, when it is moving against a rising pressure. In a real case, the element enters and proceeds within the boundary layer, and the viscous tractions prevent its motion from obeying Bernoulli's equation. Kinetic energy gathered in the first part of its passage soon flags, and the rising pressure of the second part eventually turns the element back.

Prandtl, in an analogy, has likened the circumstances to those of a ball rolling in a smooth guide of vertical wave shape, successive crests being horizontally level. With no frictional resistance of any kind, the ball, starting from rest at one wave crest, would accumulate sufficient kinetic energy in the trough just to reach the next crest. But the slightest dissipation of mechanical energy would result in the ball turning back.

Reverting to the fluid motion, a return flow near the rear part of the surface of a body wedges the boundary layer away. The position round the contour where this occurs is called the *point of break-away*. It is always found near the shoulder of a circular cylinder, except perhaps at very high Reynolds numbers, when it may move back appreciably. On the other hand, in the case of a thick strut it may be situated at only a comparatively short distance in front of the trailing edge at ordinarily high Reynolds numbers. The segregated part of the boundary layer, a film of intense vorticity,

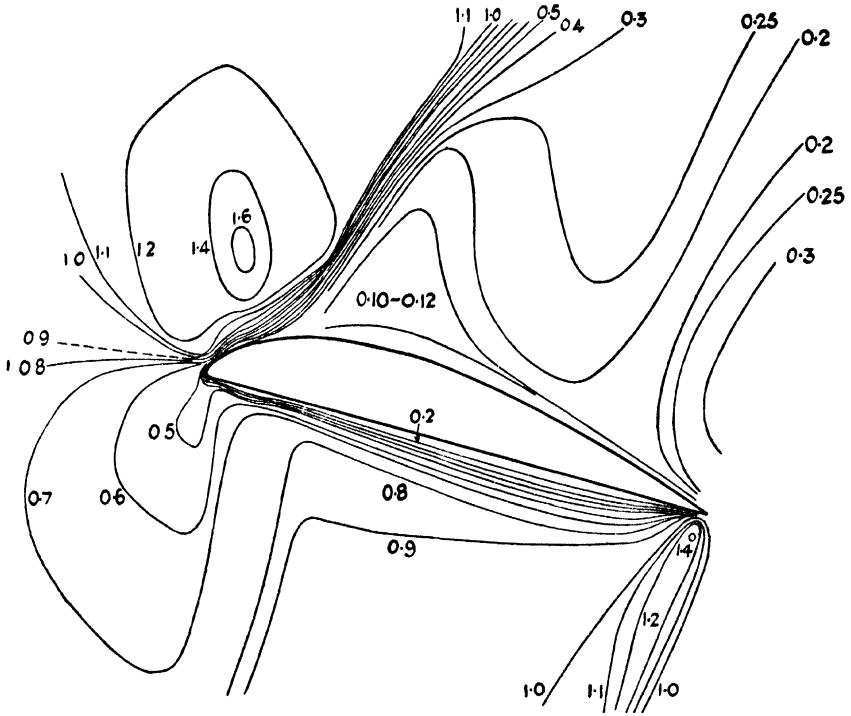

FIG. 113.—ISO-VELOCITY LINES FOR THE FLOW PAST AN AEROFOIL AT THE REYNOLDS NUMBER $2{\cdot}1 \times 10^4$ AND INCIDENCE 9·5°, SHOWING BREAK-AWAY AND THE VORTEX SHEET.

Linear scale normal to the aerofoil is magnified 8 times.

(Reproduced by permission of the Aeronautical Research Committee.)

becomes a vortex sheet in the fluid. Fig. 113 shows the break-away from the upper surface of an aerofoil * at a low Reynolds number, the vortex sheet being easily recognised by the packing together of the velocity contours. Such a flow would smooth out considerably

* Piercy and Richardson, A.R.C.R. & M., No. 1224 (1928).

with increase of Reynolds number. The flat lower surface inclined positively to the stream is free from the phenomenon, the pressure gradient not reversing here, so that the element, although moving unequally and doing work in the boundary layer, is never actually arrested.

(3) Consider a wing that has a lift. Lift can only arise, as described in Chapter II, from (upon the whole) a greater reduction of pressure on the upper surface than on the lower surface. Viewed in plan the streamlines will be inclined inwardly to a greater extent above the aerofoil than below it. Discontinuity in respect of direction of flow occurs in a sheet stretching downstream from the trailing edge, dividing the upper and lower parts of the flow where they merge behind the wing. Viscosity ensures that this surface becomes a vortex sheet. The vorticity is zero behind the centre of span, increasing in strength, but to opposite hand, towards the edges of the sheet on either side.

A characteristic of all vortex sheets is their essential instability. By this is meant that the effects of even an infinitely small disturbance instead of being damped out in course of time tend, on the contrary, to develop. In practice, therefore, only a short length of newly manufactured vortex sheet can ever be found except in peculiar circumstances. The effect of development of disturbance is to make the initially thin even spread of vorticity form marked accumulations; in other words, the sheet tends to roll up in some way. As the production of the vortex sheet goes on, so the gathering of vorticity into hoards continues. This crowding together of vortex lines in patches describes in a qualitative way the formation of discrete vortices. Their eventual disposition varies greatly, but for given cases of motion it is usually, although not always, the same. The following articles examine in some detail two arrangements which are common and important.

160. Kármán Trail

The most familiar arrangement of vortices is the procession usually known as the *vortex street*. Consisting (Fig. 114) of a moving avenue of evenly spaced staggered vortices, the two rows being of equal strength but to opposite hand, it characterises the wakes of all long cylinders of bluff section, and occasionally, at low Reynolds numbers, those of streamline cylinders. At first sight it would seem plausible to expect the vortices to be disposed opposite to one another, but such an arrangement is unstable. Kármán * showed

* *Gött. Nachrichten*, 1911. Cf. also Kármán and Rubach, *Phys. Zeits.*, 1912.

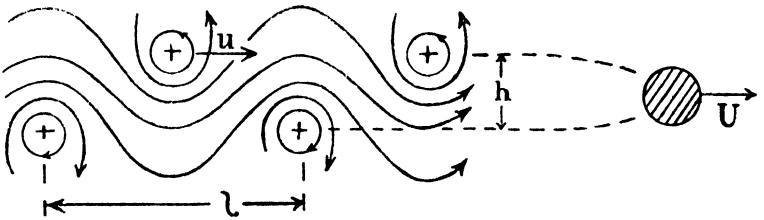

FIG. 114.—PATH-LINES OF THE VORTEX STREET BEHIND A CIRCULAR CYLINDER.

this theoretically, successfully calculating the layout of the procession necessary for stability, and also other matters to which reference will be made. Therefore, the motion is alternatively called the *Kármán trail.*

His results state first that if h is the distance between the rows and l that between successive vortices of the same row—

$$h/l = 0{\cdot}281. \quad . \quad . \quad . \quad . \quad (200)$$

Imagining the body to move at velocity U through fluid at rest at a distance, the eddy system left behind is not stationary, for each vortex has a forward velocity induced in it by all the vortices in the other row. This comparatively small velocity u is the same for all and, if K is the numerical strength of each vortex, is given by—

$$u = \frac{K}{l \,.\, 2\sqrt{2}}. \quad . \quad . \quad . \quad . \quad (201)$$

The frequency $\sim$ of generation of each pair of vortices, one vortex in each row, is clearly—

$$\sim = \frac{U - u}{l}. \quad . \quad . \quad . \quad . \quad (202)$$

The Kármán trail may be regarded as the central region of a large number of very elongated loops, all closed in a zig-zag fashion across the avenue behind the extremities of the cylinder causing them. One long vortex length matures during the short time $1/\sim$ near to the surface of the body—behind the shoulder of a circular cylinder, behind one of the sharp edges of a normal plate, or a little upstream of the tail of a cylinder of streamline section—while a fully-grown long vortex is detaching itself from the other side of the cylinder and beginning to be left behind. If a circuit be drawn round the median section of the cylinder in such a way as to include the 'bound' vortex while excluding the free vortex, conceived as having just been left in the wake, we find a circulation round the circuit. Therefore, a

transverse force on the cylinder is expected from Article 109. This will change in sign periodically, since the next vortex to mature will be situated on the opposite side of the cylinder. The periodic force exists in experiment and, in the case of fine wires, leads to singing, observation of the tone of which provides one method of finding the frequency of the eddies.

It will be noted that the above equations do not provide a solution of the problem for any particular Reynolds number. Moreover, the Reynolds number R as well as the shape of the body affect the trail, for, if b is the maximum width of section, we easily find, by the method of Article 47, that—

$$\sim = \frac{U}{b} f(R) \quad . \quad . \quad . \quad . \quad (203)$$

for a given shape. From this we can deduce the variation of $\sim$ for bodies of different sizes and the same shape at constant R, but $f(R)$ remains to be determined experimentally for each shape.

161. Application to the Circular Cylinder

Some observations with a long circular cylinder at a Reynolds number ($= Ub/\nu$, b denoting the diameter) of about 2000 gave approximately: $\sim b/U = 0{\cdot}2$ and $u/U = 0{\cdot}14$. From (202)—

$$\frac{\sim b}{U} = \frac{b}{l}\left(1 - \frac{u}{U}\right)$$

and, on substituting the above measurements—

$$l/b = 4{\cdot}3.$$

From (200)—

$$h = 0{\cdot}281\, l = 1{\cdot}21\, b$$

showing that the track of the established vortex street was, as is usual, 20 per cent. wider than the cylinder. Finally, from (201)—

$$\frac{K}{Ub} = 2\sqrt{2} \cdot \frac{u}{U} \cdot \frac{l}{b} = 1{\cdot}70$$

giving the strength of the vortices for a given speed and size of cylinder.

A first approximation to the drag is obtained as follows: the mean rate of change of impulse parallel to the direction of motion required to create the vortex loops from rest at the observed rate is, from (198)—

$$\sim \rho K h = 0{\cdot}2 \frac{U}{b} \times \rho \times 1{\cdot}7\, Ub \times 1{\cdot}21\, b$$

per unit length, giving a drag coefficient—

$$C_D = \frac{\sim Kh}{\frac{1}{2}U^2 b} \quad . \quad . \quad . \quad . \quad . \quad . \quad (204)$$

$$= \frac{\sim b}{\frac{1}{2}U} \cdot \frac{K}{Ub} \cdot \frac{h}{b} = 0{\cdot}4 \times 1{\cdot}7 \times 1{\cdot}21$$

$$= 0{\cdot}82.$$

Equation (204) may alternatively be arranged in the form—

$$C_D = \frac{2}{U^2 b}\left(\frac{U-u}{l} \times 2\sqrt{2}\,.\,ul \times 0{\cdot}281\,l\right)$$

$$= 1{\cdot}588\,\frac{l}{b}\left\{\frac{u}{U} - \left(\frac{u}{U}\right)^2\right\} \quad . \quad . \quad . \quad . \quad (205)$$

Rigorous examination by Kármán takes account of factors neglected above, and he shows that the cylinder experiences, still on account of the vortex street only, a 10 per cent. greater drag coefficient, given by—

$$C_D = 1{\cdot}588\,\frac{l}{b}\left\{\frac{u}{U} - 0{\cdot}4\left(\frac{u}{U}\right)^2\right\} \quad . \quad . \quad (206)$$

which yields the value 0·90 from the above measurements.

The drag coefficient obtained by direct weighing at this Reynolds number is 0·96, approximately. Thus vortex production accounts for nearly the whole of the drag in the case considered, and investigation at other Reynolds numbers suggests this to be generally true for the circular cylinder for $R > 100$.

Fig. 25 shows the variation of $\sim b/U$ with Ub/ν for this shape. At $R = 2 \times 10^5$, frequency begins to increase much more rapidly with U for constant diameter and fluid. The corresponding decrease in drag would be consistent with the vortex street becoming narrower by some 50 per cent.

162. Form Drag

That part of the total drag on a body which can be traced to the shedding of a vortex street is an important instance of *form drag*, which arises from a modification—sometimes a great change—of the pressure distribution pertaining to irrotational flow, illustrated in Figs. 72 and 92B. It is not always correct to ascribe the whole of the pressure drag integral (cf. Article 44), i.e. the whole difference between weighed drag and skin friction, to form drag; part may be due to a different cause, as will shortly appear, being associated with the production of lift.

The form drag of long flat plates normal to the stream is nearly 60 per cent. greater than for circular cylinders for R between 10^4 and 10^5. For the finer strut illustrated in Fig. 91, on the other hand, it is 95 per cent. less at $R = 10^5$. Thus form drag, when it is entirely parasitic in nature, can be reduced greatly by suitable streamlining. But when required for landing and slow diving it can be obtained in large measure by exposing a long normal plate (Article 76).

If the body is of short length across the stream—a body of revolution, for example, such as a sphere or an airship envelope—a vortex wake may be produced, but it has a different form. We might have expected the elongated loops of the vortex street to shrink to a succession of vortex rings, and these are observed at low velocities behind small spheres in air. But at a greater Aerodynamic scale the vortices consist of narrow loops in spiral arrangement, the whole system spinning about a central axis.

Again, breakaway may be prevented by turbulence and a wake of vorticity formed without discrete vortices.

It is convenient to leave open the question of vortex arrangement in the wake, and to define form drag as that part which is not due to skin friction or lift.

APPLICATION TO WINGS

163. Lanchester's Trailing Vortices

We turn now to the important case of Article 159 (3). The lifting wing of finite span is assumed to be of thin streamline section set at a small angle of incidence to the undisturbed wind. It is assumed to have no form drag, the wake arising from its boundary layer being neglected. The vortex sheet stretching downstream from its trailing edge, associated with the difference existing in lateral components of velocity of confluent streams from above and below, splits into two halves along the centre-line, where the vorticity vanishes, and each half rolls up about a roughly fore-and-aft axis to form downstream one member of a vortex pair. To a first approximation Fig. 106 gives the velocity distribution through a cross-section of the wake far behind a wing, where the distance between these long eddies is much less than the span of the wing. They often partly form close behind the wing-tips, and are then called *wing-tip vortices*, but the fully developed motion is a trailing vortex pair. Their presence was inferred on theoretical grounds by Lanchester in the course of his pioneering work on Aerodynamic lift.

Remembering that vortex lines cannot terminate or originate away

from the vicinity of the wing, we are faced with a question as to what may be the complete configuration of which the vortex pair forms part. Moreover, it is not clear without further examination why the wing should exert the lift on which the vortices depend. These interrelated questions are clarified by following the motion of an aerofoil from rest, again with the help of photographs of the formation of the vortex system.

164. Generation of Circulation and Lift

Let the aerofoil, of span $2s$, start from a position of rest A in stationary air and, after a brief period of rapid acceleration, be moved at constant small incidence in a straight line, assumed for convenience to be horizontal, at a velocity U of considerable magnitude. It is assumed that the time to a position H such that AH is large compared with $2s$ is sufficiently short for diffusive action of viscosity on the vortices formed to be neglected ; this is consistent with the long persistence of vortices observed in a fluid of such small viscosity as that of air.

During the period of acceleration from rest, the flow closely approximates at first to potential acyclic motion and is momentarily of the type illustrated in Fig. 97, the back stagnation line being situated on the upper surface of the aerofoil well in front of the trailing edge. The high velocity gradients caused near the trailing edge give rise to a vortex sheet which begins at once to roll up in the manner shown at (*a*) Fig. 115. A pack of vortex lines (*b*) parallel to the trailing edge begins to appear near A. This is known as the *starting vortex*. Photographs show that as soon as acceleration ends the vortex sheet ceases to be formed and the starting vortex becomes detached, as at (*c*) in the figure, and is left permanently behind at the position A.

The foregoing description applies to the vertical plane of sym-

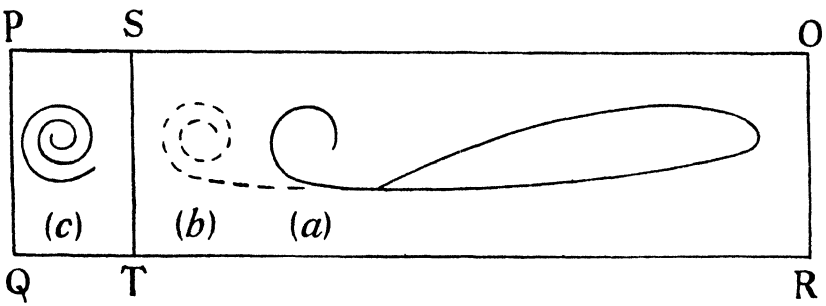

FIG. 115.—FORMATION OF THE STARTING VORTEX.

metry. Let the circuits shown in Fig. 115 be in this plane. The strength of the starting vortex is measured by the circulation $-K$ round any circuit SPQTS which encloses the vortex only. Since the trailing edge of the aerofoil was to the left of ST in the figure on starting from rest, ST has been cut by the aerofoil. But a circuit such as OSPQTRO may comprise the same fluid particles. The circulation round it was originally zero, and still remains so. Therefore, the circulation round the circuit OSTRO, or any other in the plane embracing the aerofoil but not the vortex, must be equal to K.

The vortex lines of the starting vortex cannot terminate in the fluid. We might perhaps conceive of their turning at each end and abutting on the aerofoil, although this would be difficult to imagine. The foregoing proves, however, that they must be re-entrant, their loops being closed by lengths which are 'bound' to the aerofoil surface, moving with it, in the manner shown diagrammatically in Fig. 116, all the vortex lines being required to induce a circulation equal to K round the median section of the aerofoil. It follows that the magnitude of the circulation round each member of the vortex pair is also equal to K.

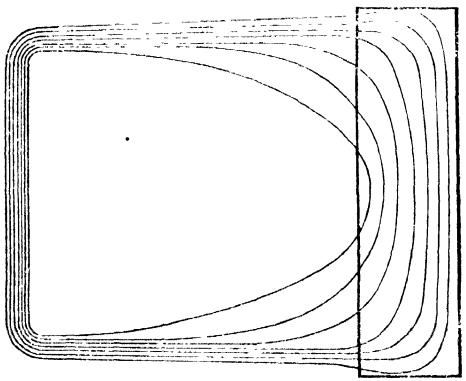

FIG. 116.—FORMATION OF THE TRAILING VORTEX PAIR OF A LIFTING WING.

Circulation applied to a two-dimensional aerofoil was shown in Article 135 to cause the back stagnation line to be displaced towards the trailing edge. The hypothesis introduced by Joukowski (Article 134), that for a steady state the back stagnation line recedes exactly to the trailing edge, assumed sharp, now receives experimental support since the starting vortex ceases to form only when this coincidence is attained.

The aerofoil now having a circulation K midway along its span combined with a steady forward velocity U, it will have locally a lift equal to ρKU per unit of span. Elsewhere along the span there will be a lift of intensity decreasing outwards because vortex lines leave before the tips are reached, as indicated in Fig. 116. The tangential trailing vortex sheet of Article 159 (3) is now identified with the sheet of escaping vortex lines which continue to accumulate into further

lengths of trailing vortex as the aerofoil proceeds along its path. No further starting vortex is formed. A picture of the vortex system anywhere between A and H is merely an extension of Fig. 116 to include a period of uniform motion.

165. Consider a region far from the start of the flight that is crossed by the lifting aerofoil. When the latter has progressed a further distance, the residual flow in the region due to the passage of the aerofoil approximates to a length of vortex pair. Thus Fig. 117 shows, as an example, the path-lines determined * experimentally 13 chords behind the wing-tip of an aerofoil of aspect ratio 6 set at 8°. The vortex sheet was found in this case to be nearly rolled up. Again, the full line of Fig. 118 gives the mean variation, experimentally determined, of the vorticity through a wing-tip vortex well behind an aerofoil. The dotted line illustrates the assumption made as an approximation, viz. that vorticity is uniform through the vortex and zero in the surrounding flow.

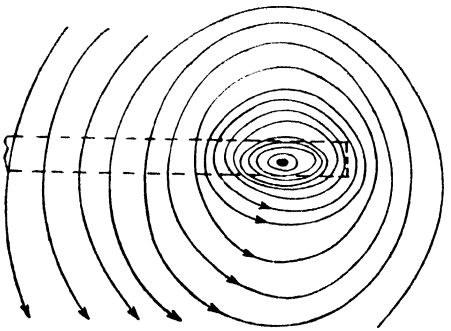

FIG. 117.—EXPERIMENTAL STREAMLINES 13 CHORDS BEHIND AN AEROFOIL (THE AEROFOIL IS SHOWN DOTTED AND ITS SPAN = 3 × WIDTH OF FIGURE).

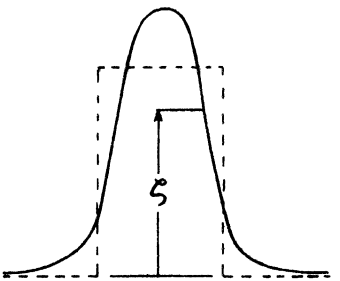

FIG. 118.—EXPERIMENTAL DISTRIBUTION OF VORTICITY THROUGH A TRAILING VORTEX.

It is easily verified that, the flight path being horizontal, the vortices are inclined downward by a small angle, of the order of 1° in a practical case, owing to their generation by successive elements. We ignore this angle, and, assuming a horizontal vortex pair, enquire what lift and drag this simplified system entails at the aerofoil. Distance from the starting-point of the flight and from the aerofoil permits the flow to be regarded as two-dimensional. Let l be the distance apart of the vortices and $2a$ the diameter of each. In calculating lift we neglect the substance of the vortices, but cannot do so in calculating drag.

From Article 157 the impulse is ρKl per unit length or, since a

* Fage and Simmons, *Phil. Trans. Roy. Soc.*, A, v. 225, p. 303, 1925.

length U is generated per second, the rate of change of impulse is ρKlU, and is directed downward. There is thus an upward reaction L on the aerofoil, balancing the external force, given by—

$$L = \rho KlU. \quad . \quad . \quad . \quad . \quad (207)$$

It is important to note that K is here the strength of the vortices.

Associated with the impulse, kinetic energy E per unit length has been generated in the region. From Article 119 by way of the artifice of Article 157, the impulse being constant between the vortices, we find—

$$E = \tfrac{1}{2}\rho K \int w dy \; . \quad . \quad . \quad . \quad (208)$$

where w is the velocity of the points of application of the distributed impulse and the integration is to extend between the vortices. Hence—

$$E = \frac{\rho K^2}{4\pi} \int_{-\frac{1}{2}l+a}^{\frac{1}{2}l-a} \left(\frac{1}{\frac{1}{2}l + y} + \frac{1}{\frac{1}{2}l - y} \right) dy$$

$$= \frac{\rho K^2}{2\pi} \log \left(\frac{l}{a} - 1 \right). \quad . \quad . \quad . \quad . \quad (209)$$

The kinetic energy E_c of the substance of the two vortex cores is not negligible, and is derived * from the original irrotational motion generated. Calculating it on the assumption of uniform angular velocity—

$$E_c = 2 \; . \; \tfrac{1}{2}\rho \; . \; 2\pi \int_0^a r \; . \; \omega^2 r^2 \, dr = \tfrac{1}{2}\pi\rho a^4 \omega^2.$$

For continuity of velocity at the periphery of the cores $\omega = K/2\pi a^2$ giving—

$$E_c = \frac{\rho K^2}{8\pi} \quad . \quad . \quad . \quad . \quad . \quad . \quad (210)$$

a result which is independent of a.

Let D_i denote the contribution to aerofoil drag associated with the continuous production of the kinetic energy of the complete residual vortex system. D_i is called the *induced drag*. We have, since work is done at the rate D_iU and kinetic energy appears at the rate $(E + E_c)U$—

$$D_i = E + E_c = \frac{\rho K^2}{2\pi} \left\{ \log \left(\frac{l}{a} - 1 \right) + \tfrac{1}{4} \right\} \; . \quad . \quad (211)$$

Induced drag is due essentially to the three-dimensional character of the flow, vanishing for aerofoils of infinite span. It appears on

* The vortex sheet behind the aerofoil cannot contain the kinetic energy in the cores of the developed vortex pair.

the wing as a modification of the pressure distribution appropriate to two-dimensional flow past the wing sections at their effective incidences. Hence a simpler but superficial definition is : induced drag is that part of the pressure drag of a wing that is caused by its lift. Another definition will become apparent in the next chapter.

To carry the foregoing expressions further and calculate the coefficient of induced drag for the wing, we should require to know its dimensions besides K, l, a, and U. The distribution of impulse along the wing will in general be quite different from that which would generate the irrotational part of the above residual motion from rest, the vortices being spread, wholly or in part, as a sheet at the wing. This we leave to the special investigations of the next chapter.

A first approximation to the size of the vortices may be noted, however. It will be shown that most practical wings have induced drags a little greater than $\pi\rho K^2/8$. Equating this minimum to (211) gives $l/a = 10{\cdot}2$. In the course of a rigorous investigation Prandtl * obtains the value 9·2, no second term appearing in the log of (211). A later, more physical enquiry by Kaden † suggests a mean value of 8·8.‡ Prandtl's result makes $2a = 0{\cdot}17 \times$ the span of the minimum drag wing. These calculations give a fair idea of the more complicated vortices found in experiment (cf. Fig. 118), and it will be observed that their size is considerable.

166. Uniform Lift

Although vortex lines leave the wing along its span, forming a trailing vortex sheet and decreasing the circulation round outboard sections, strong vortices often exist, on the other hand, close behind the wing-tips. These must not be confused with the residual vortex pair, being smaller and situated farther from the centre of span. In such cases, which are usual rather than exceptional, part of the lift is uniformly distributed along the span, an appropriate number of vortex lines remaining bound until the tips are nearly reached, when they turn a corner and crowd together suddenly to form, with a similar feature at the other wing-tip, a developed vortex pair. A weakened vortex sheet remains between to roll up farther downstream. Fig. 119 (*a*) illustrates the system diagrammatically.

We now treat of this uniform part of the lift as if it alone existed, ignoring the remaining part and its associated vortex sheet (Fig. 119 (*b*)). The circulation K' round the wing is then constant along the span and equal to K, the strength of each wing-tip vortex. Let

* *Tragflügeltheorie.* † *Ing.-Arch.*, II, 1931.
‡ *Aerodynamic Theory*, II, p. 329, 1935.

$2s$ be the span, c the chord, and A the aspect ratio $= 2s/c$, and as before let l be the distance apart of the vortices, each of diameter $2a$. According to experiment l is slightly less than $2s$, but for simplicity we ignore the difference, and also, in calculating lift, the vortex diameters. Then we have for the lift on the wing—

$$L = K'\rho U \,.\, 2s \quad . \quad . \quad . \quad (212)$$

and for the rate of change of impulse required to generate the vortex pair continuously :

$$dI/dt = K\rho Ul,$$

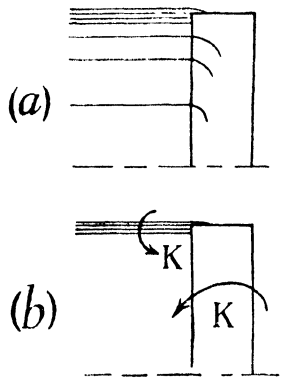

FIG. 119.

expressing equality if $K' = K$ and $2s = l$. We assume that the pair of vortices remains at $2s$ apart. Omitting the accent in (212) as no longer necessary—

$$C_L \equiv \frac{L}{\frac{1}{2}\rho U^2 \,.\, 2sc} = \frac{2K}{Uc} \quad . \quad . \quad . \quad (213)$$

and then from (211)—

$$C_{D_i} \equiv \frac{D_i}{\frac{1}{2}\rho U^2 \,.\, 2sc} = \frac{1}{4\pi A} C_L^2 \left\{ \log \left(\frac{l}{a} - 1 \right) + \tfrac{1}{4} \right\}. \quad . \quad (214)$$

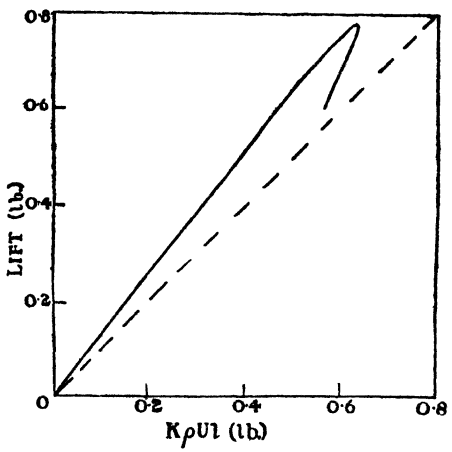

FIG. 120.—EXPERIMENTAL RELATIONSHIP BETWEEN THE LIFT OF A R.A.F. 15 AEROFOIL AND THE IMPULSE OF THE VORTEX PAIR EXISTING 2 CHORDS BEHIND IT.

Fig. 120 gives the results of experiment * with a thin aerofoil of the section known as R.A.F. 15 and $A = 6$ at a Reynolds number of $6{\cdot}3 \times 10^4$. The measurements were made at a distance of $2c$ behind the aerofoil, but little difference resulted from considerably reducing or increasing this distance. At flying incidences approximately 75 per cent. of the lift was uniform, while this percentage increased at larger incidence, past the critical. A thick aerofoil of deep camber and the same

* Piercy, *Jour. Roy. Aero. Soc.*, October 1923.

aspect ratio showed 50–60 per cent. of the lift to be of this kind at 8° incidence. A slightly weighted mean of c/a was 13, or we may take $2s/a = l/a = 78$. If C_L, C_{D_i} refer to the uniform part of the lift, we find from (214)—

$$C_{D_i} = 0{\cdot}061\, C_L^2 \quad . \quad . \quad . \quad . \quad (215)$$

For future reference it is convenient to express this result in the form—

$$C_{D_i} = \frac{1}{\pi A}\, C_L^2\, (1 + 0{\cdot}15). \quad . \quad . \quad . \quad (216)$$

The induced drag for uniform lift is distributed between the vortices in the same way as the induced velocity of the vortex pair (Fig. 121), and since $2s = l$ and the vortex pair forms immediately, we infer the same distribution along the aerofoil. It is a minimum at the centre of span, where the pressure distribution will most nearly approach that for two-dimensional flow, and increases rapidly towards the tips. Lack of knowledge of the curl and spread of the vortices at the tips prevents completion of the figure, but small areas of highly reduced pressure are commonly found here on the back part of the upper surface of an aerofoil. A great advantage of aspect ratio in reducing induced drag becomes evident when it is reflected that, for greater span, lift increases without increase of K.

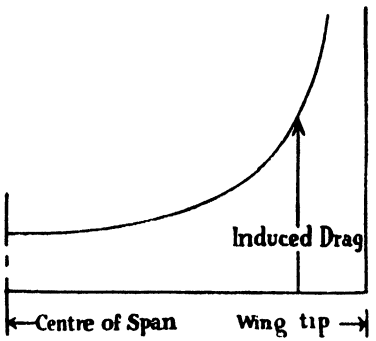

FIG. 121.—DISTRIBUTION OF INDUCED DRAG FOR UNIFORM LIFT.

Aerodynamic calculations involving a knowledge of the degree to which the vortex sheet has rolled up, e.g. on tail-setting angle, are complicated, and the assumption is sometimes adopted that the *whole* of the lift is uniform. Alternatively we may assume that the residual vortex pair is developed quickly, as tends to occur at large incidences.

167. Variation of Circulation in Free Flight

The argument of Article 164 is readily elaborated to include variation in the velocity of the aerofoil. If, after a period of steady motion, the velocity is increased, the original circulation becomes insufficient to keep the back stagnation line on the trailing edge and a new starting vortex is thrown off during the time of acceleration.

This joins together additional vortex lines packed into the trailing vortices, which are strengthened thereby, and increases the circulation round the aerofoil. A decrease of velocity produces the opposite result, a retardation vortex leaving the aerofoil to close vortex lines no longer required in the weakened trailing vortices appropriate to the reduced circulation. Such a sequence of events requires suitable variation of the external force which constrains the aerofoil, whose incidence is assumed constant, to move in a straight path in spite of variation of lift.

The same principles apply, of course, to the wings of an aeroplane in horizontal flight, but the argument needs modification to take account of the fact that the downward component of the constraining force applied to the wings is equal to the sum of the total flying weight and any downward air loads on other parts of the craft, and is approximately constant ($= W$, say).

When the velocity of an aeroplane is increased from U to U', we must have (neglecting variation of l) in order that flight may remain horizontal—

$$\rho K'U'l = \rho KUl = W$$

or—

$$K'/K = U/U' \quad . \quad . \quad . \quad \text{(i)}$$

i.e. variation of speed requires inversely proportional variation of circulation. This is secured (considering increase of speed) by such a decrease of angle of incidence as will, during the change, tend to move the back stagnation line rearwards to a greater extent than the acceleration tends to move it forwards, so that the vortex thrown off from the trailing edge is opposite in hand to a starting vortex.

In terms of the lift coefficient, we have, for steady horizontal flight—

$$C_L'\tfrac{1}{2}\rho U'^2S = C_L\tfrac{1}{2}\rho U^2S = W,$$

where S is the projected area of the wings, or, since this is constant—

$$C_L'/C_L = (U/U')^2. \quad . \quad . \quad \text{(ii)}$$

Taking for simplicity the case of uniform distribution of lift along the span and constant chord, we have, from (213)—

$$\frac{K'}{K} = \frac{C_L'U'}{C_LU},$$

agreeing with (ii) on substitution from (i).

When flight has lasted for an appreciable time, the vorticity of the original starting vortex will have diffused, through the action of viscosity, and as time proceeds, length after length of the trailing vortex pair far behind the aeroplane will similarly diffuse.

168. Example from Experiment

The following analysis of some experiments * with an aerofoil in a wind tunnel illustrates (1) approximate allowance for wall constraint (technical conversion formulæ are developed in the next chapter), (2) application of the simplified vortex configuration, (3) the Rankine vortex assumption.

The deeply cambered rectangular aerofoil, 2 ft. span and 0·33 ft. chord, was suspended symmetrically at 8° incidence in an enclosed-type tunnel 4 ft. square in section, the undisturbed air speed being 31·3 ft. per sec. Downwash angle was explored by means of the meter shown in Fig. 122, consisting of two fine tubes inclined at 45°

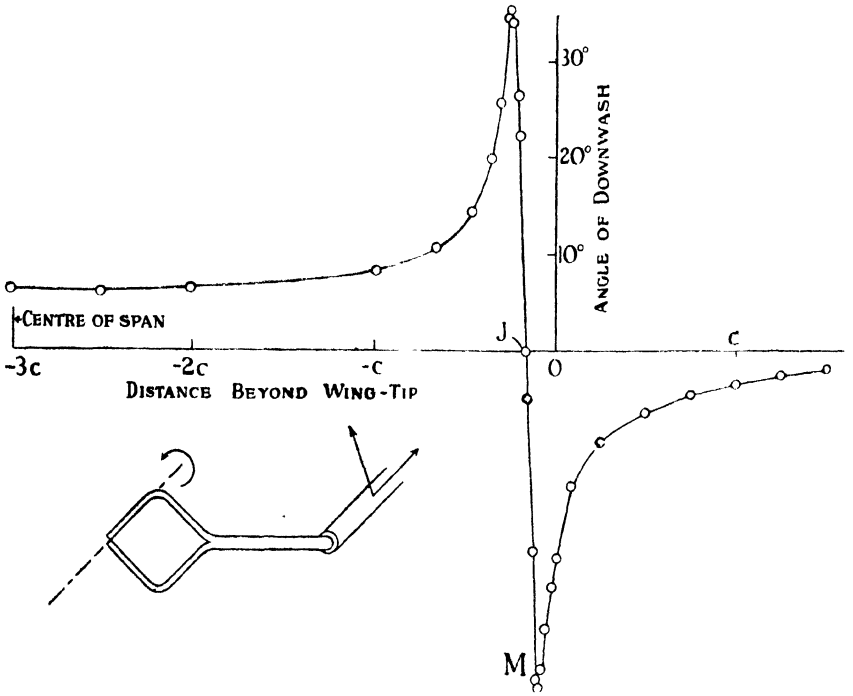

FIG. 122.—MAXIMUM DOWNWASH ANGLES OBSERVED 2 CHORDS BEHIND AN AEROFOIL BY MEANS OF THE METER SHOWN INSET.

to the stream, with their open mouths touching. This was mounted on a cranked arm turned by a micrometer wheel outside the tunnel about a centre-line passing through the point of contact. The instrument could be traversed parallel to the trailing edge of the aerofoil. The aerofoil could be traversed parallel to its lift. Thus,

* Piercy, *loc. cit.*, p. 227.

after calibration of the tunnel with the model removed, downwash angle could be measured by orienting the meter to give equal pressures in the two tubes at any point at a set distance behind the aerofoil. This distance was 0·9 ft. behind the centre of pressure of the lift, through which the bound vortex lines are assumed, in the subsequent analysis, to be concentrated.

Observed downwash angles are given in Fig. 122 for a line nearly level with the trailing edge, but adjusted to give maximum slope to JM. A vortex of 0·05 ft. diameter with centre at J and of approximately uniform angular velocity is clearly indicated. The distance l between this and the corresponding vortex behind the other wing-tip was found to be 1·89 ft.

Constraint by the floor and roof on the downwash from the bound vortex AB (Fig. 123) will be calculated from Article 155. Actually,

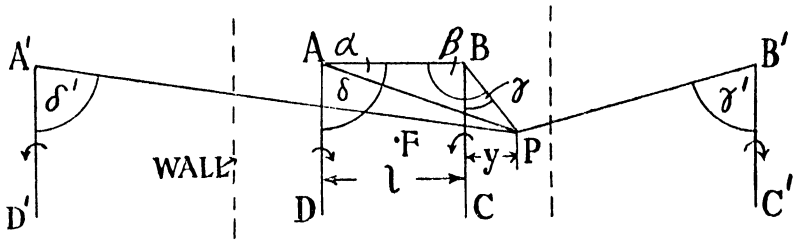

FIG. 123.

the constraint will be less owing to the short length of the aerofoil, but this correction is only 10 per cent. of that for the side walls and only 1 per cent. of the mean downwash, so that precision is unnecessary. Thus, from the figure, if w_1 is the downwash velocity from the aerofoil at P distant y from BC :

$$w_1 = \frac{K}{4\pi x}(\cos\alpha + \cos\beta)\frac{\pi x/4}{\sinh(\pi x/4)},$$

x being distance behind AB. The last factor = 0·92.

Allowance for constraint on the wing-tip vortices will be made by substituting a tunnel wall of circular section, a radius of 2·1 ft. being chosen for reasonable coincidence with the square wall

The two imaged vortices A'D', B'C' are distant $(2{\cdot}1)^2/\frac{1}{2}(1{\cdot}89) =$ 4·67 ft. from the centre of the tunnel, and lie in the plane containing the real vortices. Thus, on account of the trailing vortex system, there is at P :

(*a*) An upwash velocity $-w_2$ due to BC given by—

$$-w_2 = \frac{K}{4\pi y}(\cos\gamma + 1)$$

(*b*) A downwash velocity w_3 due to AD given by—

$$w_3 = \frac{K}{4\pi(l+y)}(\cos\delta + 1)$$

(*c*) An upwash velocity $-w_4$ due to the image B′C′ given by

$$-w_4 = \frac{K}{4\pi(4{\cdot}67 - \frac{1}{2}l - y)}(\cos\gamma' + 1)$$

(*d*) An upwash velocity $-w_5$ due to A′D′ given by—

$$-w_5 = \frac{K}{4\pi(4{\cdot}67 + \frac{1}{2}l + y)}(\cos\delta' + 1).$$

The total downwash velocity is given by—

$$w = w_1 - w_2 + w_3 - w_4 - w_5.$$

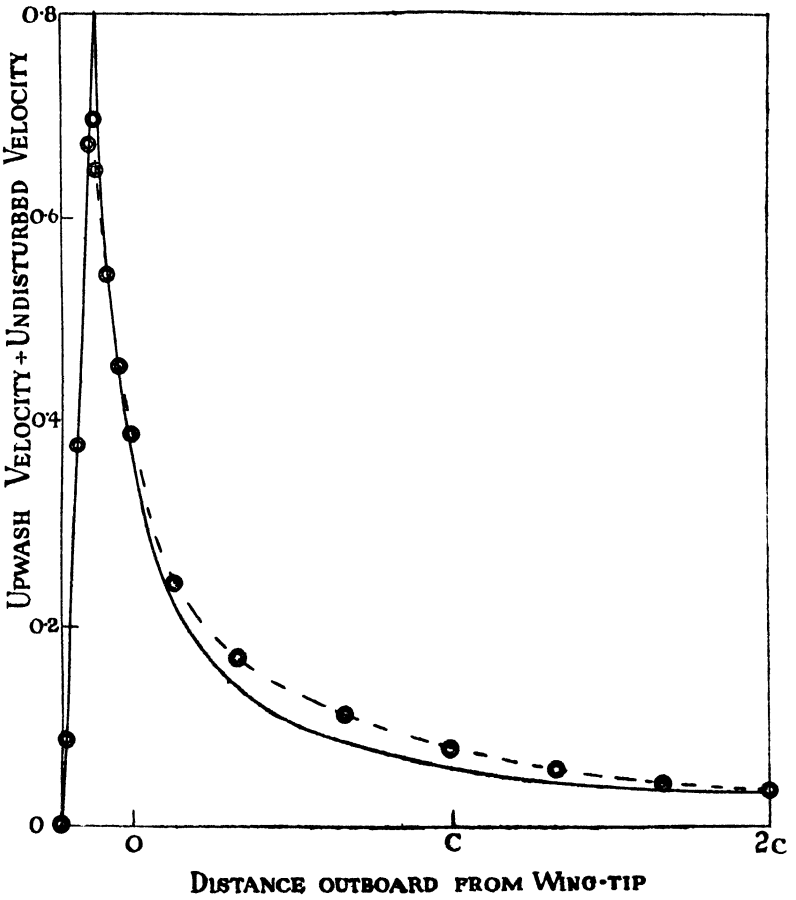

FIG. 124.

Evaluating w for a series of values of y gives the curve of Fig. 124, for which the value 4·0 has been chosen for K. The points marked about the theoretical curve are experimental, and are derived from the readings of Fig. 122 by assuming the horizontal component of velocity to be unchanged beyond the wing-tip. The ' fit ' of the curve to the observations is better near to and far from the vortex than it is at intermediate positions, but upon the whole it is fair, and $K = 4{\cdot}0$ is justified.

To obtain an independent check on this value, measurements were made of the pressure within the vortex at a number of radii. These are shown as points in Fig. 125, together with the theoretical curve

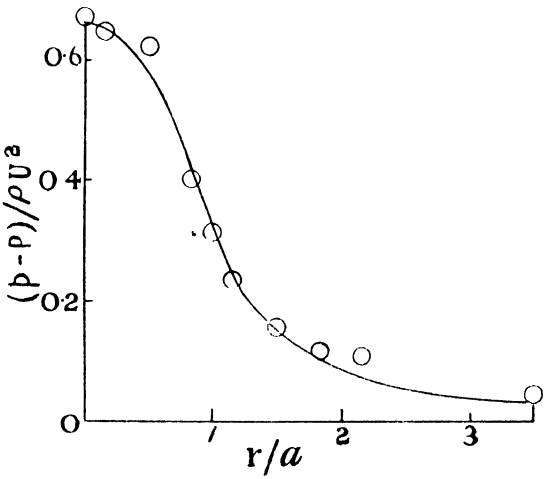

FIG. 125.—VARIATION OF STATIC PRESSURE THROUGH A TRAILING VORTEX. The curve is theoretical, the circles are observations.

obtained from (179) and (180) with $K = 4$ and $a = 0{\cdot}025$ ft. as measured. It will be seen that the check was successful.

Let us now calculate the downwash velocity w' at the point F midway between the vortices and 0·9 ft. behind the centre of pressure of the aerofoil. Denoting AF = BF by m, the expression is—

$$w' = \frac{K}{4\pi}\left\{\frac{2(\frac{1}{2}l/m)0{\cdot}92}{0{\cdot}9} + \frac{2(1+0{\cdot}9/m)}{\frac{1}{2}l} - \frac{2\{1+0{\cdot}9/\sqrt{(0{\cdot}9)^2+(4{\cdot}67)^2}\}}{4{\cdot}67}\right\},$$

where the first term gives the contribution from the circulation round the aerofoil, assumed constant and $= K$; the second that from the trailing vortices ; and the third that from their images. In round numbers this reduces to—

$$w' = \frac{K}{4\pi}(1{\cdot}48 + 3{\cdot}58 - 0{\cdot}51) = \frac{K}{4\pi} \times 4{\cdot}55$$

$$= 1{\cdot}45 \text{ ft. per sec.}$$

If the horizontal component at F were 31·3 ft. per sec., the angle of downwash there would be 2·7°. A considerably greater value than this is expected owing to the reduction of the horizontal component in the wake, but not nearly so great a value as measured, viz. 6·1°. Hence, clearly, all factors have not been taken into account. This was immediately evident on weighing the lift of the aerofoil, which came to $1{\cdot}67K\rho Ul$. The conclusion is that so close behind this aerofoil 40 per cent. of the vortex lines escaping into the wake had not yet rolled up into the vortex pair.

Chapter VIII

WING THEORY

169. The present chapter studies in more detail wings of the strictly limited span practicable for sustaining heavy flying loads. The boundary layer is supposed everywhere to be very thin, and skin friction and the viscous wake are neglected. It follows that form drag is assumed to be zero and the incidence sufficiently removed from the critical angle.

Introductory articles on the theory of the lifting monoplane have described the residual flow caused in a region of the atmosphere far behind the wing as consisting of a vortex pair, and some detailed investigation has been given to a simplified vortex configuration in which vortices are conceived to spring from the wing-tips, necessitating uniform lift along the span. We now proceed to examine the flow close to the wing with a view to investigating wing forms.

Fluid velocities are compounded of the translational velocity and a component due to the complete vortex loop, part of which is bound to the aerofoil and produces circulation round its sections. Exact calculation of the second component would be complicated, and would involve more precise knowledge of the three-dimensional distribution of the vorticity than is available. An approximation, appropriate to calculations in the vicinity of the wing, is at once suggested, however, by theory and experiment. Chapter VII clearly indicates that at a point close to a system of vorticity the velocity will be affected much less by distant parts of the system than by near parts. On the experimental side, the vortex sheet spreading behind the aerofoil has been found in some cases to roll up only slowly, apart from discrete vortices immediately formed. Consequently, a reasonable approximation for present purposes is to regard the free vortex lines as trailing behind the aerofoil perpendicular to its span. This parallel formation cannot extend indefinitely, as we have seen, but the form of (182) permits us nevertheless to regard without important error the straight vortex lines as being of semi-infinite length.

The monoplane wing is completely represented in the present investigations by its span, aspect ratio and the span-wise distribu-

tion of circulation round its sections, i.e. the grading of lift intensity. Both these quantities are at the choice of the designer within certain limits. Good approximations to a desired lift distribution can be obtained with different shapes of wing to meet other requirements.

The scope of the enquiries is expressed in the following set of general equations, whose construction will now give no difficulty, but whose solution in a given case may be attended with analytical complication. The peculiar nature of the results will fortunately enable us to avoid much of the latter when small errors can be tolerated.

170. General Equations of Monoplane Theory

Take the origin at the centre of span (Fig. 126), and denote by K the circulation round the wing at a distance y towards the starboard

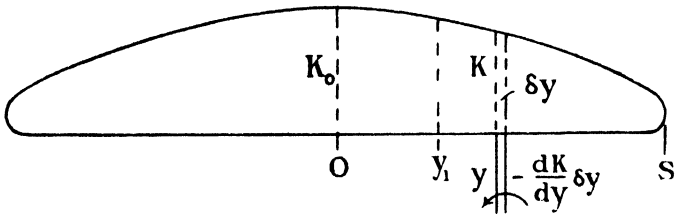

FIG. 126.

wing-tip. The circulation at $y + \delta y$ is $K + \dfrac{dK}{dy}\delta y$. It is assumed that the circulation diminishes outwards from a maximum K_0 at the centre of span. Hence, over the element of span δy, vortex lines to the strength $-\dfrac{dK}{dy}\delta y$ leave the aerofoil to form part of the vortex sheet, and the direction of rotation is such as to cause a downwash nearer the centre of span. Denoting the velocity of this downwash at y_1 along the aerofoil by δw_1, we have from (184) and by Article 169—

$$\delta w_1 = -\frac{1}{4\pi(y-y_1)}\frac{dK}{dy}\delta y. \qquad . \quad . \quad \text{(i)}$$

Trailing vortex lines arise in this way all along the span, and produce a component of the downwash velocity, which is in general variable along the span. Its value at any point is due to all the vortex lines not passing through that point. To calculate the value w_1 at y_1 we have, from (i)—

$$w_1 = -\frac{1}{4\pi}\int_{-s}^{s}\frac{dK/dy}{y-y_1}dy, \qquad . \quad . \quad (217)$$

$2s$ being the span. The integrand approaches ∞ as y approaches y_1, so that integration must be stopped short of y_1 and the limit investigated. This kind of difficulty occurs frequently in our subject; it can usually be met by considering elements close to y_1 on either side in pairs. (See also Article 140D.)

Consider the circumstances of the element at y. Its reaction amounts to $\rho Kq \,.\, \delta y$, q being the resultant of w and the translational velocity U. This reaction is perpendicular to the local relative motion, and is therefore inclined backwards from the perpendicular to U and to the span, i.e. from the direction of lift. The element δL of lift is—

$$\delta L = \rho Kq \,.\, \delta y \,.\, U/q = \rho KU \,.\, \delta y. \quad . \quad \text{(ii)}$$

There is also an element δD_i of induced drag, i.e. a component parallel to U, given by—

$$\delta D_i = \rho Kw \,.\, \delta y = \frac{w}{U}\delta L \quad . \quad . \quad . \quad \text{(iii)}$$

For the whole aerofoil—

$$L = \rho U \int_{-s}^{s} K dy \quad . \quad . \quad . \quad . \quad . \quad (218)$$

$$D_i = \rho \int_{-s}^{s} Kw dy \quad . \quad . \quad . \quad . \quad . \quad (219)$$

Again referring to the element at y, another effect of w is to reduce its incidence from α_0, the incidence it would have consistent with its lift if it formed part of a wing of infinite span so that w vanished, by the angle w/U, assuming this to be small. Hence, to realise the lift (ii), its incidence, measured from the angle for no lift, must, compared with two-dimensional conditions, be increased to α according to—

$$\alpha = \alpha_0 + w/U \quad . \quad . \quad . \quad . \quad (220)$$

171. The above alternative theory of induced drag must give the same results as that described in the last chapter. This is readily verified in the case of uniform lift, when the whole of the trailing vorticity is gathered together at the wing-tips as a vortex pair, provided we exclude a region at each tip where w cannot be determined and K is indefinite.

Let l be the distance apart of these vortices and $2a$ the diameter of each. At any position y along the span of the aerofoil—

$$w = \frac{K}{4\pi}\left(\frac{1}{\frac{1}{2}l + y} + \frac{1}{\frac{1}{2}l - y}\right),$$

provided $y < \frac{1}{2}l - a$, say, where a is the extent inwards from each vortex centre of each of the excluded regions. Hence, from (219)—

$$D_i = \rho\frac{K^2}{4\pi}\int_{-\frac{1}{2}l+a}^{\frac{1}{2}l-a}\left(\frac{1}{\frac{1}{2}l+y}+\frac{1}{\frac{1}{2}l-y}\right)dy$$
$$= \rho\frac{K^2}{2\pi}\log\left(\frac{l}{a}-1\right)$$

agreeing with the induced drag evaluated over a corresponding length of the aerofoil by the method of Article 165.

172. The ' Second Problem ' of Aerofoil Theory

We now approach the question of the distribution of a given total lift over a given span for minimum induced drag. This problem is evidently of the greatest engineering interest, provided that the distribution found can be realised in a wing which is structurally economical in weight. Investigation is possible in several ways. To introduce the method developed below, the problem may be restated as follows.

A wing traversing a region of the atmosphere at constant speed U and small positive incidence—say horizontally—exerts on the air a rate of change of impulse in a downward direction. Let I be the impulse imparted per unit length of the flight path. We have—

$$L = IU. \quad . \quad . \quad . \quad . \quad (221)$$

In the process, kinetic energy is communicated to the air at the rate E per unit length of the path. The whole flow is regarded as irrotational, the substance of the vortices formed being neglected; work is done by the impulsive action at the rate EU and, as in Article 165, we find $D_i = E$. Total lift and span being fixed, what conditions will make E a minimum? What form of wing, if any, will realise these conditions?

173. Distribution of Given Impulse for Minimum Kinetic Energy

Consider first the sum of two impulses I_1, I_2, regarded as acting on fluid masses m_1, m_2, and changing their velocities from W_1, W_2 to w_1, w_2. By Article 119—

$$I_1 = m_1(w_1 - W_1),\ I_2 = m_2(w_2 - W_2).$$

It is assumed that the sum $I_1 + I_2 = \text{const.} = C$, say, or—

$$C = m_1w_1 + m_2w_2 - (m_1W_1 + m_2W_2).$$

The work done by the total impulse is given by the change E of kinetic energy, and we have—

$$2E = m_1w_1^2 + m_2w_2^2 - (m_1W_1^2 + m_2W_2^2).$$

Therefore—

$$\begin{aligned}(m_1 + m_2)\,(2E + m_1W_1^2 + m_2W_2^2) - (C + m_1W_1 + m_2W_2)^2 \\ = (m_1 + m_2)\,(m_1w_1^2 + m_2w_2^2) - (m_1w_1 + m_2w_2)^2 \\ = m_1m_2\,(w_1^2 + w_2^2 - 2w_1w_2) \\ = m_1m_2\,(w_1 - w_2)^2.\end{aligned}$$

The last expression, being necessarily positive or zero, has a minimum value when $w_1 = w_2$. Now all the terms on the left-hand side of the equation are known and prescribed except $2E$. Hence, E is a minimum when $w_1 = w_2$, i.e. when, whatever the initial velocities, the final velocities are equal.

The corresponding result for a number of impulses $I_1, I_2, I_3 \ldots$ is proved in exactly the same way. Let these act on masses $m_1, m_2, m_3 \ldots$, changing their velocities from $W_1, W_2, W_3 \ldots$, to $w_1, w_2, w_3 \ldots$, and let—

$$\begin{aligned}I_1 + I_2 + I_3 + \ldots &= m_1\,(w_1 - W_1) + m_2\,(w_2 - W_2) \\ &\quad + m_3\,(w_3 - W_3) + \ldots \\ &= C, \text{ a constant.}\end{aligned}$$

We have—

$$2E = m_1\,(w_1^2 - W_1^2) + m_2\,(w_2^2 - W_2^2) + m_3\,(w_3^2 - W_3^2) + \ldots$$

and, therefore, writing E_0 for the original kinetic energy and M_0 for the original momentum—

$$\begin{aligned}&(\Sigma m)\,(2E + 2E_0) - (C + M_0)^2 \\ &= (\Sigma m)\,(m_1w_1^2 + m_2w_2^2 + m_3w_3^2 + \ldots) \\ &\qquad - (m_1w_1 + m_2w_2 + m_3w_3 + \ldots)^2 \\ &= m_1\,(m_2 + m_3 + \ldots)\,w_1^2 + m_2\,(m_1 + m_3 + \ldots)\,w_2^2 \\ &\qquad + m_3\,(m_1 + m_2 + m_4 + \ldots)\,w_3^2 + \ldots \\ &\qquad - 2(m_1m_2w_1w_2 + m_1m_3w_1w_3 + \ldots) \\ &= m_1m_2\,(w_1 - w_2)^2 + m_1m_3\,(w_1 - w_3)^2 + \ldots\end{aligned}$$

The right-hand side being necessarily positive or zero, the left-hand side is a minimum when $w_1 = w_2 = w_3 = \ldots$ Therefore E is a minimum under this condition.

We conclude that a distributed impulse of given total magnitude does minimum work when the final velocity of its point of application is everywhere the same.

174. The foregoing condition for minimum work done is realised when the impulse is applied through a rigid plate accelerated normally to its plane.

Considering a region of initially stationary air which has been traversed by a wing, the kinetic energy in unit length parallel to the flight path will be a minimum for a given lift and span, if the flow

there is such that it might have been generated from rest by the acceleration in a normal direction of unit length of a long plate of width equal to the wing span. Two-dimensional conditions are appropriate, the wing having passed ahead. I and E are obtained immediately from Article 120. If w is the final velocity of the plate and $2s$ its width—

$$I = \pi\rho w s^2 \quad . \quad . \quad . \quad \text{(i)}$$
$$E = \tfrac{1}{2}\pi\rho w^2 s^2 \quad . \quad . \quad . \quad \text{(ii)}$$

The distribution of I across the plate is shown in Article 120 to be elliptic.

On the plate ϕ is given by—

$$\phi = -ws\sin\eta \quad . \quad . \quad \text{(iii)}$$

η ranging from 0 to 2π round the surface. Considering two adjacent points A and B, midway between the edges and on opposite sides of the plate, the interval of ϕ between them is—

$$\phi_B - \phi_A = ws\left(\sin\frac{\pi}{2} - \sin\frac{3\pi}{2}\right)$$
$$= 2ws \quad . \quad . \quad . \quad . \quad \text{(iv)}$$

Now actually, the plate so far imagined is fluid, consisting of a vortex sheet, and this interval of ϕ is the circulation round any circuit passing through the centre line and embracing one-half of the sheet. Denote this circulation by K_0. From (iv)—

$$K_0 = 2ws$$

or—

$$w = K_0/2s \quad . \quad . \quad . \quad . \quad (222)$$

Substituting in (i) and (ii)—

$$I = \rho\frac{\pi s}{2}K_0 \quad . \quad . \quad . \quad . \quad (223)$$

$$E = \rho\frac{\pi}{8}K_0^2 \quad . \quad . \quad . \quad . \quad (224)$$

175. Elliptic Wing-loading

In applying this important result to the actual case, when the motion is generated by a wing of lift L and span $2s$, we note the following:

K_0, being the circulation round each half of the vortex sheet, must also be the circulation round the median section of the aerofoil. Hence the central intensity of the lift is $\rho K_0 U$. At outer sections

this is required to fall away elliptically, i.e. the lift intensity at y is given by—

$$\rho KU = \rho K_0 U \sqrt{1 - \frac{y^2}{s^2}}$$

$$= \rho \frac{K_0 U}{s} \sqrt{s^2 - y^2} \quad . \quad . \quad . \quad (225)$$

We note—

$$L = \rho \frac{K_0 U}{s} \int_{-s}^{s} \sqrt{s^2 - y^2} \, . \, dy$$

$$= \rho \frac{\pi s}{2} K_0 U \quad . \quad . \quad . \quad . \quad . \quad (226)$$

agreeing with (223) from (221).

The velocity w has, at the aerofoil, from Article 148, one-half its value far downstream given by (222), i.e. at the aerofoil—

$$w = K_0/4s. \quad . \quad . \quad . \quad . \quad (227)$$

Knowing this velocity to be constant along the span, we can readily recalculate its value from (217). From (225)—

$$\frac{dK}{dy} = -\frac{K_0}{s} \frac{y}{\sqrt{s^2 - y^2}}. \quad . \quad . \quad . \quad (228)$$

Hence, applying (217) to $y_1 = 0$—

$$w = \frac{K_0}{2\pi s} \int_0^s \frac{dy}{\sqrt{s^2 - y^2}} = \frac{K_0}{4s}.$$

Again, since w is constant along the span—

$$D_i = \frac{w}{U} L = \rho \frac{\pi}{8} K_0^2 \quad . \quad . \quad . \quad (229)$$

from (226) and (227), in agreement with (224), remembering that $E = D_i$. Substituting for K_0 from (226) and writing λ for the *span-loading* $L/2s$ gives—

$$D_i = 2\lambda^2/\pi\rho U^2 \quad . \quad . \quad . \quad (229a)$$

The best wing shape which, *according to theory*, should give the required uniform induced velocity at itself, is of elliptic plan-form, having geometrically similar sections, so that camber is constant, set at constant incidence along the span. This shape is quite practicable in modern wing construction. Other plan-forms can be arranged to give approximately elliptic loading by suitably gradating camber and incidence along the span, but these may hold only for a single value of the central incidence.

Criticism of the feasibility of realising the minimum of induced drag arises actually on the theoretical side. Considering again the thin flat vortex sheet, (228) shows that dK/dy tends to ∞ at the wing-tips. Essentially the same result follows alternatively from Article 124; on analogy with a plate in broadside-on motion, (153) gives the span-wise components of velocity over the faces of the sheet, which tend to ∞ at the edges. The form of vortex sheet calculated could not persist at its edges and modifications are to be expected near the wing-tips. On the other hand, we shall see shortly that (229) is not a critical minimum. Hence, while the minimum induced drag may be regarded as an ideal impossible to realise exactly, small departures from the conditions required cause increases which for some practical purposes are not important.

176. Minimum Drag Aerofoil Formulæ

Let A be the aspect ratio of the wing giving elliptic span-loading. For a rectangular plan-form of constant chord c, $A = 2s/c$. If the plan-form be shaped, having area S and mean chord c'—

$$A = \frac{2s}{c'} = \frac{4s^2}{2s \,.\, c'} = \frac{4s^2}{S}. \quad . \quad . \quad . \quad . \quad (230)$$

From (226)—

$$C_L = \frac{L}{\frac{1}{2}\rho U^2 S} = \frac{2L}{\rho U^2} \cdot \frac{A}{4s^2} = \frac{\pi}{2} \cdot \frac{K_0}{U} \cdot \frac{A}{2s}. \quad . \quad (231)$$

This may be compared with the result (213), $C_L = 2K/Uc$, for uniform lift and constant chord.

From (229)—

$$C_{Di} = \frac{D_i}{\frac{1}{2}\rho U^2 S} = \frac{2D_i}{\rho U^2} \cdot \frac{A}{4s^2} = \frac{\pi}{4} \cdot \frac{K_0^2}{U^2} \cdot \frac{A}{4s^2} = \frac{1}{\pi A} C_L^2. \quad (232)$$

by (231). Similarly for the k system of coefficients—

$$k_{Di} = 2k_L^2/\pi A.$$

Formulæ (227) and (231) yield—

$$\frac{w}{U} = \frac{1}{\pi A} C_L \quad . \quad . \quad . \quad . \quad . \quad (233)$$

Substituting in (220)—

$$\alpha = \alpha_0 + \frac{1}{\pi A} C_L \quad . \quad . \quad . \quad (234)$$

These formulæ are often employed to calculate changes consequent upon modification of aspect ratio. For this purpose we have—

$$\left.\begin{aligned} C_{Di} - C'_{Di} &= \frac{1}{\pi}\left(\frac{1}{A} - \frac{1}{A'}\right) C_L^2. \\ \alpha - \alpha' &= \frac{1}{\pi}\left(\frac{1}{A} - \frac{1}{A'}\right) C_L. \end{aligned}\right\} \quad . \quad (235)$$

By differentiation of (234)—

$$\frac{d\alpha}{dC_L} = \frac{d\alpha_0}{dC_L} + \frac{1}{\pi A} = \frac{1}{2\pi} + \frac{1}{\pi A}$$

if the theoretical slope 2π for thin aerofoils of Joukowski shape be accepted. Then—

$$\frac{dC_L}{d\alpha} = \pi \frac{2A}{2 + A} \quad . \quad . \quad . \quad . \quad (236)$$

An empirical correction is to put $dC_L/d\alpha_0 = f \,.\, 2\pi$, where $f = 0{\cdot}87$ approx. from experiment. Then $dC_L/d\alpha = 2\pi A/(2 + A/f)$.

177. Examples

The foregoing simple results are of outstanding practical importance. They are often known as 'reduction formulæ.' The following examples, illustrating their many applications, rest upon certain assumptions; e.g. the difference between elliptical and rectangular plan-forms is for the time being regarded as negligible. These are discussed after further development of the theory.

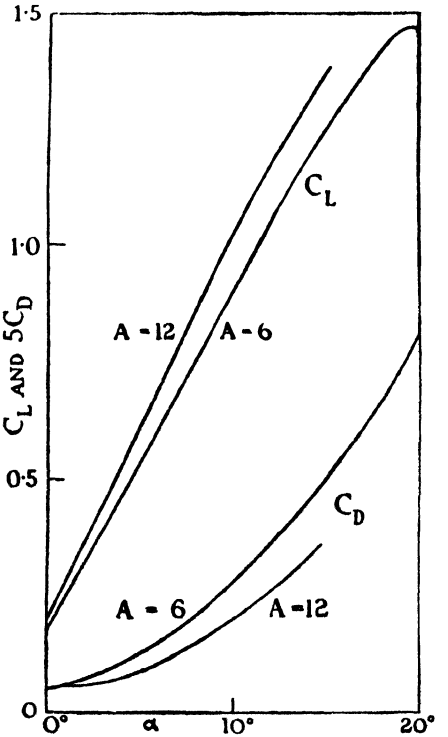

FIG. 127.

(1) The extended curves of Fig. 127 give the experimental * lift and drag coefficients at a full-scale Reynolds number for a rectangular wing of aspect ratio 6 and of

* Experimental data in this article are based on Relf, Jones, and Bell. *Loc. cit.*, p. 91.

the section shown in Fig. 42, known as R.A.F. 38 (thickness ratio $= 0{\cdot}127$). Consider the effects of increasing A from 6 to 12. Immediately from (235) $-\Delta C_{Di} = C_L^2/12\pi$, $-\Delta\alpha = C_L/12\pi$. Adding these increments to the experimental values of C_{Di} and α corresponding to any value of C_L gives one point on each of the derived curves for $A = 12$ shown. It will be noted that contributions to C_D of form drag and skin friction, necessarily included in the experimental values, are left unchanged. This will be shown to be justifiable within certain limits; the large decrease in drag at appreciable lift coefficients due to doubling the aspect ratio would be realised in practice.

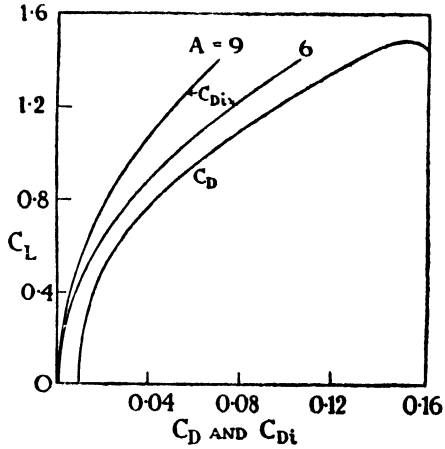

FIG. 128.

(2) Fig. 128 shows C_{Di} plotted against C_L for elliptic wings of aspect ratios 6 and 9, and also the minimum total C_D that can be expected for a rectangular wing shape of aspect ratio 6 and thickness ratio $= 0{\cdot}12$.

At moderately large lift coefficients and incidences, but appreciably below the maximum lift stage, induced drag is much greater than the sum of form drag and skin friction, and increase of aspect ratio produces marked improvement. The advantage of high aspect ratio diminishes, however, with small lift coefficients. For instance, at $C_L = 1{\cdot}0$ in the present example, C_{Di} forms nearly 80 per cent. of C_D, and increase of A from 6 to 9 would save 25 per cent. of the whole drag. But at $C_L = 0{\cdot}2$ the induced drag is only 20 per cent., and the possible saving would amount to only 7 per cent.

Consider a monoplane using this wing, of 5 tons total weight and having a minimum flying speed of 60 m.p.h. At a cruising speed of 110 m.p.h., about 180 b.h.p. would be absorbed by the wing alone, assuming an airscrew efficiency of 80 per cent. Of this, 18 per cent. could be saved by increasing A from 6 to 9. But a speed of 180 m.p.h. would require 450 b.h.p. for the wing, and a decrease of only 4 per cent. could be achieved.

It must be borne in mind that structural questions qualify the advantage of high aspect ratio. Full cantilever construction would

be too heavy, with the materials at present available, for so thin a wing as that considered with $A = 9$, and the smaller induced drag would be offset by the added drag of external bracing. A thick wing may be substituted to overcome this difficulty though form drag increases. But a point appears in favour of tapered plan-form which reduces the bending moment at the root of the wings.

(3) A monoplane weighing 9 tons has wings of aspect ratio 7 and 780 sq. ft. area. At 5000 ft. altitude its maximum rate of climb occurs at an indicated airspeed of 140 m.p.h., when $C_L = 0{\cdot}6$, and is 1080 ft. per min. Determine the aspect ratio for new wings, neglecting their increase in weight, to increase the rate of climb by 5 per cent.

The additional thrust h.p. that must be made available for climbing is—

$$\frac{0{\cdot}05 \times 20160 \times 1080}{33000} = 33{\cdot}0.$$

At 5000 ft. $\rho U^2 = 100{\cdot}3$ and $U = 205{\cdot}3/\sqrt{0{\cdot}862} = 221{\cdot}2$ ft. per sec. If A is the new aspect ratio which will lead to a saving of 33 thrust h.p.—

$$\frac{1}{\pi}\left(\frac{1}{7} - \frac{1}{A}\right)(0{\cdot}6)^2 \times \tfrac{1}{2} \times 100{\cdot}3 \times 221{\cdot}2 \times 780 = 33 \times 550$$

or—

$$A = 8{\cdot}03.$$

The above data relate to a modern craft with a usual minimum flying speed, with split flaps fitted to the wings, and whose cruising speed would be about 200 m.p.h. Let us change them to apply to a slow craft. It is only necessary to change the speed at which maximum rate of climb occurs from 140 m.p.h. to 100 m.p.h. The required increase of aspect ratio is then found to be from 7 to 10·8, owing simply to the reduction of speed, lift coefficient being supposed kept constant by reduction of minimum speed.

The foregoing examples illustrate that high aspect ratio substantially improves the speed or economy of aeroplanes of restricted speed range, and that it benefits aeroplanes of large speed range chiefly in regard to rate of climb and ability to maintain altitude when only part of their power equipment is functioning.

(4) A disadvantage of high aspect ratio arises in some cases as follows :

Wings must be made sufficiently strong to withstand the shock of flying into an upward gust, which has the effect of increasing incidence suddenly and thus momentarily increasing lift. The following

calculations are based on 25 ft. per sec. for the upward velocity of the gust, which is not excessive.

Assume the wings to have an effective maximum C_L of 1·28 and to be of aspect ratio 6 or 10, alternatively ; $dC_L/d\alpha$ is then either 4·712 or 5·236, theoretically.

Consider first a craft of 60 m.p.h. minimum flying speed encountering the gust at 120 m.p.h., so that initially $C_L = 1{\cdot}28(60/120)^2 = 0{\cdot}32$. The sharp increase of incidence comes to $25/176 = 0{\cdot}142$ radian and C_L increases by 0·670 for $A = 6$ or by 0·744 for $A = 10$, becoming 0·990 or 1·064. Thus until incidence and speed have time to change, the lift of the wings is increased in the ratio 3·10 or 3·33, approximately. The wing of the higher aspect ratio is the more severely stressed by the gust. Let us diminish the minimum flying speed to 50 m.p.h. and advance the speed range to 3. Then initially $C_L = 0{\cdot}142$, $\Delta\alpha = 0{\cdot}114$ and C_L becomes 0·680 for $A = 6$ and 0·740 for $A = 10$. The transient ' load factors ' are now 4·78 and 5·20, respectively. A factor of safety of 2 is usually called for, and this excessive loading might provide an overriding condition for the structural design of the wings, which would therefore be heavier with the larger aspect ratio on a score additional to that mentioned in (2).

178. The Arbitrary Monoplane Wing

The problem of the wing of non-elliptic form, defined by a given variation along the span of shape of section, incidence α and chord c, is somewhat complicated. A brief description is given below of a convenient method * of solution developed by Glauert, whose book † should be consulted for further details. As before, the area of the wing is written S and its span $2s$.

Change the variable so far employed to denote position along the span from y to θ, according to—

$$y = -s\cos\theta.$$

Then $\theta = 0$ when $y = -s$, i.e. at the port wing-tip, $\theta = \pi/2$ at the centre of span, $\theta = \pi$ when $y = s$, and $dy = s\sin\theta d\theta$.

The circulation K, varying along the span, is expressed in a series of Fourier type—

$$K = 4sU\Sigma C_n \sin n\theta \quad . \quad . \quad . \quad (237)$$

* An alternative method is due to Lotz; see Shenstone, *Jour. R. Ae. S.*, May 1934.

† *The Elements of Aerofoil and Airscrew Theory.*

in which for symmetry about the median plane only odd integral values of n appear. Since from (218)—

$$C_L = \frac{2L}{\rho S U^2} = 2\frac{s}{SU}\int_0^\pi K \sin\theta d\theta,$$

substituting from (237) and remembering (230) gives—

$$C_L = 2A\int_0^\pi (\Sigma C_n \sin n\theta)\sin\theta d\theta,$$

where A is the aspect ratio. This is easily evaluated, giving—

$$C_L = \pi A C_1 \quad . \quad . \quad . \quad . \quad (238)$$

The result means that the first coefficient of the Fourier series determines the total lift coefficient. It does not mean that $C_L \propto A$. C_3, C_5, . . . modify the distribution of lift along the span, but in a manner which leaves C_L constant. This distribution depends upon the shapes of the sections, their sizes and attitudes all along the span.

For an exact solution the summation should be from 1 to ∞, or at least include a considerable number of terms, each relating to a particular outboard position, i.e. to a particular value of θ. But the Fourier series often gives a good approximation when only few terms are used; the practical feasibility of the method depends upon this, and usually four or five terms are sufficient when, from symmetry, only the semi-span need be considered.

We have to find an equation for C_n which will be satisfied everywhere along the span, although in practice it will be satisfied at a few chosen positions only. In framing the equation we have to relate K to the induced velocity w, now also variable, according to the fundamental laws developed in Article 170 and Chapter VI.

At any position θ—

$$2\rho KU = C_{L\theta}\,\rho c U^2,$$

or—

$$2K = C_{L\theta}\,cU.$$

Also, if $\alpha_{0\theta}$ is the incidence under two-dimensional conditions measured from the angle of no lift—

$$C_{L\theta} = \frac{dC_{L\theta}}{d\alpha}\alpha_{0\theta}.$$

It is convenient to ignore for the moment variation of the slope of the two-dimensional lift curve from one section to another and to write for this 2π, its theoretical value for thin Joukowski shapes. Then—

$$C_{L\theta} = 2\pi\alpha_{0\theta}$$

and hence, dropping the suffix—

$$K = \pi U c \alpha_0$$

or from (220)—

$$K = \pi U c \left(\alpha - \frac{w}{U}\right). \quad . \quad . \quad . \quad (239)$$

Now, on substituting the new variable and taking account of (237), (217) can be reduced (cf. Article 140D) to—

$$\frac{w}{U} = \Sigma n C_n \frac{\sin n\theta}{\sin \theta}. \quad . \quad . \quad . \quad (240)$$

Substituting this expression for w and also for K in (239)—

$$4s \Sigma C_n \sin n\theta = \pi c \left(\alpha - \frac{\Sigma n C_n \sin n\theta}{\sin \theta}\right),$$

or—

$$\Sigma C_n \sin n\theta \left(\frac{\pi n c}{4s} + \sin \theta\right) = \frac{\pi c}{4s} \alpha \sin \theta \quad . \quad . \quad (241)$$

This is the general equation required. More accurate values of $dC_L/d\alpha$ than 2π will be known for the sections under two-dimensional conditions at the chosen θ points, and these should be substituted in practice for 2π. But we shall retain the approximation. With it, results are obtained in terms of the parameter $c/4s$, which is in general variable, but which is constant and equal to $1/2A$ for a given rectangular wing.

We are now in a position to calculate the total induced drag. After substituting for y, K and w, (219) leads to—

$$C_{Di} = \frac{D_i}{\frac{1}{2}\rho U^2 S} = 2A \int_0^\pi (\Sigma n C_n \sin n\theta)\ (\Sigma C_n \sin n\theta)\, d\theta,$$

and this reduces to—

$$C_{Di} = \pi A \Sigma n C_n^2. \quad . \quad . \quad . \quad (242)$$

179. The Elliptically Loaded Wing Compared with Others

By squaring (238) and substituting in (242) we find—

$$C_{Di} = \frac{1}{\pi A} C_L^2 \,.\, \Sigma n \left(\frac{C_n}{C_1}\right)^2. \quad . \quad . \quad . \quad (243)$$

Now the sum is obviously positive, and C_L is specified by C_1. Therefore, the induced drag is a minimum for a given lift when all coefficients subsequent to the first vanish. The sum will then

reduce to unity, and thus the minimum possible drag coefficient for any wing is given by (232), as already proved, when lift varies elliptically along the span.

The formula (243) is conveniently written—

$$C_{D_i} = \frac{1}{\pi A} C_L^2 (1 + \delta). \quad . \quad . \quad . \quad (244)$$

For elliptic loading $\delta = 0$, but for other distributions it has a positive value—a small fraction in practical cases, as will be illustrated. δ then gives the proportionate increase of induced drag above the minimum theoretically possible.

Aeroplane wings are commonly, for constructional reasons, either rectangular or straight-tapered, except for rounded tips. With square tips, these plan-forms have been investigated by Glauert,* using the method just described, and the rectangular shape by Betz † and others, employing different methods. Some load distributions

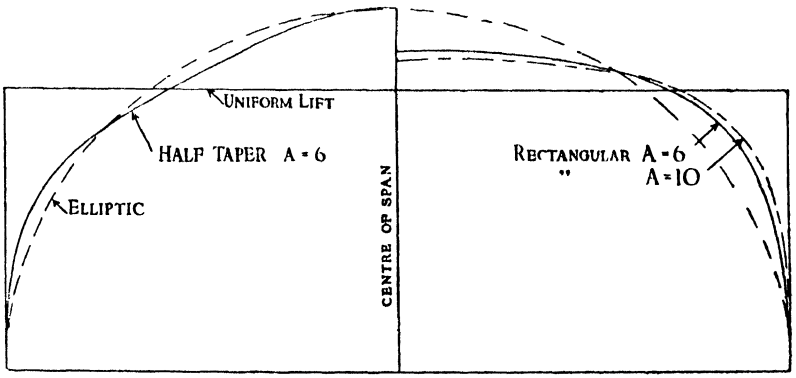

FIG. 129.—MATHEMATICAL DISTRIBUTIONS OF LIFT FOR VARIOUS PLAN-FORMS.

are illustrated in Fig. 129 for equal total lift ; uniform loading is included, although this is not a practical, nor a desirable, case. The results relate to constant shape of section and geometrical incidence along the span. The half-taper wing has a tip chord equal to one-half its central chord, and its loading approximates to elliptic loading. The distribution for a much sharper taper differs as much as does that for the rectangular shape from the ideal, but in the opposite way. Both these loadings differ widely from the elliptic considered from a structural point of view, but the question remains as to how different they may be as regards induced drag.

Loc. cit., p. 320. † *Dissertation*, Göttingen, 1919.

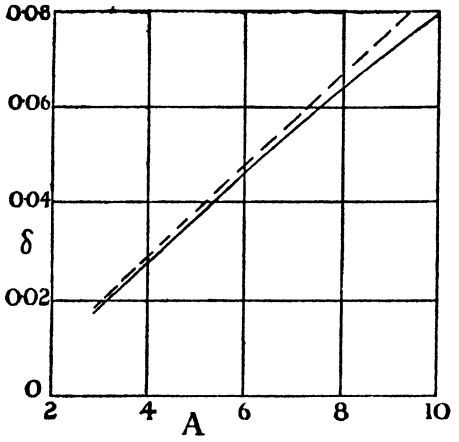

FIG. 130.

Fig. 130 indicates the theoretical variation of δ with A for rectangular wings according to Glauert (full line) and Betz (broken line), showing good agreement. The slope of the two-dimensional lift curve is assumed to be 2π; if it is less, aspect ratio should be proportionately increased. Induced drag decreases with increase of A, but not so quickly as for the elliptic wing. This is illustrated in Fig. 131, where also are shown the result estimated from experiment in Article 166 for uniform lift with $A = 6$, and a theoretical result for a pointed wing. The theoretical error in estimating induced drag for rectangular wings by (232), i.e. by assuming elliptic loading, decreases from 8 per cent. at $A = 10$, which is a large aspect ratio for aeroplane wings, to 5 per cent. at $A =$ 6–7, and to 3 per cent. at the aspect ratio 4 often employed for tail-planes.

Fig. 132 gives the variation of δ with taper for $A = 6$–7. The best taper, from the present point of view, has a tip chord somewhat less than one-half the central chord at this aspect ratio. Induced drag is then only 1 per cent. greater than for elliptic loading. Structural questions may suggest a sharper taper, but

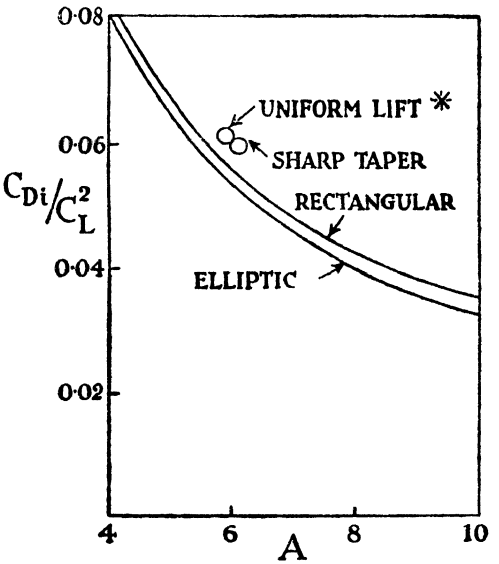

FIG. 131.—INDUCED DRAG AND ASPECT RATIO.

(* This point is estimated from experiment.)

δ then increases until, with a pointed wing, induced drag becomes as great as has been estimated for uniform lift [cf. (216)].

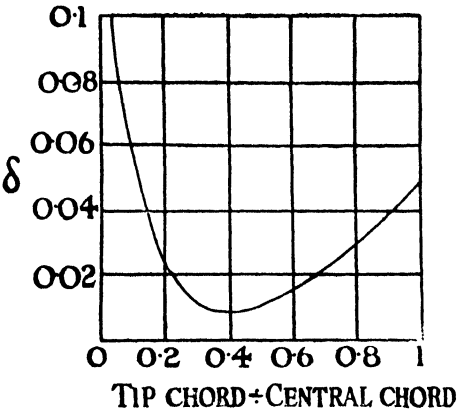

FIG. 132.

The conclusion is that the induced drag of normal types of wing, of moderate aspect ratio and taper, can be assessed to a good first approximation by the formulæ of Article 176, and especially changes due to modifications of aspect ratio provided the type of loading remains the same. More accurate reduction formulæ than (235) are, however, easily deduced by precisely the same method.

Increased induced drag implies that, to secure a specified lift coefficient, incidence must be increased more than is provided for by (234). For a full discussion of this question reference should be made to the original papers. If, on analogy with (244), we write—

$$\alpha = \alpha_0 + \frac{1}{\pi A} C_L (1 + \tau), \quad . \quad . \quad . \quad (245)$$

τ increases approximately linearly for rectangular wings from 0·1 at $A = 3$ to 0·23 at $A = 10$. Associated with this change is a decrease in the slope of the lift curve, as compared with two-dimensional conditions, greater than is calculated in (236). For rectangular aerofoils, the lift curve of whose section has a slope 2π in two-dimensional flow, the effect is approximately allowed for by substituting 3·02 for π in (236).

180. Comparison with Experiment

The solution for the rectangular wing provides convenient means for comparing the results of aerofoil theory with experiment, since aerofoils of this shape can easily be made with accuracy, and many checks of different kinds have been obtained.

The slope of the lift curves for R.A.F. 38 and Clark YH aerofoils with $A = 6$ are 0·0752 and 0·0742 per degree. A number of good aerofoils give a slope rather less than 0·076 at this aspect ratio and at fairly large Reynolds numbers. The theoretical slope for a two-dimensional slope 2π is $6{\cdot}04 \times 6/8 = 0{\cdot}453$ per radian $= 0{\cdot}079$ per

degree. It appears that at full scale a less factor than 3·02 should be used in place of π in (236), but the agreement is nevertheless quite good.

Comparisons between load grading curves are less satisfactory except at very small incidences. Fig. 133 shows as a full line the experimental distribution along the span of a rectangular aerofoil obtained by integrating the pressures over the surface, and as a dotted line the theoretical result. A marked difference will be seen to occur towards the wing-tips. The angle of incidence was 6°; the difference is typical for incidences greater than about 1°, and occurs also on tapered aerofoils. The pressure peak near the tip signalises a knuckle of hoarded vortex lines; in other words, a discrete trailing vortex of some strength exists near the trailing edge in this region (cf. Article 166). Such a departure from theory was anticipated on theoretical grounds in Article 175. Wings can be designed to eliminate this feature at cruising or climbing incidence, but the form of wing-tip required is less easy to construct and with most wings the feature is present; it has been found at full scale, and the close-up vortices must occasionally be taken into account in connection with the controls of aircraft. The peaks of pressure reduction are situated on the rear part of the upper surface, so that they lead to a large increase in drag over small areas, as described in Chapter VII. The theoretical induced drags for given shapes are ideal minima, and in actual wings apply only to part of the lift; the remaining part would appear to have a drag appropriate to uniform lift.

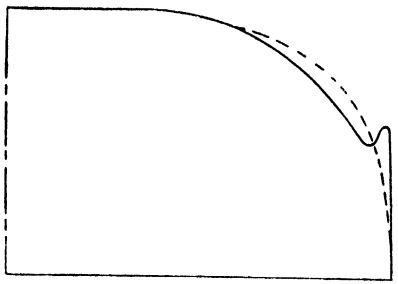

FIG. 133.—DISTRIBUTION OF LIFT ALONG RECTANGULAR WING.

Full line: experimental; broken line: theoretical. (Similar differences between theory and experiment are also found on tapered wings.)

Effects of the foregoing and other discrepancies are minimised in the principal use that is made of the theory in design, viz. to calculate relatively small differences between wings of much the same type, as illustrated in Article 177. The feasibility of this use rests upon experiment. Observations of lift and total drag coefficients are obtained on a series of aerofoils based on the same section, but of widely different aspect ratios. Plotting C_L against C_D for each results in a series of very dissimilar curves, as will be appreciated.

When, however, the reduction formulæ are used to correct every point on all the curves to some common aspect ratio, chosen as standard, the originally divergent observations are found, within certain limits, to agree with one another substantially, and all to lie within a narrow band through which a single curve may be drawn for practical purposes. The limitations are, firstly, that the aspect ratio must be greater than a minimum depending upon section and incidence; the minimum varies between 2 and 4. Secondly, incidence must in any case be restricted; the check has been successful in some cases up to 15°, but the region of maximum lift should be avoided.

BIPLANE WINGS

181. The two wings of a biplane are variously arranged as illustrated in Fig. 134. Distance between the planes is called gap (see

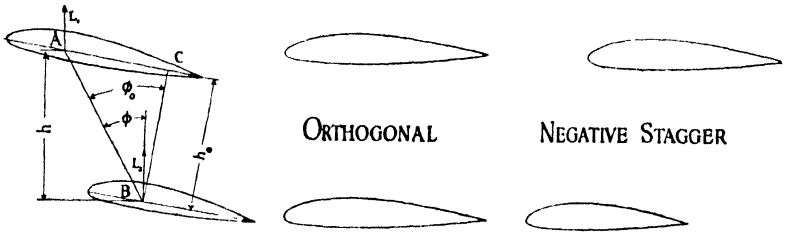

FIG. 134.—THE LEFT-HAND FIGURE ILLUSTRATES POSITIVE STAGGER, h_0 BEING THE GEOMETRIC GAP.

If A, B are the centres of pressure, h is the Aerodynamic gap and ϕ the Aerodynamic stagger. If, alternatively, A and B are fixed points, usually located at one-quarter of the chords from the leading edges, ϕ_0 is the geometric stagger.

note to figure). When the upper wing is immediately above the lower wing at 0° and has the same dimensions, the arrangement is called orthogonal. If the upper wing leads, there is said to be positive stagger, the amount being expressed as an angle. In a sesqui-plane the lower wing is of reduced span and usually of reduced chord. With positive stagger the upper wing is occasionally set at the greater incidence by 2°–3°, when the biplane is said to have *décalage*.

The two wings interfere with one another in various ways, and even in an orthogonal biplane at 0° have different lifts. Thus, considering a region of the atmosphere traversed a little time previously by a biplane, we expect to find two vortex pairs of unequal strengths. The induced drags of the wings differ from one another and from that of a similar monoplane.

Changes of Aerodynamic efficiency from one arrangement to another and in comparison with the monoplane will be studied, but it should be remembered that a particular layout may be adopted for ease of construction, restrictions on span, pilot's view, and similar practical considerations. Thinner wing sections can be used for biplanes, partly on account of decrease in span for a given lift, but more importantly by virtue of the external bracing so readily introduced. The drag and weight of the interplane bracing tend to offset this advantage, however, and also to limit the amount of stagger and gap that can usefully be employed.

182. Some General Theorems

As for the monoplane, the trailing vortex lines behind each member will, for purposes of calculation at the wings, be assumed to extend downstream parallel to the direction of motion.

A slight extension of Articles 173–4 leads to the result that minimum drag occurs for a given lift when both wings are elliptically loaded and the induced velocity is the same at each. Elliptic lift distribution will be assumed.

Introduce stagger, either positive or negative, at the same time modifying the incidence of every section of either plane in such a way as to ensure that the distribution of lift throughout the system, whatever it may be, remains unchanged. By considering a region of the atmosphere lately traversed, the kinetic energy generated within it by the biplane is clearly seen to be independent of the degree of stagger. Thus the total induced drag is, with the proviso stated, unchanged by stagger. It does not follow that the induced drag of either plane is unaffected, in fact the contrary will be found. This important theorem is known as Munk's equivalence, or stagger, theorem. It enables a staggered biplane to be replaced, for purposes of investigation, by an equivalent system of zero stagger, having the same total lift and drag, but with drag distributed between the planes in accordance with the degree of stagger.

Distinguish the upper wing by suffix 1 and the lower by suffix 2, and denote an effect on 1 by its own vortex system by the suffix 11, an effect on 1 due to the vortex system of 2 by the suffix 12, and so on. The total induced drag of the biplane is—

$$D_{iB} = D_{i11} + D_{i22} + D_{i12} + D_{i21} \quad . \quad . \quad (246)$$

The first two terms on the right-hand side are calculated as for separate monoplanes ; the last two represent the effects of interference. Regarding mutual effect, the circumstances of either wing

are modified by (*a*) the bound, and (*b*) the free vortex system of the other. We investigate the mutual effect as for (*b*) only, and introduce a correction for (*a*) later.

Divide the span of each wing of a biplane of zero stagger into a number of elements having equal small lifts. Each separate element will produce trailing vortices, appropriate to its span, which, though unequal in spacing and strength, induce equal velocities at distant corresponding points owing to the equality of the lifts. Consider a single pair of elements, one on each wing. If w' represents the induced velocity at the one element due to the trailing vorticity behind the other—

$$\frac{w'_{12}}{U}\delta L_1 = \frac{w'_{21}}{U}\delta L_2.$$

This is true of any pair of elements. Hence, if ΔD_{i12} be the whole induced drag of a chosen element of wing 1 as due not to other elements of the same wing but to the effects of all the elements of wing 2, and ΔD_{i21} be that part of the induced drag of the whole of wing 2 due to the effects on all its elements of the single chosen element of wing 1—

$$\Delta D_{i12} = \Delta D_{i21}.$$

Therefore, by summation for all elements—

$$D_{i12} = D_{i21} \quad . \quad . \quad . \quad . \quad (247)$$

Substituting in (246) we find—

$$D_{iB} = D_{i11} + D_{i22} + 2D_{i12}. \quad . \quad . \quad (248)$$

It is important to remember that this result is for zero stagger. With the aid of Munk's equivalence theorem it becomes of general utility, for by this we can replace a staggered biplane by a particular unstaggered system, to which the above result may be applied.

Now, since elliptic loading is assumed, the induced velocity at any point some distance downstream due to wing 2, say, can be calculated on the analogy between its vortex sheet and a flat plate in broadside-on motion by the methods of Article 117 or 124. The point can be moved upstream to the vertical plane containing both wings by introducing the factor $\frac{1}{2}$. Writing $2s$ for the span as before, we can then calculate for zero stagger—

$$D_{i12} = \frac{1}{U}\int_{-s_1}^{s_1} w_{12}dL_1, \quad . \quad . \quad . \quad (249)$$

and (248) can finally be evaluated with the help of the monoplane formulæ.

183. Prandtl writes (249) in the form—

$$D_{i12} = \frac{L_1 L_2}{2\pi\rho U^2 s_1 s_2}\sigma, \qquad . \quad . \quad . \quad (250)$$

where σ depends on s_1/s_2, and the ratio of gap to mean span. Fig. 135 gives his values for σ through a useful range.

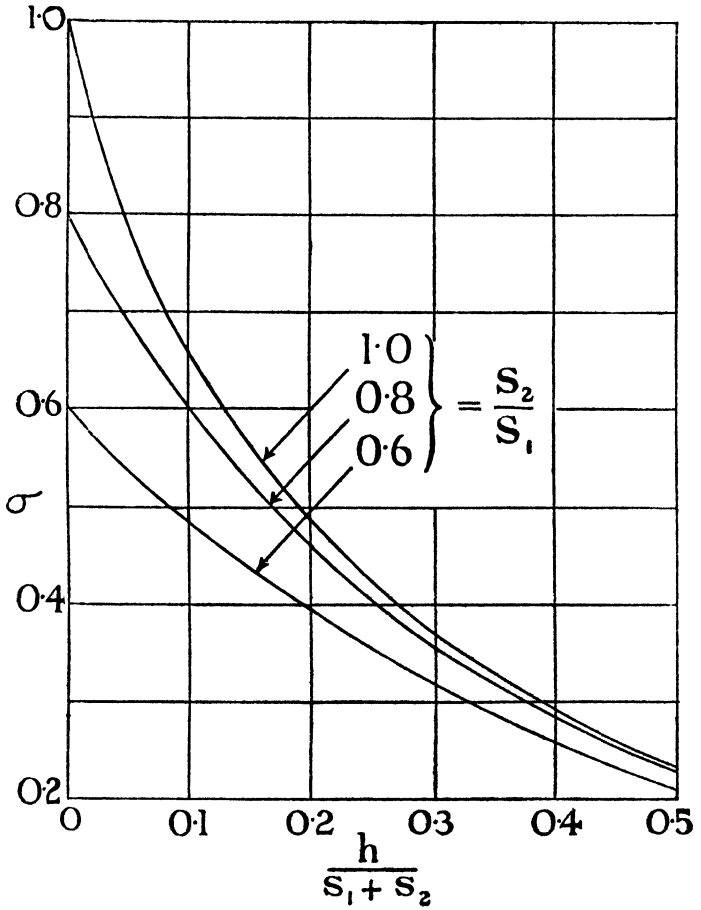

FIG. 135.—PRANDTL'S FACTOR FOR BIPLANES.

Denote the quantity lift/span for each wing by λ_1 or λ_2, so that (250) takes the form—

$$D_{i12} = \frac{2\lambda_1\lambda_2}{\pi\rho U^2}\sigma.$$

Since for a monoplane $2/\pi A = S/2\pi s^2$, the induced drag of a monoplane with elliptic loading is obtained in the same terms as—

$$D_{iM} = C_{DiM}\,\tfrac{1}{2}\rho U^2 S = \frac{S}{2\pi s^2}\frac{L^2}{\rho U^2 S}$$
$$= \frac{2\lambda_M^2}{\pi\rho U^2}. \quad . \quad . \quad . \quad (251)$$

Hence the induced drag of the complete biplane is found from (248) to be given by—

$$D_{iB} = \frac{2}{\pi\rho U^2}(\lambda_1^2 + \lambda_2^2 + 2\sigma\lambda_1\lambda_2). \quad . \quad . \quad (252)$$

This is a minimum for a given total lift when—

$$\frac{\lambda_1}{\lambda_2} = \frac{s_1 - \sigma s_2}{s_2 - \sigma s_1} \quad . \quad . \quad . \quad . \quad (253)$$

The value of the minimum is—

$$\text{min. } D_{iB} = D_{iM}\frac{1-\sigma^2}{1 - 2\sigma(s_2/s_1) + (s_2/s_1)^2}, \quad . \quad . \quad (254)$$

where the monoplane drag is for equal lift, and a span equal to that of the longer wing (1) of the biplane. The factor to be applied to D_{iM} is always < 1, so that a biplane has less drag than a monoplane of equal lift and span. This result neglects, of course, the parasitic drag of inter-plane bracing.

In the biplane of minimum induced drag and zero stagger, the mutually induced drag is divided equally between the wings, and we find—

$$\frac{(L/D_i)_1}{(L/D_i)_2} = \frac{s_1/(\lambda_1 + \sigma\lambda_2)}{s_2/(\lambda_2 + \sigma\lambda_1)} = 1$$

on substituting for λ_1 or λ_2 from (253), i.e. the wings have equal lift/drag ratios. But this is not true if the total lift is differently divided between them.

The disposition of lift required for minimum drag is usually disadvantageous from a structural point of view, since the longer wing is much the more heavily loaded. It is therefore useful to note that for practical variations the above minimum is not critical but 'flat.'

184. Examples

To illustrate the significance of the foregoing results, we consider a biplane lifting 2700 lb. at 150 ft. per sec. whose upper and lower wings are 30 ft. and 24 ft. span, respectively, with a gap of 5 ft.

For a monoplane of the same lift and 30 ft. span—

$$D_i = \frac{2 \times 8100}{\pi\rho \times 22500} = 96{\cdot}3 \text{ lb.}$$

since $\lambda_M = 90$ lb. per ft.

For 5-ft. gap $\sigma = 0{\cdot}48$, approximately, and the minimum drag is—

$$\frac{96{\cdot}3\ (1 - 0{\cdot}23)}{1 - 0{\cdot}96 \times 0{\cdot}8 + 0{\cdot}64} = 85{\cdot}0 \text{ lb.}$$

We also have—

$$\frac{\lambda_1}{\lambda_2} = \frac{15 - 5{\cdot}76}{12 - 7{\cdot}20} = 1{\cdot}925 = \frac{L_1 \times 24}{L_2 \times 30}$$

whence $L_1 = 1907$ lb., $L_2 = 793$ lb. Since $\lambda_1 = 63{\cdot}6$, $\lambda_2 = 33{\cdot}0$—

$$D_{11} = 48 \text{ lb.}, D_{22} = 13 \text{ lb.}, D_{12} + D_{21} = 24 \text{ lb.}$$

and as the biplane has zero stagger,

total induced drag, upper wing = 60 lb.
total induced drag, lower wing = 25 lb.

We note a reason for diminishing the chord of the lower wing, but that the difference in loading is rather excessive. It might be more practical to make $\lambda_2 = \frac{3}{4}\lambda_1$, so that $\lambda_1 = 56{\cdot}2$, $\lambda_2 = 42{\cdot}2$. We should then have 85·9 lb. for the total induced drag, made up as follows:

$$D_{11} = 37{\cdot}6 \text{ lb.}, D_{22} = 21{\cdot}2 \text{ lb.}, D_{12} + D_{21} = 27{\cdot}1 \text{ lb.},$$

showing 13 per cent. increase in the drag due to interference, but 1 per cent. only in the whole. Since now $L_1 = 1687$ lb. and $L_2 = 1013$ lb., it is found that for zero stagger the lift/drag (induced) ratio of the upper wing would be increased by 4 per cent. and that of the lower decreased by 8 per cent.

The loss associated with the new loading could be recovered by a small increase of gap. The only drag then affected is that mutually induced. It is easily found that, to decrease this by the small required amount, σ must be reduced to the value corresponding to a gap of 5 ft. 4 in.

185. Equal Wing Biplane—Comparison with Monoplane

Article 183 shows that minimum induced drag occurs for a given lift when the wings have equal span and λ is the same for both, i.e. their lifts are equal. We then have for the complete system—

$$D_{iB} = \frac{\lambda_B^2}{\pi\rho U^2}(1 + \sigma), \quad . \quad . \quad . \quad (255)$$

where λ_B is the *total* lift per unit span of the biplane.

An approximate expression for $1 + \sigma$ when $s_1 = s_2 = s$ is, from Prandtl, writing h for the gap—

$$1 + \sigma = \frac{2{\cdot}055 + 1{\cdot}52\ (h/s)}{1{\cdot}055 + 1{\cdot}85\ (h/s)} \quad . \quad . \quad . \quad (256)$$

The span-grading of a monoplane carrying the same load as a biplane and having the same induced drag is immediately obtained as—

$$\lambda_M = \lambda_B \sqrt{\frac{1 + \sigma}{2}} \quad . \quad . \quad . \quad . \quad (257)$$

Example.—If the gap is one-sixth of the span of the biplane, the span-grading of lift must be reduced for the monoplane by the factor 0·875.

The results may be expressed in terms of aspect ratio as follows, the aspect ratio of the biplane being defined by $A_B = 8s^2/S$, where S is the total area, so that for wings of the same dimensions A_B equals the aspect ratio of either. From—

$$C_{LB} = \frac{4s\lambda_B}{\rho U^2 S}$$

$$\lambda_B^2 = \frac{(\rho U^2)^2 S}{2A_B} C_{LB}^2.$$

Hence—

$$C_{Di_B} = \frac{1}{\pi A_B} C_{LB}^2 (1 + \sigma) \quad . \quad . \quad . \quad (258)$$

For the same lift coefficient and aspect ratio the induced drag coefficient of a biplane is greater than that of a monoplane in the ratio (256). The lifts are then different, however, for equal span. To make the lifts the same, the area of the monoplane must be doubled, whence we find that the drag of the biplane, supporting the same load at the same lift coefficient and having the same aspect ratio, is greater than that of the monoplane in the ratio $(1 + \sigma)/1$. It will be noted that the monoplane span-grading of lift is then $1/\sqrt{2}$ times that of the biplane. Let us determine the aspect ratio of the monoplane which will lead to the same induced drag at the same lift and lift coefficient. Evidently we must have—

$$\frac{A_M}{A_B} = \frac{1}{1 + \sigma}.$$

Example. For a gap-span ratio of 1/6, $A_M = 0{\cdot}653\, A_B$. This can be written, since the areas are equal, $4s_M^2 = 0{\cdot}653 \times 8s_B^2$, whence

$2s_M = 1{\cdot}143 \times 2s_B$. The chord of the monoplane is the greater by 75 per cent.

Incidence.—For biplane wings to achieve a given lift coefficient their incidence (α) must be increased from that appropriate to their sections under two-dimensional conditions (α_0) to a greater extent than monoplane wings of the same section and aspect ratio.

On account of the double trailing vortex system α is evidently increased to—

$$\alpha = \alpha_0 + \frac{1}{\pi A} C_L (1 + \sigma) \quad . \quad . \quad . \quad (259)$$

A further increase is required on account of the curvature of the streamlines in which each wing operates, due to the bound vortex system of the other. This development is left to further reading.* An approximate formula is—

$$\Delta\alpha = \frac{0{\cdot}025}{(A \times \text{gap/span})^2} C_L \quad . \quad . \quad . \quad (260)$$

Example.—For $A = 6$, $\alpha - \alpha_0$ (in radians) for a monoplane with elliptic loading $= 0{\cdot}053\ C_L$; for an equal wing biplane of gap-span ratio 1/6 it is $0{\cdot}082\ C_L$ at the lower estimate (259), which requires increasing by some 30 per cent. to take account of the neglected factor (260).

186. General Remarks

The form of (260) shows that the secondary, but important, incidence increase depends essentially upon the square of the ratio of the chord to the gap. Thus, however A is increased, the slope of the lift curve of a biplane is considerably reduced from the two-dimensional value. Formula (259) can be amended on the lines of (245) for lift distributions other than elliptic. Applying the same reasoning as to mutual effect to biplanes which, as is usual, have positive stagger, shows that the forward wing should have the smaller geometrical incidence. But the reverse is sometimes adopted, and improves the shape of the lift curve past the stall. If both wings of a staggered biplane are of equal span and carry an equal load, the forward wing is easily shown to have less induced drag than the other.

The comparisons which have been made with the monoplane neglect increase of form drag of the biplane wings due to their

* Bose and Prandtl, *Zeits. f. ang. Math. u. Mech.*, vii, 1927.

greater incidence for a given lift coefficient. They also neglect the experimental value of the maximum lift coefficient, which is the lower for the biplane and affects choice between the two in practice.

WIND-TUNNEL CORRECTIONS ON AEROFOIL TESTS

187. Enclosed Tunnel Constraint at the Aerofoil

When an aerofoil is tested in a wind tunnel of the kind in which the stream is enclosed within walls, the walls diminish the induced velocity at the aerofoil, which consequently experiences a fictitious reduction of induced drag and incidence. If the aerofoil has the same aspect ratio as the wing it represents, observations of drag and incidence must be suitably increased to apply to free air conditions. This course of correction is that usually followed. Alternatively, the measurements might be made on a model of appropriately smaller aspect ratio. The advantage of the latter method is that the aerofoil may have a larger chord, and is then easier to make accurately for small tunnels.

The constraint is often calculated with sufficient accuracy by the approximation mentioned at the end of Article 166, replacing the trailing vortex sheet by a vortex pair, and the actual tunnel wall by a circular one. The distance apart l of these vortices is determined from the lift of the aerofoil. For example—

$$\rho U l K_0 = \rho U \frac{\pi S}{2} K_0$$

if elliptic loading is assumed. Whence in this case—

$$l = \frac{\pi S}{2} \quad . \quad . \quad . \quad . \quad . \quad (261)$$

Let the radius, or effective radius, of the tunnel be a. Assuming the aerofoil to be located centrally, the images are distant $a^2/\frac{1}{2}l$ from the centre. The upward velocity at the centre due to these is—

$$-w' = 2\frac{K_0}{4\pi} \cdot \frac{\frac{1}{2}l}{a^2} = \frac{K_0 l}{4C}.$$

where C is the cross-sectional area of the tunnel. But—

$$\rho U l K_0 = \tfrac{1}{2}\rho U^2 S C_L$$

or—

$$l K_0 = \tfrac{1}{2} S U C_L$$

if C_L is the lift coefficient and S the area of the aerofoil. Substituting—

$$-w' = \frac{1}{8}\frac{S}{C} C_L U. \quad . \quad . \quad . \quad . \quad (262)$$

This result has been obtained without use of (261) and applies to any aerofoil, i.e. assumption of elliptic loading is unnecessary in the present connection.

It is usually sufficiently accurate to increase w uniformly along the span by this amount to obtain free air conditions. We then have finally—

Similarly—

$$\left.\begin{aligned} \Delta\alpha &= \frac{1}{8}\frac{S}{C} C_L, \\ \Delta C_{Di} &= \frac{1}{8}\frac{S}{C} C_L^2 \end{aligned}\right\} \quad . \quad . \quad . \quad (263)$$

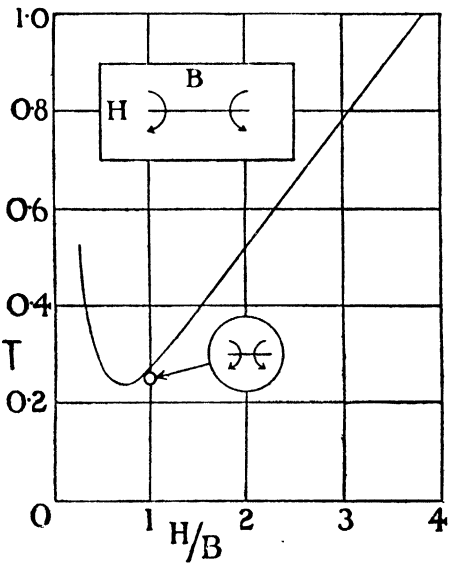

FIG. 136.

for a tunnel of circular section. It will be noticed that the distance l has vanished, and that the corrections are proportional to lift only. Thus they apply even to a biplane or triplane model, when S becomes the sum of the aerofoil areas.

Expressions of the same form are obtained by the method of Article 153 for tunnels of square or rectangular section, the numerical factor 0·125 for the circular section alone being changed. Fig. 136 shows the variation of this factor, which is denoted by $\frac{1}{2}T$, for rectangular tunnels. It will be seen that the variation from 0·125 is only 10 per cent. for open sections.* The whole correction is usually less than 10 per cent., when this variation comes to less than 1 per cent. of the final estimates. But where the clearance between the aerofoil tips and the tunnel walls becomes less than one-fifth of the span, the

* Terazawa, *Tokyo Repts.* 44, 1928.

foregoing approximate method begins to be insufficient and the form of the distribution of w' to have an appreciable effect.

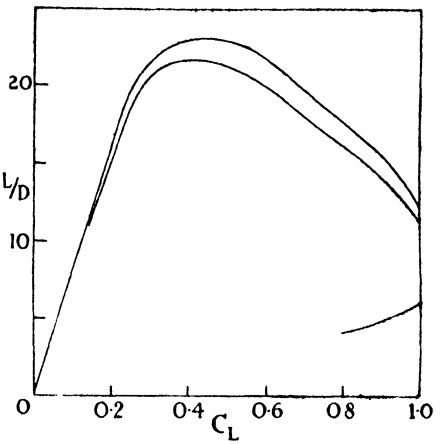

FIG. 137.

Examples. — The upper curve of Fig. 137 would be expected from an aerofoil of R.A.F. 38 section, of 4-in. chord and 24-in. span, at a speed of 150 ft. per sec. in a closed-section wind tunnel of 4-ft. diameter. $T \cdot S/C = 0{\cdot}0133$, and multiplying by half the square of lift coefficients gives increments of drag coefficient leading to the lower curve for free air conditions. Incidence would also be increased for a given C_L, e.g. at $C_L = 1{\cdot}0$, $\Delta\alpha = 0{\cdot}0066$ radian $= 0{\cdot}38°$.

What aspect ratio would a model of the same chord require for the two curves to coincide ? Comparing (263) with (235), we have, distinguishing free air conditions by the accent—

$$\frac{1}{8}\frac{S}{C} = \frac{1}{\pi}\left(\frac{1}{A} - \frac{1}{A'}\right),$$

or, since $C = \pi a^2$ and $A' = 6$—

$$\frac{1}{A} - \frac{S}{8a^2} = \frac{1}{6}.$$

By (230) $S = 4s^2/A$, while $4s^2 = A^2c^2$, c denoting the constant chord. Hence, or more directly—

$$\frac{1}{A} - \frac{Ac^2}{8a^2} = \frac{1}{6}.$$

Substituting $a = 2$, $c = 1/3$, gives $A = 5{\cdot}4$. Thus an aerofoil of 4-in. chord and 21·6-in. span in a circular-section tunnel of 4-ft. diameter would give through a limited range of incidence the same lift and drag coefficients as an aerofoil of the same section but aspect ratio 6 at the same Reynolds number in free air.

More exact conversion formulæ may be developed to take account of the actual lift distribution of the model tested. But the changes following this refinement are of the order of 10 per cent. in practice,

representing, as already mentioned, a final variation of usually less than 1 per cent.

188. Open-jet Tunnel

When aerofoils are tested in a free jet, corrections are required to allow for its limited section. These are obtained from the appropriate image system, which differs essentially, however, from that for an enclosed tunnel of the same section. Whereas in the latter case the criterion determining the image system is cancellation of velocity components normal to the walls, with the open jet it is that the pressure at the surface of the jet shall be constant and equal to the pressure of the surrounding air at a distance. The new requirement entails that the tangential velocity at the surface of the jet be reduced to its value in the absence of the aerofoil. Thus tangential, instead of normal, velocity components due to the aerofoil are to be cancelled by the image system.

To verify this, let p_0 be the pressure and U the velocity just within the jet before introducing the model, which adds small increments of velocity u, v, w there. By Bernoulli's equation—

$$p_0 + \tfrac{1}{2}\rho U^2 = p + \tfrac{1}{2}\rho\{(U+u)^2 + v^2 + w^2\}.$$

Hence—

$$p_0 - p = \rho U u,$$

neglecting squares of small quantities, so that for the pressure to remain the same as outside the jet, u must vanish.

An approximate solution is easily seen in simple cases. Take first the case of a two-dimensional aerofoil situated near a parallel flat fluid surface of infinite extent, beyond which the air is at rest. Locate the image as for a wall, i.e. at an equal distance beyond the surface, but reverse the sign of the image, so that circulation round it is in the same direction as round the aerofoil and the two form a biplane of zero stagger. The tangential velocity component due to the combination evidently, from symmetry, vanishes at the surface. The normal velocity component there is doubled, so that the surface is slightly bent, but this effect is often neglected.

The conformal transformation of Article 155 may be applied to a two-dimensional aerofoil in a two-dimensional jet, reversing the sign of the single image in the transformed plane, but not easily.

Take next the important case of a vortex pair symmetrically situated in a jet of circular section, radius a. Reversing the sign of the images at the inverse points gives the system of Fig. 138. With

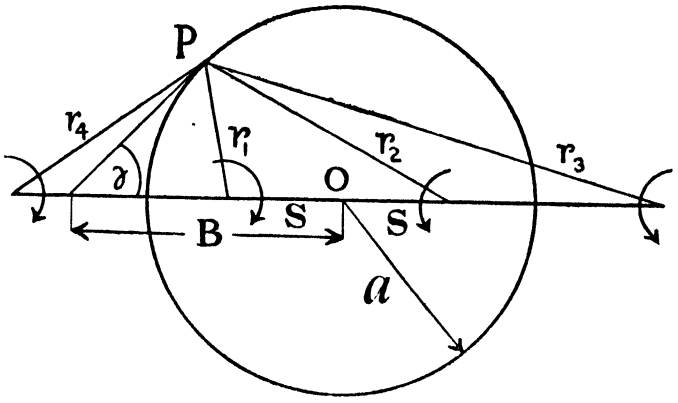

FIG. 138.

the notation of the figure it is easily verified that the tangential velocity at the general point P is proportional to—

$$\sin\gamma\left(\frac{B-s}{r_1^2}-\frac{B+s}{r_2^2}-\frac{B+a^2/s}{r_3^2}+\frac{B-a^2/s}{r_4^2}\right).$$

The expression within the brackets vanishes. Thus the artifice of changing the signs of the reflected vortices again succeeds in regard to the tangential velocity, but the normal component is again varied.

In practice, the correction formulæ of the preceding article are applied to an open jet with their signs changed. But the step is tentative and rests upon experimental justification.

This method is also used for jets of elongated section, such as elliptic or rectangular. For general treatment reference should be made to a paper by Glauert.* A simple rule appears from this and other investigations:—The correction formulæ for enclosed tunnels apply to open jets of the same sections, provided the sign is changed, and also that the aerofoil is rotated through a right angle.

If, with the last proviso, a small aerofoil is tested in an open-jet tunnel and also in an enclosed tunnel of the same size and section, the mean results should give the free air coefficients and incidence.

It must be confessed, however, that the theory of the correction for constraint, being based on ignoring the distortion of jets, is not well founded in their case.

DOWNWASH AT TAIL PLANE

189. The tail plane of an aeroplane is required to exert, with elevators neutral, zero pitching moment about the C.G. of the craft at some

* A.R.C.R. & M., No. 1470.

arranged speed and wing lift coefficient (Article 88). This is achieved by a suitable tail-setting angle. Tail planes may be adjusted (or their lift, e.g. by trimming tabs), but it is desirable to form a close estimate at the design stage of the required tail-setting angle, which depends upon the downwash at the tail position (Article 86).

Unfortunately, the magnitude of the downwash affecting the tail plane is difficult to calculate owing to the lack of precise knowledge of the trailing vortex configuration at this intermediate position behind the wing. The vortex sheet will have partly, but not completely, rolled up, while the existence of any wing-tip vortices close to the wing will affect the calculations.

A rough estimate is obtained by substituting for the actual wing a hypothetical one of equal lift distributed uniformly along a suitably reduced span $2s'$ (cf. Article 166). We then easily find that at the level of the aerofoil and at a distance x downstream from its C.P. the downwash angle is given by—

$$\varepsilon = \frac{K}{4\pi U}\left\{\frac{2s'}{x\sqrt{(s'^2+x^2)}} + \frac{2}{s'}\left[1 + \frac{x}{\sqrt{(s'^2+x^2)}}\right]\right\}.$$

The first term in the curly brackets is the contribution from the wing, the remainder that from the fully developed vortex pair, while K is the uniform circulation of the simplified vortex system. The expression reduces to—

$$\varepsilon = \frac{K}{2\pi U s'}\left\{1 + \frac{\sqrt{(s'^2+x^2)}}{x}\right\}. \quad . \quad . \quad (264)$$

This result is readily expressed in more practical terms. Let the actual wing be of span $2s$ and aspect ratio A and let C_L be its lift coefficient and α its incidence.

For uniform loading $s' = s$, and the factor $K/2\pi Us = C_L/2\pi A$.

Assume alternatively elliptic loading along $2s$. We then have for the factor—

$$\frac{K}{2\pi U s'} = \frac{2}{\pi^2 A}\cdot\frac{s}{s'}C_L$$

from (231), while from (226) $s/s' = 4/\pi$, giving for the factor $8C_L/\pi^3 A$. Then using (236)—

$$(2 + A)\frac{d\varepsilon}{d\alpha} = \frac{16}{\pi^2}\left\{1 + \frac{\sqrt{(s'^2+x^2)}}{x}\right\} \quad . \quad . \quad (265)$$

Put, for example, $x = s$ to represent a possible position of the tail plane. Then we have for that position—

$$\frac{d\varepsilon}{d\alpha} = \frac{3{\cdot}68}{2 + A}$$

giving for $A = 6$, for instance, $d\varepsilon/d\alpha = 0{\cdot}46$. But it should be remembered that such values assume a lift coefficient slope of 2π in two-dimensional flow. Results for other lift distributions along the actual wing are obtained in a similar way.

However, for the reasons stated, (264) cannot be regarded as adequate, and it is more reliable to determine ε by model experiment (Article 86). Observations of downwash require correction for wind-tunnel constraint, and the same difficulty arises in determining the amount of this. On the other hand, we then calculate only a small correction, and error is of far less significance.

190. Tunnel Constraint at Tail Plane

When a complete model of an aeroplane is tested in a wind tunnel, the downwash at the tail plane differs from that in free air. Tail-setting angles observed in an enclosed-type tunnel must be increased, and those observed in an open jet reduced, to allow for the limited expanse of the stream.

As in the preceding article, substitute for the aerofoil one of appropriately shortened span and uniform lift with a fully developed vortex pair springing from the wing-tips. Assume this to be arranged symmetrically in the tunnel and restrict attention to the constraining velocity w along the tunnel axis at distance x behind the C.P. of the aerofoil through which the bound vortex lines are supposed to be concentrated. The constraining velocity w_0, say, at the aerofoil has already received discussion, while its value w_∞ far downstream $= 2w_0$ (Article 148) ; the present problem is to determine intermediate values.

Even with the simplifications adopted analysis tends to be complicated. Glauert and Hartshorn * have obtained :

$$-\frac{w}{U} = \left(0{\cdot}137 + 0{\cdot}24\,\frac{x}{H}\right)\frac{S}{C}\,C_L \quad . \quad . \quad (266)$$

for an enclosed tunnel of square section, of side H and area of cross-section C, S being the area of the aerofoil and C_L its lift coefficient. In the above form the formula may be applied also to biplane models, and modifications of the numbers may be introduced for sections other than square. The formula is especially arranged to hold up to distances downstream representative of normal tail-plane positions, but, the approximation being linear, it must not be applied to greater values of x. Kármán and Burgers † have calculated by

* A.R.C.R. & M., 947, 1924. † *Aerodynamic Theory*, ii, 1935.

means of Bessel functions the constraint in open and enclosed tunnels of circular section. Instead of reproducing these investigations, we shall estimate in an approximate way the constraint for a circular section, using the methods of Chapter VII.

191. Estimate for Circular Section

Let a be the radius of the jet or enclosed tunnel, $2s'$ the span of the equivalent aerofoil of uniform lift, K the circulation round the simplified vortex system, w_v the velocity at x due to the images of the

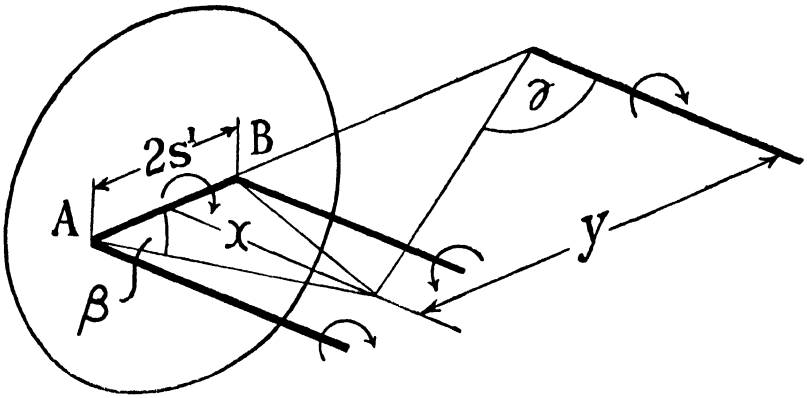

FIG. 139.

vortex pair, w_a the velocity at x due to the image system of the circulation round the aerofoil.

For the total constraining velocity w at x, which is to be subtracted from observation in a jet or added to that in a walled tunnel, we have, omitting sign, $w = w_v + w_a$. It is convenient to express velocity contributions in terms of w_∞. Thus—

$$\frac{w}{w_\infty} = \frac{w_v}{w_\infty} + \frac{w_a}{w_\infty}. \qquad . \quad . \qquad \text{(i)}$$

$w/w_\infty = \frac{1}{2}$ at the aerofoil and $= 1$ far downstream, where w_a vanishes.

Let the distance of the image of each trailing vortex from the axis, which passes through the centre of span, be y. Then $y = a^2/s'$ and—

$$w_\infty = 2\frac{K}{2\pi y} = \frac{Ks'}{\pi a^2}. \qquad . \quad . \qquad \text{(ii)}$$

From Fig. 139—

$$w_v = 2\frac{K}{4\pi y}(1 + \cos\gamma)$$

and therefore—

$$\frac{w_v}{w_\infty} = \tfrac{1}{2}(1 + \cos\gamma) \quad . \quad . \quad \text{(iii)}$$

where $\cos\gamma = x/\sqrt{(x^2 + y^2)}$.

Turning to w_a, substitute for the actual circular boundary a square contour of side H enclosing an equal area, so that—

$$H^2 = \pi a^2 \text{ or } H = a\sqrt{\pi} \quad \text{(iv)}$$

The image system of the aerofoil AB (Fig. 139) is indicated in Fig. 140 for an enclosed tunnel (cf. Article 153), both columns and rows extending infinitely.

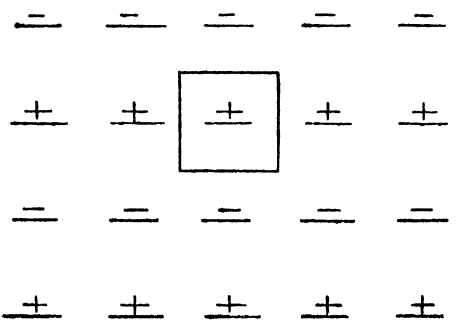

FIG. 140.

If the images in the rows were continuous and two-dimensional conditions held, the velocity at x due to the real vortex would be decreased by the walls in the ratio (cf. Article 155)—

$$\frac{\pi x/H}{\sinh(\pi x/H)}.$$

Since an image of length $2s'$ occupies each length H of the rows, we assume as an approximation that this constraint is to be reduced by the factor $2s'/H$.

The velocity at x due to AB in free air is (Fig. 139)—

$$\frac{K}{4\pi x}\, 2\cos\beta$$

where $\cos\beta = s'/\sqrt{(s'^2 + x^2)}$.

Applying the approximation gives—

$$w_a = \frac{K}{4\pi x}\, 2\cos\beta \left[1 - \frac{\pi x/H}{\sinh(\pi x/H)}\right]\frac{2s'}{H}$$

and since $w_\infty = Ks'/H^2$—

$$\frac{w_a}{w_\infty} = \tfrac{1}{2} \,.\, 2\cos\beta \left[\frac{1}{\pi x/H} - \frac{1}{\sinh(\pi x/H)}\right].$$

Hence, using (iv) and by (i) and (iii)—

$$\frac{w}{w_\infty} = \tfrac{1}{2}\left\{1 + \cos\gamma + 2\cos\beta \left[\frac{1}{x\sqrt{\pi}/a} - \frac{1}{\sinh(x\sqrt{\pi}/a)}\right]\right\}. \quad (267)$$

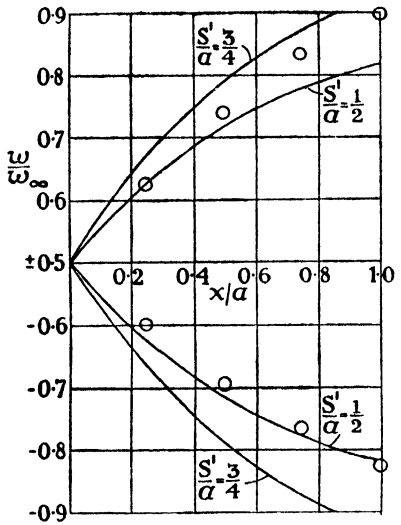

FIG. 141.—CONSTRAINT WITH A CIRCULAR STREAM.

The circles represent Kármán and Burgers' results, the curves the approximation (267). The upper curves show corrections to be added to velocities observed in an enclosed tunnel, the lower curves those to be subtracted from observations in an open jet.

Kármán and Burgers' results are given as suitable for s'/a not much exceeding $\frac{1}{2}$; they are shown as circles in Fig. 141, the upper half of the figure applying to an enclosed stream and the lower to a jet. The curves are obtained from (267) with $s'/a = \frac{1}{2}$ and $\frac{3}{4}$. The curves in the upper half of the figure for an enclosed stream are reflected in the x-axis to apply to a jet.

A model tail plane will seldom be farther downstream than $\frac{1}{2}a$ in an enclosed tunnel or $\frac{3}{4}a$ in an open jet. Thus (267) appears to give a good approximation.

191A. Application

Referring to a monoplane in free flight, let ε be the angle of downwash in the neighbourhood of the tail plane and α the incidence of the wings. A usual problem is to determine $d\varepsilon/d\alpha$ from an estimate of $d\varepsilon_0/d\alpha_0$, the corresponding quantity measured in a wind-tunnel experiment with a model. Let the working section of the tunnel be enclosed and have a cross-sectional area C, and let the area of the aerofoil be S. Then (ii) of the preceding article can be expressed in the form—

$$\frac{w_\infty}{U} = \tfrac{1}{4}\frac{S}{C}C_L,$$

as may be written down alternatively from (262). Denote by B the R.H.S. of (267), which will be known from the conditions of the experiment. Then—

$$\varepsilon = \varepsilon_0 + \frac{BS}{4C}C_L$$

and—

$$\frac{d\varepsilon}{d\alpha} = \frac{d\varepsilon}{d\alpha_0}\cdot\frac{d\alpha_0}{d\alpha} = \left(\frac{d\varepsilon_0}{d\alpha_0} + \frac{BS}{4C}\frac{dC_L}{d\alpha_0}\right)\frac{d\alpha_0}{d\alpha} \quad . \quad \text{(i)}$$

This expression gives a close estimate of $d\varepsilon/d\alpha$ provided the slope of the lift curve of the model in the tunnel is also measured. For by (263)—

$$\frac{d\alpha_0}{d\alpha} = \frac{d}{d\alpha}\left(\alpha - \frac{S}{8C}C_L\right) = 1 - \frac{S}{8C}\frac{dC_L}{d\alpha} \quad . \quad \text{(ii)}$$

and substitution for $dC_L/d\alpha$ can be made without much resulting error from (236) or a modification of that formula.

Alternatively, (i) can evidently be written—

$$\frac{d\varepsilon}{d\alpha} = \frac{d\varepsilon_0}{d\alpha_0}\frac{d\alpha_0}{d\alpha} + \frac{BS}{4C}\frac{dC_L}{d\alpha}, \quad . \quad . \quad . \quad \text{(iii)}$$

a suitable form if the slope of the lift curve is known accurately for the monoplane in free flight.

192. Tail Planes of Biplanes

Superposition of monoplane results to obtain those for multiplane wing systems has already been discussed in Article 86. It must be remembered, however, that $dC_L/d\alpha$ is less for a biplane than for one of its wings separated as a monoplane. Accordingly, $d\varepsilon/d\alpha$ is less than double its value for the monoplane. The factor 0·8 may be applied for aspect ratios in the neighbourhood of 6.

Chapter IX

VISCOUS FLOW AND SKIN DRAG

193. In Chapters V–VIII the viscosity of air was ignored, except in accounting for the production of vorticity in the simplified distributions assumed. Neglect was justified by the successful calculation of practical velocity fields, surface distributions of pressure for slim shapes, the lift and induced drag of wings, and other results of common utility. The artificiality of infinitely thin boundary layers (Article 43) prevented any investigation of skin friction. With modern aircraft of large speed range, however, owing to elimination of form drag and the small lift coefficients normally in use, skin friction is of paramount importance.

Attention is now turned to the force arising within the boundary layer as distinct from that due to pressures transmitted through it, although these two forces are not, of course, independent of one another. If the surface of the body is Aerodynamically smooth in a sense that will be explained later, the force arising is a pure skin friction, as introduced in Chapter II. But the slight roughness of surface of many aircraft bodies is not negligible, and introduces additional drag of the nature of a finely divided form drag. The two components together constitute *skin drag*. For the present we assume sufficient smoothness to avoid the second component.

On reinstating viscosity, calculation immediately becomes difficult, and a feature of our new study is that analysis alone cannot go very far. Mathematical complexity arises essentially from the fact that the flow within long boundary layers at aircraft speeds is for the most part turbulent (Article 21). On the other hand, corresponding boundary layers of experiment may be largely steady. Again, although the whole friction of a body can be measured with comparative ease, the determination of its distribution even round a model in a wind tunnel is by no means simple.

These and other difficulties necessitate oblique attack from several angles, and some of the problems studied are selected for convenience and simplicity rather than on account of their direct application to

aircraft. Such application demands greater intuition and empiricism than is usually called for in Aerodynamics.

PIPE FLOW

194. Parallel, i.e. strictly laminar, flow obtains nowhere past an aircraft, neither does the special type of turbulent flow occurring in pipes at large Reynolds numbers, which is constrained by the long parallel wall to a uniform profile of time-average velocity. The subject is of interest, however, partly as an introduction and also in view of a practical use to be deduced by semi-empirical reasoning.

In experiments with long pipes, fluid is commonly supplied to the mouth or inlet in an agitated state. Initial disturbances usually develop along the pipe into turbulent flow, but in some circumstances they are damped out. The run of pipe required to achieve damping, when this is possible, is called the stilling length. Flow for some distance from the inlet is the same as that in an enclosed-type wind tunnel ; a boundary layer lines the wall, and, increasing in thickness along the pipe, accelerates by its obstruction a central stream whose pressure diminishes according to Bernoulli's equation. After a ' transition length ' the boundary layer fills the whole of the section and, assuming damping, laminar flow becomes established. The form of the laminar flow can be calculated by a development of the method of Article 24.

Steady Flow between two Fixed Parallel Plates.—This is the simplest problem after that of uniform rate of shearing (Article 24). The plates are supposed so large compared with their distance apart h that edge effects may be neglected. Draw Ox (Fig. 142) in the direction of motion midway between the plates, and Oy perpendicular to them. If the flow is steady, the streamlines are everywhere parallel to Ox ; there is no variation of the pressure p except in the direction Ox, and this variation is a constant gradient ; i.e.—

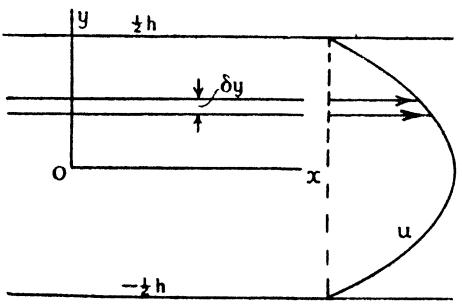

FIG. 142.

$$\frac{\partial p}{\partial y} = \frac{\partial p}{\partial z} = 0, \frac{\partial p}{\partial x} = \text{a constant} = P, \text{ say.}$$

Consider unit length and depth of a stratum of fluid parallel to the plates of thickness δy. In the direction Ox the traction on the lower face is $-\mu \frac{\partial u}{\partial y}$, while that on the upper face is $\mu \frac{\partial}{\partial y}(u + \frac{\partial u}{\partial y}\delta y)$, or there is a resultant traction $\mu \frac{\partial^2 u}{\partial y^2}\delta y$. The force exerted in this direction is $-P \,.\, \delta y$. Hence, since the motion is steady—

$$\mu \frac{\partial^2 u}{\partial y^2} - P = 0.$$

On integration—

$$u = \frac{P}{2\mu} y^2 + Ay + B \quad . \quad . \quad \text{(i)}$$

The condition of no slip at the boundaries (Article 22) states that $u = 0$ when $y = \pm \frac{1}{2}h$, giving two equations for determining the constants of integration A and B:

$$0 = \frac{P}{8\mu} h^2 \pm \frac{A}{2} h + B.$$

From these $A = 0$, $B = -Ph^2/8\mu$. Substituting in (i)—

$$u = \frac{P}{8\mu}(4y^2 - h^2). \quad . \quad . \quad . \quad (268)$$

The distribution of velocity is parabolic, as shown in the figure. For its mean value $\bar{u}$ we have—

$$\bar{u} = \frac{1}{h}\int_{-h/2}^{h/2} u\,dy = -\frac{P}{12\mu} h^2. \quad . \quad \text{(ii)}$$

The propulsive force on the whole mass of fluid per unit length and breadth of the plates is $-Ph$, and must be balanced by the traction on the two plates. Hence, if τ * is the intensity of skin friction on either plate, $-2\tau - Ph = 0$ or—

$$\tau = -\tfrac{1}{2}Ph \quad . \quad . \quad . \quad \text{(iii)}$$

Alternatively, we can calculate τ from the formula (cf. Article 24)—

$$\tau = \pm \mu \left(\frac{\partial u}{\partial y}\right)_{y=0}$$

obtaining the same result if in this case we draw y from the

* It was not possible to use this symbol for the friction per unit area in Chapter II, but the change is now made to a nomenclature which is international. Suffix 0 for the boundary value is omitted where no misconception can arise.

surface concerned into the fluid. The friction coefficient of either plate is—

$$\frac{\tau}{\rho\bar{u}^2} = -\frac{Ph}{2\rho}\left(-\frac{12\mu}{Ph^2}\right)^2 = \frac{6}{R} \quad . \quad . \quad (269)$$

where the Reynolds number $R = \bar{u}h/\nu$.

The vorticity ζ (Article 39) reduces to—

$$\zeta = -\frac{\partial u}{\partial y} = -\frac{Py}{\mu} \quad . \quad . \quad (\text{iv})$$

being zero along Ox, but, away from the axis, having values proportional to distance from it, rising to the maxima $\pm \frac{1}{2}Ph/\mu$ at the plates. If the channel formed between the plates be supposed fed with fluid in an irrotational state, vorticity is seen to be generated by the action of the boundaries and viscosity.

The above results should be compared with those of Article 24. For the same coefficient associated with the uniform rate of shearing there examined, we have, since $\bar{u} = \frac{1}{2}U$—

$$\frac{\tau}{\rho\bar{u}^2} = \frac{1}{\rho\bar{u}^2} \cdot \mu\frac{U}{h} = \frac{2}{R} \quad . \quad . \quad . \quad (270)$$

defining R in the same way as for (269). If, on the other hand, the velocity U of the moving plate were selected to specify R, which is a matter of choice, the friction coefficient would be $1/R$.

195. Steady Flow through Straight Pipe of Circular Section

The pipe is supposed to be very long and only a central length is considered. The assumption of steadiness clearly means that the pressure is constant over each section of the pipe ; its gradient in the direction of flow (Ox) is an absolute constant, P. Consider unit length of a thin concentric cylindrical shell of internal and external radii r and $r + \delta r$. The propulsive force on the shell due to the pressure gradient is $-P \cdot 2\pi r \cdot \delta r$. In the direction Ox the resultant of the internal and external tractions comes to—

$$2\pi\mu\frac{\partial}{\partial r}\left(r\frac{\partial u}{\partial r}\right)\delta r.$$

Therefore, since the flow is steady—

$$\mu\frac{\partial}{\partial r}\left(r\frac{\partial u}{\partial r}\right) - Pr = 0.$$

Integrating—

$$u = \frac{P}{4\mu}r^2 + A\log r + B \quad . \quad . \quad (\text{i})$$

Along the axis of the pipe, where $r = 0$, u cannot be infinite, so $A = 0$. Denote the bore of the pipe by D. When $r = \frac{1}{2}D$ the boundary condition of no slip states that $u = 0$, whence (i) gives $B = -\frac{PD^2}{16\mu}$. Hence the expression for the velocity reduces to—

$$u = \frac{P}{16\mu}(4r^2 - D^2) \quad . \quad . \quad . \quad . \quad (271)$$

The velocity profile is a paraboloid, the speed at the centre being twice the mean, which is given by—

$$\bar{u} = \frac{4}{\pi D^2}\int_0^{D/2} u \,.\, 2\pi r dr = -\frac{PD^2}{32\mu} \quad . \quad . \quad (ii)$$

The propulsive force on the whole mass filling the pipe is $-\frac{\pi}{4}PD^2$ per unit length, and equals the retarding traction $\tau \,.\, \pi D$ at the wall. Hence, if $R = \bar{u}D/\nu$, the friction coefficient is—

$$\frac{\tau}{\rho\bar{u}^2} = \frac{8}{R} \quad . \quad . \quad . \quad . \quad (272)$$

196. Comparison with Experiment

The laws demonstrated in the preceding article were first found to hold for small Reynolds numbers nearly a century ago by Poiseuille and Hagen experimenting independently. This early success furnished a valuable proof of the conception of zero slip at the boundary. Some fifty years later Reynolds established that if the fluid at inlet is in a disturbed state, laminar flow can only result when the Reynolds number ($\bar{u}D/\nu$) is less than 2300, approximately. Experimenting with water in a glass pipe, he showed that a little colouring liquid introduced at inlet formed, below the 'critical Reynolds number,' a steady line parallel to the axis. At greater scales the colouring matter could not be followed, becoming mixed with the stream, which developed a turbulent motion. Later on, Couette examined the jet of water issuing from the outlet end of a pipe. Well below the critical Reynolds number it was crystal clear; well above, it presented a frosted appearance, whilst at the critical stage it oscillated between these two states in a periodic manner.* Simultaneous changes in the trajectory of the jet showed a greater resistance of the pipe to turbulent than to steady flow.

By fitting a nipple at each end of a central length of a long pipe and connecting to a pressure gauge, accurate measurements are easily

* Tietjens, *Applied Hydro- and Aeromechanics*, p 37.

made of the resistance of the length through a wide range in rate of flow, the latter being measured by weighing, with a liquid, or by feeding the fluid through a calibrated orifice in the case of air. A number of such investigations has been carried out with smooth pipes, diameter and fluid being varied, and they provide an excellent check on Rayleigh's formula (Article 47). The dots given in Fig. 143 are mean values obtained from the tests of Stanton and Pannell,

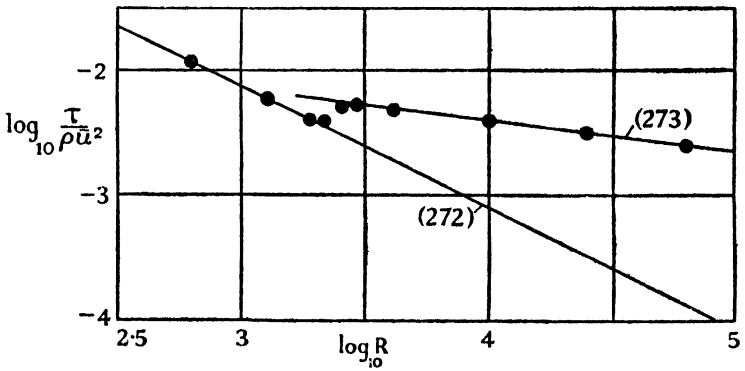

FIG. 143.—FRICTION IN STRAIGHT PIPES OF CIRCULAR SECTION WITH INITIAL TURBULENCE.

Saph and Schoder, and others. The result (272) exactly fits these readings as far $R = 2000$. The friction coefficient at the critical Reynolds number is vague, but for the turbulent flow thereafter the coefficient is increased greatly above its value for laminar flow.

Numerous investigators have demonstrated more recently that if the disturbances at inlet be reduced below a certain small maximum, laminar flow can be established at still higher Reynolds numbers, and by supplying the pipe with an extremely smooth flow the critical stage has been advanced to $R = 20{,}000$.

Experiments of the above kind are frequently undertaken as providing valuable laboratory work, and some precautions against error may be noted. The pipe should be fitted with a bell-mouth at inlet and a stilling length of at least 60 diameters allowed. It should be constrained, if necessary, to straightness; considerable curvature of the axis produces a steady streamline flow of dissimilar form, the centrifugal pressures introduced giving rise to a double corkscrew motion, increasing resistance. Commercial tubes are seldom round, but errors on this score are less important than those due to taper, when kinetic energy must be progressively added to the

stream. A similar error is caused by an insufficient transition length. The laminar velocity profile is approached only asymptotically, and meanwhile kinetic energy is added near the axis, increasing pressure drop. Pipe flow is often employed to calibrate anemometers intended for use very close to a boundary, e.g. the surface of an aerofoil. In such cases it is important to approximate closely to the calculated velocity profile, when a very generous transition length is required. If large critical Reynolds numbers are desired, great care must be exercised to free entering fluid from even such small disturbances as convection currents. In some Aerodynamic laboratories air will be used as the fluid. The orifice box surrounding the inlet should then be of ample proportions and the gauge recording intake pressure difference should be calibrated for low speeds by an aspirator method.

197. Turbulent Flow in Pipes—the Seventh-root Law

The unsteady flow beyond the critical Reynolds number is not susceptible to calculation. When referring to the velocity at any radius we mean the time-average value there. Sufficiently far from the inlet the profile across the section of the time-average velocity remains constant along the pipe ; it is much flatter than for laminar flow, the maximum velocity at the axis being approximately 1·24 times the mean, and the gradient at the wall being steep.

The simplest empirical formula for the friction coefficient (Blasius) is—

$$\frac{\tau}{\rho\bar{u}^2} = 0{\cdot}0395\, R^{-1/4} \quad . \quad . \quad . \quad (273)$$

and holds as far as $R = 10^5$ as shown in Fig. 143. A more general formula, due to Lees,* extends agreement to $R = 5 \times 10^5$, but at greater scales divergence again occurs.

On the basis of (273), if τ denote the skin friction at the wall—

$$\tau = 0{\cdot}0395\ \rho\bar{u}^2 R^{-1/4} = 0{\cdot}0395\ \rho\bar{u}^{7/4}\nu^{1/4}D^{-1/4} \qquad \text{(i)}$$

If we assume that the time-average velocity u distant y from the wall can be related to the axial value u_m by the simple formula—

$$u = u_m\,(y/a)^n = 1{\cdot}24\bar{u}\,(y/a)^n \quad . \qquad \text{(ii)}$$

where $a = \frac{1}{2}D$, the radius of the pipe, and substitute in (i), we find—

$$\tau = 0{\cdot}0228\ \rho\nu^{1/4}u^{7/4}y^{-7n/4}a^{7n/4-1/4} \quad . \qquad \text{(iii)}$$

Now it may be assumed, as an approximation, that as u increases the velocity profile retains its shape, when n in (ii) will be a constant.

* *Proc. Roy. Soc.*, A, v. 91, 1915.

If we further assume that close to the wall u is independent of a, it must follow that—

$$\tfrac{7}{4}n - \tfrac{1}{4} = 0$$

and—

$$n = \tfrac{1}{7}. \quad . \quad . \quad . \quad . \quad (274)$$

This law, due to Prandtl, is (rather surprisingly) found to hold closely throughout the greater part of the section of the pipe, breaking down only near the axis and the wall. It is restricted, of course, to the same range as (273), on which it depends, but at greater Reynolds numbers the index may be progressively decreased as an approximation ; at about 10^7 it becomes 0·10.

The great increase of resistance to turbulent as compared with laminar flow shows that molecular motion can no longer account for the transverse transport of momentum through the bulk of the stream. Past the critical Reynolds number molar masses of fluid penetrate from one radius to another and, compared with the resulting tractional stresses in the fluid, laminar friction is small. This is not the case near to the wall, however, where molar movements must eventually cease. Thus the skin friction is ultimately built up by the same mechanism as for steady flow. The thin film adjacent to the wall through which viscosity predominates is known as the laminar sub-layer, but observations with the ultra-microscope* prevent its being regarded as in a steady state.

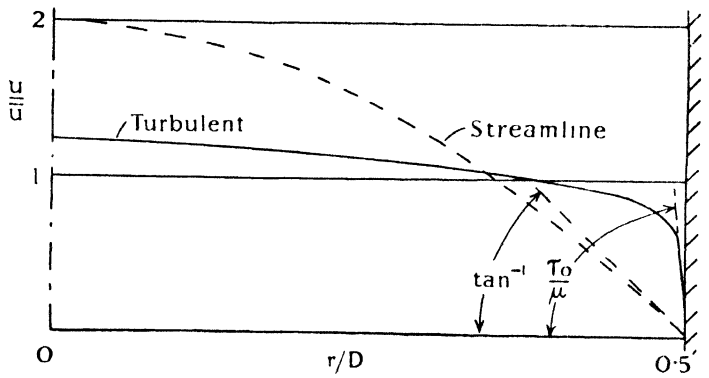

FIG. 144.—VELOCITY DISTRIBUTIONS FOR STREAMLINE AND TURBULENT FLOW THROUGH PIPES.

Through this layer the seventh-root law evidently fails, for we find on differentiating (ii) that τ becomes infinite as y vanishes. To

* Fage and Townend, *Proc. Roy. Soc.*, A, v. 135, 1932.

avoid the anomaly we suppose the velocity profile drawn in accordance with (274) to hold only from near the axis to the edge of the laminar sub-layer, and to be joined to the wall by a straight line having a slope dictated by the known value of τ (Fig. 144).

PIPES WITH CORES

198. Annular Channel

Some problems of practical Aerodynamic interest are conveniently studied in a qualitative manner, both analytically and experimentally, by considering flow through a long pipe fitted with a core that extends through its entire length. The core may be so small compared with a pipe of convenient diameter as to represent, geometrically, a very narrow body in, for example, a 5-ft. wind tunnel. In these circumstances it is possible to neglect, if required, as an approximation, effects of the core on the resistance of the pipe wall and of the general velocity profile on that of the core.

The solution for laminar flow through a circular pipe with a concentric circular core is easily deduced from Article 195. If the core is of diameter d, the constants in (i) of that article are now to be determined with the additional boundary condition : $u = 0$ when $r = \frac{1}{2}d$. To evaluate A and B we have—

$$0 = \frac{P}{16\mu} D^2 + A \log \frac{D}{2} + B$$

and a similar equation with d written for D, whence—

$$u = \frac{P}{16\mu}\left(4r^2 - D^2 + \frac{D^2 - d^2}{\log D/d} \log \frac{D}{2r}\right)$$

and for the mean velocity—

$$\bar{u} = \frac{4}{\pi(D^2 - d^2)} \int_{d/2}^{D/2} u \,.\, 2\pi r dr = -\frac{P}{32\mu}\left(D^2 + d^2 - \frac{D^2 - d^2}{\log D/d}\right).$$

Comparison with Article 195 (ii) shows that a central core of diameter only a few thousandths of that of the pipe suffices to decrease the flux for a given pressure gradient, i.e. to increase resistance, considerably. With large cores the friction approximates to that for flow between parallel planes.

According to some systematic experiments * the critical value of $\bar{u}D/\nu$ at which turbulence develops is delayed 15 per cent. by small cores, 50 per cent. where $d/D = 0{\cdot}15 - 0{\cdot}5$, and increasingly for narrower annuli. But the range for parallel flow is actually

* Piercy, Hooper, and Winny, *Phil. Mag.*, Ser. 7, v. 15, 1933. (The subsequent article is based on the same paper.)

greatly reduced by small cores, a more or less periodic motion of swaying type setting in, owing probably to small variable eccentricity, which increases resistance (such 'secondary motions' often occur in flow through other than straight circular pipes, e.g. in curved pipes, and are not to be confused with turbulence). Thus upper and lower critical speeds occur as shown in Fig. 145. The broken line in this figure illustrates a basis of approximation that is often used when, as in some applications to Aerodynamics, it is sought to correlate results for pipes and channels of different sections. This curve derives the critical values of $\bar{u}D/\nu$ on the assumption that they will vary as the *hydraulic mean depth*, defined as the ratio of the cross-section of a stream to its wetted perimeter. For annular sections this ratio is evidently $(D - d)/4$; for a pipe it is $D/4$; so that the curve gives appropriately $R'D/(D - d)$, where R' applies to the pipe without a core.

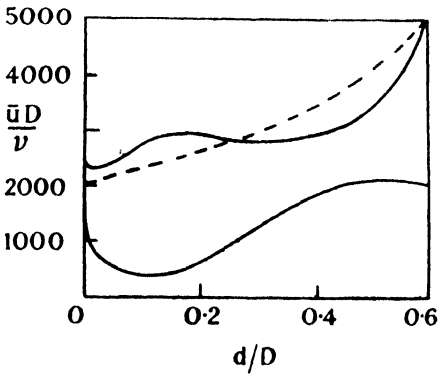

FIG. 145.—CRITICAL REYNOLDS NUMBERS FOR PIPES WITH CORES.

(The broken line gives an approximation based on hydraulic mean depth.)

(*By permission of the Phil. Mag.*)

Attempts have often been made to relate the incidence of turbulence in various cases to a common value of the skin friction coefficient. White * found that $\tau/\rho\bar{u}^2 = 0{\cdot}0045$ applied approximately in this connection to pipes of various curvatures. The value for the straight pipe $= 8/2000 = 0{\cdot}004$. For all annular channels this coefficient lies between 0·0045 and 0·0074. According to the author's experiments, turbulence is developed through wide annuli ($d/D < 0{\cdot}5$) at mean velocities—with a given fluid and pipe—that are proportional to the ratio of the whole friction to that on the pipe wall only.

199. Eccentric and Flat Cores

The analytical problem of eccentric cores and of cores of other than circular section is a little complicated, and must be left to further reading, but some results of interest will be described briefly.

* *Proc. Roy. Soc.*, A, v. 123, 1929.

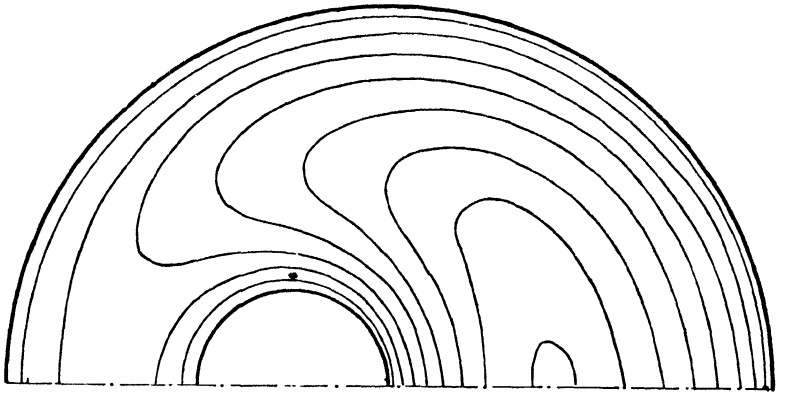

FIG. 146.—ISO-VELOCITY LINES FOR A PIPE WITH AN ECCENTRIC CORE.
(*By permission of the Phil. Mag.*)

Fig. 146 gives the velocity contours for steady flow in a typical case of eccentricity. The flow is notably reduced through the constricted side of the channel, its maximum velocity being only 30 per cent. of that on the open side. The resistance is 12 per cent. less than with the core centrally situated. A similar obstruction to flow through the passage between two bodies is often encountered in Aerodynamic circumstances beyond means of calculation, and the gap is filled in when small.

Fig. 147 shows the percentage increase of resistance to flow through a long pipe, in which there is a core of one-hundredth part its diameter, for varying eccentricity of the core. When eccentricity is a maximum and the core extends as a single corrugation along the pipe wall, the increase with steady flow is negligible. Experiments show the effect of cores to be less marked in turbulent than in streamline flow. In the absence of direct experiments, the result is reassuring as to the drag of a very shallow ridge, much less deep than the boundary layer and parallel to the flow, introduced for constructional reasons along a more or less flat surface.

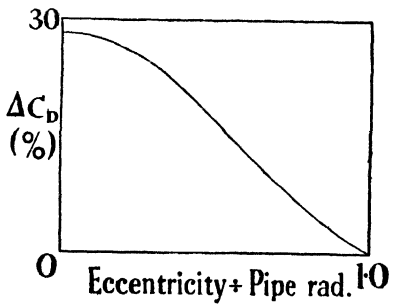

FIG. 147.

In contrast, Fig. 148 indicates the theoretical laminar flow friction variation across a flat core extending as a central strip

within an elliptic pipe. The rapid increase in friction as the sharp edges are approached will be seen, and such edges along the flow should clearly be avoided.

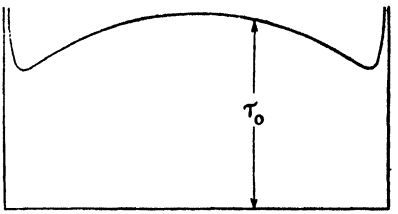

FIG. 148.—VARIATION OF FRICTION ACROSS A THIN FLAT STRIP WITHIN A PIPE OF CONFOCAL ELLIPTIC SECTION (LAMINAR FLOW).

Comparing the total friction of a long flat strip with that along the exterior of a circular cylinder, they come to the same in laminar flow if the diameter of the cylinder is one-half the width of the plate. This result was first obtained by Lees,* considering the resistance to motion of a long plate through fluid contained in a wide stationary cylinder of confocal elliptic section ; it obtains also for the corresponding case of pipe flow, provided the cores are very small.

GENERAL EQUATIONS FOR STEADY VISCOUS FLOW

200. General Motion of the Element

When the flow is steady but non-laminar in the strict sense of the word (Article 21), the element is subject to acceleration, although the velocity at any point in the field is constant. As the element proceeds on its path, it is also subject to variation of vorticity and to a certain stretching under the viscous stresses. We first reduce this compound motion to the simplest terms necessary for framing equations of motion. The matter is illustrated for steady two-dimensional flow, parallel to the xy-plane.

Let u, v be the velocity components parallel to Ox, Oy of the centre G (x, y) of any small fluid element. The component velocities at an adjacent point Q $(x + \delta x, y + \delta y)$ are :

$$u + \delta u = u + \frac{\partial u}{\partial x}\delta x + \frac{\partial u}{\partial y}\delta y,$$
$$v + \delta v = v + \frac{\partial v}{\partial x}\delta x + \frac{\partial v}{\partial y}\delta y. \qquad \text{(i)}$$

Of the terms on the right-hand sides the first represent translation of the element as a whole, which can give rise to no internal friction. The remaining terms express the velocities of Q relative to those of G. We have to deal only with these relative velocities, and may

* *Proc. Roy. Soc.*, A, v. 92, 1915.

shift the origin O to G and imagine it to move with the centre of the element.

The last two terms of the expressions include in general rotation of the element as a whole about an instantaneous axis through G, with angular velocity $\frac{1}{2}\zeta$, where ζ the vorticity $= \frac{\partial v}{\partial x} - \frac{\partial u}{\partial y}$ (Article 39). Introducing for shortness the symbols—

$$a = \frac{\partial u}{\partial x}, \quad b = \frac{\partial v}{\partial y}, \quad c = \tfrac{1}{2}\left(\frac{\partial v}{\partial x} + \frac{\partial u}{\partial y}\right) \quad . \qquad \text{(ii)}$$

equations (i) give—

$$\begin{aligned} \delta u &= a\delta x + c\delta y - \tfrac{1}{2}\zeta\delta y, \\ \delta v &= c\delta x + b\delta y + \tfrac{1}{2}\zeta\delta x \end{aligned} \quad . \quad . \qquad \text{(iii)}$$

and we note that the last terms express rotations such as a rigid body might possess, which again cannot affect internal friction.

It appears, therefore, that the stresses due to viscosity are associated solely with that part of the motion which is expressed by the terms in (iii) involving a, b, c. If δu_1, δv_1 denote components along Gx, Gy of this ' motion of distortion '—

$$\begin{aligned} \delta u_1 &= a\delta x + c\delta y, \\ \delta v_1 &= c\delta x + b\delta y. \end{aligned} \quad . \quad . \qquad \text{(iv)}$$

It is now required to find the principal axes of this motion, i.e. directions at right angles such that all lines drawn parallel to them within the element will be subject only to simple elongation or contraction. Let these axes be Gx', Gy', and let them make an angle α with the original axes. If in these directions a', b' are component *rates of strain* while $\delta u_1'$, $\delta v_1'$ are components of the motion of distortion, the above condition for principal axes is expressed as—

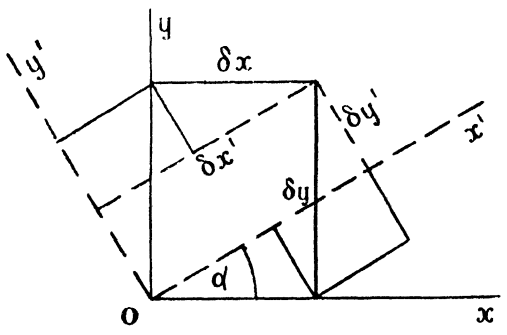

FIG. 149.

$$\delta u_1' = a'\delta x', \quad \delta v_1' = b'\delta y' \quad . \quad . \qquad \text{(v)}$$

Formulæ of transformation from the old to the new systems of axes are readily found, with the help of Fig. 149, to be—

$$\left.\begin{aligned}\delta x' &= \delta x \,.\, \cos\alpha + \delta y \,.\, \sin\alpha,\\ \delta y' &= \delta y \,.\, \cos\alpha - \delta x \,.\, \sin\alpha\end{aligned}\right\} \quad . \qquad \text{(vi)}$$

and—

$$\left.\begin{aligned}\delta u_1' &= \delta u_1 \,.\, \cos\alpha + \delta v_1 \,.\, \sin\alpha,\\ \delta v_1' &= \delta v_1 \,.\, \cos\alpha - \delta u_1 \,.\, \sin\alpha.\end{aligned}\right\} \quad . \qquad \text{(vii)}$$

Substituting for $\delta u_1'$, $\delta x'$ and $\delta v_1'$, $\delta y'$ in (v) from (vi) and (vii)—

$$\left.\begin{aligned}\delta u_1 \cos\alpha + \delta v_1 \sin\alpha &= a'\,(\delta x \cos\alpha + \delta y \sin\alpha),\\ \delta v_1 \cos\alpha - \delta u_1 \sin\alpha &= b'\,(\delta y \cos\alpha - \delta x \sin\alpha).\end{aligned}\right\} \quad \text{(viii)}$$

Eliminating δv_1, δu_1, in turn from these equations gives—

$$\left.\begin{aligned}\delta u_1 &= \delta x\,(a' \cos^2\alpha + b' \sin^2\alpha) + \delta y\,(a' - b')\sin\alpha\cos\alpha,\\ \delta v_1 &= \delta y\,(a' \sin^2\alpha + b' \cos^2\alpha) + \delta x\,(a' - b')\sin\alpha\cos\alpha.\end{aligned}\right\} \quad \text{(ix)}$$

Comparison of (ix) with (iv) shows that—

$$\left.\begin{aligned}a &= a' \cos^2\alpha + b' \sin^2\alpha,\\ b &= a' \sin^2\alpha + b' \cos^2\alpha,\\ c &= \tfrac{1}{2}(a' - b')\sin 2\alpha.\end{aligned}\right\}$$

Finally, we have, making use of the equation of continuity—

$$\left.\begin{aligned}a + b &= a' + b' = 0,\\ a &= a' \cos 2\alpha,\\ c &= a' \sin 2\alpha.\end{aligned}\right\} \quad . \quad . \qquad (275)$$

201. Application to Laminar Flow

As an important example, consider the simple type of steady motion consisting of flow in layers everywhere parallel to the plane xOz and in the direction Ox, the velocity u being a function of y only. Reference to Articles 24 or 194 shows that—

$$\left.\begin{aligned}b &= 0,\\ c &= \tfrac{1}{2}\frac{\partial u}{\partial y} = -\tfrac{1}{2}\zeta,\\ a &= a' \cos 2\alpha = 0.\end{aligned}\right\}$$

Since a' is not zero, $\alpha = 45°$ and the principal axes lie along the diagonals of an originally square element (Fig. 150). Since—

$$a' = -b' = c$$

lines drawn within the element parallel to Gx' elongate at the rate $\frac{1}{2}(\partial u/\partial y)$, while lines drawn parallel to Gy' contract at this rate. These rates of strain result from the stresses whose effects upon the element are fully represented by those of principal component stresses p_1, $-p_1$, tensile and compressive, acting parallel to the principal axes (cf. Article 26).

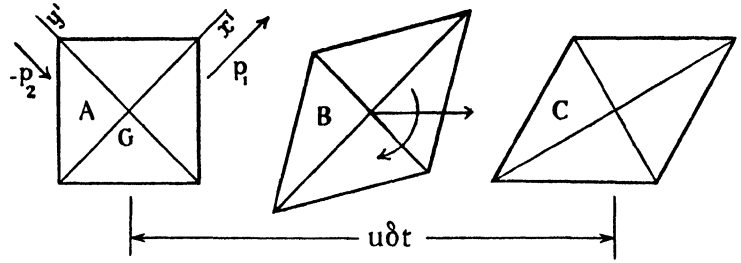

FIG. 150.

Let us follow what happens to the element during a short time δt. First ignoring rotation, it is readily calculated that the x-sides of the element at A become sloped as at B at an angle $\frac{1}{2}\frac{\partial u}{\partial y}.\delta t$. But simultaneously with the motion of distortion, the element has possessed an angular velocity $= -\frac{1}{2}\frac{\partial u}{\partial y}$. By the end of the time interval this has rotated it bodily through the angle $-\frac{1}{2}\frac{\partial u}{\partial y}\delta t$.

Thus the true orientation and shape of the element after δt is as shown at C and, diminishing δt indefinitely, we see that the x-sides of the element remain parallel to Ox consistently with the type of motion assumed in the first place.

202. Expressions for the Stresses

The foregoing analysis removes a difficulty that is sometimes felt with alternative arrangements of the proofs of Articles 24 and 194, and justifies our definition of viscosity. With the help of Article 26 we can now write down convenient formulæ for the stresses. As before, a positive sign is taken to indicate tension and a negative sign compression.

It will be found that the definition of μ requires us to write—

$$p_1 = 2\mu a' - p$$
$$p_2 = 2\mu b' - p = -2\mu a' - p$$

from (275), so that—

$$p_1 - p_2 = 4\mu a'.$$

Using (34), and subsequent formulæ of Article 26 we then find—

$$p_{xy} = \tfrac{1}{2}(p_1 - p_2)\sin 2\alpha = 2\mu c,$$
$$p_{xx} = (2\mu a' - p)\cos^2\alpha - (2\mu a' + p)\sin^2\alpha$$

$$= 2\mu a' \cos 2\alpha - p = 2\mu a - p.$$

The remaining y-component of stress is similarly dealt with.

Now substitute for a, b, c from Article 200 (ii), obtaining—

$$\left.\begin{aligned} p_{xy} &= p_{yx} = \mu\left(\frac{\partial v}{\partial x} + \frac{\partial u}{\partial y}\right), \\ p_{xx} &= 2\mu\frac{\partial u}{\partial x} - p, \\ p_{yy} &= 2\mu\frac{\partial v}{\partial y} - p. \end{aligned}\right\} \quad . \quad . \quad (276)$$

The first of these verifies consistency with the definition of μ.

203. The Equations of Motion

The general equations for *steady* viscous flow in two dimensions are now easily constructed.

Fixing attention on a rectangular element of fluid of sides δx, δy whose centre is at G, the component velocities u and v of G will change as it moves. If Du/Dt, Dv/Dt denote component accelerations, parallel to Ox, Oy, which become apparent when the motion of the element is followed, then for steady flow (Article 1401)—

$$\left.\begin{aligned} \frac{Du}{Dt} &= u\frac{\partial u}{\partial x} + v\frac{\partial u}{\partial y}, \\ \frac{Dv}{Dt} &= v\frac{\partial v}{\partial y} + u\frac{\partial v}{\partial x}. \end{aligned}\right\} \quad . \quad . \quad (i)$$

Resolving parallel to Ox, the forces due to the normal stresses on the two y-sides give a difference $\frac{\partial p_{xx}}{\partial x}\delta x \,.\, \partial y$, while the tractions on the two x-sides give a difference $\frac{\partial p_{yx}}{\partial y}\delta y \,.\, \delta x$. The sum of these is the force on the element in the x-direction, and must equal the product of its mass and acceleration in this direction, i.e.—

$$\rho \,.\, \delta x \delta y \,.\, \frac{Du}{Dt} = \frac{\partial p_{xx}}{\partial x}\delta x \delta y + \frac{\partial p_{yx}}{\partial y}\delta x \delta y$$

or—

$$\left.\begin{aligned} \rho\frac{Du}{Dt} &= \frac{\partial p_{xx}}{\partial x} + \frac{\partial p_{yx}}{\partial y}. \\ \text{Similarly—} \\ \rho\frac{Dv}{Dt} &= \frac{\partial p_{yy}}{\partial y} + \frac{\partial p_{xy}}{\partial x}. \end{aligned}\right\} \quad . \quad . \quad (ii)$$

Substituting for p_{xx}, etc., from (276)—

$$\rho \frac{Du}{Dt} = 2\mu \frac{\partial^2 u}{\partial x^2} - \frac{\partial p}{\partial x} + \mu\left(\frac{\partial^2 v}{\partial x \partial y} + \frac{\partial^2 u}{\partial y^2}\right),$$

$$\rho \frac{Dv}{Dt} = -2\mu \frac{\partial^2 u}{\partial x \partial y} - \frac{\partial p}{\partial y} + \mu\left(\frac{\partial^2 v}{\partial x^2} + \frac{\partial^2 u}{\partial x \partial y}\right).$$

Making use of the equation of continuity (61) to reduce the right-hand sides and substituting from (i) for the left-hand sides, we have finally—

$$\left.\begin{aligned} u\frac{\partial u}{\partial x} + v\frac{\partial u}{\partial y} &= \nu\nabla^2 u - \frac{1}{\rho}\frac{\partial p}{\partial x}, \\ u\frac{\partial v}{\partial x} + v\frac{\partial v}{\partial y} &= \nu\nabla^2 v - \frac{1}{\rho}\frac{\partial p}{\partial y} \end{aligned}\right\} \quad . \quad . \quad (277)$$

where $\nabla^2 = \dfrac{\partial^2}{\partial x^2} + \dfrac{\partial^2}{\partial y^2}$ and $\nu = \dfrac{\mu}{\rho}$.*

These equations may be recast in various forms. For example, eliminating p by cross differentiation and subtracting, and making use of (61) and (65), combines them into the single equation for vorticity—

$$u\frac{\partial \zeta}{\partial x} + v\frac{\partial \zeta}{\partial y} = \nu\nabla^2\zeta. \quad . \quad . \quad . \quad (278)$$

Or again they yield a single expression for the stream function ψ:

$$\frac{\partial \psi}{\partial y} \cdot \frac{\partial}{\partial x}(\nabla^2\psi) - \frac{\partial \psi}{\partial x} \cdot \frac{\partial}{\partial y}(\nabla^2\psi) = \nu\nabla^4\psi \quad . \quad . \quad (279)$$

They may also be expressed in terms of cylindrical co-ordinates. Thus if w, q denote the velocity components in the directions r, θ, respectively, so that $u = w\cos\theta - q\sin\theta$, $v = w\sin\theta + q\cos\theta$, the equations transform to—

$$\left.\begin{aligned} \frac{Dw}{Dt} - \frac{q^2}{r} &= -\frac{1}{\rho}\frac{\partial p}{\partial r} + \nu\left(\nabla^2 w - \frac{w}{r^2} - \frac{2}{r^2}\frac{\partial q}{\partial \theta}\right), \\ \frac{Dq}{Dt} + \frac{wq}{r} &= -\frac{1}{\rho r}\frac{\partial p}{\partial \theta} + \nu\left(\nabla^2 q - \frac{q}{r^2} + \frac{2}{r^2}\frac{\partial w}{\partial \theta}\right). \end{aligned}\right\} \quad . \quad (280)$$

* The equations (277), in generalised three-dimensional form, are fundamental to the theory of motion of real fluids and were evolved by Navier, Poisson, de Saint-Venant and Stokes. The simplified demonstration given is taken from an article by the author in *Aircraft Engineering*, Jan. 1933. Another proof on similar lines has been given by Prescott, *Phil. Mag.*, March 1932. It is also of interest to derive them in terms of molecular motion, as discussed by Jeans, *The Dynamical Theory of Gases.*

These alternative forms are all, of course, exactly equivalent and no simplification exists in one as compared with another.

204. Extension of Skin Friction Formula

Assuming that we can calculate from the viscous equations, and the boundary condition of absence of slip, the velocities and pressures adjacent to central parts of the surface of a long body such as a wing, Aerodynamic force follows from suitable integrations round the contour as explained in Article 44. For this purpose it is required, however, to infer the intensity of skin friction at all points from the velocity gradients, which will be known, while the only formula we have (Articles 23, 24) relates to strictly laminar flow, which will not exist.

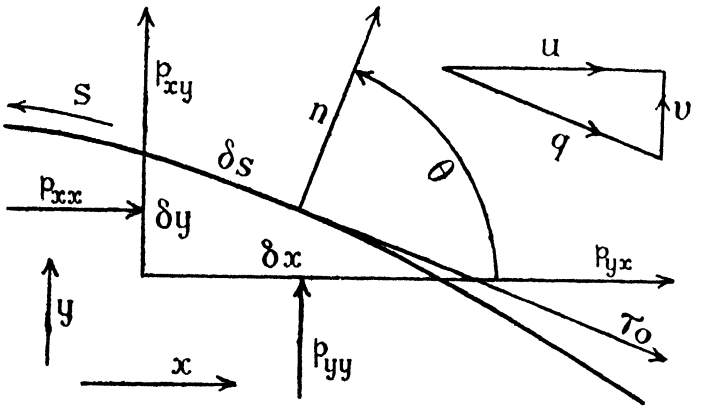

FIG. 151.

The curve in Fig. 151 represents part of the contour of a cylinder in relative motion without rotation parallel to Ox, from which the angle θ of the normal drawn outwards from the element δs is measured. Distance s round the contour is positive in the sense of θ increasing, and n outward along the normal. The force on the element is due to the stresses p_{xx} . . . as shown. If τ_0 is the intensity of skin friction at δs, acting in the direction $-s$, on the upper surface, we have from the figure—

$$\tau_0 \delta s = -\cos\theta\,(p_{xy} \cdot \delta s \cos\theta + p_{yy} \cdot \delta s \sin\theta) + \sin\theta\,(p_{xx} \cdot \delta s \cos\theta + p_{yx} \cdot \delta s \sin\theta).$$

Substituting for p_{xy} . . . from (276)—

$$\frac{\tau_0}{\mu} = \left(\frac{\partial v}{\partial x} + \frac{\partial u}{\partial y}\right)(\sin^2\theta - \cos^2\theta) + 2\left(\frac{\partial u}{\partial x} - \frac{\partial v}{\partial y}\right)\sin\theta\cos\theta. \quad \text{(i)}$$

Now adjacent to the boundary—

$$\frac{\partial}{\partial x} = \cos\theta \frac{\partial}{\partial n} - \sin\theta \frac{\partial}{\partial s},$$

$$\frac{\partial}{\partial y} = \sin\theta \frac{\partial}{\partial n} + \cos\theta \frac{\partial}{\partial s}$$

and on the boundary $\partial u/\partial s = \partial v/\partial s = 0$. Hence (i) becomes—

$$\frac{\tau_0}{\mu} = \left(\cos\theta \frac{\partial v}{\partial n} + \sin\theta \frac{\partial u}{\partial n}\right)(\sin^2\theta - \cos^2\theta) + 2\left(\cos\theta \frac{\partial u}{\partial n} - \sin\theta \frac{\partial v}{\partial n}\right)\sin\theta\cos\theta$$

$$= -\cos\theta \frac{\partial v}{\partial n} + \sin\theta \frac{\partial u}{\partial n} \quad . \quad . \quad . \quad . \quad . \quad \text{(ii)}$$

Let $q = \sqrt{(u^2 + v^2)}$ be the resultant velocity. Differentiating—

$$\frac{\partial q}{\partial n} = \frac{u}{q}\frac{\partial u}{\partial n} + \frac{v}{q}\frac{\partial v}{\partial n}.$$

But adjacent to the boundary $u = q \sin\theta$, $v = -q\cos\theta$. Substituting in (ii)—

$$\tau_0 = \mu\left(\frac{\partial q}{\partial n}\right)_{n=0} \quad . \quad . \quad . \quad (281)$$

or the skin friction is obtained from the boundary value of the velocity gradient along the normal.

This formula is equally significant as giving the skin friction from *measurements* of resultant velocity, though we shall find later on that in experiment a different method is often more convenient. It must be observed that if on the boundary $\partial u/\partial s$, $\partial v/\partial s$ fail to vanish, as, for example, in the case of a rotating cylinder, the formula does not hold.

It is easily verified that—

$$-\frac{\partial q}{\partial n} = \zeta_0$$

the boundary value of the vorticity at the position considered. Complete expressions for the drag and lift, corresponding to those of Article 44, may be left as an exercise. They come to—

$$L = \int_c p\,dx - \mu\int_c \zeta_0\,dy,$$
$$D = -\int_c p\,dy + \mu\int_c \zeta_0\,dx \quad . \quad . \quad . \quad (282)$$

the suffix indicating that the integrals are to extend completely round the contour.

VISCOUS CIRCULATION AND CURVED FLOW

205. Suppose a long circular cylinder of diameter d, pivoted axially in an unlimited expanse of still air, to be given a steady angular velocity ω_0. The boundary condition of no slip, together with the action of viscosity, will generate a motion of the fluid round it. If this becomes steady, the velocity q at any point in the fluid must evidently be perpendicular to the radius r.

We will first solve the problem as an application of the general equations of motion. Since $w = 0$ and q is independent of θ, most of the terms of (280) vanish and the equations finally reduce to—

$$\frac{q^2}{r} = \frac{1}{\rho}\frac{\partial p}{\partial r} \quad . \quad . \quad \text{(i)}$$

$$\frac{\partial^2 q}{\partial r^2} + \frac{1}{r}\cdot\frac{\partial q}{\partial r} - \frac{q}{r^2} = 0 \quad . \quad . \quad \text{(ii)}$$

the first expressing the requirement that centrifugal force per unit volume must be balanced by the pressure gradient.

Since q is a function of r only, assume as a solution $q = Ar^n$. Substituting in (ii)—

$$n(n-1)\,Ar^{n-2} + n\frac{A}{r}r^{n-1} - \frac{A}{r^2}r^n = 0$$

or—

$$n = \pm 1.$$

Hence the general solution is—

$$q = Ar + \frac{B}{r}$$

where A and B are constants to be determined by the boundary conditions, which are : $q = \frac{1}{2}\omega_0 d$, when $r = \frac{1}{2}d$, $q = 0$ when $r = \infty$. Thus $A = 0$ and $B = \frac{1}{4}\omega_0 d^2$, so that finally—

$$q = \frac{\omega_0 d^2}{4r} \quad . \quad . \quad . \quad . \quad (283)$$

or the product qr = constant.

It will be seen that the flow is identical with irrotational circulation round a circular cylinder in an inviscid fluid. Denoting by ω the angular velocity of any concentric cylindrical surface of the fluid, we have $v = \omega x$, $u = -\omega y$ (taking the origin at the centre of the cylinder) and since $\omega = q/r = B/r^2$—

$$\zeta = \frac{\partial}{\partial x}\left(\frac{Bx}{x^2+y^2}\right) + \frac{\partial}{\partial y}\left(\frac{By}{x^2+y^2}\right) = 0.$$

Hence the viscous flow is indeed irrotational.

With the viscous fluid, however, a moment M per unit length must be applied to the cylinder to maintain the motion. The traction is constant round the cylinder, and we may choose to evaluate it on the y-axis where the tractional stress in the fluid is p_{yx}. Hence from (276)—

$$\tau = \mu\left(\frac{\partial v}{\partial x} + \frac{\partial u}{\partial y}\right)_{x=0} = \left(\frac{2\mu B}{r^2}\right)_{r=d/2}$$

$$= 2\mu\omega_0. \quad . \quad . \quad \text{(iii)}$$

For the torque—

$$M = (2\pi r\tau \,.\, r)_{r=d/2} = \pi\mu\omega_0 d^2.$$

If q_0 is the peripheral speed of the cylinder and R is specified by $q_0 d/\nu$, we find the following convenient formula for the moment coefficient—

$$C_M = \frac{M}{\frac{1}{2}\rho q_0^2 d \,.\, d} = \frac{4\pi}{R}. \quad . \quad . \quad . \quad (284)$$

The above result may be more simply obtained from the consideration that the moment just calculated must be the same for all coaxial cylindrical surfaces in the fluid. If this were not so, some shell of fluid would gain or lose angular momentum, which would be contrary to the assumption of steadiness.

Putting $v = \omega x$, $u = -\omega y$, it is found that the tractional stress round a coaxial surface of radius r is $\mu r \,.\, d\omega/dr$. Hence the moment is $\mu 2\pi r^3 \,.\, d\omega/dr$ and, since this is constant—

$$\frac{d\omega}{dr} = \frac{C}{r^3}$$

where C is a constant, and on integrating—

$$\omega = -\frac{C}{2r^2} + E.$$

Applying the boundary conditions evaluates C and E, and substitution gives (283).

206. Rotating Cylinder within Fixed Concentric Cylinder

This case is readily deduced from the preceding article. Let the outer cylinder be of diameter D. Then the boundary conditions now determining A and B are the same at the inner radius but $q = 0$ when $r = \frac{1}{2}D$. Hence—

$$A = -\frac{\omega_0 d^2}{D^2 - d^2} = -\frac{4B}{D^2}$$

and substitution of these values in the expression $q = Ar + B/r$ gives—

$$q = \frac{\omega_0 d^2}{4r}\left(\frac{D^2 - 4r^2}{D^2 - d^2}\right).$$

The torque on the inner cylinder, which is equal and opposite to that on the outer one, is—

$$M = \pi\mu\omega_0 d^2 \cdot \frac{D^2}{D^2 - d^2}$$

giving a moment coefficient on the same basis as before—

$$C_M = \frac{4\pi}{R} \cdot \frac{D^2}{D^2 - d^2} \quad . \quad . \quad . \quad . \quad (285)$$

The case of the inner cylinder being fixed while the outer one rotates is solved similarly.

207. Curved Flow in Experiment

We have already seen, in examining vortices, Chapter VII, that a circulatory flow very similar to that calculated in Article 205 can exist in air. When the fluid is contained between two concentric cylinders of different sizes, revolving at different rates, qr need not be constant. The stability of this more general case was first examined by Rayleigh, ignoring viscosity.

Let it be assumed that an element of mass m and volume V, initially circulating at radius r_1 with velocity q_1, is displaced by a disturbance to a greater radius r_2 without change of its moment of momentum. For either radius the condition for equilibrium is, from Article 205 (i)—

$$m\frac{q^2}{r} = V\frac{\partial p}{\partial r}.$$

If the force on the element due to the pressure gradient, viz. $-V\dfrac{\partial p}{\partial r}$ acting inwardly, exceeds its centrifugal force at the new radius, $m\left(\dfrac{r_1}{r_2}q_1\right)^2 \cdot \dfrac{1}{r_2}$, the element will be forced back. Thus the motion is stable if—

$$\frac{q_2^2}{r_2} > \left(\frac{r_1}{r_2}q_1\right)^2 \frac{1}{r_2}$$

or—

$$r_2^2 q_2^2 > r_1^2 q_1^2$$

i.e. if the square of the circulation increase outwards. If this decrease the motion is unstable.

It is found in experiment that an outer cylinder may be revolved rapidly round a fixed one before eddying occurs in fluid contained between them. Rotation of the inner cylinder, on the other hand, the outer one being fixed, produces eddying at a comparatively low speed, although viscosity advantageously modifies the foregoing criterion.* Steady flow may be realised in a well-known type of rational viscometer the construction of which will be evident, if it is not familiar.

Rayleigh's investigation may also be applied in principle to explain a striking phenomenon that is observed in front of stagnation

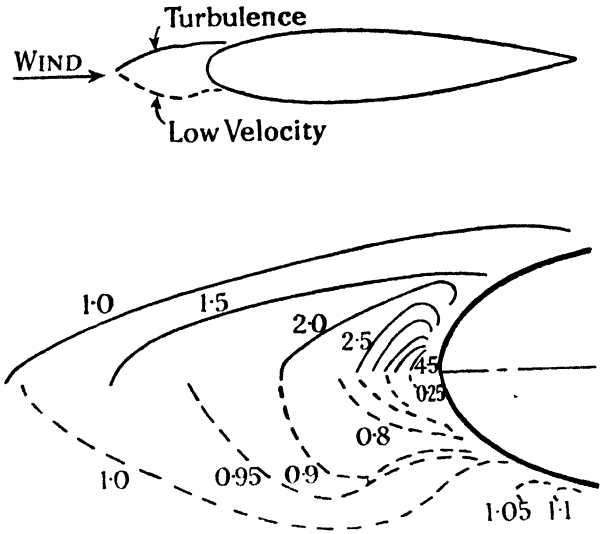

FIG. 152.—TURBULENCE SURROUNDING THE FRONT STAGNATION POINT OF A STRUT.

A similar phenomenon is observed with wings. The contours in the enlarged lower diagram give: ———— velocity amplitude; - - - - - - mean velocity.

points, at least when the oncoming stream is not specially smooth. Fluid approaching a body exerts centrifugal force towards the surface, maintaining its path against a pressure drop outwards from the stagnation point (or line). Particles approaching the surface of the body closely have their energy reduced by viscosity and, if displaced outwards by a disturbance, find themselves with insufficient centrifugal force to oppose to the pressure gradient, and so are forced

* Taylor (Sir Geoffrey), *Phil. Trans. Roy. Soc.*, A, *v.* 223, 1923.

out farther. Thus the stagnation point becomes the centre of a region of weak turbulence extending in front of the body. Farther round the contour of the body the product qr increases outwards, so that we should expect stability, and, in fact, the turbulence is damped out there.

Fig. 152 shows the region of instability and, for comparison, that of time-average velocity reduction in front of a strut. The enlarged view gives contours of mean amplitude of velocity variation, as determined by a hot wire connected with a vibration galvanometer, and also contours of time-average velocity ($R = 2{\cdot}1 \times 10^5$).* The undisturbed flow in the wind tunnel, in which the experiments were conducted, was known to be rather turbulent.

APPROXIMATIONS TO THE VISCOUS EQUATIONS

208. The general equations obtained in Article 203 are formidable, and their solution for flow past a given body, though steadiness be assumed, presents considerable difficulty. To make use of them drastic simplification is required, and various curtailed forms have been suggested as appropriate to different circumstances.

If the velocity be very small and the viscosity large, all the terms on the left-hand side of (279), having to do with the inertia of the fluid and not its viscosity, may be neglected, reducing the equation to—

$$\nabla^4\psi = 0. \quad . \quad . \quad . \quad . \quad (286)$$

This approximation is due to Stokes, and the range of Reynolds number to which it may be applied is known after him. Such motions are minute, however, even from an experimental point of view.

Another approximate form, taking considerable though incomplete account of the inertia terms, was introduced more recently by Oseen ; it is—

$$\nu\nabla^4\psi = U\nabla^2(\partial\psi/\partial x) \quad . \quad . \quad . \quad (287)$$

where U is the undisturbed velocity. This equation is appropriate to the Reynolds numbers of anemometry and has been so employed by Lamb, Bairstow, and others. Bairstow has also suggested its value for obtaining rough approximations at somewhat higher Reynolds numbers and, with Misses Cave and Lang, has developed integral equations for application to symmetrical cylinders.†

* Piercy and Richardson, *Phil. Mag.*, v. 9, 1930. Cf. also the same authors, *Phil. Mag.*, v. 6, 1928 (circular cylinder), and A.R.C.R. & M., 1224, 1928 (aerofoil).

† *Phil. Trans. Roy. Soc.*, A, v. 223, 1923.

209. Prandtl's Boundary Layer Equations

The approximation of greatest interest in Aerodynamics is that due to Prandtl, and depends upon the assumption that viscous effects are confined to a boundary layer, Article 43, a feature that is characteristic of most Aerodynamic motions. The process of simplification consists of examining the relative orders of magnitude of the various terms of (277) when a thin boundary layer exists, and will be explained for the case of flow along a flat plate.

Ox is taken in the plane of the plate parallel to the undisturbed flow and Oy perpendicular to the plate, the origin being at the nose. On account of the thinness assumed for the boundary layer, y and v are small compared with x and u, which, together with p, are taken to be of normal order. Since v is small, it follows that in the second equation of (277) all other terms may be neglected in comparison with the p-term. Hence this equation reduces to—

$$\frac{\partial p}{\partial y} = 0. \quad . \quad . \quad . \quad . \quad (288)$$

In Article 42 we found, as a matter of experiment, that the pressure generated just outside the boundary layer is transmitted through it to the surface of the body without change. The result (288) follows equally for curvilinear and unsteady flow. Thus theoretical justification exists for the experimental result.

Turning to the first equation of (277), we find that the first term of $\nabla^2 u$, viz. $\partial^2 u/\partial x^2$, is negligible in comparison with the second term : $\partial^2 u/\partial y^2$. This is the only simplification that can be made in usual circumstances, and the first equation therefore reduces to—

$$u\frac{\partial u}{\partial x} + v\frac{\partial u}{\partial y} = \nu\frac{\partial^2 u}{\partial y^2} - \frac{1}{\rho}\frac{\partial p}{\partial x}. \quad . \quad . \quad (289)$$

On account of the smallness of y, $\partial^2 u/\partial y^2$ is large and, if the order of magnitude of y be denoted by ε, it will be of order $1/\varepsilon^2$. For all the terms of the equation to be of the same order, ν requires to be of order ε^2. The thickness of the boundary layer in the y-direction is then proportional to $\sqrt{\nu}$ or, more generally, to $1/\sqrt{R}$.

FLAT PLATE SKIN FRICTION WITH STEADY FLOW

210. Application of Oseen's Approximation

The flat or tangential plate of limited chord (c) provides the easiest problem of direct Aerodynamic interest. Break-away (Article 159) does not occur, and the flow is found experimentally to remain steady

up to Reynolds numbers (Uc/ν) exceeding 5×10^5 even in moderately turbulent tunnels.

The problem has been solved * to Oseen's approximation in a general way. Although, for reasons stated in Article 208, this

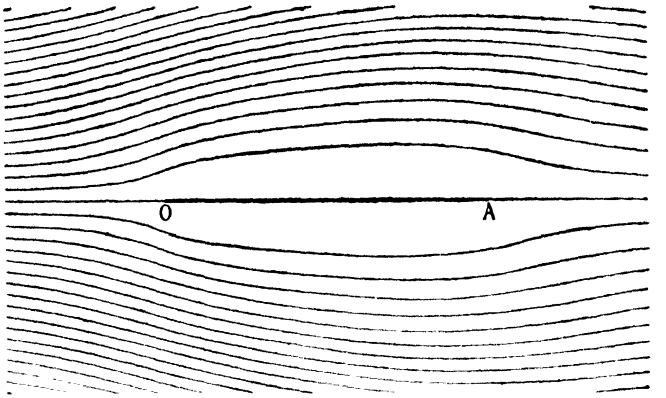

FIG. 153.—STREAMLINES TO OSEEN'S APPROXIMATION FOR A FLAT PLATE AT $R = 4$.

(*Figs* 153–5 *are reproduced by permission of the Royal Society.*)

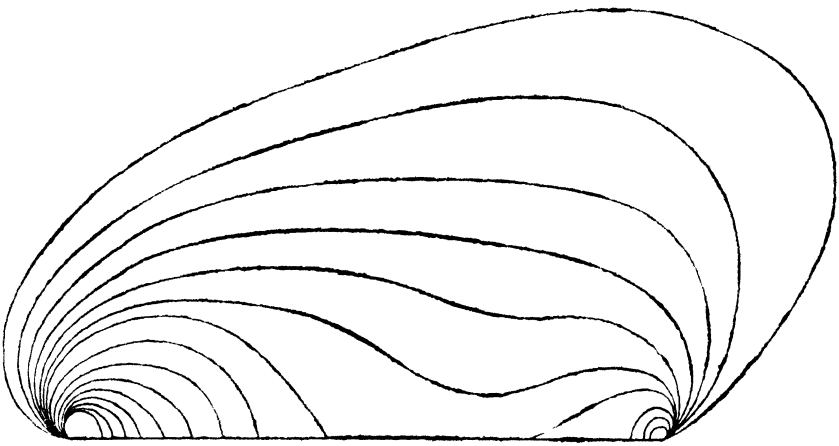

FIG. 154.—VORTICITY CONTOURS TO OSEEN'S APPROXIMATION FOR A FLAT PLATE AT $R = 4$, SHOWING THE WIDESPREAD DISTRIBUTION CHARACTERISTIC OF LOW REYNOLDS NUMBERS.

solution must diverge from fact at the larger scales, it is of interest to notice some of the results, particularly as they describe in an approximate manner how a boundary layer comes into being as Reynolds number increases.

* Piercy and Winny, *Proc. Roy. Soc.*, A, v. 140, 1933

The drag coefficient is found to be given by—

$$\tfrac{1}{2}C_D = \frac{4}{\sqrt{(\pi R)}} + \frac{1{\cdot}4839}{R}. \quad . \quad . \quad . \quad (290)$$

Thus the coefficient is large at anemometric scales. Fig. 153 shows the streamlines and Fig. 154 the vorticity contours for $R = 4$, and evidently no boundary layer has begun to form at this small scale. Fig. 155 shows in contrast the vorticity contours for $R = 4 \times 10^4$; the linear scale perpendicular to the plate is magnified in the figure

FIG. 155.—VORTICITY CONTOURS TO OSEEN'S APPROXIMATION FOR A FLAT PLATE AT $R = 4 \times 10^4$.

The linear scale perpendicular to the plate is *magnified ten times.* Comparison with Fig. 154 illustrates the growth of a boundary layer with increase of Reynolds number.

ten times, so that the boundary layer that now exists is very thin. The drag coefficient is now close to its asymptotic value, the second term of (290) almost vanishing; this value exceeds that of mean experiment by 60 per cent.

At large Reynolds numbers the velocity u at any point x, y, is given theoretically by the formula—

$$u = \frac{2U}{\sqrt{\pi}} \int_0^{\sqrt{\frac{Ry^2}{4xc}}} e^{-z^2} dz \quad . \quad . \quad . \quad (291)$$

whose values may be written down from tables of the probability integral. Thus the velocity is then a function of $y/\sqrt{\nu x/U}$ only. If we agree to mark the edge of the boundary layer by 1 per cent. decrease in velocity and denote its thickness on either side of the plate by Δ, then at distance x from the nose—

$$\Delta_x = 3{\cdot}64\sqrt{\nu x/U} \quad . \quad . \quad . \quad (292)$$

and at the trailing edge of the plate—

$$\frac{\Delta}{c} = \frac{3{\cdot}64}{\sqrt{R}}. \quad . \quad . \quad . \quad . \quad (293)$$

This result is probably within 30 per cent. of the thickness of the experimental boundary layer, which is rather thicker.

A point of particular interest may be noted at the trailing edge of

the plate in Fig. 155. The concentration of vorticity there may herald the production of an eddy at larger Reynolds numbers.

211. Application of Prandtl's Approximation

The flat plate problem has been solved to Prandtl's approximation by Blasius.* This solution, as will be anticipated, is essentially asymptotic, applying only to Reynolds numbers sufficient for a thin boundary layer to exist, and cannot be used in the anemometer range. The drag coefficient (after very slight modification by Töpfer) comes to—

$$C_D = 2{\cdot}656/\sqrt{R} \quad . \quad . \quad . \quad . \quad (294)$$

and is only some 6 per cent. less than mean experiment through the range $R = 10^4 - 5 \times 10^5$.

On the same basis as (293) the thickness at the trailing edge of the boundary layer is given by—

$$\frac{\Delta}{c} = \frac{5{\cdot}5}{\sqrt{R}} \quad . \quad . \quad . \quad . \quad (295)$$

It thickens along the plate in the same parabolic way as in (292).

It may be remarked that the convention adopted above for marking the edge of the boundary layer is arbitrary, and different writers use different systems. If a greater percentage drop in velocity is adopted, the factors in (295) and (293) are smaller.

Instead of discussing Blasius's solution, which is somewhat complex, the problem will be solved approximately by a shorter method † which is of use in some more difficult cases.

212. Method of Successive Approximation

The flow is assumed to be steady, of undisturbed velocity U, and R ($= Uc/\nu$, c being the chord of the plate) sufficiently large for a thin boundary layer to exist. The pressure is then nearly constant throughout the flow, ignoring the edges of the plate, so that Prandtl's equations reduce to—

$$u\frac{\partial u}{\partial x} + v\frac{\partial u}{\partial y} = \nu\frac{\partial^2 u}{\partial y^2}. \quad . \quad . \quad . \quad (296)$$

The boundary conditions are $u = v = 0$ on the plate and $u = U$, $v = 0$ at ∞.

* *Zeits. f. Math. u. Phys.*, 1908.
† Piercy and Preston, *Phil. Mag.*, Ser. 7, v. 21, 1936.

If u_1, v_1 are known as first approximations to u and v, the equation—

$$u_1 \frac{\partial u_2}{\partial x} + v_1 \frac{\partial u_2}{\partial y} = \nu \frac{\partial^2 u_2}{\partial y^2}$$

may be regarded as an equation for determining a second approximation u_2. A corresponding second approximation to v, viz. v_2, can then be obtained from the equation of continuity and the boundary conditions. Repeating the process gives a third approximation.

Successive approximations will not in all problems exhibit the convergence necessary for success, so that application of the method is tentative. But if they do, a sufficient number of reiterations secures what degree of accuracy may be desired in the solution of (296).

213. Transformation of the Equation

We now make the substitutions $\bar{u} = u/U$, $\bar{v} = v/U$, so that the boundary conditions become $\bar{u} = \bar{v} = 0$ on the plate, while at ∞ $\bar{u} = 1$, $\bar{v} = 0$.

Also, we transform the equations from the co-ordinates x, y to ξ, η given by—

$$\xi = \sqrt{\frac{Ry^2}{4xc}}, \quad \eta = \frac{x}{c}.$$

For this purpose we note that—

$$\frac{\partial \xi}{\partial x} = -\tfrac{1}{2}\sqrt{\frac{Ry^2}{4x^3c}} = -\frac{\xi}{2\eta c},$$

$$\frac{\partial \xi}{\partial y} = \sqrt{\frac{R}{4xc}} = \sqrt{\frac{R}{4}} \cdot \frac{1}{c\sqrt{\eta}},$$

$$\frac{\partial \eta}{\partial x} = \frac{1}{c}; \quad \frac{\partial \eta}{\partial y} = 0$$

and, since it will be found that $\partial u/\partial \eta = 0$ gives a solution satisfying the boundary conditions, that with this simplification—

$$\frac{\partial u}{\partial x} = \frac{\partial u}{\partial \xi}\frac{\partial \xi}{\partial x} + \frac{\partial u}{\partial \eta}\frac{\partial \eta}{\partial x} = -\frac{\xi}{2\eta c}\frac{\partial u}{\partial \xi},$$

$$\frac{\partial u}{\partial y} = \frac{\partial u}{\partial \xi}\frac{\partial \xi}{\partial y} + \frac{\partial u}{\partial \eta}\frac{\partial \eta}{\partial y} = \sqrt{\frac{R}{4}} \cdot \frac{1}{c\sqrt{\eta}}\frac{\partial u}{\partial \xi},$$

whence also—

$$\frac{\partial^2 u}{\partial y^2} = \frac{R}{4c^2\eta}\frac{\partial^2 u}{\partial \xi^2}.$$

We can write down from the preceding article the equation in x and y for determining the nth approximation. In terms of the non-dimensional velocities it is—

$$\bar{u}_{n-1}\frac{\partial \bar{u}_n}{\partial x} + \bar{v}_{n-1}\frac{\partial \bar{u}_n}{\partial y} = \nu\frac{\partial^2 \bar{u}_n}{\partial y^2}$$

and on transformation to ξ, η it becomes—

$$\left(-\bar{u}_{n-1}\frac{\xi}{2} + \bar{v}_{n-1}\sqrt{\frac{\overline{R\eta}}{4}}\right)\frac{d\bar{u}_n}{d\xi} = \tfrac{1}{4}\frac{d^2\bar{u}_n}{d\xi^2}. \quad . \quad (297)$$

It is required to substitute for v_{n-1} from the equation of continuity, which in terms of x and y is—

$$\frac{\partial \bar{u}_{n-1}}{\partial x} + \frac{\partial \bar{v}_{n-1}}{\partial y} = 0$$

and transforms to—

$$-\xi\frac{d\bar{u}_{n-1}}{\partial \xi} + \sqrt{R\eta}\,.\,\frac{d\bar{v}_{n-1}}{d\xi} = 0. \quad . \quad . \quad (298)$$

Hence—

$$\bar{v}_{n-1} = (R\eta)^{-1/2}\int_0^\xi \xi\frac{d\bar{u}_{n-1}}{d\xi}\,d\xi + B$$

$$= (R\eta)^{-1/2}\left(\xi\bar{u}_{n-1} - \int_0^\xi \bar{u}_{n-1}\,d\xi\right)$$

on integration by parts, the constant evidently vanishing by the boundary condition on the plate. For convenience write—

$$f_{n-1}(\xi) \equiv -2\int_0^\xi \bar{u}_{n-1}\,d\xi. \quad . \quad . \quad (299)$$

Substituting for $\bar{v}_{n-1}$ reduces (297) to the simple form—

$$\frac{d^2\bar{u}_n}{d\xi^2} = f_{n-1}(\xi)\frac{d\bar{u}_n}{d\xi}. \quad . \quad . \quad . \quad (300)$$

Integrating once—

$$\log\frac{d\bar{u}_n}{d\xi} = \int_0^\xi f_{n-1}(\xi)\,d\xi + A_n'$$

or—

$$\frac{d\bar{u}_n}{d\xi} = A_n e^{\int_0^\xi f_{n-1}(\xi)\,d\xi}.$$

Integrating again—

$$\bar{u}_n = A_n\int_0^\xi e^{\int_0^\xi f_{n-1}(\xi)\,d\xi}\,d\xi + C. \quad . \quad (301)$$

Since $\bar{u}_n = 0$ on the plate, where $\xi = 0$, evidently $C = 0$, and since $\bar{u}_n = 1$ at ∞ we have—

$$\frac{1}{A_n} = \int_0^\infty e^{\int_0^\xi f_{n-1}(\xi)\,d\xi}\,d\xi. \quad . \quad . \quad . \quad (302)$$

Formulæ for the Skin Friction

Denoting by F_n the nth approximation to the total skin friction over the plate—

$$F_n = 2\mu \int_0^c \left(\frac{\partial u_n}{\partial y}\right)_{y=0} dx.$$

In terms of the new co-ordinates this becomes—

$$F_n = 2\mu U \int_0^c \sqrt{\frac{R}{4xc}} \left(\frac{\partial \bar{u}_n}{\partial \xi}\right)_{\xi=0} dx$$

or from (301)—

$$F_n = \mu U \sqrt{\frac{R}{c}} \int_0^c \left(A_n e^{\int_0^\xi f_{n-1}(\xi)\,d\xi}\right)_{\xi=0} x^{-1/2} dx$$

$$= 2\mu U A_n \sqrt{R} \quad . \quad . \quad . \quad . \quad . \quad . \quad (303)$$

Hence—

$$\tfrac{1}{2}C_D = \frac{F_n}{\rho U^2 c} = \frac{2A_n}{\sqrt{R}}. \quad . \quad . \quad . \quad . \quad . \quad (304)$$

214. Evaluation

We have to assume a first approximation to the velocities and we take those of inviscid flow, so that $\bar{u}_1 = 1$, $\bar{v}_1 = 0$ everywhere. From (299) we then have $f_1(\xi) = -2\xi$. (302) gives—

$$\frac{1}{A_2} = \int_0^\infty e^{-\xi^2} d\xi = \frac{\sqrt{\pi}}{2}.$$

Then from (301) and (304)—

$$\bar{u}_2 = \frac{2}{\sqrt{\pi}} \int_0^\xi e^{-\xi^2} d\xi \quad . \quad . \quad . \quad . \quad (305)$$

$$\tfrac{1}{2}C_{D2} = 4/(\pi R)^{1/2} = 2{\cdot}257\ R^{-1/2}.$$

Comparing with Article 210, it appears that the second approximation is the asymptotic solution to Oseen's equation. Tables exist

for the integral in the expression for $\bar{u}_2$, but we shall approximate by expanding $e^{-\xi^2}$ and retaining only the first term, so that—

$$\bar{u}_2 = \frac{2}{\sqrt{\pi}}\,\xi.$$

Then turning to the calculation of the next approximation u_3, (299) gives—

$$f_2(\xi) = -\frac{2}{\sqrt{\pi}}\,\xi^2$$

and from (302) again—

$$\frac{1}{A_3} = \int_0^\infty e^{-\frac{2}{3\sqrt{\pi}}\xi^3} d\xi,$$

a known integral whose value is $(3\sqrt{\pi}/2)^{\frac{1}{3}}\,\Gamma(\frac{4}{3})$, where $\Gamma(\frac{4}{3})$ is the 'gamma' function whose value is 0·894, which we denote for short by k.

Proceeding in this way, we find that we can summarise the results of successive calculations as follows:

$$A_2 = \frac{2}{\sqrt{\pi}},$$

$$A_3 = \frac{1}{k}\left(\frac{A_2}{3}\right)^{1/3},$$

$$A_4 = \frac{1}{k}\left(\frac{A_3}{3}\right)^{1/3} = \frac{1}{k}\left(\frac{A_2}{3}\right)^{(1/3)^2} \cdot \left(\frac{1}{3k}\right)^{1/3},$$

. . . . . .

$$A_n = \frac{1}{k}\left(\frac{A_{n-1}}{3}\right)^{1/3} = \frac{1}{k}\left(\frac{A_2}{3}\right)^{(1/3)^n} \cdot \left(\frac{1}{3k}\right)^{1/3+(1/3)^2+\ldots(1/3)^{n-1}}.$$

The ultimate approximation obtainable by the present analytical method is found by putting $n = \infty$, which gives, since the sum to ∞ of the geometric series $= \frac{1}{2}$—

$$A_\infty = \frac{1}{\sqrt{(3k^3)}}.$$

Writing C_D for the ultimate approximation to the coefficient of the total skin friction, we find, from (304)—

$$C_D = \frac{4A_\infty}{\sqrt{R}} = \frac{2{\cdot}734}{\sqrt{R}} \quad . \quad . \quad . \quad . \quad (306)$$

a result which is only 3 per cent. in error. Such an error is negligible for most practical purposes, but a little numerical work serves * to

* Reference should be made to the paper cited (p. 373) for a convenient method.

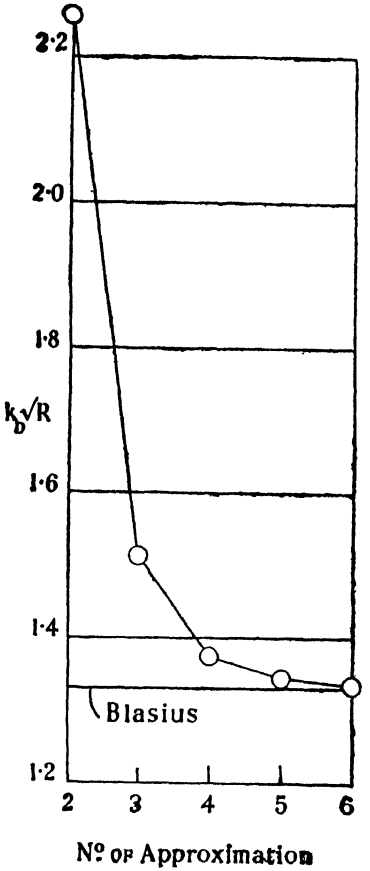

FIG. 156.

take into account the neglected terms of (305), when successive approximations are evaluated as given in Fig. 156 and agreement is reached at the eighth approximation with the elaborate solution of Blasius. Fig. 157 shows dotted the second approximation (305) to the velocity through the boundary layer and also the ultimate result. The ordinate used permits the one curve (full line) to be given for all positions along the plate. Agreement with experiment at high

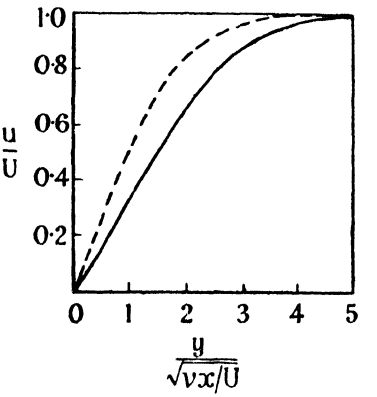

FIG. 157.

($k_D = \frac{1}{2}C_D$)

Reynolds numbers is quite close, although mean results suggest a slightly steeper curve. At small Reynolds numbers, or close to the nose in any case, the dotted line will represent fact. At the nose itself the distribution of velocity is complicated.

EXPERIMENT AND KÁRMÁN'S INTEGRATION

215. Methods of Measurement

The direct way of finding the skin friction at a point on the surface of a plate or cylinder is, from Article 204, to estimate the velocity gradient along the normal. Numerical examples worked out from the foregoing results indicate that the boundary layers of experiment are very thin ; thus at one-tenth of the way along a plate of

1-ft. chord in a stream of 100 ft. per sec. three-quarters of the entire velocity change occurs within a film 0·012 in. thick. It is seen that, to estimate the boundary value of the gradient directly, measurements require to be made within one or two thousandths of an inch from the surface.

Two methods exist for such fine work. In one a wire, of about one-thousandth inch diameter, and heated by an electric current, is held parallel to the surface and perpendicular to the stream by a rigid fork. The fork is fitted with micrometer screws enabling the clearance between surface and wire to be adjusted accurately. Velocity is estimated from the convection of heat from the wire. A serious difficulty arises from the cooling effect of the experimental surface when the clearance is small and the velocity low, and a special technique * is required to determine rather large corrections on this score.

The alternative method uses the fractional pitot tube introduced by Stanton. The specialised form is flat and sunk beneath the surface, so that only a very narrow louvre with a thin lip projects into the stream. Photographs and examples of use are given in a paper by Fage, Falkner, and Walker.† Again a difficulty arises, in that, without special calibration, it is impossible to connect the projection of the lip with effective distance from the surface ; it cannot be assumed that the pressure observed with a given setting refers, for example, to a distance from the wall equal to half the projection.

Calibration may be effected by mounting the pitot tube with the projection to be used in a long smooth pipe whose velocity profile is known.

Example.—A pitot tube 0·4 mm. diameter is calibrated in a straight pipe of 0·24 in. bore delivering 0·33 cu. ft. of air per min. When the mouth of the tube touches the pipe-wall, the pressure observed within it is 0·143 in. water head below the static pressure at a section 18 in. upstream. Show that the velocity indicated applies to a position midway between the centre of the pitot tube and its outer lip.

Since the internal radius of the pipe is 0·01 ft., the mean velocity $u = \dfrac{0{\cdot}33}{60 \times \pi \times 0{\cdot}01 \times 0{\cdot}01} = 17{\cdot}5$ ft. per sec. Assuming 15° C., $R = 17{\cdot}5 \times 0{\cdot}02/0{\cdot}000159 = 2200$ and the flow is laminar. So from Article 195, $u/\bar{u} = 2 - 8r^2/D^2$. Midway between the centre

* Piercy and Richardson, A.R.C.R. & M., 1224, 1928.
† *loc. cit.*, p. 211.

of the pitot tube and its outer lip, i.e. at 0·3 mm. = 0·001 ft. from the wall, $r = 0{\cdot}009$ ft. and $u/\bar{u}$ comes to 0·38, whence $u = 6{\cdot}65$ ft. per sec. If the pressure in the tube corresponds to this position, that pressure $= \frac{1}{2}\rho u^2 = \frac{1}{2} \times 0{\cdot}105$ lb. per sq. ft. $= 0{\cdot}0101$ in. water head above the static pressure across that section of the pipe.

Now from (272) $\tau = 8\rho\bar{u}^2/R = -PD/4$. Thus $-P = 32\rho\bar{u}^2/RD = 0{\cdot}53$ lb. per cu. ft. Hence at a distance 1·5 ft. upstream from the pitot tube section the static pressure is increased by 0·795 lb. per sq. ft. = 0·153 in. water. The static pressure is determined in this position, and the pressure in the pitot tube, situated 1·5 ft. downstream, is 0·153 − 0·0101 = 0·143 in. water head less, as stated.

With every precaution measurement of skin friction remains a difficult experiment in which to achieve accuracy. The following theorem has a particular significance as suggesting a method by which errors can be minimised, although it also has a wider interest.

216. Kármán's Theorem

Without making any assumption as to constancy of the pressure, let us write down Prandtl's equation (289) in the form—

$$\mu \frac{\partial^2 u}{\partial y^2} - \frac{\partial p}{\partial x} = \rho u \frac{\partial u}{\partial x} + \rho v \frac{\partial u}{\partial y} \quad . \qquad \text{(i)}$$

and integrate with respect to y through the boundary layer for any fixed position x. First assuming Δ const., we have—

$$\mu\left[\frac{\partial u}{\partial y}\right]_0^{\Delta} - \frac{\partial p}{\partial x}[y]_0^{\Delta} = \tfrac{1}{2}\rho \frac{\partial}{\partial x}\int_0^{\Delta} u^2 dy + \rho\,[vu]_0^{\Delta} - \rho\int_0^{\Delta} u \frac{\partial v}{\partial y}\, dy$$

the last term of (i) being integrated by parts. Considering this expression, on the right-hand side the last term is the same as the first since by the equation of continuity $\partial v/\partial y = -\partial u/\partial x$; also, regarding the middle term, $u = v = 0$ when $y = 0$ while $u = U$, $v = v_{\Delta}$, say, when $y = \Delta$. Turning to the left-hand side, the first term $= 0$ when $y = \Delta$ and is equal to the skin friction τ when $y = 0$. Putting in these limiting values, we have—

$$-\tau - \Delta \frac{\partial p}{\partial x} = \rho \frac{\partial}{\partial x}\int_0^{\Delta} u^2 dy + \rho U v_{\Delta}. \quad . \qquad \text{(ii)}$$

It is readily shown from the equation of continuity that the velocity across the edge of the boundary layer is evaluated by—

$$v_{\Delta} = -\frac{\partial}{\partial x}\int_0^{\Delta} u dy. \quad . \quad . \qquad \text{(iii)}$$

Hence finally—

$$\tau = \rho \frac{\partial}{\partial x} \int_0^\Delta (Uu - u^2)\, dy - \Delta \frac{\partial p}{\partial x} \quad . \quad . \quad . \quad (307)$$

if also U may be regarded as const. (307) is correct for Δ varying with x, additional terms arising on this score finally cancelling out.

But when the velocity (Q, say) just outside the boundary layer itself varies with x, we have in place of the integral in (307) :—

$$\rho Q \frac{\partial}{\partial x} \int_0^\Delta u dy - \rho \frac{\partial}{\partial x} \int_0^\Delta u^2 dy. \quad . \quad . \quad (307a)$$

This important result may be established in another way by considering the conditions for equilibrium of a short length δx of the boundary layer (Fig. 158). The force acting on this section in the direction Ox is $-\tau \delta x - \frac{\partial p}{\partial x} \delta x \,.\, \Delta$ and must equal the rate of increase of x-momentum within. This rate is (see figure)—

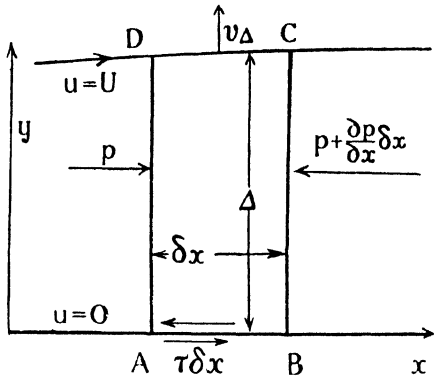

[FIG. 158.

$$-\rho \int_A^D u^2 dy + \rho \int_B^C u^2 dy + \rho U \int_D^C v_\Delta dx.$$

Hence—

$$-\tau - \Delta \frac{\partial p}{\partial x} = \frac{\rho}{\delta x} \left[\int_0^\Delta (u_{BC}^2 - u_{AD}^2)\, dy + U \int_D^C v_\Delta dx \right] \quad . \quad (308)$$

which comes to the same thing as (307) on use of (iii), if δx be small.

Now the integrals in (308) are very suitable for experimental determination, and are but little affected by errors in u close to the plate, such as would lead to large deviations in the boundary values of the velocity gradient. Thus by exploring round a transverse slice of the boundary layer perpendicular to the plate we can estimate closely the mean skin friction on the plate in this region.

Similar remarks may be made from an analytical point of view. (307) is simpler than (289) and allows of plausible assumptions being safely introduced regarding the velocity profile when it is desired to calculate approximate results.

Like Prandtl's equation from which it is derived, the foregoing

method may also be applied to the boundary layers of cylinders provided the curvature is not great.

217. Examples.—Measurements of velocity (q) across normals drawn from two points on the upper surface of an aerofoil in its median plane : A, a short distance behind the nose, and B, 0·049 ft. measured round the contour farther downstream, give (n being distance from the surface in thousandths inch and U the undisturbed velocity) :

n:	1	2	3	4	5	6	7
q/U: (A) .	0·3	0·83	0·94	1·02	1·06	1·07	1·04
(B) .	0·82	1·04	1·22	1·38	1·45	1·46	1·41

Estimate* the mean coefficient of friction between A and B.

Plotting shows the data to be inadequate for the method of Article 215 and Kármán's theorem will therefore be employed, there being evidently a boundary layer of thickness (Δ) 0·006 in. = 0·0005 ft. Write $\delta(q/U)$, etc., for increases of quantities between A and B at constant n, and Q' for the mean velocity just outside the boundary layer. (307a) leads to—

$$\frac{\tau}{\rho U^2} = \frac{1}{0{\cdot}049}\int_0^{\Delta}\left[\frac{Q'}{U}\,\delta\left(\frac{q}{U}\right) - \delta\left(\frac{q}{U}\right)^2 - \frac{\delta p}{\rho U^2}\right] dn.$$

Some assumption must be made regarding velocities very close to the surface, although what form this takes makes little difference in the end. For simplicity, assume $q \propto n$ from $n = 0$ to 0·001 in. Then integrating graphically, the first two integrals come to 0·00020 and — 0·00032, approximately, taking $Q' = 1{\cdot}23\ U$.

Now p is independent of n through the boundary layer, and, applying Bernoulli's equation, just outside it—

$$p_0 - p = \tfrac{1}{2}\rho U^2\left[\left(\frac{Q}{U}\right)^2 - 1\right]$$

where p_0 is the undisturbed pressure, whence—

$$\frac{\delta p}{\rho U^2} = \frac{p_B - p_A}{\rho U^2} = \tfrac{1}{2}\left[\left(\frac{Q_A}{U}\right)^2 - \left(\frac{Q_B}{U}\right)^2\right] = -\,0{\cdot}493.$$

Hence the value of the last integral is 0·493 × 0·0005 lb. per ft.

Finally—

$$\frac{\tau}{\rho U^2} = \frac{10^{-3}}{0{\cdot}049}\,[0{\cdot}20 - 0{\cdot}32 + (0{\cdot}493 \times 0{\cdot}5)] = 0{\cdot}0026.$$

* It should be noted that the estimate obtained is approximate only.

The second example given below illustrates the calculation of approximate values for the skin friction and boundary layer thickness along a flat plate from assumed velocity profiles.

Assume that the velocity profile can be represented with sufficient accuracy by—

$$\frac{u}{U} = A\frac{y}{\Delta} - B\left(\frac{y}{\Delta}\right)^3. \quad . \quad . \quad \text{(i)}$$

When $y = \Delta$, $u/U = 1 = A - B$, giving B in terms of A ; and when $y = 0$, $du/dy = AU/\Delta$ so that, in terms of A and Δ,

$$\frac{\tau}{\rho U^2} = \frac{\nu}{U}\cdot\frac{A}{\Delta} \quad . \quad . \quad . \quad . \quad . \quad \text{(ii)}$$

Since the pressure is constant for a flat plate, (307) reduces to—

$$\frac{\tau}{\rho U^2} = \frac{d}{dx}\int_0^\Delta \left[\frac{u}{U} - \left(\frac{u}{U}\right)^2\right] dy.$$

Substituting from (i) and integrating gives—

$$\frac{\tau}{\rho U^2} = f(A)\cdot\frac{d\Delta}{dx}, \quad . \quad . \quad . \quad . \quad \text{(iii)}$$

where—

$$f(A) = 0{\cdot}1071 + 0{\cdot}1357A - 0{\cdot}0762A^2. \quad . \quad \text{(iv)}$$

Combining this second expression for the intensity of skin friction with (ii) gives the following equation for Δ—

$$\Delta d\Delta = \frac{A}{f(A)}\cdot\frac{\nu}{U}\,dx.$$

Integrating—

$$\Delta = \left[\frac{2A}{f(A)}\cdot\frac{\nu}{U}\cdot x\right]^{1/2}. \quad . \quad . \quad . \quad \text{(v)}$$

Finally, substituting in (ii) and writing R_x for Ux/ν,

$$\frac{\tau}{\rho U^2} = [\tfrac{1}{2}Af(A)]^{1/2}\cdot R_x^{-1/2}. \quad . \quad . \quad \text{(vi)}$$

The correct value for the intensity of skin friction follows immediately from (294), which can be written—

$$C_D = \frac{2}{x}\int_0^x \frac{\tau}{\tfrac{1}{2}\rho U^2}\,dx = 2{\cdot}656\left(\frac{\nu}{U}\right)^{1/2} x^{-1/2}$$

since Blasius's solution is for a semi-infinite flat plate, i.e. one possessing a nose but no tail, and differentiating—

$$\frac{\tau}{\rho U^2} = 0{\cdot}332R_x^{-1/2}. \quad . \quad . \quad . \quad \text{(vii)}$$

It is not possible to find a value for A which will make (vi) agree with (vii), but the value involving least error is readily ascertainable ; it is $A = 1\frac{1}{2}$, giving $B = \frac{1}{2}$ and $\tau/\rho U^2 = 0{\cdot}324R_x^{-1/2}$, an error of $2\frac{1}{2}$ per cent.

The nature of the approximation is further illustrated by calculating the thickness Δ of the boundary layer either directly from (v) or by combining (v) and (vi), which yields—

$$\frac{\Delta}{x} R_x^{1/2} = \frac{\frac{\tau}{\rho U^2} R_x^{1/2}}{\frac{1}{2} f(A)} \quad . \quad . \quad . \quad \text{(viii)}$$

With $A = 1\frac{1}{2}$ this gives $\Delta/x = 4{\cdot}64R_x^{-1/2}$. The result can only roughly be compared with (295), since u/U tends to 1 asymptotically with the accurate profile. But evidently the boundary layer for $A = 1\frac{1}{2}$ is too thin, and a somewhat larger value secures better agreement in this respect, though the corresponding skin friction is in greater error.

The table below gives the results of evaluating by the above method some suggested alternatives to (i). y_1 is written for y/Δ .

$u/U =$	$(\tau/\rho U^2) \cdot R_x^{1/2}$	$(\Delta/x) \cdot R_x^{1/2}$
$2y_1 - y_1^2$ . . .	0·365	5·48
$2y_1 - 2y_1^3 + y_1^4$.	0·343	5·83
$\sin \frac{1}{2}\pi y_1$ . . .	0·328	4·79

The foregoing method may easily be formulated in general terms.

218. Transition Reynolds Number

A number of experimental investigations has been carried out on the skin friction of flat plates in steady flow, but, not unexpectedly, these fail to agree closely with one another ; the mean observations of a single experienced investigator may vary by as much as $\pm$ 7 per cent. Some different sets of observations, roughly averaged, are given as three experimental curves in Fig. 159, and there compared with the foregoing theoretical solutions. Curve (2) is excessive for $R > 30$; (1) under-estimates for $R < 10^5$. Evidence so far available points * to the empirical formula—

$$C_D = 2{\cdot}80\ R^{-1/2} \quad . \quad . \quad . \quad . \quad (309)$$

as representing mean experiment under steady conditions at large scales.

* Fage, A.R.C.R. & M., 1508, 1933.

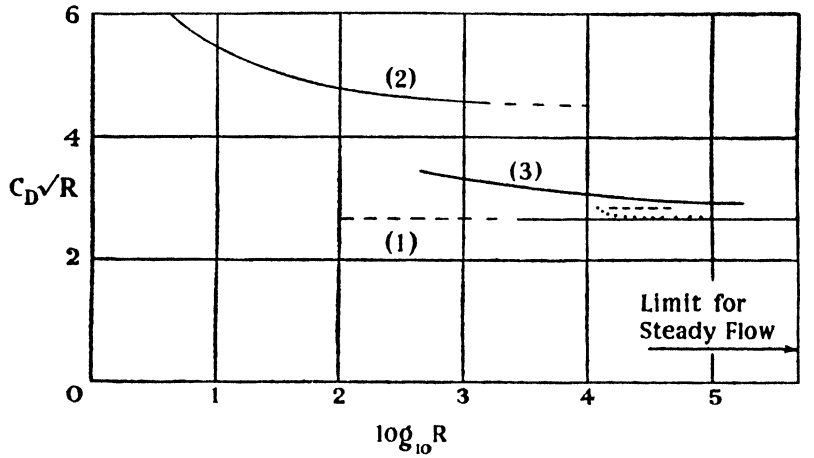

FIG. 159.—THE FLAT PLATE WITH STEADY FLOW.

(1) Prandtl (Blasius's solution); (2) Oseen (Piercy and Winny's solution). *Experimental:* (3) Fage, - - - - Miss Marshall, ... Hansen.

If a thin flat plate be held tangentially in a wind tunnel and the speed increased, the flow within the boundary layer is at first steady, but at some scale, depending on initial turbulence (large for a smooth stream) and shape of nose (large for a sharp leading edge)

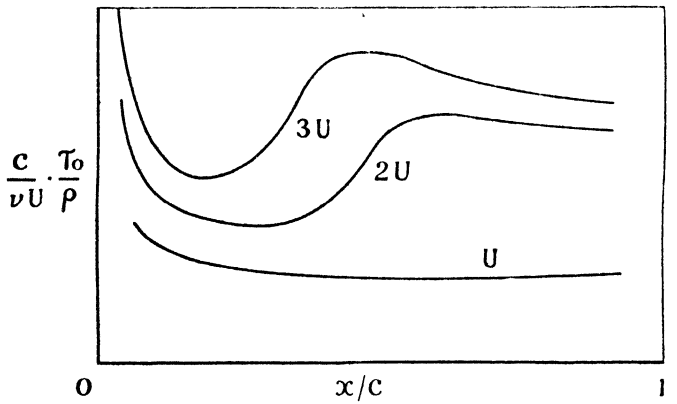

FIG. 160.—PASSAGE TO TURBULENCE IN THE BOUNDARY LAYER OF A FLAT PLATE.

the flow within the boundary layer becomes unsteady near the trailing edge. The Reynolds number, based on the length c of the plate, at which turbulence just sets in, varies from 10^5 to 5×10^6 if atmospheric steadiness be included. As speed is further

increased in a given case, the position at which streamline flow fails creeps forward. A large increase in friction occurs there. This effect is well shown by measurements of Burgers and Zijnen * from which Fig. 160 has been prepared. Thus at higher Reynolds numbers a front part of the boundary layer is steady (or laminar in the accepted sense of the word) and the remaining back part turbulent. The passage from laminar to turbulent flow in the boundary layer is called *transition* and the position at which it occurs the *transition point.* If this point is distant x from the nose of the plate, Ux/ν is called the *transition Reynolds number.* It is not easy to obtain measurements that are quantitatively consistent or to explain completely such variations as occur. But it may be assumed that under constant conditions the transition Reynolds number would be constant for wide variation of x/c. The same phenomenon occurs in the curved boundary layer of a thick body and the same definitions apply, x being measured round the profile.

218A. Detection of Transition

The above method of measuring transition Reynolds numbers is laborious and others are in use as follows.

(1) One method, developed at Cambridge, depends upon the great increase which transition causes in the thickness of the boundary layer. A fine pitot tube is located in the turbulent part of the boundary layer and moved gradually upstream at a constant distance from the friction surface. If a suitable clearance has been chosen, the tube emerges from the boundary layer at the transition point into potential flow, showing a rise of pressure.

(2) Another method, avoiding all disturbance of the flow, has been developed at Queen Mary College,† and consists of burying a very small microphone beneath the friction surface, communicating with the boundary layer through a small hole drilled in the position where transition is likely to occur. Error in this position is corrected for by adjusting the tunnel speed or other means. The transition point fluctuates slightly, causing rapid pressure changes which become audible on suitably connecting the microphone to an amplifying set.

(3) The foregoing have recently been superseded by a visual method devised by Gray ‡ at the R.A.E. for flight tests. In the form developed at the N.P.L. for use in tunnels, aerofoils are coated with an emulsion containing china clay and sprayed before a test

* *Dissertation*, Delft, 1924 ; scales are not given in the figure, since criticisms can be directed against the numerical accuracy of these early results.

† Winny, Ph.D. *thesis*, London, 1931. ‡ A.R.C. Report *Ae.* 2608, 1944.

with nitro-benzine, which has much the same refractive index and makes the white coating temporarily invisible. The nitro-benzine evaporates more quickly in turbulent than in laminar flow, and thus the white coloration first reappears under turbulent parts of the boundary layer. Other expressions of the device are also employed.

FLAT PLATE FRICTION, TURBULENT FLOW

219. Thickness of Turbulent Boundary Layer

Although turbulent boundary layer flow is familiar in Aeronautics, it is not, unfortunately, amenable to analytical treatment, and examination depends ultimately upon experiment. Independently of one another, Prandtl and v. Kármán established semi-empirical laws, known as the power formulæ, expressing the application to plates of experiments in pipes, which are easily carried out with great accuracy. As before, we choose the origin at the nose of the plate, Oy perpendicular to the plate and Ox in the direction of the undisturbed velocity U. The velocity u within the boundary layer will mean the time-average value at any point.

The underlying assumption is that u is expressible in the form—

$$u = U\left(\frac{y}{\Delta}\right)^n \quad . \quad . \quad . \quad . \quad (310)$$

where Δ is the thickness of the boundary layer and n a constant. On analogy with Article 197 it is further assumed that, through a certain range of R, $n = 1/7$. We adopt this index with the understanding that it can be varied afterwards.

Denote, as before, the local skin friction on one side only of the plate at distance x from the nose by τ. At large Reynolds numbers the pressure p is constant with turbulent as with streamline flow to a high approximation. Thus in (307) the last term can be dropped and substitution from (310) gives—

$$\frac{\tau}{\rho U^2} = \frac{\partial}{\partial x}\int_0^{\Delta}\left[\left(\frac{y}{\Delta}\right)^{1/7} - \left(\frac{y}{\Delta}\right)^{2/7}\right]dy = \frac{7}{72}\frac{d\Delta}{dx} \quad . \quad (311)$$

Now on substitution from 274), Article 197 (iii) gives—

$$\tau = 0{\cdot}0228\ \rho\nu^{1/4}u^{7/4}y^{-1/4}$$

for the pipe friction in turbulent flow at Reynolds numbers such that the seventh-root velocity formula holds. This is independent of the radius of the pipe (as originally assumed) and substituting from (310) reduces it to—

$$\frac{\tau}{\rho U^2} = 0{\cdot}0228\left(\frac{\nu}{U\Delta}\right)^{1/4} \quad . \quad . \quad . \quad (312)$$

Equating the two expressions for $\tau/\rho U^2$—

$$\Delta^{1/4}\frac{d\Delta}{dx} = 0{\cdot}235\left(\frac{\nu}{U}\right)^{1/4}.$$

Integrating—

$$\tfrac{4}{5}\,\Delta^{5/4} = 0{\cdot}235\left(\frac{\nu}{U}\right)^{1/4}x$$

or—

$$\Delta = 0{\cdot}375\left(\frac{\nu}{U}\right)^{1/5}x^{4/5} = kx^{4/5}. \quad . \quad . \quad (313)$$

for constant fluid and speed.

This result should be compared with (295), which may similarly be written $\Delta = k'x^{\frac{1}{2}}$. The turbulent part of the boundary layer increases in thickness much more rapidly along the plate than the streamline part.

220. Total Drag Coefficient

We first assume the boundary layer to be turbulent throughout. To obtain the coefficient of the total skin friction, we double τ, in order to take both sides of the plate into account, and integrate from nose to trailing edge.

Using (313), (312) becomes—

$$\frac{\tau}{\rho U^2} = 0{\cdot}029\left(\frac{\nu}{U}\right)^{1/5}x^{-1/5}.$$

Now integrating—

$$\begin{aligned} C_D &= \frac{2}{c}\int_0^c \frac{\tau}{\frac{1}{2}\rho U^2}\,dx \\ &= 0{\cdot}116\left(\frac{\nu}{U}\right)^{1/5}c^{-1/5}\times\tfrac{5}{4} \\ &= \frac{0{\cdot}144}{R^{1/5}} \quad . \quad . \quad . \quad . \quad . \quad (314) \end{aligned}$$

where $R = Uc/\nu$.

This drag coefficient is much greater than that for streamline flow at the same Reynolds number. Taking for example $R = 4{\cdot}9 \times 10^5$, when different conditions would make the boundary layer ' laminar ' or turbulent, $\sqrt{R} = 700$, $R^{1/5} = 13{\cdot}74$, and $C_D = 0{\cdot}0038$ in the former case and $= 0{\cdot}0104$ in the latter.

In the general case, as we have seen, the front part of the plate has a streamline boundary layer with a low mean drag, while the remaining back part is exposed to turbulence giving a high drag.

To apply through this ' transition range ' Prandtl has suggested for the drag coefficient of the whole plate—

$$C_D = \frac{0{\cdot}148}{R^{1/5}} - \frac{3400}{R} \quad . \quad . \quad . \quad (315)$$

where again $R = Uc/\nu$. This formula contains an empirical increase of the calculated coefficient in (314) from 0·144 to 0·148 to secure better agreement with experiment. The other coefficient is determined by the transition Reynolds number, at which (315) must agree with (294). The value 3400 is appropriate to transition at 5×10^5; it becomes 28,000 for 5×10^6.

221. Check from Direct Experiment

Regarding experimental determinations of skin friction in turbulent flow, it may be noted first that v. Kármán's theorem will apply when u is the time-average velocity (we have also to include an integral for the time change of momentum within the slice of boundary layer, but this evidently vanishes). Measurements will usually be made with a pitot tube. Since this is a ρu^2 instrument it is quite clear that the pressure within the tube will be greater than that appropriate to the time-average velocity, but examples show that the increase is small when, as is usual, the fluctuations of velocity are of the order of $\pm$ 5 per cent.

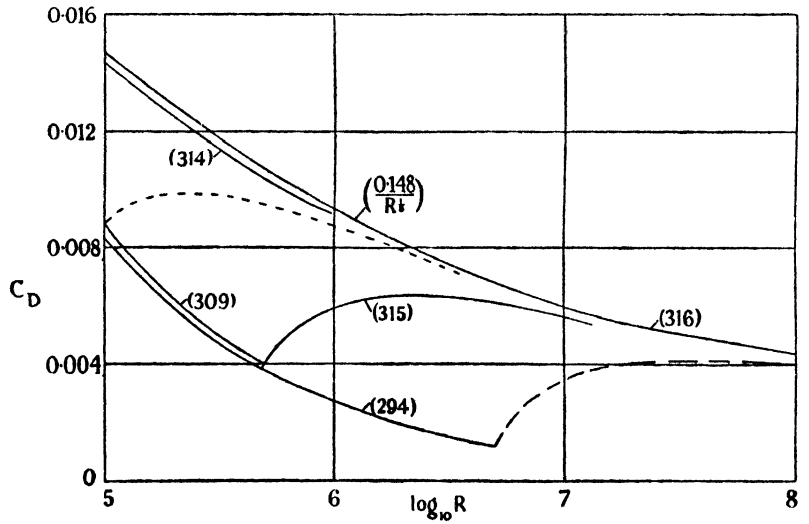

FIG. 161.—THE FRAMEWORK OF FLAT PLATE DRAG AT AERODYNAMIC REYNOLDS NUMBERS.

The four formulæ: (294), (309), (314), and (315) are plotted through a practical range of R in Fig. 161. The other curves will be described shortly.

Numerous careful investigations, some of which are listed * below, have been carried out with which the foregoing results may be compared. Variations in the conditions of the experiments, especially in the shape of the nose of the plate and the degree of turbulence in the oncoming stream, enable comparisons to be made with the several formulæ. These checks are successful up to at least $R = 5 \times 10^6$ provided the coefficient in (314) is slightly increased as described. The dotted curve to the left illustrates the change of (315) caused by, for example, an unsuitably shaped or finished nose or a very turbulent tunnel; it is obtained simply by adjusting the second coefficient in (315), as described. Beyond the above range, the formula (314) would require still further adjustment to accord approximately with experiment for completely turbulent boundary layers, and others have therefore been suggested for high Reynolds numbers, viz.—

(Kármán) $$C_D = \frac{0{\cdot}91}{(\log_{10} R)^{2{\cdot}58}} \quad . \quad . \quad . \quad (316)$$

(Falkner)† $$C_D = \frac{0{\cdot}0612}{R^{1/7}} \quad . \quad . \quad . \quad . \quad (316A)$$

Of these, Kármán's formula is most frequently adopted in elementary calculations as it is also successful at lower Reynolds numbers if the flow is turbulent. A second term may be added for the transitional range. The dotted line to the right in the figure is appropriate to the exceptionally high transition Reynolds numbers obtaining under favourable conditions with smoothly constructed and finished wings in flight. This starts at about the extremity of the range for the simple formula (314), the accurate application of which therefore tends to be restricted to wind tunnels and crudely designed or manufactured wings and other aircraft surfaces, especially those exposed to the turbulent slipstreams of airscrews. It is desirable to recall that constant pressure is assumed. Much larger transition Reynolds numbers could be secured in the absence of initial turbulence by means of a decreasing pressure along the plate.

*Blasius, *Ziets. f. Math. u. Phys.*, v. 56, 1908 (laminar and early transitional range, smooth flow); Gebers, *Schiffbau*, v. 9, 1908 (late transitional range); Baker, *Coll. Res. N.P.L.*, v. 13, 1916 (entire transitional range); Wieselsberger, *Gött. Ergebnisse*, v. 1, 1921 (plates covered with fabric, blunt nose, turbulent); Kempf, *Werft Reederei Hafen*, v. 6, 1925 (high Reynolds numbers).

† *Aircraft Engineering*, March, 1943.

221A. Displacement and Momentum Thicknesses

In approximate investigations of skin friction, particularly with turbulent flow, it is often convenient to introduce two thicknesses, δ and θ, which are measures of particular properties of the velocity profile through the boundary layer. Need for the step arises in the first place from the fact that, though the edge of the boundary layer is readily located in experiment by the method of Article 42, the corresponding analytical definition is rather uncertain since the loss of velocity caused by friction vanishes only asymptotically.

Consider a particular position x along the boundary layer. Let u be the velocity (or its time-average) at a distance y measured normally from the surface, and let U be the velocity at the same point with potential flow. One effect of retardation near the surface is to push out the streamlines of the potential flow by a distance δ, say, and we have—

$$U\delta = \int U dy - \int u dy,$$

i.e.—

$$\delta = \int \left(1 - \frac{u}{U}\right) dy, \quad . \quad . \quad . \quad \text{(i)}$$

where the integration is to extend from the surface sufficiently deeply into the fluid as to make the remainder negligible. δ is called the *displacement thickness.*

For a flat plate with a laminar boundary layer, δ may be evaluated from the curve of Fig. 157. In this case it comes to—

$$\frac{\delta}{x} = 1{\cdot}73 \left(\frac{\nu}{Ux}\right)^{1/2}, \quad . \quad . \quad . \quad \text{(ii)}$$

where x is the distance from the nose, and it is thus of the order $\Delta/3$. δ is easily estimated closely from a plausible assumption for the velocity profile ; thus the profile (i) of Article 217 changes the constant coefficient of (ii) only to 1·74 with $A = 1\frac{1}{2}$.

The loss, due to frictional effects, of momentum crossing the normal at x can be measured in terms of another length θ by equating it to $\rho U^2\theta$. Then by Article 216—

$$\theta = \frac{1}{\rho U^2}\int (\rho U u - \rho u^2) dy$$

$$= \int \frac{u}{U}\left(1 - \frac{u}{U}\right) dy. \quad . \quad . \quad . \quad \text{(iii)}$$

θ is called the *momentum thickness.*

The momentum thickness may also be illustrated, as follows, with reference to laminar flow along the flat plate with constant pressure. (307) gives—

$$\frac{\tau}{\rho U^2} = \frac{d\theta}{dx} \quad . \quad . \quad . \quad . \quad \text{(iv)}$$

and (vii) of Article 217 gives, approximately,

$$\frac{\tau}{\rho U^2} = \frac{1}{3}\left(\frac{\nu}{Ux}\right)^{1/2}.$$

Combining with (iv) and integrating—

$$\frac{\theta}{x} = \frac{2}{3}\left(\frac{\nu}{Ux}\right)^{1/2} \quad . \quad . \quad . \quad \text{(v)}$$

and eliminating x gives finally—

$$\frac{\tau}{\rho U^2} = \frac{2\nu}{9U\theta} \quad . \quad . \quad . \quad \text{(vi)}$$

The numerical factor, approximated for clearness, is readily made more accurate if desired.

221B. Alternative Form of Kármán's Equation

In the case of a flat plate with turbulent or laminar boundary layers along which there exists a pressure gradient, the asymptotic velocity Q at x will differ from U but may be calculated from the normal pressures by Bernoulli's equation. The definitions of δ and θ given by (i) and (iii) of the preceding article apply in these changed circumstances provided Q, which will be a function of x, is written for U.

Kármán's equation of Article 216 can then be arranged in the form *—

$$\frac{\tau}{\rho U^2} = \frac{d\theta}{dx} + \frac{\theta}{Q}\frac{dQ}{dx}(H + 2), \quad . \quad \text{(i)}$$

where $H = \delta/\theta$.

Now Nikuradse † and others have explored experimentally the velocity profiles for turbulent flow through slightly convergent and divergent channels. Analysis of these results shows that, though the profiles vary greatly among themselves, there occurs comparatively little variation of H from the value 1·4. It will be noticed that this value for turbulent flow is much smaller, as would be anticipated from the change in shape of the velocity profile, than

* Prandtl, *Aerodynamic Theory*, vol. III, p. 108.
† *V.D.I.*, Heft 289, 1929.

that for laminar flow, which is found to be 2·59 from the preceding article, assuming constant pressure.

Adoption of an appropriate constant value for H and other assumptions enable (i) to be employed in an approximate manner to to obtain estimations of practical utility, as will be described later.

We may conclude with an illustrative calculation based on Falkner's drag coefficient for turbulent flow along a flat plate with constant pressure, viz. $C_D = 0{\cdot}0612/R^{1/7}$. We have—

$$\frac{\tau}{\rho U^2} = \frac{d}{dx}(\tfrac{1}{4}C_D x) = 0{\cdot}0131\left(\frac{\nu}{Ux}\right)^{1/7} = \frac{d\theta}{dx}$$

whence, on integration—

$$\frac{\theta}{x} = 0{\cdot}0153\left(\frac{\nu}{Ux}\right)^{1/7}$$

and δ follows immediately. It will be observed that the procedure of Article 219 is here inverted.

APPLICATION TO CYLINDRICAL SURFACES

222. We could now proceed to calculate from Prandtl's equations the skin friction with laminar flow round cylinders of aerodynamically interesting sections. Such calculations stop at breakaway (Article 159), or at transition should the latter occur before conditions for breakaway are reached. This development of boundary layer theory must, however, be left to further reading, which may begin with the references given below *; the literature is compendious and specialised, and only a few brief remarks will be made in this book.

In the solution of the boundary layer equations for laminar flow over curved surfaces, an assumption must be made as to the distribution of pressure, and three alternatives are available. Skin friction will be most reliably estimated from pressures that have been determined experimentally. As already illustrated, these differ little from those of potential flow in the case of thin streamline cylinders, which can always be obtained, or approximated to as closely as is possible in experiment, by the methods of Chapter VI. Differences become large, however, for bluff shapes (cf. Fig. 72) owing to the thick wake. It has been suggested † that, as an alternative to the experimental pressures, those of potential flow

* Howarth, A.R.C.R. and M. No. 1632, 1934; Falkner, A.R.C.R. and M. No. 1884, 1937; Piercy, Whitehead and Tyler (being published).

† Piercy, Preston and Whitehead, *Phil. Mag.*, Ser. 7, vol. xxvi, 1938.

for an artifically modified boundary might be used in such cases, the modification consisting of an extension of the cylindrical profile backwards from the points of breakaway in order to represent the presence of the wake. Fairly close agreement with experiment is then secured. On the other hand, an already tedious calculation becomes still more involved.

The full-line curves of Fig. 162 give the distribution of skin friction along the laminar boundary layers of the flat plate, the circular cylinder,* and the elliptic cylinder of fineness ratio 3. Breakaway or separation is indicated by the position at which the skin friction becomes zero. The dotted curve refers to the circular cylinder with the potential flow pressures assumed. The chain-line curve indicates, approximately, the theoretical solution for potential flow pressures appropriate to a boundary modified, as described, to take some account of the wake.

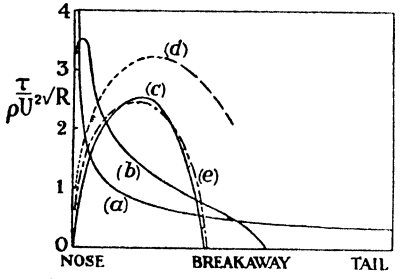

FIG. 162.—INTENSITY OF SKIN FRICTION.

(*a*) Flat plate; (*b*) Elliptic cylinder of fineness ratio 3; (*c*) Circular cylinder, experimental; (*d*) Circular cylinder, Blasuis-Heimenz solution with potential flow pressures; (*e*) Circular cylinder, Piercy, Preston and Whitehead solution with allowance for wake.

The dotted curve represents the well-known Blasius-Heimenz solution and is exact (in accordance with the pressure assumption) through the range where the dotting is close; farther away from the nose it becomes increasingly unreliable, and it cannot be used to determine the point of breakaway. As the fineness ratio of the cylindrical section increases, the range of an exact solution of the boundary layer equations becomes increasingly curtailed, until soon it extends only a short distance from the nose. Over almost the whole profile of an aerofoil, therefore, only approximate solutions of the equations can be found. Of these the oldest and best known is that due to Pohlhausen, but, though still in use, this has been superseded for some time where accuracy is required. One of the more modern approximate solutions is due to Falkner.† The determination of the separation point is of technical importance, but in its immediate vicinity the boundary layer equations become in themselves unsuitable. On the other hand, the rapid decrease of skin friction in front of this point can be estimated fairly reliably,

* From experiment by Fage and Falkner, A.R.C.R. and M. No. 1369, 1930.
† *Loc cit.*, p. 393; see also Falkner, A.R.C.R. and M. No. 1895, 1941.

and extrapolation leaves little doubt as to the approximate location of breakaway. In illustration of the physical nature of the difficulties confronting calculation in this region, Fig. 162A reproduces the results of an experiment * to investigate the fluctuation of velocity in the neighbourhood of separation. The cylinder was circular and the numbers attached to the contour lines in the figure

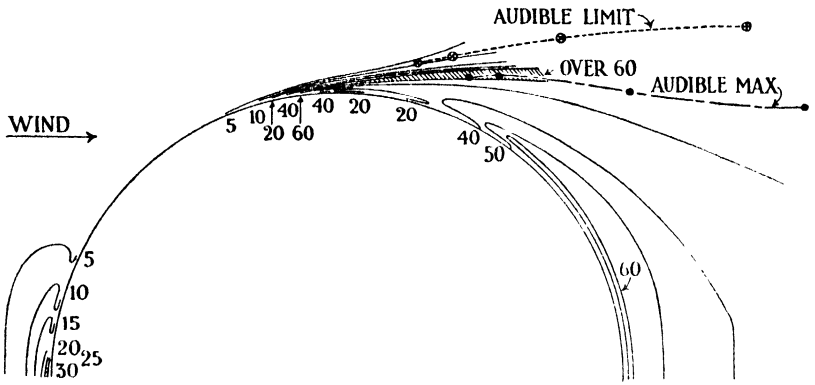

FIG. 162A.—TURBULENCE IN FLOW PAST A CIRCULAR CYLINDER.
The numbers are proportional to the amplitude of the velocity fluctuation

are roughly proportional to the velocity amplitude. Exposing a fine hot wire, connected to an amplifier, in the shaded wedge of large velocity amplitude made easily audible the passage of vortices into the Kármán trail (Article 160).

222A. As mentioned in Article 221B, the rearranged Kármán equation there given is suitable for wide employment in an approximate manner. It has been so used by Squire and Young † to estimate the skin friction of aerofoils with turbulent boundary layers, assuming that the small pressure gradients along their boundary layers at small incidences will not affect appreciably the shape of the velocity profile, so that the relationship between local values of τ, Q and θ will approximate to that for a flat plate with completely turbulent flow and a constant pressure. For further remarks on the assumptions involved in such applications of this equation, reference may be made to an article by Prandtl.‡ The method will be explained in application to laminar flow.

* Piercy and Richardson, *loc cit.*, p. 369.
† A.R.C.R. and M. 1838, 1938.
‡ *Aerodynamic Theory*, vol. III, p. 156 *et seq.*

Substituting for τ from (vi) of Article 221A, the rearranged Kármán equation becomes for laminar flow—

$$\frac{d\theta}{dx} + \frac{\theta}{Q}\frac{dQ}{dx}(H+2) = \frac{2}{9}\frac{\nu}{Q\theta}, \quad . \quad . \quad (i)$$

where $H = 2{\cdot}59$ and Q is the velocity appropriate to potential flow at a distance x measured round the profile from the front stagnation point.

This equation can be integrated by means of the substitution $\eta = \theta Q^{H+2}$, which leads to—

$$\eta\frac{d\eta}{dx} = \frac{2}{9}\nu Q^{2H+3},$$

whence—

$$\eta^2 = \frac{4}{9}\nu\int_0^x Q^{2H+3}dx$$

or *—

$$\theta^2 = \frac{4}{9}\frac{\nu}{U}\frac{1}{(Q/U)^{2(H+2)}}\int_0^x \left(\frac{Q}{U}\right)^{2H+3}dx. \quad . \quad . \quad (ii)$$

H being a known constant and Q/U an ascertainable function of x, θ is readily evaluated, whence $\tau/\rho U^2$ follows from (vi) of Article 221A in accordance with what assumptions are made. Although applicability is restricted to small pressure gradients, it is nevertheless of interest to employ the method to estimate the distribution of skin friction round the circular cylinder. The result is shown as curve (*a*) in Fig. 162B, the pressures for potential flow being implied in the simple formula for Q/U taken from Article 108. The curve (*b*) represents the most recent solution for these pressures.† The Blasius-Heimenz solution is reproduced as a dotted curve. The curve (*a*) deduced by (ii) from the very dissimilar one for the flat plate is seen to have the correct form over the front part of the cylinder. Greater accuracy cannot be expected without elaboration in view of the large variation of dp/dx in the example chosen. More elaborate approximate solutions, taking variation of H into account, duly yield a position of laminar separation, which the above first approximation fails to predict. This phenomenon occurs in a region of rising pressure and retarded flow, where

* An equation of this form with different indices is quoted by Holt, *Aircraft Engineering*, 1943, as given by Young and Winterbottom in an unpublished paper.

† Piercy, Whitehead and Tyler (in the Press).

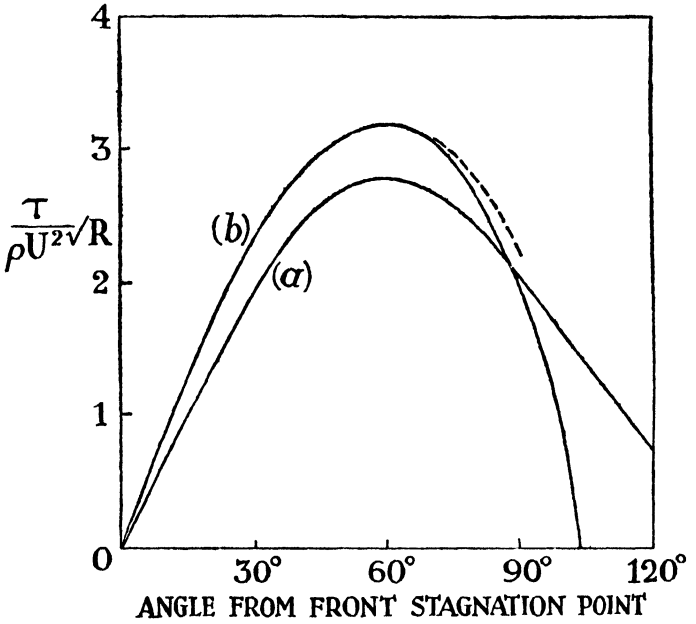

FIG. 162B.—APPLICATION OF APPROXIMATE METHOD TO CIRCULAR CYLINDER WITH POTENTIAL PRESSURES.

(*a*) First approximation deduced from flat plate ; (*b*) Correct solution.

approximate methods tend to lose accuracy, particularly as the conditions for breakaway are approached.

223. Although the local intensity of skin friction is not easy to measure accurately, no difficulty arises in determining the frictional drag of a body since it is only required to subtract from the weighed drag the drag due to the normal pressures. Many investigations have been carried out by this means to compare the frictional drag of aerofoils and streamline bodies of revolution with that of the flat plate. To take into account variation of surface area for a given chord or length, results are expressed in terms of a coefficient C_F, defined by—

$$C_F = \text{Frictional drag}/\tfrac{1}{2}\rho U^2 E,$$

where E is the ' wetted ' surface. Reynolds number continues to be based on the length of the body. Primary reference may be made to the papers cited,* from which Fig. 163 has been prepared.

* *Gött. Ergebn.*, Lfg. 3, 1926; Jones (Sir Melvill), A.R.C.R. & M., 1199, 1928; Fage, Falkner, and Walker, A.R.C.R. & M., 1241, 1929; *N.A.C.A. Tech. Rept.*, 394, 1931; Relf and Lavender, A.R.C.R. & M., 597; Jones and Williams, A.R.C.R. & M., 1804, 1937.

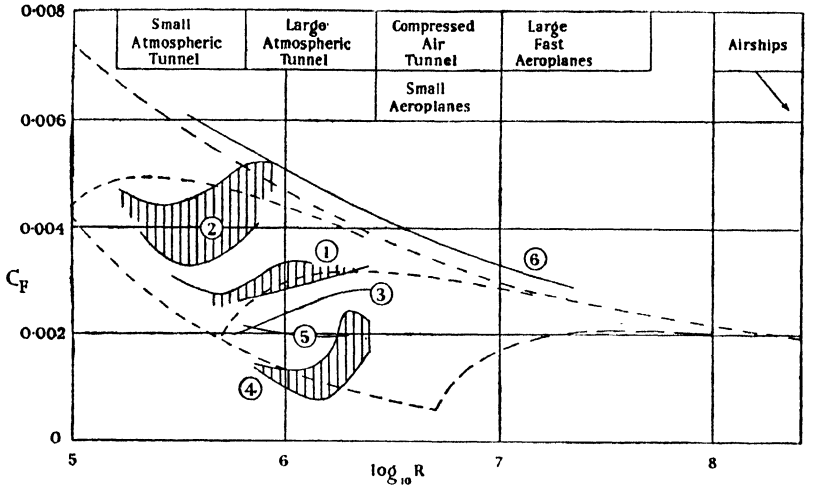

FIG. 163.—EXPERIMENTAL FRICTION IN RELATION TO THE FLAT PLATE FRAMEWORK.
(1) Thin wings; (2) thick wings and struts; (3) flat plate by extrapolation; (4) and (5) airships; (6) airship with wholly turbulent boundary layer.

These well-known investigations were carried out before the advent of low turbulence wind tunnels or laminar flow wings, but remain worthy of consideration both for their various aspects of permanent interest and also because (*a*) most wind tunnels are still fairly turbulent, (*b*) average wing construction falls rather short of theoretical requirements for maximum delay of transition.

Curves 1 (N.P.L. and Göttingen), representing ordinary symmetrical aerofoils of 5–6 per cent. thickness ratio, follow fairly well the transitional drag curve for the flat plate realised experimentally by Gebers. Still thinner aerofoils show a smaller friction, and the N.P.L. experiments allow of the prediction of flat plate friction by extrapolation on the assumption that it will be the same as for a symmetrical aerofoil of zero thickness; the curve 3 is obtained in this way. The hatched area 2 includes strut sections of 27–40 per cent. thickness (N.P.L.). It is seen that the frictional drag of aerofoils is greater than that of the flat plate, but not greatly so if allowance is made for earlier transition with thick sections. The extension of laminar flow in the boundary layers of thick sections is discussed in the next chapter.

Turning to streamline bodies of revolution, the hatched area 4 refers to a model of fineness ratio $5\frac{1}{2}$, and curve 5 to the airship R 101. These suggest remarkably little change of C_F but a greater tendency under three-dimensional conditions to maintain steady flow.

On looping a thin string round the nose of the model giving curves 4, C_F changed to curve 6, the entire boundary layer becoming turbulent. Curve 6 agrees in an average way with tests on another model (N.A.C.A.) with turbulent boundary layer. The same change can be effected for any streamline body by means of a turbulence-producing screen located upstream, and cannot be avoided with an airscrew in front of the surface.

Another matter of importance emerges from the many experiments of the above kind that have been carried out in various laboratories. If a model is suspended by a wire attached in a laminar flow region, a notable increase of friction occurs, though insufficient to accord with a wholly turbulent boundary layer. We conclude that a wedge of turbulence exists behind the wire, while at laterally displaced positions the flow remains streamline. A similar effect is caused by sharp longitudinal edges or ridges ; if the edges are widely spaced, the strips of turbulence will have limited lateral spread, though the increase of total friction may be considerable.*

It will be appreciated that through a very wide range of R, tests on the same model in different wind tunnels with different degrees of initial turbulence will disagree. Tests in a given tunnel usefully compare one model with another, but can be applied to design only when the effective turbulence is known. Since a curve of type 6 is easier to extrapolate to full scale than a transitional curve, whilst the latter depends acutely on initial turbulence, some designers having access to only small wind tunnels have in the past deliberately increased their turbulence. But the modern trend is towards exceptionally smooth streams, with large Reynolds secured, if necessary, by two-dimensional testing. This matter is returned to later on.

DEVELOPED TURBULENCE AND ROUGHNESS

224. Reynolds Equations of Mean Motion

The semi-empirical formulæ of Articles 197, 219, and 220 have been noted to be subject to rather rapid change with increase of Reynolds number, which at much larger scales is less marked. The turbulence is then said to be more fully developed and may be expected to be a little easier to analyse. Moreover, this stage is approached with modern aircraft. The following articles merely introduce what is a wide and difficult subject whose threshold has scarcely yet been

* These and similar effects can now be demonstrated visually by method (3) of Article 218A.

passed by research. We begin with an extract from a notable pioneering paper by Reynolds.*

Referring to Article 203, we must add for unsteady flow to the right-hand side of the first of equations (i) the term $\partial u/\partial t$ and to that of the second $\partial v/\partial t$. Using the equation of continuity, the first of equations (ii) can then be written as—

$$\rho \frac{\partial u}{\partial t} = \frac{\partial}{\partial x}(p_{xx} - \rho uu) + \frac{\partial}{\partial y}(p_{yx} - \rho uv) \quad . \quad (317)$$

and the second similarly. These equations are exact.

Now let $\bar{u}$, $\bar{v}$ be the mean values of u, v at any point and u', v' the added fluctuations, so that at any instant there—

$$u = \bar{u} + u', \qquad v = \bar{v} + v'$$

It is then necessary that, if the mean fluctuations be reckoned in the same way and indicated by a bar, $\bar{u}' = 0 = \bar{v}'$. For rapid fluctuations—

$$\overline{uu} = \bar{u}^2 + 2\bar{u}\bar{u}' + \overline{u'u'} = \bar{u}^2 + \overline{u'u'}.$$

Similarly,

$$\overline{uv} = \bar{u}\bar{v} + \overline{u'v'}.$$

Substituting in (317) we find *equations of mean motion*, the first being—

$$\rho \frac{\partial \bar{u}}{\partial t} = \frac{\partial}{\partial x}(\bar{p}_{xx} - \rho\bar{u}^2 - \rho\overline{u'u'}) + \frac{\partial}{\partial y}(\bar{p}_{yx} - \rho\,\bar{u}\bar{v} - \rho\overline{u'v'}). \quad (318)$$

Comparing these approximate equations for turbulent flow with (317), it is seen that additions to the stresses, represented by the last term in each of the brackets, are caused by the turbulence.

225. Eddy Viscosity and Prandtl's Mixing Length

Although viscous stresses co-exist with the turbulent stresses just found, it is assumed from experiments with pipes (cf. Article 197) that through the bulk of the flow the former are comparatively unimportant and may be neglected. This has the disadvantage that we cannot approach the boundary, where viscosity predominates, but further development is hardly concerned with establishing a mathematical theory, which has proved a difficult task, but rather with inferring from observation approximate laws of sufficient generality for use beyond the realm of the original experiments. It is also assumed that the turbulent additions to the normal stresses

* *Phil. Trans. Roy. Soc.*, 1894 (see Lamb's *Hydrodynamics*).

p_{xx}, p_{yy}, are of small account in determining the character of the motion compared with those to the shearing stresses. Thus we write approximately—

$$\tau_{yx} = -\rho\overline{u'v'} \quad . \quad . \quad . \quad \text{(i)}$$

and investigate—in the simplest possible circumstances, choosing mean motion parallel to Ox, say, with $\bar{u}$ a function of y only—the turbulent analogue of two-dimensional laminar flow. The fluctuations are treated as if they were two-dimensional, though actually an originally two-dimensional steady flow becomes three-dimensional on developing turbulence.

After Boussinesq, the following formula may be framed on analogy with the definition of the physically constant viscosity μ:

$$\tau_{yx} = \varepsilon \frac{d\bar{u}}{dy}. \quad . \quad . \quad . \quad \text{(ii)}$$

ε is called the *eddy*, or sometimes the *mechanical, viscosity*. Calculation from experimental data shows ε to be much greater than μ, as expected, and not a physical constant.

Prandtl has drawn a parallel between the interchanges from one layer to another of the molar masses (or particles) in turbulent flow and those of molecules in laminar flow, substituting a *mixing length* l (in the y-direction) in place of the mean free path of the molecules (cf. Article 23). It must be observed that in the kinetic theory of viscosity the molecules clearly suffer no change of momentum while describing their paths, but that a corresponding immunity cannot be supposed for particles. This point will be returned to. Meanwhile, it is assumed that x-momentum is conserved during the time of transference and l is regarded as a mean path consistent with this assumption. Suffix 0 indicates mean absolute values.

Then a particle penetrating a transverse distance l causes a change of velocity u' at the new position and this is equal to $l(d\bar{u}/dy)$ if l be small. Hence—

$$\tau_{yx} = -\rho\overline{v'u'} = -\rho v'_0 . l \frac{d\bar{u}}{dy}. \quad . \quad \text{(iii)}$$

Now Prandtl assumes that v' is induced by opposite values of u', proportionately great, whence—

$$\tau_{yx} = \rho l^2 \left(\frac{d\bar{u}}{dy}\right)^2. \quad . \quad . \quad . \quad (319)$$

the mixing length being adjusted, if necessary, to absorb any coefficients arising; its magnitude is not determined, and does not remain constant under given physical conditions.

226. Returning now to the question raised in the preceding article, G. I. Taylor * has suggested that, while the x-momentum of the particles may change during transference, their vorticity will remain constant, if in fact viscous effects are negligible as assumed. Exchange between the layers of the mean flow of vorticity rather than of momentum leads to a different scheme for determining a mixing length from experimental data. He obtains the equation—

$$\frac{d\rho}{dx} = -\rho v'_0 . l \frac{d^2\bar{u}}{dy^2}. \quad . \quad . \quad . \quad (320)$$

It is not yet easy to decide from experimental evidence completely in favour of the one scheme or the other.

227. Kármán's Similarity Theory

In order to carry (319) further v. Kármán has introduced the hypothesis that in every region of the turbulent motion the local flow patterns are statistically similar, scales of time and length only varying. Then a first approximation to l is obtained as—

$$l = \varkappa \frac{d\bar{u}/dy}{d^2\bar{u}/dy^2} \quad . \quad . \quad . \quad . \quad (321)$$

where $\varkappa$ is a number. Substituting in (319)—

$$\tau_{yx} = \rho\varkappa^2 \frac{(d\bar{u}/dy)^4}{(d^2\bar{u}/dy^2)^2}. \quad . \quad . \quad . \quad (322)$$

A more convenient form of this result is (dropping the suffix and bar)—

$$\sqrt{\tau/\rho} = \varkappa \frac{(du/dy)^2}{d^2u/dy^2}. \quad . \quad . \quad . \quad (323)$$

The quantity on the left-hand side has the dimensions of a velocity. Its boundary value, viz. $\sqrt{(\tau_0/\rho)}$, is often referred to as the *friction velocity*.

It is not yet known how far the similarity assumption can be justified, but v. Kármán † has applied it to the case of turbulent flow through pipes of circular section. In this case τ is proportional to radius, and replacing it by the skin friction enables (323) to be integrated, giving approximately—

$$u = \frac{\sqrt{(\tau_0/\rho)}}{\varkappa} \log \frac{y}{\delta} \quad . \quad . \quad . \quad (324)$$

* *Proc. Roy. Soc.*, A, v. 135. 1932.

† These results are taken for the most part from a paper in the *Proc. Internat. Con. f. App. Mech.* (Cambridge), 1934, to which reference should be made; original publication was in 1930.

where δ is a constant of dimensions L. With a smooth wall δ depends on τ_0, ρ and ν, and may be replaced by the quantity: const. $\times \nu/\sqrt{(\tau_0/\rho)}$, whence—

$$u = \frac{\sqrt{(\tau_0/\rho)}}{\varkappa}\left(\log \frac{y\sqrt{\tau_0/\rho}}{\nu} + \text{const.}\right). \quad . \quad . \quad (325)$$

This logarithmic formula is suggested in place of the corresponding power formula already considered when very high Reynolds numbers are concerned.

Carrying over to flat plates with the help of a further assumption explained in the next article, v. Kármán finds the approximate formula:

$$\sqrt{(2/C_F)} = \frac{1}{\varkappa}\log (RC_F) + \text{const.} \quad . \quad . \quad (326)$$

Making use of experiment—

$$1/\sqrt{C_F} = 4{\cdot}15 \log_{10} (RC_F) - 1 \quad . \quad . \quad (327)$$

where C_F is defined in Article 223.

Some other results that can be deduced are in good agreement with recent experiment at great Reynolds numbers. The value of $\varkappa$ deduced from observation appears to vary between 0·36 and 0·41; the value used in (327) is 0·39.

228. Skin Drag

An assumption involved in the preceding article is that for turbulent flow through pipes the quantity: $\frac{u_m - u}{\sqrt{(\tau_0/\rho)}}$ where u_m is the maximum mean velocity (at the axis) and u the mean velocity at radius r, is a function of r/a only, a denoting the radius of the pipe.

Experiments with rough pipes give greater resistance for a given flux than with smooth pipes, or, put another way, a rough pipe exerts the same resistance τ_0 as a smooth one of the same diameter when the mean velocities at the same radii are much smaller. The above as-

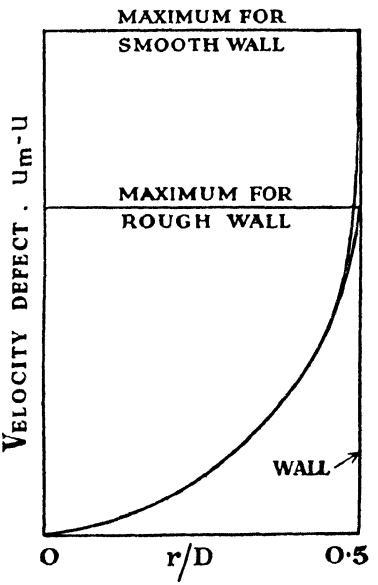

FIG. 164.—VELOCITY PROFILES (EXAGGERATED) FOR SMOOTH AND ROUGH WALLS OF EQUAL RESISTANCE.

sumption requires the profile across the section of the mean velocity to be exactly the same even in two such dissimilar cases. A number of experiments with pipes and channels of different roughness, beginning with those of Stanton,* show this to be approximately true except near the walls ; for equal resistance the *velocity defect* $u_m - u$ is the same through the bulk of the stream for equal values of r/a, though near the walls it may be greatly different (Fig. 164).

With perfect smoothness τ_0 is determined by the boundary value of the velocity gradient through the viscous film lining the walls. The gradient in the vicinity of a sufficiently rough wall is much less for the same value of τ_0, the remaining part of the resistance being due to form drag arising on the protuberances that project beyond the viscous film. Yet the mechanism of the transverse transport of momentum appears to remain approximately the same through the bulk of the flow and independent of the mechanism by which resistance is communicated to the surface. We have used τ_0 to denote this resistance however it arises, but with sufficient roughness it is no longer a pure skin friction but the sum of frictional and form drag components. This sum is termed *skin drag*.

A quite different variation of τ_0 with R is found for rough pipes, as expected. Blasius's and similar approximate laws for smooth surfaces may now be distinguished as *smooth-turbulent*. A pipe that is slightly rough, i.e. whose surface is, or may be regarded as, more or less uniformly covered with very fine grains, has a drag coefficient which at first follows the smooth-turbulent variation, the grains lying wholly within the viscous film. But at some considerable Reynolds number it begins to depart from this law, finally approximating closely to a velocity-squared law. Increasing the grain size causes earlier departure and a higher final C_F.

Formula (325) is inappropriate for asymptotic conditions when resistance is almost wholly comprised of form drag, being nearly independent of ν, and is evidently determined by some parameter k specifying the degree of roughness. Kármán suggests, therefore, for geometrically similar roughness the formula—

$$u = \frac{\sqrt{(\tau_0/\rho)}}{\varkappa}\left(\log\frac{y}{k} + \text{const.}\right). \quad . \quad . \quad (328)$$

But what precisely is meant by k is not yet quite clear.

More generally, τ_0 will depend on both ν and k ; this state appears

* *Proc. Roy. Soc.*, A, v. 85, 1911.

to be realised with well-separated grains or a waviness of surface. Although τ_0 may then be much greater than for smooth-turbulent flow, the velocity-squared law need not be approached within the range so far explored.

229. Application to Aircraft Surfaces

Prandtl and Schlichting * have applied tests on rough pipes to flat plates. Similar effects have also been found in direct experiment in compressed-air wind tunnels on aerofoils † and airship models,‡ and on aeroplane surfaces § in flight. Fig. 165 gives a qualitative || view of the general results of experiments so far published. A surface is *aerodynamically smooth*, if it exerts a pure skin friction; i.e. if its resistance coefficient follows a smooth-turbulent law. With high-speed aircraft this entails a lacquer finish, but roughness has little meaning divorced from the thickness of the boundary layer, or, more explicitly, that of the viscous sub-layer. Thus, at low speeds, doped fabric may be regarded as smooth, but a thin boundary layer makes it Aerodynamically coarsely rough. Waviness effects may be due, on high-speed craft, to such sparsely distributed roughness as the remaining projections of countersunk rivet heads.

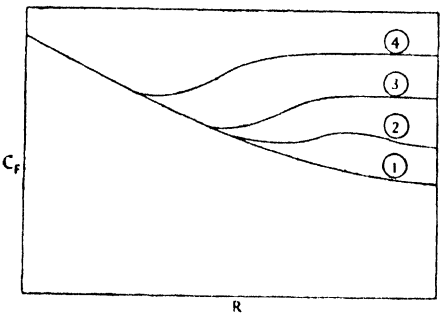

FIG. 165.—QUALITATIVE ILLUSTRATION OF ROUGHNESS EFFECTS.

(1) Aerodynamically smooth surface (smooth-turbulent friction law); (2) wavy or partly rough; (3) completely rough; (4) very rough.

Aerodynamic smoothness is not easy to secure at the Reynolds numbers of high-speed aircraft or compressed-air tunnels, and the increases of drag at stake are important. Thus a grain size amounting to no more than 0·005 in. increases drag by one-half for $R =$

* *Werft. Reed. Hafen*, 15, 1934.

† Relf, *James Forrest Lec.*, Inst.C.E., 1936; Hocker, *N.A.C.A. Tech. N.*, 457, 1933.

‡ Abbot, *N.A.C.A. Tech. R.*, 394, 1931.

§ Schrenk, *V.D.L. Jahrb.*, 1929.

|| Investigations are not sufficiently advanced to take account of several factors likely to affect the practical case. For instance, according to the explanation given, roughness might be expected to have greater significance towards the front than towards the back of the upper surface of a wing.

$5 \times 10^6 - 10^7$. At about these Reynolds numbers with speeds in the neighbourhood of 200 m.p.h. the 'permissible roughness' for the drag to be a pure skin friction is so small a grain size as 0·0005 in.

If k is the size of each of the granules which may be regarded as constituting a completely rough surface, of chord c, k/c is the 'relative roughness' and $R_k = Uk/\nu$ is the 'roughness Reynolds number.' According to some experiments the drag ceases to be a pure skin friction at $R_k = 100$ to a first approximation. Since thereafter C_F depends little on R, the following provisional empirical formula has been suggested as fitting some experiments within the range of Aerodynamic interest :

$$\log_{10} \tfrac{1}{2}C_F = 0{\cdot}188 \left(\log_{10} \frac{k}{c} - 10 \right), \quad . \quad . \quad (329)$$

provided $R_k > 100$, or, since $R_k = R \,.\, k/c$, provided $k/c > 100/R$. These results are given as indicating in a roughly approximate way the great importance of the effects concerned in connection with Aerodynamic calculations and must be regarded as of temporary value ; essential experiments, on which proper analysis depends, are still in progress.

230. Application to Model Experiment

A model of a small aeroplane wing, for a craft capable of 200 ft. per sec., could be tested in a compressed-air tunnel under dynamically similar conditions. R would be $6{\cdot}3 \times 10^6$, approximately. According to the above, the permissible roughness at full scale would be 0·001 in. Assuming this quite practical limit to be realised, the necessity for geometrical similarity would entail reduction on the model to about 0·00013 in. The requirement of smoothness of this high order is faced regarding models for compressed-air tunnels, but calls, of course, for special care in manufacture.

More frequently tunnel tests on model wings are carried out at $R < 5 \times 10^6$ and applied at full scale with $R > 10^7$. The question of geometrical similarity is not so urgent, since dynamical similarity is not attained, but it may be noted that Aerodynamic smoothness is now easily ensured on the model, but is beginning to present difficulties on the aircraft. At small lift coefficients the induced drag of wings tends to vanish, and it is frequently necessary to add considerably to extrapolated tunnel measurements of the drag coefficient in order to take account of greater effective roughness at full scale.

Before small-scale measurements can be extrapolated, it is necessary to know, in addition to full-scale roughness, the effective initial turbulence of the tunnel stream. Thus, taking two extreme cases, Fig. 163 shows that at $R = 5 \times 10^5$ the model boundary layer might be wholly streamline or almost wholly turbulent ; extrapolation of the friction would be along the transition curve in the first case and along the smooth-turbulent curve in the second, until roughness supervened.

The investigations of the present chapter suggest the following method of estimating the full-scale C_D of a wing at zero C_L from small-scale measurements. Measure C_D through a range of R including the highest value obtainable. Determine the normal pressures through a similar range of scale. Subtracting the proper integration of these enables C_F to be determined. Inspection of the C_F variation with R, together with the actual values obtained for this coefficient, in comparison with the various laws described above, will show whether the boundary layer is in a streamline, transitional, or turbulent state in the given tunnel. With this information it is possible to construct a special extrapolation curve on the framework provided by Fig. 161, assuming Aerodynamic smoothness. But it is advisable to check this prediction by direct experimental evidence from large-scale tests at zero incidence. Finally, allowance must be made for full-scale roughness. It is seen to be a question of circumstances whether C_F is greater or less for the model or the full-scale wing, but the scale effect estimated for the friction may be applied to the original measurements of C_D.* If the form drag is left unchanged, the estimate of scale effect may be regarded as conservative ; evidence regarding the implied decrease may be sought by again experimenting under two-dimensional conditions with a slice of the wing of 5-ft. or more chord in the tunnel. The investigation outlined is, of course, laborious, but when a few examples have been worked out in a given tunnel, inspection of the $C_D - R$ curve alone will often give sufficient information in subsequent cases. Collection of such data constitutes what is meant by gaining intimate acquaintance with a particular tunnel.

Comparisons of observations in a given tunnel with experiments in full-scale flight suggest the possibility of a so-called *turbulence factor* for that tunnel, the assumption being that increase of the

* The turbulence in the oncoming streams of wind tunnels is finely grained and especially apt on this score to hasten transition in boundary layers. Natural turbulence in the atmosphere, being characterised by a much larger scale, permits of delay. Model experiments are frequently corrected, therefore, in anticipation of a larger transition Reynolds number being realised in free flight.

tunnel Reynolds number by this factor will give an 'effective' Reynolds number at which agreement with flight tests can be expected. It is also hoped to determine the factor by some critical test, such as that on a sphere described in Article 65. Many questions arise, of which the most important is whether a single factor could apply to phenomena of different kinds, and the conception remains tentative.

Chapter IX A

REDUCTION OF PROFILE DRAG

230 A. Normal Profile Drag

Profile drag is defined as the sum of skin friction and form drag. The term is reserved to aerofoils and wings, though the considerations of this chapter apply in principle to all streamlined bodies.

The corresponding coefficient C_{DO} is expressed on wing area and may be estimated for a three-dimensional aerofoil by subtracting a calculated coefficient of induced drag from the total drag coefficient. The result is approximately independent of aspect ratio provided this is not very small. Again, for aerofoil sections of the type universally employed until recently, it is approximately independent of the lift coefficient provided this is not large. Such sections are likely to be superseded in the near future but are meanwhile distinguished by the term 'normal.' Thus each normal aerofoil can be regarded without much error as having, through a fairly wide range of flying incidences, a particular value of C_{DO} appropriate to the Reynolds number, and determinable directly under two-dimensional conditions.

At low Reynolds numbers the boundary layer of an aerofoil is entirely laminar, but breakaway occurs at certain positions round the section, depending upon shape and incidence, and results in a large form drag. At higher Reynolds numbers transition to turbulence usually takes place in the boundary layer before the positions of laminar breakaway can be reached. Breakaway may still occur but at least is delayed,* and is commonly prevented altogether at small incidences by turbulent mixing. In any case form drag is reduced. Skin friction, on the other hand, is much increased by transition.

Fig. 165A, based on the results of experiments at the N.P.L. with a series of Kármán-Trefftz sections, indicates the relative magnitudes of skin friction and form drag at Reynolds numbers in the neighbourhood of 1 million. There was apparently no breakaway but only a

* Experimental details for a sphere are given by Fage, A.R.C.R. and M. No. 1766, 1937.

thickened diffusion of vorticity towards the tail. The curves would be modified by increase of scale, but not very rapidly, and are fairly typical of normal aerofoils in wind tunnels except at small scales.

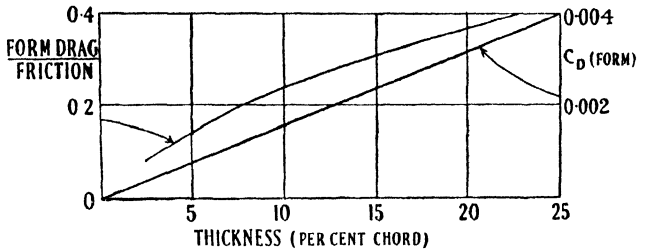

FIG. 165A.—FORM DRAG OF JOUKOWSKI SYMMETRICAL AEROFOILS AT $R = 10^6$.

The curves of Fig. 165B for C_{DO} at Reynolds numbers of 1, 10 and 20 million, respectively, are averaged results for various aerofoils, British and American, tested * by the pitot traverse method at zero lift incidence in the compressed-air tunnel at the N.P.L. They agree fairly well with Fig. 165A and may be regarded as representative of good normal aerofoils in tunnels of moderate turbulence. The enclosed points in the figure will be referred to later.

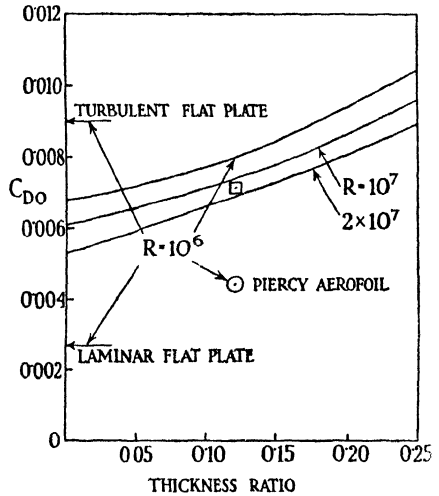

FIG. 165B.

Flight experiments on normal wings show that turbulence in the boundary layer sets in more sharply and at a rather larger transition Reynolds number than in the case of a model in a wind tunnel. The reduction of C_{DO} to be expected on this score has been investigated by Squire and Young.† Considering normal sections at a small lift coefficient, these authors assumed transition to occur at various distances up to 0·38 chord behind the nose and estimated by approximate calculation the consequent variation of profile drag.

* R. Jones and Williams, A.R.C.R. & M. No. 1804, 1937.
† A.R.C.R. & M. No. 1838, 1938; *see also* Fage, A.R.C.R. & M. No. 1852, 1938.

The front parts of the two curves in Fig. 165c (*a*) give the coefficient of (single surface) frictional drag for the upper surface only, according to these calculations. Curve (1) refers to a thickness ratio of 0·14, curve (2) to a thickness ratio of 0·25, and the Reynolds number is 10 million. The extension of these curves for transition points at greater distances than 0·38 chord behind the nose is referred to later. At (*b*) in the figure is shown the change in the distribution of skin friction following an extreme displacement of the transition point for the upper surface of a normal aerofoil, from close behind the nose in a very turbulent wind tunnel or airscrew slipstream (dotted line) to 0·4 chord behind the nose in free flight under favourable conditions (full line). A change of about half this amount can often be anticipated, and then the curves at (*a*) suggest a decrease of about 20 per cent. in the frictional drag. The authors also found, with the fixed profiles investigated, a diminution of form drag with backward displacement of transition, increasing the above improvement.

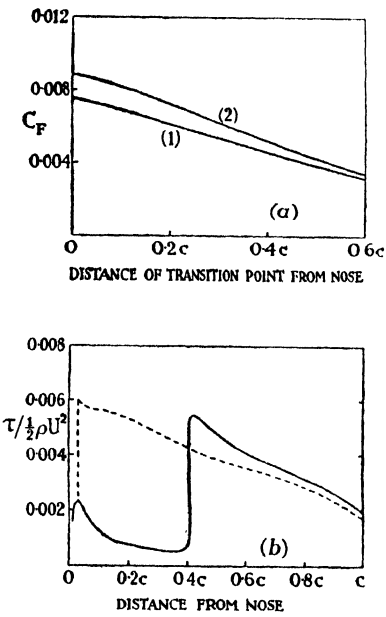

FIG. 165c.

230B. The Problem of Reduction

Until recently there appeared little promise of substantially less values of C_{DO} than those recorded in the preceding article. Nevertheless, minimising profile drag is of such importance that research into the problem has never been interrupted. In addition to testing large numbers of different aerofoil sections in the hope of discovering an abnormally good one, more scientific methods have also been employed for some years, viz. (*a*) mathematical studies aimed at determining the optimum shape for a wing section of given thickness, (*b*) improvement of the boundary layer flow by operating directly upon it, mechanically or otherwise.

These two methods are outlined separately below, but the principle primarily involved is the same. We have seen in the last article

that a restricted displacement of the transition point effects a considerable saving in frictional drag. If the restriction can be removed without undue increase of form drag, the saving in profile drag is likely to be large. The curves of Fig. 165c (*a*) have been extended to illustrate this. Displacing the transition point from 0·2 to 0·6 chord behind the nose, for instance, may be expected to halve the skin friction.

Various difficulties arise, however, in applying the principle. Re-shaping the profile for minimum drag cannot be carried to excess without introducing other disadvantages. Moreover, the practical feasibility of the method calls for an exceptionally high standard in the construction and surface finish of wings. The most promising form of method (*b*) incurs pump and duct losses which have to be minimised, and depends in the end upon the mechanical reliability of plant installed in the aeroplane. In all probability the two methods will eventually be used in conjunction with one another.

Compressibility is neglected in the following articles. Method (*a*) finds further application, however, in minimising profile drag at high subsonic speeds. This rather different problem is briefly discussed at the end of the chapter.

LAMINAR FLOW WINGS

230C. Early Example

In applying method (*a*) to the present problem the primary aim is to delay both laminar separation and transition so that the latter only just anticipates the former and occurs as far back from the nose as is possible without incurring penalties in matters other than drag.

Laminar separation can be calculated from first principles approximately, as already described, though the process is rather beyond the scope of this book ; and the conformal methods introduced in Chapter VI, or other means, can be employed to shape wing profiles in such a way as to yield far-back positions of this breakaway. Transition, on the other hand, is less perfectly understood.

Some factors tending to delay both phenomena are easily seen to be of the same nature, and an important instance is the maintenance of a negative pressure gradient. Its effect on laminar separation has already been mentioned (Article 159), while the following experiment by Dryden illustrates its effect on transition. A flat

plate tested in a moderately turbulent wind tunnel gave a transition Reynolds number of $1{\cdot}8 \times 10^6$ in the presence of the small negative pressure gradient caused by the thickening boundary layers of the tunnel, and eliminating this pressure gradient decreased the transition Reynolds number by 40 per cent. A qualitatively similar effect may be expected in flight, small irregularities of the wing surface taking the place of the initial turbulence of the wind-tunnel stream in producing disturbances. The magnitude of the negative pressure gradient necessary to damp out such disturbances, or prevent them developing, will depend upon their magnitude and nature and probably upon whether laminar separation or transition would otherwise result.

In 1939 a Piercy aerofoil of the simple family described in Article 128, with the maximum thickness of its section located at 0·4 chord behind the nose (see Fig. 92C), was tested at zero incidence in the compressed-air tunnel at the N.P.L. and gave, at a Reynolds number of 1 million, the result shown in Fig. 165B as an encircled point. Owing to differences arising from the method of testing, either this value of C_{DO} should be increased slightly or the values for the three curves in the figure reduced slightly. As the point stands in the figure, the lowest recorded value of C_{DO} for a normal aerofoil with which it can be compared is shown as the point enclosed in a square. The improvement achieved by the Piercy aerofoil is thus not less than some 35 per cent. The advantage disappeared at large scales but this is known to have been due to initial turbulence in the stream.*

The measured value of C_{DO} being less than that for a flat plate (thickness ratio zero in the figure) at the same Reynolds number in the same tunnel, the improvement was too great to be accounted for by even the total elimination of form drag, whilst actually the form drag could not have been less than about one-third normal. It immediately became apparent, therefore, that the skin friction was much less, and the transition Reynolds number much greater, than for normal aerofoils or the flat plate under the given conditions. This is explained by the exposure of a greater length of profile to a sufficiently falling pressure, see Fig. 92C.

Aerofoils of the type thus introduced are called *laminar flow aerofoils*. To measure their values of C_{DO} may require an exceptionally steady stream or flight experiments. Wind tunnels specialised to the purpose are often called *laminar flow tunnels* and were introduced in America.

*Relf, Wilbur Wright Lecture, *R.Ae.S.*, 1946.

230D. The laminar flow wing is not a particular design but a concept exerting a directive influence on the problem of shaping the profile for minimum drag under given conditions. The conditions are specified by practical needs or exigencies, which include: restriction of pitching moment, preservation of maximum lift coefficient and of control, structural requirements and constructional deficiencies. Waviness or roughness of surface must not be very unfavourable; laminar flow sections serve no useful purpose for roughly made wings or in the slipstreams of airscrews; and the surface must be kept clean.

The process of design is intimate, and potential flow theory finds an important application in enabling the effects of shape variations, however small or large, to be determined with accuracy except towards the tail. Conformal transformation, which in its highly developed modern form can encompass even such cases as the flapped wing, facilitates these calculations whilst protecting the profile from sudden changes of curvature.

The simple family of aerofoils inverted from the hyperbola has the advantage of reproducing at once a generally satisfactory section provided the position of maximum thickness is not set back farther than 0·42 chord from the nose Adjustment of the position within this practical limit is rendered possible by the fact that the family has two shape parameters in place of the single parameter of the Joukowski family.

But the family is insufficient for the full development of the laminar flow wing, which may require its maximum thickness to be located nearer to the tail than the nose, whilst the original Piercy profiles become sharp at the nose when the maximum thickness is located midway along the chord.

Additional parameters are necessary to remove this and other restrictions to shape variation. A generalisation to provide nine or more parameters, if necessary, has been effected by the author and Whitehead, yielding an exact method for extending potential flow calculations to extreme variations of profile shape.

With the profile thus made indefinitely variable, the problem of finding the optimum shape for given conditions is widened. Modifications of shape for examination by potential flow calculations may be suggested by experiment, if suitable tunnels are available, or as a result of collateral boundary layer investigations. Experiment is in any case necessary in some connections, e.g. to determine effects upon the maximum lift coefficient and form drag.

In the following brief introduction,* the above generalisation will be assumed.

230E. Incidence Effect

Casual inspection of pressure diagrams shows an acute dependence upon lift coefficient and the new aerofoils are not exceptional in this respect. Yet to be of practical interest laminar flow wings must maintain a long negative pressure gradient through a sufficient range of lift coefficient to cover ordinary variations of speed, altitude and wing-loading.

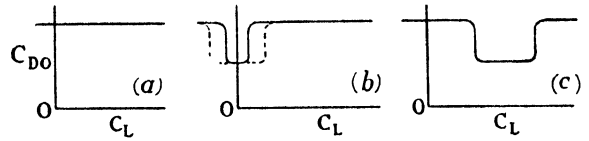

FIG. 165D.

Fig. 165D applies to ordinary flying lift coefficients and shows at (*a*) the approximately constant profile drag coefficient of normal wings, and at (*b*) the modification produced by a laminar flow symmetrical section. The interval of C_L through which C_{DO} is reduced is often called the *favourable range of lift coefficient*, or simply the favourable range. In the symmetrical case it is restricted to small lift coefficients, positive and negative, but can be sufficiently widened, as shown dotted, for application to fin and rudder design. Again, the mean value of C_L in the favourable range can be displaced from zero, as shown at (*c*) in the figure, by the addition of suitable camber.

* So far as is yet generally known, the development of laminar flow aerofoils during the war was pursued (i) at the National Physical Laboratory, (ii) in America, and (iii) in the author's temporary research school at Cambridge. The paper by Relf (*loc. cit.* p. 413) may be consulted for a description of (i), where it appears that Goldstein evolved an approximate method, based on Thin Aerofoil Theory, of calculating profiles which would reproduce pressure distributions specified beforehand from experimental or analogous considerations; for the reverse process, the potential theory of the arbitrary profile, reference may be made to Theodorsen and Garrick, N.A.C.A. Report No. 452, 1933. It is understood that (ii) relied to a considerable extent upon experiment in laminar flow wind tunnels. Preliminary descriptions of (iii) are contained in the A.R.C. Reports:—Piercy, Whitehead and Garrard, Ae. 1889, 1941; and Piercy and Whitehead, Ae. 1890, 1942: Ae. 2246, 1943: Ae. 2266, 1943. The procedure in (iii) was to employ the exact method mentioned in the text above for the potential flow calculations, so that all the wing profiles belonged to a single, though very extensive, family; and suggestions for shape variation were derived largely from mathematical investigations of the boundary layer flow.

It is too early to compare the advantages and disadvantages, the achievements and shortcomings, of these various methods, and only the barest introduction can be given in this book to a development which is prominent amongst those likely to improve aviation appreciably.

Characteristics of the new aerofoils are often exhibited by means of diagrams of the velocity ratio q/U, i.e. the velocity at the edge of the boundary layer expressed in terms of the undisturbed velocity. This system is adopted in the following figures.

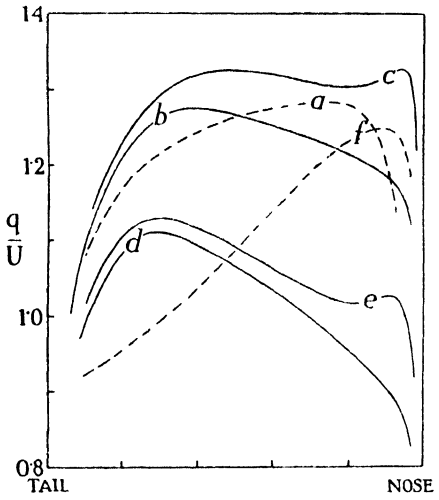

FIG. 165E.

The three curves *a*, *b*, *c*, in the upper part of Fig. 165E refer to the upper surfaces of cambered aerofoils. Curve *a* is typical of normal sections and curve *b* of laminar flow sections, both at favourable lift coefficients. The difference between these two curves is characteristic. The positions of the marking letters throughout the figure indicate where transition is to be expected.

As the lift coefficient is increased further, the negative pressure gradient implied by curve *b* is progressively reduced and ultimately suffers a reversal near the nose, as indicated at *c*. Laminar flow can survive a small localised reversal of a strongly negative gradient, the boundary layer re-attaching itself to the aerofoil surface after brief separation, but in such circumstances as are depicted by curve *c* laminar flow is impossible over the major part of the profile. Curve *a* would also become modified to a forwardly peaked form, and in practice there would be little to choose between the two sections at the higher lift coefficient.

Curve *d* in the lower part of the figure refers to the under-surface of a laminar flow section and again differs essentially from the corresponding curve *f* for a normal section. Curve *e* applies to the laminar flow section at an unfavourable lift coefficient. But the lift coefficient for the unsatisfactory curve *e* is now less than that for the satisfactory curve *d*. For skin friction to be a minimum, the velocity curves on both surfaces should be of the type *b* and *d*. Thus the favourable range is determined by the interval between the values of the lift coefficient at which the reversals shown near *c* and *e* first become appreciable, the former as incidence is increased and the latter as it is decreased. Outside this range the profile drag reverts rapidly to normal.

It follows that to be effective in flight the magnitude of the negative pressure gradient must be sufficient not only to overcome disturbances caused by slight roughness or inequalities of the wing surface but also to provide for change of incidence.

230F. Examples of Shape Effects

To illustrate preliminary steps in the design of a successful laminar flow profile, we may consider in the first place the typical problem of improving the symmetrical section distinguished by the thin full-line in Fig. 165F. As will be seen from the corresponding velocity

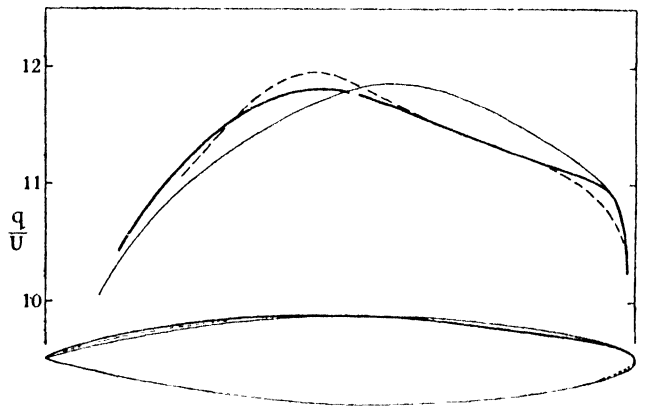

FIG. 165F.

diagram, this is already a laminar flow section, but we may suppose that excellence of construction demands a further reduction of C_{DO}.

The position of maximum velocity could be set considerably farther back by thickening the section a little in the regions of its front and rear third-chord points. We assume, however, that on trying this expedient the favourable pressure gradient, though extended, becomes too weak. It is therefore decided to locate the position of maximum thickness considerably farther back, resulting in the section and velocity curve shown by thick full-lines. The negative pressure gradient is extended without unduly decreasing its magnitude.

Is the new section satisfactory ? Three instances will be given of further modifications worth consideration.

(1) The sharp knee in the velocity curve close behind the nose probably signifies an unduly small favourable range, a matter which can be investigated by calculating parts of the velocity curves

in this region for a few small angles of incidence. Assuming that the knee develops rapidly, it must be rounded at zero incidence, and this may be achieved by sharpening the nose a little, as shown by the dotted lines near the nose. There is a consequent loss of maximum lift coefficient, however, which must be verified to be negligible or of acceptable amount.

(2) The tail of the new section is blunt, raising two associated questions. Will the back part of the boundary layer, though turbulent, break away and increase form drag ; will the power of the ailerons decrease ? Assuming that special tests or calculations return rather unfavourable replies to these questions, the section must be slightly thinned between the trailing edge and the position of maximum thickness. The new velocity curve is likely to be improved upon the whole by this change, as illustrated by the dotted lines towards the tail.

(3) Assuming that the improvement expected under (2) is realised, would it be suitable to carry the modification further by making the back part of the profile strongly concave ? This question may be considered apart from awkwardness of manufacture ; concave back parts have often been suggested for laminar flow aerofoils. Proper investigation other than by experiment is complicated, but there is easily seen to be a risk of unstable flow arising, as described in Article 207, from the streamlines becoming convex towards layers in which energy has been dissipated through friction.

Camber and Pitching Moment

The amount of camber has a special significance in the case of laminar flow aerofoils. The mean lift coefficient for the favourable range and other common requirements being specified in advance, there is usually little choice as to the camber to employ. Interest centres rather in adjusting the shape of the camber-line to reduce the moment coefficient whilst preserving a sufficient favourable range.

Geometrically, if a fairly thin section requires appreciable camber whilst its maximum thickness is located nearer to the tail than the nose, the crest of the camber-line cannot be advanced as far towards the nose as considerations of pitching moment would suggest without introducing a concavity, and part of the stabilisation must be effected by reflexure of the camber-line towards the tail. The loss of maximum lift coefficient associated with this reflexure may lead to designs in which the crest of the camber-line is edged so far forward as to cause a flat on the front part of the under-surface, as in Fig.

165G. The consequent increase of curvature along the front half of the upper-surface reduces the magnitude of the negative pressure gradient along that surface, but the gradient along the under-

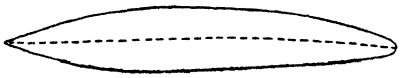

FIG. 165G.

surface is increased. Fig. 165E illustrates the effect conservatively, curve *b* having a less slope than curve *d*.

The argument may be put another way. Apart from considerations of pitching moment, both the aerofoil surfaces would be given much the same pressure gradient, and the lift would be more or less evenly distributed over a large part of the chord. In order to minimise the moment, lift is added forward of the quarter-chord point and subtracted aft of that point, a change that clearly requires the velocity curves to be adjusted in the manner described.

BOUNDARY LAYER CONTROL

230G. The method (*b*) of Article 230B, known as *boundary layer control*, is concerned with improving the operation of existing aerofoils without necessarily modifying their shape. Laminar flow sections are included since their development is otherwise limited by bluntness of tail ; boundary layer control can prevent consequent breakaway, restricting form drag and conserving the efficiency of ailerons.

Breakaway results from ' tired ' air in the boundary layer being unable to proceed very far against a rising pressure. It would appear feasible to re-energise such air by means of backwardly directed jets under pressure, but such jets tend to break up. More usually, therefore, the de-energised air is removed by sucking it into ducts within the wing. Long narrow apertures or slits may be located for the purpose close behind regions of expected breakaway, and their exhausting action, if sufficiently strong brings air unaffected by viscosity towards the surface to begin a new boundary layer. The action can be repeated farther downstream, if necessary.

The same process serves to prevent transition to turbulence, a new boundary layer being started when transition becomes imminent. The strong suction required to remove an entire boundary layer implies large pumping and duct losses. If local suction is used to prevent transition, thorough scavenging appears to be necessary in order that the following boundary layer shall be laminar, as shown

schematically for the upper surface of the aerofoil in Fig. 165H. But if most of the wing profile is already under laminar flow and only breakaway is to be prevented, the condition of the boundary layer behind the slits may be of small importance, provided the general flow closes in fairly satisfactorily, and this may be achieved without dealing with so large a flux (lower surface in the figure). Slits have also been tried in the neighbourhood of the nose.

FIG. 165H.

Alternatively to the use of isolated slits, it has often been proposed to maintain an exhausting action upon the whole of the boundary layer through a porous wing-covering. Prandtl * considers the case in which the distributed action is sufficiently powerful over regions of increasing pressure as to keep the boundary layer to a constant thickness and indicates how design calculations may proceed on this basis.

Subsequent reading must be relied upon for further information. But it is as well to realise, particularly before starting a research, that publications on boundary layer control cover only a very small fraction of the work that has been carried out on this subject in many aeronautical laboratories during the past twenty-five years. Remarkable results are easy to produce; the difficulty lies in establishing the economy and reliability of the methods by which they are obtained.

230H. Many practical applications of boundary layer control have been concerned with the delay of stalling. This aspect comes within the purview of the present chapter since stalling usually results from a rapid forward movement of breakaway, preventing which not only maintains lift but also avoids large increase of profile drag. The result may be achieved by suction methods or, as we have already seen, by slots.

It has often been proposed to apply slots to small incidences in the case of large wings. The conception leads to a succession of small wings forming a kind of cascade, Fig. 165I, and the profile drag is the sum of the skin frictions and form drags of the component members; resolved parallel to the direction of motion. In a modern form each

* Aerodynamic Theory, vol. III, p. 117; 'In all cases it can be proved that an arbitrary potential flow can be generated by the use of suitable suction methods.'

member would be designed for laminar flow with due regard, in the first place, to the resultant velocity and pressure fields caused by the other members. The schematic figure indicates that the wake of each component aerofoil is carried clear above following aerofoils. Air of undiminished energy is brought to each aerofoil by a process reverse to that described in the preceding article, avoiding the need

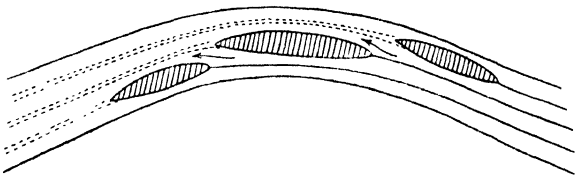

FIG. 165I.

for pumps and ducts. For small profile drag, the complete wing should comprise a sequence of long laminar boundary layers interrupted by short lengths of turbulent boundary layers, and a series of small form drags. The external flow is not entirely irrotational but contains turbulent layers of vorticity, one of the effects of which may be to produce fluctuations in the boundary layers, calling for stronger negative pressure gradients.

230I. Prediction of Lift

The advent of wing sections with blunt tails renews interest in alternatives to Joukowski's hypothesis as a means of predicting the circulation. Eventual breakaway may be permitted with some laminar flow wings, and cannot be prevented if the pumping installation should fail with wings depending upon some types of boundary layer control. In such circumstances Joukowski's hypothesis cannot be applied to a thick section with confidence. The problem is in general difficult but progress becomes possible if laminar separation can be assumed, a condition formerly realised only at small Reynolds numbers but which may now be approached in some full-scale cases.

Betz showed that the flux of vorticity across any normal section of the boundary layer is proportional to the square of the velocity at its edge. From this theorem and the reflection that in a steady state vorticity must be transported into the wake equally from the two sides of the aerofoil, Howarth * proposed that the circulation K be so determined as to make the velocities just outside the boundary layer equal at the two points of breakaway. So far, this criterion has not proved very successful, owing possibly to the necessary

* *Proc. Roy. Soc.*, A, vol. 149, 1935.

neglect of production of vorticity behind the points of breakaway and unequally on the two sides of the aerofoil.

Another method has accordingly been proposed * which is founded upon considerations affecting the wake only, so that all the vorticity from the aerofoil is included, and is related to the requirement † that the circulation round any circuit enclosing part of the wake only and cutting through it at right-angles must be zero. The application of this method to an elliptic cylinder of fineness ratio

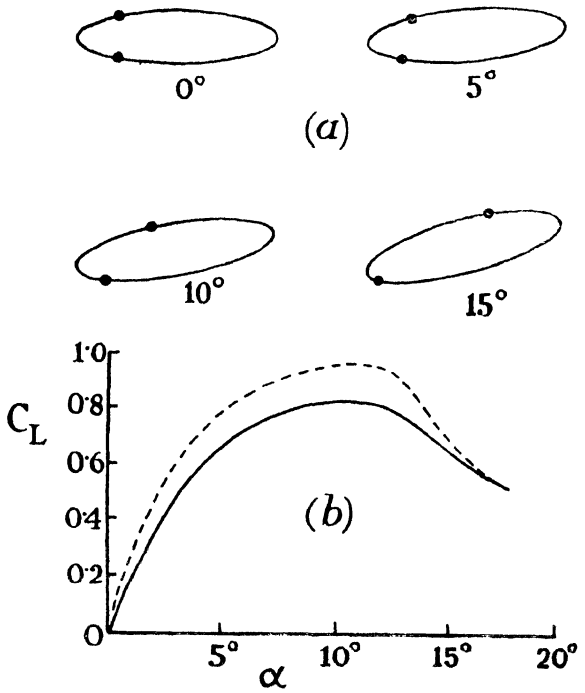

FIG. 165J.

5·4 will be briefly indicated, leaving the original paper to be consulted for further details.

Fig. 165J shows at (a) the approximate positions of laminar separation at various incidences α. The wake behind these points varies in thickness, finally gradually expanding by the diffusion of vorticity so that streamlines cross into it. Small variations in the shape and thickness of the wake are found to affect the problem only negligibly and, as an approximation, the thickness is assumed to be approximately equal to the projected distance between the points of

* Piercy, Preston and Whitehead, *loc. cit.*, p. 219.

† Taylor (Sir Geoffrey) *Phil. Trans. Roy. Soc.*, A, vol. 225, 1925.

separation, and the edges of the wake to be parallel to the streamlines. This involves that, along the wake, the velocities at its edges are equal at opposite points, leading to an unique value for K. The method is essentially one of successive approximation since the positions of laminar separation themselves depend upon K.

At (b) in the figure the full-line reproduces the lift curve so calculated and comparison is made with a wind-tunnel experiment on the cylinder by Fage * at a Reynolds number of 0·17 million. It will be seen that the stalling angle is predicted with some accuracy. Again, the difference at smaller incidences is partly due to initial turbulence in the tunnel and the approximate nature of the calculations. Whitehead† has re-examined the method in relation to a cambered aerofoil of the family described in Article 133A and found good agreement with experiment until past the stall at a sufficiently low Reynolds number as to ensure laminar flow in the tunnel used.

HIGH SPEEDS

230J. Compressibility effects at subsonic speeds have already been discussed. Experimental evidence suggests a progressive increase of C_{DO}, but also that the increment is small until the critical Mach number is approached. Minimising the increment is of little importance compared with that of delaying the occurrence of shock. The shock wave forms near the position of maximum velocity, before moving backwards with an accompanying change of the pressure distribution over the profile.

The principal consideration in profile design for high speeds is to reduce the maximum velocity ratio, which compressibility itself increases. If the assumption is made that the shock wave forms when the maximum velocity attains to the local velocity of sound, the maximum permissible velocity ratio appropriate to incompressible flow for shock to be avoided at a given Mach number is easily calculated. The result is rather low; thus an incompressible flow velocity ratio of 1·20 involves on this basis a critical Mach number of only 0·73.

The following maximum velocity ratios are typical of laminar flow sections having a thickness ratio of 0·15 chord :

Camber (per cent. of chord) ..	0	1	2	3
Maximum velocity ratio.. ..	1·18	1·23	1·28	1·33

These figures can be improved upon with a less backwardly displaced position of maximum thickness or a less pressure gradient, and

* A.R.C.R. & M. 1097, 1927. † Ph.D. *thesis*, London, 1939.

laminar flow sections restricted in this way are more suitable for high speeds than are normal sections. But for the above thickness the maximum velocity ratio even for an ellipse is 1·15, and the absolute theoretical minimum is about 1·14.* Thus there is urgent need for a drastic reduction of thickness and camber. The thin wing sections required entail the use of small aspect ratios.

230K. An aeroplane fitted with wings of a given section having a sweep-back θ, Fig. 165K (*a*), can attain without shock a larger Mach number V/a than the critical Mach number U/a without sweep-back. The effect is explained qualitatively as follows.

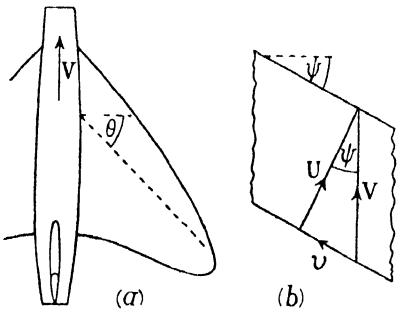

FIG. 165K.

A long straight wing in flight at velocity V and angle of yaw ψ, Fig. 165K (*b*), may be compared with the same wing flying without yaw at a velocity U and with a velocity of sideslip v. We have $\psi = \sin^{-1}(v/V)$, $U = V \cos \psi$ and, away from the wing-tips, the pressure distribution will be that appropriate to the velocity U. In so far as θ can be identified with ψ, we should expect the critical Mach number of the wings as fitted to the aeroplane to be increased in the ratio $V/U = 1/\cos \theta$. However, the correspondence is very rough.

In applying this method to estimate the rolling moment on a side-slipping aeroplane equipped with a lateral dihedral, we noted that the calculated moment might be expected to prove excessive by about one-third, owing to wing-tip and body effects. Additional cause of error arises with the swept-back aeroplane since the substitution of sideslip for yaw becomes progressively untenable as the centre-line is approached; near the body the streamlines, though convergent, cannot be deflected appreciably by sweep-back. When also the restricted aspect ratio imposed by the use of thin wing-sections is taken into account, little of the above advantage, perhaps only one-third, may remain. This can still be made considerable, however, by the use of exaggerated sweep-back. Thus with $\theta = 45°$, V/U would be 1·14 on this basis.

* Whitehead, A.R.C. Report Ae. 2073, 1942.

Chapter X

AIRSCREWS AND THE AUTOGYRO

231. The Ideal Propeller

Airscrew principles find many useful applications, but for brevity we concentrate for the most part on propulsion, recognising a need for modification of treatment in widely different circumstances. First, following Rankine and the Froudes, we investigate the characteristics of an ideal propeller of the kind which, like an airscrew, produces axial thrust by acting on the air passing through its disc. By what means this action is effected is for the moment of no concern ; different ' machines ' that may be employed for the purpose will have different efficiencies ; and to eliminate such variation the mechanical process is assumed to be perfect. Thus the propeller is represented vaguely as an *actuator disc* of diameter D, over which a thrust T is distributed. The disc will have a velocity V relative to the undisturbed air (of pressure p) consistent with the rate at which work is being done in propelling the craft. We also assume the entire flow to be steady and irrotational (though these conditions would not be satisfied with an actual airscrew).

The actuator imparts motion impulsively to the air passing through its disc, and increases its kinetic energy at a certain rate, which measures the work done by the impulse, and which for efficiency should be a minimum. We then argue, from Article 173, that the final velocity through the stream affected should be the same at all points. The flow takes the form of a jet (Fig. 166), the part behind the disc, called the slipstream, attaining a minimum section, where the velocity is V_s, a maximum. Consider any small area δS_s of this minimum section. A corresponding element of thrust δT can be calculated from the rate of change caused by the propeller of the momentum of the air crossing it, or—

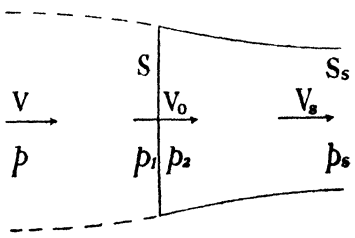

FIG. 166.

$$\delta T = \rho \delta S_s V_s (V_s - V).$$

The condition for minimum kinetic energy then leads to $\delta T \propto \delta S$, independently of the position of the element. Consequently, for maximum efficiency the thrust must be uniformly distributed, which we assume to be the case.

Let V_0 be the velocity at the actuator disc, and write S for its area. Then, on momentum considerations, since $\rho S V_0$ is the mass flow per second—

$$T = \rho S V_0 (V_s - V). \quad . \quad . \quad \text{(i)}$$

Let p_1 be the pressure on the face of the disc, and p_2 that on its back. Then an alternative expression for the thrust is—

$$T = S(p_2 - p_1). \quad . \quad . \quad \text{(ii)}$$

Now Bernoulli's equation applies with one constant outside the slipstream and with another within it. Also the velocity V_0 must be continuous through the disc, so that energy put into the stream immediately at the actuator is in the form of pressure. Therefore, applying Bernoulli's equation outside and inside the slipstream, we have—

$$p + \tfrac{1}{2}\rho V^2 = p_1 + \tfrac{1}{2}\rho V_0^2$$
$$p_s + \tfrac{1}{2}\rho V_s^2 = p_2 + \tfrac{1}{2}\rho V_0^2$$

V_0 being regarded as the equal velocity at two adjacent points on opposite faces of the disc and suffix s denoting the *vena contracta* of the slipstream as before. Here, the streamlines being parallel, the pressure has again become equal to that in the undisturbed stream. Remembering this and subtracting—

$$p_2 - p_1 = \tfrac{1}{2}\rho(V_s^2 - V^2).$$

Substituting in (ii)—

$$T = \tfrac{1}{2}\rho S(V_s^2 - V^2). \quad . \quad . \quad \text{(iii)}$$

Comparing this expression with (i), we obtain the important result—

$$V_0 = \tfrac{1}{2}(V_s + V) \quad . \quad . \quad . \quad (330)$$

i.e., of the total velocity added, one-half appears at the actuator.

It is usual to write—

$$V_0 = V(1 + a) \quad . \quad . \quad . \quad . \quad (331)$$

a being called the *inflow factor*. The addition to velocity at the disc is aV and that at the *vena contracta* $2aV$.

232. Ideal Efficiency of Propulsion

Useful work is done by the actuator at the rate TV, the drag of the craft, together with any parallel component of its weight, being equal

to T for steady motion. But the actual rate of doing work equals the rate E at which kinetic energy is increased in the fluid, assuming steady speeds, and this is—

$$E = \tfrac{1}{2}\rho S V_0 (V_s^2 - V^2) = \tfrac{1}{2} T (V_s + V)$$

by (i). Hence the efficiency η is given by—

$$\eta = \frac{TV}{E} = \frac{V}{\tfrac{1}{2}(V_s + V)} = \frac{1}{1 + a} \quad . \quad . \quad (332)$$

The result shows that, other things being equal, efficiency decreases as thrust becomes concentrated. To express this conveniently, define a thrust coefficient T_c by $T/\rho V^2 D^2$, when (iii) becomes—

$$T_c = \frac{\pi}{2} a (1 + a)$$

and (332) gives—

$$\frac{1 - \eta}{\eta^2} = \frac{2}{\pi} T_c \quad . \quad . \quad . \quad . \quad (333)$$

It is important to bear in mind that the ideal propeller should be not only uniformly loaded but as large as possible for a given thrust.

Examples.—A slow aeroplane weighing 2 tons has an over-all lift/drag ratio of 8 at 100 m.p.h. What is the ideal efficiency of its airscrew, of 10 ft. diameter, at this speed?

The drag $= T = 4480/8 = 560$ lb. and $\rho V^2 = 51{\cdot}2$, giving $T_c = 0{\cdot}109$, whence $a(1 + a) = 0{\cdot}0695$ or $a = 0{\cdot}065$. Then (332) gives $\eta = 93{\cdot}9$ per cent. This efficiency could not be surpassed under the given conditions; an airscrew for this duty might have an efficiency of 82 per cent., but the further loss would be due to its own characteristics.

It may further be noticed that since $V_0/V_s = 1{\cdot}065/1{\cdot}13$, the jet contracts to a diameter $= 0{\cdot}97\ D$; and again that, since $(V_s/V)^2 = 1{\cdot}277$, an aircraft part exposed in the slipstream may have its drag increased thereby in this ratio.

233. The Airscrew

The familiar airscrew imitates the action of the foregoing hypothetical propeller by means of blades whirled round by an engine. Considerations of efficiency and weight economy limit their number to two, three, or at most four. The ratio of the total area of the blades, counting one side only, to that of the disc of revolution swept out is known as the *solidity* of the airscrew, and is usually a small fraction. The blades support, of course, the whole thrust, in

producing which outer parts are more effective than inner, owing to their greater speeds ; over an appreciable area surrounding the boss the thrust will, in fact, be zero. Thus we now have to take into account variation of the intensity of thrust with radius, called thrust grading. Considering any concentric annulus of the disc, of small solidity, the distribution of thrust round it is periodic, being concentrated only over the blade elements, and the flow through any part of it pulsates. For the purpose of calculating the flow, we assume, however, that the thrusts of the several blade elements included in the annulus may be regarded as distributed uniformly round it, and deal with a mean flow at the given radius. This is equivalent to assuming a large number of very narrow blades.

Let the airscrew make n revolutions per second, or its angular velocity be Ω. Each element at radius r (Fig. 167), traces a helical path of pitch V/n relative to the undisturbed air. But the air at the disc is subject to inflow, and also has a slight spin in the same sense as the airscrew, defined by a certain rotational factor b, such that the angular velocity of the air just behind is $2b\Omega$. Of this one-half is due to vortices from the blades, so that the element has a forward velocity $V(1 + a)$ and an angular velocity $\Omega\,(1 - b)$. The angle ϕ which the helix makes with the plane of revolution is then given by—

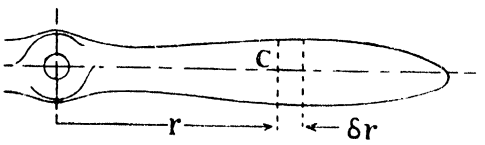

FIG. 167.

$$\tan \phi = \frac{V}{\Omega r} \cdot \frac{1 + a}{1 - b}. \quad . \quad . \quad . \quad (334)$$

The thrust of a blade element is derived from its lift, exerted perpendicularly to its path, while torque arises partly from lift and partly from drag, which acts parallel to its path. High lift/drag ratio makes for efficiency, and blade sections are shaped like those of wings and set at suitable incidences α to their helical paths. ϕ increases rapidly towards the boss, and the whole blade forms a twisted aerofoil. The angle θ between the plane of revolution and the chord of the blade at any radius, viz.—

$$\theta = \phi + \alpha \quad . \quad . \quad . \quad . \quad (335)$$

is called the blade angle.

The axial advance per revolution when $\alpha = 0$, i.e. $\phi = \theta$, depends on r, for so do a and b in (334). But we define the *geometric pitch* P

of an airscrew as this advance at a radius of 0·35 D, where D is its diameter.

By varying the throttle opening of the central unit of a three-engined craft, we could clearly vary the *effective* pitch of the central airscrew through a wide range, and in fact geometric pitch has no Aerodynamic significance. Such variation is readily carried out on a model airscrew in a wind tunnel, and thrust measured for all values of V/n. It is then found that thrust vanishes for one particular value of V/n for a given airscrew, no matter what V or n may be. This unique advance per revolution is called the *experimental mean pitch*. It is greater than P, because α will be negative, assuming cambered blade sections. The airscrew must advance a less distance per revolution, and the difference is called *slip*, although sometimes slip is reckoned from P.

It is convenient to define pitch, etc., in terms of D. The non-dimensional parameter V/nD is denoted by J.

The thrust of the whole airscrew will be denoted by T, and the torque required to maintain its rotation by Q. Then the efficiency, expressing the ratio of the rate of useful work done to power supplied, is—

$$\eta = \frac{TV}{Q\Omega} \quad . \quad . \quad . \quad . \quad (336)$$

and takes into account all losses, whether inherent in propulsion or peculiar to the airscrew.

234. Modified Blade Element Theory

Fig. 168 shows the circumstances of a blade element of chord c and span δr at radius r. Its resultant velocity W is expressible in alternative ways, e.g.—

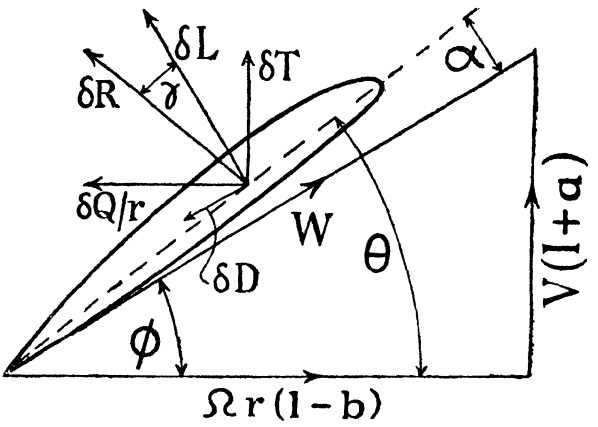

FIG. 168.

$$W = V(1 + a) \operatorname{cosec} \phi = r\Omega\,(1 - b) \sec \phi. \quad . \quad (337)$$

Let δR be the resultant force it exerts, inclined backwards from the

direction of its lift δL by the angle $\gamma = \tan^{-1}(\delta D/\delta L)$, δD being the drag. Writing $\delta T'$, $\delta Q'$ for the thrust and torque of the single element, from the figure—

$$\delta T' = \delta R \cos(\phi + \gamma), \quad \delta Q' = r\delta R \sin(\phi + \gamma), \quad \text{(i)}$$

whence at radius r—

$$\eta = \frac{V\delta T'}{\Omega\delta Q'} = \frac{1-b}{1+a} \cdot \frac{\tan\phi}{\tan(\phi+\gamma)}. \quad . \quad . \quad (338)$$

Now Lanchester and Drzewiecki introduced the assumption, since justified by experiment * for important parts of the blade, that effects of one element on another at different radius (and having in general a different lift) can be ignored. This enables us to write for any element $\delta L = C_L \tfrac{1}{2}\rho W^2(c\delta r)$, $\tan\gamma = C_D/C_L$, etc., where the coefficients are obtained by tests in the wind tunnel on aerofoils of the same section as that of the blade considered and at the same incidence. All induced velocities are included in a and b, so that tests should be made under two-dimensional conditions; it is in this respect that original blade element theories have been modified. Since tests are usually made at aspect ratio 6, conversion to infinite span is required before application to airscrews, and accurate formulæ should be used for the purpose (cf. Article 179); scale and roughness corrections should be applied to the profile drag coefficients so obtained in accordance with the concluding articles of Chapter IX.

With this understanding we proceed as follows. A B-bladed airscrew has B elements at any radius and, if δT, δQ denote their combined thrust and torque, from equations (i) or Fig. 168—

$$\delta T = B(\delta L \cos\phi - \delta D \sin\phi),$$
$$\delta Q = rB(\delta L \sin\phi + \delta D \cos\phi).$$

Substituting coefficients and diminishing δr indefinitely—

$$\frac{dT}{dr} = B(C_L \cos\phi - C_D \sin\phi)\tfrac{1}{2}\rho W^2 c \; . \quad . \quad (339)$$

$$\frac{dQ}{dr} = rB(C_L \sin\phi + C_D \cos\phi)\tfrac{1}{2}\rho W^2 c. \quad . \quad (340)$$

W is given by (337), but it will be observed that knowledge of a and b is necessary to determine ϕ. With this knowledge, thrust and torque grading can be calculated at a series of radii having known sections set at definite incidences. Fig. 169 illustrates practical thrust and torque grading curves, showing values increasing with r,

* Lock, A.R.C.R. & M., 953, 1924.

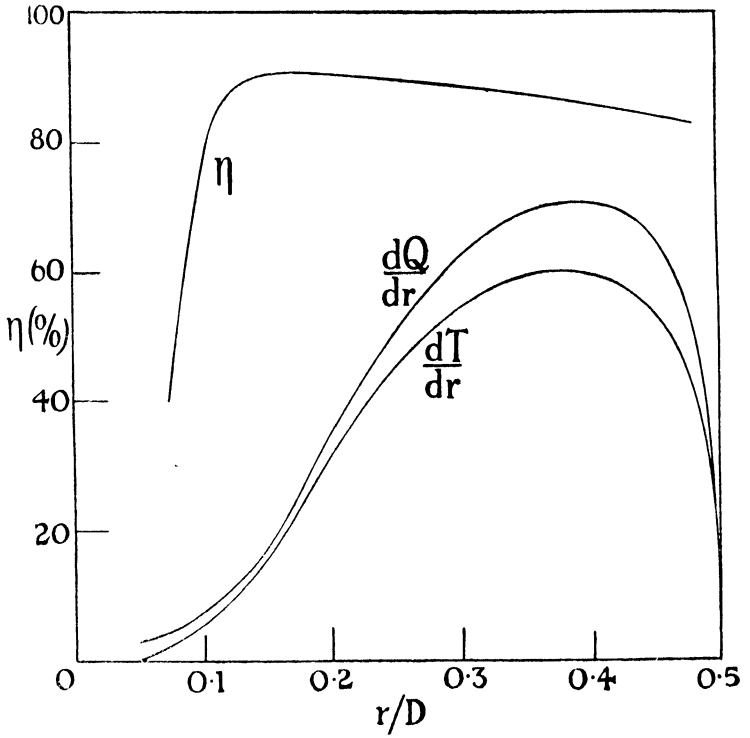

FIG. 169.—TYPICAL THRUST, TORQUE AND EFFICIENCY GRADING CURVES FOR AN AIRSCREW.

i.e. with W, until c is narrowed to form a tip. Such curves can be integrated graphically from boss to tip to give T and Q. Subject to two corrections—for tip losses and the drag of the boss, depending on the type of spinner used—the efficiency of the whole airscrew then follows from (336). Variation of efficiency along the blade is also shown.

Before proceeding to the calculation of a and b, some points of interest in (338) may be noted. Ignoring a and b, it is found by differentiation that η is a maximum when $\phi = 45°$, approximately, γ then being negligible in comparison with ϕ, whence maximum efficiency along the blade occurs at $r/D = J/2\pi$. In fixed-pitch practice r is small for this condition, e.g. taking $V = 250$ ft. per sec., $n = 25$ r.p.s. and $D = 10$ ft., $r/D = 0{\cdot}16$, and little of the thrust occurs there. The efficiency of the complete airscrew is increased by decrease of n, or increase of V, keeping n constant, i.e. by increase of pitch well towards π. Practical disadvantages exist

in the weight of the airscrew and the gearing interposed between it and the engine, but these tend to become less important with large fast craft. These results are modified by a and b (which make general investigation of the maximum possible efficiency of a practical airscrew more complicated), but the principle still applies ; decrease of efficiency with large values of $\Omega r/V$ is fundamental to the existence of γ, i.e. of form drag and skin friction. That the lift/drag ratio of sections should be high is asserted directly by (338). Provided tip speeds do not approach the velocity of sound, this is only difficult to secure near the root of the blade, where thickening is required for strength and stiffness.

235. Simplified Vortex Theory

The lift force on each blade is due to circulation round its sections whose variation with radius casts a vortex sheet from the trailing edge. This tends to roll up towards the axis and periphery of the slipstream, but meanwhile extends downstream as a screw surface which is at first not quite regular owing to contraction of the slipstream. Thus the flow approaching the airscrew ceases to be wholly irrotational on crossing its disc. It must be possible to calculate the slipstream from the distribution of vorticity within it and the circulation round the blades, if known, and this calculation would yield a and b. These quantities are now appropriately called *interference factors*. To simplify consideration, a large number of blades with suitably weakened circulation is again assumed. Irrespective of this assumption, however, it is clear that the flow far downstream cannot be affected appreciably by the circulation round the blades, while interference at the disc is due wholly to the trailing vorticity.

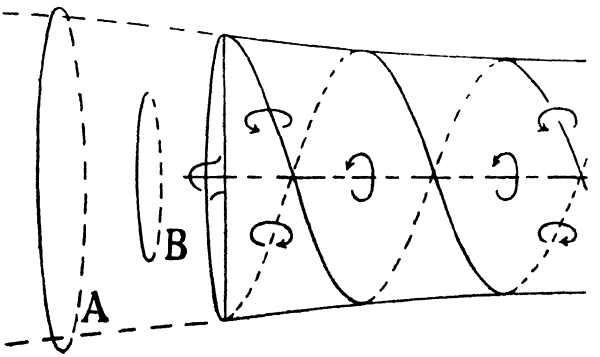

FIG. 170.

For clearness, first imagine that rolling up is complete at the blades, so that circulation is constant along them. The simple trailing system is then a shell of spiral vortices marking the boundary of the slipstream together with an axial ' shaft ' of vorticity ; it is illustrated for two blades only in Fig 170. This system can be resolved into vortex rings and longitudinal vortex lines, the first producing axial velocity, and the second rotation in the slipstream. With non-uniform circulation along the blades, the whole slipstream will be a pack of such systems. Radial velocities are dealt with later on.

Now for a lightly loaded airscrew disc we may neglect the contraction of the slipstream. Then regarding the axial disturbance, it is clear, from the theory of Chapter VII, that the velocity at any point in the disc will amount to one-half of that at the same radius far downstream. This agrees with and extends the result of Article 231.

Considering next the rotation, let us first follow a wide loop A (Fig. 170), formed always of the same particles of air. Upstream of the airscrew, its circulation is zero to accord with the irrotational flow, and this remains true, by Article 140K, as it threads over the slipstream, showing that rotation is confined to the slipstream. Now the circulations of the whirling blades are obviously trying to cause circulation in front of the disc and, for this to be zero, the tendency must be exactly balanced by an equal and opposite induction there by the trailing system. Just behind the disc, however, the circulations round the blades induce rotation about the axis in the opposite sense, and this is therefore added to the equal rotation induced by the trailing system. Thus, if we follow a narrow loop B (Fig. 170), it is set spinning at the disc, and exactly half this spin is due to the trailing system. Again, by Article 140K, the circulation round this loop of particles cannot change as it passes along the slipstream, so that, as the influence of the blades decreases, so must that of the trailing vortices increase. Hence the spin caused in the loop when at the disc, by the trailing vortices only, amounts to one-half of that induced by them far downstream. Finally, we remember from aerofoil theory that modification from two-dimensional conditions is due solely to the trailing vorticity, and deduce that the rotation interfering with the blade incidence is one-half of that at the *vena contracta.*

Summing up, if the velocities of the blades relative to the air they engage are $V(1 + a)$ and $\Omega(1 - b)$ then the velocities finally added are $2aV$ and $2b\Omega$.

236. Approximate Momentum Equations

The following treatment proceeds on the assumptions that the slipstream is sensibly parallel, that rotation is insufficient (as is known) to cause appreciable variation of pressure, and that averaging round annuli is permissible. For ordinary airscrews, at least, these assumptions appear to involve little error.

The rate at which fluid mass crosses the airscrew disc at radius r is $m = \rho \cdot 2\pi r\delta r \cdot V(1 + a)$. The velocity finally added in reaction to thrust is $2aV$. Equating thrust to rate of change of momentum—

$$\frac{dT}{dr} = 4\pi\rho r V^2(1 + a)a. \quad . \quad . \quad \text{(i)}$$

Again, the angular velocity finally given to m is $2b\Omega$, so that, considering the rate of change of angular momentum, $\delta Q = m \cdot 2b\Omega \cdot r^2$, whence—

$$\frac{dQ}{dr} = 4\pi\rho r^3 V\Omega(1 + a)b. \quad . \quad . \quad \text{(ii)}$$

Expressions for the Interference Factors

We must be able to equate the foregoing to the alternative formulæ of Article 234, whence a and b can be evaluated in a given case.

It is convenient to introduce symbols for the resolved force coefficients and the solidity of the annulus at radius r:

$$\left.\begin{aligned} 2t &= C_L \cos\phi - C_D \sin\phi \\ 2q &= C_L \sin\phi + C_D \cos\phi \\ \sigma &= Bc/2\pi r. \end{aligned}\right\} \quad . \quad . \quad . \quad (341)$$

Then equating (i) to (339) gives—

$$4\pi r V^2(1 + a)a = BtcW^2.$$

Substituting for W from (337)—

$$\frac{a}{1 + a} = \tfrac{1}{2}\sigma t \operatorname{cosec}^2\phi. \quad . \quad . \quad . \quad (342)$$

In similarly equating (ii) to (340) note that W^2 can be written—

$$W^2 = V(1 + a) \operatorname{cosec}\phi \cdot \Omega r(1 - b) \sec\phi.$$

Then it is at once found that—

$$\frac{b}{1 - b} = \sigma q \operatorname{cosec} 2\phi. \quad . \quad . \quad . \quad (343)$$

These formulæ are somewhat awkward to use; the interference factors appear in t, q and ϕ, and graphical or trial and error methods

are needed to determine them. A suitable method is described immediately after the next article.

237. Practical Formulæ

Defining thrust and torque coefficients for the complete airscrew in the usual form :

$$k_T = \frac{T}{\rho n^2 D^4}, \quad k_Q = \frac{Q}{\rho n^2 D^5}, \qquad . \quad . \quad (344)$$

thrust grading is expressed non-dimensionally as—

$$\frac{dk_T}{d(r/D)} = \frac{dT}{dr} \cdot \frac{1}{\rho n^2 D^3} = \frac{dT}{dr} \cdot \frac{4\pi^2}{\rho \Omega^2 D^3},$$

and torque grading similarly. Substitute for dT/dr, dQ/dr from (339) and (340) after using (337) to express W in terms of Ω. Then—

$$\frac{dk_T}{d(r/D)} = 8\pi^3\sigma \left(\frac{r}{D}\right)^3 t\,(1-b)^2 \sec^2\phi \quad . \quad . \quad (345)$$

and—

$$\frac{dk_Q}{d(r/D)} = 8\pi^3\sigma \left(\frac{r}{D}\right)^4 q\,(1-b)^2 \sec^2\phi \quad . \quad . \quad (346)$$

Alternative formulæ are obtainable in terms of a.

J for the airscrew is connected with ϕ and the interference factors for the element by the relationship :

$$J = \frac{V}{nD} = 2\pi \left(\frac{r}{D}\right) \frac{V}{\Omega r} = 2\pi \left(\frac{r}{D}\right) \frac{1-b}{1+a} \tan\phi \quad . \quad (347)$$

from Fig. 168.

The efficiency of the element is given by (338), but may be expressed in terms of J as follows, making use of the last formula—

$$\eta = \frac{J}{\pi} \cdot \frac{D}{2r} \cdot \cot(\phi + \gamma). \quad . \quad . \quad . \quad (348)$$

Simpler expressions for t and q than those so far given are sufficiently accurate for most purposes. Since $\tan\gamma = C_D/C_L$ the first may be written—

$$2t \cos\gamma = C_L(\cos\phi\cos\gamma - \sin\phi\sin\gamma).$$

Hence for small values of γ—

$$2t = C_L \cos(\phi + \gamma).$$

Similarly— . . . (349)

$$2q = C_L \sin(\phi + \gamma).$$

These approximations fail when α for the blade section is near the

incidence for either zero lift or the stall, and for root sections which are too thick for high lift/drag ratios.

238. Method and Example

It is usually required in practice to analyse an airscrew for several flight conditions, i.e. through a range of J. The following procedure collects the necessary data while meeting the inconvenience of (342) and (343).

Having selected a radius, subtract from the blade angle θ a series of values of α for the blade section, giving a number of ϕ's. The force coefficients will be known for each incidence and t, q follow. Then a, b, and other quantities are at once calculated and the results give curves of variation against J. The process is repeated with a number of other radii. Finally, variation against r/D is read from the curves at the constant values of J that are of interest and integration is effected by a planimeter or other means.

A fair degree of accuracy and provision for checking is required, and it will be found convenient to work out tables of 25 or 30 columns for each radius. Representative columns and rows are illustrated in Table VIII (an additional significant figure is usually attempted).

The particular case relates to two-thirds radius of a 2-bladed airscrew of 9 ft. diameter used on an aeroplane whose top speed is 160 m.p.h., the airscrew then turning at 1200 r.p.m. The pitch/diam. ratio is 1·5, so that $\tan\theta = D(P/D) \div (2\pi \,.\, \frac{1}{3}D) = 1{\cdot}5 \div \frac{2}{3}\pi$, or $\theta = 35{\cdot}6°$. The chord at $r = 3$ ft. is 0·754 ft., so that $\sigma = 0{\cdot}08$. Zero lift for the section occurs at $-2°$, while its lift coefficient slope is 0·10 per degree. Up to $C_L = 1{\cdot}2$, $\gamma = 1°$ subject to a minimum $C_D = 0{\cdot}010$. These aerofoil figures have already been duly corrected to infinite span. The third row of the table is added for comparison, taking 10° less blade angle, nothing else being changed.

TABLE VIII

θ	α	ϕ	t	q	a	b	J	η	$d/d(r/D)$: k_T	$d/d(r/D)$: k_Q
35·6°	1·6°	34°	0·146	0·105	0·019	0·009	1·37	0·92	0·153	0·0367
35·6°	10·6°	25°	0·566	0·276	0·145	0·028	0·83	0·81	0·478	0·0777
25·6°	1·6°	24°	0·162	0·078	0·041	0·008	0·89	0·89	0·140	0·0225

It has been chosen here to illustrate the efficiency of the element.

The larger value of θ gives curve (A) of Fig. 171. Zero thrust occurs at $J = 1{\cdot}6$, approximately, so that efficiency falls steeply. Curve

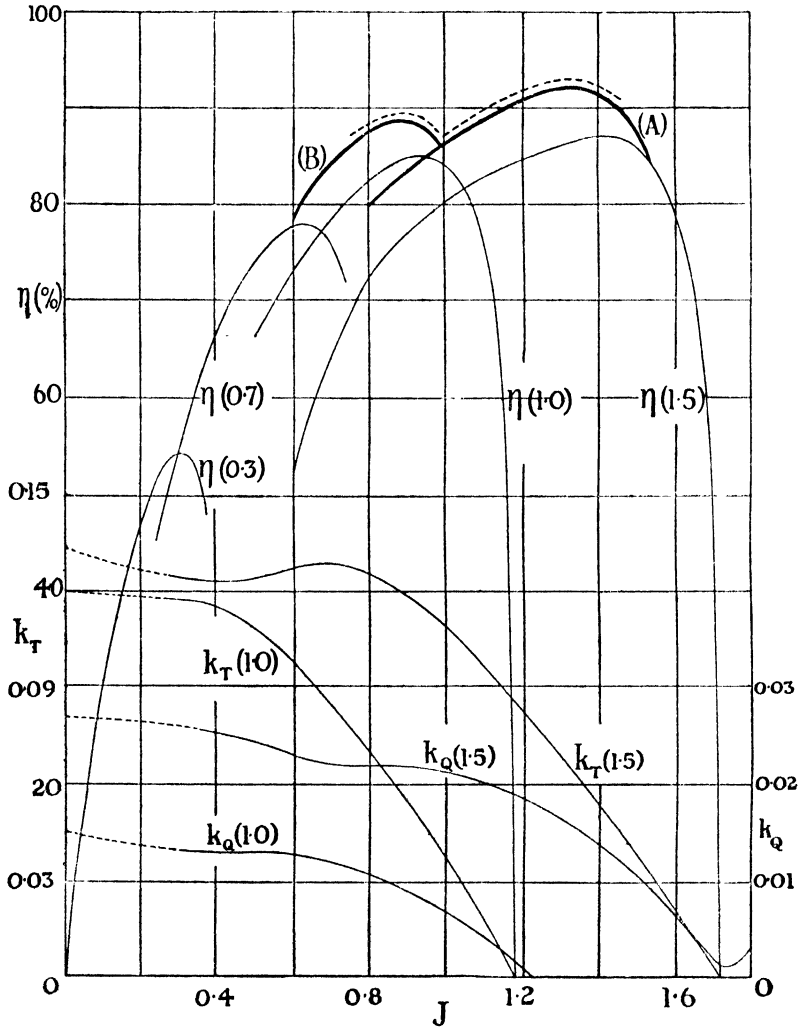

FIG. 171.—TYPICAL EXPERIMENTAL CURVES FOR AIRSCREWS.

The numbers in brackets give pitch/diameter ratios.

(B) relates to $\theta = 25{\cdot}6°$ and shows the loss in maximum efficiency due to the correspondingly smaller value of J. Increase of efficiency

with pitch is further illustrated by the group of experimental curves obtained with a family of airscrews. The dotted increase to curves (A) and (B) indicates the greater efficiency that would follow a reduction of C_D by 20 per cent. to 0·008, which by Fig. 165B is feasible for normal sections with a smooth, non-wavy surface, at the Reynolds number for the flight condition ($R = 2{\cdot}1 \times 10^6$); three times this reduction is achieved by using laminar flow sections. Referring to curve (A), the element practically attains maximum efficiency at top speed flight ($J = 1{\cdot}3$), but with $J = 0{\cdot}8$, which might correspond to maximum climb, efficiency is much reduced; the lift coefficient for the section is then about 1·28 and it is approaching stall, bearing in mind the Reynolds number. That arrest of thrust and fall in efficiency are imminent are confirmed by the experimental curves for a complete airscrew of the same P/D ratio (1·5). The table also shows that a is more important than b, which may sometimes be neglected.

239. Principle of Variable Pitch (V.P.)

In the preceding article it has been seen that the representative blade element (and we may infer the whole airscrew) designed for top speed is in a poor position to produce climb. In a V.P. airscrew the blades are socketed into the boss, and θ is increased or decreased uniformly along all blades, thus adjusting pitch, either automatically or under control. Decreasing θ by 10° increases the local efficiency in the above example from 0·80 to 0·877 at $J = 0{\cdot}8$. However, the last column of Table VIII shows that the torque coefficient would not be sufficient to absorb the full power of the engine at its maximum permissible revolutions, just as with the original pitch it would be too great to allow the engine to attain its revolutions and develop full power. When the requisite adjustment is made, there still remains an important increase in the power available for climb, though with a light aeroplane of small power it usually requires to be verified that the rate of climb is appreciably improved after taking into account the additional weight of the apparatus. But with high-duty commercial craft, and of course military aeroplanes, which are usually fitted with supercharged engines for flying at considerable altitudes, variable pitch is critically important. Apart from substantially improving climb and maintenance of altitude with partial engine failure, it may approximately double thrust during the early stages of take-off, and enable full power to be used with increase of efficiency at heights where decrease of density would

otherwise require the engines to be throttled to prevent racing. As an example, it may be mentioned that the convenient and efficient twin-engined aircraft design can be carried to considerably greater all-up weights with V.P. than with fixed-pitch airscrews.

We shall illustrate the use of variable pitch by reference to the experimental curves of Fig. 171. These do not quite accord with constant variations of blade angle, but the difference is ignored. An airscrew of 11 ft. diameter with a two-position hub is assumed, giving $P/D = 1{\cdot}0$ or $1{\cdot}5$. For simplicity, the supercharged engine of 800 b.h.p. is assumed to maintain its power at constant revolutions (25 r.p.s.) up to 11,000 ft. altitude. The most important considerations are taken to be speed at this altitude and climb at ground level, for which first estimates of A.S.I. are 300 and 200 ft. per sec. respectively.

From the engine data we find that the constant torque exerted by it is 2800 lb.-ft. and, taking account of the variation of ρ (the relative density $= 0{\cdot}71$, approximately, at 11,000 ft.), this gives *possible* torque coefficients for the airscrew of 0·0117 at G.L. climb and 0·0165 at altitude. The two values of J are 0·73 and 1·30. It is verified from the torque curves of Fig. 171 that the two pitches comply with these conditions. The efficiency at high altitude is 86 per cent. and during climb at the smaller pitch it is 80 per cent. At $J = 0{\cdot}73$ the efficiency with the larger pitch is only 67 per cent., but the torque coefficient required would be more than the engine can manage. 640 thrust h.p. is available during low-level climbing and 688 at high speed at 11,000 ft. where, however, the estimated velocity is 356 ft. per sec. Again taking account of the density, 580 thrust h.p. would produce the same level A.S.I. at low altitude ; the larger pitch would be used and the engine would slow down a little and give less power, but probably more than sufficient to maintain the A.S.I. Provision of a third pitch would improve maximum speed at low altitude.

Static Thrust

To illustrate numerically the advantage of variable pitch at the beginning of take-off requires knowledge of the variation of engine power with rotational speed—information supplied by the makers from bench tests for each engine. We shall assume the possible variation : b.h.p. $= 71{\cdot}5\, n^{3/4}$, which accords with 800 b.h.p. at 25 r.p.s., so that $Q = 550 \times$ b.h.p.$/2\pi n = 6260/n^{1/4}$ lb.-ft. Now at ground level, still with an 11-ft. airscrew, $\rho D^4 = 34{\cdot}8$ and $\rho D^5 = 383$. Assuming

first the larger pitch ($P/D = 1{\cdot}5$) we have $k_Q = 0{\cdot}0269$ at $J = 0$ from Fig. 171, whence—

$$\frac{Q}{\rho n^2 D^5} = 0{\cdot}0269 = \frac{6260}{383\, n^{9/4}}$$

giving $n = 17{\cdot}3$. Then since $k_T = 0{\cdot}133$ from the figure, $T = 1388$ lb. Repeating the calculation for $P/D = 1{\cdot}0$ ($k_Q = 0{\cdot}0151$, $k_T = 0{\cdot}120$ at $J = 0$), we find $n = 22{\cdot}3$ and $T = 2077$ lb. Thus the finer pitch gives nearly 50 per cent. greater static thrust in this instance. Most of the improvement is inherent in the smaller pitch, but part is due to the blades not being so badly stalled. This may be shown in an approximate manner as follows :

When a blade is completely stalled the Aerodynamic force acts approximately at right-angles to the chord, or $\gamma = \alpha$. Thus in equations (i) of Article 234, $\phi + \gamma = \theta$ and, since $P = 2\pi r \tan \theta$, or $\cos \theta = 2\pi r \sin \theta / P$, we have for the representative element—

$$\delta T' = \delta R \,.\, 2\pi r \sin \theta / P = \delta Q' \,.\, 2\pi / P.$$

If we assume constant pitch we can sum for all elements, obtaining—

$$T = 2\pi Q / P \quad . \quad . \quad . \quad . \quad (350)$$

for a completely stalled airscrew.

Application to the foregoing example gives approximately—

P (ft.)	16·5	11
Q (lb.-ft.)	3070	2880
T (lb.)	1169	1644

showing an improvement of 41 per cent. in the second case. Neither of the original airscrews is completely stalled, but the first is the nearer to that state.

240. Ordinary Tip Losses and Solidity

No mention has yet been made of radial components of velocity in the slipstream. Though small in its interior, these attain considerable values towards its boundary owing to the small number of blades, whose circulation diminishes towards the tips. Looked at slightly differently, the momentum equations require a factor, depending on radius, expressing that the annulus does not take up momentum quite so efficiently as supposed. The effect decreases as the number of blades increases, and a 4-bladed airscrew has an appreciable advantage in this respect over one of two blades.

Theoretical investigation must be left to further reading ; approximate treatment has been given by Prandtl * and a closer solution by

* See Glauert in *Aerodynamic Theory*, v. IV, p. 261, 1935.

Goldstein.* The simplest way of viewing the results is to conceive that the diameter of the airscrew is effectively diminished by tip losses, so that by Article 231 efficiency is decreased at given thrust coefficients. The following approximate formula results from the theory to determine D_e, the effective diameter—

$$\frac{D_e}{D} = 1 - \frac{1{\cdot}386}{B} \cdot \frac{J}{\sqrt{(\pi^2 + J^2)}} \quad . \quad . \quad . \quad (351)$$

This gives the curves in Fig. 172 for two, three, or four blades, showing that the effect becomes important for large P/D ratios; at

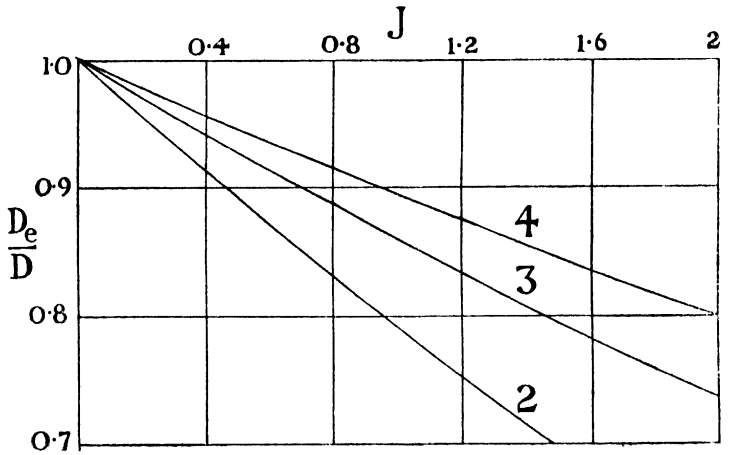

FIG. 172.—EFFECT OF TIP LOSSES.
The numbers refer to 2-, 3- or 4-bladed airscrews.

$J = 1{\cdot}3$ the loss in ideal efficiency of a 2-bladed airscrew on this score is 4 per cent.

Thus tip losses make at least three blades desirable with high pitch. It may then be necessary, however, to increase solidity, which through greater skin friction and form drag again decreases efficiency. This question is easily investigated by the methods already established, and it will be found that, although efficiency is much reduced at low P/D ratios, the correction diminishes at large ratios. It may well result in a given high-speed example that loss from greater solidity following change from two to three blades is less than one-half the gain in respect of effective diameter.

* *Proc. Roy. Soc.*, A, v. 123, 1929.

241. Compressibility and High Speed Tip Losses

Losses of a different kind are caused on the outer parts of blades by the compressibility of air when tip speeds approach the velocity of sound. In the example of flight at 11,000 ft. given in Article 239, the resultant velocity W at $r = 0{\cdot}4D$ is 777 ft. per sec. neglecting inflow; the ratio of this to the velocity of sound at the altitude is 0·72; and, without specially suitable blade sections from this radius to the tip, efficiency forecast from experiments at lower tip speeds would not be realised. At the compressibility stall, it is difficult to estimate force coefficients and equally doubtful how they may be applied to airscrew design as radial flow occurs. Study is more usefully concerned with avoiding such effects when tip speeds must be high, than with their computation. The theory of compressible flow introduced in earlier chapters is supplemented by tests on aerofoils in high-speed tunnels,* tests on model airscrews rotated at fast rates in standard wind tunnels,† on airscrews in special tunnels,‡ and in flight.§ The following description is based on these published data.

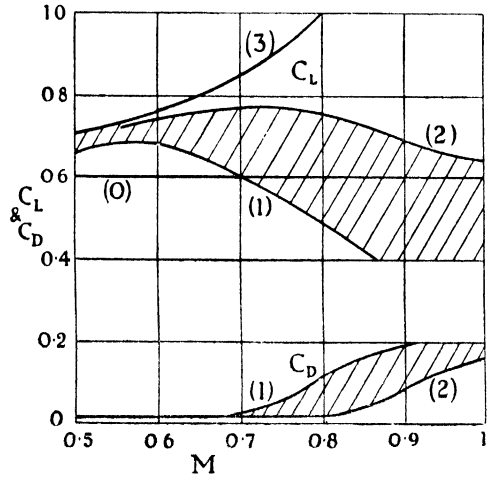

FIG. 173.—THE COMPRESSIBILITY STALL.

(0) Incompressible flow lift coefficient; (1) 10 per cent. thickness and 10 per cent. camber; (2) 10 per cent. thick symmetrical Joukowski aerofoil section; (3) Glauert's formula: $C_L \propto 1/\sqrt{(1-M^2)}$.

The symbol M will denote the ratio of the speed of a blade section at large radius to that of sound. As M increases, Glauert's theory suggests that for moderately high speeds C_L should increase in the ratio $1/\sqrt{(1-M^2)}$, and this variation is realised by some aerofoils. Drag also gradually rises, and there is an increase of thrust and torque, but with little change of efficiency. When $M = 0{\cdot}7$ to 0·8 the compressibility stall sets in, as illustrated in Fig. 173, several

* See Chapters III and VI B, C.

† Douglas and Perring, A.R.C.R. & M., 1086, 1927; Hartshorn and Douglas, A.R.C.R. & M., 1438, 1931.

‡ Weick, N.A.C.A.T.R., 302, 1928; Wood, N.A.C.A.T.R., 375, 1931.

§ Jennings, A.R.C.R. & M., 1173, 1928; E. T. Jones, A.R.C.R. & M., 1256, 1929.

reasonable sections falling within the hatched areas. At $M = 0{\cdot}8$, k_T may be falling and η still more quickly. With greater speeds these effects are accelerated, and before the velocity of sound is reached by the tips the following results are not impossible in a bad case: C_L down well below the incompressible flow value, perhaps by one-third; C_D approaching 0·2; γ passing through 20°; thrust diminished by 10 per cent., and efficiency by more than 20 per cent.

In spite of these alarming figures airscrews can be designed to attain $M = 0{\cdot}9$ at the maximum radius without loss of thrust and possibly also with little loss in efficiency, see Fig. 173A. The first precaution is to restrict thickness ratios for outer sections; 8 per cent. is a desirable limit, while decrease to 7 per cent. gives a great improvement, but such thin blades tend to flutter. Then in any case, but especially to permit increase of thickness, mathematical profiles of very small camber and minimum 'maximum velocity ratio' (Chapter VI) should be employed; thus a 10 per cent. Joukowski section has been found * to give as good results as an 8 per cent. section having a flat under-surface. Finally, solidity may be greater than for an airscrew working at lower speeds. The problem becomes most urgent, of course, in the case of fast aeroplanes at high altitudes when clearly rotational speeds should be low and pitch large.

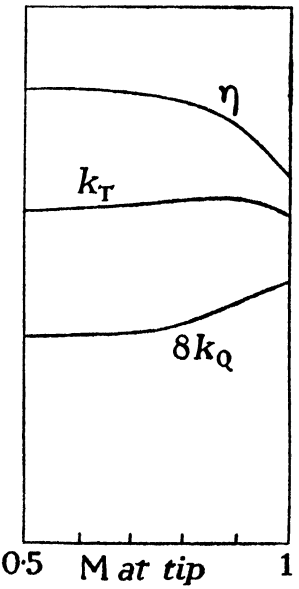

FIG. 173A.

242. Note on Preliminary Design

Systematic test results exist for families of airscrews of different P/D ratios from which may be obtained by interpolation approximate figures for a projected design. Investigation on the lines described above then determines whether the family shape can be varied advantageously in view of special conditions, but these may be so exceptional as to demand complete departure. The education of an Aeronautical Engineer commonly includes the working out of

* Douglas. *Aircraft Engineering*, March 1936.

an airscrew from first principles. The exercise loses part of its engineering value unless an attempt is made to fulfil a prescribed specification, and, to avoid disappointment, approximate analysis should precede detailed work on a proposed design.

Diameter.—Article 231 suggests a large diameter for efficiency, but limitation arises as follows: (*a*) Aero engines turn at a fast rate, and though gearing is used, its ratio is limited by weight economy; thus airscrews have a fairly high angular velocity, and diameter must be restricted to avoid the velocity of sound (low temperature cuts down this velocity, so that restriction is more severe on high-flying craft); (*b*) long narrow blades of sufficient strength and stiffness have a disadvantage in weight; (*c*) with small low-wing monoplanes having outrigged engines, D may be limited by ground clearance; in sea-going craft large clearance is necessary on account of waves. A formula in general use, as likely to lead to good performance in the various duties required of a fixed-pitch 2-bladed airscrew, is—

$$D = 43 \left(\frac{\text{b.h.p.}}{n^2 V}\right)^{1/4}.$$

This diameter may be decreased by 10 per cent. for three and by 15 per cent. for four blades.

Approximate Allowance for Inflow.—An empirical method often employed to allow roughly for inflow is as follows. An inflow factor a is calculated from the formula:

$$a(1 + 2a) = \frac{T}{1{\cdot}2\ \rho V^2 S}$$

(where S is the disc area) and is assumed to be constant from the tip circle to $r = \frac{1}{4}D$, and then to fall linearly to zero at $r = \frac{1}{6}D$. T is determined from the b.h.p. of the engine by interpolating from systematic tests an efficiency appropriate to the chosen values of J and P/D ratio. Rotational interference is ignored.

Shape.—To minimise torsional stresses, strains and oscillations, the plan form of the blade is often made symmetrical about a radial line joining the axis of rotation to the tip (cf. Fig. 167). This leaves open the question of forward or backward tilt from the plane of revolution. Forward tilt relieves radial stress, but as a rule is resorted to only as a palliative, the blade being set parallel to the disc. Highly loaded blades deflect forward appreciably, but this usually makes for safety.

Although flat-backed airscrews still occur, transverse sections should be designed from a suitable mathematical formula to keep γ and compressibility effects small. If they are transformed shapes (Chapter VI), incidences for zero lift will be known. It is essential from practical and Aerodynamic points of view that the blade be smooth and non-wavy as a whole as well as locally. In a particular design this is verified by plotting geometric contours over the blade ; these should be smooth curves and show absence of flats and concavities. Eventual contours so disappointing as to necessitate redesign are insured against by relating sections and incidences along the blade in some systematic manner. Sections should be as thin as is consistent with stiffness, especially towards the tips, but unavoidable thickness close to the boss makes it doubtful whether attempts to obtain thrust there are worth while. Fig. 174 gives the minimum C_D at $R = 10^6$ for mathematically designed symmetrical sections at zero incidence through a range of thickness ratio, maximum thickness occurring at one-third of the chord from the leading edge (a considerably farther back position is preferable).

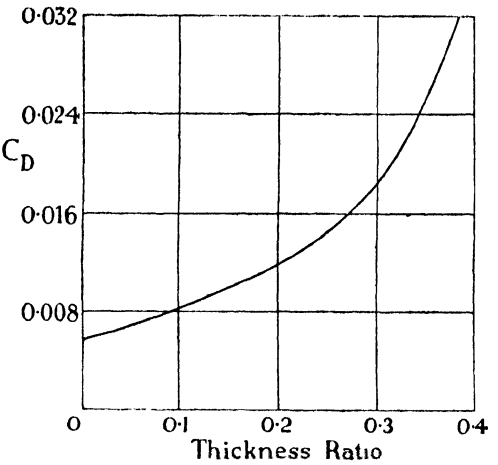

FIG. 174.

Stresses.—Radial stresses in a blade result from (*a*) bending due to Aerodynamic force, (*b*) centrifugal force, (*c*) bending due to centrifugal force. These are calculated separately for a number of radii and added together (taking the fibre stresses, of course, from the bending). A first approximation to (*a*) is found by neglecting twist and integrating, from the radius r_0 considered to the tip, the element moment $C_L \frac{1}{2}\rho W^2 c\delta r(r - r_0)$. The least second moment of area of the section is used to determine the fibre stresses. (*b*) is self-evident. (*c*) arises at r_0 only if the centroids of sections nearer the tip are displaced from a radial line parallel to the disc of revolution. The moment is resolved into components about the major and minor axes of the section, and only the first is considered.

APPLICATION TO THE AUTOGYRO

243. A *helicopter* is a craft whose lift is derived from one or more engine-driven airscrews with axes approximately vertical. The idea, like that of flapping wings, has always attracted considerable notice. Lift is said to be direct, since the craft can rise vertically. To produce forward motion the airscrew axis may be tilted slightly from the vertical. Evidently an advancing blade will then have greater lift than a retreating one, rolling the craft unless combated. Helicopters may have two concentric airscrews revolving in opposite directions. Alternatively, roll could be avoided by increasing incidence along retreating blades and decreasing that of advancing blades. A method of achieving the same end, that is slightly inferior Aerodynamically but much simpler mechanically, is to allow the blades to flap up and down about axes near their roots as they go round ; then the blade of greater lift reduces its incidence by a vertically upward velocity component until its rise is checked by a centrifugal moment about the flapping axis adjustable by stops and springs. Single-rotor helicopters may have a small anti-spin airscrew at the tail of the fuselage or an exhaust-gas jet.

The lift of an *autogyro* is derived from a windmill whose axis is inclined backward from the normal to the direction of motion. In flight, the rotor is not driven by the engine, which propels the craft in the usual way, but automatically rotates by virtue of the relative wind caused by forward or downward motion. Tilt of the axis may be controlled from the cockpit. The blades of the windmill have very small pitch, and they flap as above described. In the ' jumping ' autogyro, pitch can be reduced and the engine connected to the rotor ; high rotational speed is obtained on the ground in this way and, on suddenly increasing pitch and returning the engine to its normal duty, the craft leaps off, at first nearly vertically.

The autogyro has reached a practical stage of development in the hands of its inventor, the late J. de la Cierva. Remarks on performance appear in the next chapter. Meanwhile, we investigate its rotor lift and drag, neglecting flapping in the first instance, since the analysis is somewhat complicated.

244. Fixed-blade Inclined Windmill

In the theory * of the autogyro the lift Z and drag X are to be obtained from the axial thrust T and a component of Aerodynamic

* Glauert, A.R.C.R. & M., 1111, 1926 ; Lock, A.R.C.R. & M., 1127, 1927.

force H which acts in the plane of the rotor away from the wind. These are determined by the necessary condition for autorotation : the torque $Q = 0$. The following usual nomenclature is adopted :

R = radius of tip circle and $S = \pi R^2$;
i = incidence of disc to relative wind (of velocity V) ;
Ω = angular velocity of blades ;
$\lambda = V/\Omega R$;
$\mu = u/\Omega R$, where u = axial velocity through disc (assumed constant) ;
θ, ϕ = blade and helical angles as before ;
ψ = angle between blade and direction of motion viewed in plan ;
T_c or $H_c = T$ or $H/\rho\Omega^2R^2S$;
$Q_c = Q/\rho\Omega^2R^3S$;
k_z or $k_x = Z$ or $X/\rho V^2S$; C_z or $C_x = Z$ or $X/\frac{1}{2}\rho V^2S$.

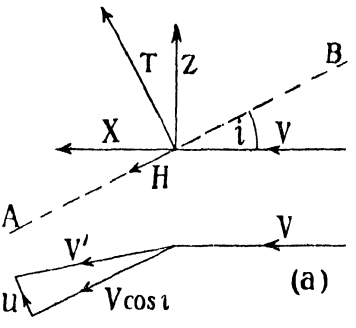

In Fig. 175 (*a*), the broken line represents the inclined windmill in side view, and V' is the resultant of u and $V\cos i$ as shown, u being assumed constant over the disc. It should be noted that u is in the direction of T as the wind is driving the rotor. If v is the axial velocity induced by the thrust, this is in the opposite direction, and

$$v = V \sin i - u.$$

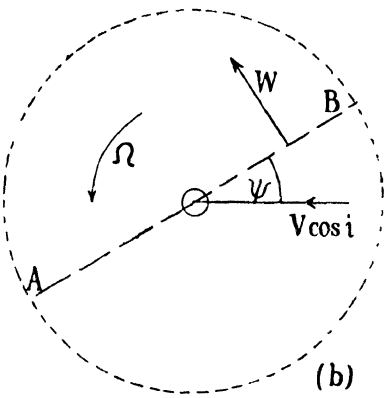

FIG. 175.

Difficulty arises on account of the deflection of the slipstream, but, on analogy with airscrews and aerofoils, it seems plausible to determine v by—

$$T = 2\rho SvV' = 2\rho S(V \sin i - u)\sqrt{(u^2 + V^2 \cos^2 i)}.$$

This gives—

$$\lambda \sin i = \frac{T_c}{2\sqrt{(\mu^2 + \lambda^2 \cos^2 i)}} + \mu \quad . \quad \text{(i)}$$

which is conveniently regarded as an equation for i, requiring knowledge of T_c and μ.

As before, let W be the velocity normal to the blade of the element at radius r (a radial component is neglected). From Fig. 175 (b), which is a plan view in the direction of the axis, W is given approximately, on neglecting u^2 in comparison with W^2, by—

$$W = \Omega r + V \cos i \sin \psi. \quad . \quad . \quad \text{(ii)}$$

For a single element, of chord c—

$$\frac{dT'}{dr} = \rho W^2 ct, \qquad \frac{dQ'}{dr} = r\rho W^2 cq \quad . \quad \text{(iii)}$$

where t and q have the meanings defined by (341). Now an autogyro rotor is of very fine pitch and, though untrue at small radii, ϕ is a small angle over important parts of the blade. Treating it as small throughout gives the approximations:

$$2t = C_L, \qquad 2q = C_L\phi + C_D.$$

As a further simplification we define θ as for zero lift of the element and take $dC_L/d\alpha$ (α being its incidence) as 6 (cf. Chapter VI). Then, since $\alpha = \theta - \phi$—

$$t = 3(\theta - \phi), \qquad q = 3\phi(\theta - \phi) + \tfrac{1}{2}C_D.$$

Hence the second of equations (iii) reduces to—

$$\frac{dQ'}{dr} = r\rho W^2 c[3\phi(\theta - \phi) + \tfrac{1}{2}C_D].$$

Now ϕ can be eliminated by the relation $\phi = -u/W$ which follows from ϕ being small, and, remembering (ii) and the definitions of λ and μ, the torque grading along one blade becomes—

$$\frac{dQ'}{dr} = r\rho c\Omega^2 [-3\mu R\theta(r + R\lambda \cos i \sin \psi) - 3\mu^2 R^2 + \tfrac{1}{2}C_D (r^2 + 2rR\lambda \cos i \sin \psi + R^2\lambda^2 \cos^2 i \sin^2 \psi)].$$

No great error is introduced by assuming c and θ constant along the blade. Then integrating with respect to r gives for one whole blade in a particular rotational position ψ:

$$Q' = \rho c\Omega^2 R^4[-\mu\theta(1 + \tfrac{3}{2}\lambda \cos i \sin \psi) - \tfrac{3}{2}\mu^2 + \tfrac{1}{2}C_D (\tfrac{1}{4} + \tfrac{2}{3}\lambda \cos i \sin \psi + \tfrac{1}{2}\lambda^2 \cos^2 i \sin^2 \psi)].$$

Now as the blade swings round and ψ varies through $\pm \pi$, clearly the terms with sin ψ as factor will give zero mean torque, but the

term with $\sin^2\psi$ as factor will give a mean torque represented by factor $\frac{1}{2}$. Thus for the whole rotor of B blades in rotation—

$$Q = B\rho c\Omega^2 R^4[-\mu\theta - \tfrac{3}{2}\mu^2 + \tfrac{1}{8}C_D(1 + \lambda^2\cos^2 i)]$$

and for a solidity $\sigma = BcR/S$—

$$Q_c = \sigma[-\mu(\theta + \tfrac{3}{2}\mu) + \tfrac{1}{8}C_D(1 + \lambda^2\cos^2 i)]. \quad . \quad (352)$$

$$T = \sigma(\theta + \tfrac{3}{2}\mu + \tfrac{3}{2}\theta\lambda^2\cos^2 i) \quad . \quad . \quad . \quad . \quad (353)$$

as approximations. Similarly—

$$H_c = \tfrac{1}{4}\sigma(C_D - 6\mu\theta)\lambda\cos i. \quad (354)$$

The essential condition $Q_c = 0$ gives the following equation for μ:

$$\mu(\theta + \tfrac{3}{2}\mu) = \tfrac{1}{8}C_D(1 + \lambda^2\cos^2 i). \quad (355)$$

Thus the problem is determinate by the tabular method of step-by-step calculation familiar in airscrew work. k_z and k_x follow from Fig. 175 (*a*).

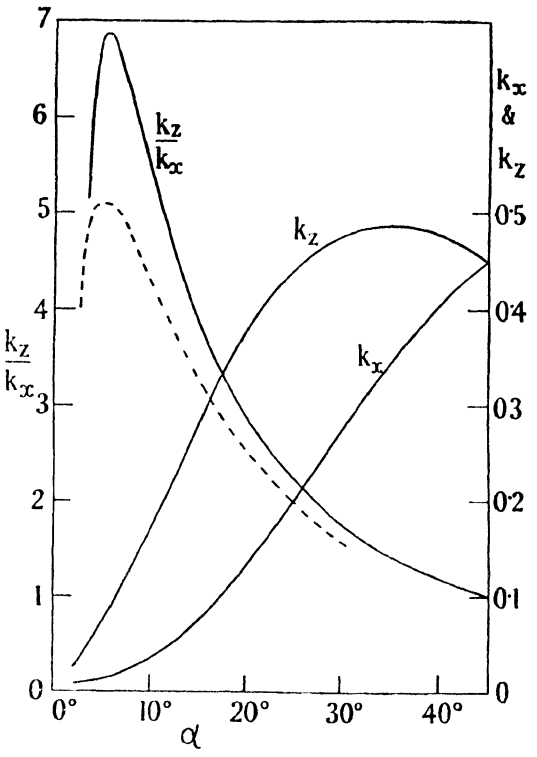

FIG. 176.—AUTOGYRO CURVES.
These are typical only and do not refer to a particular rotor. The broken line represents a complete craft.
(NOTE: $k_x = \frac{1}{2}C_x$, $k_z = \frac{1}{2}C_z$.)

245. The modification due to flapping is left to further reading. Glauert shows first that a trimming of θ sufficient to avoid rolling means increase in H_c for an autogyro (though this is not true of a helicopter), and that the alternative flapping must be rather worse. The analysis indicates on this account rather better performance than is to be expected in practice. Typical curves are shown in Fig. 176 indicating that maximum C_L occurs at a little short of 40° incidence while the drag, at first low, equals the lift at 45°. Experi-

mental results of reliability are scarce because scale effect is great under wind-tunnel conditions. Some tests in America * on 10-ft. diameter rotors in a 20-ft. wind tunnel indicated a maximum L/D of about 6. Maximum L/D occurs at a very small incidence corresponding practically to top speed of the craft, in contrast to an aeroplane; modern trend seeks to augment its value by reduction of solidity, which is already considerably smaller than for an airscrew. Decrease of solidity is compensated for by greater rotational speeds and pitch. Limitations arise through centrifugal stresses becoming great with the former variation while, in regard to the latter, pitch must remain comparatively small to secure autorotation at all.

* Wheatley and Bioletti, N.A.C.A T.R., 552, 1936.

Chapter XI

PERFQRMANCE AND EFFICIENCY

246. The General Problem

The subject of performance, dealing with steady motion characteristics of particular aircraft, has been introduced already at some length in Chapter IV. We are now in a position, however, to estimate data there assumed, and to criticise results. Critical appreciation of values helps the designer to frame a suitable craft for a specific duty, to verify that it will be successful, and to detect and locate by full-scale trials minor deficiencies in the craft built, whence engineering development follows. In the present chapter aircraft are regarded essentially as competitive engineering products, so that improvement by 1 per cent. is worth considerable endeavour.

The resistance of a complete craft when its airscrews are working at their experimental mean pitch, i.e. giving zero thrust, is known as its *glider drag*, and the first step is to assess this correctly. We may proceed from model tests and aerofoil, airscrew, and skin friction theory, calculating such scale effects as we can, and estimating others from experiment and experience. This method is essentially one of summation, approximate allowance being made by calculation or in experiment for the velocity field in which each part works. In the case of a new type no other course is open unless a compressed-air or giant tunnel is available for tests. But with a more normal aircraft we can make much greater use of experience, directing theory and experiment to assessing differences from a nearly similar craft of known performance.

Much organised experimental work has been carried out in aid of the first method, of which a brief outline is given in following articles. Uncertainty arises chiefly from scale effects on the form drags of separate component parts and the interference between one part and another, over and above that which can be allowed for by taking velocity fields into account. Form drag and interference, apart from airscrew effects, may readily absorb 25 per cent. of the power at top speed, so that resulting errors may be appreciable.

Although interference usually increases drag, this is not always the case. Exceptions include the Handley Page wing slot at large incidences and the Townend * ring for radial engines (*cf.* a paper by Otten † and several others ‡ on full-scale tests).

The second method of assessing glider drag is largely individual to the designer, being founded upon experience with different types. Fairly similar aeroplanes may be grouped and each category assigned a gross drag coefficient, which is often based on the frontally projected, or so-called ' flat plate,' area. Particular idiosyncrasies are met by adjusting the coefficient.

With glider drag known, the performance of an aeroplane in a standard atmosphere is readily forecast by taking due account of its airscrews and engines. Important interference occurs between airscrews and fuselages, or engine nacelles, a matter that is studied in a special section. Assuming reciprocating engines, their rotational speed becomes a significant variable.

The advent of jet propulsion promises some simplification of the present calculations and also justifies consideration of performance and operational efficiency from a comparatively unhampered point of view.

To be representatively intelligible, particular flight tests must be reduced to standard atmospheric conditions and the chapter concludes with a note on a suitable procedure to adopt.

COMPUTATION OF GLIDER DRAG

247. The experimental drag coefficient of wings, tail planes, and other aerofoil surfaces is usually written—

$$C_D = C_{Di} + C_{D0},$$

the first term on the right being the induced and the second the profile drag coefficient. This form is suitable when tests have been made at flight Reynolds numbers, e.g. when C.A.T. measurements are available and the craft is small and slow. Except in such circumstances, however, a more useful subdivision is—

$$C_D = C_{Di} + C_D \text{ (friction)} + C_D \text{ (form)} \quad . \quad . \quad (356)$$

The advantage and purpose of (356) is to isolate the part of the drag —the skin friction—whose scale effect is easily predicted. This term can be obtained by subtracting from the gross drag an experi-

* A.R.C.R. & M., 1267, 1929; *Aircraft Engineering*, April 1930.
† *Jour. Roy. Aero. Soc.*, November 1934.
‡ Cf. Van der Maas, 5th Int. Con., The Hague, 1930, etc.

mental form drag (Article 230), but when, as is usual, the data do not exist, an estimate can be made of one or other of the two components of profile drag. It will be assumed that only the friction is subject to increase by roughness.

The formula is not confined to aerofoil surfaces, although for others the first term will probably be negligible. With bluff components such as wheels, the last term swamps the others, and an experimental C_D is used and scale effect is neglected except in cases where it has been especially determined. Each exposed component of the craft will first be assigned a drag coefficient based on an area peculiar to itself, but in the summation a common area is more convenient. For the purpose of comparing with other aircraft or checking against experience the flat plate area of the preceding article may be used, but the area finally chosen will be the wing area. Usually this area is taken to include parts of the body and engine nacelles intercepted between the leading and trailing edges.

Airscrew effects are reserved for the next section.

248. Induced Drag

Induced drag can be neglected except on the wings, tail plane, and fin-rudder unit, although with a very large body this may not be justified. Its calculation is treated in Chapter VIII, but the following additional remarks are made.

It is convenient, in the case of a biplane, to determine the *equivalent monoplane aspect ratio*, the equivalent monoplane being defined as having the same lift and induced drag as the biplane. Denote lift and drag by L and D, span by $2s$, and $L/2s$ by λ; use suffix M to distinguish the equivalent monoplane, and 1 the longer and 2 the shorter of the biplane wings; and write μ for s_2/s_1. Now $D_{iM} = D_{iB}$, the induced drag of the whole biplane. Hence from (251) and (252)—

$$\lambda_M^2 = \lambda_1^2 + \lambda_2^2 + 2\sigma\lambda_1\lambda_2 \quad . \quad . \quad \text{(i)}$$

σ being Prandtl's factor. Let $L_1 = xL_M$. Then, since $L_1 + L_2 = L_M$, $L_2/L_1 = (1 - x)/x$. Dividing (i) through by λ_1^2 and substituting—

$$\left(\frac{1}{x} \cdot \frac{s_1}{s_M}\right)^2 = 1 + \left(\frac{1 - x}{\mu x}\right)^2 + 2\sigma \frac{1 - x}{\mu x}$$

or—

$$\frac{s_1}{s_M} = \frac{1}{\mu}\sqrt{\{x^2(\mu^2 - 2\sigma\mu + 1) + 2x(\sigma\mu - 1) + 1\}} \quad . \quad (357)$$

Writing the R.H.S. as $1/K$, $2Ks_1 = 2s_M$ is the span required.

This result can be plotted in several useful ways with the help of Fig. 135. One of these is shown in Fig. 177 which exhibits, amongst other matters, that the biplane is most efficient when $s_2/s_1 = L_2/L_1 = 1$ (Articles 183, 185).

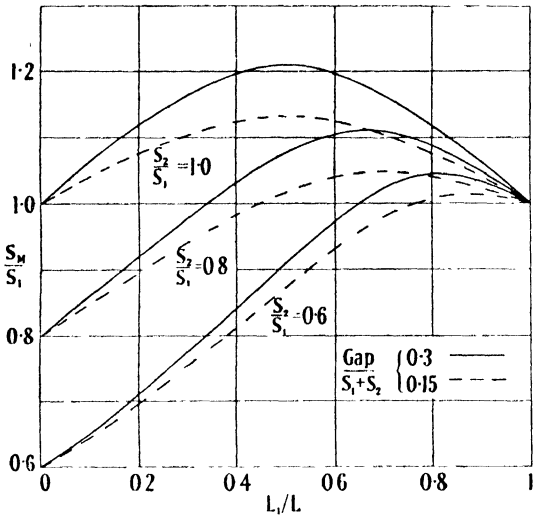

FIG. 177.—EQUIVALENT MONOPLANE ASPECT RATIO.

Once the distribution of lift between the wings has been estimated by direct experiment or otherwise,* the theoretical induced drag follows immediately from Chapter VIII. Partly for reasons discussed in Article 180, however, and partly to allow for irregularities of lift distribution arising from practical causes, the drag so calculated is regarded as a lower estimate and up to 8 per cent. added. This remark applies equally to monoplanes. Of course, should the theory be used only to assess differences between two rather similar wing arrangements, the correction would not be needed.

The induced drag of a tail plane is assessed from the $\pm$ lift it must exert to preserve equilibrium. Induced drag arises particularly on the fin and rudder when the craft is flying yawed owing to partial engine failure, a first approximation to the crosswind force being that required to balance the moment about the C.G. of the asymmetrical thrust. A small increment is due, however, to the fin being set slightly askew to balance the torque of the airscrews, which revolve all to the same hand, unless contra-propellers are used.

249. Form Drag

Chapter IX A provides data for directly estimating the profile drag of smooth normal wings at small incidences and of laminar flow wings except through the favourable range. Within this range the skin friction may be calculated approximately for laminar flow wings but the question arises as to what form drag to add, a matter on

* Diehl, N.A.C.A.T.R.'s, 458 and 501

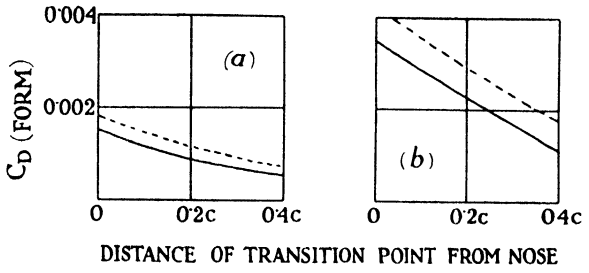

FIG. 178.—THICKNESS: (*a*) 0·14, (*b*) 0·25. *R*: - - - 10^7, —— 5×10^7.

which the experimental data generally available are not yet sufficient. Special tests can easily be made in a laminar flow tunnel, the two-dimensional conditions required enabling good Reynolds numbers to be reached, but few of these tunnels exist. Fig. 178 summarises results of Squire and Young's calculations of the form drag of normal wings, which may be used for laminar flow wings provided maximum thicknesses are only moderately displaced backward ; evidently the curves cannot be extrapolated indefinitely owing to increasing bluntness of tail.

These data can also be applied to tail-unit sections with the same restrictions, but allowances necessary for aileron, elevator and rudder angles, excrescences and roughness are commonly considerable and should be determined by test.

What has been said of aerofoil surfaces applies in principle to fuselages.* With these a tunnel test is usual, but form drag is difficult to infer. If the shape is a very good one and free of excrescences, a repeat test may be carried out after fairing in the wind screen, which commonly has a large form drag, and the whole drag then measured will be an upper limit to the skin friction. Form drag is otherwise caused by wing roots, the downwash field, the tail unit, and, in case of engine failure, by yaw (postponing discussion of slipstream effects). Failing C.A.T. or giant tunnel tests, estimates may be based on measurements with two models, a small and a very large one. The first is tested principally for pitch and yaw increases ; the second only at zero incidence. Wing roots, tail surfaces, and a model tail wheel may be offered up in the second case to give some idea of the interference drag on the body.

It will be realised that wings, tail unit, and fuselage all have

* Some recent tests of streamline bodies of revolution at Reynolds numbers (reckoned on length) between 2 and 3 $\times$ 10^6 gave for the ratio of form drag to skin friction : 0·08 with streamline, and 0·14 with turbulent oncoming flow.

different Reynolds numbers on the craft. It is profitable and entails little complication to take this into account.

250. Parasite Drag

The term *parasitic* is usually applied to the drag of all parts of an aircraft except its lifting surfaces. Thus the inter-plane bracing of biplanes, aileron control horns, tail planes, etc., contribute to parasite drag, but wings, lifting rotors, and gas envelopes do not, though part

TABLE IX

Component	Drag at optimum incidence referred to 100 m.p h.
Fuselages :	
Best, high speed	2¼ lb. per sq. ft. maximum sectional area across stream.
Exceptionally good	3 Ditto
Average	4½ Ditto
Square section with protuberances	7 Ditto
Flying-boat hull, best	*2¾–4 Ditto
Seaplane floats, good shapes	4–6 Ditto
Biplane bracing :	
Single bay, engines in body or wings	0·1 P, including interference.
Ditto, without cabane panels	0·07 P, Ditto
Two bay, with engines between wings	0·16 P, Ditto
Tail plane, fin, and rudder :	
Slow, inefficient craft	0·07–0·1 P, Ditto
High-speed craft	0·2 P, Ditto
Tail-unit hinge breaks	Add 15 per cent. to min. drag.
Shrouded aileron slot	Add 12 per cent. to min. drag of wing span affected.
Tail skids, small craft	1–4 lb.
Low-pressure tail wheel and scantlings for medium-size craft.	20 lb. (small craft, 5 lb.)
Medium-pressure wheels, faired rim to hub	11–14 lb. per sq. ft. of projected area of tyre.
Non-retractable undercarriage :	
Single-engined craft.	0·18 P, including interferences, which often contribute 15 per cent. of whole.
Twin-engined biplane	0·13 P, Ditto
Small craft, cantilever	15 lb.
,, ,, tripod	30 lb.
,, ,, inferior	40 lb.
External oil-cooler, medium-size engine	3½ lb.
Exhaust pipes, ditto engine	10 lb.
Radial engine cooling drag with ordinary cowling.	Equivalent to 7 per cent. of the b.h.p. of the engine. (*Note.*—Such losses are greatly reduced with ducted cooling.)

* Remarkably low drag of this order appears to be realised in some recent flying boats by (*a*) very careful shaping, (*b*) reducing the beam of the hull while lengthening the forebody to maintain planing surface (Gouge, lecture before the *Roy. Aero. Soc.*, December 1936).

of the resistance be form drag and perhaps reducible. Interference drag is reckoned parasitic if due to struts, fuselages, engine nacelles, etc., even though it appear as an increase in the form drag of lifting members, but it is excluded if arising between lifting surfaces, e.g. the mutual interference of the wings of a biplane.

Reference must be made to Handbooks and Laboratory Reports for design data. Table IX is intended to indicate merely the beginnings of an adequate list of notes that should be prepared and constantly revised to facilitate and check estimations. In this table 100 m.p.h. is used only as a convenient reference, and it is not implied that scale effect is to be allowed on either side of this speed. Drags are sometimes expressed as fractions of the sum of parasite drags, which is denoted by P. (The term *total parasitic drag* is reserved to include the profile drag of wings.)

251. Struts and Streamline Wires

Curve (1) (Fig. 179) shows the variation of C_D (= drag per unit length $\div \frac{1}{2}\rho V^2 T$, where T denotes the maximum thickness of the

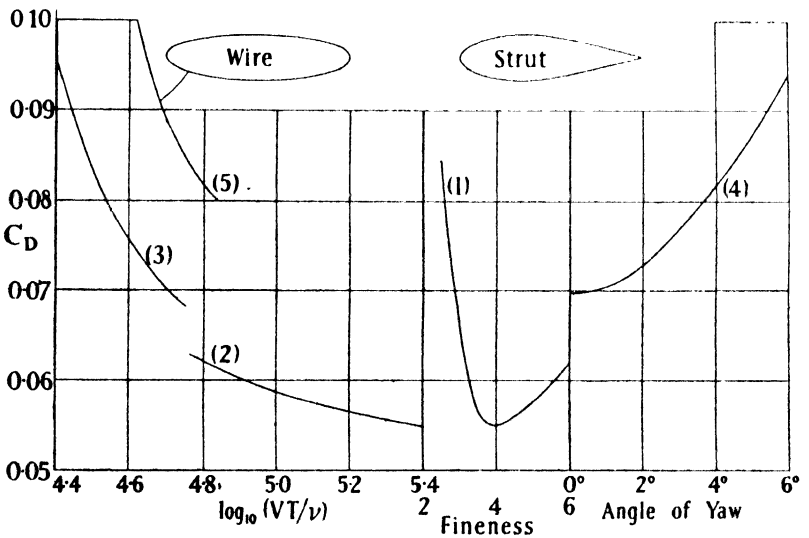

FIG. 179.—DRAG OF STRUTS AND WIRES.

section) for struts of approximately minimum drag at $\log_{10}(VT/\nu) = 5{\cdot}4$. Optimum fineness is 4; larger Reynolds numbers permit a slightly greater thickness, smaller Reynolds numbers require it to be

less. This minimum drag is plotted against R in curve (2). To secure such small values the contour must be Aerodynamically smooth and mathematically designed, although slight rounding may be introduced at the trailing edge. Curve (3) relates to the strut illustrated, which has a fineness ratio of 4, but whose section is slightly thicker at the back. Variation of the drag of this strut with yaw at $\log_{10} R$ approximately 4·7 is shown by curve (4). Although the section figured does not accord with minimum drag, it is a very good one; carelessly designed sections are often 20 per cent. wasteful.

The strut of minimum drag may not be quite the most efficient. Its weight w must be supported by the wings, say of L/D ratio r, and causes an additional drag w/r. If D is its drag, the criterion for efficiency is that $D + w/r$ be a minimum. The central cross-section of the strut will be required to have a given minimum moment of inertia; weight is saved quickly by increasing thickness for given strength, but the advantage is limited with r large. Note that any question of changing the struts on an existing craft would be differently decided, because, wing area being fixed, r would then be the over-all L/D ratio, the craft having to fly slightly faster to carry additional weight at the same incidence. Such calculations sometimes indicate, for a large, slow biplane, rather a small fineness ratio, which, however, is to be avoided, for a curious reason: the cross-wind force arising on the struts in yaw becomes uncertain in direction, i.e. it *may* act in the direction of the sideslip, and the uncertainty slightly affects lateral stability. Considerable saving results from tapering struts.

Wires of the lenticular section also illustrated in the figure give curve (5). Their drag at the smaller Reynolds numbers of usual interest is given by:

$\log_{10} R$ . . .	4·1	4·2	4·3	4·4	4·5	4·6
$C_D \times 10$ . . .	3·00	2·58	2·14	1·72	1·34	1·02

R and C_D being defined as for struts. Lenticular wires show little increase of drag for yaw of their sections up to 10°. With double wires a short distance apart, one directly behind the other, shielding to the extent of 15 per cent. may be allowed, but interference increases the drag of each with yaw > 8°.

A rough rule to allow for interference drag in the bracing of a biplane is to add 50 per cent. to the drag calculated for the interplane struts and wires.

252. The Jones Efficiency

Analysis of a number of first-class monoplanes of exceptionally fine lines and smooth surface, varying in all-up weight from 2 to 8 tons, gives the mean results of Table X. Single and twin engines are included. Top speeds vary from 200 to 250 m.p.h.; the Table applies to 220 m.p.h. with a wing loading of 21 lb. per sq. ft. and a 'power loading' of 12·3 lb. per b.h.p. Drags are expressed in round-number percentages of total drag. The large allowance under the last item includes a non-retracted tail wheel or skid, non-ducted cooling of reciprocating engines, and airscrew interference.

TABLE X

Component	Nature of Drag				Totals
	Induced	Friction	Roughness	Form and interference	
Wings and ailerons . .	7	31	5	8	51
Tail plane, fin, and rudder .	Small	8	1	3	12
Fuselage	0	14	2	3	19
Engines and miscellaneous .	0	4	Small	14	18
Totals . .	7	57	8	28	100

Points to notice in these small and lightly loaded craft are: that one-half of the thrust h.p. is expended on the wings, in spite of the fair speed; that good shaping and smoothness make pure skin friction account for more than one-half power; and that induced drag is very small at top speed (it would be substantially increased, of course, at cruising speed or with a heavier wing-loading).

Various different meanings are commonly attached to the term *efficiency*. One, which will be distinguished as the Jones efficiency, depends on the valuable conception of the *streamline aeroplane*,* and is defined as follows:

$$\eta_J = \frac{H_i + H_F}{\eta(\text{b.h.p.})} \quad . \quad . \quad . \quad . \quad (358)$$

where H_i = horsepower absorbed by induced drag.

H_F = horsepower absorbed by pure skin friction.

η = efficiency of the airscrews.

It will be seen that lack of an allowance for form drag tends to low values, the present idealisation leaving only induced drag and pure skin friction. Usually the convention is to calculate the skin friction from flat plate theory, whilst, again, the induced drag is

* Jones (Prof. Sir Melvill), *Jour. Roy. Aero. Soc.*, May 1929.

assessed from the theory of Chapter VIII. The resulting figure of merit is reduced on both these scores through lack of sufficient knowledge. However, this figure is easily calculated, and does succeed in segregating good classes of aircraft from bad, and penalties incurred by excessive form drag, slipstream effects, and roughness are made plainly evident.

From Table X we at once find, since (358) is the same as the ratio of the sum of induced drag and pure skin friction to total drag, that the monoplanes investigated have the mean efficiency of 64 per cent. Aeroplanes having an efficiency > 60 per cent. on this basis are considered satisfactory at the present time ; the slow, multi-strutted biplanes of prior to 1930 often had an efficiency of only 30 per cent. Considering the possibility of substantial improvement of efficiency, we note that the following steps promise immediate profit : (*a*) elimination of roughness drag ; (*b*) reduction to a very small minimum of eradicable parasite drags (expressively called Christmas-tree drags), as by retracting the tail wheel and closing all slots when not in use ; (*c*) reducing engine losses by ducted cooling ; (*d*) mathematical design of every contour to reduce form drag to a minimum ; (*e*) study of the manner of joining one part to another to decrease interference increments ; and finally (*f*), in the case of craft of small speed range, designing wings to approximate more closely to elliptic span distribution of lift. All these steps are in progress, and the present best efficiency of 65 per cent. need by no means be considered the maximum that can be attained.

The above method can be applied to airships, and best examples show a slightly higher efficiency, but, of course, at so low a speed that comparison with aeroplanes is not justifiable.

253. Subdivision of Parasite Drag

The number of flight conditions at which drag must be estimated are few. Normally they are : top speed, cruising, climb at low altitude, ceiling, ceiling with engine failure, coming-in incidence, nose dive or fast glide. With an efficient aircraft it is best to estimate for these conditions separately, since variation of Reynolds numbers and various small corrections are then usefully taken into account. When a large number of rather similar craft are dealt with, however, or when the type is inefficient, comprising a host of parasitic resistances whose scale variations are quite unknown, labour is saved by assembling the drags in two groups : those dependent on incidence and those which are not. Analysis shows that variation of the first group, which includes the fuselage and tail plane, may usually be

expressed as a function of $\Delta C_L/\Delta_{max}C_L$, the difference in lift coefficient being reckoned from that for top speed. The form of this function depends on the type of craft, and, unless directly calculated for a given type, must be suggested from experience. Examples are given by Kerber.*

AIRSCREW INTERFERENCE

254. In Chapter X the airscrew was regarded as isolated. A large engine nacelle or body in front of or behind the airscrew modifies its torque and thrust, while the drag of the body is increased by the acceleration of air through the disc. Theory and experiment show that the pitch of the airscrew and therefore its efficiency are apparently increased owing to the slowing up of the stream by the body. If, however, the increase of drag of the body be subtracted from the apparent thrust, to give a useful thrust, the effective efficiency is found to be less than for the isolated airscrew, unless the spinner appreciably improves a bad body shape. It will be seen that the mutual interferences are to some extent compensating, and in some flying-boat arrangements particularly, with engines carried high in separate eggs, it may be convenient to deal with an over-all correction. But more frequently we have to determine with some care increments of wing and parasite drag additional to effects on the engine housing.

Detailed investigation in practical circumstances, though possible, is very intricate, but certain simple factors have outstanding importance, and consideration of these alone is usually sufficient for performance calculations. However, unless the airscrew is designed to conform with the actual velocity field in which it works, modification of blade angles will be necessary to allow the engine to develop full power. We first neglect all aircraft parts other than the nacelle or body. Experiment shows that the *form* of the results obtained in these simplified circumstances is retained with the complete craft. Alternatively, if experimental determination of coefficients is not available, we shall be able to supplement the results by additional calculations.

Whether the body is behind or in front, some shielding takes place, either of the nacelle by the boss and blade roots in the former case or *vice versa* in the latter. Thus, usually drag is decreased on this score by a small fraction, which we shall denote by k_b. The special case where the boss is flush with the body, of whose shape the spinner forms an integral part, will be referred to later.

* *Aerodynamic Theory*, v. V, 1935.

Again, with both tractor and pusher type airscrews, the body is situated in a field of augmented velocity, increased by from aV to $2aV$ in the first case and from 0 to aV in the second, a being the axial inflow factor. We shall associate the resulting increase of drag with a certain coefficient k_v. This acceleration is accompanied by pressure variations which again increase drag.

Finally, in the case of a tractor airscrew, the sudden increase of pressure at the back of the disc, by virtue of which thrust arises, produces important mutual effects. Pressure drag increases will be connected with a coefficient k_p.

255. Tractor Arrangement

It is convenient to begin with the pressure drag last mentioned. If the flow were inviscid, a small streamline body close behind the airscrew would experience this drag in full, yet clearly the efficiency of the combination would be the same as that of the isolated airscrew, for no energy loss could be caused by the body, and the residual slipstream would be unchanged by it. We infer that the thrust of the airscrew must increase to compensate exactly for the pressure drag introduced.* Experiment bears out the practical value of this conclusion. Displacing an airscrew upstream from a body, as if it were driven through an extension shaft, decreases apparent thrust, originally high owing to interference, but also decreases the drag of the body equally, so that effective or net thrust remains unchanged.

Let T_a be the apparent thrust of the airscrew and S_e its effective disc area (Article 240) ; D_a, D the drag of the body with and without the airscrew, and S its maximum cross-sectional area. It is assumed a sufficient approximation for present purposes to regard T_a as uniformly distributed over S_e, so that pressure is proportional to T_a/S_e. Considering a proportion of S, depending on the shape of the nose of the body and the position of the airscrew, to be affected by this pressure, the interference thrust and drag increments can be expressed as equal to $T_a \,.\, k_p(S/S_e)$, and on this score only—

$$T_a = \frac{T}{1 - k_p(S/S_e)} \quad . \quad . \quad . \quad (359)$$

$$D_a - D = T_a \,.\, k_p(S/S_e). \quad . \quad . \quad (i)$$

* The argument may be illustrated by an analogy. Supposing a plumb-bob to hang from a spring balance, the decrease produced in its indicated weight on immersing it in a beaker of water is equal to the apparent increase in weight of the beaker of water due to the rise of water level. The upthrust on the plumb-bob is analogous to the increase of propeller thrust in the original case, and the increase of hydrostatic pressure integrated over the base of the beaker to the increase in drag of the streamline body.

Next, if the body were effectively wholly exposed to the ultimate slipstream velocity V_s and S were sufficiently small compared with S_e, we should have on this particular score—

$$\frac{D_a}{D} = \left(\frac{V_s}{V}\right)^2 = (1 + 2a)^2.$$

But—

$$T_a = \rho V (1 + a) S_e \,.\, 2aV$$

or—

$$2a + 2a^2 = T_a/\rho V^2 S_e.$$

Hence:

$$D_a/D = (1 + 2a)^2 = 1 + 2T_a/\rho V^2 S_e \quad . \qquad \text{(ii)}$$

To take into account throttling of the slipstream by the appreciable section of the body and other neglected factors, we write this:

$$D_a/D = 1 + k_v T_a/\rho V^2 S_e. \quad . \quad . \quad . \qquad \text{(iii)}$$

Finally, collecting from (i) and (iii), and remembering that shielding reduces drag by $k_b D$, we have—

$$D_a = D(1 - k_b) + \frac{T_a}{S_e}\left(k_p S + k_v \frac{D}{\rho V^2}\right)$$

$$= D(1 - k_b) + T_a \frac{S}{S_e}(k_p + \tfrac{1}{2} k_v C_D) \quad . \quad . \qquad (360)$$

where C_D for the body is specified on S. Alternatively—

$$\frac{D_a}{D} = (1 - k_b) + \left(2\frac{k_p}{C_D} + k_v\right)\frac{T_a}{\rho V^2 S_e} \quad . \quad . \qquad (361)$$

$$= A + B\frac{T_a}{\rho V^2 S_e}, \quad . \quad . \quad . \quad . \quad . \qquad (362)$$

say.

256. Pusher Airscrew

The case of an airscrew working behind a body differs only in detail. The body is subject to less increase of speed, which is confined to its back part, but to a fully effective pressure gradient. On the other hand, absence of a propelled body behind means that increase of thrust is no longer compensated for by increased pressure drag. These changes promise advantage to the pusher arrangement, but this tends to be lost in practice by poor streamline shape for the body and by necessary adjustment of airscrew form to ensure realising the full b.h.p. of the engine. It appears from experiment

that (362) still applies, with suitable adjustment of the coefficients, so that special investigation is unnecessary except to note that B will be smaller owing to the relative unimportance of k_v.

257. Comparison with Experiment

The simple linear relationship (362) (see Fig. 180) has been realised experimentally on many occasions during the past thirty years, and it has been found to hold for complete aeroplanes as well as in the simplified circumstances assumed for its derivation. Definition of the coefficients is slightly modified in experimental work, so that the actual airscrew disc area can be used in place of its effective area. With this understanding, tests on a biplane of very poor Aerodynamic shape gave, without the wings in position, $A = 0{\cdot}86$, $B = 1{\cdot}04$, and with the wings, $A = 0{\cdot}83$, $B = 0{\cdot}93$. In a more recent analysis k_v was found to be 2·4 (rather greater, as expected, than 2, as in (ii), Article 255) and $k_p = \frac{1}{4}$, so that with $C_D = 0{\cdot}2$, for example, B would be 4·9. Values are not yet systematised.

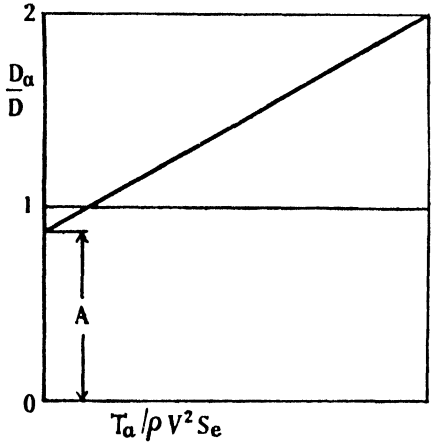

FIG. 180.

Whilst A is found to be < 1 for blunt-nosed nacelles as predicted. this no longer holds when the boss and spinner complete the lines of the streamline housing of, say, a liquid-cooled engine. k_b may then vanish; or it may change sign, and considerable positive drag then result, with fine bodies, owing to deterioration of flow.

Some pusher nacelles have given $A = 0{\cdot}97$, $B = 0{\cdot}83$ for a poor shape, and $A = 1{\cdot}05$, $B = 1{\cdot}8$ for a somewhat better one.

258. With high-speed monoplanes having two or four radial engines, the nacelles project for efficiency about one-quarter chord in front of the leading edge of the wings. Considering one of the inner engines, we have behind its airscrew a long nacelle followed by a strip of wing of approximately maximum chord and, at a little distance, possibly one-third of the tail plane area. With a single-engined aeroplane, the slipstream affects, besides the fuselage, the wing roots, tail plane, fin, and rudder and, if non-retracted, part of

the undercarriage, together with certain struts and wires in the case of a biplane. Actually, the question of precisely what components of the after-part of a craft are affected is somewhat doubtful, for slipstreams are found to wander. Associated with this question is that of what diameter to ascribe to a slipstream ; on the one hand, it contracts appreciably, especially at maximum climb, when slipstream effects are most important ; on the other, some distension is caused by the blanketing of the central part by a large bluff nacelle. It is usually sufficient to assume that parts affected lie in the projection downstream of the effective disc area, and that the additional velocity is $2aV$ spread uniformly across the slipstream. Alternatively, the method indicated in Article 242 may be applied. Comparison is made in the following example :

Example.—We take an ordinary small biplane with a single engine of 300 b.h.p. and a 9-ft. airscrew giving 240 effective thrust h.p., which provides a top speed of 150 m.p.h. ($\rho V^3 = 115$). The maximum cross-sectional area of the body is 16 sq. ft., and its drag without airscrew 166 lb., so that $C_D = 0{\cdot}18$. In order to use $\frac{1}{4}$ for k_p, we substitute S_a for S_s in (359) and, taking $S_a = 64$ sq. ft., obtain—

$$T_a = \frac{240 \times 550}{220} \div \left(1 - \tfrac{1}{4} \times \frac{16}{64}\right) = 640 \text{ lb.}$$

Thus thrust is increased by 40 lb. and the body drag by an equal amount through pressure interference. (362) gives for the fuselage on assuming $A = 0{\cdot}86$:

$$\frac{D_a}{D} = 0{\cdot}86 + \left(2{\cdot}4 + \frac{1}{4 \times 0{\cdot}09}\right) \frac{640}{115 \times 64} = 1{\cdot}31,$$

or the drag of the body alone increases by 51 lb. The glider drag of the remainder of the craft at top speed is estimated to be 360 lb., of which parts contributing 90 lb. are washed by the slipstream. By (351) and particulars of the airscrew, the effective disc area is found to be 41 sq. ft. From Article 255 (ii), $(1 + 2a)^3 = 1{\cdot}272$, and the 90 lb. drag concerned becomes 114 lb. If, alternatively, we applied the approximate method of Article 242, we should find—

$$a(1 + 2a) = T/1{\cdot}2 \times 115 \times 64$$

and since $T = 240 \times 550/220 = 600$ this would give $(1 + 2a)^3 = 1{\cdot}273$, so that in the present instance little difference would result. For the complete aircraft at top speed $D = 217$ (body) + 270 (parts out of slipstream) + 114 (other parts within slipstream) = 601 lb., and the total increase due to airscrew interference is (51 + 24)/(166

+ 360) = 14 per cent. The airscrew efficiency, provided the blade angles can be adjusted, without further loss, to absorb 300 b.h.p. at the designed engine speed, is increased from 240/300 = 80 per cent. to 640 × 220/550 × 300 = 85 per cent., the additional thrust being balanced by extra pressure drag. Much greater airscrew interference would occur, of course, at maximum climb.

SOME PERFORMANCE CALCULATIONS

259. Prediction of Speed and Climb

The only development now introduced compared with Chapter IV is in the account taken of engine and airscrew characteristics. The following are assumed: a 'polar' of $C_L \sim C_D$ for the complete aeroplane whose performance is required, all lifts and drags being referred to the wing area S; curves of variation of k_T = thrust/$\rho n^2 D^4$, and k_Q = torque/$\rho n^2 D^5$ against $J = V/nD$ for the propeller of diameter D working at n r.p.s., corrected to position on the craft; and a maker's curve (e.g. Fig. 181 (*a*)) of H_0 the b.h.p. of the engine against n at sea-level, often called the standard b.h.p. Other symbols are: L, W for total lift and weight, T for thrust, σ for relative air density, and v for rate of climb in feet per second. Suffix 0 refers to sea-level. To prepare for change of altitude we substitute $V\sqrt{\sigma}$, $n\sqrt{\sigma}$ (cf. Article 81) for V and n, when—

$$C_L = \frac{L = W}{\frac{1}{2}\rho_0 (V\sqrt{\sigma})^2 S} \quad . \quad \text{(i)}$$

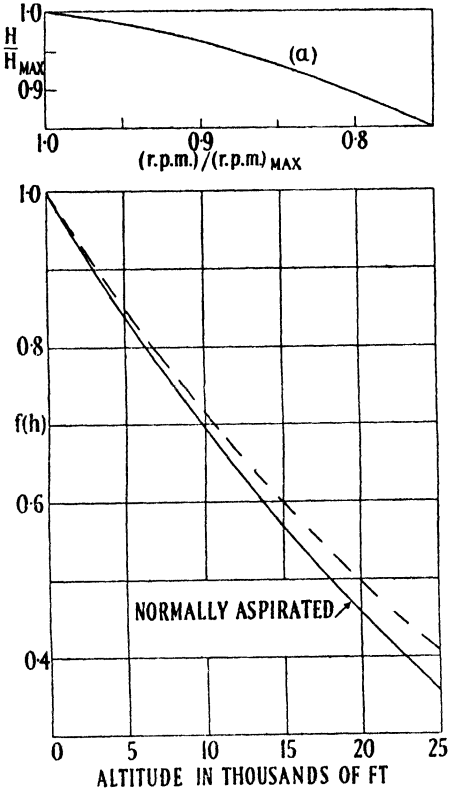

FIG. 181.—VARIATION OF ENGINE POWER WITH ALTITUDE.

The curve (*a*) is an example only of variation of power with engine speed, and must not be taken as representative.

$$k_T = \frac{T}{\rho_0 (n\sqrt{\sigma})^2 D^4} \quad . \quad . \quad \text{(ii)}$$

and similarly for other coefficients. Equation (i) is assumed as indicated to hold, with W written for L, as a sufficient approximation in level and climbing flight.

For any altitude h we write for the b.h.p. available—

$$H = H_0 \, . \, f(h) . \quad . \quad . \quad . \quad . \quad (363)$$

Different forms occur for $f(h)$. One formula in use for supercharged engines is :

$$f(h) = \frac{p}{p_0} \sqrt{\frac{\tau_0}{\tau}} \quad . \quad . \quad . \quad . \quad (364)$$

This curve is shown dotted together with another mean curve for normally aspirated engines in Fig. 181. In the formula, p of course denotes the pressure and τ the absolute temperature of the atmosphere. The torque coefficient is readily expressed in terms of (363) :

$$k_Q = \frac{550}{2\pi D^5 \rho_0 (n\sqrt{\sigma})^2} \cdot H_0 \frac{f(h)}{n} \quad . \quad . \quad . \quad (365)$$

$$= \frac{275 \, J^2}{\pi D^3 \rho_0 (V\sqrt{\sigma})^2} \cdot H_0 \frac{f(h)}{n} \quad . \quad . \quad . \quad (366)$$

These last formulæ depend only on the engine and airscrew, and hence corresponding values of n and V are known, whatever C_L or C_D may be ; knowing $f(h)$ for a particular engine, we can construct for a given airscrew a family of curves of V against n or J, one curve for each altitude, which will represent the best that the engine and airscrew can do.

Now, turning to the aircraft, unless the angle of climb is steep—

$$T = \text{drag} + W \frac{v}{V} \quad . \quad . \quad . \quad (367)$$

or in terms of coefficients * :

$$2k_T \frac{D^2}{SJ^2} = C_D + C_L \frac{v}{V} \quad . \quad . \quad . \quad (368)$$

Thus the next step is to plot a curve of k_T/J^2 against J, which follows immediately from the airscrew data.

Level Flight.—The formulæ may be used as follows. Choose a value of $V\sqrt{\sigma}$ and obtain C_L from (i) and C_D from the polar. Find k_T/J^2 from (368) and then J from the data curve mentioned. Read

* Modification for more than one airscrew will be apparent.

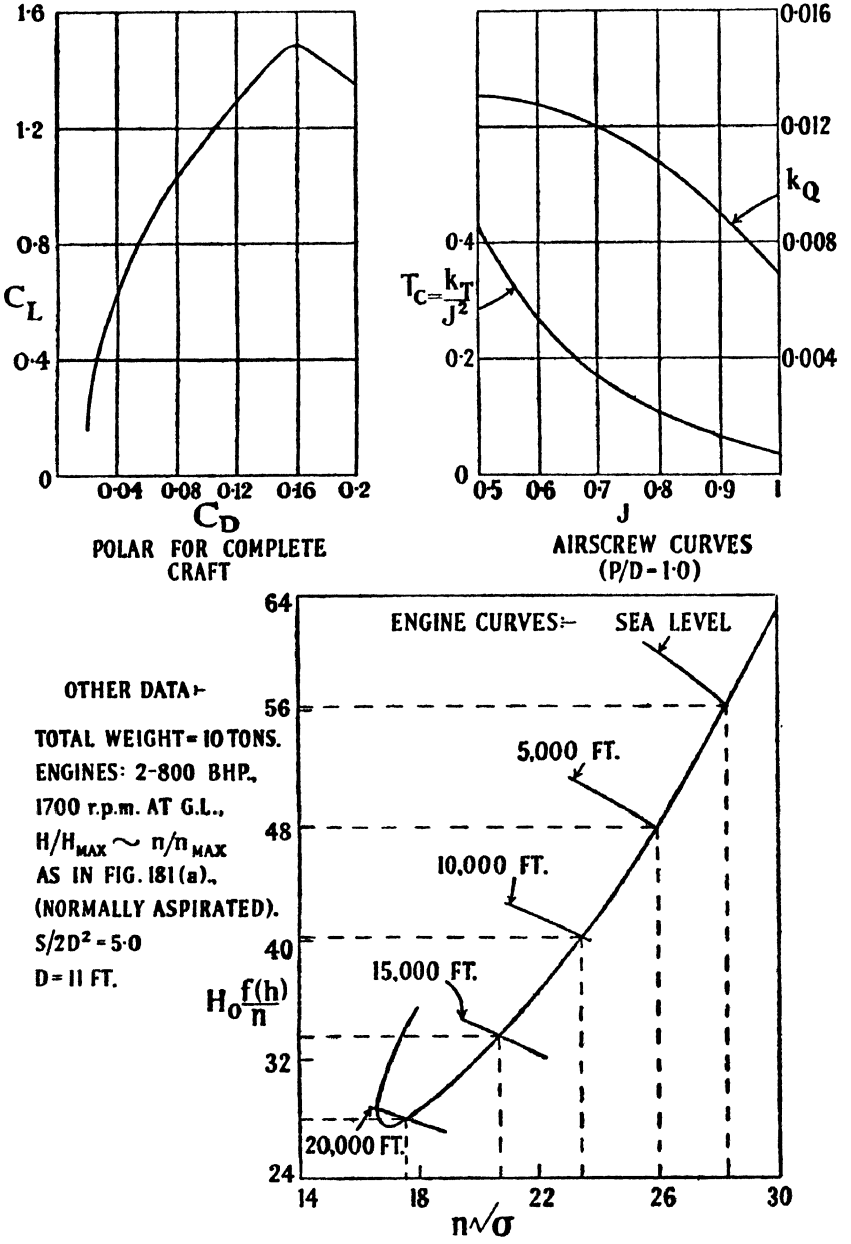

FIG. 182.—EXAMPLE OF PERFORMANCE PREDICTION.
H_0 gives the total power of the two engines.

off k_Q from the curve $k_Q \sim J$. Thence obtain $H_0 \cdot f(h)/n$ from (366). Repeat the process, and finally plot the last quantity against $n\sqrt{\sigma}$; the curve obtained is unique for the aircraft in level flight at all altitudes; an example is given in Fig. 182.

Thus we have a single curve of $H_0 \cdot f(h)/n \sim n\sqrt{\sigma}$ for the *aircraft* and airscrew.

Also, from the family of curves mentioned under (366) we can plot a family of curves of the same quantities: $H_0 \cdot f(h)/n \sim n\sqrt{\sigma}$, for the *engine*. Examples are marked in Fig. 182.

Intersections satisfy the requirement: $H\eta$ = thrust h.p. required, and represent top speeds at various altitudes. These intersections may be plotted in several ways. Since corresponding flight values of V and n are now known, we can find, for instance, a unique curve of $n\sqrt{\sigma} \sim V\sqrt{\sigma}$, each point on it representing a particular altitude; an example is given in Fig. 183, where also the ceiling is marked. It will be noticed that n falls away as h increases.

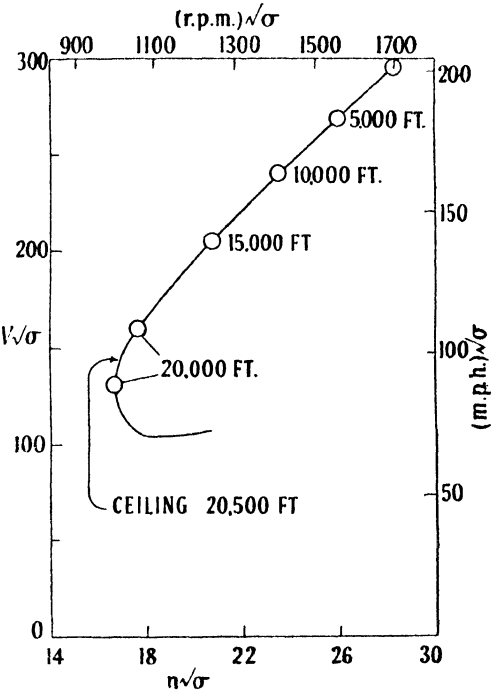

FIG. 183.—PLOTTED FROM FIG. 182.
These details relate to flaps in. The minimum flying speed with flaps out at low altitude is 60 m.p.h., approximately.

Climbing.—On assuming a value of V, the corresponding value of J follows from (365) or (366), as already traced, and thence k_T. But the value of V gives definite values of C_D and C_L. Hence v is calculated from (367) rewritten in the form:

$$\frac{v}{V} = \frac{1}{C_L}\left(2k_T \frac{D^2}{SJ^2} - C_D\right). \quad . \quad . \quad . \quad (369)$$

This calculation is, of course, appropriate to a particular altitude, and assumption of other values of V enables maximum climb at that

altitude to be found by plotting. Repetition with other densities gives the maximum rate of climb as a function of altitude, whence time of climb is estimated as in Chapter IV.

There may sometimes be slight advantage in this analysis in having V in m.p.h., n in r.p.m., or in using the geometrical pitch in place of J.

260. Another arrangement * of the foregoing process will be described briefly. Instead of k_T and k_Q we employ $T_c = T/\rho V^2 D^2$ (cf. Article 232 and note that $T_c = k_T/J^2$) and a b.h.p. coefficient $k_H = 550\ H/\rho n^3 D^5$. Both these must be plotted against J for the airscrew concerned. The new thrust coefficient can be written, since $TV/550 = \eta H$ or $T_c\ \rho V^2 D^2 = \eta k_H\ \rho n^3 D^5$, as—

$$T_c = \eta k_H / J^3 = 2\pi\eta k_Q / J^3$$

Now for any assumed value of n we can find k_{H0} with the help of the maker's engine test sheet, and thence J from the curve of $k_{H0} \sim J$, finally obtaining V, so that repetition gives a curve of $V \sim n$ for sea-level. Different curves are required for other altitudes of interest. To find these we write for altitude h:

$$k_{Hh} = k_{H0} \cdot f(h)/\sigma$$

and, knowing $f(h)$, find for each altitude a curve of $n\sqrt{\sigma} \sim V\sqrt{\sigma}$. These curves define the revolutions available for the given engine and airscrew.

Turning to the aircraft in level flight, and putting T = drag as a sufficient approximation, clearly:

$$T_c = \tfrac{1}{2} C_D \frac{S}{D^2} \quad . \quad . \quad . \quad . \quad (370)$$

A unique curve of $n\sqrt{\sigma} \sim V\sqrt{\sigma}$ is determined by assuming first some value of $V\sqrt{\sigma}$, which gives immediately C_L, and thence from the polar for the complete craft C_D, and T_c from (370), then reading off J from the curve $T_c \sim J$ and calculating $n\sqrt{\sigma}$ from the obvious relationship—

$$n\sqrt{\sigma} = V\sqrt{\sigma}/DJ. \quad . \quad . \quad . \quad (371)$$

Repeating this process gives the curve required, which holds for all altitudes.

Intersections of the engine-airscrew curves with this aircraft curve give values of $V\sqrt{\sigma}$ for various altitudes.

Climbing.—From (367) we obtain, in place of (369) (T>drag)—

$$\frac{v}{V} = \frac{1}{C_L}\left(2T_c \frac{D^2}{S} - C_D\right). \quad . \quad . \quad . \quad (372)$$

* The method of the preceding article is known as Bairstow's (cf. *Applied Aerodynamics*) and the present as the Lesley-Reid, N.A.C.A.T.N., 302, 1929.

So if we assume a value of $V\sqrt{\sigma}$, and find the engine-airscrew $n\sqrt{\sigma}$ and thence J from (371), T_c will follow, whilst C_L and C_D are known, because we are taking as a sufficient approximation that lift = weight during climbing flight. A series of values of v/V so obtained enables maximum v to be determined at the chosen altitude.

260A. More elastic methods suffice to solve isolated questions relating to the performance of an aeroplane driven by airscrews. The data provided commonly comprise, besides the all-up weight W—airscrews: the number, diameter (D), and k_T, k_Q at various values of J; engines: such particulars as enable k_Q to be related to n, the airscrew revolutions per second; wings: the plan-form together with the area (S), the span ($2s$), and possibly a polar curve of C_L plotted against C_D; extra-to-wing drag: an estimate of the glider drag apart from the wings at some intermediate speed; and lastly, information as to the fraction of the total glider parasitic drag (D_p) that is affected by slipstreams. The following discussion refers for clearness to a single-engined aeroplane, and the effect of the slipstream on the induced drag (D_i) is ignored.

The usual procedure is to work out a long table of calculations, of which the first two rows comprise the given values of J and k_Q, so that each column of the table relates to a particular value of J. In the absence of a constant-speed airscrew, row 3 lists the corresponding values of n. To obtain these it is often possible to express the engine data in the form b.h.p. $= kn^x$ for constant altitude, and equating kn^x to $2\pi n \,.\, k_Q \rho n^2 D^5/550$ gives $n = k' \,.\, (k_Q)^{-1/(3-x)}$, where k' is a known constant coefficient for the chosen altitude. Then row 4 of the table gives $V = JnD$, row 5 the full b.h.p. available at each speed, and row 6 the corresponding thrust horsepower (T.H.P.). For the last we note, if the airscrew efficiency η is not supplied, that $\eta = (J/2\pi) \,.\, k_T/k_Q$. To conclude this part of the table, row 7 may record for future use the values of $\frac{1}{2}\rho V^2$.

It is now necessary to arrive at D_p, and the first step (row 8) is to calculate $D_i = k'' \,.\, \lambda^2/(\pi \,.\, \frac{1}{2}\rho V^2)$, where $\lambda = W/2s$ for straight level flight and k'' is a coefficient, probably in the neighbourhood of 1·1, which is estimated from Chapters VII and VIII in consideration of the plan-form of the wings and what allowance should be made for wing-tip vortices. If test figures are available for the wings, row 9 will be devoted to the C_L's, row 10 to the lift/drag ratios of the wings, row 11 to their total glider drags ($W \div L/D_W$), and row 12 to their profile drags $D_0 = D_W - D_i$. Alternatively, row 8 may give C_{Di}, row 10 C_D, row 11 C_{D0} and row 12 $D_0 = C_{D0} \,.\, \frac{1}{2}\rho V^2 S$.

If test figures are not quoted for the wings, we must estimate the

profile drags by direct calculation. For this purpose it will often suffice to employ a constant profile drag coefficient obtained for some Reynolds number intermediate between those for climb and maximum speed. A first estimate results from calculating the coefficient of flat plate skin friction by Article 220, after deciding upon the probable transition Reynolds number from the wing profile and surface in order to fix the second coefficient in (315), and then adding a judicious increment (of the order of 25 per cent.) for the thickness effect on skin friction with a like increment for the form drag of normal wings. Whether wind-tunnel results or calculations are resorted to, the question of surface roughness must be faced, and some experience is necessary to forecast its effects (Article 229).

Row 13 records the part D_{P1} of the total glider parasitic drag which is not affected by the slipstream, and row 14 the remaining part D_{P2} which is to be increased on this account.

An isolated enquiry calls at this stage for choice to be exercised as to further procedure. If the enquiry relates to cruising, range, endurance, or the like, the actual slipstream drag in level flight with the engine throttled back must be obtained. But interest in preliminary calculations centres more frequently, perhaps, in top speed and climb, for which the engine will be at full throttle. Further description assumes the latter alternative.

Row 15 accordingly tabulates the maximum thrust $T = 550 \times$ T.H.P./V for each speed. The factor by which D_{P2} must be increased is, for tractor airscrews, $t = 1 + 4(a + a^2)$, where a is an average inflow factor appropriate to T uniformly distributed over an effective airscrew disc area S_e. $4(a + a^2) = T/\frac{1}{2}\rho V^2 S_e$, the values of which may be entered in row 16. Row 17 then gives $D_{P2}' = tD_{P2}$, row 18 gives $D_C = D_i + D_{P1} + D_{P2}'$, and row 19 gives $H' = D_C V/550$. H' is not the power required for straight level flight except at top speed; at lower speeds it is the thrust H.P. necessary to overcome the drag D_C when climbing.

The top speed is determined accurately by the intersection of curves of maximum T.H.P. available and H' plotted against V. The angle of climb θ is given approximately by $\sin\theta = (T - D_C)/W$; the approximation is involved in row 8 of the table, since accurately $D_i \propto L^2 \propto \cos^2\theta$. The error resulting from neglecting the difference between $\cos^2\theta$ and unity will usually be small but entails correction for large angles of climb.

If H is required for cruising conditions, the only change is that a should be calculated for a thrust $T = D = D_i + D_{P1} + D_{P2}$ $[1 + 4(a + a^2)]$, which may be solved by successive approximation.

On changing the altitude, we notice that for the same values of $\frac{1}{2}\rho V^2$, i.e. the same indicated air speeds V_i, D (but not D_C) will remain constant if further scale effects be neglected. A unique curve D against V_i can therefore be plotted and values of D read off to suit new calculations of V from J and k_Q, which take account of the supercharging of the engine and change of airscrew pitch.

The procedure can evidently be varied, and that described will not always be the shortest. But it is typical and generally useful, and has the advantage of tabulating familiar quantities, so that arithmetical errors are easily detected.

Jet propulsion involves so great a change that methods described in a later section of this chapter are preferable. To some extent this is also true of airscrews driven by gas turbines and jet-airscrew combinations.

261. Take-off and Landing Runs *

With the notation :

W = weight of aeroplane, L its lift, and D its drag ;
T = airscrew thrust and T_0 that at top speed ;
V = velocity at any instant and V_0 top speed ;
x = distance along the ground ;
μ = coefficient of friction with ground ;

we have, during the run prior to take-off—

$$\frac{W}{g}\frac{dV}{dt} = T - D - \mu(W - L). \qquad \text{(i)}$$

Write as an approximation, a and b being constants—

$$T = T_0\left[a - b\left(\frac{V}{V_0}\right)^2\right].$$

Now assume as a sufficient approximation that the tail is up during the whole run to give top-speed incidence (error here would make our estimates too small, but we shall find that they are too great), and (i) becomes :

$$\frac{1}{g}\frac{dV}{dt} = \frac{V}{g}\frac{dV}{dx} = \frac{T_0}{W}\left[a - b\left(\frac{V}{V_0}\right)^2\right] - \frac{T_0}{W}\left(\frac{V}{V_0}\right)^2 - \mu\left[1 - \left(\frac{V}{V_0}\right)^2\right] \qquad \text{(ii)}$$

Introducing the constants A and B defined as—

$$A = a(T_0/W) - \mu$$
$$B = (1 + b)\,(T_0/W) - \mu,$$

* For flying boats see Gouge, *Flight*, November 1927, or Liptrot, *Handbook of Aeronautics*.

(ii) simplifies to—

$$\frac{1}{g}\frac{dV}{dt} = \frac{V}{g}\frac{dV}{dx} = A - B\left(\frac{V}{V_0}\right)^2.$$

Integrating first to find t', the time from a standing start to take-off at speed V—

$$t' = \frac{V_0}{2g\sqrt{AB}} \log \frac{V_0\sqrt{A} + V\sqrt{B}}{V_0\sqrt{A} - V\sqrt{B}} \quad . \quad . \quad (373)$$

the integral being a standard form.

Integrating alternatively from $x = 0$, when $V = 0$ to $x = x'$ at take-off velocity V, to find the length of run—

$$x' = \frac{V_0^2}{2gB} \log \frac{AV_0^2}{AV_0^2 - BV^2} \quad . \quad . \quad . \quad (374)$$

the logs. being of course to base e.

The following values for coefficients are in general use: $a = 1{\cdot}5$, $b = 0{\cdot}8$, $\mu = 0{\cdot}05$ for average aerodrome surfaces and 0·03 for very smooth, hard surfaces, such as the deck of an aircraft carrier (a greater value is allowed over bumpy ground, for the energy then dissipated in the shock absorbers is supplied from the engine).

These simple formulæ are very difficult to apply reliably. The take-off speed would appear to be the speed for maximum climb, and the initial rate of climb to be calculable by the methods of the preceding articles, due allowance being made for wind gradient (Article 85). But lift coefficients * and lift-drag ratios are so much larger at, say, 15° incidence near the ground than in free air, that an aircraft may be well clear before reaching its normal stalling speed. Tests † of a number of aeroplanes have shown taking-off airspeeds to be less than three-quarters that for maximum climb; rates of climb at 30 ft. up have been recorded that exceed normal rates by one-third, though a considerable part of this increase is due to wind gradient and other retardation. Another factor of remarkable importance is the distance of the C.G. of the craft behind its front wheels; adding to this distance by only 2 per cent. of the wing chord may increase take-off run by 25 per cent. This is probably due to excessive incidence, a similar disadvantage resulting from keeping the tail low over rough ground to avoid risk of over-turning.

Unfortunately, different aircraft evince these non-calculable effects in different measure, and to this uncertainty must be added variation in pilots' skill. The specification of an aeroplane includes

* Mathematical investigations relating to this important problem have been carried out by Tomotika, Nagamiya, and Takenouti, *Tokyo Repts.* 97, 1933 and 120, 1935.

† Rolinson, *loc. cit.*, p. 122.

that it shall clear an obstacle height at a given distance from rest. Where there is little margin to spare, designing for this requirement calls for experience.

Many of the above remarks apply to landing runs. Force coefficients are high when undercarriages permit; retardation is greater on slightly rough ground, leading to less run, provided the wheels hold the surface. In a difficult high-speed case the angular and vertical motions of the craft after first touching must be worked out from instant to instant in connection with the proper design of the shock absorbers, smooth ground being assumed but variations of Aerodynamic force being taken into account. All high-speed craft require wheel brakes, which halve the landing run necessary when a wheel replaces a skid at the tail. Their maximum retardation is usually of the order of 4 ft. per sec.[1] With a skid and no brakes the over-all coefficient of friction is about 0·1.

262. Range * and Endurance

The practical problem of how much fuel and oil an aircraft of the aeroplane class must carry for a given length of non-stop flight is beset with uncertain factors. Consequently, approximate analysis is usually sufficient, it being understood that important factors will be introduced subsequently.

We first investigate minimum fuel for a given range. This seems to imply least work done, or drag a minimum, and with normal craft about half speed; but the engines will be throttled well back, and on this C, the specific fuel consumption, depends acutely, while the efficiency η of the airscrews is also concerned. C is defined as the lb. of fuel per b.h.p. (H) per hour, and is assumed for present purposes to include lubricant. The rate of variation of the gross weight W in regard to distance x flown through the air is $dW/dx = -CH/V$. We reckon (in this article only) V in m.p.h. so that x will be in miles, and then $\eta H = WV \div 375(L/D)$, L/D being the lift-drag ratio for the complete craft. Thus—

$$\frac{dW}{dx} = -\frac{CW}{375\eta(L/D)}.$$

Integrating on the assumption that the coefficient of W is kept constant, and changing the log. from base e—

$$x_0 = 863{\cdot}5\,\frac{\eta(L/D)}{C}\log_{10}\frac{W_1}{W_1 - w} \quad . \quad . \quad (375)$$

* An interesting discussion of extreme range has been given by Fairey (Sir Richard), *Jour. Roy. Aero. Soc.*, March 1930.

where W_1 is the initial gross weight and w the weight of fuel required for a flight of x_0 miles. w is a minimum when $\eta(L/D)/C$ is a maximum. Unfortunately, this quantity cannot be regarded as constant as assumed, although it can be evaluated at the beginning and end of the flight, and the mean used. However, it must be understood that under practical conditions of operation (375) is far too optimistic, and that w requires to be increased very considerably for safety, quite apart from risk of head winds, which is supposed to be taken into account in x_0.

To calculate roughly the minimum fuel required for a time t_0 (hours) in the air, we may proceed as follows. The equation $dW/dt = -CH$ leads to :

$$\frac{dW}{dt} = -\frac{CWV}{375\eta(L/D)}$$

$$= -\frac{CW}{375\eta(L/D)} \cdot \frac{60}{88}\sqrt{\frac{W}{C_{L\frac{1}{2}}\rho S}}$$

where S is the wing area, the factor 60/88 taking account of V being in m.p.h. Hence :

$$dt = -550\,\frac{\eta(L/D)}{C}\sqrt{C_{L\frac{1}{2}}\rho S}\,.\,\frac{dW}{\sqrt{W^3}}.$$

Integrating on a similar assumption to that used above—

$$= 1100\,\frac{\eta(L/D)}{C}\sqrt{\frac{C_{L\frac{1}{2}}\rho S}{W_1}}\left(\sqrt{\frac{W_1}{W_1 - w}} - 1\right) . \quad (376)$$

giving for maximum endurance the condition $\eta(L/D)\sqrt{\frac{1}{2}C_L}/C$ a maximum. Again we note that average values must be taken. When this is done and allowance made for operational difficulties, t_0

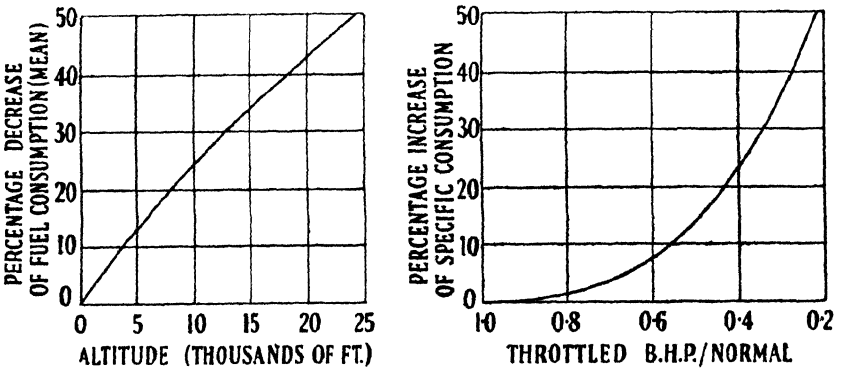

FIG. 184.—THE AVERAGE ALTITUDE VARIATION IS FOR NORMALLY ASPIRATED ENGINES AT CONSTANT R.P.M.

may amount to little more than one-half what it would be if optimum values could be maintained.

Altitude comes into both the above questions through C in the first and $\sqrt{\rho}/C$ in the second. To include this, $H \,.\, f(h)$ must be substituted for H. Introducing $\varkappa$ as an altitude factor for the specific consumption, it is required that $f(h)/\varkappa C$ be a maximum. Fig. 184 gives some average values for normally aspirated engines.

AERODYNAMIC EFFICIENCY

262A. The efficiency now to be discussed differs in nature from that described in Article 252, being the aeronautical adaptation of a universal basis on which the economy of transportation may be assessed. The load carried is compared with the work done, having due regard to the speed achieved. For general purposes, e.g. comparison between aerial and surface transport, only the useful or disposable load would be considered and the speed would be reckoned relative to the ground. But the term Aerodynamic implies that gross weight or total lift is substituted for useful or disposable load, and true air speed for ground speed. These steps can be justified from a general point of view, provided aircraft of abnormal tare weights and exceptionally low speeds are excluded (cf. Article 69), and they separate Aerodynamical from structural and mechanical considerations.

Let W be the total weight of an aircraft, including its load, and x the distance traversed horizontally through a still atmosphere at a true air speed V. Regarding W and x as of equal value, the useful result achieved is expressed by the product Wx. The work done against the drag D is Dx, but Aerodynamical losses are incurred in providing a thrust $T = D$. If the propulsive efficiency η takes separate account of these additional losses, the total work done is Dx/η, and the Aerodynamic efficiency is proportional to $\eta W/D$, i.e. to $\eta L/D$, since for straight and level flight $W = L$ the lift.

Now clearly in the case of propulsion by engines and airscrews,

$$\eta \frac{L}{D} = \frac{WV}{TV/\eta} = 6\frac{W \text{ (tons)} \times V \text{ (m.p.h.)}}{\text{b.h.p.}}$$

very closely, and with jet or other propulsion ' b.h.p.' may stand for the power of the propelling device apart from specifically Aerodynamical application. Hence, defining the *Aerodynamic efficiency* of an aircraft by—

$$\eta_A = \frac{1}{6}\eta\frac{L}{D}, \quad . \quad . \quad . \quad . \quad \text{(i)}$$

η_A is seen to be closely equal to 'ton-miles per b.h.p.-hour' and proportional to 'ton-miles per gallon.' In early days of heavier-than-air flying, η_A provided a target of 100 per cent. which was difficult for aeroplanes to surpass. But this position has long ceased to hold, and η_A has become a figure of merit, having values usually between 1 and 4.

In the first instance, Article 69 will be further developed in terms of efficiency and with the detail now possible.

It follows immediately from that article that for geometrically similar airships of size l and using the same gas, $L/D \propto L^{1/3}/V_i^2$. Thus plotting η_A/η against V_i^2 gives an hyperbola for each size. This basis is adopted in Fig. 184A in order to penalise low speeds and give weight to high speeds. The family of curves for various sizes has been prepared by scaling down known data for large airships.

It has also been seen that, considering a series of geometrically similar aeroplanes of span l in straight and level flight, their drag through the major part of the speed range can be expressed approximately as—

$$D = \frac{A}{\rho V^2}\left(\frac{L}{l}\right)^2 + B\rho V^2 l^2$$

and is a minimum when each of the terms on the right is equal to $L\sqrt{AB}$, which occurs at an indicated air speed given approximately by—

$$V_{i0} = 14\left(\frac{A}{B}\right)^{1/4}\left(\frac{L}{l^2}\right)^{1/2}.$$

Thus the maximum L/D is $1/2\sqrt{AB}$, and at any other speed—

$$\frac{L}{D} = \frac{1}{\sqrt{AB}\left[\left(\frac{V_0}{V}\right)^2 + \left(\frac{V}{V_0}\right)^2\right]} = \frac{2(L/D)\text{ max.}}{\left(\frac{V_0}{V}\right)^2 + \left(\frac{V}{V_0}\right)^2} \quad \text{(ii)}$$

For cantilever monoplanes having 'normal' wings of aspect ratio 8, a maximum L/D of at least 18 can be expected with airscrews feathered to give zero thrust, and then adding 8 per cent. to the theoretical minimum for the induced drag leads to the following:

$$(AB)^{1/2} = 1/36;\ A = 2{\cdot}16/\pi;\ V_{i0} = 24{\cdot}6w^{1/2}\ \text{(m.p.h.)};$$
$$V_0^2 = 1300\ w/\sigma\ \text{(ft. per sec.)}^2;$$

where w is the wing-loading in lb. per sq. ft. and σ the relative density of the air. These data are used for illustration below.

The straight line (a) of Fig. 184A represents the constant

maximum efficiency for aeroplanes of the given shape loaded between 20 and 50 lb. per sq. ft. The optimum true air speeds are unduly small at low altitudes even with heavy wing-loadings and, as previously noted, aeroplanes fly faster, losing efficiency but putting to use engine power provided for climbing. The expression (ii) and the above numbers lead to the curves given for $w = 20$, 30, 40, and 50 lb. per sq. ft., showing the drop in efficiency at higher speeds with these wing-loadings. The advantage achieved by decreasing the size of an aeroplane for a given total weight may be compared with that secured by increasing the size of an airship. Improvement of aeroplanes by this means is restricted by take-off and forced landing conditions (minimum flying speeds for full load vary from 56 to 88 m.p.h. through the above range of wing-loading, assuming a maximum C_L of $2\frac{1}{2}$). Improvement of airships by natural saving of surface area with increase of size is seen to become slow at the 200-ton stage. Other conclusions arrived at in Article 69 may be verified from the figure. The curves so far described apply to all altitudes if abscissæ are taken as indicated air speeds.

262B. It is of interest to trace the effect of wing-loading on the efficiency, in straight and level flight at full power, of aeroplanes having specified initial rates of climb at V_0. With airscrew effects excluded, these rates will differ little from maximum rates of climb. Let v be the rate in feet per minute. Then approximately—

$$\frac{W}{550}\left[\frac{V}{L/D} - \frac{V_0}{(L/D)_{\max.}}\right] = \frac{Wv}{33000},$$

if V is the top speed, or by (ii) of the preceding article—

$$V\left[\left(\frac{V_0}{V}\right)^2 + \left(\frac{V}{V_0}\right)^2\right] = \left(\frac{L}{D}\right)_{\max.} \cdot \frac{v}{30} + 2V_0.$$

Writing k for V_0^2/w results in the following equation for V—

$$\frac{1}{k}\left(\frac{V}{\sqrt{w}}\right)^3 + k\frac{\sqrt{w}}{V} = \frac{1}{30}\left(\frac{L}{D}\right)_{\max.} \cdot \frac{v}{\sqrt{w}} + 2\sqrt{k} \quad \text{(iii)}$$

which is in suitable form for solution by successive approximation. The above are restricted to true air speeds and cannot be interpreted as indicated air speeds.

Considering the example of Fig. 184A with $\sigma = 1$, the efficiency curves (*b*)–(*e*) are obtained for full speeds at low altitudes corresponding to initial rates of climb of 500, 1000, 1500, and 2000 ft. per min. at values of V_0 appropriate to the wing-loading. These curves are not operational but indicate the advantage of designing for high wing-loadings. Thus doubling the wing-loading from 20

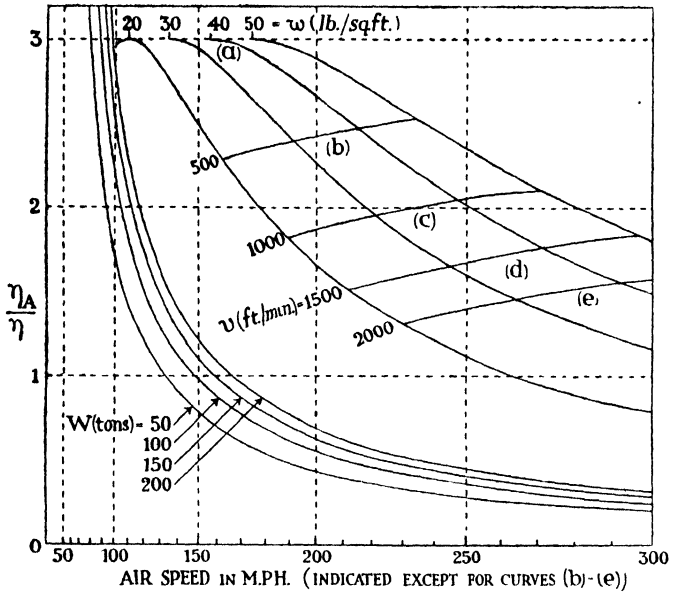

FIG. 184A.—AERODYNAMIC EFFICIENCY OF AIRSHIPS AND AEROPLANES.
v = Initial rate of climb. w = Wing loading. W = Gross weight of airship.

to 40 lb. per sq. ft. increases the ton-miles per gallon by about 16 per cent. for the same initial rate of climb, in spite of the top speed being increased by some 30 per cent.

262C. Airscrew Effects

A close network of curves of η_A/η against V^2 for constant wing-loadings and initial rates of climb provides a chart which may be used to criticise a given design or aid in a proposed one. The few curves for constant wing-loading in Fig. 184A include allowances for form drag and wing-tip vortices in the values assumed for the maximum glider L/D and A. They follow directly from these values by ignoring Aerodynamical scale effects, but may equally be plotted from an experimental curve of L/D against C_L for the given geometrical shape. Allowances have not been made, however, for slipstream effects or airscrew efficiencies, which reduce Aerodynamic efficiencies and rates of climb.

Thus taking, for example, the average lightly loaded aeroplane of merit described in Article 252, the known speed of 220 m.p.h. and wing-loading of 21 lb. per sq. ft. indicate on the chart a value of η_A/η of about 1·48. From the known power-loading (12·3 lb. per b.h.p.)—

$$\frac{\eta_A}{\eta} = \frac{\text{ton-miles per hour}}{\eta \times \text{b.h.p.}} = 1{\cdot}47,$$

on giving η the reasonable value 0·82. So far as may be determined, this typical meritorious aeroplane satisfies the chart in respect of efficiency at top speed in spite of slipstream drag. But the idealised rate of climb is seen to be more than 1600 ft. per min., whilst the actual rate would be 300–400 ft. per min. less. The large deficit will now be investigated.

Slipstream Drag.—We first determine the decreased lift/drag ratio, denoted by L/D_1, for straight and level flight at the general speed V. Neglecting change of induced drag, a fraction f of the total parasitic drag is increased by the factor $1 + 4(a + a^2)$, where a is the inflow factor determined from the thrust T on an effective airscrew disc area S_e. From airscrew theory, $4(a + a^2) = 2T/\rho V^2 S_e$. Hence the total parasitic drag is increased by the factor $1 + 2fT/\rho V^2 S_e$ and, by Article 262A,

$$\frac{L}{D_1} = \frac{2(L/D)\text{ max.}}{\left(\frac{V_0}{V}\right)^2 + \left(\frac{V}{V_0}\right)^2 + \frac{2f}{\rho V_0^2 S_e} \cdot \frac{W}{L/D_1}}$$

$$= \frac{L}{D}\left[1 - \frac{fW}{\rho V_0^2 S_e (L/D)\text{ max.}}\right], \quad . \quad . \quad \text{(i)}$$

where L/D is the glider lift/drag ratio given by (ii) of Article 262A.

For a given aeroplane and load, the percentage reduction of the glider lift/drag is the same for all speeds. For a constant geometrical shape, $\rho V_0^2 \propto w$ and the second term in the brackets of (i) $\propto fS/S_e$, where S is the wing area. The variation is obviously discontinuous and complicated. For the single-engined aeroplane with $W = 10{,}000$ lb. and $w = 20$ lb. per sq. ft., f might be equal to $\frac{1}{2}$ and S_e to 80 sq. ft., giving $L/D_1 = 0{\cdot}945(L/D)$. Doubling the weight without changing the size would have no effect unless a second engine were added, when f might become $\frac{1}{4}$ and S_e 160 sq. ft., giving $L/D_1 = 0{\cdot}972(L/D)$. Halving the wing area with the original weight and a single engine might increase f to $\frac{3}{4}$ but reduce fS/S_e by 25 per cent. Such examples verify that the effect on efficiency of slipstream variations is comparatively small in straight level flight, but it is worth remarking again that the absence of tractor airscrews altogether might improve efficiency considerably by increasing transition Reynolds numbers; such improvement would appear in the present calculations as a greater maximum lift/drag ratio.

Turning to climb at V_0, the large thrust is approximately equal to $D_2 + Wv/60V_0$, where $D_2 = W/(L/D_2)$ and is obtained from the

glider drag D at that speed by increasing the total parasitic drag by the factor—

$$1 + \frac{2fT}{\rho V_0^2 S_e} = 1 + \frac{2fW}{\rho V_0^2 S_e}\left(\frac{1}{L/D_2} + \frac{v}{60V_0}\right).$$

Thus, writing F for the factor outside the brackets, we readily find from Article 262A that—

$$\frac{L}{D_2} = \frac{2(L/D)\text{ max.}}{2 + F\left(\frac{1}{L/D_2} + \frac{v}{60V_0}\right)}$$

$$= \frac{(L/D)\text{ max.} - \frac{1}{2}F}{1 + \frac{1}{2}F \,.\, v/60V_0} \quad . \quad . \quad . \quad \text{(ii)}$$

For a 10,000-lb. aeroplane of the series to which Fig. 184A applies, and with $w = 20$ lb. per sq. ft. and $f = \frac{1}{2}$, $F = 2$, closely. Putting $v = 1500$ ft. per min. gives $L/D_2 = 14{\cdot}7$. The maximum lift/drag in level flight is reduced by slipstream drag to $0{\cdot}944 \times 18 = 17$, whence it is easily found that the increase of slipstream drag from top speed to V_0 reduces the rate of climb in this case by about 90 ft. per min., whilst the entire slipstream drag accounts for a loss of about 120 ft. per min. The remaining part of the decrease in rate of climb from the ideal value is to be traced to the loss of thrust h.p. by airscrews and is minimised by use of variable pitch, as already described.

262D. Application to Prediction

A curve of $\eta_A/\eta = \frac{1}{6}L/D_1$ against the indicated air speed V_i ($= \sigma^{1/2}V$ m.p.h.) for a given aeroplane in straight and level flight is plotted by reducing the corresponding glider curve by a factor to allow for slipstream drag. Such a corrected curve for an aeroplane is shown in Fig. 184B and, by (ii) of Article 262A and (i) of Article 262C, it is independent of altitude.

Let P be the *actual* power-loading in lb. per operative b.h.p. By Article 262A the conditions $L = W$, $T = D_1$ for straight level flight are satisfied if—

$$\frac{\eta_A}{\eta} = \frac{W\text{ (tons)} \times V_i}{\eta\sqrt{\sigma} \times \text{b.h.p.}}$$

$$= \frac{PV_i}{2240\,\eta\sqrt{\sigma}} = CV_i, \text{ say.} \quad . \quad . \quad \text{(i)}$$

Let any point A on the efficiency curve subtend at the origin the angle θ with the V_i-axis. Then the value of C required by the wing-loading and speed specified by A is equal to $(\tan\theta)\ x/y$, the

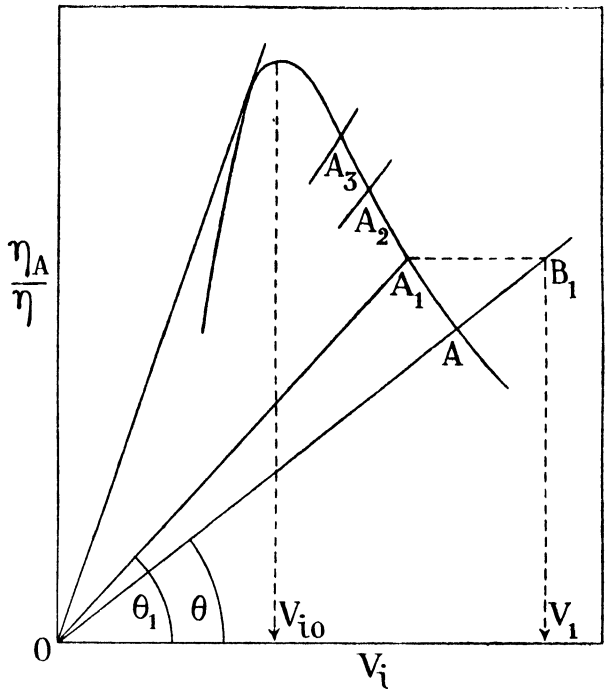

FIG. 184B.

scale of η_A/η being x units of length and that of V_i y units of length. Thus the indicated air speed for known values of P, η and σ can be found by drawing a radial line from the origin at the angle $\theta = \tan^{-1} Cy/x$ to intersect the efficiency curve. More generally, information regarding the power units enables CV_i to be plotted against V_i in Fig. 184B as a sequence of curves, one for each altitude, and the intersections A, A_1, A_2, . . . give the efficiencies and speeds of flight for those altitudes.

Increase of P (reduction of b.h.p.) and decrease of σ both increase θ, and the absolute ceiling occurs, when the radial line is tangential to the efficiency curve, as illustrated. Writing k_i for $\sigma V_0^2/w$ and V'_i for the indicated air speed in feet per second gives the following equation in place of (iii) of Article 262B—

$$\frac{1}{k_i}\left(\frac{V'_i}{\sqrt{w}}\right)^3 + k_i \frac{\sqrt{w}}{V'_i} = \frac{1}{30}\left(\frac{L}{D}\right)_{\max.} \cdot \frac{v\sqrt{\sigma}}{\sqrt{w}} + 2\sqrt{k_i},$$

whence the rate of climb at V_{i0} can be calculated for any altitude at which the top speed in level flight is known. A correction for the slipstream can be effected as already discussed.

262E. Wing-loading and High-altitude Flying

Referring again to Fig. 184B, if P and η can be regarded as constant up to a certain altitude, $C \propto 1/\sqrt{\sigma}$ through the range, and a convenient construction gives the true air speed. Let the point A in the figure represent low-altitude flight, and use suffix 1 to distinguish flight at a higher altitude. Then if V_1 is the true air speed in m.p.h.—

$$\frac{(\eta_A/\eta)_1}{V_1} = \frac{V_{i1} \tan \theta_1}{V_{i1}/\sqrt{\sigma}} = \tan \theta.$$

Hence B_1, the point on OA produced which has the same value of η_A/η as A_1, gives the true air speed V_1 on the scale of V_i.

The assumption will now be extended to a large increase of altitude and a considerable range of speed. In this form it will be representative of the reciprocating engine and airscrew, even approximately, only up to the supercharged height, but supercharging to a high altitude will also be assumed. Turbine, jet, rocket, or composite power units may make the assumption more widely representative.

In Fig. 184C, the pencil of lines radiating from the origin, marked

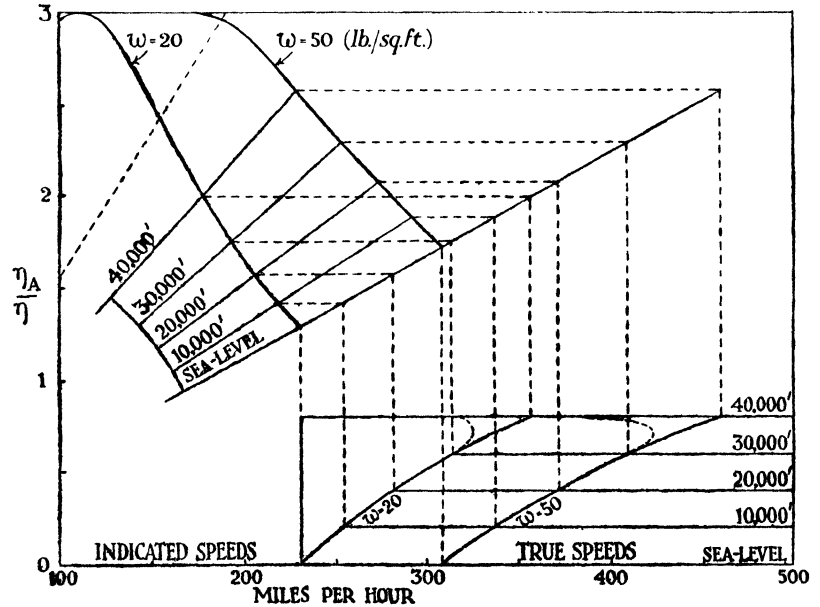

FIG. 184C.

sea-level to 40,000 ft., is appropriate to a power-loading of 10 lb. per b.h.p. Intersections with the ideal efficiency curves given for $w = 20$ and 50 lb. per sq. ft. lead, by the construction just described, to the true air speeds inset as full-line curves at the bottom of the figure. Thus the speeds marked on the scale are to be interpreted, in respect of the upper and left-hand part of the figure, as indicated air speeds, and as true air speeds in respect of the lower and right-hand part. Corrections have not been made for slipstream drag, but previous discussion has shown that they would affect the results only in degree.

The main feature evinced is the large increase of efficiency achieved at high altitudes with, at the same time, a large increase of true air speed. To the present approximation, a wing-loading of 20 lb. per sq. ft. gives at 28,000 ft. altitude the same efficiency and speed as a wing-loading of 50 lb. per sq. ft. at sea-level. At 40,000 ft. the relative density of the air is $\frac{1}{4}$, and this altitude is often regarded as suitable for long-distance flying with pressure cabins. It permits an aeroplane with a wing-loading of 50 lb. per sq. ft. to fly within 15 per cent. of the maximum possible efficiency and at twice the true air speed for the same efficiency at low altitude.

The dotted radial beyond the pencil of related lines applies to 40,000 ft. with the assumption that power is provided by reciprocating engines supercharged to rather below 30,000 ft. Associated changes in the altitude-speed curves between 30,000 and 40,000 ft. are shown dotted. The loss of power brings the aeroplane with the heavier wing-loading close to its ceiling, and the serious loss of speed ensuing at 40,000 ft. illustrates the advantage of jet or other propulsions in which the difficulty of maintaining power at high altitudes largely disappears.

262F. Laminar Flow Effect

As an example of a general kind we may consider briefly the improvement of the pre-war type of monoplane used above for illustration. Technical accuracy will not be attempted, the aim being to assess by simple means only the order of gains in efficiency up to the laminar flow stage. A Reynolds number of 15 million will be assumed for calculations and scale effects through the upper speed range neglected. Skin friction will be estimated by (315), with an allowance of 25 per cent. for thickness and a like addition for form drag in the case of normal wings, as suggested in Article 260A. The

following approximate formulæ, which can easily be verified, are adopted from *Elementary Aerodynamics*—

$$\left(\frac{L}{D}\right)_{\text{max.}} = \tfrac{1}{2}\sqrt{\frac{A}{0{\cdot}35\,C_{DP}}}, \quad . \quad . \quad . \quad . \quad . \quad \text{(i)}$$

$$V_{10} = 16{\cdot}5\sqrt{\frac{(L/D)\text{ max. } w}{A}} \quad . \quad . \quad . \quad . \quad \text{(ii)}$$

A denoting the aspect ratio (taken as 8) and C_{DP} the coefficient of total parasitic drag. The method being suitable for no more than a first approximation, only an outline of the calculations will be given and round numbers used wherever possible.

(1) For the aeroplane in its original state, (L/D)max. = 18 and (i) gives $C_{DP} = 0{\cdot}0176$. The transition Reynolds number is low on account of roughness and slipstreams, and the assumption of 1 million leads to the estimate $C_{DO} = 0{\cdot}008$, without increase for roughness drag. This leaves the value 0·0096 for C_{DB}, the coefficient of extra-to-wing drag, including roughness wherever occurring. Contributions to C_{DB} are assumed to be distributed as indicated in Table X, p. 459.

(2) Let the first improvement consist of eliminating roughness, tractor airscrews, non-ducted reciprocating engine cooling, and an exposed tail wheel. Inspection of Table X suggests a reduction of C_{DB} by about 25 per cent., i.e. to 0·0072. Another consequence is to increase the transition Reynolds number for the 'normal' wings to, say, 3 million. The revised estimate of C_{DO} is 0·0064. Hence C_{DP} becomes 0·0136 and, by (i), (L/D)max. = 20·5.

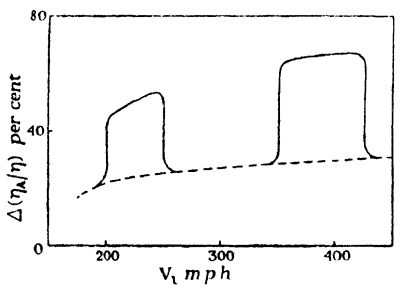

FIG. 184D.

(3) Let the second improvement be the substitution of laminar flow wings with transition at $\frac{2}{3}$ chord behind the nose. Whether the form drag is greatly less on increasing the transition Reynolds number from 3 to 10 million cannot be decided without special data, and the assumption above will still be made. Then $C_{DO} = 0{\cdot}0032$ and $C_{DP} = 0{\cdot}0104$, whence (i) gives (L/D)max. = 23·4.

Assuming further a wing-loading of 36 lb. per sq. ft., (ii) gives approximately for the most efficient speeds: $V_{10} = 148$, 158 and 169 m.p.h., for (1), (2) and (3), neglecting scale effects.

Efficiency curves for the three cases can be constructed from these data very rapidly, as described. In Fig. 184D the percentage increase of η_A/η for the two improvements is plotted against the indicated air speed. Normal wings are retained for the dotted curve, and two alternative locations are shown for the local increase of efficiency due to laminar flow wings, the one to the left in the figure being suitable for high altitude flying. The extent of the alternative favourable ranges is conjectural and remains matter for design. The figure illustrates that laminar flow wings are the more effective at small lift coefficients, as is otherwise evident.

To derive corresponding curves of η_A, we should require to take account of the variation of propulsive efficiency, not only in regard to change of speed and altitude but also as involved in the sweeping alteration introduced between cases (1) and (2).

263. The Autogyro and Helicopter

Fig. 185 is a sketch of a recent autogyro (Articles 243–4). An earlier type of these small craft has, additionally, diminutive wings with ailerons totalling some 5 per cent. of the rotor disc area. One example of this kind, of 0·7 ton all-up weight with a disc area of

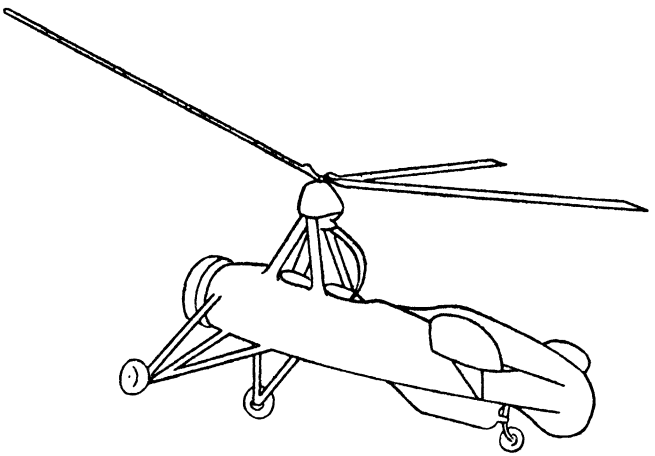

FIG. 185.—WINGLESS DIRECT-CONTROL AUTOGYRO.

900 sq. ft., gave approximately: top speed 97 m.p.h., with 110 b.h.p.; minimum horizontal speed 40 m.p.h.; minimum vertically downward component of speed 10 m.p.h. at a gliding angle of 16°; normal rotor speed 180 r.p.m. Further development is still in progress, and these figures cannot be taken as indicating either best

modern results or ultimate scope. Rotor solidity used to be as high as 0·14, then 0·07, and is still decreasing. Success with direct control tends to eliminate the auxiliary wing, though the combination has points of Aerodynamic interest. Preliminary prediction of autogyro performance follows lines already established for the aeroplane, once rotor characteristics are available from the theory of Chapter X or from model experiment freed from scale effect. It is only necessary to discuss in general terms the main differences to be expected.

The stalling disc incidence of a rotor is large, about 40°, but its lift/drag ratio, C_z/C_x, is then very small, about 1·2, and minimum horizontal speed is determined by engine power. Though this condition occasionally applies to aeroplanes (Article 77), their wings are then about to stall, while the autogyro has a large reserve.

We can verify this roughly for the above example by neglecting all parasite drag and auxiliary lift. C_z is found to be 0·42 at 40 m.p.h., corresponding to 13° incidence; C_z/C_x would then be about 3·7, giving drag = 420 lb., which would require an effective thrust h.p. of 45. That available would be about 50, leaving little margin. But a maximum C_z approaching 1·0 could be expected, so that stalling speed = 26 m.p.h. The craft could realise such low speeds in descent, gravity supplying the power required. One condition could be a vertical path, as the stall is not catastrophic. But minimum speed of descent, worked out as described in Chapter IV, would correspond to a higher forward speed and a moderately flat gliding angle, as mentioned above.

It is seen that the autogyro can use increase of power to increase its speed range by decreasing minimum speed. Also, with a quite feasible undercarriage, it can land safely in an extremely confined space. Together with use of impulsive helicopter lift as already described, to give direct take-off, these features form the distinguishing advantages of the type.

Turning to rate of climb, the type is greatly inferior to the aeroplane class, owing to very poor efficiency at the forward speed giving maximum reserve power for climbing. The L/D of a complete autogyro is then little more than 5, and consequently even an inefficient aeroplane of the same weight and power climbs twice as fast. Maximum climb will be found to occur at about two-thirds speed, as with aeroplanes.

At greater speeds the L/D of the rotor rises, attaining a maximum (say 8) just before top speed is reached. At present, the resulting decrease of rotor drag approximately offsets increase of parasite drag, so that over-all L/D is ultimately little less than at maximum

climb. This essential difference from the aeroplane, whose efficiency declines from maximum climb onward, enables the autogyro to bear comparison somewhat better at full speed, but the low L/D of about 5 still remains as an important disadvantage. Top speed L/D can doubtless be increased, but aeroplanes also have greater efficiency in prospect. Eventually, the penalty of deriving sustentation from a screw motion of the lifting surface must remain fundamental.

These comparisons between the autogyro and aeroplane are inevitable, but no more justifiable than between the airship and aeroplane. Multiple power-unit aeroplanes unquestionably provide the most efficient and the safest means of high-speed transport that at present it is possible to conceive. In this duty we have already seen that the airship cannot compete. A similar disability arises with the autogyro from the fact that disc loading must increase rapidly with increase of speed, leading to less efficiency and high minimum vertical velocity. The same need to increase loading exists with aeroplanes, but not with the same consequences. The high-speed aeroplane demands large, prepared aerodromes, a peculiar disadvantage which the autogyro and airship both avoid, the former so successfully as alone to justify this remarkable invention. Additionally, the autogyro, owing chiefly to non-stalling properties, is easy to fly in a straightforward way, although safety in manœuvres remains a matter for investigation.

A sketch of a helicopter is included in Fig. 43. It is of interest that this type of aircraft was the first to be invented (Leonardo da Vinci, *circa* A.D. 1500) and has been the last to receive practical form, a step partly due to the success of the autogyro. The example illustrated has only one lifting rotor, but a subsidiary rotor, working in a vertical plane at the tail, controls orientation of the body. In another type this control is obtained from a small jet utilising the exhaust gases of the engine. Theoretically, the helicopter is slightly more efficient than the autogyro, but until the type is further developed and performance data become available, it cannot be concluded whether this small advantage will be realised.

CORRECTION OF FLIGHT OBSERVATIONS

263A. The performance of a given aeroplane depends acutely upon the state of the atmosphere at the time of the test. In order to assess the capabilities of the aircraft, observations have therefore to be reduced to a common basis, and some standard atmosphere is chosen, such as that defined by Table III, p. 17. Methods of reduc-

tion are easily devised, and the following indicates one procedure that will often be found suitable.

Maximum Speed in Level Flight.—Data from speed tests in straight and level flight, whether automatically recorded or observed by the pilot, can be tabulated under the following headings :

TABLE A

Aneroid height. h_A (ft.)	Atmospheric temperature. θ° C.	Indicated air speed V_i (m.p.h.)	Airscrew revolutions. N (r.p.m.)

The first column of the table consists of a number of selected altitudes as given by the altimeter, and the other columns record averaged data for flight at each of these reputed altitudes. The last column will be omitted in case of jet propulsion, but airscrews will be assumed for greater generality.

The altimeter is a pressure gauge, and the pressures are correctly written down from Table III, identifying h_A with the true altitude for that purpose. But the corresponding densities would be incorrect unless the second column of Table A happened to accord with the standard atmosphere. The true values of the relative density are obtained from

$$\sigma = \frac{\rho}{\rho_0} = \frac{288}{273 + \theta} \cdot \frac{p}{p_0},$$

in which the suffix refers to conditions at the foot of the standard atmosphere, where $\theta = 15°$ C.

It is necessary to determine the brake horsepowers actually expended at the various aneroid heights. These can always be found from records of ' bench ' tests carried out on the power units at various air pressures, knowing the pressure, density, and temperature during flight. For instance, reciprocating engines often give, for normal aspiration or above the rated altitude, a linear relationship between the b.h.p. and the variable $\sqrt{(\sigma p/p_0)}$ at constant r.p.m., and the actual b.h.p. can be read by interpolation from charts prepared on this basis.

On multiplying the b.h.p. and N by $\sqrt{\sigma}$ in accordance with Article 259, a new table with headings as follows results from Table A :

TABLE B

p/p_0	σ	V_i	$N\sqrt{\sigma}$	b.h.p. $\sqrt{\sigma}$.

The original data have now been expressed in terms of the actual pressure, density, and temperature during flight, with the actual horsepowers added.

Let any true altitude h be chosen. Corresponding values of p, ρ, and θ appropriate to the standard atmosphere are written down from Table III, and the b.h.p. available at any r.p.m. immediately follows. The values of b.h.p.$\sqrt{\sigma}$ and $N\sqrt{\sigma}$ required to satisfy Table B with the new values of σ and θ are then found by plotting, and the solution gives the corresponding indicated air speeds without further work. The calculations are repeated for other true altitudes.

Maximum Climb.—Flight records regarding climb are presented in the form :

TABLE C

h_A	θ	V_i	N	Time to h_A t (min.)

The aneroid rate of climb is readily found, with the help of (99) p. 145, for heights above the rated altitude. It is required to deduce true rates of climb at true altitudes. It is assumed in the following that the rows of Table C differ by only short intervals of h_A and t; otherwise the records may be plotted and small changes read from the curves. The nature of the correction required may be visualised from the reflection that an aneroid rate of climb would be registered for level flight if the density decreased at the altitude concerned.

Through a restricted change of height, the pressure and density are related by the hydrostatic equation (2), p. 5, i.e. $\Delta h = -\Delta p/\rho g$. The mean value of ρ during a short interval of time is readily deduced from changes in the altimeter and thermometer readings, by use of the equation of state (9), p. 13. Hence the actual climb Δh follows, and we have, if σ' is the standard relative density used in calibrating the altimeter,

$$\Delta h\sigma = -\Delta p/g\rho_0 = \Delta h_A\sigma',$$

whence the true rate of climb is given by

$$\frac{dh}{dt} = \frac{\sigma'}{\sigma} \cdot \frac{dh_A}{dt}.$$

This equation may be used to correct the recorded time intervals to standard atmospheric conditions, and then the true time to a given altitude, or required to traverse a given change of altitude,

follows by summation. The graphical representation of altitude plotted against time is often called the climb diagram (*cf.* also Article 81).

The remaining data of Table C can now be used to reduce the corrected rates of climb to standard atmospheric conditions by obtaining the horsepowers available at various true altitudes under those conditions, the calculations being the same as for maximum speed in level flight. A graphical solution for the new values of σ gives corresponding values of V_i, $N\sqrt{\sigma}$ and the rate of climb $x\sqrt{\sigma}$, whence Table C may be standardised.

Plotting.—In Fig. 185A (*a*), curve 1 is plotted from the last two columns of Table B, whilst curve 2 is obtained from the engine data for any chosen altitude in the standard atmosphere by assuming some likely values of N. The intersection determines the b.h.p.

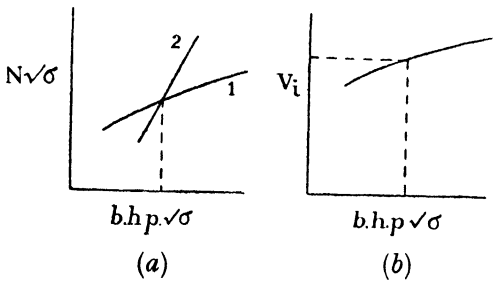

Fig. 185A.

required for straight and level flight at maximum speed under standard conditions. The speed is read from (*b*) in the figure, which is also plotted from Table B. Repetition for other altitudes standardises maximum speed performance. Simple development extends the method to climb.

Chapter XII

SAFETY IN FLIGHT

264. Complete discussion of aerial safety would involve such matters as engine reliability, structural design, life of materials, and the direction of flying routes. Aerodynamics is concerned mainly with three other factors, as will be described.

A craft should be capable of flying itself, in the sense of maintaining a particular mode of flight, for which its controls have been arranged, without further assistance from the pilot. This faculty might be secured by a mechanical or robot pilot, when the craft is said to be *automatically stable.* But we shall study only the case where no substitution for the pilot is necessary, the craft possessing an inherent stability by virtue of judicious shaping and distribution of its mass. *Inherent stability* in aeroplanes must be limited by both flight variation and violence of disturbance. Beyond this range, and during manœuvres, safety against disturbance lies in the hands of the pilot, and depends upon the provision of controls which will remain adequate in rather extreme circumstances. The third Aerodynamic consideration is concerned with specifying what accelerations are to be expected from the response of a craft to disturbances (such as gusts) or the reasonable exercise of its controls, so that the structure may be designed to have sufficient strength.

After introductory articles, we shall proceed, in the first place, to rigorous study of inherent stability in straight flight. The theory and application of the method are due, following pioneering work by Lanchester and others, to Bryan,* and to Bairstow † and his collaborators at the N.P.L. As shown by the dates given, the theory is one of the oldest of Aerodynamics. But, though not difficult mathematically, the subject is very complicated, and only recently has it been recast into a form suitable for discussion and use by the designer. This step is due to Glauert.‡

Aeroplanes are examined theoretically for response to very small

* *Stability in Aviation*, 1911.

† *Adv. Com. for Aeronautics*, 1912–13 ; also *Applied Aerodynamics*, 1920.

‡ A.R.C.R. & M., 1093, 1927. For the most recent general account see B. M. Jones, *Aerodynamic Theory*, vol. v, 1935.

disturbances, and practical utility depends on the assumption that they will behave similarly in face of the disturbances encountered in normally bumpy weather. This assumption is sanctioned by full-scale experience ; it fails in some cases, but usually for specific reasons that are apparent on inspection. Maintenance of flight is not continuous, a stable craft requiring time to recover from disturbance. Recovery is achieved by a natural manœuvre, in which the C.G. is displaced from the course of mean motion, variable linear and angular velocities being superposed. Damping out the effects of disturbance may occupy a fraction of a second or more than a minute. Space is required and, when this is lacking, as on landing, it is essential for a pilot to be able to supersede stability by control. Even with no restriction on freedom of movement, a tedious response by a stable aeroplane will usually be corrected by control at an early stage. Thus, stability moments should be light and easily overridden. But this requirement follows also from the fact that too strong a response to one kind of disturbance may involve instability in regard to another. Thus, designing for stability does not lend itself to the employment of large margins to cover error, but calls for careful compromise between conflicting factors. Evidence of static stability is often a poor guide to the possession of the dynamic stability with which we are now concerned.

Longitudinal stability deals with changes in the plane of symmetry, such as of pitch or air speed ; *lateral* stability includes all asymmetric movements, such as roll or sideslip. Great simplification follows mathematically from the assumption of initially straight flight : longitudinal and lateral stability do not affect one another, and may be discussed separately. We do not attempt to follow the complicated motion that would develop in an unstable craft without control : we are concerned only with the way in which instability, if any, first occurs and from what causes. A large number of factors affect stability, and all must be retained in the examination of a border-line case. But several are of little importance, and may be omitted from the approximate solutions that often suffice in practice.

265. Axes and Notation

The motion of the C.G. of an aeroplane is determined by the resultant force and the rotation by the resultant couple about the C.G. We use a right-handed system of axes (Fig. 186), with the origin at the C.G. : Oz lies in the plane of symmetry and is directed approximately downwards in normal flight ; Ox points forward and

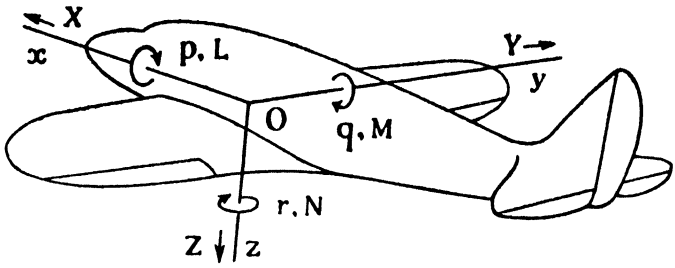

FIG. 186.

Oy to starboard. These axes are fixed relative to the craft and move with it. *Ox* may be chosen (whence the others follow) as a principal axis of inertia, or arbitrarily (e.g. parallel to the wing chord or the airscrew axis), or parallel to the undisturbed motion. The last choice is usually most convenient, and the axes are then known as *wind axes*. Positive pitch increases angle of incidence, α, positive bank (ϕ) and yaw (ψ) are those for a right-hand turn, and positive moments increase these angular displacements. Moments are denoted by L about Ox (rolling), M about Oy (pitching), N about Oz (yawing), and the corresponding angular velocities by p, q, and r. The components of Aerodynamic force in the directions of the axes are X, Y, and Z per unit mass of the craft. The transverse moment of inertia, approximately about Ox, is denoted by A, the longitudinal by B, and the directional by C.

V represents the resultant velocity of the aeroplane and U or u, v, W or w, velocity components along the axes. u, v, w are always small, but δU, δw may be used for infinitesimal increments. W is also used for the weight of the aeroplane, but no confusion will arise. A small increase of incidence $= w/V$, a small positive angle of yaw $= -v/V$.

Damping Factor.—Let w_1 be the initial value of a disturbance w, which varies exponentially with time. Writing $w = w_1 e^{\lambda t}$, λ (or its real part) is called the damping factor. Assuming the motion to be damped, let us calculate the time at which w will have decayed to $\frac{1}{2}w_1$. Taking logarithms, $\log \frac{1}{2} = \lambda t$, or—

$$t = -\frac{0{\cdot}69}{\lambda}.$$

For the disturbance to be damped, the real part of λ must be negative, and then the time to half-disturbance varies inversely as the damping factor. If the motion is unstable, the time to double disturbance follows in a similar way.

If λ be wholly real, the disturbance decays or grows continuously, and the motion is called a subsidence or a divergence, respectively. If λ be complex, let $\lambda = A + iB$. Then

$$e^{\lambda t} = e^{(A+iB)t} = e^{At}(\cos Bt + i \sin Bt)$$

and, as t increases, $e^{\lambda t}$ is seen to oscillate in value with a period $2\pi/B$ and an amplitude e^{At}. Thus if A—i.e. the real part of λ—be negative, the amplitude of successive oscillations decreases. The disturbance is then damped, the time required to halve the amplitude being $-0{\cdot}69/A$. A positive value of A indicates increasing amplitude and an unstable motion. Thus if λ be complex, its real part is the damping factor. It is possible for A to be zero, when the oscillation maintains constant amplitude ; in accordance with the preceding article, we regard this case also as indicating instability in connection with flight.

Immediate Notation.—Numerous symbols will be defined later as they arise, but the following are required for immediate use :

W = Weight of aeroplane.
S = Area of wings (of chord c).
l = Effective lever-arm of tail plane about C.G.
$\mu = W/g\rho Sl$, called the relative density of the aeroplane.
S' = Area of tail plane.
$\tau = S'l/Sc$, called the tail volume ratio.
a = Slope of lift curve $(dk_L/d\alpha)$ for wings.
a' = Slope of lift curve $(dk'_L/d\alpha')$ for tail.
α_t = Tail setting angle (angle between wing and tail chords).
ε = Angle of downwash.
k_m = Pitching moment coefficient : $M/\rho V^2 Sc$.
k = Radius of gyration about transverse axis through C.G.

INTRODUCTION TO LONGITUDINAL STABILITY

266. The Longitudinal Dihedral

A necessary, though insufficient, condition for longitudinal stability has been described in Article 87 : the rate of increase of $-M$ due to the tail must exceed that of M due to wings, body, etc. Neglecting all forces other than the lifts of wings and tail, and considering only normal incidences for which a, a', and $d\varepsilon/d\alpha$ remain constant, the argument may be arranged in convenient terms. It concerns the upward vee, or longitudinal dihedral, between wings and tail. Geometrically this $= \alpha_t$, but Aerodynamically it is more complicated.

If the C.G. is distant bc behind the quarter-chord point (the 'Aerodynamic centre') of the wings and k_{m_0} is the wing moment coefficient at the incidence α_0 of zero lift, we can write for the wings only—

$$k_m = k_{m_0} + bk_L.$$

For equilibrium at V and α—

$$\text{Tail lift} \times \frac{l}{\rho V^2 Sc} = k_{m_0} + bk_L.$$

On assuming a symmetrical section for the tail plane, so that its lift vanishes at zero local incidence, this expression leads at once to (cf. Article 87)—

$$\tau a' (\alpha + \alpha_t - \varepsilon) = k_{m_0} + ba(\alpha - \alpha_0).$$

On transference to the L.H.S., k_{m_0} can be represented by an additional angle e of the tail plane, giving—

$$\tau a' (\alpha + \alpha_t - \varepsilon + e) = ba(\alpha - \alpha_0). \quad . \quad \text{(i)}$$

Existence of a righting moment requires the L.H.S. of (i) to increase more rapidly with α than the R.H.S., i.e. differentiating with respect to α—

$$\tau a' \left(1 - \frac{d\varepsilon}{d\alpha}\right) > ba \quad . \quad . \quad . \quad . \quad \text{(ii)}$$

or from (i) again—

$$(\alpha - \alpha_0) \left(1 - \frac{d\varepsilon}{d\alpha}\right) > \alpha + \alpha_t - \varepsilon + e$$

i.e.—

$$-\alpha_t > \alpha_0 + e. \quad . \quad \text{(iii)}$$

In Fig. 187 the tail moment curve is plotted with its sign changed, so that intersection with the wing curve represents zero resultant moment and equilibrium on this account. The apparent or geometric dihedral—α_t is increased first by $-\alpha_0$ (α_0 being negative) and then by e, to give the effective dihedral, for only when the wings are at incidence $\alpha_0 - e$ will their moment vanish.

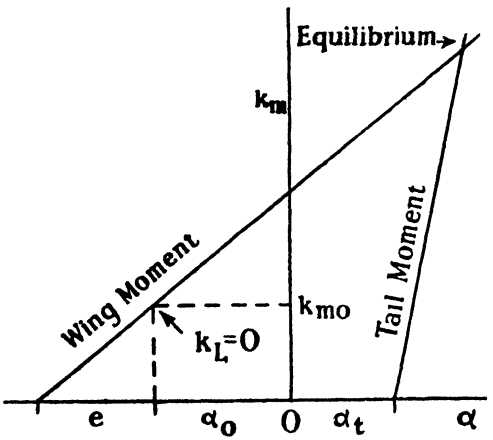

FIG. 187.—THE LONGITUDINAL AERODYNAMIC DIHEDRAL.

It will be seen that (iii) is independent of downwash, assuming $d\varepsilon/d\alpha$ constant. However, from (ii) the righting moment is proportional to—

$$\tau a' \left(1 - \frac{d\varepsilon}{d\alpha}\right) - ba \quad . \quad . \quad . \quad . \quad (377)$$

and the factor within the brackets is about 0·65 for normal monoplanes and 0·5 for biplanes (Articles 189, 192), so that S' must be increased on this score. The same principle holds for 'tail-first' aeroplanes, an old type recently revived and improved, but their forward stabilisers work in an upwash which, in contrast with downwash, increases efficiency (usually by some 7 per cent.).*

It is to be noted that the simple idea developed in this article, though useful in connection with certain compact types of craft, cannot be applied directly to modern high-speed monoplanes, in which the unstable moment of body and engine nacelles alone may easily exceed that of the wings.†

267. The Short Oscillation

The foregoing considerations are static, the C.G. being constrained and angular velocity zero. We now remove these restrictions, and examine in a preliminary manner ‡ the initial response of a stable aeroplane in straight horizontal flight to a transient vertical gust. The two moments of the last article, together with any other pitching moments arising on the craft, are assumed added algebraically to give a resultant static moment M, of which the coefficient is k_m. It is clear that the craft will nose into the relative wind. The C.G. receives a vertical acceleration, while there also occur changes both of pitch and pitching.

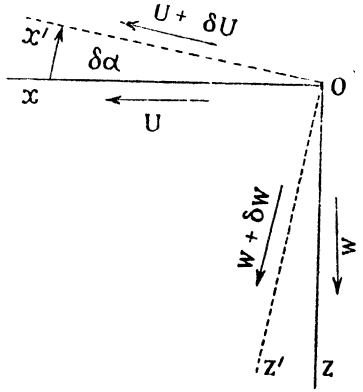

FIG. 188.

Shortly after the impulse, when U, w are the velocity components along Ox, Oz, let the craft pitch through the small angle $\delta\alpha$ in the short time δt, the directions of the axes changing from Ox, Oz to Ox', Oz' (Fig. 188), while the velocity components increase to $U + \delta U$ and $w + \delta w$. Resolving in the

* Bryant, *Aircraft Engineering*, July 1933.
† Cf. Lachmann, *R. Ae. S.*, 1936.
‡ The approximate treatment in this article is based on a paper by Munk.

original direction Oz, the increase of velocity in δt is $\delta w \cos \delta\alpha - (U + \delta U) \sin \delta\alpha = \delta w - U\delta\alpha$ to the first order of small quantities. Hence the acceleration in the direction Oz comes to $dw/dt - U \,.\, d\alpha/dt$. V and q can be written without serious error for U and $d\alpha/dt$, when the acceleration becomes—

$$\frac{dw}{dt} - Vq.$$

The increase of downward force is $-\rho V^2 S \,.\, a\Delta\alpha$, while $\Delta\alpha = w/V$. Therefore—

$$\frac{W}{g}\left(\frac{dw}{dt} - Vq\right) = -\rho V S a w. \quad . \quad . \quad \text{(i)}$$

The angular acceleration is dq/dt. One moment in this direction is $\rho V^2 Sc(dk_m/d\alpha)\Delta\alpha$. Others arise in a complicated way, but the most important of these is due to the increase of incidence of the tail plane by lq/V, and amounts to $-\rho V^2 S' l \,.\, a'(lq/V)$ in the sense of α increasing. Hence to the present approximation—

$$\frac{Wk^2}{g}\frac{dq}{dt} = \rho V^2\left(\frac{dk_m}{d\alpha} Sc \frac{w}{V} - S'la' \frac{lq}{V}\right). \quad . \quad \text{(ii)}$$

The two equations (i) and (ii) are conveniently written—

$$\mu\left(\frac{dw}{dt} - Vq\right) = -\frac{a}{l} Vw \quad . \quad . \quad \text{(iii)}$$

$$\frac{\mu k^2}{Vc}\frac{dq}{dt} = \frac{w}{l}\frac{dk_m}{d\alpha} - \tau a' q. \quad . \quad \text{(iv)}$$

From these follow two expressions for q:

$$q = \frac{1}{V}\frac{dw}{dt} + \frac{a}{\mu l} w = \frac{1}{\tau a'}\left(\frac{w}{l}\frac{dk_m}{d\alpha} - \frac{\mu k^2}{Vc}\frac{dq}{dt}\right). \quad \text{(v)}$$

Differentiate (iii) and substitute for dq/dt from (v), obtaining—

$$\frac{d^2 w}{dt^2} + \xi V \frac{dw}{dt} + \eta V^2 w = 0 \quad . \quad . \quad \text{(378)}$$

where—

$$\xi = \frac{1}{\mu}\left(\frac{\tau a' c}{k^2} + \frac{a}{l}\right),$$

$$\eta = \frac{c}{\mu l k^2}\left(\frac{\tau a a'}{\mu} - \frac{dk_m}{d\alpha}\right). \quad . \quad . \quad \text{(vi)}$$

A similar differential equation may be obtained for q.

Substituting from $w = w_1 e^{\lambda t}$ in (378) gives the following equation for the damping factor :

$$\left(\frac{\lambda}{V}\right)^2 + \xi\frac{\lambda}{V} + \eta = 0 \quad . \quad . \quad . \quad (379)$$

whence—

$$\frac{\lambda}{V} = \frac{-\xi \pm \sqrt{\xi^2 - 4\eta}}{2}.$$

The form of the roots follows for a given craft at a particular speed, enabling stability in the present connection to be examined.

If, for instance, $\eta = 0$, one root is zero and the other $= -\xi$. The motion is then not an oscillation, but a stable *subsidence* or an unstable *divergence* according to the sign of ξ.

Usually, however, $4\eta > \xi^2$, when a pair of complex roots results, which indicates an oscillation. Writing these roots—

$$\lambda/V = -\tfrac{1}{2}\xi \pm i\beta,$$

$-\frac{1}{2}\xi V$ is the damping factor and $2\pi/\beta V$ is the periodic time.

268. Examples

The following particulars relate to a small, slow, lightly loaded biplane at 100 m.p.h. :

μ	c	S/S'	k/c	l/c	τ	a	a'	$dk_m/d\alpha$
6	5 ft.	10	1·0	2·8	0·28	2	1·5	− 0·12

From (vi) of the preceding article we find $\xi = 0{\cdot}0378$, $\eta = 0{\cdot}00062$. Hence—

$$\lambda/V = -0{\cdot}0189 \pm 0{\cdot}0162i.$$

The time t of a complete oscillation $= 2\pi/(0{\cdot}0162 \times 146{\cdot}7) = 2{\cdot}64$ secs. The damping factor $= -0{\cdot}0189 \times 146{\cdot}7 = -2{\cdot}77$. The time to half-disturbance $= 0{\cdot}69/2{\cdot}77 = 0{\cdot}25$ sec., or $< 0{\cdot}1\ t$. Thus the oscillation is very heavily damped.

Let us next suppose that at 50 m.p.h. the aeroplane is approaching its stall, and that a, a' are then reduced by 80 per cent. ; for simplicity $dk_m/d\alpha$ will be kept the same. We find that t is doubled, while λ is reduced by 90 per cent., so that before 50 per cent. of the initial disturbance is damped out, nearly half a complete oscillation is described, or the craft travels 183 ft. If, at a still lower speed, both wings and tail arrived at a flat stall, a damping factor would cease to exist. The formula for ξ shows, in short, that causes of decrease in damping are : increase of μ, i.e. increase of wing loading

or altitude, or too short a fuselage ; increase of moment of inertia ; decrease of tail volume ; decrease of lift-angle slopes.

We must not strain this approximate analysis too far in seeking to apply it to practical flight. But the following conclusions which it demonstrates are well established. The immediate response of a stable aeroplane at high speed to a vertical gust or like disturbance is an exceedingly rapid dead beat adjustment into the wind ; damping becomes light at low speed near the stall, and an oscillation may develop, of period usually less than 5 secs.

269. Lanchester's Phugoid Oscillation

In this article we assume the short oscillation to be damped. Considering the effect of a transient upgust on initially steady horizontal flight, the craft, turning almost instantly into the relative wind as described in the preceding article, proceeds to fall and gather speed. The resulting increase of lift provides an upward acceleration, eventually stopping the fall and sloping the path upwards again. The airscrew axis, which at first dipped, recovers and passes through its original inclination to the horizon. Speed decreases and, as the craft completes its small climb, becomes low, so that the aeroplane must dive again to recover speed. Unless damped out or corrected by the pilot, the cycle of changes repeats itself with a period seldom less than 15 secs. This is called the long, slow, or (after Lanchester) the phugoid oscillation.

For the present we shall be content to examine a greatly simplified, or idealised form of the phugoid oscillation, following closely Lanchester's * original demonstration. The simplifying assumptions are : constant incidence to instantaneous flight path, a propeller thrust that *always* exactly balances drag, small size of craft compared with the minimum radius of curvature of the flight path, and negligible moment of inertia. Then the Aerodynamic force is perpendicular to the path, and varies with the square of the speed. But the angle θ between the vertical and the normal to the flight path is assumed to be sufficiently small for the difference between $\cos\theta$ and unity to be neglected, so that the vertical component of the Aerodynamic force is sensibly equal to the lift. It is implied that the oscillation is of small amplitude, and it follows that squares of velocity increments are negligible.

The motion is governed by an alternating exchange of potential

* *Aerial Flight*, v, 2 : " Aerodonetics," 1908. In this historic work Lanchester proceeded to introduce corrections for moment of inertia, etc., but such development will be approached in another way.

and kinetic energy, which is conservative. Let the altitude of the craft increase by h while speed increases by u. The K.E. increases from $WV^2/2g$ to $W(V+u)^2/2g$, i.e. by WVu/g, and—

$$Wh + WVu/g = 0. \quad . \quad . \quad . \quad (i)$$

Owing to constancy of k_L—

$$\text{Lift } (L) = W(V+u)^2/V^2 = W + W \,.\, 2u/V$$

or—

$$\delta L = L - W = -W \,.\, 2gh/V^2 \quad . \quad . \quad (ii)$$

on substituting for u from (i). Hence the vertical force increment varies (sensibly) as the vertical displacement of the craft from a mean level; the oscillation is simple-harmonic with period—

$$t = 2\pi\sqrt{\left(\frac{1}{g}\cdot\frac{V^2}{2g}\right)} = \pi\sqrt{2}\cdot\frac{V}{g} = 0{\cdot}138\ V. \quad . \quad (380)$$

Form of the Oscillation.—From (i), $-u/h = g/V$ = constant, whence the velocity variation is also simple-harmonic, 90° out of phase with the vertical displacement. Let u_1 be the maximum velocity variation and x_1, h_1 the semi-amplitudes of the motion of the C.G. of the craft relative to axes moving uniformly with velocity V and periodically coinciding with axes fixed in the craft. We have $x_1 = u_1 t/2\pi$ or, since $u_1 = -gh_1/V$ and from (380)—

$$-h_1 = \sqrt{2}\cdot x_1.$$

Thus the superimposed motion of the C.G. is elliptical, the vertical amplitude being $\sqrt{2}$-times the horizontal amplitude. This result

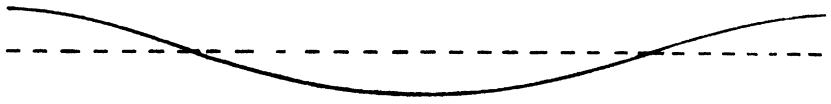

FIG. 189.—EXAMPLE OF PHUGOID OSCILLATION.

enables a phugoid oscillation of chosen length and vertical amplitude to be traced; an example is shown in Fig. 189.

The simple formula (380) indicates at 60 m.p.h., for example, 12·1 secs. for the time of a complete oscillation and 0·2 mile for its length. This estimate would not be widely wrong for an aeroplane of low minimum flying speed. But (380) would normally give much too small values at, say, twice the above speed, when the oscillation may exceed a mile in length. Since, in a real aeroplane, propeller thrust $\propto 1/V$ and drag $\propto V^2$ at constant incidence, damping of speed

changes would evidently occur. Other damping arises from incidence changes, here excluded. It is not necessary for the phugoid oscillation to exist ; two subsidences may take its place at high speed.

THEORY OF LONGITUDINAL STABILITY

270. The Classical Equations

As already mentioned, the theory of stability is founded on the assumption that it is sufficient to examine the response of the craft to small disturbances only from steady flight. We restrict investigation to straight flight, and in this case it was first remarked by Bryan and can readily be verified that a generalised disturbance may be resolved into components which affect the symmetric and asymmetric stability of the craft quite separately. Thus we are able to consider longitudinal stability without reference to lateral stability.

Considering an aeroplane climbing steadily at angle θ_0 to the horizon, with Ox in the direction of motion, the conditions for equilibrium are—

$$\begin{aligned} -g \sin \theta_0 + X_0 &= 0 \\ g \cos \theta_0 + Z_0 &= 0 \\ M_0 &= 0, \end{aligned} \qquad \text{(i)}$$

the components of Aerodynamic force being reckoned per unit mass. The latter are different functions of U_0, W_0, the steady values of the velocity components U, W. Obviously, $q = 0$.

Resulting from disturbance let U_0, W_0, and θ_0 increase by the small quantities u, w, and θ, and let q appear as variable. Equations (i) are no longer satisfied, accelerations appearing along Ox, Oz, and about Oy. These are found, as in Article 267, to be—

$$dU/dt + Wq = du/dt + Wq, \quad dW/dt - Uq, \quad dq/dt.$$

Each of the air forces, as well as the pitching moment, is affected by u, w, and q, unless shown otherwise ; for the increase of X to the first order we have—

$$\delta X = \frac{\partial X}{\partial U}\delta U + \frac{\partial X}{\partial W}\delta W + \frac{\partial X}{\partial q}\delta q.$$

Also the gravity components receive small increments. We write X_u for $\partial X/\partial U$, M_w for $\partial M/\partial W$, and so on. In this notation the force along Ox, for example, becomes—

$$-g \sin \theta_0 + X_0 - g \cos \theta_0 \,.\, \theta + uX_u + wX_w + qX_q$$

and the first two terms vanish by (i). Hence we have the following equations—

$$\begin{aligned} du/dt + Wq + g\cos\theta_0 \,.\, \theta &= uX_u + wX_w + qX_q \\ dw/dt - Uq + g\sin\theta_0 \,.\, \theta &= uZ_u + wZ_w + qZ_q \\ B \,.\, dq/dt &= uM_u + wM_w + qM_q. \end{aligned} \quad . \quad (381)$$

It is to be noticed that we can substitute $\int q dt$ for θ in these linear differential equations. They are founded on the assumption that u, w, q are so small after the impulsive disturbance that second order terms may be neglected. Recently, this assumption has been found to be insufficient for a peculiar reason in regard to the last equation, and the addition of the term $\dot{w}M_{\dot{w}}$ to be necessary, where $\dot{w} = dw/dt$. This will be discussed in detail later and an appropriate correction introduced. We might also add to the last equation a term representing an instantaneous movement of the elevator; a fourth equation might be framed for the propeller thrust.

Equations (381) determine u, w, q as functions of t. Any two variables may be eliminated in turn in the usual manner, and a differential equation of the same form results for u, w, or q, viz.—

$$f(D) \,.\, (u, w, \text{or } q) = 0,$$

where $f(D)$ contains powers up to the fourth of the differential operator. The solution of this equation is known to be of the form—

$$u = u_1 e^{\lambda_1 t} + u_2 e^{\lambda_2 t} + u_3 e^{\lambda_3 t} + u_4 e^{\lambda_4 t},$$

where u_1, etc., are constant coefficients derived from initial values, and λ_1, etc., are the roots of the equation $f(\lambda) = 0$. Since $De^{\lambda t} = \lambda e^{\lambda t}$, $D^2 e^{\lambda t} = \lambda^2 e^{\lambda t}$, etc., λu may be substituted for du/dt, etc., whence from (381) we find * for $f(\lambda) = 0$ the equation—

$$\begin{vmatrix} \lambda - X_u & -X_w & g\cos\theta_0 - \lambda(X_q - W_0) \\ -Z_u & \lambda - Z_w & g\sin\theta_0 - \lambda(Z_q + U_0) \\ -M_u & -M_w & \lambda^2 B - \lambda M_q \end{vmatrix} = 0 \quad (382)$$

On expansion this equation may be arranged as:

$$A_0\lambda^4 + B_0\lambda^3 + C_0\lambda^2 + D_0\lambda + E_0 = 0 \quad . \quad . \quad (383)$$

where the coefficients of λ, called the stability coefficients, are functions of X_u, M_q, B, θ_0, etc., all of which can be ascertained for a given aeroplane under particular conditions. The response of the aeroplane to small disturbance is investigated from the nature of the

* For a more detailed demonstration see Cowley and Levy, *Aeronautics in Theory and Experiment*, 1918.

roots of this equation, which may be real or complex. Stability occurs if, as before, their real parts are negative. The algebraic condition for this result is that all the stability coefficients—together with Routh's discriminant :

$$R_0 = B_0C_0D_0 - A_0D_0^2 - B_0^2E_0 \quad . \quad . \quad (384)$$

are required to be positive.

The demonstration is completed with expressions for the stability coefficients. It is convenient, however, to delay these until the equations are expressed in more convenient units.

271. Glauert's Non-dimensional System

It will be seen that the stability equations are rather complicated. Their discussion is greatly facilitated by adoption at once of the dimensionless system of units due to Glauert.*

The quantities X_u, M_q, etc., are called *resistance derivatives* ; the first named is further distinguished as a *force-velocity* derivative, the second as a *moment-rotary* derivative ; to take another example, X_q is called a *force-rotary* derivative. Inspection at once shows that the derivatives depend on ρVS (not on ρV^2S), S being taken for convenience as the wing area, and we accordingly divide by this quantity. Again, it is inconsistent to reckon forces per unit mass of the craft, and yet to leave moments as actual moments. Finally, most of the old derivatives are negative, and it makes for clearness to change their signs.

Consider, for example, the force derivative X_u. When U_0 changes to $U_0 + u$, X_0 changes to X as given by—

$$X = X_0\left(\frac{U_0 + u}{U_0}\right)^2 = X_0\left(1 + \frac{2u}{U_0}\right).$$

But, if m is the mass of the aeroplane, $mX_0 = -k_D\rho U_0^2S$, provided k_D is calculated to include parasitic drag. Hence—

$$mX_u = m\frac{2X_0}{U_0} = -2k_D\rho U_0S.$$

It is evidently suitable, therefore, to replace X_u by the non-dimensional coefficient x_u defined (if W is the weight) by—

$$x_u = -\frac{W}{g}\cdot\frac{X_u}{\rho VS} = 2k_D\ (= C_D). \quad . \quad . \quad (385)$$

Now X_u has the dimensions $1/T$. Hence an appropriate unit of time t_0 in the non-dimensional system is—

$$t_0 = W/g\rho VS. \quad . \quad . \quad . \quad . \quad (386)$$

* *Loc. cit.*, p. 381

Lengths must be expressed in terms of some representative length, and the effective lever-arm l of the tail plane from the C.G. is chosen.

It follows that the unit of velocity is l/t_0, and this $= V/\mu$ ft. per sec. if—

$$\mu = W/g\rho Sl \quad . \quad . \quad . \quad . \quad (387)$$

as in Article 267. The significance of μ, the *relative density of the aeroplane*, will already have partly appeared ; it collects the effects of size, wing loading, and altitude. But the following is of interest. Let us define k_R, the *coefficient of resultant air reaction*, by—

$$k_R\rho V^2S = W\cos\theta_0 \quad . \quad . \quad . \quad (388)$$

For small values of θ_0, k_R closely equals the lift coefficient, and, if $\cos\theta_0 = 1$—

$$\frac{\mu}{k_L} = \frac{\rho V^2S}{W}\cdot\frac{W}{g\rho Sl} = \frac{V^2}{gl}, \quad . \quad . \quad . \quad (389)$$

The quantity on the R.H.S. will be recognised as the appropriate parameter (cf. Article 66) for similar motions that are affected by gravity.

A non-dimensional force-rotary derivative is obtained by dividing that of the old system by ρVSl, multiplying by m, and changing sign, e.g.—

$$x_q = -mX_q/\rho VSl.$$

Finally, moments of inertia are expressed in the form—

$$B = k_B ml^2,$$

the coefficient being called an *inertia coefficient*, and the moment-velocity and moment-rotary derivatives of longitudinal stability are—

$$m_w = -\frac{M_w}{k_B\rho VSl}, \quad m_q = -\frac{M_q}{k_B\rho VSl^2} \quad . \quad . \quad (390)$$

272. Recast Stability Equation

In terms of the non-dimensional system the equation (382) becomes—

$$\begin{vmatrix} \lambda + x_u & x_w & \mu k_R + \lambda\left(x_q + \mu\dfrac{W_0}{V}\right) \\ z_u & \lambda + z_w & \mu k_R\tan\theta_o + \lambda\left(z_q - \mu\dfrac{U_0}{V}\right) \\ m_u & m_w & \lambda^2 + \lambda m_q \end{vmatrix} = 0 \quad . \quad (391)$$

This is simplified further by (*a*) introducing wind axes, (*b*) neglecting the derivatives x_q, z_q, which are always small. The result is—

$$\begin{vmatrix} \lambda + x_u & x_w & \mu k_R \\ z_u & \lambda + z_w & \mu(k_R \tan \theta_0 - \lambda) \\ m_u & m_w & \lambda^2 + \lambda m_q \end{vmatrix} = 0 \quad . \quad (392)$$

Expansion gives—

$$\lambda^4 + B_1\lambda^3 + C_1\lambda^2 + D_1\lambda + E_1 = 0 \quad . \quad (393)$$

in which—

$$\begin{aligned} B_1 &= x_u + z_w + m_q \\ C_1 &= x_u z_w - x_w z_u + m_q(x_u + z_w) + \mu m_w \; [= z_w m_q + \mu m_w, \text{ approx.}] \\ D_1 &= m_q(x_u z_w - x_w z_u) + \mu\{m_w(x_u - k_R \tan \theta_0) - m_u(x_w + k_R)\} \\ E_1 &= \mu k_R\{m_w(z_u - x_u \tan \theta_0) - m_u(z_w - x_w \tan \theta_0)\} \\ &\quad [= \mu k_L(z_u m_w - z_w m_u), \text{ approx.}] \quad . \quad . \quad . \quad . \quad . \quad (394) \end{aligned}$$

For stability, all the coefficients and Routh's discriminant must be positive.

273. These criteria for stability, though greatly simplified, are still rather involved. But the following may be noted at once.

It is generally true that D_1 and E_1 are small compared with B_1 and C_1, enabling (393) to be factorised approximately as—

$$(\lambda^2 + B_1\lambda + C_1)\left(\lambda^2 + \frac{C_1D_1 - B_1E_1}{C_1^2}\lambda + \frac{E_1}{C_1}\right) = 0 \quad . \quad (395)$$

The first factor equated to zero gives the short oscillation (cf. Article 267), the second the phugoid oscillation or the subsidences which may take its place. Now, Routh's discriminant has to do with oscillations. Unless an oscillation increases in amplitude through the discriminant becoming negative, instability must first appear (in a nearly stable aeroplane) through E_1 becoming negative. To the approximation in (395) the conditions for stability are—

$$E_1 \text{ and } (C_1D_1 - B_1E_1) \text{ both positive.} \quad . \quad . \quad (396)$$

The first of these conditions means m_w positive, in horizontal flight, and so refers to the investigation of Article 266.

It is seen that μ is always associated with m_w or m_u, in which it might be included. This usefully localises effects of wing loading and altitude.

Since the scale of time is changed, the new damping factor and the new period of oscillation are (if the accent refers to the old)—

$$\lambda = \lambda' t_0, \quad t = t'/t_0 \quad . \quad . \quad . \quad (397)$$

and we have, if σ is the relative density of the air—

$$t_0 = \frac{1}{g\rho_0\sigma VS}\sqrt{W \cdot k_L \rho V^2 S} = 0{\cdot}637\sqrt{\frac{W}{S}\cdot\frac{k_L}{\sigma}} \quad . \quad (398)$$

ENGINE-OFF STABILITY

274. Force Derivatives

Certain practically useful formulæ will now be obtained that are restricted to normal flight incidences with engines off (often known as glider stability).

In steady flight with wind axes $-mX = D$, the total drag, and $-mZ = L$, the lift. But angle disturbance causes the directions of X and Z to cease to coincide with those of D and L. If incidence increase by the small angle w/V, we have—

$$-mX = D - \frac{w}{V}L, \quad . \quad . \quad . \quad (i)$$

$$-mZ = L + \frac{w}{V}D. \quad . \quad . \quad . \quad (ii)$$

Z and X, called the normal and longitudinal forces, respectively, can evidently be plotted from lift and drag data, and slopes at the undisturbed incidence measured. But we can calculate approximately as follows. By differentiation of (i)—

$$-mX_w = \frac{\partial}{\partial w}\left(D - \frac{w}{V}L\right) = \frac{1}{V}\left(\frac{dD}{d\alpha} - L\right)$$

whence—

$$x_w = -\frac{mX_w}{\rho VS} = \frac{dk_D}{d\alpha} - k_L \quad . \quad . \quad . \quad (iii)$$

This result is simplified by the substitution, appropriate to moderately small incidences (cf. Articles 176, 247): $k_D = k_0 + k_1 k_L^2$, giving $dk_D/d\alpha = 2k_1 k_L a$, a denoting $dk_L/d\alpha$ as before. k_0 will include parasite drag.

Proceeding in this way we find—

$$\begin{aligned} x_u &= 2k_D = 2(k_0 + k_1 k_L^2)\ (= C_L) \\ x_w &= \frac{dk_D}{d\alpha} - k_L = k_L(2k_1 a - 1) \\ z_u &= 2k_L\ (= C_L) \\ z_w &= a + k_0 + k_1 k_L^2 = a, \text{ approx.}, \end{aligned} \quad . \quad . \quad (399)$$

while it will be remembered that $x_q = z_q = 0$, approximately.

275. Moment Derivatives

One moment, m_u, vanishes in gliding flight. Another, m_w, is easily determined by experiment, or can be calculated roughly, in favourable circumstances, on lines indicated by Article 266. If k_m is the coefficient of resultant moment, we have—

$$m_w = -\frac{M_w}{k_B \rho V S l} = \frac{1}{k_B \rho V^2 S l}\frac{\partial M}{\partial \alpha} = \frac{c}{k_B l}\frac{dk_m}{d\alpha} \quad . \quad \text{(i)}$$

and now if only wings and tail contribute, we have clearly, from Article 266—

$$m_w = \frac{c}{k_B l}\left\{\tau a'\left(1 - \frac{d\varepsilon}{d\alpha}\right) - ba\right\}. \quad . \quad . \quad . \quad . \quad (400)$$

But in regard to modern high-speed monoplanes, this formula suffers from the restriction mentioned at the end of Article 266.

The remaining derivative, m_q, must be obtained from experiment, unless correction factors are available from experience, and presents a difficulty which leads to the introduction of another derivative, $m_{\dot{w}}$, as anticipated in Article 270. These are discussed in the next article.

276. m_q and $m_{\dot{w}}$.

The basic data for m_q are obtained by oscillating in a wind tunnel a more or less complete model of the aeroplane concerned about the transverse axis through its C.G. Two methods are in use. The model may be oscillated freely by means of a spring and the logarithmic decrement of the damping estimated by measuring the amplitudes of successive swings. Mechanical friction accounts for some of the observed damping, but is allowed for by repeating the experiment in still air. In the alternative forced oscillation method, the model is oscillated through a spring and wire by a crank (Fig. 190); the frequency of the applied oscillation is

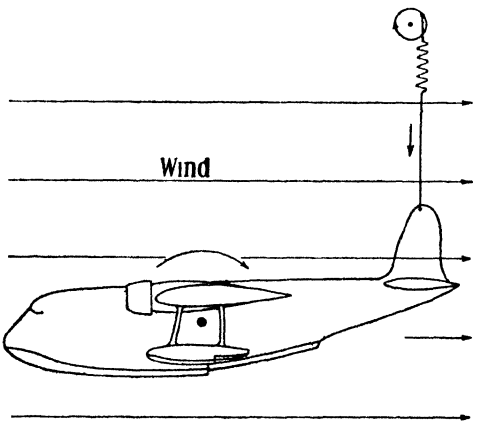

FIG. 190.—AN ARRANGEMENT FOR MEASURING AIR DAMPING.

gradually increased until the model attains a maximum synchronous vibration, the amplitude (θ_m) and period (t) of which are observed. If ν denote the damping due to the wind, ν_1 that due to friction, and θ_1 the amplitude of the forcing oscillation, it is nearly true that—

$$\nu + \nu_1 = \frac{t}{2\pi} \cdot \frac{\theta_1}{\theta_m} \quad . \quad . \quad . \quad (401)$$

ν_1 is extracted, as before, by repeating without the wind.

Either of these methods determines ν satisfactorily. But it does not follow that the air-damping is the same as M_q; in fact, these two quantities are essentially different from one another. The reason is as follows. M_q, like other derivatives, must be evaluated with other variables kept constant. But in the experiment α varies as well as q. Moreover, the time δt taken by a change of downwash $\delta\varepsilon$ due to change of wing incidence to travel from wings to tail is so considerable that the tail meanwhile changes its incidence appreciably. Now M_q results almost entirely from the tail, and downwash decreases tail incidence, which is increased, therefore, by the lag.

During δt let incidence increase by $\delta\alpha$. With the approximation $\delta t = l/V$, we find $\delta\alpha = \dot{\alpha}\ (l/V)$ and tail incidence is increased from lq/V to—

$$\frac{lq}{V} + \frac{d\varepsilon}{d\alpha}\,\delta\alpha = \frac{lq}{V} + \frac{d\varepsilon}{d\alpha} \cdot \dot{\alpha}\,\frac{l}{V} = \frac{l}{V}\,\dot{\alpha}\left(1 + \frac{d\varepsilon}{d\alpha}\right)$$

since $q = d\alpha/dt$. Thus the efficiency of the tail is increased by the factor within the brackets, and approximately—

$$M_q = \frac{\nu}{1 + d\varepsilon/d\alpha} \quad . \quad . \quad . \quad . \quad (402)$$

i.e. the measured air-damping is to be decreased by about one-third. Experiment affords support of this conclusion.* Finally,

$$m_q = -\frac{\nu}{k_B \rho V S l^2 (1 + d\varepsilon/d\alpha)} \quad . \quad (403)$$

Experimental determination takes account of interference from the wings (due to wake velocity reduction) and from the body, and includes damping from parts other than the tail represented in the model. If we neglect small contributions, and can introduce a factor I for interference, we calculate as follows. We have—

$$M_q = \frac{\partial M}{\partial q} = -\frac{l}{V}\frac{\partial M}{\partial \alpha} = -I\rho V S' a' l^2$$

* *Aerodynamic Theory*, vol. v, p. 51.

whence—

$$m_q = I \frac{c}{k_B l} \tau a^1 \quad . \quad . \quad . \quad . \quad (404)$$

No downwash factor appears, because incidence is assumed constant.

It remains to deal with the remainder of the air-damping, ν, i.e. the last term of—

$$\nu = M_q + M_{\dot{q}}(d\varepsilon/d\alpha)$$

which follows from (402). Since $q = \dot{\alpha}$ and α (when $q = 0$) $= w/V$, $\dot{\alpha} = \dot{w}/V$ and—

$$M_{\dot{w}} = \frac{1}{V} M_{\dot{\alpha}} = \frac{1}{V} M_{\dot{q}} \frac{d\varepsilon}{d\alpha}$$

Hence—

$$m_{\dot{w}} = -\frac{M_{\dot{w}}}{k_B \rho S l^2} = -\frac{M_{\dot{q}}(d\varepsilon/d\alpha)}{k_B \rho V S l^2}$$

$$= m_{\dot{q}} \cdot (d\varepsilon/d\alpha). \quad . \quad . \quad . \quad . \quad (405)$$

The effect on the stability equation of including this additional derivative is to add the term $\lambda m_{\dot{w}}$ to m_w in (392).

277. Example

Further discussion will be illustrated by reference to a monoplane of wing loading 13·8 lb. per sq. ft. at 150 ft. per sec., to which the following particulars apply :

μ	$c/k_B l$	τ	a	a''	b	k_L'	k_D	k_1	$d\epsilon/d\alpha$
12	3	$\frac{1}{3}$	2	1	0·075	0·258	0·025	0·1	0·35

It is assumed for simplicity in this example that formulæ (400) and (404) without an interference factor are suitable, provided a'' is substituted for a'. Hence—

$$m_w = 3(0{\cdot}333 \times 0{\cdot}65 - 0{\cdot}15) = 0{\cdot}2 \; ; \; m_q = 1.$$

We also have to a close approximation $k_R \tan \theta_0 = -k_L \cdot k_D/k_L = -k_D$, while $m_u = 0$ in gliding flight.

Neglecting $m_{\dot{w}}$, we find for the approximate stability coefficients of (394) :

$$B_1 = 2k_D + a + m_q = 3{\cdot}05,$$

$$C_1 = am_q + \mu m_w = 4{\cdot}4,$$

$$D_1 = m_q\{2k_D a - 2k_L^2(2k_1 a - 1)\} + 3\mu k_D m_w = 0{\cdot}36.$$

$$E_1 = 2\mu k_L^2 m_w = 0{\cdot}32.$$

All the coefficients are positive. Routh's discriminant—

$$B_1C_1D_1 - D_1^2 - B_1^2E_1 = 4{\cdot}83 - 0{\cdot}13 - 2{\cdot}98$$

is also positive, and the craft is stable.

Short Oscillation.—From (395) this is given by—

$$\lambda^2 + 3{\cdot}05\lambda + 4{\cdot}4 = 0$$

or—

$$\lambda = -1{\cdot}525 \pm \tfrac{1}{2}\sqrt{9{\cdot}30 - 17{\cdot}6} = -1{\cdot}525 \pm 1{\cdot}44i.$$

The period is—

$$t\ (\text{sec.}) = \frac{2\pi}{1{\cdot}44}\,t_0 = 5{\cdot}2,$$

because $t_0 = 13{\cdot}8/g\rho V = 1{\cdot}2$. The time to half-disturbance is $\frac{1}{2}$ sec.

278. The Long Oscillation.

To the approximation of (395) the period of the phugoid is—

$$t\ (\text{sec.}) = 2\pi t_0\sqrt{C_1/E_1}. \qquad . \qquad . \qquad . \qquad (406)$$

nearly. For the example this gives—

$$t\ (\text{sec.}) = 2{\cdot}4\pi\sqrt{4{\cdot}4/0{\cdot}32} = 28.$$

Similarly, the damping factor in common units is—

$$-\frac{1}{t_o}\cdot\frac{C_1D_1 - B_1E_1}{2C_1^2} \qquad . \qquad . \qquad . \qquad (407)$$

evaluating to—

$$-\frac{1}{1{\cdot}2}\times\frac{4{\cdot}4\times 0{\cdot}36 - 3{\cdot}05\times 0{\cdot}32}{2\times 19{\cdot}36} = -0{\cdot}0131$$

and the time to half-disturbance is $0{\cdot}69/0{\cdot}0131 = 53$ secs.

It is of interest, however, to develop approximate formulæ in terms of the derivatives for gliding flight. Substituting in (406)—

$$t\ (\text{sec.}) = 2\pi\frac{W}{g\rho SV}\sqrt{\left(\frac{\mu m_w + z_w m_q}{\mu k_L z_u m_w}\right)}$$

$$= \frac{\pi\cdot\sqrt{2}}{g}V\sqrt{\left(1 + \frac{am_q}{\mu m_w}\right)}. \qquad . \qquad . \qquad . \qquad (408)$$

This result should be compared with (380); that simple and preliminary estimate of the period is to be increased by the factor under the radical. A rough formula for the second term of this factor in the case of a monoplane having unimportant pitching moments from the body and engine nacelles is easily obtained from (400) and

(404) as $(a/\mu)/(0{\cdot}65 - \beta b)$, where β will be of the order 6. Thus, considering a craft of given weight and shape, moving the C.G. back may soon produce a long period. If m_w vanish, no oscillation will occur. Then E_1 is no longer positive, and the motion is a weak divergence. If, on the other hand, the C.G. is far forward and m_w large while (owing to small tail volume) m_q becomes small, a large moment of inertia is likely to make the oscillation increase in amplitude.

SOME STALLING AND ENGINE-ON EFFECTS

279. The foregoing analysis may be employed for gliding flight up to 8° or 10° incidence, but errors then begin to become appreciable. The method ceases to be useful near the stall. Nothing serious happens to the phugoid, as a rule, on reaching the stall, but the short oscillation may become unstable through a narrow range of speed. Effects primarily resulting from large decreases in a and a', and from reversal of sign of the former, will easily be followed out. Some notes are given below on other effects.

Tail Level.—The efficiency of a tail plane is reduced by the wings on account of their downwash and wake. It is not feasible to obviate the first loss except by ' tail-first ' layout. The second may involve a factor so low as 0·75 through decreased air speed if the tail plane is directly in the wake, but can be avoided at small incidences by carrying the tail plane either high or low. Now wings which approach a rectangle in plan-form stall first near the centre of span, several degrees earlier than the incidence for maximum lift. Downwash then decreases at the tail plane, while the wake thickens and lifts—two changes which are conflicting in regard to tail efficiency. The high tail plane suddenly becomes poorly situated at large incidences through passing into the wake, decrease of downwash failing to compensate for loss of speed ; the tail plane which is normally level with the wings may run through the wake and become more efficient. These effects are illustrated in Fig. 191.

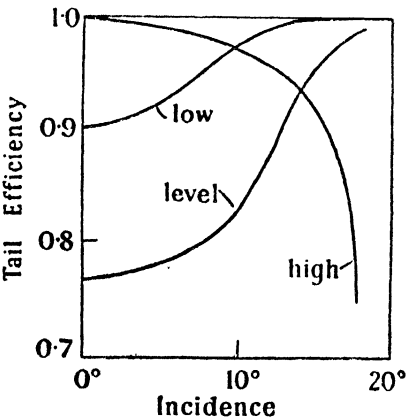

FIG. 191.—EFFECTS OF TAIL LEVEL ON ITS EFFICIENCY.

With wings having very sharp taper, stall may set in from the tips * and the above transition be delayed. Sharp taper is also associated with a concentration of downwash behind the central part of the span. Tail location for biplanes is governed by the fact that the lower wing usually stalls late.

It will be deduced that a rather low position for the tail plane is usually preferable from the present point of view. However, this frequently tends to increase parasite drag and to introduce landing difficulties.

280. Effects of Stalling on Moment Derivatives

In regard to m_w, most aeroplanes have such strong static stability at large incidences that elevators of normal size soon fail to be able to depress the tail further.

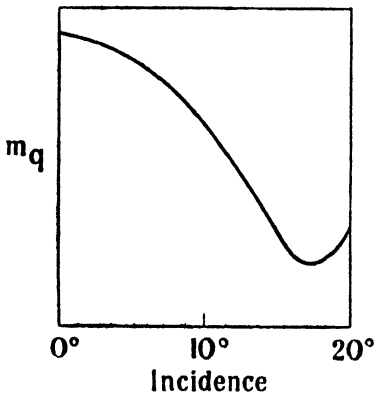

FIG. 192.—VARIATION OF m_q WITH INCIDENCE (TYPICAL).

Variation of m_q, or $m_q + m_{\dot{w}}$, normally takes the form illustrated in Fig. 192. Near the stall, damping passes through a sharply defined minimum, which has little to do with the tail, but is due essentially to rapid changes in the pitching moment of the wings. Instability may result from this cause through a narrow range of low speeds. First approximations to the damping factors of the short and long oscillations are, respectively, m_q and a becoming small—

$$-\tfrac{1}{2}(m_q + a) \quad \text{and} \quad -3k_D/2.$$

The large increase of drag at stall tends to keep the phugoid stable, and the trouble is seen to be concerned with the short oscillation, normally so strongly damped. The question is intimately concerned with the shape of the lift curve at the critical angle, i.e. on the violence of the stall. This is less severe if burbling creeps forward from the trailing edge than if, as happens with some aerofoil shapes, it sets in near the nose.

281. Level Flight

It is by no means certain that an aeroplane which is satisfactory when gliding will maintain stability when the engines are opened out

* Nazir, *Jour. R.Ae.S.*, August 1935.

for level flight. The chief differences that occur are summarised below; further study may conveniently proceed by a method of graphical analysis which will be described later.

The first change to note is that $\theta_0, = -\tan^{-1}(k_D/k_L)$ during gliding, vanishes, thereby reducing the stability coefficient D_1.

Several important changes affect the tail plane, assumed to lie in the slipstream. The first is an increase of downwash, which is difficult to calculate as local changes of trailing vorticity are involved; at present this is best estimated from special experiments (the cautionary note may be made that increases are often surprisingly larger than would be indicated by simplified theories). The chief result is a decrease of static stability through modification of m_w. Secondly, the tail plane is subjected to an increase of speed, which may be calculated by the methods of Chapter XI, and has the effect of increasing m_q. Thirdly, we note that the slipstream will vary with small changes of V due to variation of propeller thrust T, and that m_u will take up values in consequence. It is not difficult to estimate dT/dV from Chapter X, constant engine torque being assumed for this purpose. But if the speed at the tail plane increase from V to $V\sqrt{r}$, a formula for m_u is—

$$m_u = \frac{c}{lk_B} \cdot \frac{V}{r} \cdot \frac{dr}{dV} \tau k'_L. \quad . \quad . \quad . \quad (409)$$

Besides its effect on m_u, dT/dV directly modifies the gliding formula for x_u to

$$x_u = 2k_D - \frac{1}{\rho VS} \frac{dT}{dV}. \quad . \quad . \quad . \quad (410)$$

It should be observed that k_D is not the same in this formula as in that for gliding, because of the elimination of the idle airscrew drag of the latter case. For this reason, x_u is often much the same in the two cases.

282. High Speeds

On resolving (407) in terms of derivatives, a long expression results for the damping factor of the phugoid oscillation. This at once simplifies, however, if k_L become very small, corresponding to high speeds. Damping is then found to be proportional to k_D as a first approximation, a result that may be compared with a remark at the end of Article 269. It is somewhat unfortunate that stability, from the present point of view, decreases as the craft becomes more efficient.

Putting $a = 2$, the approximate expression for E_1 is—

$$E_1 = 2\mu(k_L^2 m_w - k_L m_u). \quad . \quad . \quad (411)$$

On k_L decreasing, the first term loses importance, and stability, as depending upon the sign of E_1, becomes more and more determined by that of m_u. m_u may change sign as speed attains high values and so produce instability. Possession of static stability does not guard against this eventuality.

283. Free Elevators

It is desirable, chiefly in order to reduce fatigue during long flights, for craft to be stable when elevators are released. The foregoing methods suffice to investigate this question in a given case, provided allowance is made for loss of efficiency by the tail plane. Following disturbance, free elevators will normally change their incidence by a less angle than if they were fixed, moving relative to the fixed part of the tail plane until the moment about their hinges again vanishes. The loss in tail efficiency may be as great as one-third. However, suitable balancing or springs can obviously be arranged to prevent the loss, or even to increase stability with free elevators by causing them to move through a greater angle than the craft on disturbance. This is a principal consideration in favour of minimising the chord of elevators.

284. Climbing

Referring to (394), climbing—θ_0 positive—is seen to diminish D_1 and E_1. The latter effect is usually negligible, and hence the result is to decrease the damping of the phugoid. The amount of the decrease is approximately $\mu m_w k_L \tan \theta_0 / C_1$.

285. Graphical Analysis

An ingenious and rapid means of examining stability by graphical means has been devised by Gates.* If we define—

$$X_0 = bl^2/k^2, \quad Y_0 = \tau a' \, . \, cl/k^2 \qquad . \qquad . \quad (412)$$

where k is the radius of gyration, so that $X_0 = 0$ is the Aerodynamic centre, we find that m_w and m_q will depend on X_0 and Y_0, but the other derivatives on k_L. The question of stability can be exhibited by plotting curves against X_0, Y_0 as co-ordinates, k_L and μ being supposed constant. The composite curve: Routh's discriminant $R_1 = 0$ and $E_1 = 0$, will represent a dividing line or boundary between stability and instability.

If, for example, we assume (400) and (404) to hold without an

* A.R.C.R. & M., 1118, 1927.

interference factor for a particular monoplane in which $a = 2{\cdot}5 = l/c$ and $d\varepsilon/d\alpha = 0{\cdot}35$, we have, during gliding:

$$m_q = Y_0, \qquad m_w = 0{\cdot}65\ Y_0 - X_0$$

and $E_1 = 0$ gives $X_0 = 0{\cdot}65\ Y_0$, independent of k_L and μ. But $R_1 = 0$ clearly depends on k_L and μ.

Fig. 193 illustrates the form of the boundary curve for gliding flight, as varying with k_L. The broken line indicates the approximation to $R_1 = 0$ given in (396). Crossing $E_1 = 0$ towards the right in the figure means that a divergence occurs, the curves being shaded towards the stable region, and both $C_1 = 0$ and $D_1 = 0$ lying to the right of $E_1 = 0$. $B_1 = 0$ lies far below the figure, parallel to the X_0 axis, and the possibility of B_1 becoming negative need not be considered. Crossing $R_1 = 0$ downwards signifies that an oscillation increases in amplitude. It will be seen that this eventuality is much less probable at high speeds than at low. Fig. 194 shows the effects of increasing μ at a low speed (k_L

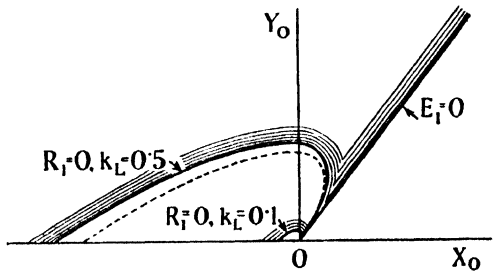

FIG. 193.—TYPICAL STABILITY CHART.

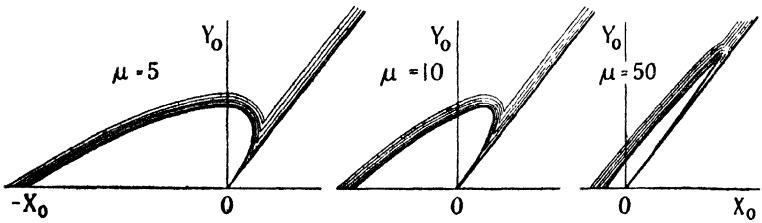

FIG. 194.

constant and fairly large); with a high wing loading, especially at great altitude, $E_1 = 0$ approximates to the complete conditions for stability. These illustrations are based on diagrams given by Gates,* who also obtains typical boundary curves for level flight, showing in particular a restriction of the stable region for high-powered craft.

* This and some other writers on stability employ k_B to denote the radius of gyration about the transverse axis, instead of k as in the above. Reservation of this symbol for the inertia coefficient: k^2/l^2, has been adopted in this chapter for ease of reference to Jones's account of the subject, *loc. cit.*, p. 493.

LATERAL STABILITY

286. Introduction

From a mathematical point of view, the conditions for asymmetric stability are, with little error in normal flight, formally the same as those for longitudinal stability. The quite different relationships between corresponding derivatives, however, change the physical aspect completely.

The aeroplane is conceived to be flying straight in its plane of geometric symmetry when lateral balance is disturbed. The asymmetric motion that results comprises three responses, which develop at such very different rates that we can follow them in turn. If a vertical gust strike a wing-tip a rolling about Ox will first occur. The moment damping this formed the subject of investigation in Article 93, being found to have a large magnitude except near or past the stall. It is associated with the derivative L_p. Thus, normally, the rolling subsides extremely rapidly, leaving the craft with slight roll (list) and yaw. The sideslip that ensues generates a rather complicated lateral oscillation—the only oscillation that arises from asymmetric disturbance ; its period may be 5 or 6 secs., and, with a stable craft, it may diminish to half-amplitude in about double this time. The craft is then left with a sluggish spiral motion, associated with sideslip and yawing, which is slow to develop or to decay.

Since the rolling subsidence is inherent in all aeroplanes at normal incidences, asymmetric stability is concerned with the oscillation and the spiral motion, and these depend largely on the disposition of the vertical fins. The *effective* fins of primary importance are (*a*) the actual fin together with the rudder, usually situated above the tail plane, (*b*) the transverse dihedral angle of the wings. The significance of the latter as a fin was seen in Article 95, from which (or otherwise) will be apparent that fins in general lead to both roll and yaw. Thus arise the derivatives L_v and N_v. Secondary fins include the body, engine nacelles and airscrews. These are by no means negligible, especially in the case of high-speed monoplanes of modern types. (*a*) and (*b*) alone, however, are at the designer's disposal in regard to stability ; they are adjusted to take secondary fin effects into account and the latter will be omitted from discussion for clearness.

It is important to realise that fore-and-aft balancing of fin surface is critical. A craft left with positive roll sideslips to the right, and the equivalent yaw produces lateral forces on the fins. That on the rear

fin (comprising the actual fin and the rudder) turns the craft into a right-hand turn suitable for the existing bank. The left-hand wing-tip now moves with excess speed, and asymmetric lift may increase both bank and sideslip. The resulting spiral flight is seen to follow too strong a directional stability in the static sense. On the other hand, much too far forward a position for the C.P. of the lateral forces—strong directional instability—leads rapidly to a fast, spinning dive. No definite result can be drawn from these simple considerations ; it is not clear that any static directional righting couple is desirable, slight directional instability of the static kind often proving an advantage dynamically.

The above illustrations tacitly assume a weak or absent transverse dihedral. As we have seen, a dihedral rolls a craft away from the sideslip and turn. The outer wing-tip of the turn thus comes to be at the lower level, though its greater speed soon raises it again. Reversal of the sideslip leads to the lateral oscillation. This would not occur in a craft that was prone to spin. The latter defect being, however, uncommon, the oscillation is usually present, and may, on occasion, become noticeable, when sufficient (though not too great) static instability exists, together with an exaggerated dihedral.

287. The Asymmetric Equations

Mass distribution is now defined by A and C, the transverse and directional moments of inertia. For precision we have also to include E, the product of inertia along Oy, though terms containing this as factor may be neglected in normal flight. The gravity force is in the direction Oy and amounts to $g \cos \theta_0 . \phi$ per unit mass. Construction of the classical equations for small oscillations follows precisely the lines explained in Article 270 for longitudinal disturbances, and the reader will have no difficulty in verifying the following group in place of (381) :

$$\begin{aligned} dv/dt + U_0 r - W_0 p - g \cos \theta_0 . \phi &= vY_v + pY_p + rY_r \\ A . dp/dt - E . dr/dt &= vL_v + pL_p + rL_r \\ C . dr/dt - E . dp/dt &= vN_v + pN_p + rN_r \end{aligned} \quad . \quad (413)$$

in which, since $p = d\phi/dt - \sin \theta_0 \, d\psi/dt$ and $r = \cos \theta_0 \, d\psi/dt$ while $d\phi/dt = \lambda\phi$, we can substitute for ϕ from—

$$\cos \theta_0 . \phi = \frac{p}{\lambda} \cos \theta_0 + \frac{r}{\lambda} \sin \theta_0. \quad . \quad . \quad (414)$$

Treating these equations in the same way as (381) gives for the damping factor λ the equation—

$$\begin{vmatrix} \lambda - Y_v & -g\cos\theta_0 - \lambda(Y_p + W_0) & -g\sin\theta_0 - \lambda(Y_r - U_0) \\ -L_v & \lambda^2 A - \lambda L_p & -\lambda^2 E - \lambda L_r \\ -N_v & -\lambda^2 E - \lambda N_p & \lambda^2 C - \lambda N_r \end{vmatrix} = 0 \quad (415)$$

Expressed in the non-dimensional system, this equation can be arranged in the form *—

$$\begin{vmatrix} \lambda + l_p & -\lambda\dfrac{E}{C} + n_p & \mu k_R - \lambda\left(y_p - \mu\dfrac{W_0}{V}\right) \\ -\lambda\dfrac{E}{A} + l_r & \lambda + n_r & k_R\tan\theta_0 - \lambda\left(y_r + \mu\dfrac{U_0}{V}\right) \\ -l_v & -n_v & \lambda^2 + \lambda y_v \end{vmatrix} = 0 \quad (416)$$

Away from the stall, terms containing E as factor may be neglected. Comparison with (391) then shows formal agreement to exist according to the scheme :

	u	w	q
x	l_p	n_p	$-y_p$
z	l_r	n_r	$-y_r$
m	$-l_v$	$-n_v$	y_v

by which is meant that n_r takes the place of z_w, $-y_p$ that of x_q, etc.

288. Solution with Wind Axes

Introducing wind axes as in the longitudinal case, so that $U_0 = V$ and $W_0 = 0$, and taking approximately $E = y_p = y_r = 0$, (416) reduces to—

$$\begin{vmatrix} \lambda + y_v & -\mu k_R & \mu(\lambda - k_R\tan\theta_0) \\ l_v & \lambda^2 + \lambda l_p & \lambda l_r \\ n_v & \lambda n_p & \lambda^2 + \lambda n_r \end{vmatrix} = 0 \quad (417)$$

which expands to—

$$\lambda^4 + B_2\lambda^3 + C_2\lambda^2 + D_2\lambda + E_2 = 0 \quad . \quad . \quad (418)$$

where, writing k_L as an approximation to k_R—

$$\begin{aligned} B_2 &= l_p + n_r + y_v \qquad (= l_p, \text{ approx.}) \\ C_2 &= (l_p n_r - l_r n_p) + y_v(l_p + n_r) - \mu n_v \\ D_2 &= y_v(l_p n_r - l_r n_p) - \mu n_v(l_p - k_L\tan\theta_0) + \mu l_v(n_p + k_L) \\ E_2 &= \mu k_L\{(l_v n_r - l_r n_v) - \tan\theta_0(l_v n_p - l_p n_v)\}. \end{aligned} \quad . \quad (419)$$

These expressions should be compared with (394).

* Glauert, *loc. cit.*, p. 493.

The aircraft is stable if the stability coefficients and $R_2 = B_2C_2D_2 - D_2^2 - B_2^2E_2$ are all positive.

289. Approximate Factorisation

Arising from the overwhelming rolling subsidence there is in normal flight always one large root of (418), viz. $-B_2 = -l_p$, approximately, enabling the factor $(\lambda + l_p)$ to be divided out.

Associated with the spiral disturbance a small root occurs, closely of value $-E_2/D_2$, which can also be extracted.

There is left a quadratic, representing in usual circumstances the lateral oscillation. To a first and rather rough approximation this is—

$$\lambda^2 + \frac{C_2}{B_2}\lambda + \frac{D_2}{B_2} = 0. \quad . \quad . \quad . \quad (420)$$

The magnitude of the damping factor calculated from this approximation errs on the wrong side for safety. If the quadratic has real roots, it represents the spinning divergence.

290. Discussion in Terms of the Derivatives

The condition for E_2 to be positive in level flight is—

$$l_v n_r > l_r n_v \quad . \quad . \quad . \quad . \quad (421)$$

and instability is usually traced to a failure here. The first two derivatives are usually positive, the third considerably larger and negative, so that n_v, if negative, must be small. This means that static directional stability must be limited, though it is to be remarked that increase of $-n_v$ is accompanied by increase of n_r. More generally, the above condition is—

$$l_v(n_r - n_p \tan \theta_0) > n_v(l_r - l_p \tan \theta_0) \quad . \quad . \quad (422)$$

which intimates that stability is a little more difficult to secure during climbing.

The quadratic (420) is easily investigated once the stability coefficients have been evaluated in a given case. That it should have a pair of complex roots will be found to depend on n_v, if positive, not exceeding a small fraction of l_v. This value must be reduced considerably if the oscillation is to decay quickly, though it need not become negative, i.e. static directional stability may not be necessary.

Change of sign of l_p near the stall has consequences traced in Article 93.

291. Example

Some plausible numerical values are—

μ	k_L	l_v	l_p	l_r	n_v	n_p	n_r	y_v
8	$\frac{1}{4}$	$\frac{1}{2}$	6	-2	$-\frac{1}{4}$	$\frac{1}{2}$	$\frac{1}{3}$	$\frac{1}{8}$

These give for level flight—

B_3	C_3	D_3	E_3
6·46	5·79	15·38	−0·67

The craft is spirally unstable, to correct which a larger dihedral would be required. Routh's discriminant is—

$$6{\cdot}46 \times 5{\cdot}79 \times 15{\cdot}38 - (15{\cdot}38)^2 + (6{\cdot}46)^2 \times 0{\cdot}67,$$

so that the oscillation is damped. Inserting values in (420) we have approximately—

$$\lambda^3 + 0{\cdot}9\lambda + 2{\cdot}4 = 0$$

or—

$$\lambda = -0{\cdot}45 \pm 1{\cdot}45i.$$

The true damping would be appreciably less than as here estimated.

292. Evaluation of Derivatives

The only effective force derivative, y_v, is easily deduced from a tunnel experiment in which a complete model is yawed at a succession of small angles to the wind.

The strip method, introduced in Article 93 and employed in the Theory of Airscrews, is available for the approximate calculation of moment derivatives which depend largely on the wings. It is readily arranged to take account of non-uniform grading of air load along the span in steady flight. This is best seen from an example.

Let l_r be required at a mean lift coefficient k_{L0}. Neglecting contribution from a possibly high fin, consider two wing strips of chord c distant $\pm y$ from the longitudinal axis. Owing to change of local speed only, there arises an element rolling moment :

$$\delta L_{(r)} = \rho c \delta y k_L y \{(V + ry)^2 - (V - ry)^2\} = 4\rho V r k_L c y^2 \delta y.$$

If c and k_L may be assumed constant, this integrates at once to—

$$L_{(r)} = \tfrac{4}{3}\rho V r k_{L0} c s^3 = \tfrac{2}{3}\rho V r k_{L0} S s^2$$

where s is the semi-span and S the total area. Otherwise, considering the integral—

$$\int_0^s c k_L y^2 dy,$$

we note that—

$$k_{L0} = \frac{2}{S}\int_0^s c k_L dy$$

whence, if y_0 be the radius of gyration of the lift-grading diagram appropriate to the plan form and sections in steady flight,

$$L_{(r)} = 2\rho V r k_{L0} S y_0^2.$$

Finally—

$$l_r = -\frac{1}{\rho V S l^2 k_A}\frac{\partial L_{(r)}}{\partial r} = -\frac{2}{l^2 k_A} k_{L0} y_0^2 \quad . \quad . \quad (423)$$

In the absence of precise data, elliptic loading may be assumed, for which $y_0 = \frac{1}{2}s$.

Rotary derivatives can be determined experimentally by the oscillation method (Article 276)* or, in the case of l_p and n_p, by measurements during continuous rotation of the model about the wind direction. n_r depends principally on the fin and rudder and is analogous to m_q.

CONTROLS

293. The functions of Aerodynamic controls in steady flight under various conditions have already been described. The subject of aerobatics is beyond our scope. We now discuss the requirements and limitations of controls during disturbed flight, examining the first principles of their design in connection with the dynamic features of the craft. Several preliminary considerations are grouped together in this article.

Power.—In deciding the power for an Aerodynamic control, we note first that the size of elevators, given the leverage, determines the maximum angle of incidence of flight. These might be so diminished as to render impossible the deliberate stalling of the craft. Such a policy has adherents on the Continent, but opposed to it is the consideration that small elevators deprive the pilot of the means of quick recovery from accidental stall, caused, for example, by the sudden failure of an engine with a high thrust line. The ailerons, having a strong adverse rolling moment to overcome at normal speeds, must be many times as powerful as the rudder, for little resistance opposes yawing. Use of ordinary ailerons induces an adverse yawing moment, i.e. one which turns the craft to the wrong hand for the imposed bank ; this is natural, since the wing with the greater lift exerts the greater drag. The yawing is corrected by use of the rudder. The necessity for this correction may be overcome by a spoiler operating on the depressed wing, but synchronous rudder movement appears to have become instinctive with pilots.

* Relf, Lavender, and Ower, A.R.C.R. & M. 809, 1921.

The hinge moment of a control surface should be reduced by balancing to small magnitude, determined by the force a pilot can exert on the control column without fatigue. This balancing is Aerodynamic and will not be confused with mass balancing, introduced to prevent elastic flutter. It is achieved by locating the hinge line well aft of the effective nose of the control surface. There is some danger of over-balancing when fine limits are attempted for a very large craft ; moreover, balancing commonly fails at some moderately large control angle. For these and other reasons, the control surfaces of heavy aeroplanes are often servo operated, which usually means that the control column moves a tab, or diminutive surface attached to a control, in the wrong direction, and the tab generates sufficient Aerodynamic moment to operate the real control. There are two general points to notice. Aeroplane controls are 'reversible,' the pilot feeling a moment proportional to that applied. He is usually able, from the point of view of strength, to operate controls quickly through wide angles.

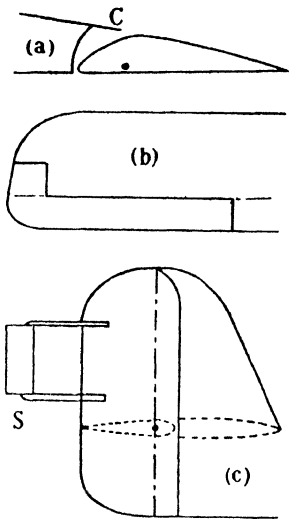

FIG. 195.—(*a*) FRISE TYPE AILERON ; THE NOSE ACTS AS A SPOILER ON THE DEPRESSED WING ; C, CURTAIN OR SHROUD. (*b*) HORN BALANCED AILERON. (*c*) OUTRIGGED SERVO (S) OPERATING THE PARTLY BALANCED RUDDER OF A LARGE CRAFT.

Stalling of Controls.—It is clearly important for controls to stall later than the wing. Consider, as one of many examples that might be chosen, the case of an aeroplane which is approaching a confined landing space steeply with its wings at large incidence ; a wing-tip that suddenly rotates downwards through a gust is momentarily at still greater incidence and yet must be lifted by its aileron. The remarkable efficiency of Handley Page slots both in delaying aileron stall and in curing adverse yawing moment at high incidences has been described in Article 94. Stalling of a control is also delayed by the so-called 'cut slot,' which may be arranged to open between a deflected control and the fixed member to which it is attached. Fore-and-aft location of a cut slot and also its shaping need care ; this is work for the wind tunnel, but experience is necessary to allow for scale effect on both variables. Slots should be closed when not in use.

Rudder and elevators lose efficiency when the wings stall. ' Shadowing ' by the wings may be so marked during a spin that the rudder is commonly set as high as structural considerations allow.

294. Relation to Stability

In normal disturbed flight, controls are used to correct a tedious, though safe, response of a stable aeroplane and also to supplement its stability if this be restricted.

Elevator control cannot vie with the speed of the short, damped oscillation—a chief reason for limiting longitudinal static stability, excess creating a discomfort in bumpy weather which is beyond the power of the pilot to ease. If the oscillation becomes unstable near the stall (Article 280), there results a lag in the response of the craft to the elevators, making steady flight difficult or impossible. Special modifications to controls have been suggested.*

The sluggish phugoid can be corrected at an early stage.

Turning to asymmetric disturbances, there is ample time to correct by control movements both the lateral oscillation and the slow spiral motion. But it is doubtful whether a pilot can act sufficiently rapidly to prevent failure by the spinning divergence, if this supersedes the lateral oscillation, especially as the cause is likely to be too small a rudder. It is noteworthy that since the spinning divergence may double disturbance every two seconds, whilst spiral instability, due to too great static righting moments, develops only very slowly, there exists a mathematical explanation of the pilot's well-known distrust of a weak rudder. Possession of too powerful a rudder prevents flying with all controls released, yet nearly all aeroplanes are so characterised, and it is probable that spiral instability will remain a general feature until amateur, fair-weather flying greatly increases.

In favourable circumstances, a stable aeroplane will fly itself just as steadily as a pilot can contrive ; it is equally true that an unstable aeroplane can be flown satisfactorily with skill and good controls, provided it is not wilfully unstable. An important aspect of stability is to provide relief for the pilot, and this will not be necessary during manœuvring. Thus a craft may be stabilised for level and gliding flight, but left to control during climb.

The investigation of this chapter is restricted to symmetric flight, and an aeroplane designed in accordance with the theory given might become unstable if, for example, it were turned into horizontal circling flight, when the damping is redistributed between the short

* Garner and Wright, A.R.C.R. & M., 1193, 1928.

and long oscillations. Extension of the theory is possible, but simplicity is lost through coupling of longitudinal and lateral effects. If it be thought that so restricted a study of the subject loses practical utility, it should also be realised that knowledge of a craft's symmetric stability will often suggest a modification to correct faulty behaviour in a manœuvre.

295. Large Disturbances

Experience has shown that most craft, when subjected to common disturbances, behave in much the same way as calculated by the theory of small oscillations. But guidance through very large disturbances must be left to the pilot; it is just in these circumstances that he stands most in need of unfailing controls; and the obvious deduction is that their efficiency should be ensured under extreme conditions. Aeroplanes are controllably safe in this wider view except as regards recovery from a possible type of motion known as the flat spin.

The flat spin may arise as a development of the slower spin described in Articles 92–94. When this ordinary spin speeds up and narrows, large centrifugal couples tend to lift the nose of the craft, and in some cases to increase the rate of spin rapidly. At a large incidence, in the neighbourhood of 45°, the elevators may not be able to check this tendency. The rate of descent then decreases, but the rate of spin increases from perhaps 20 r.p.m. to 60 r.p.m., and the only chance of control lies in the rudder. Detailed analysis must be left to further reading, but has not yet proceeded very far. An excellent experimental method of investigation is provided by the free spinning of light models in a vertical tunnel (cf. Article 66), although the usual difficulties exist in carrying over such small-scale experiments to full scale. The distribution of mass in the craft appears to be of great importance.

THE LOAD FACTOR

296. Whilst structural design is no part of our subject, Aerodynamics specifies largely what load each member of the craft should be able to withstand. The possibility of large transient accelerations makes a wide margin of strength especially desirable in aircraft, but the imperative need to save weight must narrow this down to the safe minimum. An over-all factor of safety, such as is commonly used in engineering design, would obviously be wasteful, and, as a rule, the maximum load that each part of a craft is likely

to be called upon to withstand is carefully assessed before applying an over-riding factor to allow for defects in design, material, and workmanship. It is unnecessary to consider the matter in detail, since rules are laid down by the competent Government authority, which take account of the duties which a given craft will normally discharge, and we shall consider only some principles.

Instances have appeared in Chapter IV and elsewhere, e.g. during steady or unsteady turning, where clearly the wings support a load equal to several times the dead weight of the craft. The ratio of this load to that supported in straight level flight is called the *load factor*. Considering all cases that may be specified by the acceleration of the C.G., we easily find that the load factor is the ratio of the abnormal to the normal lift coefficients, change of speed being neglected, and that its maximum value is the ratio of the maximum lift coefficient to the normal. The critical condition arises in pulling out from a steep dive, when k_L is initially very small, and simple calculations show that the load factor might then exceed 50 if the elevators were suddenly operated by radio from a distance. But a personal load factor of 5 would cause acute physical discomfort to a pilot, who therefore straightens out much more gradually. Thus the pilot acts as a safety valve against excessive load factors.

The *accelerometer* records the variation of load factor during flight. This instrument may consist of a short fine wire clamped at the ends like a beam to a frame secured to the aeroplane and with its length perpendicular to the direction of the acceleration to be measured. The wire bends under its own weight and centrifugal force, and the deflection is photographed on a moving film. Fig. 196 is a typical

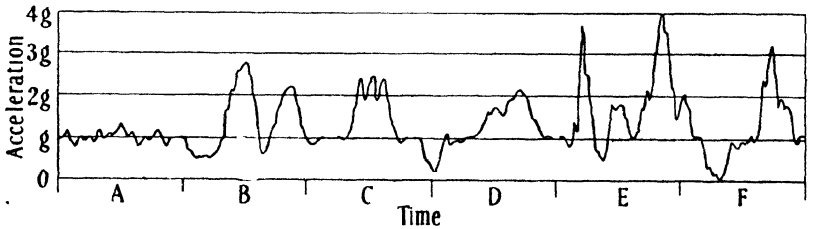

FIG. 196.—VARIATION OF LOAD FACTOR DURING FLIGHT.

Each of the intervals A, B, . . . is 30 sec. A, bad atmospheric bumps; B, loop; C, spin; D, dive and flatten out; E and F, mock fighting.

record for aerobatic flight, with the added zest of mock fighting; unit spacing in the vertical scale represents the maximum deflection of the wire under its own weight, i.e. due to the acceleration g. Even in this fairly severe test, the pilot kept C.G. accelerations

between 0 and $4g$. A specially trained pilot may nerve himself to $7g$ in cornering during a race, but such occasions are very exceptional, and it appears that in ordinary flight the variation of load factor, as due to control, is much less than might be expected. The accelerations of parts far from the C.G. vary through a wider range. It should be noticed that the accelerometer can be arranged to measure these, and also the component acceleration in any desired direction.

The response of a stable aeroplane to disturbance creates stresses, but the uncontrollable load factors may be more severe if the craft be unstable. A growing upgust, for example, will generate excess lift as indicated in Article 177, and this will be all the more marked if the craft noses away from the relative wind.

* * * * *

To trace reliably the load factors arising from a gust of given structure, as also to investigate many problems of control, we require to follow the disturbed motion of the craft. Problems frequently arising are concerned with the effects, over a comparatively brief interval of time, of forces and moments suddenly applied, e.g., by dropping a load by parachute, or, in military aeronautics, by firing a gun of considerable calibre. Others, as the analysis of spinning, involve longer periods Such studies call for wider reading than the foregoing treatment. Representation of the general motion of an aeroplane following small disturbances leads to eight simultaneous linear differential equations, though in some instances a smaller number will suffice. The labour of solution is greatly reduced by use of the method of operators introduced by Heaviside,* the theory of which has been given by Jeffreys.† Applications of operational methods to aircraft have been described by Bryant and Williams,‡ Klemin,§ and others.

* *Proc. Roy. Soc.*, A, 1893–4.
† *Operational Methods in Mathematical Physics*, 1927.
‡ A.R.C.R. & M., 1346, 1930.
§ *Jour. Aeronautical Sciences*, May 1936.

AUTHOR INDEX

The numbers refer to pages.

SUBJECT INDEX

The numbers refer to pages.